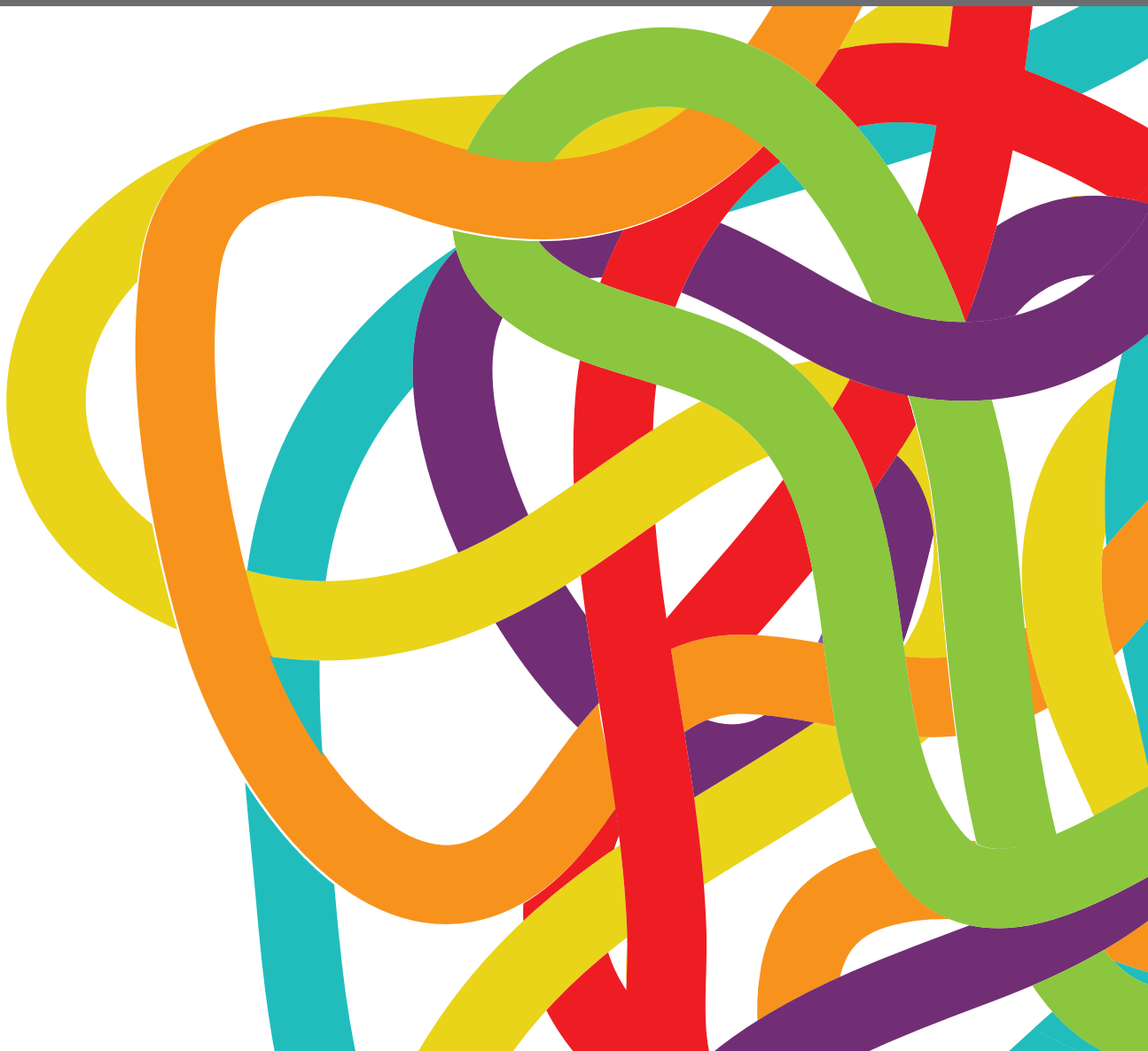


# IDENTIFICATION OF NOVEL BIOMARKERS FOR PANCREATIC AND HEPATOCELLULAR CANCERS

EDITED BY: Brendan Jenkins, Alessandro Passardi, Qingfeng Zhu and  
Zhaohui Huang  
PUBLISHED IN: Frontiers in Oncology





# frontiers

## Frontiers eBook Copyright Statement

The copyright in the text of individual articles in this eBook is the property of their respective authors or their respective institutions or funders. The copyright in graphics and images within each article may be subject to copyright of other parties. In both cases this is subject to a license granted to Frontiers.

The compilation of articles constituting this eBook is the property of Frontiers.

Each article within this eBook, and the eBook itself, are published under the most recent version of the Creative Commons CC-BY licence.

The version current at the date of publication of this eBook is CC-BY 4.0. If the CC-BY licence is updated, the licence granted by Frontiers is automatically updated to the new version.

When exercising any right under the CC-BY licence, Frontiers must be attributed as the original publisher of the article or eBook, as applicable.

Authors have the responsibility of ensuring that any graphics or other materials which are the property of others may be included in the CC-BY licence, but this should be checked before relying on the CC-BY licence to reproduce those materials. Any copyright notices relating to those materials must be complied with.

Copyright and source acknowledgement notices may not be removed and must be displayed in any copy, derivative work or partial copy which includes the elements in question.

All copyright, and all rights therein, are protected by national and international copyright laws. The above represents a summary only. For further information please read Frontiers' Conditions for Website Use and Copyright Statement, and the applicable CC-BY licence.

ISSN 1664-8714

ISBN 978-2-83250-836-7

DOI 10.3389/978-2-83250-836-7

## About Frontiers

Frontiers is more than just an open-access publisher of scholarly articles: it is a pioneering approach to the world of academia, radically improving the way scholarly research is managed. The grand vision of Frontiers is a world where all people have an equal opportunity to seek, share and generate knowledge. Frontiers provides immediate and permanent online open access to all its publications, but this alone is not enough to realize our grand goals.

## Frontiers Journal Series

The Frontiers Journal Series is a multi-tier and interdisciplinary set of open-access, online journals, promising a paradigm shift from the current review, selection and dissemination processes in academic publishing. All Frontiers journals are driven by researchers for researchers; therefore, they constitute a service to the scholarly community. At the same time, the Frontiers Journal Series operates on a revolutionary invention, the tiered publishing system, initially addressing specific communities of scholars, and gradually climbing up to broader public understanding, thus serving the interests of the lay society, too.

## Dedication to Quality

Each Frontiers article is a landmark of the highest quality, thanks to genuinely collaborative interactions between authors and review editors, who include some of the world's best academicians. Research must be certified by peers before entering a stream of knowledge that may eventually reach the public - and shape society; therefore, Frontiers only applies the most rigorous and unbiased reviews.

Frontiers revolutionizes research publishing by freely delivering the most outstanding research, evaluated with no bias from both the academic and social point of view. By applying the most advanced information technologies, Frontiers is catapulting scholarly publishing into a new generation.

## What are Frontiers Research Topics?

Frontiers Research Topics are very popular trademarks of the Frontiers Journals Series: they are collections of at least ten articles, all centered on a particular subject. With their unique mix of varied contributions from Original Research to Review Articles, Frontiers Research Topics unify the most influential researchers, the latest key findings and historical advances in a hot research area! Find out more on how to host your own Frontiers Research Topic or contribute to one as an author by contacting the Frontiers Editorial Office: [frontiersin.org/about/contact](http://frontiersin.org/about/contact)



# IDENTIFICATION OF NOVEL BIOMARKERS FOR PANCREATIC AND HEPATOCELLULAR CANCERS

Topic Editors:

**Brendan Jenkins**, Hudson Institute of Medical Research, Australia

**Alessandro Passardi**, Department of Medical Oncology, Scientific Institute of Romagna for the Study and Treatment of Tumors (IRCCS), Italy

**Qingfeng Zhu**, Johns Hopkins Medicine, United States

**Zhaohui Huang**, Affiliated Hospital of Jiangnan University, China

**Citation:** Jenkins, B., Passardi, A., Zhu, Q., Huang, Z., eds. (2022). Identification of Novel Biomarkers for Pancreatic and Hepatocellular Cancers.

Lausanne: Frontiers Media SA. doi: 10.3389/978-2-83250-836-7

# Table of Contents

- 05 Editorial: Identification of Novel Biomarkers for Pancreatic and Hepatocellular Cancers**  
Laura Matteucci, Ilario Giovanni Rapposelli and Alessandro Passardi
- 08 Identification of Novel Biomarkers in Pancreatic Tumor Tissue to Predict Response to Neoadjuvant Chemotherapy**  
Sumit Sahni, Christopher Nahm, Christoph Krisp, Mark P. Molloy, Shreya Mehta, Sarah Maloney, Malinda Itchins, Nick Pavlakis, Stephen Clarke, David Chan, Anthony J. Gill, Viive M. Howell, Jaswinder Samra and Anubhav Mittal
- 18 Dysregulated microRNAs in Hepatitis B Virus-Related Hepatocellular Carcinoma: Potential as Biomarkers and Therapeutic Targets**  
Jinghang Xu, Ping An, Cheryl A. Winkler and Yanyan Yu
- 34 New Blood Biomarkers for the Diagnosis of AFP-Negative Hepatocellular Carcinoma**  
Ting Wang and Kun-He Zhang
- 51 A Prognostic Prediction Model Developed Based on Four CpG Sites and Weighted Correlation Network Analysis Identified DNAJB1 as a Novel Biomarker for Pancreatic Cancer**  
Lingming Kong, Peng Liu, Xiang Fei, Tianyu Wu, Zhongpeng Wang, Baohui Zhang, Jiatong Li and Xiaodong Tan
- 67 HILPDA Is a Prognostic Biomarker and Correlates With Macrophage Infiltration in Pan-Cancer**  
Chengdong Liu, Xiaohan Zhou, Hanyi Zeng, Dehua Wu and Li Liu
- 77 Serum Biomarker Panel for Diagnosis and Prognosis of Pancreatic Ductal Adenocarcinomas**  
Shreya Mehta, Nazim Bhimani, Anthony J. Gill, Jaswinder S. Samra, Sumit Sahni and Anubhav Mittal
- 83 Preoperative Serum Prealbumin Level and Adverse Prognosis in Patients With Hepatocellular Carcinoma After Hepatectomy: A Meta-Analysis**  
Yu Fan, Yimeng Sun, Changfeng Man and Yakun Lang
- 90 ZCCHC17 Served as a Predictive Biomarker for Prognosis and Immunotherapy in Hepatocellular Carcinoma**  
Fahui Liu, Jiadong Liang, Puze Long, Lilan Zhu, Wanyun Hou, Xueming Wu and Chunying Luo
- 104 FAM21C Promotes Hepatocellular Carcinoma Invasion and Metastasis by Driving Actin Cytoskeleton Remodeling via Inhibiting Capping Ability of CAPZA1**  
Yao Lu, Deng Huang, Baolin Wang, Bowen Zheng, Jialong Liu, Juxian Song and Shuguo Zheng
- 117 Metabolism-Associated Gene Signatures for FDG Avidity on PET/CT and Prognostic Validation in Hepatocellular Carcinoma**  
Hyunjong Lee, Joon Young Choi, Je-Gun Joung, Jae-Won Joh, Jong Man Kim and Seung Hyup Hyun

- 128 ***HER2 Aberrations as a Novel Marker in Advanced Biliary Tract Cancer***  
Hongsik Kim, Ryul Kim, Hye Ryeon Kim, Hyunji Jo, Hana Kim, Sang Yun Ha, Joon Oh Park, Young Suk Park and Seung Tae Kim
- 135 ***Glypican-3: A Novel and Promising Target for the Treatment of Hepatocellular Carcinoma***  
Xiufeng Zheng, Xun Liu, Yanna Lei, Gang Wang and Ming Liu
- 146 ***The Value of Serum Tumor Markers and Blood Inflammation Markers in Differentiating Pancreatic Serous Cystic Neoplasms and Pancreatic Mucinous Cystic Neoplasms***  
Huan Wang, Sihai Chen, Xu Shu, Zhijian Liu, Pi Liu, Yong Zhu, Yin Zhu and Huifang Xiong
- 153 ***A Promising Preoperative Prediction Model for Microvascular Invasion in Hepatocellular Carcinoma Based on an Extreme Gradient Boosting Algorithm***  
Weiwei Liu, Lifan Zhang, Zhaodan Xin, Haili Zhang, Liting You, Ling Bai, Juan Zhou and Binwu Ying
- 165 ***Diagnostic Value, Prognostic Value, and Immune Infiltration of LOX Family Members in Liver Cancer: Bioinformatic Analysis***  
Chenyu Sun, Shaodi Ma, Yue Chen, Na Hyun Kim, Sujatha Kailas, Yichen Wang, Wenchao Gu, Yisheng Chen, John Pocholo W. Tuason, Chandur Bhan, Nikitha Manem, Yuting Huang, Ce Cheng, Zhen Zhou, Qin Zhou and Yanzhe Zhu
- 184 ***Proteomic Analyses Identify Therapeutic Targets in Hepatocellular Carcinoma***  
Abdulkadir Elmas, Amaia Lujambio and Kuan-lin Huang
- 193 ***Sarcopenia and Systemic Inflammation Response Index Predict Response to Systemic Therapy for Hepatocellular Carcinoma and Are Associated With Immune Cells***  
Man Zhao, Xiaoling Duan, Xin Han, Jinfeng Wang, Guangjie Han, Lili Mi, Jianfei Shi, Ning Li, Xiaolei Yin, Jiaojiao Hou and Fei Yin
- 204 ***Challenges and Opportunities Associated With Platelets in Pancreatic Cancer***  
Zhou Chen, Xiaodong Wei, Shi Dong, Fangfang Han, Ru He and Wence Zhou
- 219 ***COMMD2 Upregulation Mediated by an ncRNA Axis Correlates With an Unfavorable Prognosis and Tumor Immune Infiltration in Liver Hepatocellular Carcinoma***  
Weidan Fang, Yu Gan, Ling Zhang and Jianping Xiong



## OPEN ACCESS

EDITED AND REVIEWED BY  
Khurum Hayat Khan,  
University College London,  
United Kingdom

\*CORRESPONDENCE  
Ilario Giovanni Rapposelli  
ilario.rapposelli@airst.emr.it

†These authors have contributed  
equally to this work and share  
first authorship

SPECIALTY SECTION  
This article was submitted to  
Gastrointestinal Cancers: Hepato  
Pancreatic Biliary Cancers,  
a section of the journal  
Frontiers in Oncology

RECEIVED 28 September 2022  
ACCEPTED 24 October 2022  
PUBLISHED 08 November 2022

CITATION  
Matteucci L, Rapposelli IG and  
Passardi A (2022) Editorial:  
Identification of novel biomarkers for  
pancreatic and hepatocellular cancers.  
*Front. Oncol.* 12:1056002.  
doi: 10.3389/fonc.2022.1056002

COPYRIGHT  
© 2022 Matteucci, Rapposelli and  
Passardi. This is an open-access article  
distributed under the terms of the  
[Creative Commons Attribution License](#)  
(CC BY). The use, distribution or  
reproduction in other forums is  
permitted, provided the original  
author(s) and the copyright owner(s)  
are credited and that the original  
publication in this journal is cited, in  
accordance with accepted academic  
practice. No use, distribution or  
reproduction is permitted which does  
not comply with these terms.

# Editorial: Identification of novel biomarkers for pancreatic and hepatocellular cancers

Laura Matteucci<sup>†</sup>, Ilario Giovanni Rapposelli<sup>\*,†</sup>  
and Alessandro Passardi

Department of Medical Oncology, IRCCS Istituto Romagnolo per lo Studio dei Tumori (IRST) "Dino Amadori", Meldola, Italy

## KEYWORDS

pancreatic cancer, hepatocellular carcinoma, biomarkers, prognosis, predictive, translational oncology

## Editorial on the Research Topic

Identification of novel biomarkers for pancreatic and hepatocellular cancers

Pancreatic and hepatocellular cancers are among the most aggressive human malignancies and a major cause of cancer mortality in the world (1). Although groups at high risk for these malignancies have been recognized, screening and early detection strategies have not been successful yet. For both tumors, diagnosis often comes at advanced stage, and systemic therapy is the only treatment option. Unfortunately, systemic treatments such as chemotherapy, targeted therapies and immunotherapy often have limited clinical benefit. Hopefully, our evolving understanding of the disease biology and the advancements of molecular biology will provide new approaches for early detection and tailored therapy. In particular there is an increasing interest in the identification of potential novel diagnostic, prognostic and/or predictive biomarkers in the field of pancreatic and hepatocellular cancers, with the aim to improve patient prognosis and overall survival rates.

*Pancreatic cancer* (PC) has the highest mortality rate of all major cancers and it is currently the third leading cause of cancer-related death after lung and colon cancers (1). Even in the resectable setting, high rates of recurrences confer a dismal prognosis. Therefore, in the last years there has been an increasing trend toward neoadjuvant chemotherapy (NAC) for resectable and borderline resectable disease, in order to control possible micrometastases and select patients with potential benefit from radical resection (Oba et al.). However, a subset of patients does not benefit from NAC, and the optimal treatment schedule is not yet defined. Thus predictive markers are awaited to identify patients who may benefit from NAC. In this context, a proteomic analysis was performed by Sahni et al. from tissue samples of PC patients treated with NAC: GRP78, CADM1, PGES2, and RUXF were shown to be the best predictors of poor response to treatment. Notably, pathway analysis indicated an activation of immune response pathways in good

responders, highlighting the fundamental role of cross-talk of PC cells and immune microenvironment (2).

The evaluation of diagnostic and prognostic markers to better identify and stratify patients with PC is another important field of research, and in the present special issue some preclinical trials have been presented. Wang et al. explored the value of serum biomarkers in the differential diagnosis between serous and mucinous pancreatic cystic neoplasms. They showed that 'lymphocyte  $\times$  ALB' decrease and CA19.9 increase had good differential diagnostic efficacy, being relevant risk factors for mucinous cystic neoplasms. Kong et al. developed a prognostic prediction model based on four CpG sites using the Cancer Genome Atlas (TCGA) and the International Cancer Genome Consortium (ICGC) datasets as discovery and validation cohorts, respectively. They identified DNAB1, a suppressor of p53-mediated apoptosis (3), as a potential diagnostic and prognostic biomarker for PC. Next, a nomogram model based on the independent prognostic factors was constructed, leading to a new method for predicting the prognosis of patients with PC. The protein hypoxia-inducible lipid droplet-associated (HILPDA) expression was analyzed in pan-cancer data from The Cancer Genome Atlas (TCGA) database. It was shown to be a marker of poor prognosis (Liu et al.). Interestingly, Kong et al. reported high immune infiltration in the low-risk group, while Liu et al. showed the association of the poor prognosis marker HILPDA with tumor-associated macrophage infiltration and the expression of immunosuppressive factors, underscoring once again the importance of the interplay with immune system for PC progression (4). A panel of four serum biomarkers (S100A2, S100A4, Ca-125 and Ca 19-9) was tested in PC patients and healthy controls, providing the potential, to be validated in larger cohorts, to diagnose and stratify PC patients based on their prognostic outcomes (Mehta et al.). This study pursues the promising strategy of early detection of PC by liquid biopsy (5). Chen et al. provided an interesting review on the impact of platelets on PC, including the molecular mechanisms of cancer onset, fibrosis and thrombosis, immune escape, as well as drug resistance mechanisms and targeted therapy (Chen et al.).

Hepatocellular carcinoma (HCC) accounts for about 85–90% of all primary liver cancers and is the fourth cause of cancer-related mortality worldwide (1). Most cases of HCC occur in patients with chronic liver disease and may present with non-specific symptoms such as jaundice, abdominal pain, nausea and vomiting, or fatigue. The prognosis of HCC is affected by tumor stage and liver function, therefore early diagnosis and correct management of liver disease are crucial. However, the diagnosis of HCC, in particular those cases with negative alpha-fetoprotein, is often challenging, and new diagnostic biomarkers are awaited (Wang et al.). To this end, it is essential to boost studies aimed at defining the molecular mechanisms underlying the development of HCC. Luet al.

carried out a preclinical study on the role of FAM21C in promoting malignant progression of HCC both *in vitro* and *in vivo*. FAM21C led to the inhibition of the capping protein CAPZA1, which drives F-actin cytoskeleton remodelling, and thus promoted invasion and migration of HCC cells. Xu et al. carried out an interesting review on the miRNAs that are most commonly up-regulated or downregulated in liver tumor tissues and plasma/serum of hepatitis B virus (HBV)-related HCC patients. Indeed, patterns of miRNA expression in HCC differ according to HCC aetiology (e.g., viral, alcoholic liver disease, nonalcoholic steatohepatitis) (6). Indeed, miRNAs, isolated from serum or from extracellular vesicles, have a promising role both as early detection biomarkers and as therapeutic targets (7, 8). Liu et al. explored the role of the RNA binding protein Zinc Finger CCHC-Type Containing 17 (ZCCHC17) in the diagnosis and prognosis of HCC. They found that protein and mRNA levels of ZCCHC17 were significantly higher in tumor than in normal tissues, moreover HCC patients with high ZCCHC17 expression had a worse prognosis. The authors also highlighted a possible role of the protein in the regulation of immune cells in the tumor microenvironment, suggesting future applications in the immunotherapy of HCC.

Surgical resection or ablation of the tumor are the treatment of choice for HCC, but only 5–15% of patients are suitable for surgical resection due to the extent of disease or poor liver function, moreover among operated patients long-term survival rates remain unsatisfactory because of high recurrence rates (9). Presence of microvascular invasion (MVI) is considered one of the most important risk factors related to tumor recurrence (10). For this reason non-invasive preoperative prediction of MVI might be vital for precise surgical decision-making and patient prognosis definition: the identification of such predictive model by means of a machine learning algorithm (Liu et al.) gives an outlook of the potential impact of artificial intelligence in the management of HCC (11). In order to further refine the management of resectable disease, Fan et al. performed a meta-analysis of 11 studies with 7,442 HCC patients undergoing hepatectomy, and found that a low preoperative serum prealbumin level was significantly associated with poor overall and recurrence-free survival.

In the disease which has spread beyond the liver, treatment with tyrosine kinase inhibitors (TKIs) or immune checkpoint inhibitors (ICIs) is recommended (12–14). Despite the increasing number of therapeutic options, predictive markers of efficacy are still lacking. Zhao et al. evaluated the role of sarcopenia and systemic inflammation response index (SIRI) with encouraging results. Interestingly, sarcopenia and high SIRI were associated with reduced survival in HCC patients treated with TKIs and ICIs. Also, they show that sarcopenia may affect inflammatory states and immune microenvironment, a crucial effect if considering the increasing immunotherapeutic options in HCC (15).

However, there is great interest in expanding our knowledge about potentially druggable alterations in HCC (Niu et al.). HER2 aberrations have been observed in about 14.9% of advanced biliary tract tumors (Kim et al.) and are present in even lower percentages in HCC. With the aim to identify new potential targets, Elmas et al. performed a proteomics analysis on 260 HBV-related HCC and identified some overexpressed targets which deserve further studies such as PDGFRB, FGFR4, ERBB2/3, CDK6 kinases and MFAP5, HMCN1, and Hsp. Furthermore, the expression of FGFR4 and Hsp were significantly associated with response to their inhibitors. Glypican-3 (GPC3) has been recently studied as a potential marker of diagnosis and prognosis of HCC, as well as a potential target for targeted treatments, as reviewed by Zheng et al. Lysyl oxidase (LOX) and copper metabolism MURR1 domain (COMMD) family members are being developed with the same potential (Sun et al., Fang et al.). A different, interesting approach for targeted therapy of HCC exploits FDG PET/CT: indeed, metabolism-associated gene signatures showed prognostic value, and a potential utility for the identification of appropriate patients for metabolism-targeted therapy (Lee et al.).

## References

1. Siegel RL, Miller KD, Fuchs HE, Jemal A. Cancer statistics, 2022. *CA Cancer J Clin* (2022) 72(1):7–33. doi: 10.3322/caac.21708
2. Huber M, Brehm CU, Gress TM, Buchholz M, Alashkar Alhamwe B, von Strandmann EP, et al. The immune microenvironment in pancreatic cancer. *Int J Mol Sci* (2020) 21(19):7307. doi: 10.3390/ijms21197307
3. Cui X, Choi HK, Choi YS, Park SY, Sung GJ, Lee YH, et al. DNAB1 destabilizes PDCD5 to suppress p53-mediated apoptosis. *Cancer Lett* (2015) 357(1):307–15. doi: 10.1016/j.canlet.2014.11.041
4. Sideras K, Braat H, Kwekkeboom J, van Eijck CH, Peppelenbosch MP, Sleijfer S, et al. Role of the immune system in pancreatic cancer progression and immune modulating treatment strategies. *Cancer Treat Rev* (2014) 40(4):513–22. doi: 10.1016/j.ctrv.2013.11.005
5. Kamyabi N, Bernard V, Maitra A. Liquid biopsies in pancreatic cancer. *Expert Rev Anticancer Ther* (2019) 19(10):869–78. doi: 10.1080/14737140.2019.1670063
6. Morishita A, Oura K, Tadokoro T, Fujita K, Tani J, Masaki T. MicroRNAs in the pathogenesis of hepatocellular carcinoma: A review. *Cancers (Basel)* (2021) 13(3):514. doi: 10.3390/cancers13030514
7. Zhang Y, Li T, Qiu Y, Zhang T, Guo P, Ma X, et al. Serum microRNA panel for early diagnosis of the onset of hepatocellular carcinoma. *Med (Baltimore)* (2017) 96(2):e5642. doi: 10.1097/MD.00000000000005642
8. Sorop A, Constantinescu D, Cojocaru F, Dinischiotu A, Cucu D, Dima SO. Exosomal microRNAs as biomarkers and therapeutic targets for hepatocellular carcinoma. *Int J Mol Sci* (2021) 22(9):4997. doi: 10.3390/ijms22094997
9. Poon RT, Fan ST, Lo CM, Liu CL, Wong J. Intrahepatic recurrence after curative resection of hepatocellular carcinoma: long-term results of treatment and prognostic factors. *Ann Surg* (1999) 229:216–22. doi: 10.1097/0000658-199902000-00009
10. Lim KC, Chow PK, Allen JC, Chia GS, Lim M, Cheow PC, et al. Microvascular invasion is a better predictor of tumor recurrence and overall survival following surgical resection for hepatocellular carcinoma compared to the Milan criteria. *Ann Surg* (2011) 254:108–13. doi: 10.1097/SLA.0b013e31821ad884
11. Calderaro J, Seraphin TP, Luedde T, Simon TG. Artificial intelligence for the prevention and clinical management of hepatocellular carcinoma. *J Hepatol* (2022) 76(6):1348–61. doi: 10.1016/j.jhep.2022.01.014
12. Llovet J, Ricci S, Mazzaferro V, Hilgard P, Gane E, Blanc JF, et al. "Sorafenib in advanced hepatocellular carcinoma". *N Engl J Med* (2008) 359(4):378–90. doi: 10.1056/nejmoa0708857
13. Kudo M, Finn RS, Qin S, Han KH, Ikeda K, Piscaglia F, et al. Lenvatinib versus sorafenib in first-line treatment of patients with unresectable hepatocellular carcinoma: A randomised phase 3 non-inferiority trial. *Lancet*. (2018) 391(10126):1163–73. doi: 10.1016/S0140-6736(18)30207-1
14. Finn RS, Qin S, Ikeda M. "Atezolizumab plus bevacizumab in unresectable hepatocellular carcinoma". *N Engl J Med* (2020) 382(20):1894–905. doi: 10.1056/nejmoa1915745
15. Abou-Alfa GK, Lau G, Kudo M, Chan SL, Kelley RK, Furuse J, et al. Tremelimumab plus durvalumab in unresectable hepatocellular carcinoma. *NEJM Evid*; (2022) 1:(8). doi: 10.1056/EVIDoa2100070

## Author contributions

AP wrote the first draft of the manuscript, LM and IGR contributed to manuscript revision, read, and approved the submitted version.

## Conflict of interest

The authors declare that the research was conducted in the absence of any commercial or financial relationships that could be construed as a potential conflict of interest.

## Publisher's note

All claims expressed in this article are solely those of the authors and do not necessarily represent those of their affiliated organizations, or those of the publisher, the editors and the reviewers. Any product that may be evaluated in this article, or claim that may be made by its manufacturer, is not guaranteed or endorsed by the publisher.





# Identification of Novel Biomarkers in Pancreatic Tumor Tissue to Predict Response to Neoadjuvant Chemotherapy

Sumit Sahni<sup>1,2,3</sup>, Christopher Nahm<sup>1,2,3</sup>, Christoph Krisp<sup>4</sup>, Mark P. Molloy<sup>1,5,6</sup>, Shreya Mehta<sup>1,2,3</sup>, Sarah Maloney<sup>1,2</sup>, Malinda Itchins<sup>1,2,7,8</sup>, Nick Pavlakis<sup>1,2,7,8</sup>, Stephen Clarke<sup>1,2,7,8</sup>, David Chan<sup>1,2,7,8</sup>, Anthony J. Gill<sup>1,9</sup>, Viive M. Howell<sup>1,2</sup>, Jaswinder Samra<sup>1,3,10</sup> and Anubhav Mittal<sup>1,3,10\*</sup>

<sup>1</sup> Northern Clinical School, Faculty of Medicine and Health, University of Sydney, Camperdown, NSW, Australia, <sup>2</sup> Bill Walsh Translational Cancer Research Laboratory, Kolling Institute of Medical Research, University of Sydney, Camperdown, NSW, Australia, <sup>3</sup> Australian Pancreatic Centre, Sydney, NSW, Australia, <sup>4</sup> Center for Diagnostics, Clinical Chemistry and Laboratory Medicine, University Medical Center Hamburg – Eppendorf, Hamburg, Germany, <sup>5</sup> Bowel Cancer and Biomarker Research Laboratory, Kolling Institute of Medical Research, Royal North Shore Hospital, St Leonards, NSW, Australia, <sup>6</sup> Australian Proteome Analysis Facility (APAF), Macquarie University, Sydney, NSW, Australia, <sup>7</sup> Northern Sydney Cancer Center, Royal North Shore Hospital, St Leonards, NSW, Australia, <sup>8</sup> Northern Cancer Institute, St Leonards and Frenchs Forest, St Leonards, NSW, Australia, <sup>9</sup> Cancer Diagnosis and Pathology Group, Kolling Institute of Medical Research, Royal North Shore Hospital, St Leonards, NSW, Australia, <sup>10</sup> Upper GI Surgical Unit, Royal North Shore Hospital and North Shore Private Hospital, Sydney, NSW, Australia

## OPEN ACCESS

### Edited by:

Qingfeng Zhu,  
Johns Hopkins Medicine,  
United States

### Reviewed by:

Savio George Barreto,  
Medanta the Medicity, India  
Hirdesh Kumar,  
National Institute of Allergy and  
Infectious Diseases (NIAID),  
United States

### \*Correspondence:

Anubhav Mittal  
anubhav.mittal@sydney.edu.au

### Specialty section:

This article was submitted to  
Gastrointestinal Cancers,  
a section of the journal  
Frontiers in Oncology

Received: 03 October 2019

Accepted: 12 February 2020

Published: 04 March 2020

### Citation:

Sahni S, Nahm C, Krisp C, Molloy MP, Mehta S, Maloney S, Itchins M, Pavlakis N, Clarke S, Chan D, Gill AJ, Howell VM, Samra J and Mittal A (2020) Identification of Novel Biomarkers in Pancreatic Tumor Tissue to Predict Response to Neoadjuvant Chemotherapy. *Front. Oncol.* 10:237. doi: 10.3389/fonc.2020.00237

**Background:** Neoadjuvant chemotherapy (NAC) has been of recent interest as an alternative to upfront surgery followed by adjuvant chemotherapy in patients with pancreatic ductal adenocarcinoma (PDAC). However, a subset of patients does not respond to NAC and may have been better managed by upfront surgery. Hence, there is an unmet need for accurate biomarkers for predicting NAC response in PDAC. We aimed to identify upregulated proteins in tumor tissue from poor- and good-NAC responders.

**Methods:** Tumor and adjacent pancreas tissue samples were obtained following surgical resection from NAC-treated PDAC patients. SWATH-MS proteomic analysis was performed to identify and quantify proteins in tissue samples. Statistical analysis was performed to identify biomarkers for NAC response. Pathway analysis was performed to characterize affected canonical pathways in good- and poor-NAC responders.

**Results:** A total of 3,156 proteins were identified, with 19 being significantly upregulated in poor-responders compared to good-responders ( $\log_2$  ratio  $> 2$ ,  $p < 0.05$ ). Those with the greatest ability to predict poor-NAC response were GRP78, CADM1, PGES2, and RUXF. Notably, canonical pathways that were significantly upregulated in good-responders included acute phase signaling and macrophage activation, indicating a heightened immune response in these patients.

**Conclusion:** A novel biomarker signature for poor-NAC response in PDAC was identified.

**Keywords:** pancreatic ductal adenocarcinoma, biomarkers, neoadjuvant chemotherapy, proteomics, SWATH-MS

## INTRODUCTION

Pancreatic ductal adenocarcinoma (PDAC) has the lowest survival rate of all major cancers (~6% at 5 years post-diagnosis) and is projected to become the second most common cause of cancer related death by 2030 (1, 2). Intrinsic chemotherapy-resistance is one of the major clinical problems associated with PDAC, resulting in the failure of currently available therapeutic options (3). Adjuvant chemotherapy in patients with resected PDAC has been shown to extend survival over surgery alone, and more recently, more intensive regimens such as FOLFIRONOX have been shown to be even more effective (4). However, not all patients are capable of commencing let alone completing chemotherapy after surgery for PDAC. As such, there has been an increasing trend toward neoadjuvant chemotherapy (NAC), i.e., pre-operative chemotherapy, in order to effectively deliver systemic chemotherapy since improvements in nodal status and resection margin status have been observed (5, 6). However, a subset of patients can be classified as “poor responders” to NAC, failing to demonstrate tumor response with subsequent early disease recurrence and shortened overall survival time (7). While genetic classification of PDAC may help identify a high risk squamous or basal subtype (8), the high costs of these methodologies have prohibited the general clinical use of genetic analysis of individual PDAC patients to help guide therapy. Therefore, there is a need for discovering more readily applicable tissue and/or blood-based secreted biomarkers that can predict a NAC response, which may be detected by more cost-effective tests.

Recently, there has been a surge in interest in the “-omics” approach to biomarker discovery in cancer research. Such approaches allow identification of a myriad of genes, transcripts, proteins and metabolites unique to cancer. They are therefore an invaluable first-step in the process of biomarker identification and validation. SWATH-MS (Sequential Window Acquisition of all Theoretical fragment ion spectra—Mass Spectrometry) is a high throughput quantitative mass spectrometry method for proteome analysis (9). This technology allows permanent recording of all peptide fragment ions in biological samples, which imparts the advantages of a high throughput shotgun approach, with the consistency and data reproducibility of selective reaction monitoring (SRM) proteomics (10). Here, we report on the use of SWATH-MS as a discovery proteomics approach to identify differences in proteomic profile of good- and poor-NAC responders in PDAC.

## MATERIALS AND METHODS

### Participants and Tissue Collection

Patients who presented with histologically confirmed PDAC at a tertiary centre [Royal North Shore Hospital (RNSH) and North Shore Private Hospital (NSP), Sydney, Australia] were included in the study between 04/03/2016 and 18/07/2017. All patients selected were treated with NAC before surgical resection, following individual discussion by our multidisciplinary team. The NAC regimen was at the discretion of the oncologist. Tumor tissue and adjacent normal pancreas were obtained

from patients during the surgical intervention. Pathologically confirmed tumor and adjacent normal pancreas tissue were cut into 2 mm<sup>3</sup> portions and stored in cryotubes in a –80°C freezer for later analysis.

The NAC response was determined based on the residual tumor viability, as described previously (7). Briefly, at the time of initial surgical pathology reporting, the residual tumor viability was assessed by the reporting pathologist. All histological slides were reviewed to estimate the viable residual tumor as a percentage of the estimated original tumor volume. A case with no response to NAC was recorded as 100% viable and a case with complete regression after treatment was recorded 0% viable.

### Ethics Approval and Consent to Participate

This study was approved by the RNSH and NSP institutional ethics committees under references HREC/16/HAWKE/105 and NSPHEC 2016-007, respectively. Informed written consent was obtained from all participants and/or their designated surrogate. North Sydney Local Health District (NSLHD) reference: RESP/16/76.

### Proteomic Sample Preparation and SWATH-MS Analysis

#### Protein Digestion and LC-MS/MS Analysis

All tissue samples were lysed in 100 mM triethylammonium bicarbonate (TEAB) and 1% sodium deoxycholate buffer using a probe sonicator. Protein concentrations were estimated using the bicinchoninic acid protein assay (Thermo Scientific, Waltham, MA). The cysteine residues were reduced in the presence of 10 mM dithiothreitol (DTT, Bio-Rad, Hercules, CA) at 60°C and alkylated with 10 mM iodoacetamide (IAA, Bio-Rad) at room temperature in the dark. Trypsin (sequencing grade; Promega, Madison, WI) was added in a 1:50 ratio and proteins were enzymatically degraded overnight at 37°C. By adding 1 µL formic acid (FA; Thermo Scientific) the digestion was quenched and the sodium deoxycholate (SDC) precipitated and removed by centrifugation (14,000 rpm) for 5 min. Samples were lyophilized and reconstituted in 2% acetonitrile (ACN; Sigma Aldrich, St. Louis, MO) and 0.1% FA.

Liquid Chromatography-Tandem Mass Spectrometry (LC-MS/MS) analysis for tissue samples were performed on an Eksport NanoLC 400 with cHiPLC system (SCIEX, Framingham, MA) coupled to a TripleTOF 6600 mass spectrometer (SCIEX). A 200 µm × 0.5 mm nano cHiPLC trap column and 15 cm × 200 µm nano cHiPLC columns (ChromXP™ C18-CL 3 µm 120 Å) were used with 140 min ACN gradients.

Digested samples were pooled, by combining a small fraction of each tissue sample from the tumor and adjacent normal pancreas, and subjected them to basic reverse phase chromatography high performance liquid chromatography (HPLC), using an extended C18 column 2.1 mm × 150 mm, 3.5 µm (Agilent, Santa Clara, CA), on an Agilent 1200 series HPLC. One hundred microgram of peptides per pool were pre-cleaned with Sep-Pak C18 and then injected at a flow rate of 0.3 mL/min at room temperature onto the column. The peptides were separated over a 1 h gradient from using Buffer A of 5 mM ammonia at approximately pH 10.4 and Buffer B of



90% ACN/5 mM ammonia, and eluting peptides were collected in fractions of 1 min. Concatenated pooling of the fractions was performed.

For data dependent MS/MS acquisition to build a spectral library of the basic reverse phase fractionated samples, the 20 most intense  $m/z$  values exceeding a threshold  $>250$  cps on the TripleTOF 6600 with charge stages between 2+ and 4+ were selected for analysis from a full MS survey scan and excluded from analysis for 20 s to minimize redundant precursor sampling.

In data independent acquisition, a 100 variable window method was used over a range of 400–1,250  $m/z$  with window sizes based on precursor densities in the LC-MS/MS acquisition. Collision energies were calculated for 2+ precursors with  $m/z$  values of lowest  $m/z$  in window + 10% of the window width. The data were acquired over an 80 min ACN gradient.

### Protein Identification and Quantification

Spectral libraries for SWATH-MS quantitation were generated with ProteinPilot™ software 5.0 using the Paragon™ algorithm

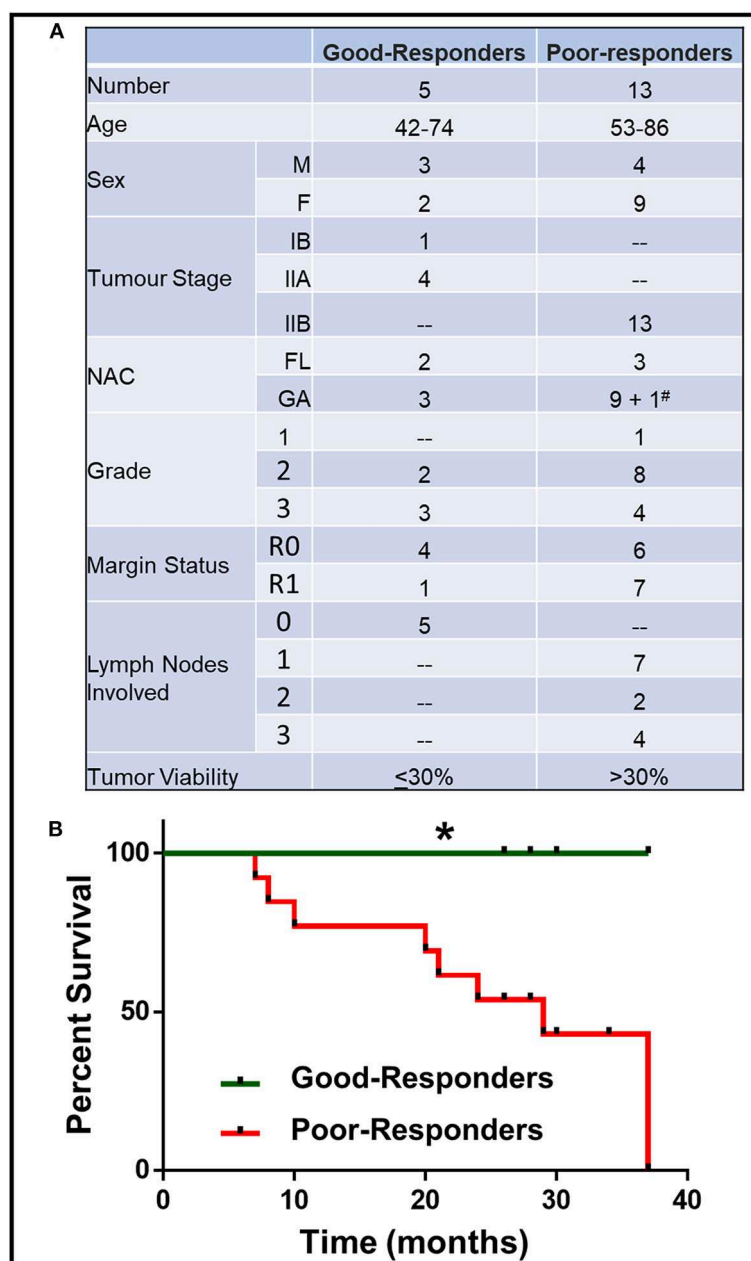


**FIGURE 1 |** Characteristics of patient with good and poor NAC response. **(A)** Details of patient age, sex, tumor stage, grade, margin status, number of lymph nodes involved, neoadjuvant chemotherapy (NAC) received (FL, Florfirinox; GA, Gemcitabine/Abraxane; # Patient initially received FL followed by GA) and residual tumor cell viability. **(B)** Kaplan-Meier survival curve for good- and poor-NAC responders. \* $p < 0.05$ .

(SCIEX) in the thorough ID mode including biological modifications and chemical modifications. MS/MS data were searched against the human UniProt database (release February 2016, 20,198 entries) with carbamidomethyl as a fixed modification for cysteine residues. An Unused Score cut-off was set to 0.05 and the false discovery rate (FDR) analysis was enabled.

Generated Paragon group files were imported into PeakView™ software 2.1 using the SWATH MicroApp 2.0 (release 25/08/2014) to generate a sample specific spectral library which was matched against SWATH-MS data. After retention time calibration with endogenous peptides, data were processed using following processing settings; 100 maximal peptides per protein, maximal 6 transitions per peptide, peptide confidence threshold of 99%, transition false discovery rate < 1%, 5 min extraction window and fragment extraction tolerance of 75 ppm.

## Data Analysis

Survival data was compared using Kaplan-Meier curve analysis. The statistical differences in the survival curve were analyzed by the Log-rank test. Proteomic data was initially analyzed by the principal component analysis (PCA) to observe inherent groupings within the data set. Further, proteins which were markedly up- or down-regulated ( $\log_2 \geq 2$  or  $\leq -2$ ) were compared using multiple *t*-test analysis ( $p < 0.05$ ;  $q < 0.1$ ; false discovery rate was determined with  $Q = 1\%$ ). The predictive model for selected proteins was validated by the Area Under the Receiver Operating Characteristic (AUROC) curve. All analysis was performed using either GraphPad Prism (GraphPad Software, San Diego, California) or JMP (SAS Institute, Cary, North Carolina) statistical software. Pathway analysis was performed using Ingenuity Pathway Analysis (IPA; Qiagen Bioinformatics, Redwood City, CA) (11). The proteins which were markedly ( $\log_2 \geq 2$  or  $\leq -2$ ) and significantly ( $p < 0.05$ ;  $q < 0.1$ ) differentially expressed were inputted into IPA.

Protein secretion prediction was performed using Proteinside software (12).

## RESULTS

### Population Demographics and Survival Data

A total of 18 PDAC patients (7 males, 11 females) were recruited for this study. All PDAC patients underwent neoadjuvant chemotherapy (NAC) before surgical resection. Patient characteristics (age, sex, tumor stage, NAC received, residual tumor viability) are described in **Figure 1A**.

The patients were divided on the basis of their response to NAC, which was determined by the residual tumor viability in the specimen. Based on the previously described classification methods (13), the tumors with  $\leq 30\%$  viable tumor cells (i.e., HTRG grade 0, CAP grade 0; HTRG grade 1, CAP grade 1; and HTRG grade 2, CAP grade 2: complete to moderate response) were graded “good-responders,” while tumors with  $> 30\%$  viable tumor cells (HTRG grade 2, CAP grade 3; poor response) were graded as “poor-responders.” The good-responders had significantly ( $p < 0.05$ ) longer overall survival compared to poor-responders (**Figure 1B**).

### Principal Component Analysis: Distinct Tissue Samples

Using SWATH-MS analysis, a total of 3,156 proteins were identified in both tumor tissue and adjacent normal pancreas. Principal component analysis (PCA) was performed on the proteomic data obtained by SWATH-MS analysis of tumor tissue and adjacent normal pancreas. PCA is an unsupervised class recognition approach, to observe inherent groupings (14). Tissues were observed to be clustered according to their class grouping (i.e., tumor tissue or adjacent normal pancreas) for all patients together (**Figure 2A**), good-responders (**Figure 2B**),

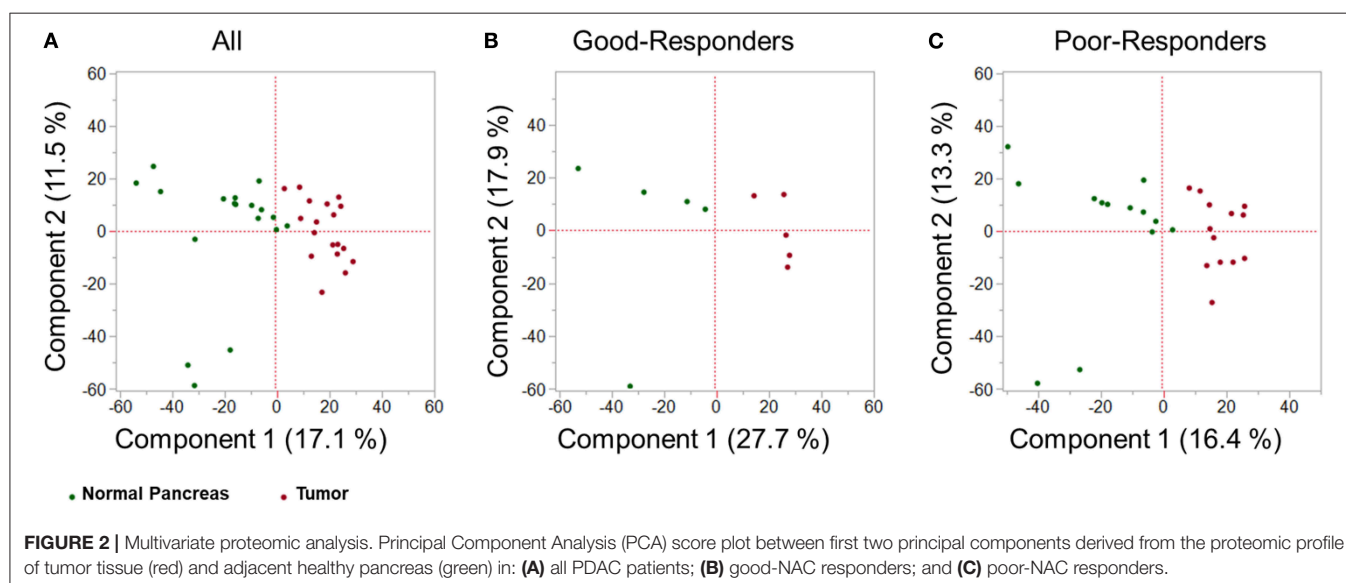


**TABLE 1** | Over-expressed and under-expressed proteins in good-responders.

Good-responders				
Protein name	Uniprot accession	Log <sub>2</sub> ratio	P-value	q-value
<b>OVER-EXPRESSED</b>				
Rho guanine nucleotide exchange factor 18	ARHGI_HUMAN	4.915	0.004	0.011
CDP-diacylglycerol-glycerol-3-phosphate 3-phosphatidyltransferase	PGS1_HUMAN	4.222	0.003	0.010
Prolargin	PRELP_HUMAN	4.115	0.009	0.017
Versican core protein	CSPG2_HUMAN	4.109	0.003	0.010
Alpha-1-antitrypsin	A1AT_HUMAN	3.935	0.007	0.015
Apolipoprotein A-I	APOA1_HUMAN	3.735	0.003	0.010
Hemopexin	HEMO_HUMAN	3.590	0.006	0.014
Collagen alpha-1(III) chain	CO3A1_HUMAN	3.588	0.012	0.019
Inter-alpha-trypsin inhibitor heavy chain H1	ITI1_HUMAN	3.538	0.005	0.012
Fibulin-1	FBLN1_HUMAN	3.457	0.007	0.015
<b>UNDER-EXPRESSED</b>				
Pancreatic alpha-amylase	AMYP_HUMAN	-6.333	4.19E-05	3.14E-03
Chymotrypsin-like elastase family member 3A	CEL3A_HUMAN	-6.245	4.48E-05	3.14E-03
Carboxypeptidase B	CBPB1_HUMAN	-5.428	5.75E-05	3.14E-03
Trypsin-1	TRY1_HUMAN	-5.346	1.26E-03	8.63E-03
Pancreatic lipase-related protein 2	LIPR2_HUMAN	-4.847	3.67E-04	6.36E-03
Bile salt-activated lipase	CEL_HUMAN	-4.775	2.50E-03	9.68E-03
Protein disulfide-isomerase A2	PDIA2_HUMAN	-4.757	2.52E-03	9.68E-03
Carboxypeptidase A1	CBPA1_HUMAN	-4.748	1.18E-02	1.85E-02
Carboxypeptidase A2	CBPA2_HUMAN	-4.395	1.25E-03	8.63E-03
Chymotrypsin-C	CTRC_HUMAN	-4.249	3.48E-03	1.03E-02

or poor-responders (**Figure 2C**). These results indicate that a clearly distinct tumor and adjacent normal tissue specimens were obtained from the patients.

## Differentially Regulated Proteins

There were 236 differentially expressed ( $\log_2 > 2$ ;  $p < 0.05$ ) proteins in the tumor tissue in good-responders compared to their adjacent normal pancreas (**Supplementary Table 1**). Of these, 134 proteins were over-expressed and 102 proteins were under-expressed in the tumor tissue. In poor-responders, only 67 proteins were differentially expressed (23 over-expressed and 44 under-expressed; **Supplementary Table 2**).

The top 10 over- and under-expressed proteins for both good- and poor-responders based on fold-change are reported in **Tables 1, 2**. The over-expressed proteins in good- and poor-responders showed distinct functional activity. In contrast, the majority of proteins which were under-expressed in both good- and poor-responders, shared similar functional (proteases or peptidase) activity with 7 out of top 10 proteins being the same.

## Comparative Pathway Analysis

Next, based on the identified differentially regulated proteins in both good- and poor-NAC responders, pathway analysis was performed using Ingenuity Pathway Analysis. A number of canonical pathways were observed to be differentially regulated in good- and poor-NAC responders (**Figure 3A** and **Supplementary Table 3**). Notably, immune response pathways,

such as acute phase signaling and macrophage mediated nitric oxide and reactive oxygen species production, were upregulated in good responders but remained unaffected in poor-responders. Similarly, analysis of predicted disease and functions based on differential protein expression using IPA, supported an immunogenic phenotype in good-responders, while poor-responders showed only mild inflammatory response and phagocyte migration (**Figure 3B**).

## Biomarker Analysis

There were 19 proteins which were markedly ( $\log_2 > 2$ ) and significantly ( $p < 0.05$ ) over-expressed in tumor from the poor-responders compared to good-responders (**Table 3**). The ability to these proteins to predict chemo-resistance to NAC was determined by area under the receiver operator characteristic (AUROC) curve. Four biomarkers, namely GRP78, CADM1, PGES2, and RUXF, demonstrated very high predictive performance with AUROC  $\geq 0.92$ .

Notably, four proteins, i.e., TMED2, AGR2, JTB, and CADM1, were predicted as secreted proteins, with SignalP score of 0.908, 0.856, 0.759, and 0.699, respectively.

## DISCUSSION

Neoadjuvant chemotherapy (NAC) is being increasingly given to PDAC patients with borderline/locally advanced disease and is also being evaluated in upfront operable patients. Previous

**TABLE 2 |** Over-expressed and under-expressed proteins in poor-responders.

Poor-responders				
Protein name	Uniprot accession	Log <sub>2</sub> ratio	P-value	q-value
<b>OVER-EXPRESSED</b>				
Periostin	POSTN_HUMAN	2.789	6.94E-06	1.45E-05
Filamin-A	FLNA_HUMAN	2.700	3.44E-05	5.12E-05
Ras-related C3 botulinum toxin substrate 2	RAC2_HUMAN	2.613	2.80E-07	9.38E-07
Proteasome subunit beta type-10	PSB10_HUMAN	2.555	3.31E-05	5.04E-05
Collagen alpha-1(XII) chain	COCA1_HUMAN	2.482	2.64E-07	9.31E-07
Versican core protein	CSPG2_HUMAN	2.436	6.80E-07	1.98E-06
Collagen alpha-2(V) chain	CO5A2_HUMAN	2.388	3.71E-04	4.60E-04
CDP-diacylglycerol-glycerol-3-phosphate 3-phosphatidyltransferase	PGS1_HUMAN	2.373	4.31E-04	5.25E-04
Apolipoprotein A-I	APOA1_HUMAN	2.354	7.56E-04	8.30E-04
Syntenin-1	SDCB1_HUMAN	2.345	6.97E-05	9.16E-05
<b>UNDER-EXPRESSED</b>				
Trypsin-3	TRY3_HUMAN	-5.124	1.41E-08	1.58E-07
Chymotrypsinogen B2	CTRB2_HUMAN	-5.067	4.56E-05	6.49E-05
Pancreatic alpha-amylase	AMYP_HUMAN	-4.988	3.63E-08	2.70E-07
Chymotrypsin-like elastase family member 3A	CEL3A_HUMAN	-4.933	2.35E-09	5.57E-08
Protein disulfide-isomerase A2	PDIA2_HUMAN	-4.859	2.19E-08	1.84E-07
Trypsin-1	TRY1_HUMAN	-4.471	2.18E-09	5.57E-08
Carboxypeptidase A1	CBPA1_HUMAN	-4.463	4.03E-06	8.72E-06
Chymotrypsin-C	CTRC_HUMAN	-4.390	2.99E-09	5.57E-08
Serine protease inhibitor Kazal-type 1	ISK1_HUMAN	-4.212	4.16E-09	5.57E-08
Carboxypeptidase B	CBPB1_HUMAN	-4.187	1.89E-07	7.44E-07

studies have shown that patients who respond to NAC have an overall survival benefit compared to non-responders (7). There are currently no validated biomarkers readily available for predicting NAC response in these patients. This study identified a panel of potential biomarkers which correlate with resistance to NAC in PDAC patients. The top four biomarkers for NAC resistance, namely, GRP78, CADM1, PGES2, and RUXF demonstrated very high predictive ability for chemo-resistance with AUROC > 0.92. Notably, GRP78 has been previously demonstrated to play an important role in mediating chemo-resistance in PDAC (15–17). Moreover, RUXF and PGES2 are known to be involved in chemo-resistance in ovarian and colorectal cancer, respectively (18, 19). On the other hand, CADM1 is shown to be a good prognostic marker in other cancers (20, 21).

Four proteins (i.e., TMED2, AGR2, JTB, and CADM1) among the over-expressed proteins in poor-responders (Table 3) were predicted to be secreted extracellularly. This is important, as detection of these proteins in plasma/serum from the PDAC patients could be used to develop a simple blood-based test for determining NAC response in PDAC patients. Of note, TMED2, AGR2, and JTB are known to be associated with poor prognosis in other cancers (22–24) and thus, could be explored as novel biomarkers for predicting chemo-resistance in PDAC. Future studies, assessing the levels of these biomarkers in serum or plasma from the NAC-treated PDAC patients, will be required to confirm the clinical utility of these biomarkers as an indicator of chemo-resistance in PDAC.

This study also compared tumor tissue with adjacent normal pancreas in both good- and poor- NAC responders. A distinct proteomic profile of over-expressed proteins in tumors was observed in good- and poor-NAC responders compared to the adjacent normal pancreas. Rho guanine nucleotide exchange factor 18 (Uniprot: ARHGE18\_Human) was the most over-expressed protein in good-responders. This latter protein is known to be up-regulated in response to reactive oxygen species (25), which are known to be increased in tumor tissue treated with chemotherapy (26). Periostin (Uniprot: POSTN) was identified as the highest over-expressed protein in poor-NAC responders. Periostin is an extracellular matrix protein, which is known to play an important role in cancer progression (27). Notably, periostin expression has also been shown to be associated with chemo-resistance in pancreatic and other cancers (28–30). Previous studies have also demonstrated periostin as a poor prognostic biomarker in PDAC and other cancers (31–34). In PDAC, periostin is produced by pancreatic stellate cells and it is shown to establish a microenvironment that is supportive for cancer growth and progression (31, 35). Identification of periostin as a highly over-expressed protein in poor-NAC responders in this study further supports its important role in PDAC chemo-resistance.

The majority of proteins under-expressed in both good- and poor-NAC responders were pancreas specific peptidases or proteases (e.g., CEL3A, CBPB1, CBPA1, CBPA2, etc.). Notably, several previous studies also have shown that pancreatic

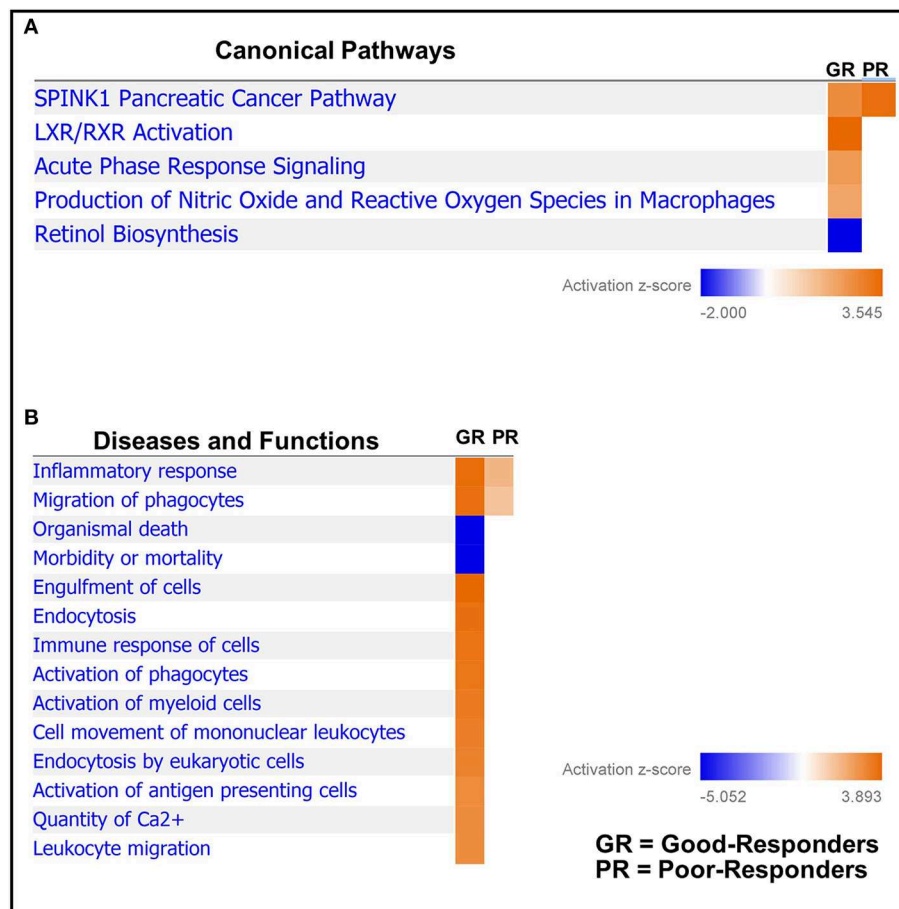


**FIGURE 3 |** Comparative pathways and associated disease/functions between good- and poor-NAC Responders. Ingenuity pathway analysis was performed to identify **(A)** canonical pathways; and **(B)** associated disease/function affected in the tumor tissue of good- and poor-NAC responding PDAC patients, compared to adjacent normal pancreas.

proteases or peptidases are downregulated in PDAC tumor compared adjacent normal pancreas (33, 36, 37).

Assessment of pathway analysis revealed that the SPINK1 pathway was upregulated in both good- and poor-NAC responders, with the latter having more pronounced involvement of this pathway. SPINK1 is a serine protease inhibitor which has an anti-trypsin activity and is known to play an important role in protecting the normal pancreatic tissue from inadvertent activation of trypsin (38). Moreover, SPINK1 is also shown to play a role in cancer cell survival and progression (39–41). In this study, we observed that levels of SPINK1 (Uniprot: ISK1\_Human) were decreased in tumor tissue compared to adjacent normal pancreas. This is consistent with previous studies demonstrating higher levels of SPINK1 in normal pancreatic tissue compared to tumor (42, 43).

The pathway analysis further demonstrated that innate immune response was highly activated in tumors from the good-NAC responders, while only moderate immune activity was observed in poor-NAC responders. It can be postulated that initial response to NAC in good-responders could have resulted in a heightened immune infiltration into these tumors, resulting

in an overall increased anti-tumor response. Studies have also shown similar immune-stimulatory effect of chemotherapy in other cancers (44, 45), but this is the first study to observe this effect in PDAC.

The main limitation of this study is a relatively small cohort size. Future multi-institutional studies with a larger group of patients will be required to independently validate the identified proteins and their predictive value. This study utilized tumor specimens obtained at the time of surgical resection after chemotherapy treatment. Future studies will be required to further validate these findings using pre-NAC endoscopic ultrasound (EUS) core biopsies. Notably, EUS core biopsy provides sufficient amount of protein (~1 µg) required for SWATH-MS analysis, which highlights the future clinical utility of these biomarkers in selecting patients for NAC prior to surgery.

## CONCLUSION

Overall, this exploratory study has demonstrated the successful application of SWATH-MS proteomic analysis to pancreatic



**TABLE 3 |** Biomarkers to predict poor-NAC response.

Protein name	Uniprot accession	Log <sub>2</sub> ratio	P-value	q-value	AUROC
Endoplasmic reticulum chaperone BiP	GRP78_HUMAN	2.139	0.009	0.028	0.954
Cell adhesion molecule 1	CADM1_HUMAN	2.424	0.007	0.028	0.923
Prostaglandin E synthase 2	PGES2_HUMAN	2.359	0.001	0.028	0.923
Small nuclear ribonucleoprotein F	RUXF_HUMAN	2.144	0.009	0.028	0.923
ATP-binding cassette sub-family D member 3	ABCD3_HUMAN	2.060	0.005	0.028	0.892
START domain-containing protein 10	PCTL_HUMAN	2.261	0.006	0.028	0.876
39S ribosomal protein L37	RM37_HUMAN	2.986	0.012	0.030	0.862
Protein enabled homolog	ENAH_HUMAN	2.956	0.003	0.028	0.862
Transmembrane emp24 domain-containing protein 2	TMED2_HUMAN	2.193	0.039	0.061	0.862
Anterior gradient protein 2 homolog	AGR2_HUMAN	2.036	0.027	0.045	0.862
Glutamate decarboxylase 2	DCE2_HUMAN	3.225	0.016	0.034	0.846
Acyl-coenzyme A synthetase ACSM3	ACSM3_HUMAN	2.241	0.013	0.030	0.831
Epiplakin	EPIPL_HUMAN	2.106	0.026	0.045	0.831
SCY1-like protein 2	SCYL2_HUMAN	3.729	0.004	0.028	0.815
Synaptosomal-associated protein 29	SNP29_HUMAN	2.279	0.013	0.030	0.800
Protein JTB	JTB_HUMAN	2.449	0.044	0.062	0.785
MARCKS-related protein	MRP_HUMAN	2.206	0.045	0.062	0.785
60S ribosomal protein L38	RL38_HUMAN	2.061	0.047	0.062	0.785
YTH domain-containing family protein 3	YTHD3_HUMAN	2.175	0.022	0.042	0.738

tumor and normal pancreas tissue samples, resulting in the identification of novel potential biomarkers which may predict for a chemo-resistant tumor phenotype in PDAC patients treated with NAC. Further research in a larger patient cohort is required to validate these findings.

## DATA AVAILABILITY STATEMENT

The datasets generated for this study can be found in the ProteomeXchange via the PRIDE database (46) (Accession: PXD017051).

## ETHICS STATEMENT

The studies involving human participants were reviewed and approved by Royal North Shore Hospital Institutional Ethics Committee, RNSH, St Leonards, Australia and North Shore Private Hospital Institutional Ethics Committee, NSP, St Leonards, Australia. The patients/participants provided their written informed consent to participate in this study.

## AUTHOR CONTRIBUTIONS

SS, CN, MM, and AM were involved in the design of the study. CN and CK performed the proteomic experiments. AG analyzed the residual tumor viability. SS, SMe, SMa, and AM were involved in the statistical analysis and interpretation of data. MI, NP, SC,

DC, JS, and AM enrolled patients. SS and AM wrote the draft manuscript. All authors helped with the manuscript editing. All authors read and approved the final manuscript.

## FUNDING

This study was supported by philanthropic donations received by JS and AM.

## ACKNOWLEDGMENTS

AM would like to thank Sydney Vital for the Translational Centre for Excellence in Pancreatic Cancer Grant and R. T. Hall Trust for the R. T. Hall Trust grant. SS would like to thank Mr. Guy Boncardo for the Boncardo Pancreatic Cancer Fellowship. SS would also like to thank AMP Foundation for the AMP Tomorrow Grant and Cancer Australia and Cure Cancer Australia for the Young Investigator PdCCRS grant. CN would like to thank the Van Beek Family for the van Beek Memorial Fund Scholarship. MM acknowledges support from Cancer Institute NSW through a research equipment grant.

## SUPPLEMENTARY MATERIAL

The Supplementary Material for this article can be found online at: <https://www.frontiersin.org/articles/10.3389/fonc.2020.00237/full#supplementary-material>

## REFERENCES

- Ilic M, Ilic I. Epidemiology of pancreatic cancer. *World J Gastroenterol.* (2016) 22:9694–705. doi: 10.3748/wjg.v22.i44.9694
- Rahib L, Smith BD, Aizenberg R, Rosenzweig AB, Fleshman JM, Matrisian LM. Projecting cancer incidence and deaths to 2030: the unexpected burden of thyroid, liver, and pancreas cancers in the United States. *Cancer Res.* (2014) 74:2913–21. doi: 10.1158/0008-5472.CAN-14-0155
- Aslan M, Shahbazi R, Ulubayram K, Ozpolat B. Targeted therapies for pancreatic cancer and hurdles ahead. *Anticancer Res.* (2018) 38:6591–606. doi: 10.21873/anticancer.13026
- Conroy T, Hammel P, Hebbar M, Ben Abdelghani M, Wei AC, Raoul J-L, et al. FOLFIRINOX or gemcitabine as adjuvant therapy for pancreatic cancer. *N Engl J Med.* (2018) 379:2395–406. doi: 10.1056/NEJMoa1809775
- Roland CL, Yang AD, Katz MHG, Chatterjee D, Wang H, Lin H, et al. Neoadjuvant therapy is associated with a reduced lymph node ratio in patients with potentially resectable pancreatic cancer. *Ann Surg Oncol.* (2015) 22:1168–75. doi: 10.1245/s10434-014-4192-6
- Itchins M, Arena J, Nahm CB, Rabindran J, Kim S, Gibbs E, et al. Retrospective cohort analysis of neoadjuvant treatment and survival in resectable and borderline resectable pancreatic ductal adenocarcinoma in a high volume referral centre. *Eur J Surg Oncol.* (2017) 43:1711–7. doi: 10.1016/j.ejso.2017.06.012
- Townend P, de Reuver PR, Chua TC, Mittal A, Clark SJ, Pavlakakis N, et al. Histopathological tumour viability after neoadjuvant chemotherapy influences survival in resected pancreatic cancer: analysis of early outcome data. *ANZ J Surg.* (2018) 88:E167–72. doi: 10.1111/ans.13897
- Bailey P, Chang DK, Nones K, Johns AL, Patch AM, Gingras MC, et al. Genomic analyses identify molecular subtypes of pancreatic cancer. *Nature.* (2016) 531:47–52. doi: 10.1038/nature16965
- Gillet LC, Navarro P, Tate S, Rost H, Selevsek N, Reiter L, et al. Targeted data extraction of the MS/MS spectra generated by data-independent acquisition: a new concept for consistent and accurate proteome analysis. *Mol Cell Proteomics.* (2012) 11:O111.016717. doi: 10.1074/mcp.O111.016717
- Guo T, Kouvonen P, Koh CC, Gillet LC, Wolski WE, Rost HL, et al. Rapid mass spectrometric conversion of tissue biopsy samples into permanent quantitative digital proteome maps. *Nat Med.* (2015) 21:407–13. doi: 10.1038/nm.3807
- Kramer A, Green J, Pollard J Jr, Tugendreich S. Causal analysis approaches in ingenuity pathway analysis. *Bioinformatics.* (2014) 30:523–30. doi: 10.1093/bioinformatics/btt703
- Kaspric N, Picard B, Reichstadt M, Tournayre J, Bonnet M. ProteINSIDE to easily investigate proteomics data from ruminants: application to mine proteome of adipose and muscle tissues in bovine fetuses. *PLoS ONE.* (2015) 10:e0128086. doi: 10.1371/journal.pone.0128086
- Lee SM, Katz MH, Liu L, Sundar M, Wang H, Varadhachary GR, et al. Validation of a proposed tumor regression grading scheme for pancreatic ductal adenocarcinoma after neoadjuvant therapy as a prognostic indicator for survival. *Am J Surg Pathol.* (2016) 40:1653–60. doi: 10.1097/PAS.0000000000000738
- David CC, Jacobs DJ. Principal component analysis: a method for determining the essential dynamics of proteins. *Methods Mol Biol.* (2014) 1084:193–226. doi: 10.1007/978-1-62703-658-0\_11
- Gifford JB, Huang W, Zeleniak AE, Hindoyan A, Wu H, Donahue TR, et al. Expression of GRP78: master regulator of the unfolded protein response, increases chemoresistance in pancreatic ductal adenocarcinoma. *Mol Cancer Ther.* (2016) 15:1043–52. doi: 10.1158/1535-7163.MCT-15-0774
- Dauer P, Sharma NS, Gupta VK, Nomura A, Dudeja V, Saluja A, et al. GRP78-mediated antioxidant response and ABC transporter activity confers chemoresistance to pancreatic cancer cells. *Mol Oncol.* (2018) 12:1498–512. doi: 10.1002/1878-0261.12322
- Clarke WR, Amundadottir L, James MA. CLPTM1L/CRR9 ectodomain interaction with GRP78 at the cell surface signals for survival and chemoresistance upon ER stress in pancreatic adenocarcinoma cells. *Int J Cancer.* (2019) 144:1367–78. doi: 10.1002/ijc.32012
- Peters D, Freund J, Ochs RL. Genome-wide transcriptional analysis of carboplatin response in chemosensitive and chemoresistant ovarian cancer cells. *Mol Cancer Ther.* (2005) 4:1605–16. doi: 10.1158/1535-7163.MCT-04-0311
- Cao B, Luo L, Feng L, Ma S, Chen T, Ren Y, et al. A network-based predictive gene-expression signature for adjuvant chemotherapy benefit in stage II colorectal cancer. *BMC Cancer.* (2017) 17:844. doi: 10.1186/s12885-017-3821-4
- Hartsough EJ, Weiss MB, Heilman SA, Purwin TJ, Kugel CH 3rd, Rosenbaum SR, et al. CADM1 is a TWIST1-regulated suppressor of invasion and survival. *Cell Death Dis.* (2019) 10:281. doi: 10.1038/s41419-019-1515-3
- Ito T, Nakamura A, Tanaka I, Tsuboi Y, Morikawa T, Nakajima J, et al. CADM1 associates with Hippo pathway core kinases; membranous co-expression of CADM1 and LATS2 in lung tumors predicts good prognosis. *Cancer Sci.* (2019) 110:2284–95. doi: 10.1111/cas.14040
- Pan JS, Cai JY, Xie CX, Zhou F, Zhang ZP, Dong J, et al. Interacting with HBsAg compromises resistance of jumping translocation breakpoint protein to ultraviolet radiation-induced apoptosis in 293FT cells. *Cancer Lett.* (2009) 285:151–6. doi: 10.1016/j.canlet.2009.05.009
- Lin X, Liu J, Hu SF, Hu X. Increased expression of TMED2 is an unfavorable prognostic factor in patients with breast cancer. *Cancer Manag Res.* (2019) 11:2203–14. doi: 10.2147/CMAR.S192949
- Tian SB, Tao KX, Hu J, Liu ZB, Ding XL, Chu YN, et al. The prognostic value of AGR2 expression in solid tumours: a systematic review and meta-analysis. *Sci Rep.* (2017) 7:15500. doi: 10.1038/s41598-017-15757-z
- Yi YW, Oh S. Comparative analysis of NRF2-responsive gene expression in AcPC-1 pancreatic cancer cell line. *Genes Genomics.* (2015). 37:97–109. doi: 10.1007/s13258-014-0253-2
- Yang H, Villani RM, Wang H, Simpson MJ, Roberts MS, Tang M, et al. The role of cellular reactive oxygen species in cancer chemotherapy. *J Exp Clin Cancer Res.* (2018) 37:266. doi: 10.1186/s13046-018-0909-x
- González-González L, Alonso J. Periostin: a matricellular protein with multiple functions in cancer development and progression. *Front Oncol.* (2018) 8:225. doi: 10.3389/fonc.2018.00225
- Nakazawa Y, Taniyama Y, Sanada F, Morishita R, Nakamori S, Morimoto K, et al. Periostin blockade overcomes chemoresistance via restricting the expansion of mesenchymal tumor subpopulations in breast cancer. *Sci Rep.* (2018) 8:4013. doi: 10.1038/s41598-018-22340-7
- Liu Y, Li F, Gao F, Xing L, Qin P, Liang X, et al. Periostin promotes the chemotherapy resistance to gemcitabine in pancreatic cancer. *Tumour Biol.* (2016) 37:15283–91. doi: 10.1007/s13277-016-5321-6
- Ryner L, Guan Y, Firestein R, Xiao Y, Choi Y, Rabe C, et al. Upregulation of periostin and reactive stroma is associated with primary chemoresistance and predicts clinical outcomes in epithelial ovarian cancer. *Clin Cancer Res.* (2015) 21:2941–51. doi: 10.1158/1078-0432.CCR-14-3111
- Erkan M, Kleeff J, Gorbachevski A, Reiser C, Mitkus T, Esposito I, et al. Periostin creates a tumor-supportive microenvironment in the pancreas by sustaining fibrogenic stellate cell activity. *Gastroenterology.* (2007) 132:1447–64. doi: 10.1053/j.gastro.2007.01.031
- Dong D, Zhang L, Jia L, Ji W, Wang Z, Ren L, et al. Identification of serum periostin as a potential diagnostic and prognostic marker for colorectal cancer. *Clin Lab.* (2018) 64:973–81. doi: 10.7754/Clin.Lab.2018.171225
- Song Y, Wang Q, Wang D, Junqiang L, Yang J, Li H, et al. Label-free quantitative proteomics unravels carboxypeptidases as the novel biomarker in pancreatic ductal adenocarcinoma. *Transl Oncol.* (2018) 11:691–9. doi: 10.1016/j.tranon.2018.03.005
- Tian B, Zhang Y, Zhang J. Periostin is a new potential prognostic biomarker for glioma. *Tumour Biol.* (2014) 35:5877–83. doi: 10.1007/s13277-014-1778-3
- Liu Y, Li F, Gao F, Xing L, Qin P, Liang X, et al. Role of microenvironmental periostin in pancreatic cancer progression. *Oncotarget.* (2017) 8:89552–65. doi: 10.18632/oncotarget.11533
- Lu Z, Hu L, Evers S, Chen J, Shen Y. Differential expression profiling of human pancreatic adenocarcinoma and healthy pancreatic tissue. *Proteomics.* (2004) 4:3975–88. doi: 10.1002/pmic.200300863
- Chung JC, Oh MJ, Choi SH, Bae CD. Proteomic analysis to identify biomarker proteins in pancreatic ductal adenocarcinoma. *ANZ J Surg.* (2008) 78:245–51. doi: 10.1111/j.1445-2197.2008.04429.x
- Mehner C, Radisky ES. Bad tumors made worse: SPINK1. *Front Cell Dev Biol.* (2019) 7:1–5. doi: 10.3389/fcell.2019.00010

39. Ozaki N, Ohmuraya M, Hirota M, Ida S, Wang J, Takamori H, et al. Serine protease inhibitor Kazal type 1 promotes proliferation of pancreatic cancer cells through the epidermal growth factor receptor. *Mol Cancer Res.* (2009) 7:1572–81. doi: 10.1158/1541-7786.MCR-08-0567
40. Wang C, Wang L, Su B, Lu N, Song J, Yang X, et al. Serine protease inhibitor Kazal type 1 promotes epithelial-mesenchymal transition through EGFR signaling pathway in prostate cancer. *Prostate.* (2014) 74:689–701. doi: 10.1002/pros.22787
41. Tiwari R, Pandey SK, Goel S, Bhatia V, Shukla S, Jing X, et al. SPINK1 promotes colorectal cancer progression by downregulating Metallothioneins expression. *Oncogenesis.* (2015) 4:e162. doi: 10.1038/oncsis.2015.23
42. Marks WH, Ohlsson K, Polling A. Immunocytochemical distribution of trypsinogen and pancreatic secretory trypsin inhibitor in normal and neoplastic tissues in man. *Scand J Gastroenterol.* (1984) 19:673–6. doi: 10.1080/00365521.1984.12005792
43. Haglund C, Huhtala ML, Halila H, Nordling S, Roberts PJ, Scheinin TM, et al. Tumour-associated trypsin inhibitor, TATI, in patients with pancreatic cancer, pancreatitis and benign biliary diseases. *Br J Cancer.* (1986) 54:297–303. doi: 10.1038/bjc.1986.176
44. Sherif A, Winerdal M, Winqvist O. Immune responses to neoadjuvant chemotherapy in muscle invasive bladder cancer. *Bladder Cancer.* (2018) 4:1–7. doi: 10.3233/BLC-170123
45. Parra ER, Villalobos P, Behrens C, Jiang M, Pataer A, Swisher SG, et al. Effect of neoadjuvant chemotherapy on the immune microenvironment in non-small cell lung carcinomas as determined by multiplex immunofluorescence and image analysis approaches. *J Immunother Cancer.* (2018) 6:48. doi: 10.1186/s40425-018-0368-0
46. Vizcaino JA, Cote RG, Csordas A, Dienes JA, Fabregat A, Foster JM, et al. The PRoteomics IDentifications (PRIDE) database and associated tools: status in 2013. *Nucleic Acids Res.* (2013) 41:D1063–9. doi: 10.1093/nar/gks1262

**Conflict of Interest:** The authors declare that the research was conducted in the absence of any commercial or financial relationships that could be construed as a potential conflict of interest.

Copyright © 2020 Sahni, Nahm, Krisp, Molloy, Mehta, Maloney, Itchins, Pavlakis, Clarke, Chan, Gill, Howell, Samra and Mittal. This is an open-access article distributed under the terms of the Creative Commons Attribution License (CC BY). The use, distribution or reproduction in other forums is permitted, provided the original author(s) and the copyright owner(s) are credited and that the original publication in this journal is cited, in accordance with accepted academic practice. No use, distribution or reproduction is permitted which does not comply with these terms.





# Dysregulated microRNAs in Hepatitis B Virus-Related Hepatocellular Carcinoma: Potential as Biomarkers and Therapeutic Targets

Jinghang Xu<sup>1,2†</sup>, Ping An<sup>2\*†</sup>, Cheryl A. Winkler<sup>2</sup> and Yanyan Yu<sup>1\*</sup>

<sup>1</sup> Department of Infectious Diseases, Center for Liver Diseases, Peking University First Hospital, Peking University, Beijing, China, <sup>2</sup> Basic Research Laboratory, Molecular Genetic Epidemiology Section, Basic Science Program, Frederick National Laboratory for Cancer Research, Frederick, MD, United States

## OPEN ACCESS

### Edited by:

Zhaohui Huang,  
Affiliated Hospital of Jiangnan  
University, China

### Reviewed by:

Shuai Zhang,  
Tianjin University of Traditional  
Chinese Medicine, China  
Shenglin Huang,  
Fudan University, China

### \*Correspondence:

Ping An  
anp@mail.nih.gov  
Yanyan Yu  
yyy@bjmu.edu.cn

<sup>†</sup>These authors have contributed  
equally to this work

### Specialty section:

This article was submitted to  
Gastrointestinal Cancers,  
a section of the journal  
Frontiers in Oncology

**Received:** 15 January 2020

**Accepted:** 19 June 2020

**Published:** 28 July 2020

### Citation:

Xu J, An P, Winkler CA and Yu Y  
(2020) Dysregulated microRNAs in  
Hepatitis B Virus-Related  
Hepatocellular Carcinoma: Potential  
as Biomarkers and Therapeutic  
Targets. *Front. Oncol.* 10:1271.  
doi: 10.3389/fonc.2020.01271

MicroRNAs (miRNAs) are non-coding small RNAs that can function as gene regulators and are involved in tumorigenesis. We review the commonly dysregulated miRNAs in liver tumor tissues and plasma/serum of hepatitis B virus (HBV)-related hepatocellular carcinoma (HCC) patients. The frequently reported up-regulated miRNAs in liver tumor tissues include miR-18a, miR-21, miR-221, miR-222, and miR-224, whereas down-regulated miRNAs include miR-26a, miR-101, miR-122, miR-125b, miR-145, miR-199a, miR-199b, miR-200a, and miR-223. For a subset of these miRNAs (up-regulated miR-222 and miR-224, down-regulated miR-26a and miR-125b), the pattern of dysregulated circulating miRNAs in plasma/serum is mirrored in tumor tissue based on multiple independent studies. Dysregulated miRNAs target oncogenes or tumor suppressor genes involved in hepatocarcinogenesis. Normalization of dysregulated miRNAs by up- or down-regulation has been shown to inhibit HCC cell proliferation or sensitize liver cancer cells to chemotherapeutic treatment. miRNAs hold as yet unrealized potential as biomarkers for early detection of HCC and as precision therapeutic targets, but further studies in diverse populations and across all stages of HCC are needed.

**Keywords:** biomarkers, hepatitis B virus, hepatocellular carcinoma, microRNA, gene expression, early diagnosis, prognosis

## INTRODUCTION

Hepatocellular carcinoma (HCC) is one of the most common and deadly cancers in the world (1, 2). Major risk factors for HCC are chronic infection by hepatitis B virus (HBV) or hepatitis C virus (HCV) (3). HCC is usually diagnosed at the late stages, due to the low sensitivity of the current diagnostic methods, which include imaging and quantification of alpha-fetoprotein (AFP) levels. Although recent advances in genomic technology have identified a variety of genetic alterations in HCC tissues, convenient biomarkers with sufficient sensitivity and specificity for early diagnosis of HCC are still lacking.

Detection of microRNAs (miRNAs) has recently gained increasing attention for their potential utility in the early diagnosis of HCC. miRNAs are one of the major post-transcriptional regulators of gene expression. As non-coding small endogenous RNAs with ~22 nucleotides, miRNAs silence genes by binding to the 3' untranslated region (3' UTR) of messenger RNAs (mRNAs)

and triggering mRNA degradation or translational repression (4–6). To date, more than 2,600 mature human miRNAs have been listed on the miRbase database (<http://www.mirbase.org>). Each miRNA can target multiple mRNAs with varying effects and a single mRNA may be targeted by multiple miRNAs. miRNAs modulate various biological molecular pathways and cellular processes, including cell proliferation, differentiation, development, apoptosis, angiogenesis, metabolism, and immune responses (7–10). Dysregulated miRNAs have been implicated in the development of a variety of tumors, including HCC, and may serve as robust biomarkers for cancer diagnosis and prognosis (11–14).

Given that miRNAs expression levels might differ among HCC patients with different etiological factors (15) and that HBV is the predominant risk factor for HCC (16), the present review focuses on miRNAs involved with HBV-related HCC

(HBV-HCC). We have assessed patterns of reported dysregulated miRNAs in the HBV-HCC patients and present the mechanisms and potential applications of miRNAs in the diagnosis, prognosis, and treatment of HBV-HCC (**Figure 1**).

## DYSREGULATED miRNAs IN HBV-HCC

Comparisons of HBV-HCC tumor tissue to either matched non-tumor tissue or liver tissue from healthy controls indicate that a subset of miRNAs is differentially expressed between health and tumor tissues. In **Table 1**, we list miRNAs that have been replicated in at least two HBV-HCC studies. Commonly reported up-regulated miRNAs include miR-18a, miR-21, miR-221, miR-222, and miR-224, whereas down-regulated miRNAs include miR-26a, miR-101, miR-122, miR-125b, miR-145, miR-199a, miR-199b, miR-200a, and miR-223 (17–36).

Due to limited liver tissue accessibility and the invasive nature of biopsy, studies assessing circulating miRNAs in plasma or serum from patients with HBV-HCC have increased dramatically in recent years. Cellular miRNAs from tumors leak into the circulation system following cell injury, apoptosis, and necrosis or by secretion through cell-derived exosomes and shedding vesicles (37). Circulating miRNAs in serum or plasma are stable (38), suggesting that circulating miRNAs may be accessible and quantifiable cancer diagnostic or prognostic biomarkers. Commonly reported dysregulated circulating miRNAs from patients with HBV-HCC include miR-21, miR-26, miR-122, miR-125b, miR-192, miR-206, miR-222, miR-223, and miR-224 (28, 29, 39–46) (**Table 2**).

For a subset of the miRNAs [e.g., up-regulated miR-18a, miR-221, miR-222, miR-224, and down-regulated miR-26a and miR-125b (**Table 3**)], dysregulated patterns were consistent among multiple independent studies and between tumor tissue and serum/plasma. These microRNAs may be of more translational

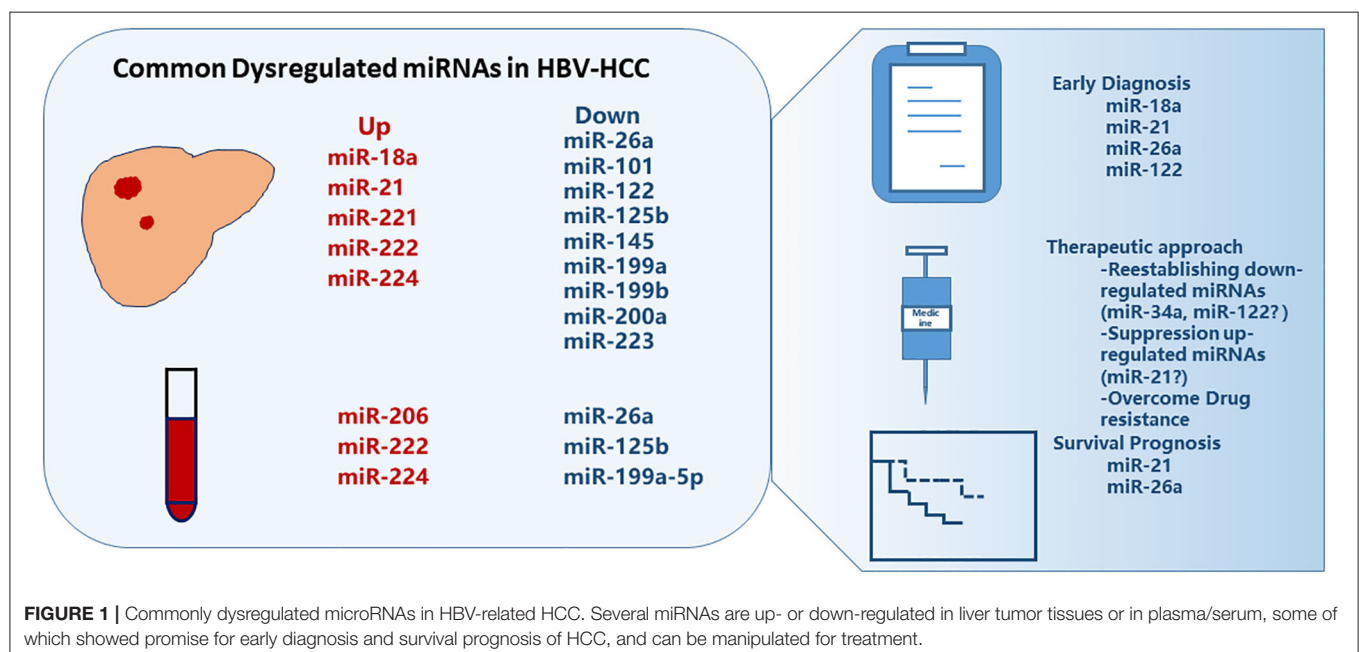


**TABLE 1 |** Dysregulated microRNAs in the tissue of predominantly HBV-related HCC.

miRNAs	Dysregulation type	Fold change	Case vs. control	Samples details		References
				Size and HBV status	Underlying cirrhosis % (n)	
miR-18a	Up-regulated	0.585 <sup>a</sup>	HCC vs. ANT	78 HCC (62 HBV)	51% (40/78)	(17)
	Up-regulated	3.223 <sup>b</sup>	HCC vs. ANT	22 HCC (20 HBV)	NA	(18)
miR-21	Up-regulated	2.29 <sup>a</sup>	HCC vs. ANT	100 HCC (58 HBV, 8 HCV, 27 NBNC, 27 Unknown)	46% (46/100)	(19)
	Up-regulated	3.67 <sup>b</sup>	HCC vs. ANT	115 HCC (101 HBV)	51% (59/115)	(20)
	Up-regulated	NA	HCC vs. ANT	148 HCC (82 HBV)	41% (45/109)	(21)
	Up-regulated	NA	HCC vs. ANT	31 HBV-HCC	NA	(22)
	Up-regulated	NA	HCC vs. ANT	24 HBV-DNs, 29 small HBV-HCC nodules, 38 HBV-ANTs	92% (22/24) in DNs 93% (27/29) in HCC	(23)
	Up-regulated	3.72 <sup>b</sup>	HCC vs. ANT	42 HBV-HCC	NA	(24)
miR-221	Up-regulated	1.51 <sup>a</sup>	HCC vs. ANT	100 HCC (58 HBV, 8 HCV, 27 NBNC, 27 Unknown)	46% (46/100)	(19)
	Up-regulated	NA	HCC vs. ANT	135 HCC (96 HBV)	95% (128/135)	(25)
	Up-regulated	4.00 <sup>b</sup>	HCC vs. ANT	115 HCC (101 HBV)	51% (59/115)	(20)
	Up-regulated	NA	HCC vs. ANT	31 HBV-HCC	NA	(22)
	Up-regulated	NA	HCC vs. ANT	24 HBV-DNs, 29 small HBV-HCC Nodules, 38 HBV-ANTs	92% (22/24) in DNs 93% (27/29) in HCC	(23)
miR-222	Up-regulated	1.57 <sup>a</sup>	HCC vs. ANT	78 HCC (62 HBV)	51% (40/78)	(17)
	Up-regulated	1.41 <sup>a</sup>	HCC vs. ANT	78 HCC (62 HBV)	51% (40/78)	(17)
	Up-regulated	4.44 <sup>b</sup>	HCC vs. ANT	115 HCC (101 HBV)	51% (59/115)	(20)
	Up-regulated	4.964 <sup>b</sup>	HCC vs. ANT	22 HCC (20 HBV)	NA	(18)
	Up-regulated	NA	HCC vs. ANT	42 HCC (33 HBV), 6 HCV, 3 NBNC-HCC	85% (28/33)	(26)
miR-224	Up-regulated	NA	HCC vs. ANT	24 HBV-DNs, 29 small HBV-HCC Nodules, 38 HBV-ANTs	92% (22/24) in DNs 93% (27/29) in HCC	(23)
	Up-regulated	27.231 <sup>b</sup>	HCC vs. ANT	22 HCC (20 HBV)	NA	(18)
miR-26a	Up-regulated	0.903 <sup>a</sup>	HCC vs. ANT	78 HCC (62 HBV)	51% (40/78)	(17)
	Down-regulated	0.37 <sup>b</sup>	HCC vs. ANT	455 HCC (412 HBV)	88% (400/455)	(27)
	Down-regulated	−1.59 <sup>a</sup>	HCC vs. ANT	100 HCC (58 HBV, 8 HCV, 27 NBNC, 27 Unknown)	46% (46/100)	(19)
miR-101	Down-regulated	NA	HCC vs. ANT	25 HCC (20 HBV), 20 HC (HBV negative)	72% (18/25)	(28)
	Down-regulated	NA	HCC vs. HC HCC vs. CHB HCC vs. LC	67 HBV-HCC, 61 HBV-LC, 79 CHB, 30 Normal control	NA	(29)
miR-122	Down-regulated	0.214 <sup>b</sup>	HCC vs. ANT	22 HCC (20 HBV)	NA	(18)
	Down-regulated	−0.958 <sup>a</sup>	HCC vs. ANT	78 HCC (62 HBV)	51% (40/78)	(17)
	Down-regulated	−1.67 <sup>a</sup>	HCC vs. ANT	100 HCC (58 HBV, 8 HCV, 27 NBNC, 27 Unknown)	46% (46/100)	(19)
	Down-regulated	NA	HCC vs. ANT	97 HCC (84 HBV)	NA	(30)
	Down-regulated	NA	HCC vs. ANT, HBV-HCC vs. non-HBV-HCC	142 HCC (103 HBV)	58% (82/142)	(31)
	Down-regulated	NA	HCC vs. ANT	24 HBV-DNs, 29 small HBV-HCC Nodules, 38 HBV-ANTs	92% (22/24) in DNs 93% (27/29) in HCC	(23)
miR-125b	Down-regulated	0.60 <sup>b</sup>	Venous metastases vs. solitary tumors	214 HBV-HCC	93% (199/214)	(32)
	Down-regulated	−0.893 <sup>a</sup>	HCC vs. ANT	78 HCC (62 HBV)	51% (40/78)	(17)
	Down-regulated	NA	HCC vs. ANT	97 HCC (84 HBV)	NA	(30)
	Down-regulated	0.58 <sup>b</sup>	Venous metastases vs. solitary tumors	214 HBV-HCC	93% (199/214)	(32)

(Continued)

**TABLE 1 |** Continued

miRNAs	Dysregulation type	Fold change	Case vs. control	Samples details		References
				Size and HBV status	Underlying cirrhosis % (n)	
miR-145	Down-regulated	NA	HCC vs. ANT LGDN vs. ANT HGDN vs. ANT	24 HBV-DNs, 29 small HBV-HCC Nodules, 38 HBV-ANTs	92% (22/24) in DNs 93% (27/29) in HCC	(23)
		0.28 <sup>b</sup>	HCC vs. ANT	42 HBV-HCC	NA	(24)
miR-145-5P	Down-Regulated	−2.39 <sup>a</sup>	HCC vs. ANT	100 HCC (58 HBV, 8 HCV, 27 NBNC, 27 Unknown)	46% (46/100)	(19)
miR-199a	Down-regulated	0.149 <sup>b</sup>	HCC vs. ANT	22 HCC (20 HBV)	NA	(18)
	Down-regulated	NA	HCC vs. ANT	97 HCC (84 HBV)	NA	(30)
miR-199a-5P	Down-regulated	−4.51 <sup>a</sup>	HCC vs. ANT	100 HCC (58 HBV, 8 HCV, 27 NBNC, 27 Unknown)	46% (46/100)	(19)
miR-199a-3P	Down-regulated	−2.78 <sup>a</sup>	HCC vs. ANT	100 HCC (58 HBV, 8 HCV, 27 NBNC, 27 Unknown)	46% (46/100)	(19)
miR-199b	Down-regulated	NA	HCC vs. ANT LGDN vs. ANT HGDN vs. ANT	24 HBV-DNs, 29 small HBV-HCC Nodules, 38 HBV-ANTs	92% (22/24) in DNs 93% (27/29) in HCC	(23)
miR-200a	Down-regulated	NA	HCC vs. ANT	120 HCC (97 HBV)	78% (93/120)	(33)
	Down-regulated	0.421 <sup>b</sup>	HCC vs. ANT	101 HCC (71 HBV)	NA	(34)
	Down-regulated	0.522 <sup>b</sup>	HCC vs. ANT	95 HCC (78 HBV)	47% (45/95)	(35)
miR-223	Down-regulated	−1.92 <sup>a</sup>	HCC vs. ANT	100 HCC (58 HBV)	46% (46/100)	(19)
	Down-regulated	0.267 <sup>b</sup>	HCC vs. ANT	22 HCC (20 HBV)	NA	(18)
	Down-regulated	0.20 <sup>b</sup>	HCC vs. ANT	42 HCC (33 HBV), 6 HCV, 3 NBNC-HCC	85% (28/33)	(26)

Fold changes were based on the original report; <sup>a</sup>Log<sub>2</sub> fold change.

<sup>b</sup>Regular fold change.

ANT, adjacent non-cancerous tissue; CHB, chronic hepatitis B; DN, dysplastic nodules; HBV, hepatitis B virus; HC, healthy control; HCC, hepatocellular carcinoma; HCV, hepatitis C virus; HGDN, high-grade dysplastic nodule; LC, liver cirrhosis; LGDN, low-grade dysplastic nodule; NA, not available; NBNC, non-HBV non-HCV.

value in the diagnosis, differential diagnosis or even therapy for HBV-HCC. However, other miRNAs showed inconsistent or contrasting profiles of dysregulation among studies or between tumor tissue and serum/plasma (Tables 1, 2). For example, downregulation of miR-122 was common in HCC tissue (19, 23, 32), but circulating miRNA levels were upregulated in some studies (39, 42, 43) and downregulated in others (45). Based on the observation that increased serum miR-122 is presented in both HCC patients and chronic hepatitis patients, some researchers speculate that higher levels of miR-122 in serum may result from liver injury rather than HCC itself (42, 43). It is also likely that factors governing the expression of miRNAs in the tissues and sera of HCC patients might differ. Additional factors that may contribute to discordant findings among these results include differences in patient selection, tumor stage, biological sample handling, and storage, miRNA probes employed, sample size, or genetic background of study populations (49).

## MECHANISM OF miRNA DYSREGULATION IN HCC

It's not fully understood if miRNA dysregulation in HCC is the cause, consequence of HCC development or both. Accumulating evidence indicates that some dysregulated miRNAs are active

players in tumor initiation and progression. The direct targets of miRNAs may be protein-coding genes involved in any or all pathophysiological mechanisms of cancer development, including cell growth, apoptosis, invasion, and metastasis. miRNAs may function as either tumor promoters or tumor suppressors depending on their target genes (50). miRNAs in HCC that target and suppress oncogenes may be down-regulated, while miRNAs that target suppressor genes may be up-regulated during tumor development (Figure 2). The miR-122 expression is largely liver-specific and under transcriptional control by the liver-enriched transcription factors HNF1A, HNF3A, and HNF3B (51). miR-122 can function as a tumor suppressor by suppressing HCC growth, invasion, migration, angiogenesis and by increasing HCC apoptosis and cell cycle arrest (52). miRNA-122 targets multiple genes, including *BCL9*, *Bcl-w*, *NDRG3*, cyclin G1, *ADAM17*, *ADAM10*, *G6PD*, and pituitary tumor-transforming gene 1 (*PTTG1*) binding factor (*PBF*), all of which have been implicated in tumor development (53–60). Other miRNAs such as miRNA-21 function as oncogenes by stimulating HCC growth, invasion, and migration (23, 61, 62). The inhibition of miR-21 suppresses HCC tumor growth (63).

Dysregulated miRNAs affect key cellular pathways that play a role in the pathogenesis of HBV-HCC (Figure 2). The commonly targeted pathways by dysregulated miRNAs in HBV-HCC include the Janus kinase/signal transducer (JAK/STAT),

**TABLE 2 |** Dysregulated microRNAs in the plasma/serum of patients with HBV-related HCC.

miRNAs	Dysregulation type	Fold change	Case vs. control	Samples details	References
miR-18a	Up-regulated	NA	HCC vs. HC, HCC vs. (CHB + LC)	101 HBV-HCC, 30 CHB or HBV-LC, 60 HC	(44)
miR-192	Up-regulated	1.4 <sup>b</sup>	HCC vs. (LC+CHB+HC)	457 HBV-HCC, 141 HBV-LC, 169 CHB, 167 HC	(45)
miR-206	Up-regulated	9.94 <sup>b</sup>	HCC vs. HC	261 HBV-HCC, 173 HC	(46)
	Up-regulated	3.51 <sup>b</sup>	HCC vs. LC	261 HBV-HCC, 233 HBV-LC	(46)
	Up-regulated	2.98 ± 3.94 <sup>b</sup>	HCC vs. matched control	55 HBV-HCC, 50 age and gender-matched control	(39)
miR-221	Up-regulated	4.83 <sup>b</sup>	HCC vs. HC	46 HCC (30 HBV), 20 HC	(41)
miR-222	Up-regulated	NA	HCC vs. HC	70 HBV-HCC, 48 CHB, 34 HC	(43)
	Up-regulated	3.01 <sup>b</sup>	HCC vs. HC	46 HCC (30 HBV), 20 HC	(41)
miR-224	Up-regulated	1.88 <sup>b</sup>	HCC vs. HC	46 HCC (30 HBV), 20 HC	(41)
miR-21	Up-regulated	1.9 <sup>b</sup>	HCC vs. (LC+CHB+HC)	457 HBV-HCC, 141 HBV-LC, 169 CHB, 167 HC	(45)
	Up-regulated	NA	HCC vs. HC	97 HCC (60 HBV), 30 HC	(47)
	Up-regulated	2.85 <sup>b</sup>	HCC vs. HC	46 HCC (30 HBV), 20 HC	(41)
	Up-regulated	NA	HCC vs. HC	101 HCC (76 HBV), 48 CHB, 89 HC	(42)
	Down-regulated	NA	HCC vs. CHB	101 HCC (76 HBV), 48 CHB, 89 HC	(42)
miR-122	Up-regulated	4.09 ± 5.38 <sup>b</sup>	HCC vs. HBV (ASC +CHB)	65 HBV-HCC, 160 controls	(39)
	Up-regulated	NA	HCC vs. HC	70 HBV-HCC, 48 CHB, 34 HC	(43)
	Up-regulated	NA	HCC vs. HC	101 HCC (76 HBV), 48 CHB, 89 HC	(42)
	Down-regulated	0.7 <sup>b</sup>	HCC vs. (LC+CHB+HC)	457 HBV-HCC, 141 HBV-LC, 169 CHB, 167 HC	(45)
	Down-regulated	NA	HCC vs. CHB	101 HCC (76 HBV), 48 CHB, 89 HC	(42)
miR-192-5p	Up-regulated	1.71 <sup>b</sup>	HCC vs. HC	212 HBV-HCC, 110 HC	(48)
	Up-regulated	1.97 <sup>b</sup>	HCC vs. LC	212 HBV-HCC, 106 HBV-LC	(48)
	Down-regulated	0.85 <sup>b</sup>	HCC vs. LC	261 HBV-HCC, 233 HBV-LC	(46)
	Down-regulated	0.77 <sup>b</sup>	HCC vs. HC	261 HBV-HCC, 173 HC	(46)
miR-223	Up-regulated	NA	HCC vs. HC	101 HCC (76 HBV), 89 HC	(42)
	Up-regulated	2.97 ± 1.67 <sup>b</sup>	HCC vs. HC	65 HBV-HCC, 160 controls	(39)
	Up-regulated	NA	HCC vs. HC	70 HBV-HCC, 34 HC	(43)
	No difference	NA	HCC vs. CHB	101 HCC (76 HBV), 48 CHB	(42)
	Down-regulated	0.3 <sup>b</sup>	HCC vs. (LC+CHB+HC)	457 HBV-HCC, 141 HBV-LC, 169 CHB, 167 HC	(45)
	Down-regulated	NA	HCC vs. HBV (ASC +CHB)	65 HBV-HCC, 135 HBV (55 ASC+ 80 CHB)	(39)
miR-26a	Down-regulated	0.2 <sup>b</sup>	HCC vs. (LC+CHB+HC)	457 HBV-HCC, 141 HBV-LC, 169 CHB, 167 HC	(45)
miR-26a-5p	Down-regulated	0.65 <sup>b</sup>	HCC vs. HC	261 HBV-HCC, 173 HC	(46)
	Down-regulated	0.54 <sup>b</sup>	HCC vs. LC	261 HBV-HCC, 233 HBV-LC	(46)
miR-122-5p	Down-regulated	0.27 <sup>b</sup>	HCC vs. HC	261 HBV-HCC, 173 HC	(46)
	Down-regulated	0.54 <sup>b</sup>	HCC vs. LC	261 HBV-HCC, 233 HBV-LC	(46)
miR-125b	Down-regulated	0.26 ± 0.46 <sup>b</sup>	HCC vs. HBV (ASC +CHB)	65 HBV-HCC, 135 HBV (55 ASC+ 80 CHB)	(39)
	Down-regulated	NA	HCC vs. LC	30 HCC (28 HBV), 30 LC (27 HBV)	(40)
	Down-regulated	NA	HCC vs. CHB	30 HCC (28 HBV), 30 CHB	(40)
miR-199a-5p	Down-regulated	0.58 <sup>b</sup>	HCC vs. HC	261 HBV-HCC, 173 HC	(46)
	Down-regulated	0.87 <sup>b</sup>	HCC vs. LC	261 HBV-HCC, 233 HBV-LC	(46)

Fold changes were based on the original report; <sup>a</sup>Log<sub>2</sub> fold change.

<sup>b</sup>Regular fold change.

ASC, asymptomatic carrier; CHB, chronic hepatitis B; HBV, Hepatitis B virus; HBV-HCC, HBV-related HCC; HBV-LC, HBV-related LC; HC, healthy control; HCC, hepatocellular carcinoma; LC, liver cirrhosis; NA, not available.

phosphoinositide 3-kinase/mitogen-activated protein kinase (PI3K)/AKT and MAPK, Wingless-related integration site/beta-catenin (WNT/β-Catenin) and TP-53 pathways (40, 64–73).

## Interaction of miRNAs and HBV in HBV-HCC

HBV can directly regulate cellular miRNAs levels. miR-122 is targeted and inhibited by HBV mRNA, which harbors a miR-122 complementary site, leading to the upregulation of the PTTG1-binding protein and promotion of HCC tumor growth

and cell invasion (57). Down-regulation of miR-122 occurs mainly in HBV-HCCs but not in HCV-infected HCCs (74). HBV downregulates miR-101 expression by directly inhibiting its promoter activity (75). Hepatitis B X antigen (HBx) increases the expression of miR-21 and subsequently promotes the progression of HCC by targeting *PTEN* and the tumor suppressor *PDCD4* (61). HBx suppresses p53-mediated activation of miR-148a thereby promoting tumor growth and metastasis; expression of miR-148a reduced tumor growth and invasion. In patients with HBV-HCC, miR-148a was down-regulated. These results suggest



that activation of miRNA-148a or down-regulation of its targeted pathways may have a role in HCC treatment (76).

In contrast, cellular miRNAs, including miR-122, and miR-125 and miR-199 family members, affect HBV replication (77). miR-125a-5p, markedly downregulated in HCC, inhibits HBsAg expression and secretion (78).

Using RNA deep sequencing and northern blotting, HBV-encoded miRNAs were recently identified. HBV-miR-3 was shown to restrict HBV replication, by targeting the region of HBV 3.5-kb mRNA encoding HBV core antigen (HBc) (79). Another HBV-encoded miRNA, HBV-miR-2, can promote the oncogenic activity of liver cancer cells (80). HBV-encoded miRNAs likely contribute to HBV-specific HCC development.

**TABLE 3 |** Common consistently dysregulated microRNAs between tumor tissue and serum/plasma in HBV- HCC.

Dysregulation miRNAs type		Publication numbers* (in tissue)	Publication numbers* (in serum/plasma)
Up-regulated	miR-18a	2	1
	miR-221	6	1
	miR-222	4	2
	miR-224	3	1
	miR-26a	2	1
Down-regulated	miR-125b	3	3

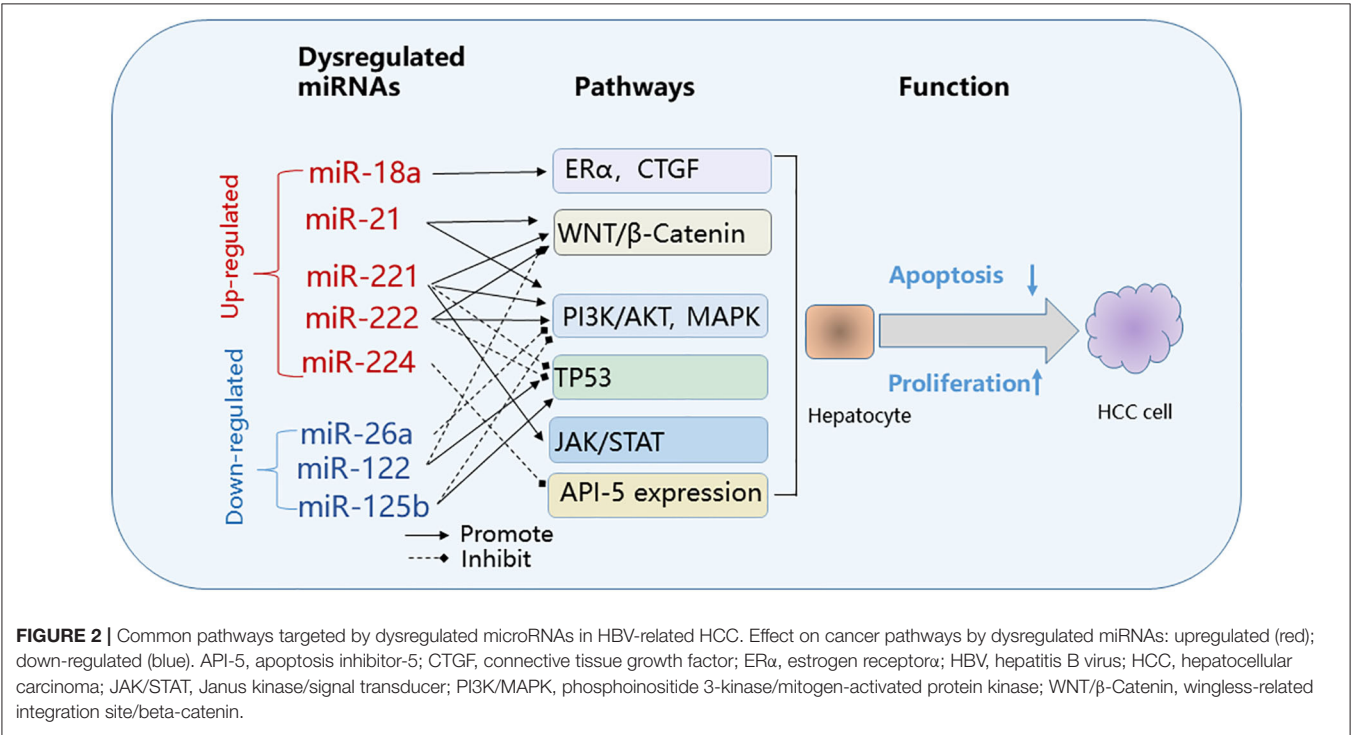
\*Publications cited in **Table 1** and **Table 2**. Results in tissue and serum/plasma don't necessarily origin from the same study.

The complex interactions and molecular interactions among cellular miRNAs and HBV have been reviewed in (73, 81–83).

Dysregulated miRNAs in Liver Cancer Stem Cells (LCSCs)

Cancer stem cells are small subpopulations of tumor-initiating cells within tumors that capable of self-renewal, differentiation, and proliferation. LCSCs can be identified by several highly expressed stem cell surface markers including epithelial cell adhesion molecule (EpCAM), CD90, CD44, CD133, and CD13 (84, 85). The other reported LCSC surface markers include OV6, DLK1, ABCG2, ALDH, and CD24 (84–87). LCSCs are responsible for tumor initiation, metastasis, relapse, and chemo- and radiation-therapy resistance in liver cancer (87). The specific influence of HBV on LCSCs remains largely unknown. Liver inflammatory damage induced by chronic HBV and HCV infection and liver toxins can induce somatic mutations, genomic instability, and epigenetic perturbations, resulting in the deregulation of self-renewal and differentiation signaling pathways of activated liver progenitor cells, which promotes the transformation of liver progenitor cells into LCSCs (84). It has been reported that HBx promotes the stem-like properties of OV6<sup>+</sup> CSCs in HBV-related HCC via MDM2 independent of p53 (88). Concomitant elevated expression of HBx and OV6 predicts a poor prognosis for patients with HBV- HCC (88).

Multiple miRNAs have been reported to regulate a variety of biological behaviors of LCSCs, including let-7, miR-200, miR-122, miR-181, miR-1246, miR-152, miR-145, miR-217, miR-500a-3p, and miR-148 (87). miRNAs affect the CSC phenotype by regulating the expression of oncogenes and stem



cell-related genes (85). These miRNAs target key molecules in the following pathways involved in carcinogenesis: *Wnt*/beta-catenin signaling, TGF-beta signaling, JAK/STAT signaling, epithelial-mesenchymal transition (EMT) in LCSCs (87). miRNA profiling comparisons between CSC<sup>+</sup> and CSC<sup>-</sup> HCCs, as separated by hepatic CSC biomarkers (EpCAM, CD133, CD90, CD44, and CD24), identified aberrant downregulation of liver-specific miR-192-5p in HCC cells, which correlated with increased CSC populations with stemness features and shorter survival in HCC patients (89). Over-expression of miR-192-5p inhibited the stemness features of human liver cancer cell lines, with decreased spheroid formation, decreased CSC number and diversity and decreased expression of CSC biomarkers and increased expression of genes related to hepatocyte metabolism (89). Hepatitis B virus X protein (HBx) induces expression of EpCAM by upregulating miR-181 to promote stemness in hepatocarcinogenesis (90, 91). The knockdown of miR-181 significantly reduces the EpCAM<sup>+</sup> LCSCs and tumor-initiating ability (92).

Targeting the regulation of these miRNAs or their pathways may serve as a potential therapeutic strategy to inhibit or eradicate LCSCs (87). Restoring of miR-122 has been demonstrated to suppresses stem-like HCC cells (93). It would be interesting to explore the clinical utility of restoring the miR-192-5p for riding of LCSCs (89).

## Epigenetic Alterations and miRNAs in HCC

Epigenetic alterations such as DNA methylation and histone modification are essential for chromatin remodeling and regulation of both coding genes and miRNAs. Abnormal DNA methylation patterns of a number of miRNAs in HCC have been reported for hypermethylation of miR-1, miR-9, miR-10a, miR-10b, miR-124, miR-125b, miR-132, miR-148a, miR-195, miR-196b, miR-203, miR-320, miR-375, miR-378, miR-497, miR-596, miR-663, and miR-1247, and for hypomethylation of miR-23a, miR-25, miR-27a, miR-93, and miR-106b (94). Among these miRNAs, only miR-125b presents consistent dysregulation pattern of expression, and was down-regulated both in tissue (17, 30, 32) and serum (39, 40) of patients with HCC. The expression of miR-125b was significantly increased by the methylation inhibitor 5-aza-2'-deoxycytidine in HCC cells, suggesting the epigenetically modulation of the expression of miR-125b (95).

Histone modifications, including acetylation, methylation, and phosphorylation of lysine residues, play an important role in expression regulation of genes including miRNAs in HCC tumor tissue. For example, levels of hsa-miR-449a in HCC cell lines was enhanced significantly by inhibiting histone deacetylases (HDACs), which were up-regulated in HCC tissue (96). Reduced expression of miR-199a/b-3p, one of the consistently and markedly decreased miRNA in HCC, is mediated by histone methylation and independent of DNA methylation (97). On the other hand, some miRNAs have been reported to be involved in hepatocarcinogenesis by regulating histone deacetylases (HDACs), including miR-1, miR-22, and miR-200a targeting HDAC4, miR-31 and miR-145 targeting HDAC2, miR-221 targeting HDAC6, miR-29c targeting SIRT1,

miR-125a-5p, and miR-125b targeting SIRT7, suggesting the potential use of miRNA-based therapies in HCC (98).

Chromatin modifiers or remodelers regulate accessibility to chromatin and positioning of nucleosome in the DNA. Upregulated enhancer of zeste homolog 2 (EZH2) in HCC, a well-studied chromatin modifier which mediates gene silencing in HCC, represses miR-622 by enhancing H3K27 trimethylation, and is correlated with unfavorable HCC prognosis (32). CCCTC-binding factor (CTCF) is a highly conserved insulator-binding protein with an enhancer-blocking function and contributes to the epigenetic regulation of some miRNAs (99). In breast cancer cells, disruption of CTCF binding at miR-125b1 CpG island (CGI) is associated with CGI methylation and the gain of the repressive histone marks including H3K9me3 and H3K27me3, and induces silencing of miR-125b1 expression (100). Considering the miR-125b is consistently down-regulated in HCC tissue (17, 30, 32) and serum (39, 40), disruption of CTCF binding might modulate HCC development.

Circular RNAs (circRNAs) are a class of highly conserved, stable and abundant non-coding RNAs (ncRNAs) that can regulate gene expression at transcriptional or post-transcriptional levels. The majority of circRNAs function as sponges of miRNA (101) and deregulation of a number of circRNAs have been reported in HCC. For example, circHIPK3 can sponge 9 miRNAs with 18 potential binding sites, including directly binding to the well-known tumor suppressor miR-124, reducing its activity (102). circTRIM33-12 acts as the sponge of miR-191 to suppress HCC (103). Artificial circRNAs which bind and sponge specific miRNAs can be constructed to achieve better inhibitory effects on oncogenic or pathogenic miRNAs, indicating a promising strategy to treat HCC.

## REGULATING miRNA AS A THERAPEUTIC APPROACH FOR HCC

Normalization of dysregulated miRNAs in patients with HBV-HCC, by either up- or down-regulation of dysregulated miRNAs, is a plausible therapeutic approach in treating HCC.

Preliminary studies suggest that reestablishing the expression of down-regulated miRNAs might restore the tumor-suppressing function of miRNAs. In a first-in-human Phase 1 trial of a miRNA therapy using a liposomal miR-34a mimic in patients with advanced solid tumors including HBV-HCC, the miR-34a mimic showed antitumor activity (104). In another study upregulation of miR-122, which is frequently down-regulated in HCC patients, suppressed the proliferation and invasion capability of HCC-derived cells and increased sensitivity to chemotherapy (31, 105–107). Restoring miR-122 in stem-like HCC cells was shown to decrease cell proliferation and reduce tumor size in a mouse model (93). Besides miR-122, other miRNAs may have value in treating HCC. A recent study showed that injection of exosomal miR-335-5p, a tumor suppressor, can inhibit HCC cell proliferation and invasion as well as result in slower cancer growth (108). On the other hand, suppression of miR-21, which is frequently up-regulated in patients with HCC, leads to increased sensitivity to chemotherapeutic drugs (21).

In addition to direct targeting of miRNA, modulating the upstream genes that control miRNA expression is another therapeutic strategy. Upregulation of miR-122 by activating the farnesoid X receptor transcription factor (FXR), suppressed the proliferation of HCC cells *in vitro* and reduced the growth of HCC xenografts *in vivo* (109).

The crosstalk between epigenetics and miRNA related to HCC provides new opportunities for the development of more effective therapy for HCC by targeting epigenetic modulation of miRNAs as discussed above. Restoring the expression of tumor suppressor miRNA by inhibitors of DNA methylation and histone deacetylase, and inhibiting the expression of oncogenes by artificial circRNAs sponging specific miRNAs may be promising therapeutic strategies for HCC.

Regulating miRNA-mediated immune response in HCC may prove to be a promising therapeutic strategy. Most recently, Tian's group demonstrated that HBV mediates PD-L1-induced T cell immune exhaustion through the interaction of the oncofetal gene SALL4 and miR-200c (110). They showed that miR-200c controls PD-L1 expression by directly targeting the 3'-UTR of PD-L1 and that overexpression of miR-200c antagonizes HBV-mediated PD-L1 expression and reverses antiviral CD8<sup>+</sup> T cell exhaustion.

A group of miRNAs are involved either directly or indirectly in drug resistance and either suppressing or activating miRNAs may reduce drug resistance. For example, a recent study reported that some miRNAs contribute to drug resistance to sorafenib. Targeting these miRNAs by the artificial long non-coding RNA improved treatment response in patients with HCC (111). Other studies found that restoration of miR-122 can sensitize HCC cancer cells to adriamycin and vincristine (112) as well as reverse doxorubicin-resistance in HCC cells (113). MiR-101 was shown to sensitize liver cancer cells to chemotherapeutic treatment (114).

The risk of undesirable effects of miRNA targeting, due in large part to off-target binding, is challenging. Adverse events were common in the miR-34a mimic trial, the first clinical trial for the treatment of HBV-HCC (104) and the trial was recently terminated due to immune-related serious adverse events (115). Of the clinical trials using miRNAs that are dysregulated in HBV-HCC, one phase II trial of miR-122 as a treatment modality for HCV has been completed and a miR-21 phase II trial for Alports syndrome was suspended (115). The application of miRNA-targeting therapy has strong potential in personalized medicine, although off-target effects remains a significant hurdle.

## miRNAs AS BIOMARKERS IN HBV-HCC

Early diagnosis of HCC, crucial for treatment outcome, remains challenging. The limitations of imaging technology and AFP detection to diagnose small and atypical HCC calls for more sensitive and specific biomarkers. Based on reports that many miRNAs are expressed differentially in HBV-HCC patients (Tables 1, 2) and miRNAs dysregulation is an early event in hepatocarcinogenesis occurring in pre-malignant dysplastic nodules (23, 47), the detection of miRNAs, especially circulating

miRNAs levels, is gaining increasing recognition and attention for their potential clinical utility as biomarkers in screening and early diagnosis of HBV-HCC and predicting HCC prognosis as well.

## miRNAs as Diagnostic Biomarkers in HBV-HCC

Potential single miRNAs and miRNA panels that have been proposed as early diagnostic biomarkers for HBV-HCC are summarized in Table 4. Circulating miRNAs, including miR-18a, miR-21, miR-101, miR-122, miR-139, miR-223, and some miRNA panels may have diagnostic utility in distinguishing HBV-HCC patients from patients with chronic HBV infection (CHB) or liver cirrhosis (LC). Complicating the consensus and interpretation of the results of the studies (Table 4) are the differences in control groups employed [i.e., HBV-negative or HBV infected persons (CHB or LC) (22, 29, 42–46, 48, 116–118)].

A recent study revealed that a seven-miRNA classifier (miR-29a, miR-29c, miR-133a, miR-143, miR-145, miR-192, and miR-505) had significantly higher sensitivity than AFP to discriminate between HCC and healthy controls, inactive HBsAg carriers, CHB patients, and HBV-cirrhosis patients. Critically this miRNA classifier was the first biomarker to diagnosis preclinical HCC, which was detected in eight of 27 HBV infected individuals 12 months before clinical diagnosis of HCC. This miRNA classifier holds promise for improving clinical outcomes by early HCC detection and curative treatment (117).

Among these miRNAs and miRNA panels, miR-122 is the most replicated miRNA biomarker in HCC, which has a sensitivity ranging from 71 to 81%, specificity from 59 to 83%, and an AUC from 0.63 to 0.87 to distinguish HBV-HCC from controls (42, 43). miR-122 is also included in two miRNA panels for HBV-HCC (45, 46). However, the diagnostic utility of miR-122 in HBV-HCC also extends to other HCCs (119).

Multiple approaches may be taken to improve the diagnostic performance of miRNA biomarkers in HBV-HCC. The type of biological sample is one of the key factors influencing sensitivity and specificity.

Exosomes are secreted by most cell types including cancer cells. Serum exosomes are highly enriched in miRNAs and exosomes can transfer miRNAs between cells, thus affecting HCC cancer proliferation, migration, metastasis, drug resistance (120). A meta-analysis published in 2019 suggested that exosomal miRNAs have superior diagnostic value in prostate cancer patients (121). With regard to diagnosis of HBV-HCC, recent studies indicate that exosomal miRNAs might also be a better choice than miRNAs from whole serum or plasma for early diagnosis. Wang et al. found that the detection of exosomal miR-21, which is enriched in exomes, had improved sensitivity over the whole serum (122). Similarly, miR-125b levels in exosomes were significantly lower than in serum from patients with HBV-HCC when compared to patients with CHB or LC, which explains, at least in part, why miR-125b levels in exosomes, but not in serum, independently predict HCC progression (40). Another study comparing HBV-HCC to CHB or LC, found a greater difference in



**TABLE 4 |** Diagnostic value of miRNAs in HBV-related HCC.

miRNA	Sample details				Diagnostic value				References
	Sample type	Size of case	Underlying cirrhosis, %	Control	Specificity (%)	Sensitivity (%)	AUC	CI of AUC	
miR-18a	S	101 HBV-HCC	NA	60 HC	75.0	86.1	0.881	0.829–0.933	(44)
		101 HBV-HCC	NA	30 CHB or LC	70.0	77.2	0.775	0.681–0.869	(44)
miR-21	S	101 HCC (76 HBV)	NA	89 HC	73.5	84	0.87	0.81–0.93	(42)
		57 HBV-HCC	NA	30 HC + 29 HBV	71.2	89.5	0.865	NA	(116)
miR-101	S	67 HBV-HCC	NA	30 HC	70.0	76.1	0.788	0.693–0.865	(29)
		67 HBV-HCC	NA	79 CHB	62.0	88.1	0.777	0.701–0.842	(29)
		67 HBV-HCC	NA	61 HBV-LC	90.2	95.5	0.976	0.931–0.995	(29)
miR-122	S	70 HBV-HCC	75% (51/68)	34 HC	83.3	81.6	0.869	0.786–0.952	(43)
		70 HBV-HCC	75% (51/68)	48 CHB	57.8	77.6	0.63	0.516–0.743	(43)
		101 HCC (76 HBV)	NA	89 HC	69.1	70.7	0.79	0.71–0.86	(42)
miR-139	P	31 HBV-HCC	NA	31 CHB	58.1	80.6	0.761	0.643–0.878	(22)
miR-223	S	101 HCC (76 HBV)	NA	89 HC	80	76.5	0.86	0.80–0.92	(42)
miR-15b and miR-130b	S	57 HBV-HCC	NA	30 HC + 29 HBV	91.5	98.3	0.981	NA	(116)
miR-27b-3p, miR-192-5p	S	212 HBV-HCC	NA	110 HC + 106 HBV- LC	91.2	68.6	0.836	0.783–0.880	(48)
				110 HC	95.2	68.5	0.823	0.748–0.866	
				106 HBV-LC	79.3	78.5	0.859	0.804–0.906	
				60 HC + 68 CHB + 71 HBV-LC	88.9	74.5	0.817	0.769–0.865	(117)
miR-29a, miR-29c, miR-133a, miR-143, miR-145, miR-192, miR-505	S	153 HBV-HCC	NA	68 CHB + 71 HBV-LC	89.9	74.5	0.822	0.772–0.873	
		49 HBV-HCC	NA	48 HC + 42 inactive HBsAg carrier +	91.1	85.7	0.884	0.818–0.951	
		49 HBV-HCC	NA	42 inactive HBsAg carrier	83.3	85.7	0.845	0.758–0.932	
		27 HBV-HCC	NA	135 matched CHB	80.0	70.4	0.752	0.644–0.860	
miR-122, miR-192, miR-21, miR-223, miR-26a, miR-27a, miR-801	P	457 HBV-HCC	NA	141 HBV-LC + 169 CHB + 167 HC	83.5	81.8	0.888	0.852–0.917	(45)
				167 HC	93.9	83.2	0.941	0/905–0.966	
				169 CHB	76.4	79.1	0.842	0.792–0.883	
				141 HBV-LC	91.1	75	0.884	0.838–0.921	
miR122, miR1228, miR141, miR192, miR199a, miR206, miR26a, miR433	S	261 HBV-HCC	NA	173 HC + 233 HBV-LC	76.2	90.3	0.879	0.842–0.941	(46)
				173 HC	83.3	82.8	0.893	0.849–0.94	
				233 HBV-LC	84.6	81.6	0.892	0.844–0.939	
miR-20a-5p, miR-25-3p, miR-30a-5p, miR-92a-3p, miR-132-3p, miR-185-5p, miR-320a, miR-324-3p	P	67 HBV-HCC	NA	82 HBV	64.6	86.6	0.802	NA	(118)

When data from training set and validation set are available, only the latter is presented. AUC, area under the curve; CHB, chronic hepatitis B; CI, confidence interval; HBV, Hepatitis B virus; HC, healthy control; HCC, hepatocellular carcinoma; LC, liver cirrhosis; NA, not available; P, plasma; S, serum.

miRNA levels in exosomes compared to whole serum (123). Combinations of miRNAs with other classic serum markers, i.e., AFP, is another approach to increase sensitivity and specificity of blood-based early detection of HBV-HCC (117,

118), especially for atypical HCC cases with lower serum AFP levels. The better performance of this add-on strategy was demonstrated in HCC cases caused by non-HBV factors as well (124).

**TABLE 5 |** Prognostic value of miRNAs in HBV-related HCC.

Sample			miRNA panels	Risk/protective factor	HR/RR	CI	P-value	Outcome	References
Type	Size of case	Underlying cirrhosis, %							
P/S	97 HCC (60 HBV)	32.0% (31/97)	miR-21	Risk	2.229	1.328–3.743	0.002	OS	(47)
P/S	136 HCC (129 HBV)	NA	miR-200a	Risk	1.75	1.45–2.11	<0.001	OS	(125)
P/S	62 HCC (40 HBV)	NA	miR-1246	Risk	10.24	1.39–75.67	0.023	OS	(126)
P/S	62 HCC (40 HBV)	NA	miR-1246	Risk	10.12	1.45–70.47	0.020	DFS	(126)
P/S	120 HBV-HCC	85.8% (103/120)	miR-26a	Protective	0.29	0.11–0.76	0.011	LT-free survival	(127)
P/S	120 HBV-HCC	85.8% (103/120)	miR-29a	Protective	0.36	0.15–0.91	0.030	LT-free survival	(127)
Exosome	128 HCC (121 HBV)	76% (97/128)	miR-125b	Protective	0.36	0.18–0.74	0.005	OS	(40)
T	148 HCC (82 HBV)	41% (45/109)	miR-21	Risk	NA	1.19–1.47	0.004	DFS	(21)
T	140 HBV-HCC	NA	miR-21	Risk	1.509	1.079–2.112	0.016	3-years OS	(128)
T	108 HBV-HCC	NA	miR-21	Risk	1.416	1.057–1.897	0.020	5-years OS	(128)
T	115 HCC (101 HBV)	51% (59/115)	miR-221	Risk	2.09	1.09–4.04	0.027	MFS	(20)
T	135 HCC (96 HBV)	95% (128/135)	miR-221	Risk	2.846	1.564–5.181	0.001	DFS	(25)
T	135 HCC (96 HBV)	95% (128/135)	miR-221	Risk	2.969	1.629–5.408	<0.001	OS	(25)
T	166 HCC (146 HBV)	84% (139/166)	20-miRNA prognostic signature*	Risk	2.75	1.58–4.79	<0.001	OS	(129)
T	214 HBV-HCC	93% (199/214)	20-miRNA metastasis signature#	Risk	2.1	1.2–3.6	0.01	OS	(32)
T	455 HCC (412 HBV)	88% (400/455)	miR-26a	Protective	0.48	0.21–1.0	0.05	OS	(27)
T	455 HCC (412 HBV)	88% (400/455)	miR-26b	Protective	0.48	0.20–0.91	0.04	OS	(27)
T	142 HCC (103 HBV)	58% (82/142)	miR-122	Protective	NA	NA	0.001	OS	(31)
T	120 HCC (97 HBV)	78% (93/120)	miR-200a	Protective	0.382	0.215–0.896	0.004	OS	(33)
T	101 HCC (71 HBV)	NA	miR-200a	Protective	0.403	0.242–0.670	<0.001	OS	(34)
T	66 HCC (64 HBV)	NA	miR-203	Protective	0.202	0.064–0.638	0.006	RFS	(130)
T	66 HCC (64 HBV)	NA	miR-203	Protective	0.332	0.139–0.793	0.013	OS	(130)

\*miR-708, miR-34c-3p, miR-584, miR-4310, miR-744, miR-141, let-7d, miR-15a, miR-142-3p, miR-10b, let-7e, miR-28-3p, miR-193b, miR-101, miR-451, miR-142-5p, miR-26b, miR-497, miR-29c, miR-140-3p.

#miR-338, miR-219-1, miR-207, miR-185, miR-30c-1, miR-1-2, miR-34a, miR-19a, miR-148a, miR-124a-2, miR-9-2, miR-148b, miR-122a, miR-125b-2, miR-194, miR-30a, miR-126, let-7g, miR-15a, miR-30e.

CI, confidence interval; DFS, disease-free survival; HBV, Hepatitis B virus; HR, hazard ratio; HCC, hepatocellular carcinoma; LT, liver transplantation; MFS, metastasis-free survival; OS, overall survival; P/S, plasma or serum; Ref, reference; RFS, recurrence-free survival; RR, relative risk; T, tissue.

## miRNAs as Biomarkers for HBV-HCC Prognosis

Expression levels of several miRNAs in liver tissue or circulation were correlated with disease severity and survival of HBV-HCC patients. Commonly reported single miRNAs and miRNA biomarker panels in predicting the survival of HBV-HCC are summarized in **Table 5**. Single miRNAs and miRNA panels associated with shorter survival include miR-21, miR-221, and two 20-mer miRNA signature profiles (20, 21, 25, 32, 47, 128, 129); miR-26a, miR-26b, miR-122, miR-125b, and miR-203 were associated with longer survival (27, 31, 40, 130). Among these miRNAs, miR-21 was the most replicated with a hazard ratio (HR) ranging from 1.4 to 2.2 in predicting the long-term progression of HBV-HCC (**Table 5**); miR-21 was also associated with HCCs (131). Given the enrichment of miRNAs in serum exosomes, detection of serum exosomal miRNAs can be used to predict prognosis of HCC patients (40).

It should also be noted that other studies found no significant associations with survival between HBV-HCC patients with high or low levels of miRNAs, (i.e., miR-21, miR-122, and

miR-125b) (126, 132, 133). These disparate results may be due to differences in study design, analysis, and participant characteristics. For example, the cut-off value used to divide high and low miRNA-expressed population varies among studies and can be quite arbitrary [e.g., using a fixed value or average value or optimal cut-off value from Youden index analysis, or a ratio comparison to adjacent non-tumor tissue] (20, 21, 40, 126). The outcome events also varied, including overall survival (OS), disease-free survival (DFS), recurrence-free survival (RFS), and liver transplantation (LT)-free survival. These differences among studies make comparison challenging. These limitations will need to be addressed to establish reliable diagnostic and prognostic miRNA biomarker panels for HBV-HCC.

## DYSREGULATED miRNAS IN HCV-HCC

Since effective HCV-curative, direct-acting antiviral agents (DAA) are widely used worldwide in recent years (134, 135), fewer cases of HCC will be caused by HCV infection in the future. Subsequently, HBV infection will likely be the predominant cause

**TABLE 6 |** Common microRNAs dysregulated consistently in HBV-HCC and HCV-HCC.

Dysregulation type	miRNAs	Publications in HBV-HCC	Publications in HCV-HCC
Up-regulated	miR-18a	(17, 18, 44)	(136)
	miR-221	(17, 19, 20, 22, 23, 25, 41)	(137)
	miR-224	(17, 18, 23, 41)	(15, 138, 139)
Down-regulated	miR-199a-5p	(19)	(136)

of HCC worldwide. The pattern of dysregulated miRNAs in HCV-HCC, nevertheless, may still shed insights on the HBV-HCC pathogenesis as the comparison may reveal pathogen-specific and pathogen-independent tumorigenic pathways.

Several miRNAs showed similar dysregulation patterns in HCV- HCC and HBV-HCC (Table 6), including up-regulation of miR-18 (136), miR-221 (137) and miR-224 (15, 138, 139), and down-regulation of miR-199a-5p (136). These miRNAs may be involved in key cancer pathways that are shared by HBV- and HCV-HCC, including the WNT/ $\beta$ -Catenin and TP53 pathways. These miRNA and pathways may, therefore, be putative common targets for diagnostic, prognostic, and therapeutic interventions. Direct comparisons of miRNAs in HBV- and HCV-HCCs are lacking. In a small study comparing HBV-HCC and HCV-HCC tumor samples, the abundance of miR-122 was significantly reduced in HBV-HCC but not HCV-HCC, providing evidence of pathogen-specific dysregulation of miRNAs (74).

## CHALLENGES AND FUTURE DIRECTIONS

Accumulating evidence indicates that miRNAs, which function as gene regulators at the post-transcriptional level, are involved in the development of HBV-HCC. The expression levels of some single miRNAs or miRNA panels have the specificity and sensitivity to diagnose HCC and to predict survival; therefore, miRNA profiling panels are promising biomarkers for early diagnosis and survival prediction of HCC (Figure 1). Clinical trials to establish the utility of these panels in clinical practice are warranted.

However, there are several limitations and knowledge gaps in the current literature. In HBV-HCC, most HCC arise from cirrhotic tissues, thus miRNA changes may originate from either or both HCC and cirrhotic tissues. Underlying cirrhosis was present in 45–95% of HCC cases among studies that reported this information (Table 1), other studies did not report cirrhosis status. How miRNA profiles differ between cirrhotic and non-cirrhotic HBV-HCC remains largely unexplored (140).

The heterogeneity of methodologies in control selection, miRNA detecting technologies, case and control characteristics, and biostatistical analyses in studies also contribute to different results among studies. Failure to replicate findings may be due to small sample size affecting power leading to type 1 and type 2 errors. A major confounder among the studies is the selection of control tissue or sample. For example, comparisons may be made between tumor and non-tumor tissues from the same patients or different individuals. qRT-PCR quantification

methods and platforms for miRNAs vary in their sensitivity and breadth. Technical replication to control for between and within-sample variation was lacking in some studies (42). Although most studies use internal controls to normalize miRNA expression levels of target genes (e.g., U6 SnRNA, GAPDH, miR-16, RNU43, cel-miRNA-39, or synthetic cel-miR-67), no universal internal references are used making comparisons among studies challenging (32, 36, 42, 47, 117, 122, 141, 142). Reviewers and journals are aware that a lack of replication in clinical research is a growing area of concern. A common set of internal controls would facilitate the replication and validation of informative miRNAs. Another source of failure to replicate is that the coverage of the miRNA arrays varies by more than 2-fold (308 to 829 miRNAs) (17–19, 32, 45). Definitions of differential expression vary from >2-fold change to <1.5 change in others. Over conservative cut-offs tend to lead to type 2 errors while less conservative cut-offs tend to increase type 1 errors. Next-generation sequencing is particularly prone to mis-annotations of microRNAs, which may lead to false-positive (143) or false-negative findings (144).

Before miRNAs can be used in a clinical setting, standardized methods for sample collection and handling should be implemented. Clinical trials will need to be conducted to assess the performance of miRNA biomarkers in addition to or in place of current diagnostic methods before their acceptance into surveillance or screening programs or for clinical management of HCC. We consider design issues and knowledge gaps that warrant attention in future investigations.

- (1) Sample size: is a major factor affecting power and validity. Since most miRNA have a moderate (<3-fold) difference between cases and controls and both large intra-individual and inter-individual variation, large sample sizes are required for sufficient power to minimize type 1 and II errors. Replication using public datasets [e.g., the Cancer Genome Atlas (TCGA) database] may provide additional supporting evidence (145, 146).
- (2) Validation for circulating miRNAs: To develop liquid biopsies for detection, diagnosis, and prognosis, miRNAs identified from serum/plasma should be validated to miRNAs obtained from tumor tissue before clinical evaluation as biomarkers. Non-specific circulating miRNAs may originate from other high blood-flow organs and tissue (147).
- (3) Clinical trials: Promising miRNAs markers must be tested for efficacy vs. standard of care (imaging and AFP levels) in randomized clinical trials before entering clinical practice.
- (4) HCC early detection: Since HCC is usually diagnosed mid to late-stage HCC, early HCC is rarely studied for miRNAs. Data comparing miRNAs expression levels in LC and early HCC groups is scarce and is urgently needed, as most HBV-HCCs develop from cirrhotic liver tissue. Clinical trials for miRNA early-diagnosis should focus on patients with HBV, HCV, or liver cirrhosis at high risk for HCC.
- (5) miRNA profiling for HBV-HCC: Evaluation of differences and commonalities of miRNA profiles in HCCs arising from HBV and other underlying liver diseases
- (6) Personalized medicine: Basic and clinical investigations for the clinical utility of precision miRNA-targeting therapies.

- (7) Diversity of miRNA investigations: Most HBV-HCC studies have enrolled Asian patients because of their high carrier rate for HBV. However, it is unknown if miRNA results are similar across diverse populations, particularly in Africa where HBV prevalence is also high (73). The generalizability of findings in Asians needs to be tested in other global populations.

Taken together, the recent studies in miRNAs provide encouraging evidence that miRNAs detection may aid in the diagnosis, survival prediction, and treatment of HBV-HCC. More well-designed and well-powered case-control or longitudinal studies in diverse populations are critically needed to validate the utility of miRNAs in HCC and translate miRNA into clinical use.

## AUTHOR CONTRIBUTIONS

JX and PA conceived idea, prepared the tables, and wrote the manuscript. YY and CW revised the manuscript. All authors read and approved the final manuscript.

## REFERENCES

- Torre LA, Bray F, Siegel RL, Ferlay J, Lortet-Tieulent J, Jemal A. Global cancer statistics, 2012. *CA Cancer J Clin.* (2015) 65:87–108. doi: 10.3322/caac.21262
- El-Serag HB. Hepatocellular carcinoma. *N Engl J Med.* (2011) 365:1118–27. doi: 10.1056/NEJMra1001683
- Bruix J, Reig M, Sherman M. Evidence-based diagnosis, staging, and treatment of patients with hepatocellular Carcinoma. *Gastroenterology.* (2016) 150:835–53. doi: 10.1053/j.gastro.2015.12.041
- Bartel DP. MicroRNAs: target recognition and regulatory functions. *Cell.* (2009) 136:215–33. doi: 10.1016/j.cell.2009.01.002
- Lee RC, Feinbaum RL, Ambros V. The *C. elegans* heterochronic gene lin-4 encodes small RNAs with antisense complementarity to lin-14. *Cell.* (1993) 75:843–54. doi: 10.1016/0092-8674(93)90529-Y
- Iwakawa HO, Tomari Y. The functions of microRNAs: mRNA decay and translational repression. *Trends Cell Biol.* (2015) 25:651–65. doi: 10.1016/j.tcb.2015.07.011
- Shi Y, Jin Y. MicroRNA in cell differentiation and development. *Sci China C Life Sci.* (2009) 52:205–11. doi: 10.1007/s11427-009-0040-5
- Mehta A, Baltimore D. MicroRNAs as regulatory elements in immune system logic. *Nat Rev Immunol.* (2016) 16:279–94. doi: 10.1038/nri.2016.40
- Su Z, Yang Z, Xu Y, Chen Y, Yu Q. MicroRNAs in apoptosis, autophagy and necroptosis. *Oncotarget.* (2015) 6:8474–90. doi: 10.18632/oncotarget.3523
- Landskroner-Eiger S, Moneke I, Sessa WC. miRNAs as modulators of angiogenesis. *Cold Spring Harb Perspect Med.* (2013) 3:a006643. doi: 10.1101/cshperspect.a006643
- Wang S, Claret FX, Wu W. MicroRNAs as therapeutic targets in nasopharyngeal carcinoma. *Front Oncol.* (2019) 9:756. doi: 10.3389/fonc.2019.00756
- Bandini E, Fanini F. MicroRNAs and androgen receptor: emerging players in breast cancer. *Front Genet.* (2019) 10:203. doi: 10.3389/fgene.2019.00203
- Fortunato O, Gasparini P, Boeri M, Sozzi G. Exo-miRNAs as a new tool for liquid biopsy in lung cancer. *Cancers.* (2019) 11:888. doi: 10.3390/cancers11060888
- Sasaki R, Osaki M, Okada F. MicroRNA-based diagnosis and treatment of metastatic human osteosarcoma. *Cancers.* (2019) 11:553. doi: 10.3390/cancers11040553
- Ladeiro Y, Couchy G, Balabaud C, Bioulac-Sage P, Pelletier L, Rebouissou S, et al. MicroRNA profiling in hepatocellular tumors is associated with clinical

## FUNDING

This project has been funded in whole or in part with Federal funds from the Frederick National Laboratory for Cancer Research, National Institutes of Health, under contract HHSN261200800001E. This research was supported in part by the Intramural Research Program of NIH, Frederick National Lab, Center for Cancer Research. The content of this publication does not necessarily reflect the views or policies of the Department of Health and Human Services, nor does mention of trade names, commercial products or organizations imply endorsement by the US Government. This research was supported in part by the China 13th 5-years science and technology major project on the prevention and treatment of major infectious diseases (2017ZX10202202).

## ACKNOWLEDGMENTS

We thank Brean Derrett, an NIH CRTA Postbaccalaureate Fellow, for technical assistance.

- features and oncogene/tumor suppressor gene mutations. *Hepatology.* (2008) 47:1955–63. doi: 10.1002/hep.22256
- WHO. *Global Hepatitis Report 2017*. Geneva: World Health Organization (2017). Available online at: <http://www.who.int/hepatitis/publications/global-hepatitis-report2017/en/> (accessed July 22, 2017).
  - Li W, Xie L, He X, Li J, Tu K, Wei L, et al. Diagnostic and prognostic implications of microRNAs in human hepatocellular carcinoma. *Int J Cancer.* (2008) 123:1616–22. doi: 10.1002/ijc.23693
  - Su H, Yang JR, Xu T, Huang J, Xu L, Yuan Y, et al. MicroRNA-101, down-regulated in hepatocellular carcinoma, promotes apoptosis and suppresses tumorigenicity. *Cancer Res.* (2009) 69:1135–42. doi: 10.1158/0008-5472.CAN-08-2886
  - Thurnherr T, Mah WC, Lei Z, Jin Y, Rozen SG, Lee CG. Differentially expressed miRNAs in hepatocellular carcinoma target genes in the genetic information processing and metabolism pathways. *Sci Rep.* (2016) 6:20065. doi: 10.1038/srep20065
  - Yoon SO, Chun SM, Han EH, Choi J, Jang SJ, Koh SA, et al. Deregulated expression of microRNA-221 with the potential for prognostic biomarkers in surgically resected hepatocellular carcinoma. *Hum Pathol.* (2011) 42:1391–400. doi: 10.1016/j.humpath.2010.12.010
  - He X, Li J, Guo W, Liu W, Yu J, Song W, et al. Targeting the microRNA-21/AP1 axis by 5-fluorouracil and pirarubicin in human hepatocellular carcinoma. *Oncotarget.* (2015) 6:2302–14. doi: 10.18632/oncotarget.2955
  - Li T, Yin J, Yuan L, Wang S, Yang L, Du X, et al. Downregulation of microRNA-139 is associated with hepatocellular carcinoma risk and short-term survival. *Oncol Rep.* (2014) 31:1699–706. doi: 10.3892/or.2014.3032
  - Gao P, Wong CC, Tung EK, Lee JM, Wong CM, Ng IO. Deregulation of microRNA expression occurs early and accumulates in early stages of HBV-associated multistep hepatocarcinogenesis. *J Hepatol.* (2011) 54:1177–84. doi: 10.1016/j.jhep.2010.09.023
  - Dundar HZ, Aksoy F, Aksoy SA, Tasar P, Ugras N, Tunca B, et al. Overexpression of miR-21 is associated with recurrence in patients with Hepatitis B virus-mediated hepatocellular carcinoma undergoing liver transplantation. *Transplant Proc.* (2019) 51:1157–61. doi: 10.1016/j.transproceed.2019.01.089
  - Chen F, Li XF, Fu DS, Huang JG, Yang SE. Clinical potential of miRNA-221 as a novel prognostic biomarker for hepatocellular carcinoma. *Cancer Biomark.* (2017) 18:209–14. doi: 10.3233/CBM-161671
  - Wong QW, Lung RW, Law PT, Lai PB, Chan KY, To KF, et al. MicroRNA-223 is commonly repressed in hepatocellular carcinoma and



- potentiates expression of Stathmin1. *Gastroenterology*. (2008) 135:257–69. doi: 10.1053/j.gastro.2008.04.003
27. Ji J, Shi J, Budhu A, Yu Z, Forgues M, Roessler S, et al. MicroRNA expression, survival, and response to interferon in liver cancer. *N Engl J Med*. (2009) 361:1437–47. doi: 10.1056/NEJMoa0901282
  28. Fu Y, Wei X, Tang C, Li J, Liu R, Shen A, et al. Circulating microRNA-101 as a potential biomarker for hepatitis B virus-related hepatocellular carcinoma. *Oncol Lett*. (2013) 6:1811–15. doi: 10.3892/ol.2013.1638
  29. Xie Y, Yao Q, Butt AM, Guo J, Tian Z, Bao X, et al. Expression profiling of serum microRNA-101 in HBV-associated chronic hepatitis, liver cirrhosis, hepatocellular carcinoma. *Cancer Biol Ther*. (2014) 15:1248–55. doi: 10.4161/cbt.29688
  30. Burchard J, Zhang C, Liu AM, Poon RT, Lee NP, Wong KF, et al. microRNA-122 as a regulator of mitochondrial metabolic gene network in hepatocellular carcinoma. *Mol Syst Biol*. (2010) 6:402. doi: 10.1038/msb.2010.58
  31. Wu Q, Liu HO, Liu YD, Liu WS, Pan D, Zhang WJ, et al. Decreased expression of hepatocyte nuclear factor 4alpha (Hnf4alpha)/microRNA-122 (miR-122) axis in hepatitis B virus-associated hepatocellular carcinoma enhances potential oncogenic GALNT10 protein activity. *J Biol Chem*. (2015) 290:1170–85. doi: 10.1074/jbc.M114.601203
  32. Budhu A, Jia HL, Forgues M, Liu CG, Goldstein D, Lam A, et al. Identification of metastasis-related microRNAs in hepatocellular carcinoma. *Hepatology*. (2008) 47:897–907. doi: 10.1002/hep.22160
  33. Xiao F, Zhang W, Zhou L, Xie H, Xing C, Ding S, et al. microRNA-200a is an independent prognostic factor of hepatocellular carcinoma and induces cell cycle arrest by targeting CDK6. *Oncol Rep*. (2013) 30:2203–10. doi: 10.3892/or.2013.2715
  34. Yang X, Wang J, Qu S, Zhang H, Ruan B, Gao Y, et al. MicroRNA-200a suppresses metastatic potential of side population cells in human hepatocellular carcinoma by decreasing ZEB2. *Oncotarget*. (2015) 6:7918–29. doi: 10.18632/oncotarget.3486
  35. Liu Y, Ren F, Rong M, Luo Y, Dang Y, Chen G. Association between underexpression of microRNA-203 and clinicopathological significance in hepatocellular carcinoma tissues. *Cancer Cell Int*. (2015) 15:62. doi: 10.1186/s12935-015-0214-0
  36. Connolly E, Melegari M, Landgraf P, Tchaikovskaya T, Tennant BC, Slagle BL, et al. Elevated expression of the miR-17-92 polycistron and miR-21 in hepatitis B virus-associated hepatocellular carcinoma contributes to the malignant phenotype. *Am J Pathol*. (2008) 173:856–64. doi: 10.2353/ajpath.2008.080096
  37. Valadi H, Ekstrom K, Bossios A, Sjostrand M, Lee JJ, Lotvall JO. Exosome-mediated transfer of mRNAs and microRNAs is a novel mechanism of genetic exchange between cells. *Nat Cell Biol*. (2007) 9:654–9. doi: 10.1038/ncb1596
  38. Chen X, Ba Y, Ma L, Cai X, Yin Y, Wang K, et al. Characterization of microRNAs in serum: a novel class of biomarkers for diagnosis of cancer and other diseases. *Cell Res*. (2008) 18:997–1006. doi: 10.1038/cr.2008.282
  39. Li LM, Hu ZB, Zhou ZX, Chen X, Liu FY, Zhang JF, et al. Serum microRNA profiles serve as novel biomarkers for HBV infection and diagnosis of HBV-positive hepatocarcinoma. *Cancer Res*. (2010) 70:9798–807. doi: 10.1158/0008-5472.CAN-10-1001
  40. Liu W, Hu J, Zhou K, Chen F, Wang Z, Liao B, et al. Serum exosomal miR-125b is a novel prognostic marker for hepatocellular carcinoma. *Oncotargets Ther*. (2017) 10:3843–51. doi: 10.2147/OTT.S140062
  41. Li J, Wang Y, Yu W, Chen J, Luo J. Expression of serum miR-221 in human hepatocellular carcinoma and its prognostic significance. *Biochem Biophys Res Commun*. (2011) 406:70–3. doi: 10.1016/j.bbrc.2011.01.111
  42. Xu J, Wu C, Che X, Wang L, Yu D, Zhang T, et al. Circulating microRNAs, miR-21, miR-122, and miR-223, in patients with hepatocellular carcinoma or chronic hepatitis. *Mol Carcinog*. (2011) 50:136–42. doi: 10.1002/mc.20712
  43. Qi P, Cheng SQ, Wang H, Li N, Chen YF, Gao CF. Serum microRNAs as biomarkers for hepatocellular carcinoma in Chinese patients with chronic hepatitis B virus infection. *PLoS ONE*. (2011) 6:e28486. doi: 10.1371/journal.pone.0028486
  44. Li L, Guo Z, Wang J, Mao Y, Gao Q. Serum miR-18a: a potential marker for hepatitis B virus-related hepatocellular carcinoma screening. *Dig Dis Sci*. (2012) 57:2910–6. doi: 10.1007/s10620-012-2317-y
  45. Zhou J, Yu L, Gao X, Hu J, Wang J, Dai Z, et al. Plasma microRNA panel to diagnose hepatitis B virus-related hepatocellular carcinoma. *J Clin Oncol*. (2011) 29:4781–8. doi: 10.1200/JCO.2011.38.2697
  46. Tan Y, Ge G, Pan T, Wen D, Chen L, Yu X, et al. A serum microRNA panel as potential biomarkers for hepatocellular carcinoma related with hepatitis B virus. *PLoS ONE*. (2014) 9:e107986. doi: 10.1371/journal.pone.0107986
  47. Wang X, Zhang J, Zhou L, Lu P, Zheng ZG, Sun W, et al. Significance of serum microRNA-21 in diagnosis of hepatocellular carcinoma (HCC): clinical analyses of patients and an HCC rat model. *Int J Clin Exp Pathol*. (2015) 8:1466–78. Available online at: <http://www.ijcep.com/files/ijcep0004608.pdf>
  48. Zhu HT, Liu RB, Liang YY, Hasan AME, Wang HY, Shao Q, et al. Serum microRNA profiles as diagnostic biomarkers for HBV-positive hepatocellular carcinoma. *Liver Int*. (2017) 37:888–96. doi: 10.1111/liv.13356
  49. Fornari F, Ferracin M, Trere D, Milazzo M, Marinelli S, Galassi M, et al. Circulating microRNAs, miR-939, miR-595, miR-519d and miR-494, identify cirrhotic patients with HCC. *PLoS ONE*. (2015) 10:e0141448. doi: 10.1371/journal.pone.0141448
  50. Peng Y, Croce CM. The role of MicroRNAs in human cancer. *Signal Transduct Target Ther*. (2016) 1:15004. doi: 10.1038/sigtrans.2015.4
  51. Coulouarn C, Factor VM, Andersen JB, Durkin ME, Thorgeirsson SS. Loss of miR-122 expression in liver cancer correlates with suppression of the hepatic phenotype and gain of metastatic properties. *Oncogene*. (2009) 28:3526–36. doi: 10.1038/ncr.2009.211
  52. Bandiera S, Pfeffer S, Baumert TF, Zeisel MB. miR-122—a key factor and therapeutic target in liver disease. *J Hepatol*. (2015) 62:448–57. doi: 10.1016/j.jhep.2014.10.004
  53. Fan CG, Wang CM, Tian C, Wang Y, Li L, Sun WS, et al. miR-122 inhibits viral replication and cell proliferation in hepatitis B virus-related hepatocellular carcinoma and targets NDRG3. *Oncol Rep*. (2011) 26:1281–6. doi: 10.3892/or.2011.1375
  54. Wang S, Qiu L, Yan X, Jin W, Wang Y, Chen L, et al. Loss of microRNA 122 expression in patients with hepatitis B enhances hepatitis B virus replication through cyclin G(1)-modulated P53 activity. *Hepatology*. (2012) 55:730–41. doi: 10.1002/hep.24809
  55. Tsai WC, Hsu PW, Lai TC, Chau GY, Lin CW, Chen CM, et al. MicroRNA-122, a tumor suppressor microRNA that regulates intrahepatic metastasis of hepatocellular carcinoma. *Hepatology*. (2009) 49:1571–82. doi: 10.1002/hep.22806
  56. Bai S, Nasser MW, Wang B, Hsu SH, Datta J, Kutay H, et al. MicroRNA-122 inhibits tumorigenic properties of hepatocellular carcinoma cells and sensitizes these cells to sorafenib. *J Biol Chem*. (2009) 284:32015–27. doi: 10.1074/jbc.M109.016774
  57. Li C, Wang Y, Wang S, Wu B, Hao J, Fan H, et al. Hepatitis B virus mRNA-mediated miR-122 inhibition upregulates PTTG1-binding protein, which promotes hepatocellular carcinoma tumor growth and cell invasion. *J Virol*. (2013) 87:2193–205. doi: 10.1128/JVI.02831-12
  58. Lin CJ, Gong HY, Tseng HC, Wang WL, Wu JL. miR-122 targets an anti-apoptotic gene, Bcl-w, in human hepatocellular carcinoma cell lines. *Biochem Biophys Res Commun*. (2008) 375:315–20. doi: 10.1016/j.bbrc.2008.07.154
  59. Luna JM, Barajas JM, Teng KY, Sun HL, Moore MJ, Rice CM, et al. Argonaute CLIP defines a deregulated miR-122-bound transcriptome that correlates with patient survival in human liver cancer. *Mol Cell*. (2017) 67:400–10.e7. doi: 10.1016/j.molcel.2017.06.025
  60. Barajas JM, Reyes R, Guerrero MJ, Jacob ST, Motiwala T, Ghoshal K. The role of miR-122 in the dysregulation of glucose-6-phosphate dehydrogenase (G6PD) expression in hepatocellular cancer. *Sci Rep*. (2018) 8:9105. doi: 10.1038/s41598-018-27358-5
  61. Meng F, Henson R, Wehbe-Janek H, Ghoshal K, Jacob ST, Patel T. MicroRNA-21 regulates expression of the PTEN tumor suppressor gene in human hepatocellular cancer. *Gastroenterology*. (2007) 133:647–58. doi: 10.1053/j.gastro.2007.05.022
  62. Asangani IA, Rasheed SA, Nikolova DA, Leupold JH, Colburn NH, Post S, et al. MicroRNA-21 (miR-21) post-transcriptionally downregulates tumor suppressor Pdc4 and stimulates invasion, intravasation and metastasis in colorectal cancer. *Oncogene*. (2008) 27:2128–36. doi: 10.1038/sj.onc.1210856
  63. Wagenaar TR, Zabudoff S, Ahn SM, Allerson C, Arlt H, Baffa R, et al. Anti-miR-21 suppresses hepatocellular carcinoma growth via broad

- transcriptional network deregulation. *Mol Cancer Res.* (2015) 13:1009–21. doi: 10.1158/1541-7786.MCR-14-0703
64. Liu WH, Yeh SH, Lu CC, Yu SL, Chen HY, Lin CY, et al. MicroRNA-18a prevents estrogen receptor- $\alpha$  expression, promoting proliferation of hepatocellular carcinoma cells. *Gastroenterology.* (2009) 136:683–93. doi: 10.1053/j.gastro.2008.10.029
  65. Liu X, Zhang Y, Wang P, Wang H, Su H, Zhou X, et al. HBx protein-induced downregulation of microRNA-18a is responsible for upregulation of connective tissue growth factor in hbv infection-associated hepatocarcinoma. *Med Sci Monit.* (2016) 22:2492–500. doi: 10.12659/MSM.895943
  66. Chen JJ, Tang YS, Huang SF, Ai JG, Wang HX, Zhang LP. HBx protein-induced upregulation of microRNA-221 promotes aberrant proliferation in HBV-related hepatocellular carcinoma by targeting estrogen receptor- $\alpha$ . *Oncol Rep.* (2015) 33:792–8. doi: 10.3892/or.2014.3647
  67. Rong M, Chen G, Dang Y. Increased miR-221 expression in hepatocellular carcinoma tissues and its role in enhancing cell growth and inhibiting apoptosis *in vitro*. *BMC Cancer.* (2013) 13:21. doi: 10.1186/1471-2407-13-21
  68. Huang S, Zhou D, Li YX, Ming ZY, Li KZ, Wu GB, et al. *In vivo* and *in vitro* effects of microRNA-221 on hepatocellular carcinoma development and progression through the JAK-STAT3 signaling pathway by targeting SOCS3. *J Cell Physiol.* (2019) 234:3500–14. doi: 10.1002/jcp.26863
  69. Bandopadhyay M, Banerjee A, Sarkar N, Panigrahi R, Datta S, Pal A, et al. Tumor suppressor micro RNA miR-145 and onco micro RNAs miR-21 and miR-222 expressions are differentially modulated by hepatitis B virus X protein in malignant hepatocytes. *BMC Cancer.* (2014) 14:721. doi: 10.1186/1471-2407-14-721
  70. Yang YF, Wang F, Xiao JJ, Song Y, Zhao YY, Cao Y, et al. MiR-222 overexpression promotes proliferation of human hepatocellular carcinoma HepG2 cells by downregulating p27. *Int J Clin Exp Med.* (2014) 7:893–902. Available online at: <http://www.ijcem.com/files/ijcem0000090.pdf>
  71. Wong QW, Ching AK, Chan AW, Choy KW, To KF, Lai PB, et al. MiR-222 overexpression confers cell migratory advantages in hepatocellular carcinoma through enhancing AKT signaling. *Clin Cancer Res.* (2010) 16:867–75. doi: 10.1158/1078-0432.CCR-09-1840
  72. Yang HI, Yeh SH, Chen PJ, Iloeje UH, Jen CL, Su J, et al. Associations between hepatitis B virus genotype and mutants and the risk of hepatocellular carcinoma. *J Natl Cancer Inst.* (2008) 100:1134–43. doi: 10.1093/jnci/djn243
  73. Sartorius K, Sartorius B, Kramvis A, Singh E, Turchinovich A, Burwinkel B, et al. Circulating microRNAs as a diagnostic tool for hepatocellular carcinoma in a hyper endemic HIV setting, KwaZulu-natal, South Africa: a case control study protocol focusing on viral etiology. *BMC Cancer.* (2017) 17:894. doi: 10.1186/s12885-017-3915-z
  74. Spaniel C, Honda M, Selitsky SR, Yamane D, Shimakami T, Kaneko S, et al. microRNA-122 abundance in hepatocellular carcinoma and non-tumor liver tissue from Japanese patients with persistent HCV versus HBV infection. *PLoS ONE.* (2013) 8:e76867. doi: 10.1371/journal.pone.0076867
  75. Sheng Y, Li J, Zou C, Wang S, Cao Y, Zhang J, et al. Downregulation of miR-101-3p by hepatitis B virus promotes proliferation and migration of hepatocellular carcinoma cells by targeting Rab5a. *Arch Virol.* (2014) 159:2397–410. doi: 10.1007/s00705-014-2084-5
  76. Xu X, Fan Z, Kang L, Han J, Jiang C, Zheng X, et al. Hepatitis B virus X protein represses miRNA-148a to enhance tumorigenesis. *J Clin Invest.* (2013) 123:630–45. doi: 10.1172/JCI64265
  77. Lamontagne J. Hepatitis B virus and microRNAs: complex interactions affecting hepatitis B virus replication and hepatitis B virus-associated diseases. *World J Gastroenterol.* (2015) 21:7375. doi: 10.3748/wjg.v21.i24.7375
  78. Potenza N, Papa U, Mosca N, Zerbini F, Nobile V, Russo A. Human microRNA hsa-miR-125a-5p interferes with expression of hepatitis B virus surface antigen. *Nucleic Acids Res.* (2011) 39:5157–63. doi: 10.1093/nar/gkr067
  79. Yang X, Li H, Sun H, Fan H, Hu Y, Liu M, et al. Hepatitis B virus-encoded microRNA controls viral replication. *J Virol.* (2017) 91:e01919–16. doi: 10.1128/JVI.01919-16
  80. Yao L, Zhou Y, Sui Z, Zhang Y, Liu Y, Xie H, et al. HBV-encoded miR-2 functions as an oncogene by downregulating TRIM35 but upregulating RAN in liver cancer cells. *EBioMedicine.* (2019) 48:117–29. doi: 10.2139/ssrn.3365052
  81. Zhang X, Hou J, Lu M. Regulation of hepatitis B virus replication by epigenetic mechanisms and microRNAs. *Front Genet.* (2013) 4:202. doi: 10.3389/fgene.2013.00202
  82. Liu WH, Yeh SH, Chen PJ. Role of microRNAs in hepatitis B virus replication and pathogenesis. *Biochim Biophys Acta.* (2011) 1809:678–85. doi: 10.1016/j.bbagr.2011.04.008
  83. Sagnelli E, Potenza N, Onorato L, Sagnelli C, Coppola N, Russo A. MicroRNAs in hepatitis B virus-related chronic liver diseases and hepatocellular carcinoma. *World J Hepatol.* (2018) 10:558–70. doi: 10.4254/wjh.v10.i9.558
  84. Zhou G, Wilson G, George J, Qiao L. Targeting cancer stem cells as a therapeutic approach in liver cancer. *Curr Gene Ther.* (2015) 15:161–70. doi: 10.2174/1566523214666141224095938
  85. Qiu L, Li H, Fu S, Chen X, Lu L. Surface markers of liver cancer stem cells and innovative targeted-therapy strategies for HCC. *Oncol Lett.* (2018) 15:2039–48. doi: 10.3892/ol.2017.7568
  86. Ma S, Chan KW, Hu L, Lee TK, Wo JY, Ng IO, et al. Identification and characterization of tumorigenic liver cancer stem/progenitor cells. *Gastroenterology.* (2007) 132:2542–56. doi: 10.1053/j.gastro.2007.04.025
  87. Lou W, Liu J, Gao Y, Zhong G, Ding B, Xu L, et al. MicroRNA regulation of liver cancer stem cells. *Am J Cancer Res.* (2018) 8:1126–41. Available online at: <http://www.ajcr.us/files/ajcr0079739.pdf>
  88. Wang C, Wang MD, Cheng P, Huang H, Dong W, Zhang WW, et al. Hepatitis B virus X protein promotes the stem-like properties of OV6(+) cancer cells in hepatocellular carcinoma. *Cell Death Dis.* (2017) 8:e2560. doi: 10.1038/cddis.2016.493
  89. Gu Y, Wei X, Sun Y, Gao H, Zheng X, Wong LL, et al. miR-192-5p silencing by genetic aberrations is a key event in hepatocellular carcinomas with cancer stem cell features. *Cancer Res.* (2019) 79:941–53. doi: 10.1158/0008-5472.CAN-18-1675
  90. Arzumanyan A, Friedman T, Ng IO, Clayton MM, Lian Z, Feitelson MA. Does the hepatitis B antigen HBx promote the appearance of liver cancer stem cells? *Cancer Res.* (2011) 71:3701–8. doi: 10.1158/0008-5472.CAN-10-3951
  91. Ji J, Zheng X, Forgues M, Yamashita T, Wauthier EL, Reid LM, et al. Identification of microRNAs specific for epithelial cell adhesion molecule-positive tumor cells in hepatocellular carcinoma. *Hepatology.* (2015) 62:829–40. doi: 10.1002/hep.27886
  92. Ji J, Yamashita T, Budhu A, Forgues M, Jia HL, Li C, et al. Identification of microRNA-181 by genome-wide screening as a critical player in EpCAM-positive hepatic cancer stem cells. *Hepatology.* (2009) 50:472–80. doi: 10.1002/hep.22989
  93. Boix L, Lopez-Oliva JM, Rhodes AC, Bruix J. Restoring miR122 in human stem-like hepatocarcinoma cells, prompts tumor dormancy through Smad-independent TGF-beta pathway. *Oncotarget.* (2016) 7:71309–29. doi: 10.18632/oncotarget.11885
  94. Nasr MA, Salah RA, Abd Elkodous M, Elshenawy SE, El-Badri N. Dysregulated microRNA fingerprints and methylation patterns in hepatocellular carcinoma, cancer stem cells, and mesenchymal stem cells. *Front Cell Dev Biol.* (2019) 7:229. doi: 10.3389/fcell.2019.00229
  95. Alpini G, Glaser SS, Zhang JP, Francis H, Han Y, Gong J, et al. Regulation of placenta growth factor by microRNA-125b in hepatocellular cancer. *J Hepatol.* (2011) 55:1339–45. doi: 10.1016/j.jhep.2011.04.015
  96. Buurman R, Gurlevik E, Schaffer V, Eilers M, Sandbothe M, Kreipe H, et al. Histone deacetylases activate hepatocyte growth factor signaling by repressing microRNA-449 in hepatocellular carcinoma cells. *Gastroenterology.* (2012) 143:811–20.e15. doi: 10.1053/j.gastro.2012.05.033
  97. Hou J, Lin L, Zhou W, Wang Z, Ding G, Dong Q, et al. Identification of miRNomes in human liver and hepatocellular carcinoma reveals miR-199a/b-3p as therapeutic target for hepatocellular carcinoma. *Cancer Cell.* (2011) 19:232–43. doi: 10.1016/j.ccr.2011.01.001
  98. Kim HS, Shen Q, Nam SW. Histone deacetylases and their regulatory microRNAs in hepatocarcinogenesis. *J Korean Med Sci.* (2015) 30:1375–80. doi: 10.3346/jkms.2015.30.10.1375
  99. Saito Y, Saito H. Role of CTCF in the regulation of microRNA expression. *Front Genet.* (2012) 3:186. doi: 10.3389/fgene.2012.00186

100. Soto-Reyes E, Gonzalez-Barrios R, Cisneros-Soberanis F, Herrera-Goepfert R, Perez V, Cantu D, et al. Disruption of CTCF at the miR-125b1 locus in gynecological cancers. *BMC Cancer*. (2012) 12:40. doi: 10.1186/1471-2407-12-40
101. Qiu L, Xu H, Ji M, Shang D, Lu Z, Wu Y, et al. Circular RNAs in hepatocellular carcinoma: biomarkers, functions and mechanisms. *Life Sci*. (2019) 231:116660. doi: 10.1016/j.lfs.2019.116660
102. Zheng Q, Bao C, Guo W, Li S, Chen J, Chen B, et al. Circular RNA profiling reveals an abundant circHIPK3 that regulates cell growth by sponging multiple miRNAs. *Nat Commun*. (2016) 7:11215. doi: 10.1038/ncomms11215
103. Zhang PF, Wei CY, Huang XY, Peng R, Yang X, Lu JC, et al. Circular RNA circTRIM32-12 acts as the sponge of microRNA-191 to suppress hepatocellular carcinoma progression. *Mol Cancer*. (2019) 18:105. doi: 10.1186/s12943-019-1031-1
104. Beg MS, Brenner AJ, Sachdev J, Borad M, Kang YK, Stoudemire J, et al. Phase I study of MRX34, a liposomal miR-34a mimic, administered twice weekly in patients with advanced solid tumors. *Invest New Drugs*. (2017) 35:180–8. doi: 10.1007/s10637-016-0407-y
105. Xu Q, Zhang M, Tu J, Pang L, Cai W, Liu X. MicroRNA-122 affects cell aggressiveness and apoptosis by targeting PKM2 in human hepatocellular carcinoma. *Oncol Rep*. (2015) 34:2054–64. doi: 10.3892/or.2015.4175
106. Jin Y, Wang J, Han J, Luo D, Sun Z. MiR-122 inhibits epithelial-mesenchymal transition in hepatocellular carcinoma by targeting Snail1 and Snail2 and suppressing WNT/beta-cadherin signaling pathway. *Exp Cell Res*. (2017) 360:210–7. doi: 10.1016/j.yexcr.2017.09.010
107. Fornari F, Gramantieri L, Giovannini C, Veronese A, Ferracin M, Sabbioni S, et al. MiR-122/cyclin G1 interaction modulates p53 activity and affects doxorubicin sensitivity of human hepatocarcinoma cells. *Cancer Res*. (2009) 69:5761–7. doi: 10.1158/0008-5472.CAN-08-4797
108. Wang F, Li L, Piontek K, Sakaguchi M, Selaru FM. Exosome miR-335 as a novel therapeutic strategy in hepatocellular carcinoma. *Hepatology*. (2018) 67:940–54. doi: 10.1002/hep.29586
109. He J, Zhao K, Zheng L, Xu Z, Gong W, Chen S, et al. Upregulation of microRNA-122 by farnesoid X receptor suppresses the growth of hepatocellular carcinoma cells. *Mol Cancer*. (2015) 14:163. doi: 10.1186/s12943-015-0427-9
110. Sun C, Lan P, Han Q, Huang M, Zhang Z, Xu G, et al. Oncofetal gene SALL4 reactivation by hepatitis B virus counteracts miR-200c in PD-L1-induced T cell exhaustion. *Nat Commun*. (2018) 9:1241. doi: 10.1038/s41467-018-03584-3
111. Tang S, Tan G, Jiang X, Han P, Zhai B, Dong X, et al. An artificial lncRNA targeting multiple miRNAs overcomes sorafenib resistance in hepatocellular carcinoma cells. *Oncotarget*. (2016) 7:73257–69. doi: 10.18632/oncotarget.12304
112. Xu Y, Xia F, Ma L, Shan J, Shen J, Yang Z, et al. MicroRNA-122 sensitizes HCC cancer cells to adriamycin and vincristine through modulating expression of MDR and inducing cell cycle arrest. *Cancer Lett*. (2011) 310:160–9. doi: 10.1016/j.canlet.2011.06.027
113. Pan C, Wang X, Shi K, Zheng Y, Li J, Chen Y, et al. MiR-122 reverses the doxorubicin-resistance in hepatocellular carcinoma cells through regulating the tumor metabolism. *PLoS ONE*. (2016) 11:e0152090. doi: 10.1371/journal.pone.0152090
114. Xu L, Beckebaum S, Jacob S, Wu G, Kaiser GM, Radtke A, et al. MicroRNA-101 inhibits human hepatocellular carcinoma progression through EZH2 downregulation and increased cytostatic drug sensitivity. *J Hepatol*. (2014) 60:590–8. doi: 10.1016/j.jhep.2013.10.028
115. Hanna J, Hossain GS, Kocerha J. The potential for microRNA therapeutics and clinical research. *Front Genet*. (2019) 10:478. doi: 10.3389/fgene.2019.00478
116. Liu AM, Yao TJ, Wang W, Wong KF, Lee NP, Fan ST, et al. Circulating miR-15b and miR-130b in serum as potential markers for detecting hepatocellular carcinoma: a retrospective cohort study. *BMJ Open*. (2012) 2:e000825. doi: 10.1136/bmjopen-2012-000825
117. Lin XJ, Chong Y, Guo ZW, Xie C, Yang XJ, Zhang Q, et al. A serum microRNA classifier for early detection of hepatocellular carcinoma: a multicentre, retrospective, longitudinal biomarker identification study with a nested case-control study. *Lancet Oncol*. (2015) 16:804–15. doi: 10.1016/S1470-2045(15)00048-0
118. Wen Y, Han J, Chen J, Dong J, Xia Y, Liu J, et al. Plasma miRNAs as early biomarkers for detecting hepatocellular carcinoma. *Int J Cancer*. (2015) 137:1679–90. doi: 10.1002/ijc.29544
119. Huang JT, Liu SM, Ma H, Yang Y, Zhang X, Sun H, et al. Systematic review and meta-analysis: circulating miRNAs for diagnosis of hepatocellular Carcinoma. *J Cell Physiol*. (2016) 231:328–35. doi: 10.1002/jcp.25135
120. Xu X, Tao Y, Shan L, Chen R, Jiang H, Qian Z, et al. The role of microRNAs in hepatocellular Carcinoma. *J Cancer*. (2018) 9:3557–69. doi: 10.7150/jca.26350
121. Yang B, Xiong WY, Hou HJ, Xu Q, Cai XL, Zeng TX, et al. Exosomal miRNAs as biomarkers of cancer: a meta-analysis. *Clin Lab*. (2019) 65:181011. doi: 10.7754/Clin.Lab.2018.181011
122. Wang H, Hou L, Li A, Duan Y, Gao H, Song X. Expression of serum exosomal microRNA-21 in human hepatocellular carcinoma. *Biomed Res Int*. (2014) 2014:864894. doi: 10.1155/2014/864894
123. Sohn W, Kim J, Kang SH, Yang SR, Cho JY, Cho HC, et al. Serum exosomal microRNAs as novel biomarkers for hepatocellular carcinoma. *Exp Mol Med*. (2015) 47:e184. doi: 10.1038/emmm.2015.68
124. Tomimaru Y, Eguchi H, Nagano H, Wada H, Kobayashi S, Marubashi S, et al. Circulating microRNA-21 as a novel biomarker for hepatocellular carcinoma. *J Hepatol*. (2012) 56:167–75. doi: 10.1016/j.jhep.2011.04.026
125. Liu M, Liu J, Wang L, Wu H, Zhou C, Zhu H, et al. Association of serum microRNA expression in hepatocellular carcinomas treated with transarterial chemoembolization and patient survival. *PLoS ONE*. (2014) 9:e109347. doi: 10.1371/journal.pone.0109347
126. Ng KT, Lo CM, Wong N, Li CX, Qi X, Liu XB, et al. Early-phase circulating miRNAs predict tumor recurrence and survival of hepatocellular carcinoma patients after liver transplantation. *Oncotarget*. (2016) 7:19824–39. doi: 10.18632/oncotarget.7627
127. Cho HJ, Kim SS, Nam JS, Kim JK, Lee JH, Kim B, et al. Low levels of circulating microRNA-26a/29a as poor prognostic markers in patients with hepatocellular carcinoma who underwent curative treatment. *Clin Res Hepatol Gastroenterol*. (2017) 41:181–9. doi: 10.1016/j.clinre.2016.09.011
128. Shi KQ, Lin Z, Chen XJ, Song M, Wang YQ, Cai YJ, et al. Hepatocellular carcinoma associated microRNA expression signature: integrated bioinformatics analysis, experimental validation and clinical significance. *Oncotarget*. (2015) 6:25093–108. doi: 10.18632/oncotarget.4437
129. Wei R, Huang GL, Zhang MY, Li BK, Zhang HZ, Shi M, et al. Clinical significance and prognostic value of microRNA expression signatures in hepatocellular carcinoma. *Clin Cancer Res*. (2013) 19:4780–91. doi: 10.1158/1078-0432.CCR-12-2728
130. Chen HY, Han ZB, Fan JW, Xia J, Wu JY, Qiu GQ, et al. miR-203 expression predicts outcome after liver transplantation for hepatocellular carcinoma in cirrhotic liver. *Med Oncol*. (2012) 29:1859–65. doi: 10.1007/s12032-011-0031-9
131. Wang WY, Zhang HF, Wang L, Ma YP, Gao F, Zhang SJ, et al. miR-21 expression predicts prognosis in hepatocellular carcinoma. *Clin Res Hepatol Gastroenterol*. (2014) 38:715–9. doi: 10.1016/j.clinre.2014.07.001
132. Cho HJ, Kim JK, Nam JS, Wang HJ, Lee JH, Kim BW, et al. High circulating microRNA-122 expression is a poor prognostic marker in patients with hepatitis B virus-related hepatocellular carcinoma who undergo radiofrequency ablation. *Clin Biochem*. (2015) 48:1073–8. doi: 10.1016/j.clinbiochem.2015.06.019
133. Kim SS, Nam JS, Cho HJ, Won JH, Kim JW, Ji JH, et al. Plasma microRNA-122 as a predictive marker for treatment response following transarterial chemoembolization in patients with hepatocellular carcinoma. *J Gastroenterol Hepatol*. (2017) 32:199–207. doi: 10.1111/jgh.13448
134. American Association for the Study of Liver Diseases and Infectious Diseases Society of America. *HCV Guidance: Recommendations for Testing, Managing, and Treating Hepatitis C*. Alexandria, VA: AASLD-IDS (2020). Available online at: <http://www.hcvguidelines.org> (accessed January 2, 2020).
135. Chinese Society of Hepatology and Chinese Society of Infectious Diseases, and Chinese Medical Association. Guidelines for the prevention and treatment of hepatitis C (2019 version). *Zhonghua Gan Zang Bing Za Zhi*. (2019) 27:962–79. doi: 10.3760/cma.j.issn.1007-3418.2019.12.008

136. Morita K, Shirabe K, Taketomi A, Soejima Y, Yoshizumi T, Uchiyama H, et al. Relevance of microRNA-18a and microRNA-199a-5p to hepatocellular carcinoma recurrence after living donor liver transplantation. *Liver Transpl.* (2016) 22:665–76. doi: 10.1002/lt.24400
137. El-Garem H, Ammer A, Shehab H, Shaker O, Anwer M, El-Akel W, et al. Circulating microRNA, miR-122 and miR-221 signature in Egyptian patients with chronic hepatitis C related hepatocellular carcinoma. *World J Hepatol.* (2014) 6:818–24. doi: 10.4254/wjh.v6.i11.818
138. Diaz G, Melis M, Tice A, Kleiner DE, Mishra L, Zamboni F, et al. Identification of microRNAs specifically expressed in hepatitis C virus-associated hepatocellular carcinoma. *Int J Cancer.* (2013) 133:816–24. doi: 10.1002/ijc.28075
139. Murakami Y, Yasuda T, Saigo K, Urashima T, Toyoda H, Okanou T, et al. Comprehensive analysis of microRNA expression patterns in hepatocellular carcinoma and non-tumorous tissues. *Oncogene.* (2006) 25:2537–45. doi: 10.1038/sj.onc.1209283
140. Fittipaldi S, Vasuri F, Bonora S, Degiovanni A, Santandrea G, Cucchetti A, et al. miRNA signature of hepatocellular carcinoma vascularization: how the controls can influence the signature. *Dig Dis Sci.* (2017) 62:2397–407. doi: 10.1007/s10620-017-4654-3
141. Karakatsanis A, Papaconstantinou I, Gazouli M, Lyberopoulou A, Polymeneas G, Voros D. Expression of microRNAs, miR-21, miR-31, miR-122, miR-145, miR-146a, miR-200c, miR-221, miR-222, and miR-223 in patients with hepatocellular carcinoma or intrahepatic cholangiocarcinoma and its prognostic significance. *Mol Carcinog.* (2013) 52:297–303. doi: 10.1002/mc.21864
142. Wang G, Dong F, Xu Z, Sharma S, Hu X, Chen D, et al. MicroRNA profile in HBV-induced infection and hepatocellular carcinoma. *BMC Cancer.* (2017) 17:805. doi: 10.1186/s12885-017-3816-1
143. Schopman NC, Heynen S, Haasnoot J, Berkhout B. A miRNA-tRNA mix-up: tRNA origin of proposed miRNA. *RNA Biol.* (2010) 7:573–6. doi: 10.4161/rna.7.5.13141
144. Hansen TB, Bramsen JB, Kjems J. Re-inspection of small RNA sequence datasets reveals several novel human miRNA genes. *PLoS ONE.* (2010) 5:e10961. doi: 10.1371/journal.pone.0010961
145. Zhen Y, Xinghui Z, Chao W, Yi Z, Jinwen C, Ruifang G, et al. Several microRNAs could predict survival in patients with hepatitis B-related liver cancer. *Sci Rep.* (2017) 7:45195. doi: 10.1038/srep45195
146. Mei Y, You Y, Xia J, Gong JP, Wang YB. Identifying differentially expressed microRNAs between cirrhotic and non-cirrhotic hepatocellular carcinoma and exploring their functions using bioinformatic analysis. *Cell Physiol Biochem.* (2018) 48:1443–56. doi: 10.1159/000492254
147. Zhang YC, Xu Z, Zhang TF, Wang YL. Circulating microRNAs as diagnostic and prognostic tools for hepatocellular carcinoma. *World J Gastroenterol.* (2015) 21:9853–62. doi: 10.3748/wjg.v21.i34.9853

**Conflict of Interest:** The authors declare that the research was conducted in the absence of any commercial or financial relationships that could be construed as a potential conflict of interest.

Copyright © 2020 Xu, An, Winkler and Yu. This is an open-access article distributed under the terms of the Creative Commons Attribution License (CC BY). The use, distribution or reproduction in other forums is permitted, provided the original author(s) and the copyright owner(s) are credited and that the original publication in this journal is cited, in accordance with accepted academic practice. No use, distribution or reproduction is permitted which does not comply with these terms.





# New Blood Biomarkers for the Diagnosis of AFP-Negative Hepatocellular Carcinoma

Ting Wang and Kun-He Zhang\*

Department of Gastroenterology, Jiangxi Institute of Gastroenterology & Hepatology, The First Affiliated Hospital of Nanchang University, Nanchang, China

## OPEN ACCESS

### Edited by:

Zhaohui Huang,  
Affiliated Hospital of Jiangnan  
University, China

### Reviewed by:

Jian Tu,  
Guilin Medical University, China  
Mengsen Li,  
Hainan Medical University, China

### \*Correspondence:

Kun-He Zhang  
khzhang@ncu.edu.cn

### Specialty section:

This article was submitted to  
Gastrointestinal Cancers,  
a section of the journal  
Frontiers in Oncology

Received: 11 March 2020

Accepted: 24 June 2020

Published: 14 August 2020

### Citation:

Wang T and Zhang K-H (2020) New  
Blood Biomarkers for the Diagnosis of  
AFP-Negative Hepatocellular  
Carcinoma. *Front. Oncol.* 10:1316.  
doi: 10.3389/fonc.2020.01316

An early diagnosis of hepatocellular carcinoma (HCC) followed by effective treatment is currently critical for improving the prognosis and reducing the associated economic burden. Alpha-fetoprotein (AFP) is the most widely used biomarker for HCC diagnosis. Based on elevated serum AFP levels as well as typical imaging features, AFP-positive HCC (APHC) can be easily diagnosed, but AFP-negative HCC (ANHC) is not easily detected due to lack of ideal biomarkers and thus mainly reliance on imaging. Imaging for the diagnosis of ANHC is probably insufficient in sensitivity and/or specificity because most ANHC tumors are small and early-stage HCC, and it is involved in sophisticated techniques and high costs. Moreover, ANHC accounts for nearly half of HCC and exhibits a better prognosis compared with APHC. Therefore, the diagnosis of ANHC in clinical practice has been a critical issue for the early treatment and prognosis improvement of HCC. In recent years, tremendous efforts have been made to discover new biomarkers complementary to AFP for HCC diagnosis. In this review, we systematically review and discuss the recent advances of blood biomarkers for HCC diagnosis, including DNA biomarkers, RNA biomarkers, protein biomarkers, and conventional laboratory metrics, focusing on their diagnostic evaluation alone and in combination, in particular on their diagnostic performance for ANHC.

**Keywords:** hepatocellular carcinoma, AFP-negative, diagnosis, blood biomarkers, DNA, RNA, protein

## INTRODUCTION

According to GOLOBOCAN 2018 (1), liver cancer is estimated to be the sixth most commonly diagnosed cancer and the fourth leading cause of cancer deaths globally, with 841,080 new cases and 781,631 deaths, and hepatocellular carcinoma (HCC) is the dominant histological type of liver cancer (accounting for ~75–85% of all liver cancer cases), with the highest prevalence in Asian and Eastern African countries. In addition to clinical burden, HCC also poses substantial and increasing economic burden due to healthcare expenditures; the annual cost of HCC in the USA has been estimated at more than \$450 million (2). The early diagnosis and effective treatment of HCC could impact both clinical outcomes and the economic burden of HCC.

Serum alpha-fetoprotein (AFP) is by far the most widely used biomarker for HCC screening, early diagnosis, and evaluation of therapeutic efficacy and prognosis (3). However, not all HCCs secrete AFP, and AFP may be elevated in cirrhosis or hepatitis cases. A systematic review showed that the sensitivity of AFP was 41–65%, with a specificity of 80–94% when using the commonly used positive cutoff value (AFP level  $\geq 20$  ng/mL) for HCC (4). A large-scale prospective multicenter

study showed that the positive rates of AFP ( $\geq 11$  ng/ml as the cutoff value) were 46% (616/1338) for all HCC and 23.4% (150/641) for small HCC ( $< 2$  cm) (5). Another large multicentric survey showed that AFP-negative ( $< 20$  ng/mL) rates were found in 52% (261/502) patients with small HCCs ( $< 3$  cm), in 53.5% (51/95) patients at TNM stage I, in 48% (314/656) patients with Okuda stage 1, and in some advanced HCC patients [41.5% (24/58) at TNM stage IV and 28% (17/61) at Okuda stage 3] (6), indicating that nearly a half of HCC patients are AFP-negative, especially early and small HCCs.

The diagnosis of HCC is easy when significantly increased serum AFP levels and definitive imaging features are present. However, AFP-negative hepatic cancer (ANHC) is not as easily diagnosed, as most ANHCs are early and small HCCs, often without typical imaging characteristics. Liver nodular lesions may also have HCC-like imaging findings, making ANHC patients easily misdiagnosed (7). Due to a range of influential factors on ultrasonographic diagnosis, a systematic review, and economic analysis suggested that ultrasound should not be routinely offered to patients with ANHC (8). However, the diagnosis of ANHC is important in clinical practice, because ANHC patients have a better prognosis compared with those with AFP-positive HCC (APHC) (6, 9, 10). An et al. (11) found that the 1-, 3-, and 5-year recurrence-free survival rates were 78.1, 57.5, and 40.6% in the AFP-negative group and 61.8, 37.7, and 31.4% in the AFP-positive group, respectively, while the corresponding overall survival rates were 94.4, 83.8, and 62.3% in the AFP-negative group and 87.2, 60.0, and 36.7% in the AFP-positive group, respectively. Thus, the diagnosis of ANHC is important for the improvement of prognosis in HCC patients.

Imaging techniques are useful for HCC diagnosis. Digital subtraction angiography, dynamic contrast-enhanced magnetic resonance imaging, contrast-enhanced ultrasound, and positron-emission tomography-computed tomography were found with sensitivity of 88.2, 93.9, 88.9, and 88.9%, respectively, for the diagnosis of AFP-negative small hepatic lesions (12). However, these tools are expensive and unsuitable for screening or for a first-line diagnosis of HCC. Blood biomarkers are non-invasive, safe, convenient, economic, and easy-to-repeat tools for tumor diagnosis, and compared with imaging, biomarkers in blood can be measured repeatedly with accuracy and with a relatively rapid clinical turnaround time to monitor disease progression. In this review, we describe the clinical characteristics of ANHC and systematically review and discuss recent advances in the use of blood biomarkers for HCC diagnosis, including DNA biomarkers, RNA biomarkers, protein biomarkers and conventional laboratory metrics, and their diagnostic evaluation alone and in combination, focusing on their diagnostic performance for ANHC.

## CHARACTERISTICS OF ANHC

The symptoms of ANHC are generally mild and non-specific, and ANHC has better clinicopathological features compared with APHC. Compared with ANHC patients, APHC cases were more likely to feature a higher female-to-male ratio, a younger age,

higher HBV-positive rate, larger tumor diameter, more cirrhosis nodules, more liver capsule invasions, higher tumor multiplicity, more carcinoma cell emboli, lower differentiation grade, later BCLC stage and TNM stage, poor Edmondson–Steiner grade, poor liver function, higher short-term recurrence, and lower overall survival and disease-free survival rates after hepatectomy or radiofrequency ablation (11, 13–18). APHC patients may need comprehensive/individualized adjuvant therapy besides surgical resection and close follow-up compared with ANHC (9). In addition, patients with ANHC at the time of diagnosis are more likely to be eligible for liver transplant (19), which may be related to the high expression of the CC genotype of mannose-binding lectin-2 gene in ANHC (20). Therefore, ANHC patients can benefit more from treatment.

The reduced malignancy of ANHC may be related to the reduced expression of related proteins, such as AFP and secretory protein c19orf10. AFP levels in HCC patients have strong relationships with unfavorable tumor features (such as histological grade, tumor size, and vascular invasion) and staging classification (9, 11, 21–23). AFP has oncogenic effects on promoting the proliferation and metastasis of HCC cells (24, 25). AFP can induce cell proliferation, migration, and invasion in ANHC (26). Overexpression of secretory protein c19orf10 can enhance ANHC cell proliferation via the activation of Akt/mitogen-activated protein kinase pathways (27). In addition, the development of ANHC is associated with DNA hydromethylation-mediated dysregulation of associated genes, such as leucine-rich repeat protein phosphatase 1 and actin-dependent regulator of chromatin, subfamily A, member 2, and associated trans-regulatory factors, such as nuclear factor I and GATA-binding protein 3, which may be a novel epigenetic regulation mechanism and potential diagnostic and prognostic biomarker of ANHC (28).

Slight differences in immunophenotypic features are also found between ANHC and APHC. CD44 positivity and higher tumor histological grade are more frequent in APHC, while nuclear beta-catenin positivity is more common in ANHC (29). In the ultrastructural morphology by transmission electron microscopy, the positive rate of Tn protein (Thomsen–Friedenreich-related antigen) was markedly higher in ANHC than in APHC, while AFP showed the opposite expression pattern; in addition, most ANHC cells were dispersed loosely with simple organelles but with abundant free polyribosomes (30); however, the APHC cells were all linked closely together and had rich organelles in their cytoplasm, especially the rough endoplasmic reticula, mitochondria, and complex Golgi, which might be related to the role of AFP in promoting cell proliferation.

## BLOOD BIOMARKERS FOR ANHC DIAGNOSIS

The detection of disease-related molecules in blood is simple and non-invasive and is widely regarded as the best choice for disease screening and diagnosis. In recent years, many biomarkers in blood have been identified and evaluated for the diagnosis of

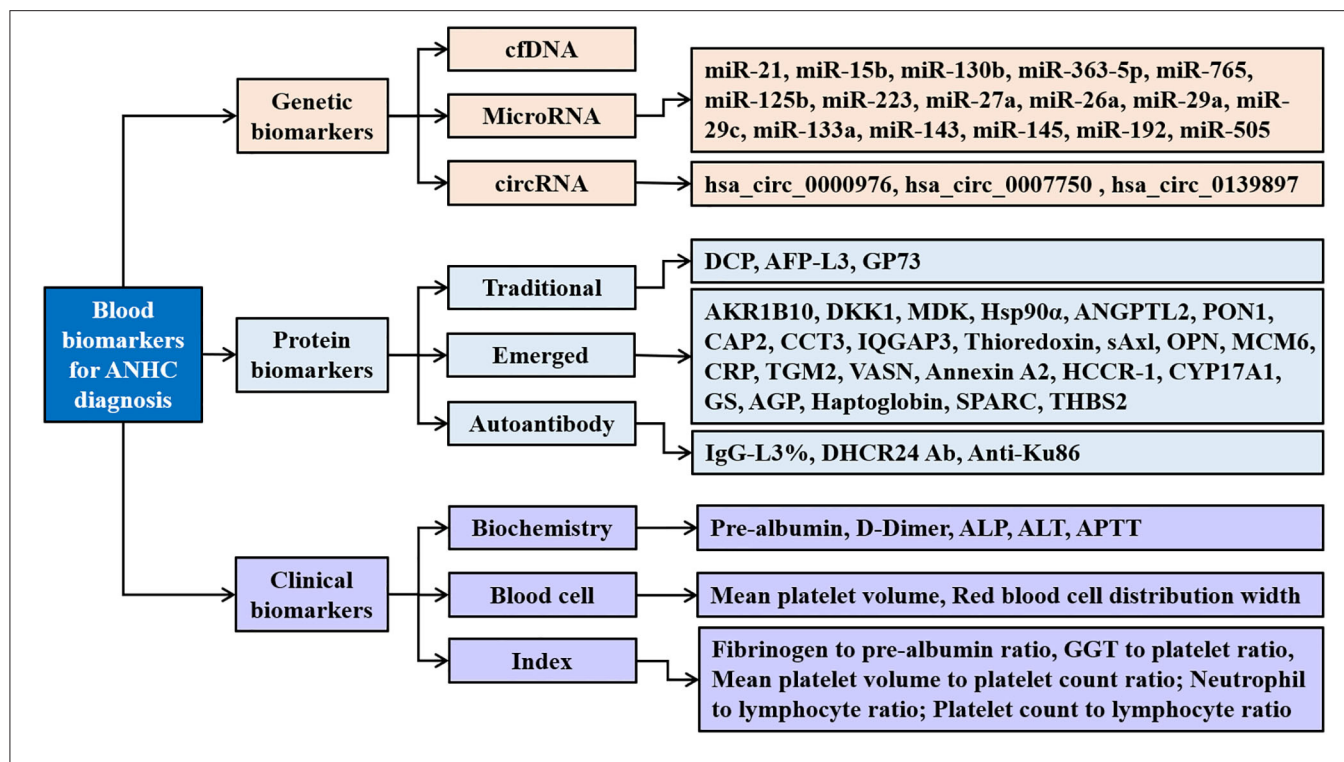


**FIGURE 1 |** Blood biomarkers for AFP-negative hepatocellular carcinoma. ANHC, alpha-fetoprotein-negative hepatocellular carcinoma; cfDNA, circulating cell-free DNA; circRNAs, circular RNAs; DCP, des-gamma-carboxy prothrombin; AFP-L3,  $\alpha$ -fetoprotein fraction L3; GP73, golgi protein 73; AKR1B10, aldo-keto reductase family 1 member B10; DKK1, dickkopf-1; MDK, midkine; Hsp90 $\alpha$ , heat shock protein 90alpha; ANGPTL2, angiopoietin-like protein 2; PON1, paraoxonase 1; CAP2, cyclase-associated protein 2; CCT3, chaperonin containing TCP1 complex subunit 3; IQGAP3, IQ-motif-containing GTPase-activating protein-3; sAxI, soluble transforming receptor tyrosine kinase; OPN, osteopontin; MCM6, minichromosome maintenance complex component 6; CRP, c-reactive protein; TGM2, tissue transglutaminase 2; VASN, vasorin; HCCR-1, human cervical cancer oncogene 1; CYP17A1, the cytochrome P450, family 17, subfamily A, polypeptide 1; GS, glutamine synthetase; AGP, alpha-1 acid glycoprotein; THBS2, thrombospondin-2; IgG, immunoglobulin G; DHCR24 Ab, 3 $\beta$ -hydroxysterol  $\Delta$ 24-reductase antibody; ALP, alkaline phosphatase; ALT, alanine aminotransaminase; APTT, activated partial thromboplastin time; GGT, gamma-glutamyl transpeptidase.

ANHC (Figure 1), such as genetic biomarkers, proteins, and also metabolic biomarkers (31).

## Genetic Biomarkers

The development of ANHC is a chronic process and involves complicated genetic changes. Zhang et al. (28) identified 615 differentially hydroxymethylated regions from ANHC tissues compared to adjacent normal tissues, which were significantly enriched in gene ontology functions, and they found that some hydroxymethylated genes were involved in ANHC development. Lu et al. (32) found that a panel based on four candidate genes (COL5A1, HLA-DQB1, MMP2, and CDK4) was valuable for the diagnosis of ANHC patients [with an area under the receiver operating characteristic curve (AUROC) of 0.768], and Zheng et al. (33) also found that a blood-based 22-gene signature was valuable for ANHC screening (AUROC of 0.93, sensitivity of 91.3%, specificity of 83.2%). Circulating cell-free DNA (cfDNA), microRNAs, and circular RNAs are easily detected genetic biomarkers that are valuable for the diagnosis of HCC, including ANHC.

## Circulating Cell-Free DNA

cfDNA are extracellular DNA molecules released into blood from apoptotic or necrotic cells or tissues (34). cfDNA is elevated in

various malignancies, including HCC, and has cancer-specific DNA alterations, including DNA strand integrity, mutation frequency, microsatellite abnormalities, and gene methylation, and is regarded as diagnostic, prognostic, and monitoring biomarkers for cancers (35). Many methods with high sensitivity and specificity facilitate the use of cfDNA as a “liquid biopsy” for the diagnosis, prognosis, and monitoring of therapeutic response in HCC with advantages of real time and minimal invasion (36). Xiong et al. (37) found that plasma cfDNA mutations in HCC were valuable for the diagnosis of HCC, with an AUROC of 0.92, sensitivity of 65%, and specificity 100% compared with healthy controls. During the combination of cfDNA somatic mutations with AFP, they found that the AUROC was 0.96 with a sensitivity of 73% and specificity of 100% for ANHC, while for APHC, the AUROC was 0.86, with a sensitivity of 53% and a specificity of 100%. Moreover, cfDNA could predict HCC recurrence, that is, the patients with recurrent HCC showed significantly higher somatic mutation frequency of cfDNA than those without recurrence, of which the TP53 gene was the most frequently mutated gene in majority of the HCC patients (21/33, 64%).

In addition, the expression levels of cfDNA were not associated with patient age, gender, TNM stage, or AFP levels or protein induced by vitamin K absence (PIVKA-II) (38), and serum cfDNA levels could be directly, simply,

and accurately detected by a real-time PCR system, which enhances their clinical application for the diagnosis of ANHC. We found that cfDNA-related fluorescence intensity and serum autofluorescence intensity were of value for the diagnosis of early, small, AFP-negative, and all primary hepatic carcinomas from liver cirrhosis (LC), chronic hepatitis, and normal control, with an AUROC value of 0.777–0.963 in the training set and 0.764–0.972 in the validation set, of which the two fluorescence intensity indicators had an AUROC of 0.836, a sensitivity of 73.6%, a specificity of 79.7%, and an accuracy of 78.6% for differentiating ANHC from non-HCC (39, 40), and their diagnostic value could be improved by combination with AFP, hepatic function tests, and/or blood cell analyses.

## MicroRNA

MicroRNAs (miRNAs) are a family of endogenous, small (20–25 nucleotides in length), non-coding RNAs that regulate posttranscriptional gene expression by repressing messenger RNA (mRNA) translation mainly via binding at the complementary 3'-untranslated region and are well-known to play a role in human hepatocarcinogenesis. miRNAs serve as promising cancer biomarkers for diagnosis and therapy response monitoring (41), and circulating miRNAs are stable and able to be detected and quantified, which gives them either diagnostic value for an ANHC diagnosis or an additive value.

MiR-21 has been found to be dysregulated in several cancers and is associated with tumor proliferation, invasion, and metastasis (42). Serum levels of miR-21 were higher in HCC than in controls, with an AUROC of 0.849, sensitivity of 82.1%, and specificity of 83.9% for the diagnosis of HCC, which were higher than those of AFP (AUROC 0.722, sensitivity 68.7%, specificity 62.5%) (43), and the serum levels of miR-21 were also significantly related to clinical stage and distant metastasis (positive in 83.3% HCC patients) but not with AFP. MiR-21 had a positive rate of 77.6% (45/58) in the ANHC group and an AUROC of 0.831, sensitivity of 81.2%, and specificity of 83.2% for the diagnosis of ANHC (43). Additionally, the serum levels of miR-21 were significantly decreased after surgery in patients with HCC (43), indicating that miRNAs can be used for monitoring treatment response.

The combination analysis of miRNAs can complement each other and effectively improve their diagnostic performance for ANHC. A classifier established by the combination of miR-15b and miR-130b had an AUROC of 0.980 (96.7% sensitivity and 91.5% specificity) for detecting ANHC (44), and this miRNA classifier could identify 44 of 45 (97.8%) HCC cases with tumor-node-metastasis stages I and II, whereas serum AFP (cutoff value 20 ng/ml) could only detect 22 of 45 (48.9%) of the same cases; also, miR-15b and miR-130b were markedly reduced after surgery. Tian et al. (45) combined miR-363-5p and miR-765 with PIVKA-II and established a logistic regression model for predicting ANHC and found that the model had the AUROC of 0.930, sensitivity of 79.4%, and specificity of 95.4% in the testing set, higher than any single indicator, and AUC of 0.936, sensitivity of 83.6%, and specificity of 94.7% in the validation set. The combination of four miRNAs (miR-125b, miR-223, miR-27a, and miR-26a) showed an AUROC of 0.849, sensitivity of 80.0%, and

specificity of 89.4% for distinguishing HBV-related AFP-negative early-stage HCC and the non-cancer subjects (46); interestingly, the panel that combined two miRNAs (miR-125b and miR-27a) also had comparable diagnostic performance to the four-miRNA panel above, with an AUROC of 0.845, sensitivity of 80.0%, and specificity of 87.2% for differentiating HBV-related early-stage ANHC from non-cancer, indicating that selecting appropriate complementary biomarkers for combined detection can not only simplify detection methods but also reduce detection costs.

MiRNAs have the ability to detect small-size, early-stage, AFP-negative HCC, which provides a chance of curative resection for HCC patients. Lin et al. (47) conducted a large-scale, multicenter nested case-control study to evaluate a seven-miRNA classifier (miR-29a, miR-29c, miR-133a, miR-143, miR-145, miR-192, and miR-505) for HCC in at-risk patients. The authors found that the miRNA classifier had an AUROC of 0.825 for detecting ANHC, with sensitivities of 78.8, 75.8, and 80.0% and specificities of 86.3, 88.2, and 91.1% in the training cohort, validation cohort 1, and validation cohort 2, respectively, and had an AUROC of 0.812 to identify ANHC from at-risk controls, and this classifier also had larger AUROCs than did AFP to detect small-size (AUROC 0.833 vs. 0.727) and early-stage (AUROC 0.824 vs. 0.754) HCC.

## Circular RNAs

Circular RNAs (circRNAs) are covalently closed, single-stranded, and stable transcripts (48) that have been found to play important roles in the diagnosis of various cancers, including gastric cancer (49–51), breast cancer (52), lung cancer (53, 54), pancreatic cancer (55), and HCC (56, 57). A large-scale, multicenter study successfully validated three circRNAs (hsa\_circ\_0000976, hsa\_circ\_0007750, and hsa\_circ\_0139897) in the plasma of the hepatitis B virus-related HCC patients, and their plasma levels positively correlated with HCC tissue levels and significantly decreased after hepatectomy (58), and the CircPanel developed by using binary logistic regression based on the three circRNAs showed a significantly higher accuracy than AFP to differentiating HCC patients from controls in all three sets (AUROC, 0.863 vs. 0.790 in the training set; 0.843 vs. 0.747 in validation set 1 and 0.864 vs. 0.769 in validation set 2). The CircPanel also had a high diagnostic accuracy in the diagnosis of ANHC and AFP-negative small-HCC (all AUROCs ranged from 0.823 to 0.902, sensitivity ranged from 74.0 to 82.2%, specificity ranged from 90.6 to 97.7%) (58). Therefore, circRNAs may be potential diagnostic and therapeutic response biomarkers for HCC and ANHC.

## Protein Biomarkers for ANHC Diagnosis

### Traditional Serum Protein Biomarkers

Several well-known traditional serum biomarkers used for the diagnosis of HCC have been explored for detecting ANHC alone or in combination (59). Prothrombin induced by vitamin K absence II (PIVKA-II), also named des-gamma-carboxy prothrombin (DCP), was found to be expressed significantly higher in early-stage HBV-related HCC than in chronic hepatitis B and to be valuable for the diagnosis of ANHC, with an AUROC of 0.73, sensitivity of 51.0%, and specificity of 84.5–94.3% (60, 61), and patients with poorly differentiated or undifferentiated



HCC and microvascular invasion exhibited higher levels of PIVKA-II. Another large-scale, multicenter study found that DCP could be complementary to AFP in detecting ANHC and excluding LC with AFP positivity (62) and is also beneficial for HCC surveillance, early diagnosis, and monitoring treatment response and recurrence in the HBV-infected population, with positive rates of 63.2–76.3% in ANHC and an AUROC of 0.856, sensitivity of 76.3%, and specificity of 89.1% for the diagnosis of ANHC, and better than AFP in the surveillance of early HCC (AUROC 0.837 vs. 0.650) and discriminating HCC from LC (accuracy: 92.9 vs. 64.7%), and moreover, higher DCP levels were associated with worse clinical behaviors and shorter disease-free survival. These results indicate that serum PIVKA-II is a potential early diagnostic and prognostic biomarker for HCC, including ANHC.

Alpha-fetoprotein fraction L3 (AFP-L3) is a traditional diagnostic marker for HCC, but the conventional AFP-L3 detection methods are insufficiently sensitive in patients with low-level AFP. With a highly sensitive method, AFP-L3% had a sensitivity of 41.5% and a specificity of 85.1% for the diagnosis of ANHC (63), and the combination of AFP-L3% and DCP effectively improved the diagnostic value for ANHC (sensitivity of 44.9–90.6%). Additionally, the survival rate of patients with high AFP-L3% ratio ( $\geq 5\%$ ) was significantly lower than that of patients with low AFP-L3% ( $< 5\%$ ) (63).

Another study (64) found that PIVKA-II was not correlated with AFP, AFP-L3, and tumor characteristics, and the combination of PIVKA-II and AFP-L3 was capable of improving HCC detection regardless of AFP levels, with an AUROC of 0.939, sensitivity of 92.1%, and specificity of 79.7% in ANHC, which was higher than that of AFP-L3 alone (AUROC 0.824, sensitivity 71.1%, and specificity 83.8%) and PIVKA-II alone (AUROC 0.774, sensitivity 57.9%, and specificity 95.9%). Moreover, the two biomarkers in combination could detect 81.8% of early-stage HCC, 86.7% of small HCC, and 91.7% of single tumor of HCC in the ANHC group (64).

As a single biomarker has insufficient sensitivity and/or specificity for the diagnosis of ANHC, a combination of multiple biomarkers is usually used to effectively improve diagnostic efficacy (65). An integrated parameter AFP/GP73 (Golgi protein 73) was created to magnify the differential diagnosis of ANHC in terms of better sensitivity and specificity (66), which had an AUROC of 0.662, sensitivity of 68.6%, and specificity of 58.8% for differentiating ANHC from LC and an AUROC of 0.796, sensitivity of 81.4%, and specificity of 70.0% for differentiating metastatic ANHC from adenocarcinomas; these values were slightly higher than those of GP73 alone (AUROC of 0.747, sensitivity of 57.7%, and specificity of 87.0%). AFP-L3 combined with GP73 was also evaluated for the diagnostic accuracy of ANHC (67): both serum AFP-L3 and GP73 had a higher positive rate in ANHC than in non-HCC patients, with respective AUROC values of 0.609 and 0.781, sensitivity of 50 and 66%, specificity of 97.5 and 96.2%, and accuracy of 79.2 and 84.6% for the diagnosis of ANHC, while the sensitivity, specificity, and accuracy achieved 40, 100, and 76.9%, respectively, when AFP-L3 and GP73 were used in combination, indicating that AFP-L3 or GP73 could be used

as a biomarker for ANHC diagnosis, but their combined use does not significantly improve diagnostic performance for ANHC.

### Emergent Serum Protein Biomarkers

Although traditional biomarkers have certain diagnostic values for HCC, none of them was ideal in clinical practice. Therefore, new biomarkers are continuing to be explored.

#### AKR1B10

Aldo-keto reductase family 1 member B10 (AKR1B10) is a novel secretory protein that is overexpressed in multiple tumors, including lung cancer, breast cancer, and colorectal cancer (68, 69), and is a potential diagnostic and prognostic biomarker for HCC (70–73). A multicenter study (74) with 1,244 participants found that serum AKR1B10 levels were significantly increased in HCC patients compared with those in non-HCC and were associated with AFP, alanine aminotransaminase, aspartate aminotransaminase, and tumor size, but not with tumor number, vascular invasion, and TNM stage, with an AUROC of 0.896, sensitivity of 72.7%, and specificity of 95.7% for the diagnosis of HCC, and these values were better than those of AFP (AUROC 0.816, sensitivity 65.1%, and specificity 88.9%), and for ANHC cases, AKR1B10 exhibited a promising diagnostic value (AUROC 0.891, sensitivity 71.2%, and specificity 92.6%), and a similar diagnostic performance was observed in AFP-negative early-stage HCC (AUROC 0.839, sensitivity 63.4%, and specificity 90.7%). Moreover, serum AKR1B10 levels dramatically decreased 1 day after surgery and returned nearly back to normal at 3 days after surgery, indicating that AKR1B10 may also be a potential diagnostic, metastasis, and/or recurrence biomarker for ANHC (74).

#### DDK1

Dickkopf-1 (DKK1) is a 266-amino acid (35-kDa) secreted glycoprotein that is expressed in a variety of human tumors, including the pancreas, stomach, liver, bile duct, breast, cervix, esophageal, and prostate (75–77) and plays a functional role in human HCC cell migration, invasion, and tumor growth (78). Serum DKK1 levels demonstrated high diagnostic and prognostic values for HCC, especially for ANHC and early-stage HCC (79, 80). A large-scale, multicenter validation study (81) noted that serum DKK1 levels were significantly higher in HCC than in chronic HBV infection, cirrhosis, and healthy controls and were valuable for differentiating ANHC from all controls, with an AUROC of 0.841, sensitivity of 70.4%, and specificity of 90.0% in the test cohort and similar results in the validation cohort (0.869, 66.7, and 87.2%, respectively) and in the test cohort (0.870, 73.1, and 90.0%, respectively). For early-stage HCC patients in the validation cohort, DKK1 also had a good diagnostic performance (AUROC 0.893, sensitivity 72.2%, and specificity 87.2%) (81). DKK1 may also be a useful biomarker to predict the therapeutic response, as its serum levels dropped after surgery (81). However, other studies showed that plasma DKK1 levels may not be valuable for diagnosing ANHC (AUROC 0.551–0.620, sensitivity 54.4–89.1%, and specificity 37.9–61.5%) (82, 83).



### MDK

Midkine (MDK) is a heparin-binding growth factor with multiple functions, including anti-apoptotic, migratory ion-promoting, angiogenic, and antimicrobial effects and is strongly expressed during embryogenesis and most malignant tumors, but in normal adult tissues, it is weak or undetectable (84). A large-scale, multicenter validation study (85) found that serum MDK is expressed higher in HCC than in gastrointestinal malignant tumors and in non-HCC controls, and there was no significant correlation with clinicopathological features, such as histological differentiation, stage, microvascular invasion, tumor size, and serum AFP levels, and MDK had a higher sensitivity (86.9 vs. 51.9%) but similar specificity (83.9 vs. 86.3%) for HCC diagnosis compared with AFP, even in very early-stage HCC (87.1 vs. 46.7%), and in particular, MDK had an outstanding performance for distinguishing ANHC from non-HCC controls (AUROC, 0.926) and from LC (AUROC, 0.931), with sensitivity as high as 89.2%; serum MDK levels were significantly decreased in HCC patients after curative resection and re-elevated with tumor relapse. A systematic review and meta-analysis also confirmed that MDK had AUROC of 0.91, sensitivity of 88.5%, and specificity of 83.9% for detecting ANHC (86). These results indicate that MDK could be a sensitive tumor marker for diagnosis, treatment response, and recurrence in patients with HCC, including ANHC.

### Hsp90 $\alpha$

Heat shock protein 90alpha (Hsp90 $\alpha$ ) is a conserved molecular chaperone that is significantly increased in various tumors and positively correlates with tumor malignancy and metastatic ability (87), and therefore, it is regarded as a potentially important target for tumor therapy. A large-scale, multicenter clinical study (88) found that plasma Hsp90 $\alpha$  concentrations were significantly elevated in liver cancer patients, with no significant differences among different tumor types and differentiation grades, but was positively associated with tumor staging. Hsp90 $\alpha$  was more valuable for distinguishing HCC from non-liver cancer controls than AFP, with an AUROC of 0.965, sensitivity of 93.3%, and specificity of 90.3% (for AFP, AUROC 0.887, sensitivity 61.1%, specificity 96.3%) and exhibited a remarkable discriminating performance in early-stage liver cancer (AUROC 0.963, sensitivity 91.4%, specificity 91.3%) and in ANHC (AUROC 0.971, sensitivity 93.9%, and specificity 91.3%); similar results were observed in small liver cancers. This study also found that plasma Hsp90 $\alpha$  dropped after treatment and increased with tumor recurrence. Plasma Hsp90 $\alpha$  may represent an effective and timely “liquid biopsy” means for the diagnosis and therapeutic efficacy of liver cancer.

### ANGPTL2

Angiopoietin-like protein 2 (ANGPTL2) is a secretory glycoprotein involved in vascular biology, inflammation, and tumor development (89). ANGPTL2 is overexpressed in HCC tissues compared with non-cancerous liver tissues and able to promote HCC migration and invasion (90). Zhou. et al. (91) found that serum levels of ANGPTL2 is gradually elevated with the liver injury progression and reached a peak in HCC patients

with chronic HBV infection, with better diagnostic performance (AUROC 0.952, sensitivity 95.2%, specificity 81.8%, and accuracy 90.7%) than AFP (AUROC 0.824, sensitivity 71.4%, specificity 95.5%, and accuracy 81.5%) for the differentiation of HCC from healthy controls. ANGPTL2 also showed good performance for the differentiation of HCC from chronic liver diseases, with an AUROC of 0.831, sensitivity of 68.3%, specificity of 87.3%, and accuracy of 80.4%, which was also better than that of AFP (AUROC 0.777, sensitivity 42.9%, specificity 93.3%, and accuracy 79.2%), for the diagnosis of ANHC, with an AUROC of 0.919 for differentiating ANHC from healthy controls and an AUROC of 0.798 (95% CI 0.710–0.886) for differentiating ANHC from high-risk controls. Thus, ANGPTL2 may be a potential diagnostic biomarker in detecting AFP-negative HBV-related HCC.

### PON1

Abnormal protein glycosylation is involved in different diseases, especially cancers (92). Serum paraoxonase 1 (PON1) is a highly fucosylated glycoprotein in HCC compared with LC, with an AUROC of 0.892, sensitivity of 71.4%, and specificity of 94.7% in differentiating early HCC from LC (93). For differentiating AFP-negative early HCC ( $n = 20$ ) from LC ( $n = 20$ ), PON1 exhibited an AUROC of 0.850, sensitivity of 90.0%, specificity of 75.0%, and accuracy of 82.5% (94). Shu et al. (95) used Fuc-PON1 (the ratio of fucosylated PON1 to total serum PON1) to differentiate AFP-negative early HCC ( $n = 76$ ) from AFP-negative LC ( $n = 76$ ) and found that Fuc-PON1 had an AUROC of 0.78, sensitivity of 62.2%, specificity of 67.7%, and accuracy of 64.5%, while the concentration alterations of AFP-L3 and glypican-3 (GPC3) in ANHC patients were not remarkable, indicating that Fuc-PON1 is useful in the diagnosis of AFP-negative early HCC.

### CAP2

Cyclase-associated protein 2 (CAP2), a conserved protein, takes part in the regulation of actin cytoskeleton that is involved in cellular functions, including morphogenesis, cytokinesis, and cell migration (96). CAP2 is upregulated in multiple tumors, such as breast cancer, gastric cancer, malignant melanoma (97), and it is also upregulated in early HCC and to a greater extent in advanced HCC (98). CAP2 expression in HCC correlated with tumor size, histological grade, and clinical stage, but not with plasma AFP level, HBV infection status, and patient's gender and age (99), and higher levels of CAP2 were found in HCC compared with cirrhosis patients, with better performance than AFP for diagnosing general HCC (AUROC 0.86 vs. 0.75, sensitivity 82.6 vs. 59.3%, specificity 79.3 vs. 83.1%) and for diagnosing early-stage HCC patients (AUROC 0.81 vs. 0.67, sensitivity 78.6 vs. 40.4%, specificity 81.4 vs. 83.1%). CAP2 had an AUROC of 0.84, sensitivity of 82.9%, and specificity of 79.6% for the detection of ANHC ( $n = 35$ ), and for the detection of AFP-negative early HCC, CAP2 also presented a good performance (AUROC 0.80, sensitivity 80.0%, and specificity 79.6% (99). The results above suggest that CAP2 may be a potential diagnostic biomarker for ANHC.

### CCT3 and IQGAP3

Chaperonin containing TCP1 complex subunit 3 (CCT3) is a crucial subunit in the complexes and involved in tumor cell proliferation and the tumorigenesis (100). Overexpressed CCT3 is associated with HCC progression (101, 102). IQ-motif-containing GTPase-activating protein-3 (IQGAP3) is involved in the proliferation of epithelial cells (103) and liver regeneration (104). Both CCT3 and IQGAP3 genes, localized on 1q22, were upregulated in HCC (105). Qian et al. (106) found that both plasma CCT3 and IQGAP3 levels were higher in HCC than in non-HCC, correlated well with each other ( $r = 0.824$ ), and associated with HCC etiology, tumor size and number, and Child–Pugh classification. Plasma CCT3 and IQGAP3 were both valuable for differentiating ANHC ( $n = 38$ ) from LC ( $n = 88$ ) (CCT3 with an AUROC of 0.871, sensitivity of 92.1%, and specificity of 70.5% and IQGAP3 with an AUROC of 0.804, sensitivity of 81.6%, and specificity of 71.6%) and differentiating small HCC ( $n = 47$ ) from LC (CCT3 with an AUROC of 0.761, sensitivity of 76.6%, and specificity of 70.5% and IQGAP3 with an AUROC of 0.753, sensitivity of 74.5%, and specificity of 71.6%), which were better than that of AFP (AUROC 0.707, sensitivity 53.2%, and specificity 68.2%) (106). For the diagnosis of AFP-negative small HCC ( $n = 27$ ), CCT3 exhibited an AUROC of 0.84, sensitivity of 88.9%, and specificity of 70.5%, and IQGAP3 exhibited an AUROC of 0.822, sensitivity of 85.2%, and specificity of 71.6%) (106). The combination of AFP, CCT3, and IQGAP3 was significantly superior to AFP alone in discriminative ability (AUROC 0.954 vs. 0.815), indicating that the expression of CCT3 and IQGAP3 is independent of AFP and thus complementary to AFP for AFP-negative and small HCC diagnosis.

### Thioredoxin

Thioredoxin is a thiol oxidoreductase that is ubiquitously expressed and is highly expressed in a variety of malignancies and associated with aggressive tumor growth and poor survival (107–109). Its expression level positively correlated with tumor size, Child–Pugh classification, or tumor stage of HCC, but not with age, sex, HBV infection time, etiology, alanine aminotransaminase, aspartate aminotransaminase, total bilirubin, prothrombin time, and AFP levels (110). Serum thioredoxin levels were significantly higher in HCC compared with chronic liver diseases and exhibited positive rates of 72.7% (40 of 55) and 69.2% (18 of 26) in ANHC and very early-stage ANHC, respectively (110). For differentiating very early HCC from non-HCC, thioredoxin had an AUROC of 0.901, sensitivity of 75.2%, and specificity of 88.9%, which were higher than that of AFP (AUROC 0.769, sensitivity 70.1%, specificity 79.4%) (110). These findings indicate that thioredoxin has the advantage over AFP for HCC detection, particularly for very early ANHC.

### sAxl

The transforming receptor tyrosine kinase (Axl) is a member of the tumor-associated macrophage family and upregulates in several types of cancer and correlated with poor prognosis and metastasis of cancers (111, 112). The extracellular portion of Axl

can be cleaved from the membrane to generate soluble Axl (sAxl) that can be detected in serum. A retrospective multicenter study found that sAxl was significantly increased in HCC compared with healthy or cirrhotic subjects and continuously elevated with the progression of HCC (113), and HCC patients with high serum sAxl levels exhibited a significantly reduced overall survival compared with low-level sAxl patients (median, 25.37 vs. 88.56 months). sAxl outperformed AFP for the detection of very early HCC (BCLC 0) (AUROC 0.848 vs. 0.797; sensitivity 76.9 vs. 38.5%), and the combination of sAxl and AFP exhibited an AUROC of 0.937, a sensitivity of 84.5%, and a specificity of 92.3% in diagnosing HCC (113). In ANHC, sAxl was also indicated as a valid diagnostic biomarker (AUROC 0.803, sensitivity 73.0%, and specificity 70.8%), and in very early ANHC, sAxl presented an even higher diagnostic value (AUROC 0.863, sensitivity 80%, and specificity 69.2%) (113). A recent study also found that sAxl had an AUROC of 0.898, sensitivity 84.6%, and specificity 76.3% for the diagnosis of ANHC and had a higher diagnostic performance (AUROC 0.881, sensitivity 94.1%, and specificity 74.2%) than that of AFP (AUROC 0.705, sensitivity 58.8%, and specificity 73.3%) for early HCC (114). These findings implicate that sAxl is a diagnostic biomarker with high accuracy for very early HCC and ANHC.

### OPN

Osteopontin (OPN), a secreted phosphoprotein, is associated with tumor invasion, progression, or metastasis in multiple types of cancer and has been considered to be a promising target for cancer therapy (115, 116). HCC patients with elevated plasma levels of OPN were more likely to exhibit intrahepatic metastasis, early recurrence, and a worse prognosis (117). OPN was also found to be a potential biomarker complementary to AFP for HCC diagnosis. A pilot study with a small sample size found that plasma OPN levels were significantly higher in HCC patients than in cirrhosis patients, chronic hepatitis patients, and healthy controls (118), with a greater AUROC than AFP in discriminating HCC and cirrhosis patients (0.76 vs. 0.71), in discriminating early-stage HCCs and cirrhosis patients (0.73 vs. 0.68), and in discriminating ANHC and cirrhosis patients (0.75 vs. 0.59), and furthermore, in another cohort, an AUROC of 0.87 was observed for distinguishing ANHC from cirrhosis and chronic HBV. OPN was also found to be able to detect preclinical tumors, that is, 87% of patients within 2 years preceding HCC diagnosis exhibited OPN levels above cutoff value (118). Similar results were found in another study (with AUROC of 0.851, sensitivity of 79.2%, and specificity of 80.5% for diagnosing HCC and AUROC of 0.838, sensitivity of 78.3%, and specificity of 79.6% for diagnosing ANHC) (83). A meta-analysis including 8 studies ( $N = 1,399$ ) found that serum/plasma OPN had a ability for predicting survival of HCC patients and an accuracy comparable to AFP for HCC diagnosis (the pooled sensitivity and specificity for OPN and AFP were 88 vs. 68% and 87 vs. 97%, respectively) (119); however, there is only one study to evaluate OPN for the diagnosis of early or AFP-negative HCC in this meta-analysis, so further assessment for the diagnostic value of plasma OPN in early and AFP-negative HCC is required.

### MCM6

Minichromosome maintenance complex component 6 (MCM6) is a member of minichromosome maintenance proteins, which is indispensable for DNA replication during the initiation of S phase of the cell cycle (120). Plasma MCM6 mRNA and protein levels were significantly upregulated in HCC and correlated with vascular invasion, tumor progression, and lymph node metastasis but not with AFP levels or clinical features (age, gender, tumor size, HBV or HCV infection status, or Child–Pugh score) (121), with a sensitivity of 67.2% and a specificity of 89.8% for MCM6 protein to discriminating HCC from non-HCC. Both of MCM6 mRNA and protein were positive in 76.9% of ANHC patients and in 64.3 and 71.4% of small HCC patients, respectively (121). However, the sample size of this study is very small; hence, further studies are required to confirm the diagnostic value of MCM6 in HCC patients.

### CRP

C-reactive protein (CRP) is a non-specific acute-phase protein produced by the liver in response to acute and chronic inflammation, and elevated CRP expression has been detected in multiple tumors and is associated with poor prognosis (122–125). Ma et al. (126) used a high-sensitivity CRP (hs-CRP) assay, which could be quantified as low as 0.04 mg/L of CRP and found that serum hs-CRP levels were significantly elevated in the HCC group compared with those in the non-HCC group and did not correlate with tumor Edmondson grade, TNM stage, or AFP status. Serum hs-CRP had a better performance than AFP (AUROC 0.903 vs. 0.824, sensitivity 84.2 vs. 74.4%, specificity 61.6 vs. 55.6%) for diagnosing HCC, and the diagnostic performance improved when the two indicators were combined (AUROC = 0.998, sensitivity = 94.1%), with similar positive rates between APHC and ANHC patients (86.9 vs. 84.6%) (126), indicating that serum hs-CRP level may be a useful diagnostic biomarker complementary to AFP for ANHC diagnosis. Another study also found that serum CRP-positive rate was significantly higher in the HCC than in the LC (64.15 vs. 37.97%) (127), and serum CRP levels were similar between ANHC and APHC patients. The combination of serum CRP with liver stiffness could be complementary to AFP in the identification of ANHC patients and help to distinguish HCC from LC.

### TGM2

Tissue transglutaminase 2 (TGM2) is a stress-regulated protein that is associated with matrix stabilization, cell adhesion and migration, and cell death and survival (128). TGM2 in the tumor stroma can inhibit tumor growth and metastasis (129, 130). TGM2 is overexpressed in many types of cancer, including pancreatic carcinoma (131), breast cancer (132), ovarian carcinoma (133), and lung cancer (134). Interestingly, TGM2 expression in liver tissues showed an inverse correlation with serum AFP levels in HCC patients (135), and TGM2 was overexpressed in some AFP-deficient HCC cell lines (SK-HEP-1 and Bel-7402) and approximately half (17/32) of ANHC tissues but trace-expressed in APHC (3/29). Serum TGM2 levels were significantly higher in HCC patients and positively correlated with the histological grade and tumor size (135), indicating

that TGM2 may be a useful histological and serologic candidate biomarker for ANHC diagnosis, although more studies are required to confirm the value of TGM2 in ANHC diagnosis.

### VASN

Vasorin (VASN) is a secreted cell surface protein that is associated with vascular injury repair through inhibiting the TGF- $\beta$  signaling pathway (136), and its overexpression in some human tumors can stimulate malignant progression and angiogenesis (137). In hepatoma, VASN is capable of promoting cell proliferation and migration and inhibiting cell apoptosis and is regarded as a promising biological treatment target for HCC. Higher VASN levels were verified in HCC serum compared with that in control cohorts, with an AUROC of 0.770, sensitivity of 69%, and specificity of 80.5% for the diagnosis of HCC; VASN was positive in 62% (23/37) of ANHC cases, indicating that VASN may be a potential biomarker for HCC diagnosis (138).

### Annexin A2

Annexin A2 is a calcium-dependent, phospholipid-binding protein expressed on the surface of endothelial cells and most epithelial cells (139, 140). It upregulates in multiple tumors and plays various roles in tumorigenic processes, such as cell proliferation, apoptosis, migration, adhesion, invasion, and angiogenesis (141–143). Serum annexin A2 levels were significantly higher in HCC patients compared with non-HCC controls and did not correlate with gender, age, tumor size, differentiation degree, BCLC staging, and AFP levels (144), with a better performance than AFP (AUROC 0.800 vs. 0.690) for distinguishing HCC from hepatitis and cirrhosis. For early-stage HCC, annexin A2 also had a better diagnostic performance (AUROC 0.79, sensitivity 83.2%, and specificity 67.5%) compared with AFP (AUROC 0.73, sensitivity 54.7%, and specificity 81.3%), and the combination of annexin A2 with AFP improved the sensitivity and specificity up to 87.4 and 68.3% for early-stage HCC (144). Importantly, in ANHC patients ( $n = 74$ ), annexin A2 had an AUROC of 0.77, sensitivity of 89.2%, and specificity of 58.5% (144). Thus, annexin A2 might be an important candidate biomarker for the diagnosis of ANHC and early-stage HCC.

### HCCR-1

Human cervical cancer oncogene 1 (HCCR-1) is a novel human oncoprotein associated with human cervical cancer and upregulated in various human tumors in tumorigenesis and tumor progression (145, 146). HCCR-1 expression is high in HCC, moderate in LC, and at basal levels in normal control and chronic hepatitis, with higher detection accuracy (78.2%) than AFP (64.6%) for discrimination between HCC and LC. Serum HCCR was positive in 76.9% (40 of 52) ANHC patients (147); in addition, nine patients with metastatic lesions who were negative for AFP were positive for HCCR. However, another study showed that HCCR-1 has a positive rate of only 48.5% (63 of 130) in ANHC (148). In a multicenter prospective study (5), HCCR-1 levels did not significantly correlate with HCC clinicopathological characteristics such as age, gender, tumor size, and lymph node metastasis, but positively correlated with histological grading. Interestingly, AFP was positive in 97 of 164



(59.1%) HCCR-1-negative HCC patients, and the positive rate was up to 77.2% in combination of both AFP and HCCR-1, indicating that HCCR-1 expression is not associated with AFP levels in many HCC cases and thus HCCR-1 can be complementary to AFP for ANHC diagnosis.

### CYP17A1

The cytochrome P450, family 17, subfamily A, polypeptide 1 (CYP17A1), is a secretory protein that is overexpressed in the liver tissues of HCC model mice at both preneoplastic and neoplastic stages and in human HCC tissues compared with paired non-tumor tissues and other malignant tumors (lung cancer and prostate cancer) (149). Serum CYP17A1 exhibited better diagnostic performance than did AFP in differentiating HCC vs. healthy controls, with an AUROC of 0.91, sensitivity of 86.9%, and specificity of 76.8% for CYP17A1 and an AUROC of 0.78, sensitivity of 65.6%, and specificity of 65.6% for AFP (149). More importantly, serum CYP17A1 levels were positive in 89.1% of ANHC cases and not significantly different between ANHC and APHC (149), indicating that CYP17A1 is a promising biomarker for ANHC detection.

### GS

Glutamine synthetase (GS) is a metabolic enzyme that catalyzes the synthesis of glutamine (a major energy source of tumor cells) and has been revealed as a sensitive and specific indicator for the development of HCC (150). Liu et al. (151) found that the serum levels of GS in HCC patients were higher compared with liver cirrhosis patients and healthy controls, and the AUROCs of GS and AFP for HCC diagnosis were 0.848 and 0.861, respectively, while the AUROC was 0.913 (sensitivity 81.9%, specificity 100%) for differentiating ANHC from healthy control, and the sensitivity and specificity achieved to 82.5 and 93% when combining GS with AFP. Those results indicate that GS may be a valuable biomarker for HCC diagnosis, especially for ANHC.

### AGP

Alpha-1 acid glycoprotein (AGP) is an acute-phase glycoprotein synthesized mainly by hepatocytes and has different glycoforms dependent on the pathophysiological conditions (152), and multifuosylated AGP can be used as a novel biomarker for HCC (153). Liang et al. (154) found the trifucosylated N-glycan of AGP presented in HCC patients but absent in healthy controls and most cirrhosis patients and could differentiate HCC from cirrhosis with AUROCs of 0.707–0.751 in various causes of liver diseases and exhibited an AUROC of 0.709, sensitivity of 52%, and specificity of 80% for differentiating ANHC from LC. These results suggest that the AGP could serve as a potential marker for diagnosing HCC, including ANHC.

### Serum Autoantibodies

At a relatively early stage of carcinogenesis, a small amount of tumor antigens can be produced by tumor cells and leads to the generation of autoantibodies. These autoantibodies are stable in blood circulation and remain elevated for a long time. Therefore, the detection of autoantibodies can improve the early detection of tumors that are difficult to detect directly (155). Many autoantibodies have been investigated for the early detection of

ANHC, such as autoantibodies to centromere protein F and heat shock protein (HSP60), which were found to be positive in 73.6 and 79.3% cases of early-stage ANHC, respectively (156).

### IgG-L3%

HCC-derived immunoglobulin G (IgG) and its abnormal glycosylations are related to carcinogenesis. The fraction of Lens culinaris agglutinin binding IgG (IgG-L3) among total serum IgG (IgG-L3%) was found to gradually increase from healthy volunteers, HBV carriers, and patients with LC to HCC patients, including ANHC patients, and to be more valuable than AFP for the diagnosis of HBV-related HCC (157), with an AUROC 0.835 vs. 0.718, accuracy 81.3 vs. 78.0%, sensitivity 86.7 vs. 66.7%, and specificity 77.8 vs. 85.6%, and also to be valuable for distinguishing ANHC ( $n = 123$ ) from non-HCC ( $n = 234$ ) (AUROC of 0.795, sensitivity of 80.5%, specificity of 70.0%) and from LC ( $n = 71$ ) (AUROC of 0.711, sensitivity of 80.5%, specificity of 58.6%). In addition, patients with a high IgG-L3% value had a significantly lower overall survival rate than patients with low IgG-L3% value, and serum IgG-L3% values reduced after surgery and increased with recurrence. These results indicate that IgG-L3% could be a potential diagnostic and prognostic biomarker in HBV-related HCC.

### DHCR24 Ab

Serum  $3\beta$ -hydroxysterol  $\Delta 24$ -reductase antibody (DHCR24 Ab) is an autoimmune protein that is remarkably upregulated in HCV-infection patients and can be exploited as diagnostic biomarker for HCV-mediated HCC, but not for HBV-related diseases (158), with a higher AUROC than AFP and PIVKA-II in discriminating HCV-mediated chronic hepatitis from HCV-mediated HCC patients (0.860 vs. 0.840 and 0.780) and no correlation with serum AFP or PIVKA-II levels. It was revealed that 73.4% (58/79) of ANHC patients exhibited elevated serum DHCR24 Ab levels. Serum DHCR24 Ab may represent a potential biomarker for the diagnosis of HCV-related HCC with negative AFP.

### Anti-Ku86

Ku86 is the regulatory region of a DNA-dependent protein kinase that is involved in multiple biological processes, including DNA double-strand break repair, recombination, telomere length maintenance, cell cycle progression, and transcriptional regulation (159). Its autoantibody, serum anti-Ku86, is significantly elevated in HCC patients compared with LC patients and decreased after surgical resection with a positive rate of 60.7% in small early-stage HCC with 90% specificity, whereas the sensitivities of AFP and PIVKA-II were 17.8 and 21.4%, respectively. Anti-Ku86 was not correlated with AFP and was positive in 61.7% (37/60) of ANHC cases (159). Therefore, the serum anti-Ku86 antibody may be a potential biomarker for the early detection of ANHC (160).

Some studies have shown low sensitivities of autoantibodies for ANHC diagnosis. The sensitivities of three autoantibodies (against nucleophosmin1, 14-3-3zeta, and mouse double minute 2 homolog proteins) for diagnosing ANHC ranged from 19.6 to 21.4%, with a specificity of 95% (161). Using a mini-array

of multiple tumor-associated antigens as target antigens could enhance the detection of autoantibodies in cancer (162). In addition, a study found that the combination of autoantibodies against multiple TAAs was positive in 7 of 8 ANHC patients and in 6 of 8 small HCC patients, indicating that the combination analysis of anti-TAAs appears to be able to improve the diagnosis performance for ANHC (163).

### New Protein Biomarkers Identified by “omics”

The proteome is a collection of all proteins in a biological sample. Tumor cells can secrete proteins or shed proteins from its surface into body fluids as a source for the discovery of potential cancer biomarkers (164, 165). With the development of proteomics technology, numerous proteomic studies have been performed to examine specific protein profiles for the early detection of ANHC. Wu et al. (166) found 45 differentially changed serum protein/peptide peaks in HCC compared with LC using mass spectrometry techniques, and the most significant peak, 3,892, yielded 69.0% sensitivity, 83.3% specificity, and 80% positive predictive value in distinguishing HCC from LC and a favorable positive value for ANHC patients (6/8). He et al. (167) quantitatively screened out 24 differentially expressed proteins from patients with HBV-related ANHC, HBV without HCC, and healthy control subjects by using the combination of liquid chromatography and tandem mass spectrometry with isobaric tags for relative and absolute quantitation, of which 15 proteins were upregulated and 9 downregulated, but their diagnostic significance is to be assessed. She et al. (168) also revealed 14 abnormally expressed proteins specific to HCC by mass spectrometry and found CRP for the diagnosis of ANHC with an AUROC of 0.724, sensitivity of 73.0%, and specificity of 60.0%. Haptoglobin was identified with an AUROC of 0.763 for the diagnosis of ANHC ( $n = 49$ ) from LC ( $n = 86$ ) (169).

In addition to serum, tissue interstitial fluid was also used to identify differentially expressed proteins. Zhang et al. (170) found that two overexpressed extracellular matrix proteins from tissue interstitial fluid, SPARC (a glycoprotein involved in cell growth regulation through interactions with the ECM and cytokines), and thrombospondin-2 (THBS2) were valuable for HCC diagnosis. The combination of serum SPARC and THBS2 for distinguishing HCC ( $n = 44$ ) with an AUROC of 0.97, sensitivity of 86%, and specificity of 100% and ANHC ( $n = 22$ ) with an AUROC of 0.95, sensitivity of 91%, and specificity of 93% from healthy controls ( $n = 30$ ) (170), and HCC patients with high THBS2 levels had significantly shorter disease-free survival and overall survival than those with low THBS2 levels, indicating that serum THBS2 could be used as a novel indicator for a poor prognosis of HCC.

### Conventional Laboratory Tests

Routine laboratory tests are a large pool of data that contain much disease-related information that can be used for the diagnosis and prognosis of diseases. Jing et al. (7) found that routine laboratory test indicators, serum pre-albumin and D-Dimer, were valuable for diagnosing ANHC, with an AUROC of 0.900, sensitivity of 90.1%, and specificity of 86.3% for pre-albumin

and 0.868, sensitivity of 73.8%, and specificity of 87.1% for D-Dimer, and the combination of these two indicators provided an AUROC of 0.941, sensitivity of 85.7%, and specificity of 89.2% for the diagnosis of ANHC. Moreover, low levels of pre-albumin and high levels of D-Dimer were independent predictors of an unfavorable outcome for ANHC (7). Huang et al. (171) also found that the combination of fibrinogen to pre-albumin ratio and gamma-glutamyl transpeptidase to platelet ratio had a good ability to detect ANHC from the control group (AUROC = 0.977), AFP-negative chronic hepatitis (AUC = 0.745), and AFP-negative LC (AUC = 0.666) and possessed a larger area (0.943, 0.971) than fibrinogen to pre-albumin ratio and gamma-glutamyl transpeptidase to platelet ratio alone for differentiating small or early ANHC.

Mining the hidden information from abundant routine laboratory tests and establishing disease-predictive models can exhibit advantages of a least costly and noninvasive method. Data mining has been shown to be a successful way that automates analysis of data repositories and establishes models to make predictions, classifications, clustering, and clinical decision-making based on the core methodology called machine learning (172, 173). Best et al. (174) established a diagnostic algorithm based on age, sex, and tumor biomarkers of AFP, AFP-L3, and DCP for the diagnosis of HCC, and the model showed a sensitivity of 67.5% and specificity over 90% for diagnosing ANHC and an AUROC of 0.924, specificity of 93.3%, and sensitivity of 85.6% for diagnosing early-stage HCC.

Incorporation of some new biomarkers into a diagnostic model may be valuable to improve the diagnostic performance of the model. Wang et al. (175) found that fucosylation was elevated in HCC patients compared with cirrhotic patients and developed a diagnostic model that incorporated fucosylated kininogen with age, gender, serum alkaline phosphatase, alanine aminotransaminase levels, and AFP for predicting HCC incidence. This model has an AUROC of 0.970 and a true positive rate of 89% for detecting ANHC and early-stage HCC patients, whereas the AUROC of AFP was 0.597 with a true positive rate of 0% at a 5% false positive rate and presented better diagnostic performance compared with their previous model based on simple clinical metrics.

Conventional demographic and clinical characteristics also had been used for the diagnosis of ANHC. For a non-invasive prediction of ANHC, Luo et al. (176) developed a logistic regression model based on the combination of multiple hematological parameters including mean platelet volume, red blood cell distribution width, mean platelet volume to platelet count ratio, neutrophil/lymphocyte ratio, and platelet count/lymphocyte ratio, and this model presented superior diagnostic efficiency with an AUROC of 0.922, sensitivity of 83.0%, and specificity of 93.1%, and high diagnostic efficiency for the early diagnosis of ANHC and was confirmed in four validation sets from different hospitals, with AUROCs of 0.839–0.901, sensitivities of 78.3–87.7%, and specificities of 88.9–92.5%. We also used clinical metrics to establish a model for identifying HCC at various AFP levels in cirrhotic patients by binary logistic stepwise regression analysis (177), and the model incorporating 6 parameters (indicators of age, AFP, Na<sup>+</sup>, Cl<sup>-</sup>,



**TABLE 1 |** New blood biomarkers with potential value for AFP-negative hepatocellular carcinoma diagnosis.

Biomarkers	Molecule type	Method	Subject number	Diagnostic performance			References
				AUROC	Sensitivity (%)	Specificity (%)	
Mutations of circulating cell-free DNA	DNA	Next-generation sequencing	Cases: 33 Controls: 37	0.960	73.0	100	(37)
Circulating cell-free DNA	DNA	Fluorescence intensity measurement	Cases: 193 Controls: 876	0.836	73.6	79.7	(39)
miR-21	RNA	Quantitative RT-PCR	Cases: 58 Controls: 278	0.831	81.2	83.2	(43)
miR-15b and miR-130b classifier	RNA	Qpcr	Cases: 30 Controls: 59	0.980	96.7	91.5	(44)
miR-363-5p, miR-765 with PIVKA-II	RNA+ protein	Qrt-PCR+ ELISA	Cases: 214 Controls: 410	0.930	79.4	95.4	(45)
miR-125b and miR-27a	RNA	Qrt-PCR	Cases: 38 Controls: 48	0.845	80.0	87.2	(46)
miRNA classifier (miR-29a, miR-29c, miR-133a, miR-143, miR-145, miR-192, and miR-505)	RNA	Qpcr	Cases: 66 Controls: 199	0.825	75.8	88.2	(47)
CircPanel (hsa_circ_0000976, hsa_circ_0007750, and hsa_circ_0139897)	circRNAs	Qpcr	Cases: UK Controls: 236	0.851	83.0	87.3	(58)
DCP/PIVKA-II	Protein	ECLIA CLEIA	Cases: 76 Controls: 285	0.856	76.3	89.1	(62)
AFP-L3	Protein	Microchip capillary electrophoresis and liquid-phase binding assay	Cases: 270 Controls: 396	0.707	41.5	85.1	(63)
AFP-L3+ PIVKA-II	Protein	Microchip capillary electrophoresis and liquid-phase binding assay	Cases: 38 Controls: 74	0.939	92.1	79.7	(64)
AKR1B10	Protein	Time-resolved fluorescent kit	Cases: 73 Controls: 280	0.891	71.2	92.6	(74)
DKK1	Glycoprotein	ELISA	Cases: 179 Controls: 407	0.841	70.4	90.0	(81)
MDK	Protein	ELISA	Cases: 121 Controls: 455	0.926	89.2	UK	(85)
Hsp90 $\alpha$	Protein	ELISA	Cases: 197 Controls: 743	0.971	93.9	91.3	(88)
ANGPTL2	Glycoprotein	ELISA	Cases: 30 Controls: 35	0.919	NA	NA	(91)
CAP2	Protein	ELISA	Cases: 35 Controls: 49	0.840	82.9	79.6	(99)
CCT3	Protein	ELISA	Cases: 38 Controls: 88	0.871	92.1	70.5	(106)
IQGAP3	Protein	ELISA	Cases: 38 Controls: 88	0.804	81.6	71.6	(106)
Soluble Axl	Protein	ELISA	Cases: 137 Controls: 65	0.803	73.0	70.8	(113)
OPN	Phosphoprotein	ELISA	Cases: 20 Controls: 23	0.870	AN	NA	(118)
MCM6	Protein	ELISA	Cases: 13 Controls: 59	0.857	76.9	89.8	(121)
CRP	Protein	Laser nephelometry	Cases: 65 Controls: 64	UK	95.9	92.2	(126)
Annexin A2	Protein	ELISA	Cases: 74 Controls: 123	0.770	89.2	58.5	(144)

(Continued)

TABLE 1 | Continued

Biomarkers	Molecule type	Method	Subject number	Diagnostic performance			References
				AUROC	Sensitivity (%)	Specificity (%)	
CYP17A1	Protein	ELISA	Cases: 267 Controls: 366	NA	89.1	NA	(149)
GS	Protein	ELISA	Cases: 75 Controls: 57	0.913	81.9	100	(151)
AGP	glycoprotein	ELISA	Cases: 44 Controls: 58	0.709	52.0	80.0	(154)
Pre-albumin	Protein	Turbidimetry	Cases: 214 Controls: 210	0.900	90.1	86.3	(7)
D-Dimer	Protein	Immunoturbidimetry	Cases: 214 Controls: 210	0.868	73.8	87.1	(7)

AUROC, area under the receiver operating characteristic curve; DCP, des-gamma-carboxy prothrombin; PIVKA-II, prothrombin induced by vitamin K absence II; AFP-L3,  $\alpha$ -fetoprotein fraction L3; AKR1B10, aldo-keto reductase family 1 member B10; DKK1, dickkopf-1; MDK, midkine; Hsp90 $\alpha$ , heat shock protein 90 $\alpha$ ; ANGPTL2, angiopoietin-like protein 2; PON1, paraoxonase 1; CAP2, cyclase-associated protein 2; CCT3, chaperonin containing TCP1 complex subunit 3; IQGAP3, IQ-motif-containing GTPase-activating protein-3; Axl, the transforming receptor tyrosine kinase; OPN, osteopontin; MCM6, minichromosome maintenance complex component 6; CRP, c-reactive protein; TGM2, tissue transglutaminase 2; CYP17A1, the cytochrome P450, family 17, subfamily A, polypeptide 1; GS, glutamine synthetase; AGP, alpha-1 acid glycoprotein; UK, unknown; qPCR, real-time quantitative PCR; qRT-PCR, quantitative real-time polymerase chain reaction; ECLIA, electrochemiluminescence immunoassay; CLEIA, chemiluminescence enzyme immunoassay.

alkaline phosphatase, and activated partial thromboplastin time) showed an AUROC of 0.854, 68.5% sensitivity, 86.6% specificity, and 80.0% accuracy for the identification of cirrhotic patients with ANHC.

## SUMMARY AND CONCLUSIONS

Because the diagnosis of ANHC is a challenge in clinical practice, many studies have been conducted to identify new blood biomarkers complementary to AFP for the diagnosis of HCC, including ANHC. The new blood biomarkers with potential value for ANHC diagnosis are summarized in **Table 1**. These new blood biomarkers consist of three types: DNA, RNA, and protein. Although these new biomarkers appear valuable for ANHC diagnosis, the results were usually obtained from monometer, preclinical studies with small sample sizes; therefore, further assessment in studies with large sample sizes, multiple centers, and a more rigorous design should be performed to validate the clinical diagnostic value of these biomarkers. A single biomarker alone is usually insufficient in sensitivity and

specificity for the clinical detection of ANHC. The combination of several biomarkers including clinical variables could enhance the diagnostic performance for ANHC detection; thus, the development and validation of diagnostic models may be a promising approach to achieve a high efficiency for ANHC diagnosis. Conclusively, it remains a challenge to diagnose ANHC using blood biomarkers, and continuous efforts should be made in discovering new biomarkers, validating current biomarkers, and incorporating multiple biomarkers.

## AUTHOR CONTRIBUTIONS

TW wrote the initial draft. K-HZ revised the review. All authors checked and approved the final version.

## FUNDING

This work was supported by the National Natural Science Foundation of China (81760536) and Jiangxi Provincial Department of Science and Technology, China (20171ACB21055 and 20192BBG70048).

## REFERENCES

- Bray F, Ferlay J, Soerjomataram I, Siegel RL, Torre LA, Jemal A. Global cancer statistics 2018: GLOBOCAN estimates of incidence and mortality worldwide for 36 cancers in 185 countries. *CA Cancer J Clin.* (2018) 68:394–424. doi: 10.3322/caac.21492
- Sayiner M, Golabi P, Younossi ZM. Disease burden of hepatocellular carcinoma: a global perspective. *Dig Dis Sci.* (2019) 64:910–7. doi: 10.1007/s10620-019-05537-2
- Terentiev AA, Moldogazieva NT. Alpha-fetoprotein: a renaissance. *Tumor Biol.* (2013) 34:2075–91. doi: 10.1007/s13277-013-0904-y
- Gupta S, Bent S, Kohlwes J. Test characteristics of alpha-fetoprotein for detecting hepatocellular carcinoma in patients with hepatitis C: a systematic review and critical analysis. *Ann Intern Med.* (2003) 139:46–50. doi: 10.7326/0003-4819-139-1-200307010-00012
- Zhang G, Ha SA, Kim HK, Yoo J, Kim S, Lee YS, et al. Combined analysis of AFP and HCCP-1 as an useful serological marker for small hepatocellular carcinoma: a prospective cohort study. *Dis Markers.* (2012) 32:265–71. doi: 10.1155/2012/964036
- Farinati F, Marino D, de Giorgio M, Baldan A, Cantarini M, Cursaro C, et al. Diagnostic and prognostic role of alpha-fetoprotein in hepatocellular carcinoma: both or neither? *Am J Gastroenterol.* (2006) 101:524–32. doi: 10.1111/j.1572-0241.2006.00443.x
- Jing W, Peng R, Zhu M, Lv S, Jiang S, Ma J, et al. Differential expression and diagnostic significance of pre-albumin, fibrinogen combined with D-dimer in AFP-negative hepatocellular carcinoma. *Pathol Oncol Res.* (2019) 26:1669–76. doi: 10.1007/s12253-019-00752-8

8. Thompson CJ, Rogers G, Hewson P, Wright D, Anderson R, Cramp M, et al. Surveillance of cirrhosis for hepatocellular carcinoma: systematic review and economic analysis. *Health Technol Assess.* (2007) 11:1–206. doi: 10.3310/hta11340
9. Bai DS, Zhang C, Chen P, Jin SJ, Jiang GQ. The prognostic correlation of AFP level at diagnosis with pathological grade, progression, and survival of patients with hepatocellular carcinoma. *Sci Rep.* (2017) 7:12870. doi: 10.1038/s41598-017-12834-1
10. Carr BI, Guerra V. Low alpha-fetoprotein levels are associated with improved survival in hepatocellular carcinoma patients with portal vein thrombosis. *Digest Dis Sci.* (2016) 61:937–47. doi: 10.1007/s10620-015-3922-3
11. An SL, Xiao T, Wang LM, Rong WQ, Wu F, Feng L, et al. Prognostic significance of preoperative serum alpha-fetoprotein in hepatocellular carcinoma and correlation with clinicopathological factors: a single-center experience from China. *Asian Pac J Cancer Prev.* (2015) 16:4421–7. doi: 10.7314/APJCP.2015.16.10.4421
12. Xu Y, Lu X, Mao Y, Sang X, Zhao H, Du S, et al. Clinical diagnosis and treatment of alpha-fetoprotein-negative small hepatic lesions. *Chin J Cancer Res.* (2013) 25:382–8. doi: 10.3978/j.issn.1000-9604.2013.08.12
13. Xu J, Liu C, Zhou L, Tian F, Tai MH, Wei JC, et al. Distinctions between clinicopathological factors and prognosis of alpha-fetoprotein negative and positive hepatocellular carcinoma patients. *Asian Pac J Cancer Prev.* (2012) 13:559–62. doi: 10.7314/APJCP.2012.13.2.559
14. Li SP, Wu LQ. [Impact of serum alpha-fetoprotein level on short-term recurrence after R0 resection in primary hepatocellular carcinoma]. *Zhonghua Wai Ke Za Zhi.* (2013) 51:600–3. doi: 10.3760/cma.j.issn.0529-5815.2013.07.006
15. Zhou J, Yan T, Bi X, Zhao H, Huang Z, Zhang Y, et al. Evaluation of seven different staging systems for alpha-fetoprotein expression in hepatocellular carcinoma after hepatectomy. *Tumour Biol.* (2013) 34:1061–70. doi: 10.1007/s13277-013-0646-x
16. Wang NY, Wang C, Li W, Wang GJ, Cui GZ, He H, et al. Prognostic value of serum AFP, AFP-L3, and GP73 in monitoring short-term treatment response and recurrence of hepatocellular carcinoma after radiofrequency ablation. *Asian Pac J Cancer Prev.* (2014) 15:1539–44. doi: 10.7314/APJCP.2014.15.4.1539
17. Xia Y, Yan ZL, Xi T, Wang K, Li J, Shi LH, et al. A case-control study of correlation between preoperative serum AFP and recurrence of hepatocellular carcinoma after curative hepatectomy. *Hepatogastroenterology.* (2012) 59:2248–54. doi: 10.5754/hge11978
18. Bi X, Yan T, Zhao H, Zhao J, Li Z, Huang Z, et al. [Correlation of alpha fetoprotein with the prognosis of hepatocellular carcinoma after hepatectomy in an ethnic Chinese population]. *Zhonghua Yi Xue Za Zhi.* (2014) 94:2645–9. doi: 10.3760/cma.j.issn.0376-2491.2014.34.002
19. Singal AG, Chan V, Getachew Y, Guerrero R, Reisch JS, Cuthbert JA. Predictors of liver transplant eligibility for patients with hepatocellular carcinoma in a safety net hospital. *Dig Dis Sci.* (2012) 57:580–6. doi: 10.1007/s10620-011-1904-7
20. Eurich D, Boas-Knoop S, Morawietz L, Neuhaus R, Somasundaram R, Ruehl M, et al. Association of mannose-binding lectin-2 gene polymorphism with the development of hepatitis C-induced hepatocellular carcinoma. *Liver Int.* (2011) 31:1006–12. doi: 10.1111/j.1478-3231.2011.02522.x
21. Liu C, Xiao GQ, Yan LN, Li B, Jiang L, Wen TF, et al. Value of alpha-fetoprotein in association with clinicopathological features of hepatocellular carcinoma. *World J Gastroenterol.* (2013) 19:1811–9. doi: 10.3748/wjg.v19.i11.1811
22. Ilikhan SU, Bilici M, Sahin H, Akca AS, Can M, Oz II, et al. Assessment of the correlation between serum prothrombin and alpha-fetoprotein levels in patients with hepatocellular carcinoma. *World J Gastroenterol.* (2015) 21:6999–7007. doi: 10.3748/wjg.v21.i22.6999
23. Abbasi A, Bhutto AR, Butt N, Munir SM. Correlation of serum alpha fetoprotein and tumor size in hepatocellular carcinoma. *J Pak Med Assoc.* (2012) 62:33–6.
24. Tang H, Tang XY, Liu M, Li X. Targeting alpha-fetoprotein represses the proliferation of hepatoma cells via regulation of the cell cycle. *Clin Chim Acta.* (2008) 394:81–8. doi: 10.1016/j.cca.2008.04.012
25. Lu Y, Zhu M, Li W, Lin B, Dong X, Chen Y, et al. Alpha fetoprotein plays a critical role in promoting metastasis of hepatocellular carcinoma cells. *J Cell Mol Med.* (2016) 20:549–58. doi: 10.1111/jcmm.12745
26. Parpart S, Roessler S, Dong F, Rao V, Takai A, Ji J, et al. Modulation of miR-29 expression by alpha-fetoprotein is linked to the hepatocellular carcinoma epigenome. *Hepatology.* (2014) 60:872–83. doi: 10.1002/hep.27200
27. Sunagozaka H, Honda M, Yamashita T, Nishino R, Takatori H, Arai K, et al. Identification of a secretory protein c19orf10 activated in hepatocellular carcinoma. *Int J Cancer.* (2011) 129:1576–85. doi: 10.1002/ijc.25830
28. Zhang L, Wang K, Deng Q, Li W, Zhang X, Liu X. Identification of key hydroxymethylated genes and transcription factors associated with alpha-fetoprotein-negative hepatocellular carcinoma. *Dna Cell Biol.* (2019) 38:1346–56. doi: 10.1089/dna.2019.4689
29. Gorog D, Regoly-Merei J, Paku S, Kopper L, Nagy P. Alpha-fetoprotein expression is a potential prognostic marker in hepatocellular carcinoma. *World J Gastroenterol.* (2005) 11:5015–8. doi: 10.3748/wjg.v11.i32.5015
30. Zheng M, Ruan Y, Yang M, Guan Y, Wu Z. The comparative study on ultrastructure and immunohistochemistry in AFP negative and positive hepatocellular carcinoma. *J Huazhong Univ Sci Technol Med Sci.* (2004) 24:547–9. doi: 10.1007/BF02911350
31. Sun J, Zhao Y, Qin L, Li K, Zhao Y, Sun H, et al. Metabolomic profiles for HBV related hepatocellular carcinoma including alpha-fetoproteins positive and negative subtypes. *Front Oncol.* (2019) 9:1069. doi: 10.3389/fonc.2019.01069
32. Lu Y, Fang Z, Li M, Qian C, Zeng T, Lu L, et al. Dynamic edge-based biomarker noninvasively predicts hepatocellular carcinoma with hepatitis B virus infection for individual patients based on blood testing. *J Mol Cell Biol.* (2019) 11:665–77. doi: 10.1093/jmcb/mjz025
33. Zheng J, Zhu MY, Wu F, Kang B, Liang J, Heskia F, et al. A blood-based 22-gene expression signature for hepatocellular carcinoma identification. *Ann Transl Med.* (2020) 8:195. doi: 10.21037/atm.2020.01.93
34. Fleischhacker M, Schmidt B. Circulating nucleic acids (CNAs) and cancer—a survey. *Biochim Biophys Acta.* (2007) 1775:181–232. doi: 10.1016/j.bbcan.2006.10.001
35. Jung K, Fleischhacker M, Rabien A. Cell-free DNA in the blood as a solid tumor biomarker—a critical appraisal of the literature. *Clin Chim Acta.* (2010) 411:1611–24. doi: 10.1016/j.cca.2010.07.032
36. Ye Q, Ling S, Zheng S, Xu X. Liquid biopsy in hepatocellular carcinoma: circulating tumor cells and circulating tumor DNA. *Mol Cancer.* (2019) 18:114. doi: 10.1186/s12943-019-1043-x
37. Xiong Y, Xie CR, Zhang S, Chen J, Yin ZY. Detection of a novel panel of somatic mutations in plasma cell-free DNA and its diagnostic value in hepatocellular carcinoma. *Cancer Manag Res.* (2019) 11:5745–56. doi: 10.2147/CMAR.S197455
38. Iizuka N, Sakaida I, Moribe T, Fujita N, Miura T, Stark M, et al. Elevated levels of circulating cell-free DNA in the blood of patients with hepatitis C virus-associated hepatocellular carcinoma. *Anticancer Res.* (2006) 26:4713–9.
39. Wang T, Zhang KH, Hu PP, Huang ZY, Zhang P, Wan QS, et al. Simple and robust diagnosis of early, small and AFP-negative primary hepatic carcinomas: an integrative approach of serum fluorescence and conventional blood tests. *Oncotarget.* (2016) 7:64053–70. doi: 10.18632/oncotarget.11771
40. Wang T, Zhang KH, Hu PP, Wan QS, Han FL, Zhou JM, et al. Combination of dual serum fluorescence, AFP and hepatic function tests is valuable to identify HCC in AFP-elevated liver diseases. *Oncotarget.* (2017) 8:97758–68. doi: 10.18632/oncotarget.22050
41. Callegari E, Elamin BK, Sabbioni S, Gramantieri L, Negrini M. Role of microRNAs in hepatocellular carcinoma: a clinical perspective. *Onco Targets Ther.* (2013) 6:1167–78. doi: 10.2147/OTT.S36161
42. Feng YH, Tsao CJ. Emerging role of microRNA-21 in cancer. *Biomed Rep.* (2016) 5:395–402. doi: 10.3892/br.2016.747
43. Guo X, Lv X, Lv X, Ma Y, Chen L, Chen Y. Circulating miR-21 serves as a serum biomarker for hepatocellular carcinoma and correlated with distant metastasis. *Oncotarget.* (2017) 8:44050–8. doi: 10.18632/oncotarget.17211
44. Liu AM, Yao TJ, Wang W, Wong KF, Lee NP, Fan ST, et al. Circulating miR-15b and miR-130b in serum as potential markers for detecting hepatocellular carcinoma: a retrospective cohort study. *BMJ Open.* (2012) 2:e825. doi: 10.1136/bmjopen-2012-000825
45. Tian Z, Yu T, Wei H, Ning N. Clinical value of LHP-associated microRNAs combined with protein induced by vitamin K deficiency or antagonist-II in

- the diagnosis of alpha-fetoprotein-negative hepatocellular carcinoma. *J Clin Lab Anal.* (2020) 34:e23071. doi: 10.1002/jcla.23071
46. Zuo D, Chen L, Liu X, Wang X, Xi Q, Luo Y, et al. Combination of miR-125b and miR-27a enhances sensitivity and specificity of AFP-based diagnosis of hepatocellular carcinoma. *Tumor Biol.* (2015) 37:6539–49. doi: 10.1007/s13277-015-4545-1
  47. Lin X, Chong Y, Guo Z, Xie C, Yang X, Zhang Q, et al. A serum microRNA classifier for early detection of hepatocellular carcinoma: a multicentre, retrospective, longitudinal biomarker identification study with a nested case-control study. *Lancet Oncol.* (2015) 16:804–15. doi: 10.1016/S1470-2045(15)00048-0
  48. Chen LL. The biogenesis and emerging roles of circular RNAs. *Nat Rev Mol Cell Biol.* (2016) 17:205–11. doi: 10.1038/nrm.2015.32
  49. Sun H, Tang W, Rong D, Jin H, Fu K, Zhang W, et al. Hsa\_circ\_0000520, a potential new circular RNA biomarker, is involved in gastric carcinoma. *Cancer Biomark.* (2018) 21:299–306. doi: 10.3233/CBM-170379
  50. Li P, Chen S, Chen H, Mo X, Li T, Shao Y, et al. Using circular RNA as a novel type of biomarker in the screening of gastric cancer. *Clin Chim Acta.* (2015) 444:132–6. doi: 10.1016/j.cca.2015.02.018
  51. Li T, Shao Y, Fu L, Xie Y, Zhu L, Sun W, et al. Plasma circular RNA profiling of patients with gastric cancer and their droplet digital RT-PCR detection. *J Mol Med.* (2018) 96:85–96. doi: 10.1007/s00109-017-1600-y
  52. Yin WB, Yan MG, Fang X, Guo JJ, Xiong W, Zhang RP. Circulating circular RNA hsa\_circ\_0001785 acts as a diagnostic biomarker for breast cancer detection. *Clin Chim Acta.* (2018) 487:363–8. doi: 10.1016/j.cca.2017.10.011
  53. Zhu X, Wang X, Wei S, Chen Y, Chen Y, Fan X, et al. hsa\_circ\_0013958: a circular RNA and potential novel biomarker for lung adenocarcinoma. *FEBS J.* (2017) 284:2170–82. doi: 10.1111/febs.14132
  54. Hang D, Zhou J, Qin N, Zhou W, Ma H, Jin G, et al. A novel plasma circular RNA circFARSA is a potential biomarker for non-small cell lung cancer. *Cancer Med.* (2018) 7:2783–91. doi: 10.1002/cam4.1514
  55. Yang F, Liu DY, Guo JT, Ge N, Zhu P, Liu X, et al. Circular RNA circ-LDLRAD3 as a biomarker in diagnosis of pancreatic cancer. *World J Gastroenterol.* (2017) 23:8345–54. doi: 10.3748/wjg.v23.i47.8345
  56. Zhang X, Xu Y, Qian Z, Zheng W, Wu Q, Chen Y, et al. circRNA\_104075 stimulates YAP-dependent tumorigenesis through the regulation of HNF4a and may serve as a diagnostic marker in hepatocellular carcinoma. *Cell Death Dis.* (2018) 9:1091. doi: 10.1038/s41419-018-1132-6
  57. Li Z, Zhou Y, Yang G, He S, Qiu X, Zhang L, et al. Using circular RNA SMARCA5 as a potential novel biomarker for hepatocellular carcinoma. *Clin Chim Acta.* (2019) 492:37–44. doi: 10.1016/j.cca.2019.02.001
  58. Yu J, Ding WB, Wang MC, Guo XG, Xu J, Xu QG, et al. Plasma circular RNA panel to diagnose hepatitis B virus-related hepatocellular carcinoma: a large-scale, multicenter study. *Int J Cancer.* (2019) 146:1754–63. doi: 10.1002/ijc.32647
  59. Luo P, Wu S, Yu Y, Ming X, Li S, Zuo X, et al. Current status and perspective biomarkers in AFP negative HCC: towards screening for and diagnosing hepatocellular carcinoma at an earlier stage. *Pathol Oncol Res.* (2019) 26:599–603. doi: 10.1007/s12253-019-00585-5
  60. Wang X, Zhang W, Liu Y, Gong W, Sun P, Kong X, et al. Diagnostic value of prothrombin induced by the absence of vitamin K or antagonist-II (PIVKA-II) for early stage HBV related hepatocellular carcinoma. *Infect Agents Cancer.* (2017) 12:47. doi: 10.1186/s13027-017-0153-6
  61. Liu Z, Wu M, Lin D, Li N. Des-gamma-carboxyprothrombin is a favorable biomarker for the early diagnosis of alfa-fetoprotein-negative hepatitis B virus-related hepatocellular carcinoma. *J Int Med Res.* (2020) 48:1220702127. doi: 10.1177/0300060520902575
  62. Ji J, Wang H, Li Y, Zheng L, Yin Y, Zou Z, et al. Diagnostic evaluation of des-gamma-carboxy prothrombin versus alpha-fetoprotein for hepatitis B virus-related hepatocellular carcinoma in China: a large-scale, multicentre study. *PLoS ONE.* (2016) 11:e153227. doi: 10.1371/journal.pone.0153227
  63. Toyoda H, Kumada T, Tada T, Kaneoka Y, Maeda A, Kanke F, et al. Clinical utility of highly sensitive Lens culinaris agglutinin-reactive alpha-fetoprotein in hepatocellular carcinoma patients with alpha-fetoprotein <20 ng/mL. *Cancer Sci.* (2011) 102:1025–31. doi: 10.1111/j.1349-7006.2011.01875.x
  64. Choi JY, Jung SW, Kim HY, Kim M, Kim Y, Kim DG, et al. Diagnostic value of AFP-L3 and PIVKA-II in hepatocellular carcinoma according to total-AFP. *World J Gastroenterol.* (2013) 19:339–46. doi: 10.3748/wjg.v19.i3.339
  65. Chen H, Zhang Y, Li S, Li N, Chen Y, Zhang B, et al. Direct comparison of five serum biomarkers in early diagnosis of hepatocellular carcinoma. *Cancer Manag Res.* (2018) 10:1947–58. doi: 10.2147/CMAR.S167036
  66. Tian L, Wang Y, Xu D, Gui J, Jia X, Tong H, et al. Serological AFP/Golgi protein 73 could be a new diagnostic parameter of hepatic diseases. *Int J Cancer.* (2011) 129:1923–31. doi: 10.1002/ijc.25838
  67. Zhang Z, Zhang Y, Wang Y, Xu L, Xu W. Alpha-fetoprotein-L3 and Golgi protein 73 may serve as candidate biomarkers for diagnosing alpha-fetoprotein-negative hepatocellular carcinoma. *Onco Targets Ther.* (2016) 9:123–9. doi: 10.2147/OTT.S90732
  68. Ma J, Yan R, Zu X, Cheng JM, Rao K, Liao DF, et al. Aldo-keto reductase family 1 B10 affects fatty acid synthesis by regulating the stability of acetyl-CoA carboxylase-alpha in breast cancer cells. *J Biol Chem.* (2008) 283:3418–23. doi: 10.1074/jbc.M707650200
  69. Yan R, Zu X, Ma J, Liu Z, Adeyanju M, Cao D. Aldo-keto reductase family 1 B10 gene silencing results in growth inhibition of colorectal cancer cells: implication for cancer intervention. *Int J Cancer.* (2007) 121:2301–6. doi: 10.1002/ijc.22933
  70. Matkowskyj KA, Bai H, Liao J, Zhang W, Li H, Rao S, et al. Aldoketoreductase family 1B10 (AKR1B10) as a biomarker to distinguish hepatocellular carcinoma from benign liver lesions. *Hum Pathol.* (2014) 45:834–43. doi: 10.1016/j.humpath.2013.12.002
  71. Schmitz KJ, Sotiropoulos GC, Baba HA, Schmid KW, Muller D, Paul A, et al. AKR1B10 expression is associated with less aggressive hepatocellular carcinoma: a clinicopathological study of 168 cases. *Liver Int.* (2011) 31:810–6. doi: 10.1111/j.1478-3231.2011.02511.x
  72. Han C, Gao L, Bai H, Dou X. Identification of a role for serum aldo-keto reductase family 1 member B10 in early detection of hepatocellular carcinoma. *Oncol Lett.* (2018) 16:7123–30. doi: 10.3892/ol.2018.9547
  73. Zhu R, Xiao J, Luo D, Dong M, Sun T, Jin J. Serum AKR1B10 predicts the risk of hepatocellular carcinoma - a retrospective single-center study. *Gastroenterol Hepatol.* (2019) 42:614–21. doi: 10.1016/j.gastrohep.2019.06.007
  74. Ye X, Li C, Zu X, Lin M, Liu Q, Liu J, et al. A large-scale multicenter study validates AKR1B10 as a new prevalent serum marker for detection of hepatocellular carcinoma. *Hepatology.* (2019) 69:2489–501. doi: 10.1002/hep.30519
  75. Sato N, Yamabuki T, Takano A, Koinuma J, Aragaki M, Masuda K, et al. Wnt inhibitor Dickkopf-1 as a target for passive cancer immunotherapy. *Cancer Res.* (2010) 70:5326–36. doi: 10.1158/0008-5472.CAN-09-3879
  76. Rachner TD, Thiele S, Gobel A, Browne A, Fuessel S, Erdmann K, et al. High serum levels of Dickkopf-1 are associated with a poor prognosis in prostate cancer patients. *BMC Cancer.* (2014) 14:649. doi: 10.1186/1471-2407-14-649
  77. Peng YH, Xu YW, Guo H, Huang LS, Tan HZ, Hong CQ, et al. Combined detection of serum Dickkopf-1 and its autoantibodies to diagnose esophageal squamous cell carcinoma. *Cancer Med.* (2016) 5:1388–96. doi: 10.1002/cam4.702
  78. Tung EK, Mak CK, Fatima S, Lo RC, Zhao H, Zhang C, et al. Clinicopathological and prognostic significance of serum and tissue Dickkopf-1 levels in human hepatocellular carcinoma. *Liver Int.* (2011) 31:1494–504. doi: 10.1111/j.1478-3231.2011.02597.x
  79. Fatima S, Luk JM, Poon RT, Lee NP. Dysregulated expression of dickkopfs for potential detection of hepatocellular carcinoma. *Expert Rev Mol Diagn.* (2014) 14:535–48. doi: 10.1586/14737159.2014.915747
  80. Yang H, Chen GD, Fang F, Liu Z, Lau SH, Zhang JF, et al. Dickkopf-1: as a diagnostic and prognostic serum marker for early hepatocellular carcinoma. *Int J Biol Markers.* (2013) 28:286–97. doi: 10.5301/IBM.5000015
  81. Shen Q, Fan J, Yang XR, Tan Y, Zhao W, Xu Y, et al. Serum DKK1 as a protein biomarker for the diagnosis of hepatocellular carcinoma: a large-scale, multicentre study. *Lancet Oncol.* (2012) 13:817–26. doi: 10.1016/S1470-2045(12)70233-4
  82. Mao L, Wang Y, Wang D, Han G, Fu S, Wang J. TEMs but not DKK1 could serve as complementary biomarkers for AFP in diagnosing AFP-negative hepatocellular carcinoma. *PLoS ONE.* (2017) 12:e183880. doi: 10.1371/journal.pone.0183880
  83. Zhu M, Zheng J, Wu F, Kang B, Liang J, Heskia F, et al. OPN is a promising serological biomarker for hepatocellular carcinoma diagnosis. *J Med Virol.* (2020). doi: 10.1002/jmv.25704. [Epub ahead of print].



84. Muramatsu T, Kadomatsu K. Midkine: an emerging target of drug development for treatment of multiple diseases. *Br J Pharmacol.* (2014) 171:811–3. doi: 10.1111/bph.12571
85. Zhu WW, Guo JJ, Guo L, Jia HL, Zhu M, Zhang JB, et al. Evaluation of midkine as a diagnostic serum biomarker in hepatocellular carcinoma. *Clin Cancer Res.* (2013) 19:3944–54. doi: 10.1158/1078-0432.CCR-12-3363
86. Lu Q, Li J, Cao H, Lv C, Wang X, Cao S. Comparison of diagnostic accuracy of Midkine and AFP for detecting hepatocellular carcinoma: a systematic review and meta-analysis. *Biosci Rep.* (2020) 40:BSR20192424. doi: 10.1042/BSR20192424
87. Wang X, Song X, Zhuo W, Fu Y, Shi H, Liang Y, et al. The regulatory mechanism of Hsp90 $\alpha$  secretion and its function in tumor malignancy. *Proc Natl Acad Sci USA.* (2009) 106:21288–93. doi: 10.1073/pnas.0908151106
88. Fu Y, Xu X, Huang D, Cui D, Liu L, Liu J, et al. Plasma heat shock protein 90 $\alpha$  as a biomarker for the diagnosis of liver cancer: an official, large-scale, and multicenter clinical trial. *Ebiomedicine.* (2017) 24:56–63. doi: 10.1016/j.ebiom.2017.09.007
89. Endo M. The roles of ANGPTL families in cancer progression. *J UOEH.* (2019) 41:317–25. doi: 10.7888/juoh.41.317
90. Gao L, Ge C, Fang T, Zhao F, Chen T, Yao M, et al. ANGPTL2 promotes tumor metastasis in hepatocellular carcinoma. *J Gastroenterol Hepatol.* (2015) 30:396–404. doi: 10.1111/jgh.12702
91. Zhou J, Yang W, Zhang S, He X, Lin J, Zhou T, et al. Diagnostic value of angiopoietin-like protein 2 for CHB-related hepatocellular carcinoma. *Cancer Manag Res.* (2019) 11:7159–69. doi: 10.2147/CMAR.S217170
92. Stowell SR, Ju T, Cummings RD. Protein glycosylation in cancer. *Annu Rev Pathol.* (2015) 10:473–510. doi: 10.1146/annurev-pathol-012414-040438
93. Sun C, Chen P, Chen Q, Sun L, Kang X, Qin X, et al. Serum paraoxonase 1 heteroplasmon, a fucosylated, and sialylated glycoprotein in distinguishing early hepatocellular carcinoma from liver cirrhosis patients. *Acta Biochim Biophys Sin.* (2012) 44:765–73. doi: 10.1093/abbs/gms055
94. Zhang S, Jiang K, Zhang Q, Guo K, Liu Y. Serum fucosylated paraoxonase 1 as a potential glycoprotein biomarker for clinical diagnosis of early hepatocellular carcinoma using ELISA Index. *Glycoconjugate J.* (2015) 32:119–25. doi: 10.1007/s10719-015-9576-8
95. Shu H, Li W, Shang S, Qin X, Zhang S, Liu Y. Diagnosis of AFP-negative early-stage hepatocellular carcinoma using Fuc-PON1. *Discov Med.* (2017) 23:163–8.
96. Peche V, Shekar S, Leichter M, Korte H, Schroder R, Schleicher M, et al. CAP2, cyclase-associated protein 2, is a dual compartment protein. *Cell Mol Life Sci.* (2007) 64:2702–15. doi: 10.1007/s00018-007-7316-3
97. Li L, Fu LQ, Wang HJ, Wang YY. CAP2 is a valuable biomarker for diagnosis and prognostic in patients with gastric cancer. *Pathol Oncol Res.* (2020) 26:273–9. doi: 10.1007/s12253-018-0450-4
98. Shibata R, Mori T, Du W, Chuma M, Gotoh M, Shimazu M, et al. Overexpression of cyclase-associated protein 2 in multistage hepatocarcinogenesis. *Clin Cancer Res.* (2006) 12:5363–8. doi: 10.1158/1078-0432.CCR-05-2245
99. Chen M, Zheng T, Han S, Zhang L, Bai Y, Fang X, et al. A preliminary study of plasma cyclase-associated protein 2 as a novel biomarker for early stage and alpha-fetoprotein negative hepatocellular carcinoma patients. *Clin Res Hepatol Gastroenterol.* (2015) 39:215–21. doi: 10.1016/j.clinre.2014.08.006
100. Boudiaf-Benmammar C, Cresteil T, Melki R. The cytosolic chaperonin CCT/TRiC and cancer cell proliferation. *PLoS ONE.* (2013) 8:e60895. doi: 10.1371/journal.pone.0060895
101. Zhang Y, Wang Y, Wei Y, Wu J, Zhang P, Shen S, et al. Molecular chaperone CCT3 supports proper mitotic progression and cell proliferation in hepatocellular carcinoma cells. *Cancer Lett.* (2016) 372:101–9. doi: 10.1016/j.canlet.2015.12.029
102. Cui X, Hu ZP, Li Z, Gao PJ, Zhu JY. Overexpression of chaperonin containing TCP1, subunit 3 predicts poor prognosis in hepatocellular carcinoma. *World J Gastroenterol.* (2015) 21:8588–604. doi: 10.3748/wjg.v21.i28.8588
103. Nojima H, Adachi M, Matsui T, Okawa K, Tsukita S, Tsukita S. IQGAP3 regulates cell proliferation through the Ras/ERK signalling cascade. *Nat Cell Biol.* (2008) 10:971–8. doi: 10.1038/ncb1757
104. Kunimoto K, Nojima H, Yamazaki Y, Yoshikawa T, Okanoue T, Tsukita S. Involvement of IQGAP3, a regulator of Ras/ERK-related cascade, in hepatocyte proliferation in mouse liver regeneration and development. *J Cell Physiol.* (2009) 220:621–31. doi: 10.1002/jcp.21798
105. Skawran B, Steinemann D, Weigmann A, Flemming P, Becker T, Flik J, et al. Gene expression profiling in hepatocellular carcinoma: upregulation of genes in amplified chromosome regions. *Mod Pathol.* (2008) 21:505–16. doi: 10.1038/modpathol.3800998
106. Qian EN, Han SY, Ding SZ, Lv X. Expression and diagnostic value of CCT3 and IQGAP3 in hepatocellular carcinoma. *Cancer Cell Int.* (2016) 16:55. doi: 10.1186/s12935-016-0332-3
107. Welsh SJ, Bellamy WT, Briehl MM, Powis G. The redox protein thioredoxin-1 (Trx-1) increases hypoxia-inducible factor 1 $\alpha$  protein expression: Trx-1 overexpression results in increased vascular endothelial growth factor production and enhanced tumor angiogenesis. *Cancer Res.* (2002) 62:5089–95.
108. Kakolyris S, Giatromanolaki A, Koukourakis M, Powis G, Souglakos J, Sivridis E, et al. Thioredoxin expression is associated with lymph node status and prognosis in early operable non-small cell lung cancer. *Clin Cancer Res.* (2001) 7:3087–91.
109. Raffel J, Bhattacharyya AK, Gallegos A, Cui H, Einspahr JG, Alberts DS, et al. Increased expression of thioredoxin-1 in human colorectal cancer is associated with decreased patient survival. *J Lab Clin Med.* (2003) 142:46–51. doi: 10.1016/S0022-2143(03)00068-4
110. Li J, Cheng ZJ, Liu Y, Yan ZL, Wang K, Wu D, et al. Serum thioredoxin is a diagnostic marker for hepatocellular carcinoma. *Oncotarget.* (2015) 6:9551–63. doi: 10.18632/oncotarget.3314
111. Gjerdrum C, Tiron C, Hoiby T, Stefansson I, Haugen H, Sandal T, et al. Axl is an essential epithelial-to-mesenchymal transition-induced regulator of breast cancer metastasis and patient survival. *Proc Natl Acad Sci USA.* (2010) 107:1124–9. doi: 10.1073/pnas.0909333107
112. Ishikawa M, Sonobe M, Nakayama E, Kobayashi M, Kikuchi R, Kitamura J, et al. Higher expression of receptor tyrosine kinase Axl, and differential expression of its ligand, Gas6, predict poor survival in lung adenocarcinoma patients. *Ann Surg Oncol.* (2013) 20(Suppl. 3):S467–76. doi: 10.1245/s10434-012-2795-3
113. Reichl P, Fang M, Starlinger P, Stauder K, Nenutil R, Muller P, et al. Multicenter analysis of soluble Axl reveals diagnostic value for very early stage hepatocellular carcinoma. *Int J Cancer.* (2015) 137:385–94. doi: 10.1002/ijc.29394
114. Song X, Wu A, Ding Z, Liang S, Zhang C. Soluble Axl is a novel diagnostic biomarker of hepatocellular carcinoma in Chinese patients with chronic hepatitis B virus infection. *Cancer Res Treat.* (2020) 52:789–97. doi: 10.4143/crt.2019.749
115. Anborgh PH, Mutrie JC, Tuck AB, Chambers AF. Role of the metastasis-promoting protein osteopontin in the tumour microenvironment. *J Cell Mol Med.* (2010) 14:2037–44. doi: 10.1111/j.1582-4934.2010.01115.x
116. Johnston NI, Gunasekharan VK, Ravindranath A, O'Connell C, Johnston PG, El-Tanani MK. Osteopontin as a target for cancer therapy. *Front Biosci.* (2008) 13:4361–72. doi: 10.2741/3009
117. Pan HW, Ou YH, Peng SY, Liu SH, Lai PL, Lee PH, et al. Overexpression of osteopontin is associated with intrahepatic metastasis, early recurrence, and poorer prognosis of surgically resected hepatocellular carcinoma. *Cancer Am Cancer Soc.* (2003) 98:119–27. doi: 10.1002/cncr.11487
118. Shang S, Plymoth A, Ge S, Feng Z, Rosen HR, Sangrajang S, et al. Identification of osteopontin as a novel marker for early hepatocellular carcinoma. *Hepatology.* (2012) 55:483–90. doi: 10.1002/hep.24703
119. Cheng J, Wang W, Sun C, Li M, Wang B, Lv Y. Meta-analysis of the prognostic and diagnostic significance of serum/plasma osteopontin in hepatocellular carcinoma. *J Clin Gastroenterol.* (2014) 48:806–14. doi: 10.1097/MCG.0000000000000018
120. Ogawa Y, Takahashi T, Masukata H. Association of fission yeast Orp1 and Mcm6 proteins with chromosomal replication origins. *Mol Cell Biol.* (1999) 19:7228–36. doi: 10.1128/MCB.19.10.7228
121. Zheng T, Chen M, Han S, Zhang L, Bai Y, Fang X, et al. Plasma minichromosome maintenance complex component 6 is a novel biomarker for hepatocellular carcinoma patients. *Hepatol Res.* (2014) 44:1347–56. doi: 10.1111/hepr.12303
122. Shibutani M, Maeda K, Nagahara H, Ohtani H, Sugano K, Ikeya T, et al. Elevated preoperative serum C-reactive protein levels are associated with



- poor survival in patients with colorectal cancer. *Hepatogastroenterology*. (2014) 61:2236–40.
123. Chen W, Wang JB, Abnet CC, Dawsey SM, Fan JH, Yin LY, et al. Association between C-reactive protein, incident liver cancer, and chronic liver disease mortality in the Linxian nutrition intervention trials: a nested case-control study. *Cancer Epidemiol Biomarkers Prev*. (2015) 24:386–92. doi: 10.1158/1055-9965.EPI-14-1038
  124. Hefler LA, Concin N, Hofstetter G, Marth C, Mustea A, Sehouli J, et al. Serum C-reactive protein as independent prognostic variable in patients with ovarian cancer. *Clin Cancer Res*. (2008) 14:710–4. doi: 10.1158/1078-0432.CCR-07-1044
  125. Xu M, Zhu M, Du Y, Yan B, Wang Q, Wang C, et al. Serum C-reactive protein and risk of lung cancer: a case-control study. *Med Oncol*. (2013) 30:319. doi: 10.1007/s12032-012-0319-4
  126. Ma LN, Liu XY, Lu ZH, Wu LG, Tang YY, Luo X, et al. Assessment of high-sensitivity C-reactive protein tests for the diagnosis of hepatocellular carcinoma in patients with hepatitis B-associated liver cirrhosis. *Oncol Lett*. (2017) 13:3457–64. doi: 10.3892/ol.2017.5890
  127. Liu XY, Ma LN, Yan TT, Lu ZH, Tang YY, Luo X, et al. Combined detection of liver stiffness and C-reactive protein in patients with hepatitis B virus-related liver cirrhosis, with and without hepatocellular carcinoma. *Mol Clin Oncol*. (2016) 4:587–90. doi: 10.3892/mco.2016.742
  128. Belkin AM. Extracellular TGF $\beta$ : emerging functions and regulation. *FEBS J*. (2011) 278:4704–16. doi: 10.1111/j.1742-4658.2011.08346.x
  129. Mangala LS, Arun B, Sahin AA, Mehta K. Tissue transglutaminase-induced alterations in extracellular matrix inhibit tumor invasion. *Mol Cancer*. (2005) 4:33. doi: 10.1186/1476-4598-4-33
  130. Xu L, Begum S, Hearn JD, Hynes RO. GPR56, an atypical G protein-coupled receptor, binds tissue transglutaminase, TGF $\beta$ , and inhibits melanoma tumor growth and metastasis. *Proc Natl Acad Sci USA*. (2006) 103:9023–8. doi: 10.1073/pnas.0602681103
  131. Verma A, Wang H, Manavathi B, Fok JY, Mann AP, Kumar R, et al. Increased expression of tissue transglutaminase in pancreatic ductal adenocarcinoma and its implications in drug resistance and metastasis. *Cancer Res*. (2006) 66:10525–33. doi: 10.1158/0008-5472.CAN-06-2387
  132. Mehta K, Fok J, Miller FR, Koul D, Sahin AA. Prognostic significance of tissue transglutaminase in drug resistant and metastatic breast cancer. *Clin Cancer Res*. (2004) 10:8068–76. doi: 10.1158/1078-0432.CCR-04-1107
  133. Hwang JY, Mangala LS, Fok JY, Lin YG, Merritt WM, Spannuth WA, et al. Clinical and biological significance of tissue transglutaminase in ovarian carcinoma. *Cancer Res*. (2008) 68:5849–58. doi: 10.1158/0008-5472.CAN-07-6130
  134. Park KS, Kim HK, Lee JH, Choi YB, Park SY, Yang SH, et al. Transglutaminase 2 as a cisplatin resistance marker in non-small cell lung cancer. *J Cancer Res Clin Oncol*. (2010) 136:493–502. doi: 10.1007/s00432-009-0681-6
  135. Sun Y, Mi W, Cai J, Ying W, Liu F, Lu H, et al. Quantitative proteomic signature of liver cancer cells: tissue transglutaminase 2 could be a novel protein candidate of human hepatocellular carcinoma. *J Proteome Res*. (2008) 7:3847–59. doi: 10.1021/pr800153s
  136. Ikeda Y, Imai Y, Kumagai H, Nosaka T, Morikawa Y, Hisaoka T, et al. Vasorin, a transforming growth factor beta-binding protein expressed in vascular smooth muscle cells, modulates the arterial response to injury *in vivo*. *Proc Natl Acad Sci USA*. (2004) 101:10732–7. doi: 10.1073/pnas.0404117101
  137. Liang W, Guo B, Ye J, Liu H, Deng W, Lin C, et al. Vasorin stimulates malignant progression and angiogenesis in glioma. *Cancer Sci*. (2019) 110:2558–72. doi: 10.1111/cas.14103
  138. Li S, Li H, Yang X, Wang W, Huang A, Li J, et al. Vasorin is a potential serum biomarker and drug target of hepatocarcinoma screened by subtractive-EMSA-SELEX to clinic patient serum. *Oncotarget*. (2015) 6:10045–59. doi: 10.18632/oncotarget.3541
  139. Sharma MC, Sharma M. The role of annexin II in angiogenesis and tumor progression: a potential therapeutic target. *Curr Pharm Des*. (2007) 13:3568–75. doi: 10.2174/138161207782794167
  140. Lokman NA, Ween MP, Oehler MK, Ricciardelli C. The role of annexin A2 in tumorigenesis and cancer progression. *Cancer Microenviron*. (2011) 4:199–208. doi: 10.1007/s12307-011-0064-9
  141. Sharma MR, Koltowski L, Ownbey RT, Tuszyński GP, Sharma MC. Angiogenesis-associated protein annexin II in breast cancer: selective expression in invasive breast cancer and contribution to tumor invasion and progression. *Exp Mol Pathol*. (2006) 81:146–56. doi: 10.1016/j.yexmp.2006.03.003
  142. Shiozawa Y, Havens AM, Jung Y, Ziegler AM, Pedersen EA, Wang J, et al. Annexin II/annexin II receptor axis regulates adhesion, migration, homing, and growth of prostate cancer. *J Cell Biochem*. (2008) 105:370–80. doi: 10.1002/jcb.21835
  143. Diaz VM, Hurtado M, Thomson TM, Reventos J, Paciucci R. Specific interaction of tissue-type plasminogen activator (t-PA) with annexin II on the membrane of pancreatic cancer cells activates plasminogen and promotes invasion *in vitro*. *Gut*. (2004) 53:993–1000. doi: 10.1136/gut.2003.026831
  144. Sun Y, Gao G, Cai J, Wang Y, Qu X, He L, et al. Annexin A2 is a discriminative serological candidate in early hepatocellular carcinoma. *Carcinogenesis*. (2013) 34:595–604. doi: 10.1093/carcin/bgs372
  145. Meng K, Yuan M, Xu S, Wang L, Li Z, Wang M, et al. Human cervical cancer oncogene-1 over expression in colon cancer and its clinical significance. *Int J Clin Exp Med*. (2015) 8:939–43.
  146. Liu Y, Li K, Ren Z, Li S, Zhang H, Fan Q. Clinical implication of elevated human cervical cancer oncogene-1 expression in esophageal squamous cell carcinoma. *J Histochem Cytochem*. (2012) 60:512–20. doi: 10.1369/0022155412444437
  147. Yoon SK, Lim NK, Ha SA, Park YG, Choi JY, Chung KW, et al. The human cervical cancer oncogene protein is a biomarker for human hepatocellular carcinoma. *Cancer Res*. (2004) 64:5434–41. doi: 10.1158/0008-5472.CAN-03-3665
  148. Jirun P, Zhang G, Kim HK, Ha SA, Zhongtian J, Shishi Q, et al. Clinical utility of alpha fetoprotein and HCCR-1, alone or in combination, in patients with chronic hepatitis, liver cirrhosis and hepatocellular carcinoma. *Dis Markers*. (2011) 30:307–15. doi: 10.1155/2011/698975
  149. Wang F, Huang J, Zhu Z, Ma X, Cao L, Zhang Y, et al. Transcriptome analysis of WHV/c-myc transgenic mice implicates cytochrome P450 enzyme 17A1 as a promising biomarker for hepatocellular carcinoma. *Cancer Prev Res*. (2016) 9:739–49. doi: 10.1158/1940-6207.CAPR-16-0023
  150. Wasfy RE, Shams EA. Roles of combined glypican-3 and glutamine synthetase in differential diagnosis of hepatocellular lesions. *Asian Pac J Cancer Prev*. (2015) 16:4769–75. doi: 10.7314/APJCP.2015.16.11.4769
  151. Liu P, Lu D, Al-Ameri A, Wei X, Ling S, Li J, et al. Glutamine synthetase promotes tumor invasion in hepatocellular carcinoma through mediating epithelial-mesenchymal transition. *Hepatol Res*. (2020) 50:246–57. doi: 10.1111/hepr.13433
  152. Fournier T, Medjoubi-N N, Porquet D. Alpha-1-acid glycoprotein. *Biochim Biophys Acta*. (2000) 1482:157–71. doi: 10.1016/S0167-4838(00)00153-9
  153. Tanabe K, Kitagawa K, Kojima N, Iijima S. Multifucosylated alpha-1-acid glycoprotein as a novel marker for hepatocellular carcinoma. *J Proteome Res*. (2016) 15:2935–44. doi: 10.1021/acs.jproteome.5b01145
  154. Liang J, Zhu J, Wang M, Singal AG, Odewole M, Kagan S, et al. Evaluation of AGP fucosylation as a marker for hepatocellular carcinoma of three different etiologies. *Sci Rep*. (2019) 9:11580. doi: 10.1038/s41598-019-48043-1
  155. Tan HT, Low J, Lim SG, Chung MC. Serum autoantibodies as biomarkers for early cancer detection. *FEBS J*. (2009) 276:6880–904. doi: 10.1111/j.1742-4658.2009.07396.x
  156. Hong Y, Long J, Li H, Chen S, Liu Q, Zhang B, et al. An analysis of immunoreactive signatures in early stage hepatocellular carcinoma. *Ebiomedicine*. (2015) 2:438–46. doi: 10.1016/j.ebiom.2015.03.010
  157. Yi CH, Weng HL, Zhou FG, Fang M, Ji J, Cheng C, et al. Elevated core-fucosylated IgG is a new marker for hepatitis B virus-related hepatocellular carcinoma. *Oncoimmunology*. (2015) 4:e1011503. doi: 10.1080/2162402X.2015.1011503
  158. Ezzikouri S, Kimura K, Sunagazaka H, Kaneko S, Inoue K, Nishimura T, et al. Serum DHCR24 auto-antibody as a new biomarker for progression of hepatitis C. *Ebiomedicine*. (2015) 2:604–12. doi: 10.1016/j.ebiom.2015.04.007
  159. Nomura F, Sogawa K, Noda K, Seimiya M, Matsushita K, Miura T, et al. Serum anti-Ku86 is a potential biomarker for early detection of hepatitis C virus-related hepatocellular carcinoma. *Biochem Biophys Res Commun*. (2012) 421:837–43. doi: 10.1016/j.bbrc.2012.04.099

160. Chu L, Zhang X, Wang G, Zhou W, Du Z, Liu A, et al. [Serum anti-Ku86: a potential biomarker for early detection of hepatocellular carcinoma]. *Zhonghua Zhong Liu Za Zhi.* (2014) 36:123–7. doi: 10.3760/cma.j.issn.0253-3766.2014.02.011
161. Wang T, Liu M, Zheng SJ, Bian DD, Zhang JY, Yao J, et al. Tumor-associated autoantibodies are useful biomarkers in immunodiagnosis of alpha-fetoprotein-negative hepatocellular carcinoma. *World J Gastroenterol.* (2017) 23:3496–504. doi: 10.3748/wjg.v23.i19.3496
162. Zhang JY. Mini-array of multiple tumor-associated antigens to enhance autoantibody detection for immunodiagnosis of hepatocellular carcinoma. *Autoimmun Rev.* (2007) 6:143–8. doi: 10.1016/j.autrev.2006.09.009
163. Himoto T, Kuriyama S, Zhang JY, Chan EK, Kimura Y, Masaki T, et al. Analyses of autoantibodies against tumor-associated antigens in patients with hepatocellular carcinoma. *Int J Oncol.* (2005) 27:1079–85. doi: 10.3892/ijo.27.4.1079
164. Hanash SM, Pitteri SJ, Faca VM. Mining the plasma proteome for cancer biomarkers. *Nature.* (2008) 452:571–9. doi: 10.1038/nature06916
165. Makridakis M, Vlahou A. Secretome proteomics for discovery of cancer biomarkers. *J Proteomics.* (2010) 73:2291–305. doi: 10.1016/j.jprot.2010.07.001
166. Wu C, Wang Z, Liu L, Zhao P, Wang W, Yao D, et al. Surface enhanced laser desorption/ionization profiling: new diagnostic method of HBV-related hepatocellular carcinoma. *J Gastroenterol Hepatol.* (2009) 24:55–62. doi: 10.1111/j.1440-1746.2008.05580.x
167. He X, Wang Y, Zhang W, Li H, Luo R, Zhou Y, et al. Screening differential expression of serum proteins in AFP-negative HBV-related hepatocellular carcinoma using iTRAQ -MALDI-MS/MS. *Neoplasma.* (2014) 61:17–26. doi: 10.4149/neo\_2014\_001
168. She S, Xiang Y, Yang M, Ding X, Liu X, Ma L, et al. C-reactive protein is a biomarker of AFP-negative HBV-related hepatocellular carcinoma. *Int J Oncol.* (2015) 47:543–54. doi: 10.3892/ijo.2015.3042
169. Shu H, Kang X, Guo K, Li S, Li M, Sun L, et al. Diagnostic value of serum haptoglobin protein as hepatocellular carcinoma candidate marker complementary to alpha fetoprotein. *Oncol Rep.* (2010) 24:1271–6. doi: 10.3892/or\_00000982
170. Zhang J, Hao N, Liu W, Lu M, Sun L, Chen N, et al. In-depth proteomic analysis of tissue interstitial fluid for hepatocellular carcinoma serum biomarker discovery. *Br J Cancer.* (2017) 117:1676–84. doi: 10.1038/bjc.2017.344
171. Huang L, Mo Z, Hu Z, Zhang L, Qin S, Qin X, et al. Diagnostic value of fibrinogen to prealbumin ratio and gamma-glutamyl transpeptidase to platelet ratio in the progression of AFP-negative hepatocellular carcinoma. *Cancer Cell Int.* (2020) 20:77. doi: 10.1186/s12935-020-1161-y
172. Lo CM, Iqbal U, Li YJ. Cancer quantification from data mining to artificial intelligence. *Comput Methods Prog Biomed.* (2017) 145:A1. doi: 10.1016/S0169-2607(17)30594-1
173. Chen LA, Fawcett TN. Using data mining strategies in clinical decision making: a literature review. *Comput Inform Nurs.* (2016) 34:448–54. doi: 10.1097/CIN.0000000000000282
174. Best J, Bilgi H, Heider D, Schotten C, Manka P, Bedreli S, et al. The GALAD scoring algorithm based on AFP, AFP-L3, and DCP significantly improves detection of BCLC early stage hepatocellular carcinoma. *Z Gastroenterol.* (2016) 54:1296–305. doi: 10.1055/s-0042-119529
175. Wang M, Sanda M, Comunale MA, Herrera H, Swindell C, Kono Y, et al. Changes in the glycosylation of Kininogen and the development of a kininogen-based algorithm for the early detection of HCC. *Cancer Epidemiol Biomarkers Prev.* (2017) 26:795–803. doi: 10.1158/1055-9965.EPI-16-0974
176. Luo CL, Rong Y, Chen H, Zhang WW, Wu L, Wei D, et al. A logistic regression model for noninvasive prediction of AFP-negative hepatocellular carcinoma. *Technol Cancer Res Treat.* (2019) 18:1078114280. doi: 10.1177/1533033819846632
177. Zhang X, Wang T, Zhang KH, Chen SH, He YT, Wang YQ. Simple clinical metrics enhance AFP to effectively identify cirrhotic patients with complicating hepatocellular carcinoma at various AFP levels. *Front Oncol.* (2019) 9:1478. doi: 10.3389/fonc.2019.01478

**Conflict of Interest:** The authors declare that the research was conducted in the absence of any commercial or financial relationships that could be construed as a potential conflict of interest.

Copyright © 2020 Wang and Zhang. This is an open-access article distributed under the terms of the Creative Commons Attribution License (CC BY). The use, distribution or reproduction in other forums is permitted, provided the original author(s) and the copyright owner(s) are credited and that the original publication in this journal is cited, in accordance with accepted academic practice. No use, distribution or reproduction is permitted which does not comply with these terms.



# A Prognostic Prediction Model Developed Based on Four CpG Sites and Weighted Correlation Network Analysis Identified *DNAJB1* as a Novel Biomarker for Pancreatic Cancer

Lingming Kong<sup>1†</sup>, Peng Liu<sup>1†</sup>, Xiang Fei<sup>1</sup>, Tianyu Wu<sup>1</sup>, Zhongpeng Wang<sup>2</sup>, Baohui Zhang<sup>3</sup>, Jiatong Li<sup>4</sup> and Xiaodong Tan<sup>1\*</sup>

<sup>1</sup> Department of General Surgery, Shengjing Hospital of China Medical University, Shenyang, China, <sup>2</sup> Department of Cardiology, The First Affiliated Hospital of China Medical University, Shenyang, China, <sup>3</sup> Department of Physiology, School of Life Sciences, China Medical University, Shenyang, China, <sup>4</sup> Department of Orthopedics, The First Affiliated Hospital of China Medical University, Shenyang, China

## OPEN ACCESS

### Edited by:

Alessandro Vanoli,  
University of Pavia, Italy

### Reviewed by:

Claudio Luchini,  
University of Verona, Italy  
Yuangen Yao,  
Huazhong Agricultural University,  
China

### \*Correspondence:

Xiaodong Tan  
tanxdcmu@163.com

<sup>†</sup> These authors have contributed  
equally to this work

### Specialty section:

This article was submitted to  
Gastrointestinal Cancers,  
a section of the journal  
Frontiers in Oncology

**Received:** 20 April 2020

**Accepted:** 31 July 2020

**Published:** 25 August 2020

### Citation:

Kong L, Liu P, Fei X, Wu T,  
Wang Z, Zhang B, Li J and Tan X  
(2020) A Prognostic Prediction Model  
Developed Based on Four CpG Sites  
and Weighted Correlation Network  
Analysis Identified *DNAJB1* as  
a Novel Biomarker for Pancreatic  
Cancer. *Front. Oncol.* 10:1716.  
doi: 10.3389/fonc.2020.01716

**Background:** The prognosis of pancreatic cancer, which is among the solid tumors associated with high mortality, is poor. There is a need to improve the overall survival rate of patients with pancreatic cancer.

**Materials and Methods:** The Cancer Genome Atlas (TCGA) dataset with 153 samples and the International Cancer Genome Consortium (ICGC) dataset with 235 samples were used as the discovery and validation cohorts, respectively. The least absolute shrinkage and selection operator regression was used to construct the prognostic prediction model based on the DNA methylation markers. The predictive efficiency of the model was evaluated based on the calibration curve, concordance index, receiver operating characteristic curve, area under the curve, and decision curve. The xenograft model and cellular functional experiments were used to investigate the potential role of *DNAJB1* in pancreatic cancer.

**Results:** A prognostic prediction model based on four CpG sites (cg00609645, cg13512069, cg23811464, and cg03502002) was developed using TCGA dataset. The model effectively predicted the overall survival rate of patients with pancreatic cancer, which was verified in the ICGC dataset. Next, a nomogram model based on the independent prognostic factors was constructed to predict the overall survival rate of patients with pancreatic cancer. The nomogram model had a higher predictive value than TCGA or ICGC datasets. The low-risk group with improved prognosis exhibited less mutational frequency and high immune infiltration. The brown module with 247 genes derived from the WGCNA analysis was significantly correlated with the prognostic prediction model, tumor grade, clinical stage, and T stage. The bioinformatic analysis indicated that *DNAJB1* can serve as a novel biomarker for pancreatic cancer. *DNAJB1* knockdown significantly inhibited the proliferation, migration, and invasion of pancreatic cancer cells *in vivo* and *in vitro*.

**Conclusion:** The prognostic prediction model based on four CpG sites is a new method for predicting the prognosis of patients with pancreatic cancer. The molecular characteristic analyses, including Gene Ontology, Gene Set Enrichment Analysis, mutation spectrum, and immune infiltration of the subgroups, stratified by the model provided novel insights into the initiation and development of pancreatic cancer. *DNAJB1* may serve as diagnostic and prognostic biomarkers for pancreatic cancer.

**Keywords:** LASSO, WGCNA, pancreatic cancer, DNA methylation, prognostic prediction, *DNAJB1*

## INTRODUCTION

Pancreatic cancer, which is one of the gastrointestinal tract malignancies associated with high mortality, is the fourth most common cause of cancer-related deaths in the United States of America (1). Due to the specific anatomical position and malignant phenotype of pancreatic cancer, most patients exhibit insidious onset and unspecific clinical symptoms at the earlier stage of pancreatic cancer. Large proportions of patients with pancreatic cancer are diagnosed at an advanced stage along with early distant metastasis and neural or vascular invasion. Thus, patients with pancreatic cancer exhibit a low survival rate with a 5-year survival rate of less than 5% (2, 3). Currently, the classical TNM staging and blood tumor markers (CA 19-9, CA 125, and CEA) are used to assess the risk level in patients with pancreatic cancer and predict the prognosis, which are not highly efficient or accurate (4, 5). There is an urgent need to devise strategies to increase the overall survival rate of patients with pancreatic cancer, which can be achieved by developing a sensitive and specific risk prediction model for prognosis. The novel biomarkers derived from the risk prediction model can serve as diagnostic, therapeutic, and prognostic biomarkers for pancreatic cancer.

The initiation and progression of various cancers are reported to be regulated by epigenetic alterations. DNA methylation, an important epigenetic regulation, silences tumor suppressor genes, and upregulates oncogenic genes through hypermethylation and hypomethylation of the corresponding CpG islands in the promoter regions, respectively. Several studies have demonstrated that numerous genes with deregulated methylation status, such as *KRAS*, *CDKN2A*, *TP53*, *CD1D*, *MUC4*, and *MUC1* play vital roles in the progression of pancreatic cancer (6–8). Moreover, specific DNA methylation signatures in the circulating DNA from pancreatic juice and plasma can be used as novel biomarkers for pancreatic cancer (9, 10). Several prognostic prediction models using DNA methylation data have been proposed for prostate, gastric, colorectal, and esophageal cancers (11–14). These studies indicated that the DNA methylation status is closely associated with the prognosis of multiple cancers. The development of high-throughput sequencing and construction of large cancer genome databases, such as The Cancer Genome Atlas (TCGA) and International Cancer Genome Consortium (ICGC) have enabled access to massive sequencing data and the corresponding clinical data. This study aimed to explore the potential prognostic

values of prognostic prediction model generated based on CpG sites in pancreatic cancer.

In this study, a prognostic prediction model based on four CpG sites was established using TCGA dataset. The conclusion of this model was verified in the external ICGC dataset. Next, this study demonstrated that the nomogram model generated using the independent prognostic factors can be used as an efficient tool for prognostic prediction. Additionally, the comparisons between molecular subgroups based on the prognostic prediction model identified novel biomarkers and therapeutic targets for pancreatic cancer. The molecular characteristic analyses among subgroups may aid in elucidating the mechanisms underlying pancreatic cancer.

## MATERIALS AND METHODS

### Downloading and Preprocessing Data

The DNA methylation, RNA sequencing (RNA-Seq; HTSeq counts type), single nucleotide variation (MuTect type) data of patients with pancreatic cancer were downloaded from TCGA database<sup>1</sup>. The latest clinicopathological information and clinical follow-up data of patients with pancreatic cancer in TCGA were downloaded on 13 November 2019 (15). The DNA methylation status and clinical data of patients with pancreatic cancer in the ICGC database (the Australian Pancreatic Cancer Genome Initiative, <https://icgc.org>) were used as the validation cohort (16). In the DNA methylation data, the CpG sites with absent values in >70% of the samples were removed and the K-nearest neighbor algorithm was used to estimate and replace the missing values. The probes from upstream 2 kb to downstream 200 bp of the transcription start site region were used for further analysis. In the RNA-Seq data, the genes with missing values in >50% of the total samples were deleted. The silent mutation and mutation in the intron region of single nucleotide variation data were deleted (17). The detailed information of the pancreatic cancer samples obtained from TCGA and ICGC databases is shown in **Supplementary Tables 1, 2**, respectively.

### Construction of the Prognostic Prediction Model Based on CpG Sites

The Cancer Genome Atlas dataset was used as the discovery cohort. The differentially methylated CpG sites between 10

<sup>1</sup><https://portal.gdc.cancer.gov/>



normal and 185 tumor samples were identified from TCGA database. The R package “minfi” was used to normalize the  $\beta$ -values of methylation data. The Mann–Whitney  $U$  test was performed to select the differentially methylated CpG sites with adjusted  $p$ -value  $< 0.05$  and  $|\log_2 \text{fold-change}| > 2$  (11, 18). The samples of patients with pancreatic cancer exhibiting survival time of less than 30 days were removed. In total, 153 samples were selected to identify the survival-related CpG sites. The CpG sites with  $p$ -value  $< 0.05$  in both Cox and log-rank tests were used for the generation of prognostic prediction model. The least absolute shrinkage and selection operator (LASSO) regression was used to construct the prognostic prediction model using the R package “glmnet” (19, 20). To verify the effectiveness of the model, the ICGC dataset with 235 pancreatic cancer samples was used as the validation cohort.

### Nomogram Model Development

To comprehensively utilize the clinicopathological data to increase the predictive ability of the LASSO model, the independent prognostic factors were identified based on the univariate and multivariate Cox analyses. The nomogram was generated based on the selected independent prognostic factors and used to predict the 1-, 3-, and 5-year overall survival rates of patients with pancreatic cancer. The discriminative ability of the nomogram model was evaluated based on the calibration curve, concordance index (C-index), receiver operator characteristic (ROC) curve, and area under the curve (AUC). The decision curve analysis (DCA) was used to compare the clinical benefits among these models. The R packages “rms,” “survcomp,” “timeROC,” “survival,” and “stdca.R” were used for the analysis (21–23).

### Molecular Characteristic Analyses of the Prognostic Prediction Model

To further explore the mechanisms underlying the prognostic prediction model, several molecular characteristic analyses were performed using the high-risk and low-risk groups depending on the model. The immunological infiltrations of six types of immune cells were calculated using TIMER (Tumor Immune Estimation Resource, <https://cistrome.shinyapps.io/timer/>) (24, 25). The R package “maftools” was used to perform the mutation spectrum analysis (26). The R packages “clusterProfiler” and “ggplot2” were utilized to perform and visualize the results of Gene Ontology (GO) analysis and Gene Set Enrichment Analysis (GSEA) (27, 28).

### Weighted Correlation Network Analysis (WGCNA) to Identify the Hub Genes Associated With the Model

The prognostic prediction model effectively predicted the prognosis of the patients with pancreatic cancer and categorized the samples into high-risk and low-risk groups. The differentially expressed genes between the high-risk and low-risk groups may play a vital role in the progression of pancreatic cancer. The differentially expressed genes between different groups were calculated and selected using the R package “DESeq2”

with an adjusted  $p$ -value  $< 0.05$  and  $|\log_2 \text{fold-change}| > 1$  (29). To identify the most relevant genes of the model, weighted correlation network analysis (WGCNA) was performed according to the official guideline of the R package “WGCNA” (30, 31). The parameters used in the analysis were set as follows: best soft power threshold, 4; minimum module size, 30; merge cut height, 0.25. The Cytoscape software (version 2.8.3) was used to calculate and visualize the hub genes in the gene network (32, 33).

### Gene Expression Profiling Interactive Analysis (GEPIA), Kaplan-Meier (KM) Plotter, and TISIDB Databases

The Gene expression profiling interactive analysis (GEPIA) website provided the differentially expressed genes between 179 pancreatic tumor samples and 171 normal samples based on the integrated RNA-Seq data from TCGA and Genotype-Tissue Expression (GTEx) databases (34). The KM plotter website provided the genes associated with overall survival and relapse-free survival of patients from TCGA dataset (35). The TISIDB website was used to analyze the relationship between clinicopathological information and gene expression (36).

### Cell Culture and Transfection

The four human pancreatic cancer cell lines (AsPC-1, Capan-2, MIA PaCa-2, and SW1990) and one human normal pancreatic cell line (hTERT-HPNE) used in this study were purchased from the American Type Culture Collection (ATCC). The cells were cultured following the official guidelines provided in the ATCC website at 37°C and 5% CO<sub>2</sub>. The pHBLV-U6-ZsGreen-puro lentiviral RNAi expression system containing the *DNAJB1* shRNA sequence (5'-GGTGCCAATGGTACCTCTTTC-3') were designed and provided by Hanbio Biotechnology Co. Ltd. (Shanghai, China).

### Western Blotting and Immunohistochemical Assay

The western blotting analysis was performed following the methods of a previous study (37). Equal amounts (30  $\mu$ g) of protein were subjected to sodium dodecyl sulfate-polyacrylamide gel electrophoresis (SDS-PAGE) using a 10% gel. The following primary antibodies used for the western blotting analysis were purchased from Proteintech Group (Rosemont, United States): anti-DNAJB1 (Catalog number: 13174-1-AP; 1:1000); and anti-alpha tubulin (Catalog number: 11224-1-AP; 1:3000) antibodies. The immunohistochemical assay was performed following the methods of a previous study (38).

### Cell Proliferation, Invasion, and Migration Assays

The CCK-8 and colony formation assays were used to estimate the proliferative ability of different groups. For CCK-8 assay, 2000 cells of different groups were seeded into a 96-well plate. The cells in each well were incubated with 10  $\mu$ L of CCK-8 solution (Beyotime biotechnology Co. Ltd., Shanghai, China) for 60 min. The optical density of the mixture was measured at 450 nm using a microplate spectrophotometer. The colony formation assay was



performed using 1000 cells of different groups seeded in a 6-well plate. The culture medium was replaced every 3 days. After the appearance of visible colonies, 4% paraformaldehyde and crystal violet were used to fix and stain the colonies. The transwell and wound healing assays were used to analyze the cellular invasion and cellular migration, respectively. These assays were performed following the methods described in a previous study (37). The 96-well plates, 6-well plates, transwell system, and cell culture flask were purchased from Guangzhou Jet Bio-Filtration Co., Ltd.

## Xenograft Tumor Mouse Model

The subcutaneous tumor mouse model was used to assess the tumor cell proliferative ability *in vivo* following the method described in a previous study (39). Twelve BALB/c nude mice (4-week-old, female) were purchased from Huafukang Biotechnology Co. Ltd. (Beijing, China). The cells ( $1 \times 10^6$ ) of different groups in 100  $\mu$ L phosphate buffer solution were injected into the right axillary area of each nude mouse. The subcutaneous tumor volume was measured and recorded once a week. The tumor volume was measured as follows: volume =  $0.5 \times L \times W^2$ , where L is the long axis of the tumor and W is the short axis of the tumor.

## Statistical Analysis

The statistical analyses were performed in the R software (version 3.5.3) and RStudio software. The data were analyzed by two-tailed Student's *t*-test and one-way analysis of variance (ANOVA). The difference was considered statistically significant when the *p*-value was less than 0.05.

## RESULTS

### Construction of the Prognostic Prediction Model Based on Four CpG Sites

To establish the prognostic prediction model based on CpG sites, 3173 differentially methylated CpG sites were identified among 10 normal and 185 tumor samples from TCGA dataset (Supplementary Table 3). Next, 1325 prognosis-related CpG sites with *p*-value < 0.05 in both Cox and log-rank tests were selected for further LASSO regression analysis (Supplementary Table 4). After the LASSO regression analysis, a prognostic model based on four CpG sites, namely cg00609645, cg13512069, cg23811464, and cg03502002, was developed (Figures 1A,B). The detailed information on the four CpG sites is shown in Supplementary Table 5. Based on the four CpG site  $\beta$  values and the corresponding risk coefficients, each patient was assigned a risk score according to the following formula: risk score = (cg00609645  $\times$  1.461) + (cg13512069  $\times$  1.226) + (cg23811464  $\times$  0.539) + (cg03502002  $\times$  0.519). As shown in Figures 1C–E, the samples from TCGA dataset were separated into high-risk and low-risk groups based on the median of the risk scores (cutoff value: 0.694). In order to improve the universality of the prognostic model, the same cutoff value was used in the ICGC dataset. The analysis revealed that

the risk score was significantly associated with the overall survival of patients with pancreatic cancer [Hazard ratio (HR), 11; 95% confidence interval (CI), 5.5–21; *p* < 0.001] in the TCGA discovery dataset. Similarly, the risk score also significantly predicted the overall survival of patients with pancreatic cancer (HR, 2; 95% CI: 1.4–3; *p* < 0.001) in the ICGC validation cohort (Figures 1D–F). These results suggested that the prediction model based on four CpG sites can be an effective tool to predict the prognosis of patients with pancreatic cancer.

### Construction of Nomogram Model Based on the Independent Prognosis-Related Factors

To develop the nomogram model for predicting the prognosis of patients with pancreatic cancer, the univariate and multivariate Cox analyses were performed using the risk score and other clinicopathological factors. The univariate Cox analysis based on TCGA dataset revealed that the risk score (HR, 10.72; 95% CI, 5.52–20.80; and *p* < 0.001), age (HR, 1.03; 95% CI, 1.01–1.05; and *p* = 0.016), tumor grade (HR, 1.80; 95% CI, 1.29–2.50; and *p* < 0.001), clinical stage (HR, 1.54; 95% CI, 1.03–2.29; and *p* = 0.035), T stage (HR, 2.26; 95% CI, 1.28–4.00; and *p* = 0.005), N stage (HR, 2.47; 95% CI, 1.31–4.66; and *p* = 0.005), site of resection (HR, 0.50; 95% CI, 0.27–0.92; and *p* = 0.026), and radiation therapy (HR, 0.21; 95% CI, 0.07–0.68; and *p* = 0.009) can serve as prognosis-associated factors. According to the general rule, the multivariate Cox analysis was performed using these prognosis-associated factors to avoid the overfitting of the multivariable Cox model. The multivariate Cox analysis revealed that the risk score (HR, 24.68; 95% CI, 7.70–79.14; and *p* < 0.001), tumor grade (HR, 2.33; 95% CI, 1.16–4.65; and *p* = 0.017), and radiation therapy (HR, 0.14; 95% CI 0.04–0.50; and *p* = 0.003) were independent prognosis-related factors (Table 1). The nomogram model was constructed using these independent prognosis factors to predict the 1-, 3-, and 5-year survival rates of patients with pancreatic cancer (Figure 2A).

To compare the predictive efficiency among the nomogram model, TCGA dataset, and ICGC dataset, the AUC of ROC curve was used to assess the discriminative ability. The nomogram model (1-year: 0.81, 3-year: 0.91, and 5-year: 0.89) exhibited better performance in predicting the survival rates than TCGA dataset (1-year: 0.76, 3-year: 0.87, and 5-year: 0.82) and ICGC dataset (1-year: 0.64, 3-year: 0.76, and 5-year: 0.55; Figures 2B–D). The calibration curve of the three models exhibited satisfactory consistency between the predicted survival rate and the actual survival rate. However, the C-index of the nomogram model (C-index, 0.83; 95% CI, 0.78–0.88) was higher than that of TCGA dataset (C-index, 0.79; 95% CI, 0.73–0.85) and ICGC dataset (C-index, 0.60; 95% CI, 0.56–0.65; Figures 2E–G). Moreover, the DCA curve revealed that the predicted clinical benefits of the nomogram model were better than those of TCGA dataset and ICGC dataset (Figure 2H). These results suggested that the prognostic prediction model based on four CpG sites can serve as an effective model for predicting prognosis in patients

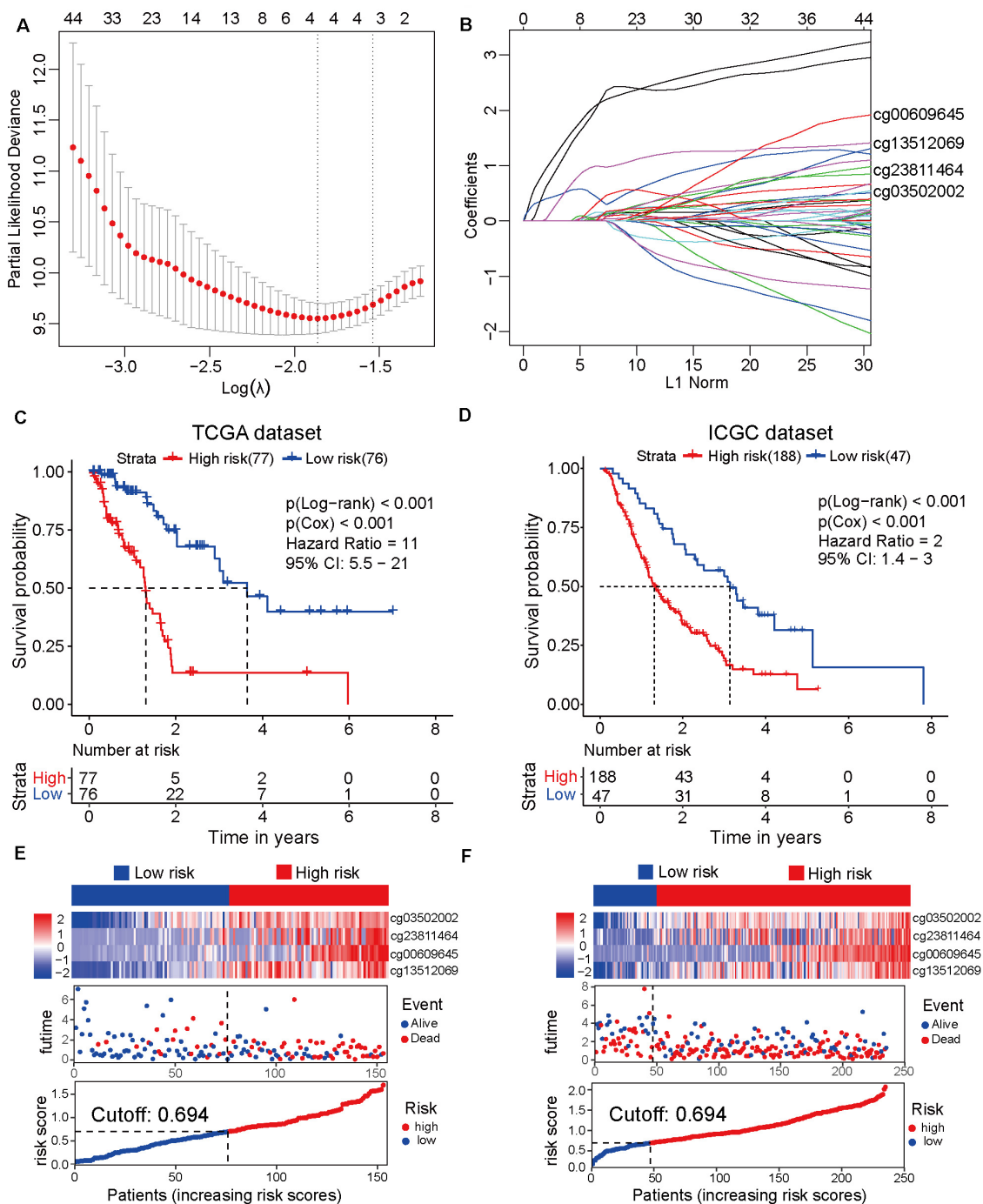


**FIGURE 1 |** Development and verification of the prognostic prediction model based on four CpG sites by least absolute shrinkage and selection operator (LASSO) regression. **(A)** The selection of tuning parameter ( $\lambda$ ) in the LASSO model based on the 10-fold cross-validation with minimum criteria. The  $\log(\lambda)$  value of -1.863678 is used for further analysis. **(B)** The four CpG sites (cg00609645, cg13512069, cg23811464, and cg03502002) and their coefficients were used to construct the model. **(C)** The Cancer Genome Atlas (TCGA) dataset (discovery cohort) is divided into high-risk ( $N = 77$ ) and low-risk ( $N = 76$ ) groups based on the risk scores generated from the LASSO model. The Kaplan-Meier survival plots of high-risk and low-risk groups. **(D)** The Kaplan-Meier survival plot of the high-risk ( $N = 188$ ) and low-risk ( $N = 47$ ) groups of the International Cancer Genome Consortium (ICGC) dataset (validation cohort). **(E)** From top to bottom, the heatmap of the four CpG sites in the high-risk and low-risk groups of TCGA dataset (top). The distribution plot of survival time and survival status of high-risk and low-risk groups of TCGA dataset (middle). The X-axis is the patients' number with increasing risk scores and the Y-axis is the survival time. The distribution plot of the risk scores of the high-risk and low-risk groups of TCGA dataset (bottom). **(F)** The heatmap of the four CpG sites of the high-risk and low-risk groups of the ICGC dataset (top). The distribution plot of survival time and survival status of the high-risk and low-risk groups of the ICGC dataset (middle). The distribution plot of the risk scores of the high-risk and low-risk groups of the ICGC dataset (bottom).

**TABLE 1 |** Univariate and multivariate Cox analyses of clinicopathological information and risk score of the prognostic prediction model.

Prognostic factors	Univariate Cox regression			Multivariate Cox regression		
	HR	95% CI	P-value	HR	95% CI	P-value
Risk score	10.72	5.52–20.80	<0.001	24.68	7.70–79.14	<0.001
Age	1.03	1.01–1.05	0.016	1.00	0.96–1.04	0.977
Gender	0.82	0.49–1.35	0.428			
Grade	1.80	1.29–2.50	<0.001	2.33	1.16–4.65	0.017
Stage (AJCC 7th)	1.54	1.03–2.29	0.035	0.87	0.23–3.23	0.836
T	2.26	1.28–4.00	0.005	1.80	0.51–6.31	0.360
M	0.55	0.07–4.08	0.560			
N	2.47	1.31–4.66	0.005	1.50	0.59–3.78	0.395
Alcohol history	1.28	0.72–2.26	0.402			
Alcoholic exposure	0.88	0.70–1.10	0.266			
Site of resection	0.50	0.27–0.92	0.026	0.48	0.22–1.05	0.066
Radiation therapy	0.21	0.07–0.68	0.009	0.14	0.04–0.50	0.003
Smoking history	0.90	0.75–1.08	0.273			
Histologic grading	0.71	0.35–1.45	0.346			

with pancreatic cancer. The nomogram model based on the risk score and other independent factors improved the efficiency of the prediction model based on four CpG sites.

## Molecular Characteristics of the Subgroups Based on the Prognostic Prediction Model

The Cancer Genome Atlas dataset was divided into the high-risk and low-risk groups based on the risk score obtained from the prognostic prediction model based on four CpG sites. As the model was significantly associated with the prognosis, it is important to explore the underlying molecular mechanisms. The top 10 results of GO analysis of high-risk and low-risk groups, including molecular function (MF), biological process (BP), and cellular component (CC), are shown in **Figure 3A**. The GO terms were enriched in several important molecular mechanisms, such as regulation of ion transmembrane transport, regulation of *trans*-synaptic signaling, signal release, presynapse, ion channel complex, postsynaptic membrane, ion channel activity, cation channel activity, and potassium channel activity, which indicated a close relationship between cell signaling transduction and the model. As shown in **Figure 3B**, the GSEA revealed that glycolysis, MYC targets, Notch signaling, base excision repair, nucleotide excision repair, and p53 signaling pathway were significantly activated, whereas pancreas beta cells, ABC transporters, calcium signaling pathway, neuroactive ligand-receptor interaction, and type II diabetes mellitus were significantly inhibited in the high-risk group. The comparative mutation spectrum analysis identified genes with different mutational frequencies between the high-risk and low-risk groups (**Supplementary Table 6**). The top 10 genes are shown in **Figure 3C**. The classical genes associated with the progression of pancreatic cancer, such as *KRAS*, *TP53*, and *CDKN2A* exhibited increased mutational frequency in the high-risk group. Next, the immune cell infiltration was analyzed using the TIMER website. The immune scores of CD4 T cell, CD8 T cell, and macrophage in the high-risk

group were significantly lower than those in the low-risk group. This indicated the immunological enhancement of the low-risk group (**Figure 3D** and **Supplementary Table 7**).

## Hub Genes Associated With the Prognosis Model Were Identified by WGCNA

The differentially expressed genes between high-risk and low-risk groups were calculated based on the RNA-Seq data from TCGA dataset. In total, 1861 differentially expressed genes with adjusted *p*-value < 0.05 and |log<sub>2</sub> fold-change| > 1 (**Supplementary Table 8** and **Figure 4A**) were obtained. These differentially expressed genes were used as input data for WGCNA to identify the correlations between gene co-expression modules and clinical traits. The best soft power threshold of WGCNA was set as 4 to maintain the scale-free topology and competent connectivity (**Figures 4B,C**). The hierarchical clustering of WGCNA was utilized to construct five gene co-expression networks (**Figure 4D**). As shown in **Figure 4E**, the brown module was significantly correlated with the risk score (correlation coefficient = 0.6, *p* = 6e–16). Moreover, the brown module was significantly positively correlated with tumor grade, clinical stage, and T stage (**Figure 4E**). These results suggested that the 247 genes in the brown module played a significant role in the progression of pancreatic cancer. The detailed information on the genes of brown module is provided in **Supplementary Table 9**. To further identify the hub genes of the brown module, the correlation between module membership and gene significance for risk score (**Figure 4F**) was analyzed. The top 15 hub genes were obtained using the Cytoscape software and *DNAJB1* served as the hub gene of the network (**Figure 4G**).

## DNAJB1 Was Identified as a Novel Biomarker for Pancreatic Cancer

To comprehensively analyze the role of *DNAJB1* and its family members in the progression of pancreatic cancer,

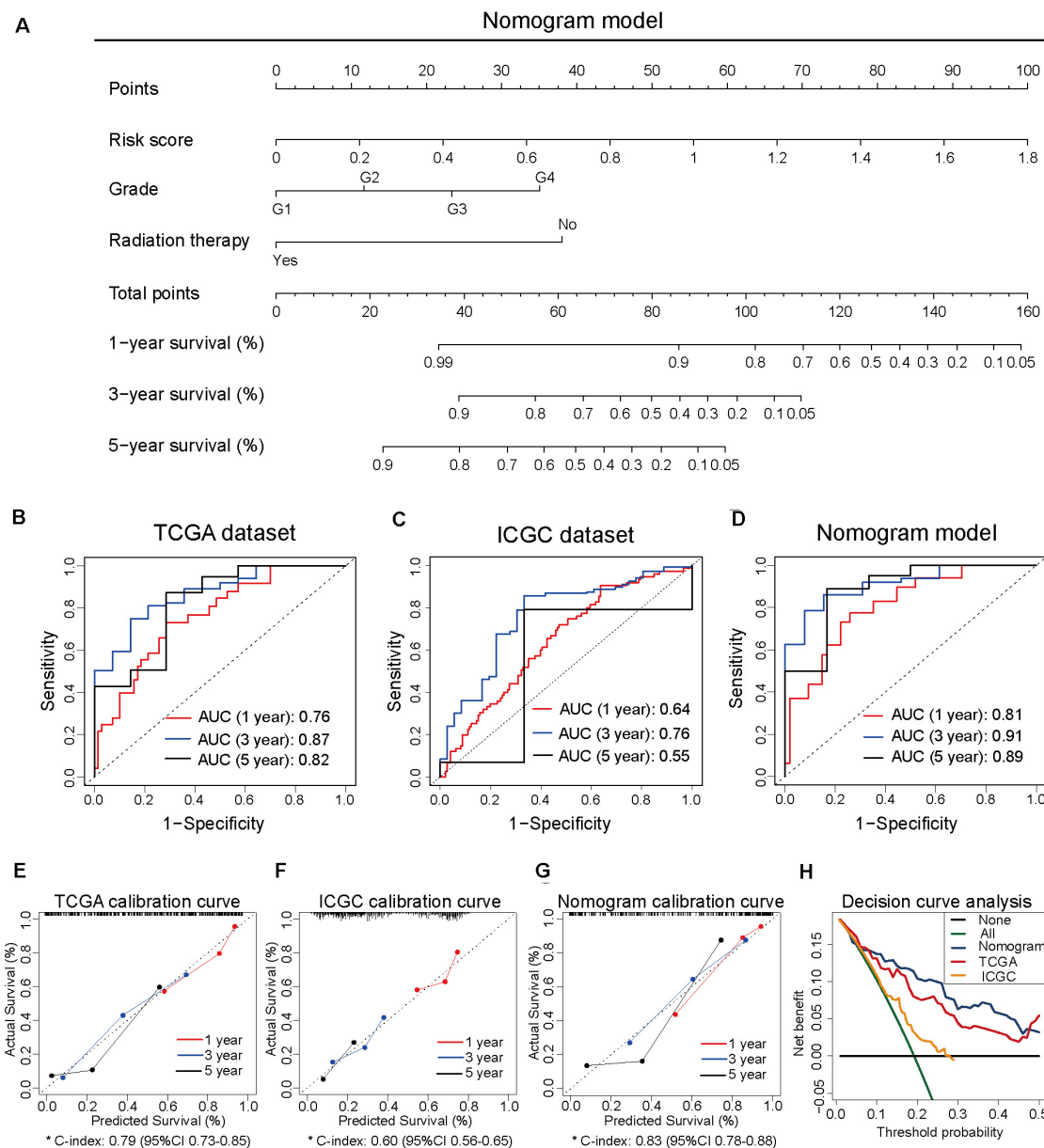


**FIGURE 2 |** Construction of the nomogram model based on three independent prognosis-related factors. **(A)** The nomogram model developed to predict 1-, 3-, and 5-year survival rates of patients with pancreatic cancer from The Cancer Genome Atlas dataset. **(B)** The receiver operating characteristic (ROC) curves of TCGA dataset to predict the 1-, 3-, and 5-year survival rates. **(C)** The ROC curves of the International Cancer Genome Consortium (ICGC) dataset to predict the 1-, 3-, and 5-year survival rates. **(D)** The ROC curves of the nomogram model to predict the 1-, 3-, and 5-year survival rates. **(E)** The calibration curves for predicting the 1-, 3-, and 5-year survival rates of patients from TCGA dataset. **(F)** The calibration curves for predicting the 1-, 3-, and 5-year survival rates of patients from ICGC dataset. **(G)** The calibration curves for predicting the 1-, 3-, and 5-year survival rates in the nomogram model. **(H)** Decision curve analysis of TCGA, ICGC, and nomogram models.

a systematic analysis of the *DNAJB* gene family members (*DNAJB1-DNAJB9* and *DNAJB11-DNAJB14*) was performed. These differentially expressed genes were all obtained from patients with pancreatic cancer based on the stratification of risk score. To verify the diagnostic value of specific genes, the RNA-Seq data of 179 pancreatic cancer tissues and 171 normal pancreatic tissues from TCGA and GTEx databases (Figure 5A)

were integrated. As shown in Figure 5B and Supplementary Figure 1A, the expression levels of *DNAJB1*, *DNAJB5*, *DNAJB6*, *DNAJB11*, *DNAJB12*, *DNAJB13*, and *DNAJB14* were significantly upregulated in the tumor tissues. The expression of *DNAJB1* and *DNAJB13* was positively correlated with the clinical stage (Figure 5D and Supplementary Figure 1B,  $p < 0.05$ ). The members of *DNAJB* gene family associated with overall survival



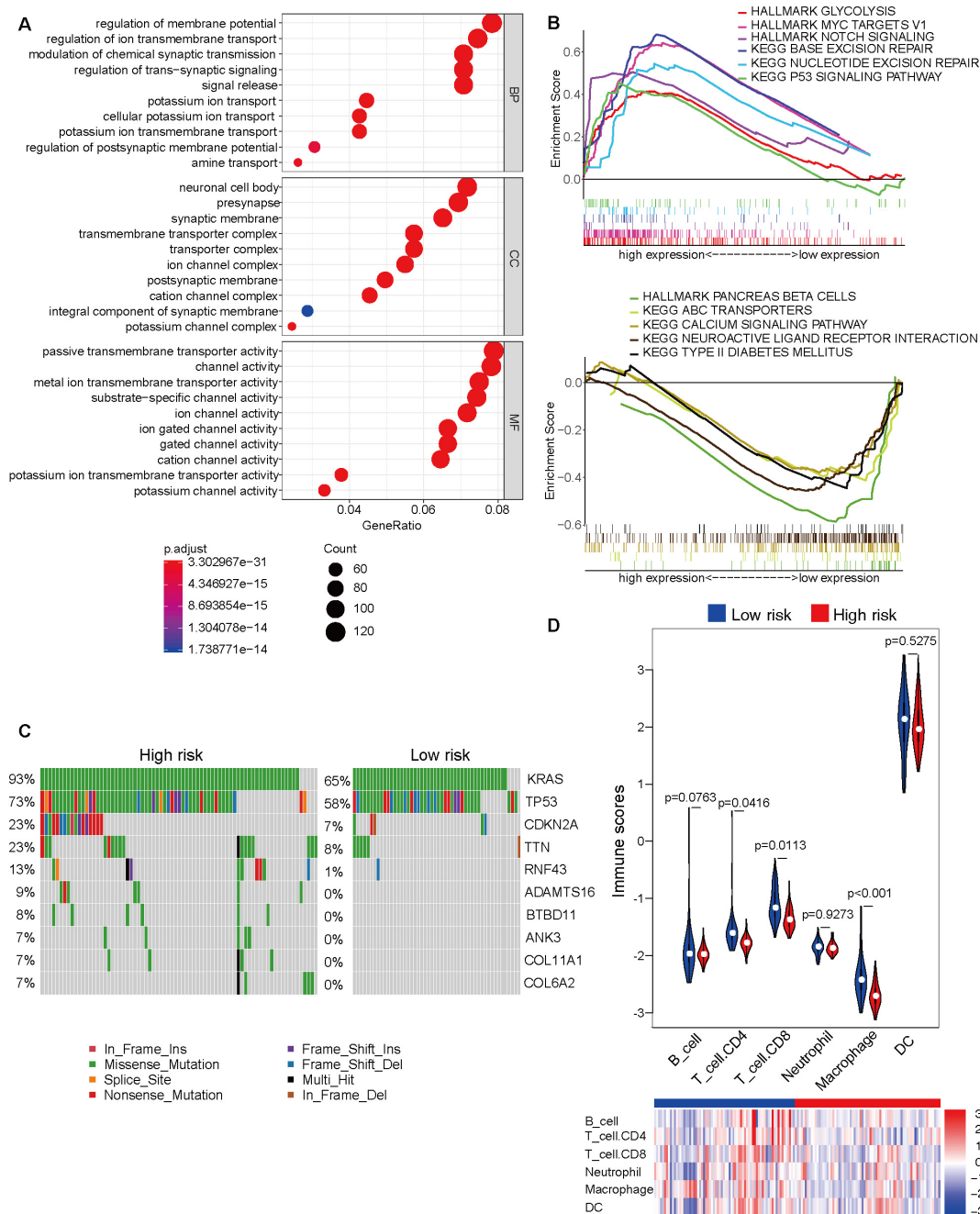


**FIGURE 3 |** Molecular characteristic analyses of the high-risk and low-risk groups based on the prognostic prediction model. **(A)** The results of Gene Ontology analysis of the high-risk and low-risk groups, including biological process (BP), cellular component (CC), and molecular function (MF). **(B)** The activated (top) and inhibited (bottom) signaling pathways in the high-risk and low-risk groups were subjected to Gene Set Enrichment Analysis (GSEA). **(C)** The comparative mutation spectrum analysis of the top 10 genes in the high-risk and low-risk groups. **(D)** The immune infiltration analysis of six immune cell types in the high-risk and low-risk groups based on the Tumor Immune Estimation Resource (TIMER) website.

and relapse-free survival were analyzed. The detailed information is provided in **Figures 5G–J** and **Supplementary Figure 2**. The results indicated that only *DNAJB1* could serve as an unfavorable prognostic factor for overall survival and relapse-free survival. In contrast, *DNAJB2*, *DNAJB5*, and *DNAJB7* served

as favorable prognostic factors for overall survival and relapse-free survival. These results demonstrated that *DNAJB1* might serve as a novel biomarker for pancreatic cancer. The diagnostic ROC curve revealed that *DNAJB1* can be used as an effective diagnostic marker, which had a diagnostic value of 4.8 and AUC



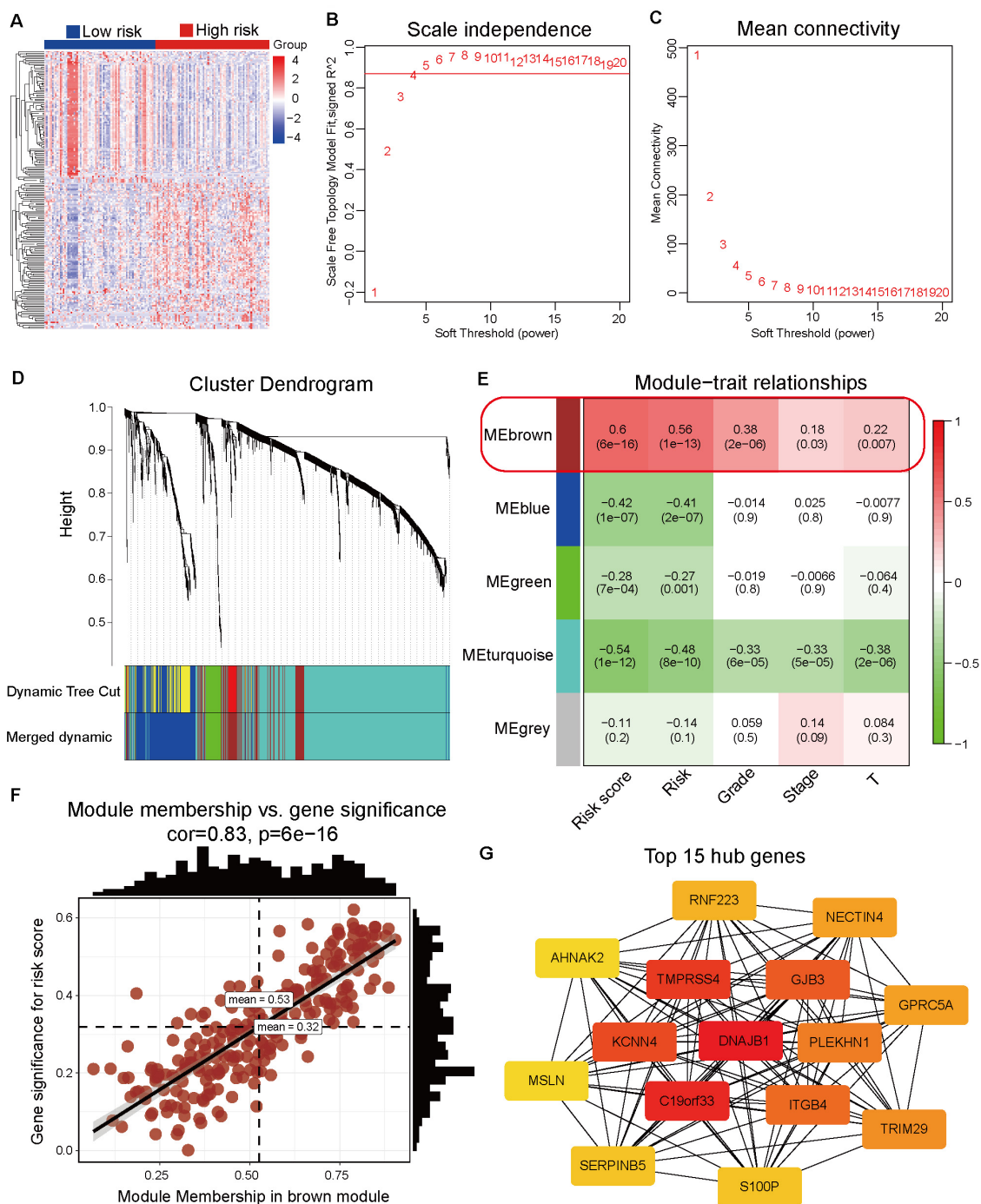


**FIGURE 4 |** Identification of hub genes associated with the prognosis model by weighted correlation network analysis (WGCNA). **(A)** Heatmap of the differentially expressed genes between the high-risk and low-risk groups. **(B)** The correlation between soft threshold power and scale-free topology model fit. **(C)** The correlation between soft threshold power and mean connectivity. **(D)** Identification of co-expression modules by the hierarchical cluster tree. **(E)** The relationships between gene modules and clinical traits. The correlation coefficient (top) and  $p$ -value (bottom) of each cell display in the corresponding cell. **(F)** The correlation between module membership and gene significance of the brown module. **(G)** The top 15 hub genes of the brown module are calculated and visualized using the Cytoscape software.

of 91.6% (95% CI: 82.5–93.3%, **Figure 5C**). To confirm whether *DNAJB1* can be used as a novel biomarker in the plasma, the plasma exosomal RNA-Seq data of 6 healthy donors and 14

patients with pancreatic carcinoma from the GSE106804 (40) and GSE100232 (41) datasets were downloaded and integrated. The principal component analysis suggested that RNA-Seq data of

healthy donors and patients with pancreatic carcinoma clustered separately (Figure 5E). The expression level of exosomal *DNAJB1* was upregulated in patients with pancreatic cancer. A large cohort study is needed to further investigate its diagnostic value (Figure 5F).

In addition to the top 15 hub genes, the other genes also deserved to be investigated. The expression levels of *TMPRSS4*, *KCNN4*, *GJB3*, *ITGB4*, *PLEKHN1*, *TRIM29*, *GPRC5A*, and *NECTIN4* were also significantly upregulated in the pancreatic cancer tissues (Figure 6A). Moreover, the overall survival analysis indicated that these genes can be used as unfavorable prognostic factors (Figure 6B). These results suggested that WGCNA can effectively select survival-related genes. The detailed roles of these genes in pancreatic cancer should be investigated in future studies.

## DNAJB1 Knockdown Inhibits Malignant Phenotype of Pancreatic Cancer *in vitro* and *in vivo*

To evaluate the specific role of *DNAJB1* in pancreatic cancer, the relative expression level of *DNAJB1* in the four pancreatic cancer cell lines (AsPC-1, Capan-2, MIA PaCa-2, and SW1990) and a hTERT-HPNE was analyzed. The expression level of *DNAJB1* in the AsPC-1 and MIA PaCa-2 cell lines was higher than that in the other cell lines (Figure 7A). Therefore, the AsPC-1 and MIA PaCa-2 cell lines were chosen for further functional assays. The efficiency of *DNAJB1* knockdown was detected by western blotting (Figure 7B). The results of CCK8 and colony formation assays indicated that *DNAJB1* knockdown significantly inhibited the proliferation and colony formation rate of AsPC-1 and MIA PaCa-2 cells (Figures 7C–E). The results of transwell assay revealed that the AsPC-1 and MIA PaCa-2 cells exhibited markedly decreased invasion upon *DNAJB1* knockdown (Figures 7F,G). The results of wound healing assay demonstrated that the knockdown of *DNAJB1* significantly decreased the migration of AsPC-1 and MIA PaCa-2 cells (Figures 7H,I). The subcutaneous xenograft model was utilized to detect the cellular proliferation ability *in vivo*. The group injected with *DNAJB1* knockdown AsPC-1 cells exhibited significantly smaller tumoral volumes than the negative control group (Figures 7J,K). The relative expression of *DNAJB1* was detected by the immunohistochemical assay (Figure 7L). These results indicated that *DNAJB1* may be a novel promoter of pancreatic cancer. Further studies are needed to elucidate the underlying molecular mechanisms.

## DISCUSSION

Pancreatic cancer, a malignancy associated with high mortality, has high heterogeneity. The patients with pancreatic cancer receiving similar therapies exhibit varied clinical outcomes (42). Therefore, the development of a risk stratification model may help clinicians to design personalized treatment programs for different patients. Previous studies have proposed various risk stratification models for the diagnosis, prognosis, and recurrence of pancreatic cancer, which exhibited better efficiency than

the classical TNM stage (43–45). The rapid development of sequencing techniques has enabled the access to multi-omics data and high-quality clinical information through different databases, such as TCGA, ICGC, and Gene Expression Omnibus (17, 46, 47). These resources provide novel insights into the initiation and progression of multiple cancers. There is an urgent need to devise strategies to increase the overall survival of patients with pancreatic cancer. The development of a prognosis prediction model based on genome data can be a useful tool for molecular and precise medicine.

Several recent studies have demonstrated that the prognosis model based on DNA methylation data can be used to predict the prognosis of patients with various cancers with satisfactory efficiency. The circulating tumor DNA methylation markers can be utilized to generate a risk model for the diagnosis and prognosis prediction of ovarian cancer, colorectal cancer, and hepatocellular carcinoma (13, 48, 49). Additionally, the DNA methylation markers originating from tissues can also be employed to construct a prognosis prediction model for esophageal, gastric, and prostate cancers (11, 12, 14). These studies demonstrated that the DNA methylation status can serve as novel biomarkers to generate the prognosis prediction model. However, there are limited studies that have reported the significance of prognosis prediction model in pancreatic cancer. In this study, a prognostic prediction model based on four CpG sites, namely cg00609645, cg13512069, cg23811464, and cg03502002, was established. The model was generated based on TCGA dataset and the conclusion was verified in the external ICGC dataset. Next, a nomogram model was constructed based on the independent prognostic factors of pancreatic cancer. Chen H, et al. used three hypomethylated genes (*SULT1E1*, *IGF2BP3*, and *MAP4K4*) to construct a prognostic prediction model using the AUC (1-year: 0.62, 3-year: 0.69, and 5-year: 0.69) (50). Liao X, et al. had constructed a prognostic model comprising 9 hub genes and reported that the AUC for 1-, 3-, and 5-year was 0.641, 0.623, and 0.554, respectively (51). Compared to these two models, the nomogram model exhibited better prediction ability using the AUC (1-year: 0.81, 3-year: 0.91, and 5-year: 0.89). These results suggested that the nomogram model can be employed as an effective instrument for prognosis prediction in patients with pancreatic cancer. The model can be improved with increased access to sequencing data and clinical information.

To further elucidate the molecular mechanisms underlying the prognostic model, the GO, GSEA, mutation spectrum, and immune infiltration analyses were performed on the subgroups stratified by the prognostic prediction model. The low-risk group with improved prognosis exhibited less mutational frequency and high immune cell infiltration. The analysis of several important signaling pathways in the subgroups can aid in a better molecular understanding of the prognostic model.

Furthermore, the WGCNA was performed using the clinical traits and differentially expressed genes. The brown module containing 247 genes was significantly correlated with the prognostic model, tumor grade, clinical stage, and T stage. Next, *DNAJB1* was identified as the hub gene of the brown gene module. These results indicated that *DNAJB1* can play a vital role in pancreatic cancer. Previous studies have reported that

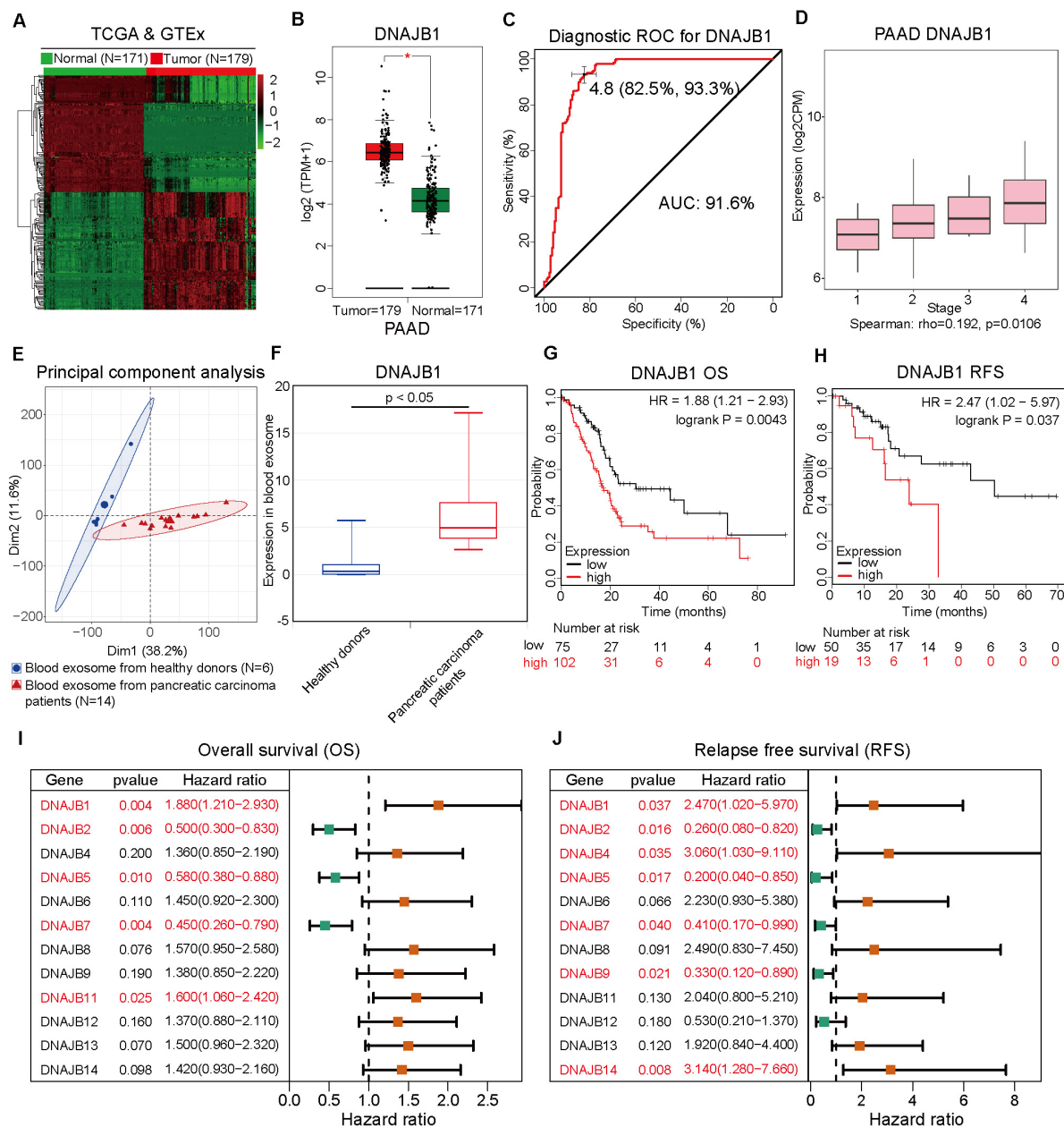


**FIGURE 5 |** *DNAJB1* serves as a novel biomarker for pancreatic cancer. **(A)** Heatmap of the differentially expressed genes between 171 normal pancreatic tissues and 179 pancreatic cancer tissues based on the integrated analysis of The Cancer Genome Atlas (TCGA) and Genotype-Tissue Expression (GTEx) datasets. **(B)** The relative expression level of *DNAJB1* in 171 normal pancreatic tissues and 179 pancreatic cancer tissues. **(C)** The diagnostic receiving operating characteristic (ROC) curve of *DNAJB1* based on the integrated data from TCGA and GTEx datasets. **(D)** The relationship between *DNAJB1* expression level and different clinical stages of pancreatic cancer. **(E)** The principal component analysis of the blood exosome RNA sequencing (RNA-seq) data of healthy donors ( $N = 6$ ) and patients with pancreatic carcinoma ( $N = 14$ ). **(F)** The relative expression level of *DNAJB1* in the blood exosome of healthy donors ( $N = 6$ ) and patients with pancreatic carcinoma ( $N = 14$ ). **(G)** The overall survival analysis of patients from TCGA dataset based on *DNAJB1* expression. **(H)** The relapse-free survival analysis of patients from TCGA dataset based on *DNAJB1* expression. **(I)** The forest plot shows the overall survival analyses of patients from TCGA dataset based on the expression of *DNAJB* gene family. **(J)** The forest plot demonstrates the relapse-free survival of patients from TCGA dataset based on the expression of *DNAJB* gene family members.

*DNAJB1* expression, which is upregulated in the tissues, cell lines, and bile of cholangiocarcinoma, can serve as a new biomarker for cholangiocarcinoma (52). *DNAJB1-PRKACA* gene fusion is reported to play an oncogenic promoter role in fibrolamellar

hepatocellular carcinoma (53, 54). In addition, several researches have demonstrated that the *DNAJB1-PRKACA* gene fusion can also be found in the pancreatic and biliary intraductal oncocytic papillary neoplasm (IOPN), as well as in the intraductal papillary

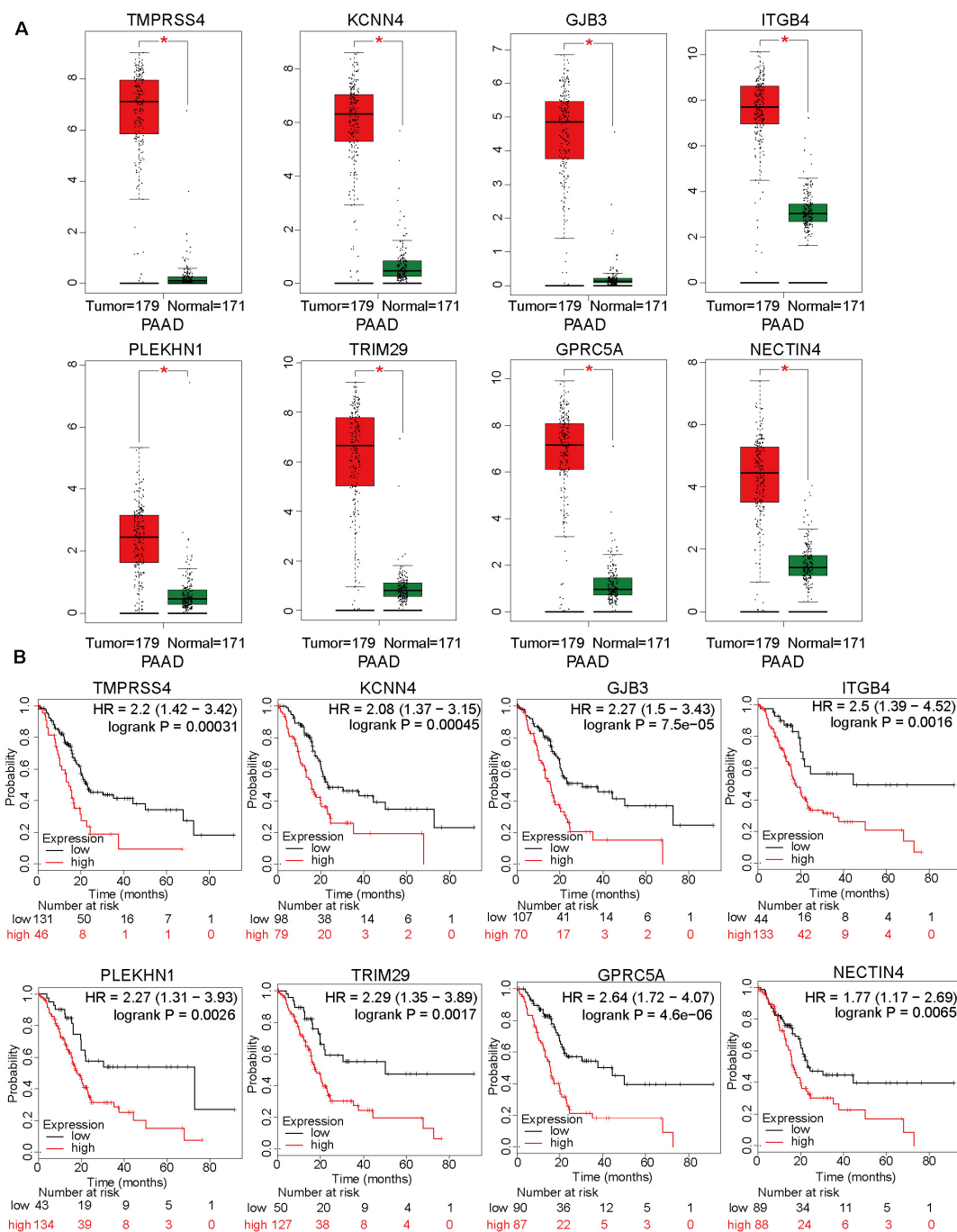


**FIGURE 6 |** The differential expression levels of top 15 hub genes, except for *DNAJB1*, and analysis of overall survival based on these genes. **(A)** The relative expression levels of *TMPRSS4*, *KCNN4*, *GJB3*, *ITGB4*, *PLEKHN1*, *TRIM29*, *GPRC5A*, and *NECTIN4* in 171 normal pancreatic tissues and 179 pancreatic cancer tissues based on the integrated data from The Cancer Genome Atlas (TCGA) and Genome-Tissue Expression (GTEx) datasets. **(B)** The overall survival analyses of patients from TCGA dataset based on the expression of *TMPRSS4*, *KCNN4*, *GJB3*, *ITGB4*, *PLEKHN1*, *TRIM29*, *GPRC5A*, and *NECTIN4*.

mucinous neoplasm (IPMN) of pancreas and pancreatic ductal adenocarcinoma. The specific functions of the gene fusion in the initiation and progression of IOPNs, IPMNs, and their associated neoplasms need further research (55, 56). Cui X, et al. reported that *DNAJB1* can suppress apoptosis and promote cancer cell

proliferation via ubiquitin degradation of PDCD5 in the lung cancer cell line (A549) (57). To identify the specific role of *DNAJB1* in pancreatic cancer, a systematic analysis of *DNAJB1* family members was performed. The analysis indicated that *DNAJB1* may serve as a novel biomarker for the diagnosis and



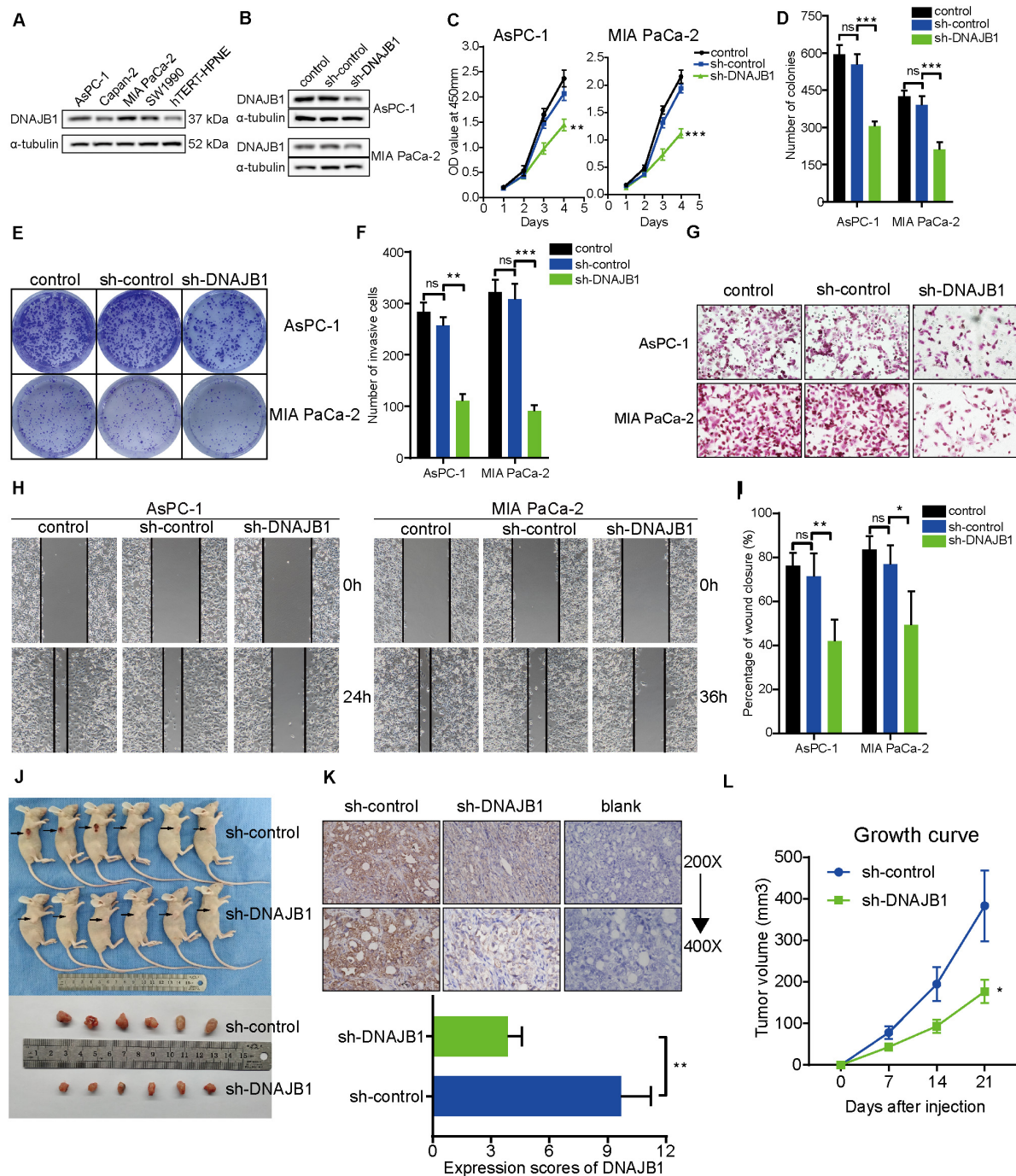


**FIGURE 7 |** Knockdown of *DNAJB1* inhibits proliferation, migration, and invasion of pancreatic cancer cells *in vitro* and *in vivo*. **(A)** The relative expression level of *DNAJB1* in the AsPC-1, Capan-2, MIA PaCa-2, SW1990, and hTERT-HPNE cell lines detected by western blotting. **(B)** The transfection efficiency of sh-DNAJB1 in the AsPC-1 and MIA PaCa-2 cell lines detected by western blotting. **(C)** The CCK-8 assay was used to detect the effect of *DNAJB1* knockdown on the proliferation of AsPC-1 and MIA PaCa-2 cell lines. **(D)** Statistical analysis of the colony formation assay results after knockdown of *DNAJB1* in the AsPC-1 and MIA PaCa-2 cell lines. **(E)** Representative images of the colony formation assay, including control, sh-control, and sh-DNAJB1 groups. **(F)** Statistical analysis of the transwell assay results after knockdown of *DNAJB1* in the AsPC-1 and MIA PaCa-2 cell lines. **(G)** Representative images of the transwell assay. **(H)** Representative images of the wound healing assay. **(I)** Statistical analysis of the wound healing assay results after knockdown of *DNAJB1*. **(J)** Subcutaneous tumor tissues of sh-control and sh-DNAJB1 groups at 3 weeks after initial implantation. **(K)** Relative *DNAJB1* expression in the tumor tissues excised from sh-control and sh-DNAJB1 groups was detected by immunohistochemical assay. **(L)** The growth curve of subcutaneous tumor tissues of sh-control and sh-DNAJB1 groups. \* $p < 0.05$ , \*\* $p < 0.01$ , and \*\*\* $p < 0.001$ .

prognosis of pancreatic cancer. The role of *DNAJB1* in the proliferation, migration, and invasion of pancreatic cancer cells was verified *in vivo* and *in vitro*. The molecular mechanisms of *DNAJB1* in pancreatic cancer must be elucidated in future studies.

## CONCLUSION

A novel prognostic prediction model was established based on four CpG sites for pancreatic cancer. The molecular characteristic analyses based on the model provided new insights into the initiation and development of pancreatic cancer. The WGCNA can serve as an excellent tool to identify the genes correlated with specific clinical traits. *DNAJB1* can serve as a potential diagnostic and prognostic biomarker for pancreatic cancer.

## DATA AVAILABILITY STATEMENT

All datasets presented in this study are included in the article/**Supplementary Material**.

## ETHICS STATEMENT

The animal study was reviewed and approved by the Ethics Committee of Shengjing Hospital of China Medical University.

## AUTHOR CONTRIBUTIONS

LK, PL, and XT contributed to conception and design of the study. XF, TW, and ZW organized the database. LK and PL

performed the statistical analysis. LK and PL wrote the first draft of the manuscript. LK, PL, BZ, and JL wrote sections of the manuscript. All authors contributed to manuscript revision, read, and approved the submitted version.

## FUNDING

This study was supported by the National Natural Science Foundation of China (grant numbers 81902953 and 30973501); Natural Science Foundation of Liaoning Province (grant number 180530068); the Outstanding Young Doctor Fund of China Medical University (grant number QGZD2018050); Liaoning BaiQianWan Talents Program (grant number 3200417003); and 345 Talent Project of Shengjing Hospital of China Medical University. The sponsors had no involvement in any of the stages from study design to submission of the manuscript for publication.

## ACKNOWLEDGMENTS

We would like to thank Editage ([www.editage.cn](http://www.editage.cn)) for English language editing. The results published here are in whole or part based upon data generated by the TCGA Research Network: <https://www.cancer.gov/tcga>.

## SUPPLEMENTARY MATERIAL

The Supplementary Material for this article can be found online at: <https://www.frontiersin.org/articles/10.3389/fonc.2020.01716/full#supplementary-material>

## REFERENCES

1. Siegel RL, Miller KD, Jemal A. Cancer statistics, 2020. *CA Cancer J Clin.* (2020) 70:7–30. doi: 10.3322/caac.21590
2. Liu P, Kong L, Liang K, Wu Y, Jin H, Song B, et al. Identification of dissociation factors in pancreatic Cancer using a mass spectrometry-based proteomic approach. *BMC Cancer.* (2020) 20:45. doi: 10.1186/s12885-020-6522-3
3. Pereira SP, Oldfield L, Ney A, Hart PA, Keane MG, Pandol SJ, et al. Early detection of pancreatic cancer. *Lancet Gastroenterol Hepatol.* (2020) 5:698–710. doi: 10.1016/S2468-1253(19)30416-9
4. Chang JC, Kundranda M. Novel diagnostic and predictive biomarkers in pancreatic adenocarcinoma. *Int J Mol Sci.* (2017) 18:667. doi: 10.3390/ijms18030667
5. Swords DS, Firpo MA, Scaife CL, Mulvihill SJ. Biomarkers in pancreatic adenocarcinoma: current perspectives. *Onco Targets Ther.* (2016) 9:7459–67. doi: 10.2147/OTT.S100510
6. Kiesel JB, Raimondo M, Taylor WR, Yab TC, Mahoney DW, Sun Z, et al. New DNA methylation markers for pancreatic cancer: discovery, tissue validation, and pilot testing in pancreatic juice. *Clin Cancer Res.* (2015) 21:4473–81. doi: 10.1158/1078-0432.CCR-14-2469
7. Natale F, Vivo M, Falco G, Angrisano T. Deciphering DNA methylation signatures of pancreatic cancer and pancreatitis. *Clin Epigenetics.* (2019) 11:132. doi: 10.1186/s13148-019-0728-8
8. Yokoyama S, Higashi M, Kitamoto S, Oeldorf M, Knippschild U, Kornmann M, et al. Aberrant methylation of MUC1 and MUC4 promoters are potential prognostic biomarkers for pancreatic ductal adenocarcinomas. *Oncotarget.* (2016) 7:42553–65. doi: 10.18632/oncotarget.9924
9. Singh N, Rashid S, Rashid S, Dash NR, Gupta S, Saraya A. Clinical significance of promoter methylation status of tumor suppressor genes in circulating DNA of pancreatic cancer patients. *J Cancer Res Clin Oncol.* (2020) 146:897–907. doi: 10.1007/s00432-020-03169-y
10. Majumder S, Raimondo M, Taylor WR, Yab TC, Berger CK, Dukek BA, et al. Methylated DNA in pancreatic juice distinguishes patients with pancreatic cancer from controls. *Clin Gastroenterol Hepatol.* (2020) 18:676–83.e3. doi: 10.1016/j.cgh.2019.07.017
11. Zhang E, Hou X, Hou B, Zhang M, Song Y. A risk prediction model of DNA methylation improves prognosis evaluation and indicates gene targets in prostate cancer. *Epigenomics.* (2020) 12:333–52. doi: 10.2217/epi-2019-0349
12. Peng Y, Wu Q, Wang L, Wang H, Yin F. A DNA methylation signature to improve survival prediction of gastric cancer. *Clin Epigenetics.* (2020) 12:15. doi: 10.1186/s13148-020-0807-x
13. Luo H, Zhao Q, Wei W, Zheng L, Yi S, Li G, et al. Circulating tumor DNA methylation profiles enable early diagnosis, prognosis prediction, and screening for colorectal cancer. *Sci Transl Med.* (2020) 12:eaax7533. doi: 10.1126/scitranslmed.aax7533
14. Li D, Zhang L, Liu Y, Sun H, Onwuka JU, Zhao Z, et al. Specific DNA methylation markers in the diagnosis and prognosis of esophageal cancer. *Aging.* (2019) 11:11640–58. doi: 10.18632/aging.102569
15. Cancer Genome Atlas Research Network. Electronic address aadhe, cancer genome atlas research n. integrated genomic characterization of pancreatic

- ductal adenocarcinoma. *Cancer Cell*. (2017) 32:185–203.e13. doi: 10.1016/j.ccell.2017.07.007
16. International Cancer Genome Consortium, Hudson TJ, Anderson W, Artez A, Barker AD, Bell C, et al. International network of cancer genome projects. *Nature*. (2010) 464:993–8. doi: 10.1038/nature08987
  17. Kong L, Liu P, Zheng M, Xue B, Liang K, Tan X. Multi-omics analysis based on integrated genomics, epigenomics and transcriptomics in pancreatic cancer. *Epigenomics*. (2020) 12:507–24. doi: 10.2217/epi-2019-0374
  18. Aryee MJ, Jaffe AE, Corrada-Bravo H, Ladd-Acosta C, Feinberg AP, Hansen KD, et al. Minfi: a flexible and comprehensive Bioconductor package for the analysis of Infinium DNA methylation microarrays. *Bioinformatics*. (2014) 30:1363–9. doi: 10.1093/bioinformatics/btu049
  19. Simon N, Friedman J, Hastie T, Tibshirani R. Regularization paths for Cox's proportional hazards model via coordinate descent. *J Stat Softw*. (2011) 39:1–13. doi: 10.18637/jss.v039.i05
  20. Friedman J, Hastie T, Tibshirani R. Regularization paths for generalized linear models via coordinate descent. *J Stat Softw*. (2010) 33:1–22.
  21. Blanche P, Dartigues JF, Jacqmin-Gadda H. Estimating and comparing time-dependent areas under receiver operating characteristic curves for censored event times with competing risks. *Stat Med*. (2013) 32:5381–97. doi: 10.1002/sim.5958
  22. Schroder MS, Culhane AC, Quackenbush J, Haibe-Kains B. survcomp: an R/Bioconductor package for performance assessment and comparison of survival models. *Bioinformatics*. (2011) 27:3206–8. doi: 10.1093/bioinformatics/btr511
  23. Vickers AJ, Cronin AM, Elkin EB, Gonen M. Extensions to decision curve analysis, a novel method for evaluating diagnostic tests, prediction models and molecular markers. *BMC Med Inform Decis Mak*. (2008) 8:53. doi: 10.1186/1472-6947-8-53
  24. Li T, Fan J, Wang B, Traugh N, Chen Q, Liu JS, et al. TIMER: a web server for comprehensive analysis of tumor-infiltrating immune cells. *Cancer Res*. (2017) 77:e108–10. doi: 10.1158/0008-5472.CAN-17-0307
  25. Li B, Severson E, Pignon JC, Zhao H, Li T, Novak J, et al. Comprehensive analyses of tumor immunity: implications for cancer immunotherapy. *Genome Biol*. (2016) 17:174. doi: 10.1186/s13059-016-1028-7
  26. Mayakonda A, Lin DC, Assenov Y, Plass C, Koeffler HP. Maftools: efficient and comprehensive analysis of somatic variants in cancer. *Genome Res*. (2018) 28:1747–56. doi: 10.1101/gr.239244.118
  27. Subramanian A, Tamayo P, Mootha VK, Mukherjee S, Ebert BL, Gillette MA, et al. Gene set enrichment analysis: a knowledge-based approach for interpreting genome-wide expression profiles. *Proc Natl Acad Sci USA*. (2005) 102:15545–50. doi: 10.1073/pnas.0506580102
  28. Yu G, Wang LG, Han Y, He QY. clusterProfiler: an R package for comparing biological themes among gene clusters. *OMICS*. (2012) 16:284–7. doi: 10.1089/omi.2011.0118
  29. Love MI, Huber W, Anders S. Moderated estimation of fold change and dispersion for RNA-seq data with DESeq2. *Genome Biol*. (2014) 15:550. doi: 10.1186/s13059-014-0550-8
  30. Langfelder P, Horvath S. WGCNA: an R package for weighted correlation network analysis. *BMC Bioinformatics*. (2008) 9:559. doi: 10.1186/1471-2105-9-559
  31. Langfelder P, Horvath S. Fast R functions for robust correlations and hierarchical clustering. *J Stat Softw*. (2012) 46:i11.
  32. Otasek D, Morris JH, Boucas J, Pico AR, Demchak B. Cytoscape automation: empowering workflow-based network analysis. *Genome Biol*. (2019) 20:185. doi: 10.1186/s13059-019-1758-4
  33. Shannon P, Markiel A, Ozier O, Baliga NS, Wang JT, Ramage D, et al. Cytoscape: a software environment for integrated models of biomolecular interaction networks. *Genome Res*. (2003) 13:2498–504. doi: 10.1101/gr.1239303
  34. Tang Z, Li C, Kang B, Gao G, Li C, Zhang Z. GEPIA: a web server for cancer and normal gene expression profiling and interactive analyses. *Nucleic Acids Res*. (2017) 45:W98–102. doi: 10.1093/nar/gkx247
  35. Nagy A, Lanczky A, Menyhart O, Györffy B. Validation of miRNA prognostic power in hepatocellular carcinoma using expression data of independent datasets. *Sci Rep*. (2018) 8:9227. doi: 10.1038/s41598-018-27521-y
  36. Ru B, Wong CN, Tong Y, Zhong JY, Zhong SSW, Wu WC, et al. TISIDB: an integrated repository portal for tumor-immune system interactions. *Bioinformatics*. (2019) 35:4200–2. doi: 10.1093/bioinformatics/btz210
  37. Qian S, Tan X, Liu X, Liu P, Wu Y. Exosomal Tenascin-c induces proliferation and invasion of pancreatic cancer cells by WNT signaling. *Oncotargets Ther*. (2019) 12:3197–205. doi: 10.2147/OTT.S192218
  38. Wu Y, Tan X, Liu P, Yang Y, Huang Y, Liu X, et al. ITGA6 and RPSA synergistically promote pancreatic cancer invasion and metastasis via PI3K and MAPK signaling pathways. *Exp Cell Res*. (2019) 379:30–47. doi: 10.1016/j.yexcr.2019.03.022
  39. Jin H, Liu P, Wu Y, Meng X, Wu M, Han J, et al. Exosomal zinc transporter ZIP4 promotes cancer growth and is a novel diagnostic biomarker for pancreatic cancer. *Cancer Sci*. (2018) 109:2946–56. doi: 10.1111/cas.13737
  40. Reategui E, van der Vos KE, Lai CP, Zeinali M, Atai NA, Aldikacti B, et al. Engineered nanointerfaces for microfluidic isolation and molecular profiling of tumor-specific extracellular vesicles. *Nat Commun*. (2018) 9:175. doi: 10.1038/s41467-017-02261-1
  41. Li S, Li Y, Chen B, Zhao J, Yu S, Tang Y, et al. exoRBase: a database of circRNA, lncRNA and mRNA in human blood exosomes. *Nucleic Acids Res*. (2018) 46:D106–12. doi: 10.1093/nar/gkx891
  42. Peng J, Sun BF, Chen CY, Zhou JY, Chen YS, Chen H, et al. Single-cell RNA-seq highlights intra-tumoral heterogeneity and malignant progression in pancreatic ductal adenocarcinoma. *Cell Res*. (2019) 29:725–38. doi: 10.1038/s41422-019-0195-y
  43. Xiao D, Dong Z, Zhen L, Xia G, Huang X, Wang T, et al. Combined exosomal GPC1, CD82, and serum CA19-9 as multiplex targets: a specific, sensitive, and reproducible detection panel for the diagnosis of pancreatic cancer. *Mol Cancer Res*. (2020) 18:300–10. doi: 10.1158/1541-7786.MCR-19-0588
  44. Yan X, Wan H, Hao X, Lan T, Li W, Xu L, et al. Importance of gene expression signatures in pancreatic cancer prognosis and the establishment of a prediction model. *Cancer Manag Res*. (2019) 11:273–83. doi: 10.2147/CMAR.S185205
  45. Tanaka M, Mihaljevic AL, Probst P, Heckler M, Klaiber U, Heger U, et al. Meta-analysis of recurrence pattern after resection for pancreatic cancer. *Br J Surg*. (2019) 106:1590–601. doi: 10.1002/bjs.11295
  46. Edgar R, Domrachev M, Lash AE. Gene expression omnibus: NCBI gene expression and hybridization array data repository. *Nucleic Acids Res*. (2002) 30:207–10. doi: 10.1093/nar/30.1.207
  47. Barrett T, Wilhite SE, Ledoux P, Evangelista C, Kim IF, Tomashevsky M, et al. NCBI GEO: archive for functional genomics data sets—update. *Nucleic Acids Res*. (2013) 41:D991–5. doi: 10.1093/nar/gks1193
  48. Widschwendter M, Zikan M, Wahl B, Lempiainen H, Paprotka T, Evans I, et al. The potential of circulating tumor DNA methylation analysis for the early detection and management of ovarian cancer. *Genome Med*. (2017) 9:116. doi: 10.1186/s13073-017-0500-7
  49. Xu RH, Wei W, Krawczyk M, Wang W, Luo H, Flagg K, et al. Circulating tumour DNA methylation markers for diagnosis and prognosis of hepatocellular carcinoma. *Nat Mater*. (2017) 16:1155–61. doi: 10.1038/nmat4997
  50. Chen H, Kong Y, Yao Q, Zhang X, Fu Y, Li J, et al. Three hypomethylated genes were associated with poor overall survival in pancreatic cancer patients. *Aging*. (2019) 11:885–97. doi: 10.18632/aging.101785
  51. Liao X, Huang K, Huang R, Liu X, Han C, Yu L, et al. Genome-scale analysis to identify prognostic markers in patients with early-stage pancreatic ductal adenocarcinoma after pancreaticoduodenectomy. *Oncotargets Ther*. (2017) 10:4493–506. doi: 10.2147/OTT.S142557
  52. Ren H, Luo M, Chen J, Zhou Y, Li X, Zhan Y, et al. Identification of TPD52 and DNAJB1 as two novel bile biomarkers for cholangiocarcinoma by iTRAQ-based quantitative proteomics analysis. *Oncol Rep*. (2019) 42:2622–34. doi: 10.3892/or.2019.7387
  53. Kasthuber ER, Lalazar G, Houlihan SL, Tschaharganeh DF, Baslan T, Chen CC, et al. DNAJB1-PRKACA fusion kinase interacts with beta-catenin and the liver regenerative response to drive fibrolamellar hepatocellular carcinoma. *Proc Natl Acad Sci USA*. (2017) 114:13076–84. doi: 10.1073/pnas.1716483114
  54. Engelholm LH, Riaz A, Serra D, Dagnaes-Hansen F, Johansen JV, Santoni-Rugiu E, et al. CRISPR/Cas9 engineering of adult mouse liver demonstrates that the dnajb1-prkaca gene fusion is sufficient to induce tumors resembling fibrolamellar hepatocellular carcinoma. *Gastroenterology*. (2017) 153:1662–73.e10. doi: 10.1053/j.gastro.2017.09.008

55. Vyas M, Hechtman JF, Zhang Y, Benayed R, Yavas A, Askan G, et al. DNAB1-PRKACA fusions occur in oncocytic pancreatic and biliary neoplasms and are not specific for fibrolamellar hepatocellular carcinoma. *Mod Pathol.* (2020) 33:648–56. doi: 10.1038/s41379-019-0398-2
56. Singhi AD, Wood LD, Parks E, Torbenson MS, Felsenstein M, Hruban RH, et al. Recurrent rearrangements in PRKACA and PRKACB in intraductal oncocytic papillary neoplasms of the pancreas and bile duct. *Gastroenterology.* (2020) 158:573–82.e2. doi: 10.1053/j.gastro.2019.10.028
57. Cui X, Choi HK, Choi YS, Park SY, Sung GJ, Lee YH, et al. DNAB1 destabilizes PDCD5 to suppress p53-mediated apoptosis. *Cancer Lett.* (2015) 357:307–15. doi: 10.1016/j.canlet.2014.11.041

**Conflict of Interest:** The authors declare that the research was conducted in the absence of any commercial or financial relationships that could be construed as a potential conflict of interest.

Copyright © 2020 Kong, Liu, Fei, Wu, Wang, Zhang, Li and Tan. This is an open-access article distributed under the terms of the Creative Commons Attribution License (CC BY). The use, distribution or reproduction in other forums is permitted, provided the original author(s) and the copyright owner(s) are credited and that the original publication in this journal is cited, in accordance with accepted academic practice. No use, distribution or reproduction is permitted which does not comply with these terms.





# HILPDA Is a Prognostic Biomarker and Correlates With Macrophage Infiltration in Pan-Cancer

Chengdong Liu<sup>††</sup>, Xiaohan Zhou<sup>2†</sup>, Hanyi Zeng<sup>1</sup>, Dehua Wu<sup>2\*</sup> and Li Liu<sup>1\*</sup>

<sup>1</sup> Department of Infectious Diseases, Nanfang Hospital, Southern Medical University, Guangzhou, China, <sup>2</sup> Department of Radiation Oncology, Nanfang Hospital, Southern Medical University, Guangzhou, China

## OPEN ACCESS

### Edited by:

Alessandro Passardi,  
Romagnolo Scientific Institute for the  
Study and Treatment of Tumors  
(IRCCS), Italy

### Reviewed by:

Xiao Xu,  
Zhejiang University, China  
Gao Liu,  
Meizhou People's Hospital, China

### \*Correspondence:

Li Liu  
liuli@i.smu.edu.cn  
Dehua Wu  
wudehua.gd@gmail.com

<sup>†</sup>These authors have contributed  
equally to this work

### Specialty section:

This article was submitted to  
Gastrointestinal Cancers,  
a section of the journal  
Frontiers in Oncology

Received: 22 August 2020

Accepted: 22 February 2021

Published: 18 March 2021

### Citation:

Liu C, Zhou X, Zeng H, Wu D and  
Liu L (2021) HILPDA Is a Prognostic  
Biomarker and Correlates With  
Macrophage Infiltration in Pan-Cancer.  
Front. Oncol. 11:597860.  
doi: 10.3389/fonc.2021.597860

**Background:** The protein hypoxia-inducible lipid droplet-associated (HILPDA) is differentially expressed in various tumors. However, its role and correlation with immune cell infiltration in most tumors remain unclear.

**Methods:** HILPDA expression was analyzed in pan-cancer data from The Cancer Genome Atlas (TCGA) database. The influence of HILPDA in clinical prognosis was evaluated using clinical survival data from TCGA. Enrichment analysis of HILPDA was conducted using the R package “clusterProfiler.” We downloaded the immune cell infiltration score of TCGA samples from published articles and analyzed the correlation between the magnitude of immune cell infiltration and HILPDA expression.

**Results:** HILPDA was highly expressed and associated with worse overall survival, disease-specific survival, and progression-free interval in most tumor types. In addition, HILPDA expression was significantly associated with the glycolysis pathway and infiltration of immune cells. Tumor-associated macrophage (TAM) infiltration increased in tissues with high HILPDA expression in most tumor types. Immunosuppressive genes, such as *PD-L1*, *PD-1*, *TGFB1*, and *TGFBR1* were positively correlated with HILPDA.

**Conclusions:** Our study suggests that HILPDA is a marker of poor prognosis. High HILPDA may contribute to TAM infiltration and be associated with tumor immunosuppression status.

**Keywords:** HILPDA, pan-cancer, tumor associated macrophages, TCGA, immunosuppression

## INTRODUCTION

Hypoxia-inducible lipid droplet associated protein (HILPDA) plays an oncogenic role in various tumor types. For example, HILPDA is overexpressed in colorectal cancer and promotes cancer progression via hypoxia-dependent and independent pathways (1). Interestingly, high HILPDA expression was reported to predict worse patient survival in renal cell carcinoma, in which it may

**Abbreviations:** ACC, Adrenocortical carcinoma; BLCA, Bladder Urothelial Carcinoma; BRCA, Breast invasive carcinoma; CESC, Cervical squamous cell carcinoma and endocervical adenocarcinoma; CHOL, Cholangiocarcinoma; COAD, Colon adenocarcinoma; DLBC, Lymphoid Neoplasm Diffuse Large B-cell Lymphoma; ESCA, Esophageal carcinoma; GBM, Glioblastoma multiforme; HNSC, Head and Neck squamous cell carcinoma; KICH, Kidney Chromophobe; KIRC, Kidney renal clear cell carcinoma; KIRP, Kidney renal papillary cell carcinoma; LAML, Acute Myeloid Leukemia; LGG, Lower Grade Glioma; LIHC, Liver hepatocellular carcinoma; LUAD, Lung adenocarcinoma; LUSC, Lung squamous cell carcinoma; MESO, Mesothelioma; OV, Ovarian serous cystadenocarcinoma; PAAD, Pancreatic adenocarcinoma; PCPG, Pheochromocytoma and Paraganglioma; PRAD, Prostate adenocarcinoma; READ, Rectum adenocarcinoma; SARC, Sarcoma; SKCM, Skin Cutaneous Melanoma; STAD, Stomach adenocarcinoma; TGCT, Testicular Germ Cell Tumor; THCA, Thyroid carcinoma; THYM, Thymoma; UCEC, Uterine Corpus Endometrial Carcinoma; UCS, Uterine Carcinosarcoma; UVM, Uveal Melanoma.

become a potential target for molecular therapy (2). However, the roles of HILPDA in most tumor types remain unclear.

Complex tumor microenvironment (TME), especially tumor immune microenvironment (TIME), is the main factor for poor prognosis of tumor patients (3). Tumor associated macrophages (TAMs) constitute the plasticity and heterogeneity of TME, which can account for 50% of some solid tumors (4). TAMs, especially M2-like TAMs, play an important role in tumor progression. Many oncogenes can promote the infiltration of TAMs in TME to accelerate tumor progression. However, the association between HILPDA expression and the infiltration of TAMs has not been explored.

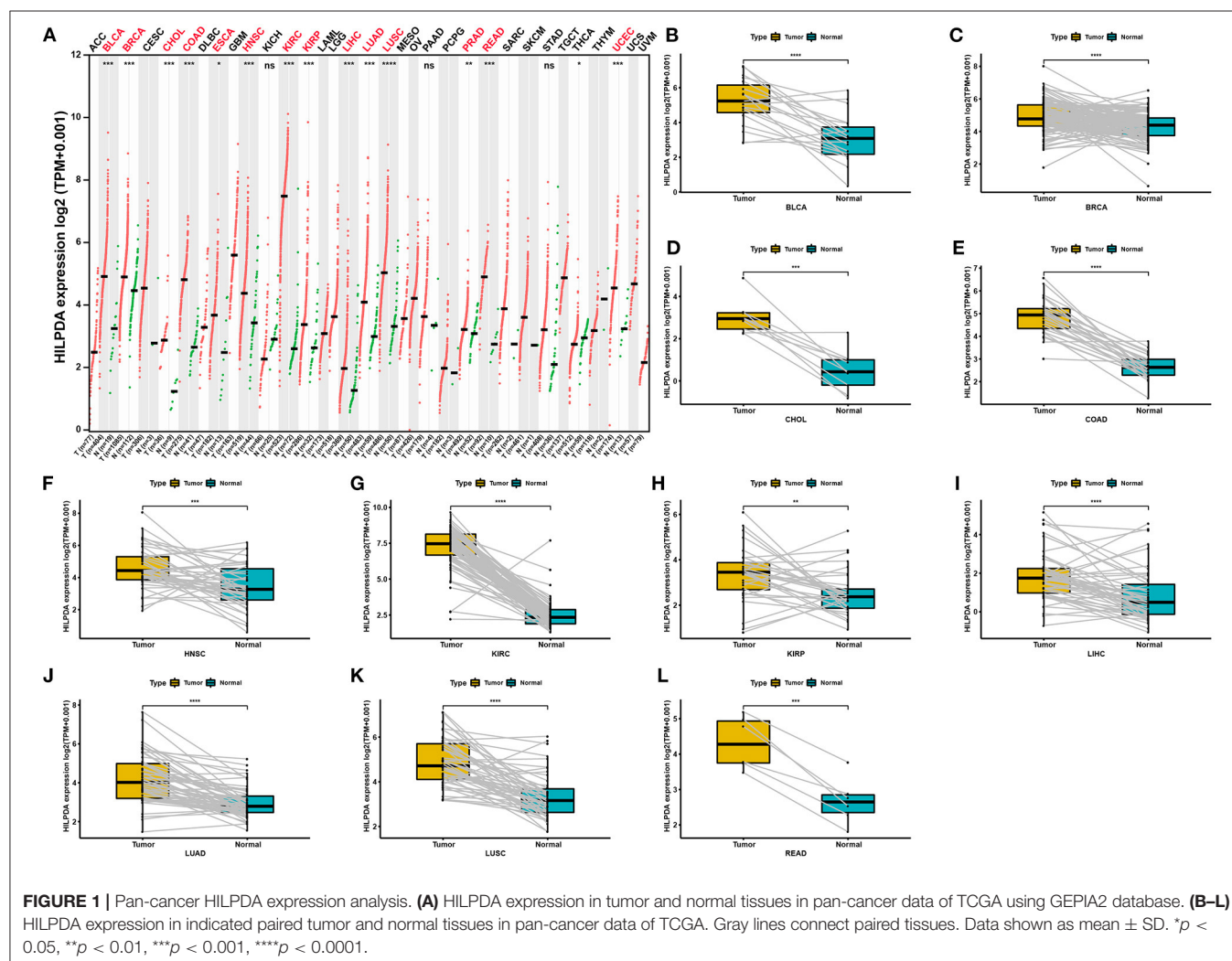
In this study, we evaluated HILPDA expression in different tumor types from The Cancer Genome Atlas (TCGA) database and its association with tumor stage and prognosis of patients. We found that HILPDA is overexpressed in 14 tumor types. Additionally, high HILPDA expression was associated with worse overall survival (OS), disease-specific survival (DSS), and progression-free intervals (PFI) in most tumor types. HILPDA was predicted to participate in pathways related to the cell

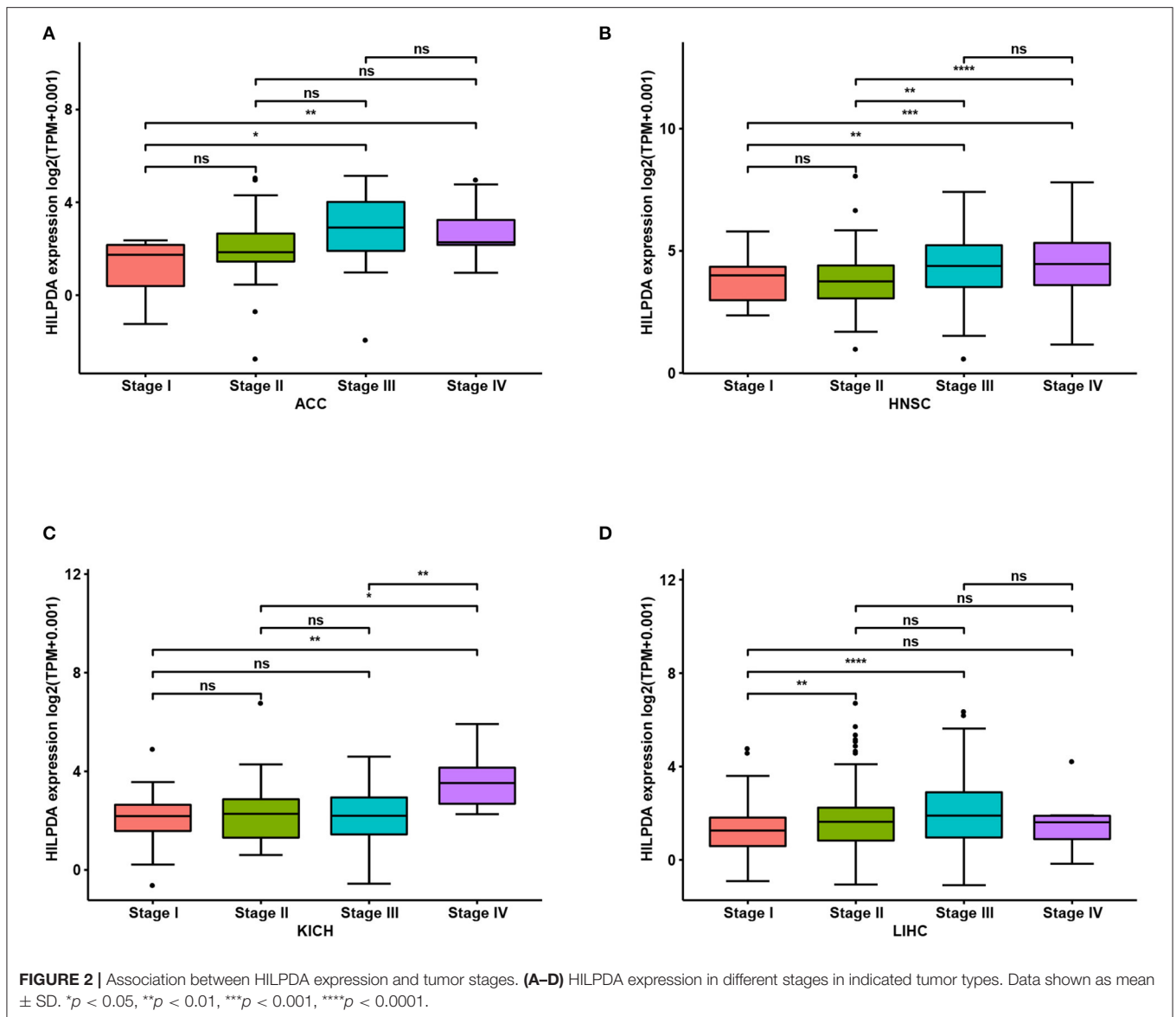
cycle and tumor immunity. As of immune cell infiltration is an important prognostic factor in tumor progression (5, 6), we examined the correlation between HILPDA expression and immune cell infiltration score and found that tumor associated macrophages (TAM) infiltration significantly increased in tissues with high HILPDA expression. Moreover, HILPDA was positively correlated with immunosuppressive gene, such as PD-L1, PD-1, TGFBI, and TGFBR1. Our results offer novel insights into the functional role of HILPDA and further highlight a potential mechanistic basis whereby HILPDA influences TAM infiltration and immunosuppressive gene expression in tumor microenvironment.

## MATERIALS AND METHODS

### Data Collection and Analysis of HILPDA Expression

HILPDA expression profiles and clinical information of TCGA pan-cancer data were downloaded from the UCSC Xena (<https://xenabrowser.net/datapages/>) database. A total of 10496





patients with expression profiles and corresponding clinical data were included in our study. For HILPDA expression analysis in paired tumor and normal tissues, we selected a total of 1,362 patients with expression profiles of both tumor and adjacent normal tissues. For HILPDA expression analysis in different WHO stages, we selected a total of 7,105 patients with completed stage information. For survival analysis, 9,637, 9,165, and 9,479 patients with overall survival, disease-specific survival, and progression-free interval information were selected, respectively.

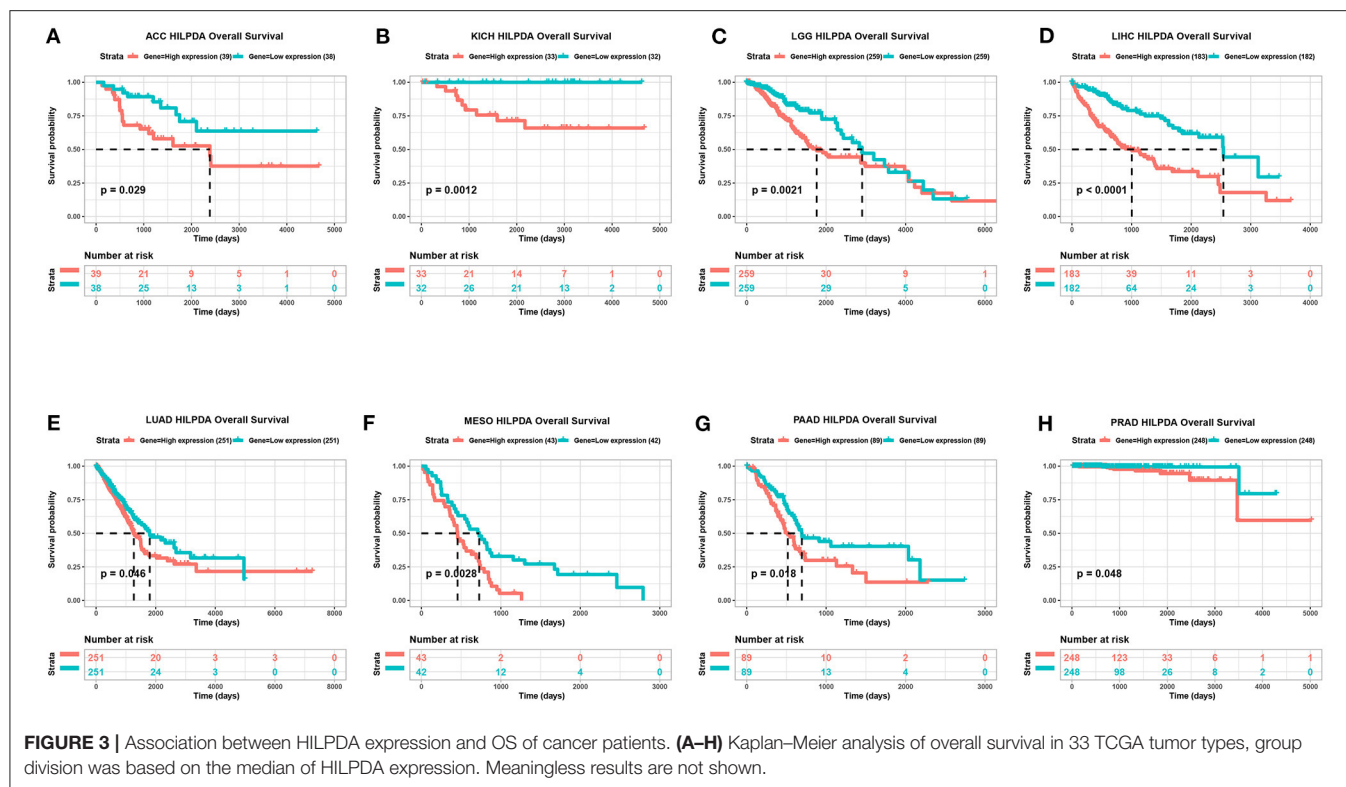
## Correlation and Enrichment Analyses

The correlation analysis of HILPDA was performed using TCGA LIHC data. The Pearson correlation coefficient was calculated. The top 300 genes most positively correlated with HILPDA were selected for enrichment analysis to reflect the

function of HILPDA. Gene Set Variation Analysis (GSVA) was conducted using the R package “GSVA” to calculate the pathway score of each sample based on the MSigDB database v7.1 (<https://www.gsea-msigdb.org/gsea/msigdb/index.jsp>). Gene set enrichment analyses (GSEA) were conducted using the R package “clusterProfiler,” with the following parameters:  $nPerm = 1,000$ ,  $minGSSize = 10$ ,  $maxGSSize = 1,000$ , and  $p\text{-value-Cutoff} = 0.05$ .

## Immune Cell Infiltration

TCGA pan-cancer immune cell infiltration score was downloaded from the published study “The Immune Landscape of Cancer” (7), in which immune cell infiltration score was estimated using CIBERSORT. Samples of TCGA were divided into two groups (high HILPDA group and low HILPDA group) based on the median of HILPDA expression to compare the level of immune cell infiltration.



## Tumor Mutation Burden Calculation

TCGA somatic mutation data was downloaded from the UCSC XENA database. Tumor mutation burden (TMB) was calculated as the number of mutated bases per million bases, based on somatic mutation data in each tumor. The TMB results are shown in **Supplementary Table 1**.

## Statistical Analysis

Data are presented as the mean  $\pm$  standard deviation (SD). Student's *t*-test (two-tailed) was used to analyze differences between two groups using R software (version: 3.6.2).  $p < 0.05$  was considered statistically significant: \* $p < 0.05$ ; \*\* $p < 0.01$ ; \*\*\* $p < 0.001$ ; and \*\*\*\* $p < 0.0001$ .

## Human Tissue Samples

The experiments involving human samples in our study were in accordance with the principles of the Declaration of Helsinki, and approved by the Institutional Review Board of Nanfang Hospital, Southern Medical University of Guangdong, China (NFEC-201208-K3). A total of 13 liver cancer and paired non-cancerous tissues were collected and used for qRT-PCR.

## qRT-PCR

TRIzol<sup>®</sup> reagent (TaKaRa, Tokyo, Japan), PrimeScript<sup>™</sup> 1st Strand cDNA Synthesis Kit (TaKaRa, Tokyo, Japan), and SYBR<sup>®</sup> Green PCR kit (TaKaRa, Tokyo, Japan) were used to perform the extraction of total RNA, synthesization of First-strand cDNA, and Real-time PCR, respectively. Primers as follows:

ACTB:

Forward Primer CATGTACGTTGCTATCCAGGC,  
Reverse Primer CTCCTTAATGTCACGCACGAT  
HILPDA:

Forward Primer AAGCATGTGTTGAACCTCTACC  
Reverse Primer TGTGTTGGCTAGTTGGCTTCT  
CD274:

Forward Primer TGGCATTGCTGAACGCATTT  
Reverse Primer TGCAGCCAGGTCTAATTGTTTT  
TGFB1:

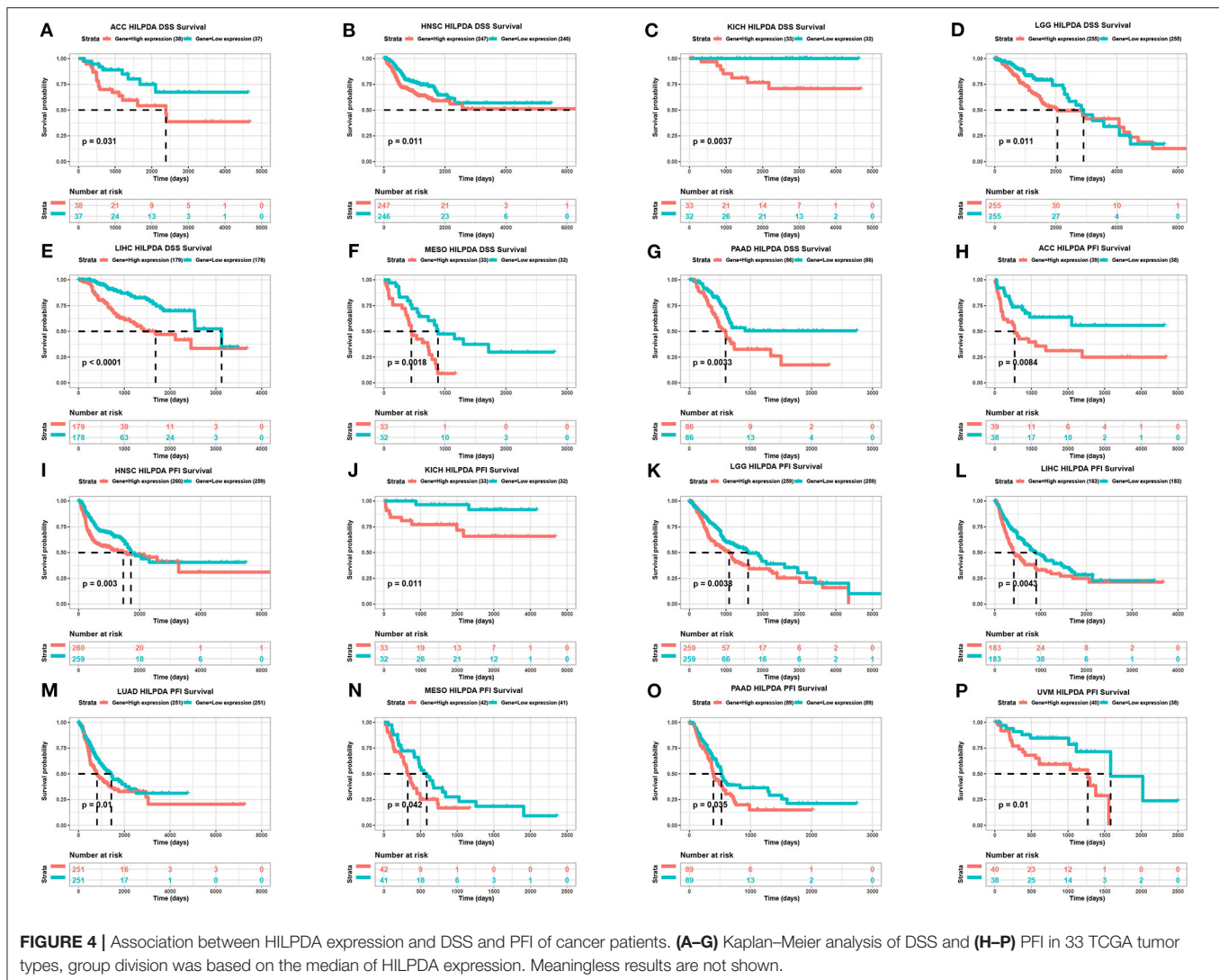
Reverse Primer TGCAGCCAGGTCTAATTGTTTT  
Reverse Primer GTGGGTTTCCACCATTAGCAC.

## RESULTS

### HILPDA Expression Is High in Several Tumor Types and Correlates With Clinical Stage

We first assessed HILPDA expression in pan-cancer data from TCGA. The analysis results revealed that HILPDA expression was higher in 14 tumors, including Bladder Urothelial Carcinoma (BLCA), Breast Invasive Carcinoma (BRCA), Cholangiocarcinoma (CHOL), Colon Adenocarcinoma (COAD), Esophageal Carcinoma (ESCA), Head and Neck Squamous Cell Carcinoma (HNSC), Kidney Renal Clear Cell Carcinoma (KIRC), Kidney Renal Clear Cell Carcinoma (KIRP), Liver Hepatocellular Carcinoma (LIHC), Lung Adenocarcinoma (LUAD), Lung Squamous Cell Carcinoma (LUSC), Prostate Adenocarcinoma (PRAD), Prostate Adenocarcinoma (READ), and Uterine Corpus Endometrial Carcinoma (UCEC), while





lower expression was observed in Thyroid Carcinoma (THCA) (Figure 1A). For paired tumors and normal tissues, HILPDA was overexpressed in tumor tissues of BLCA, BRCA, CHOL, COAD, HNSC, KIRC, KIRP, LIHC, LUAD, LUSC, and READ (Figures 1B–L). In addition, the expression of HILPDA was closely related to the clinical stage, being higher in patients with relatively high stages of several tumor types, including Adrenocortical Carcinoma (ACC), HNSC, Kidney Chromophobe (KICH), and LIHC (Figures 2A–D).

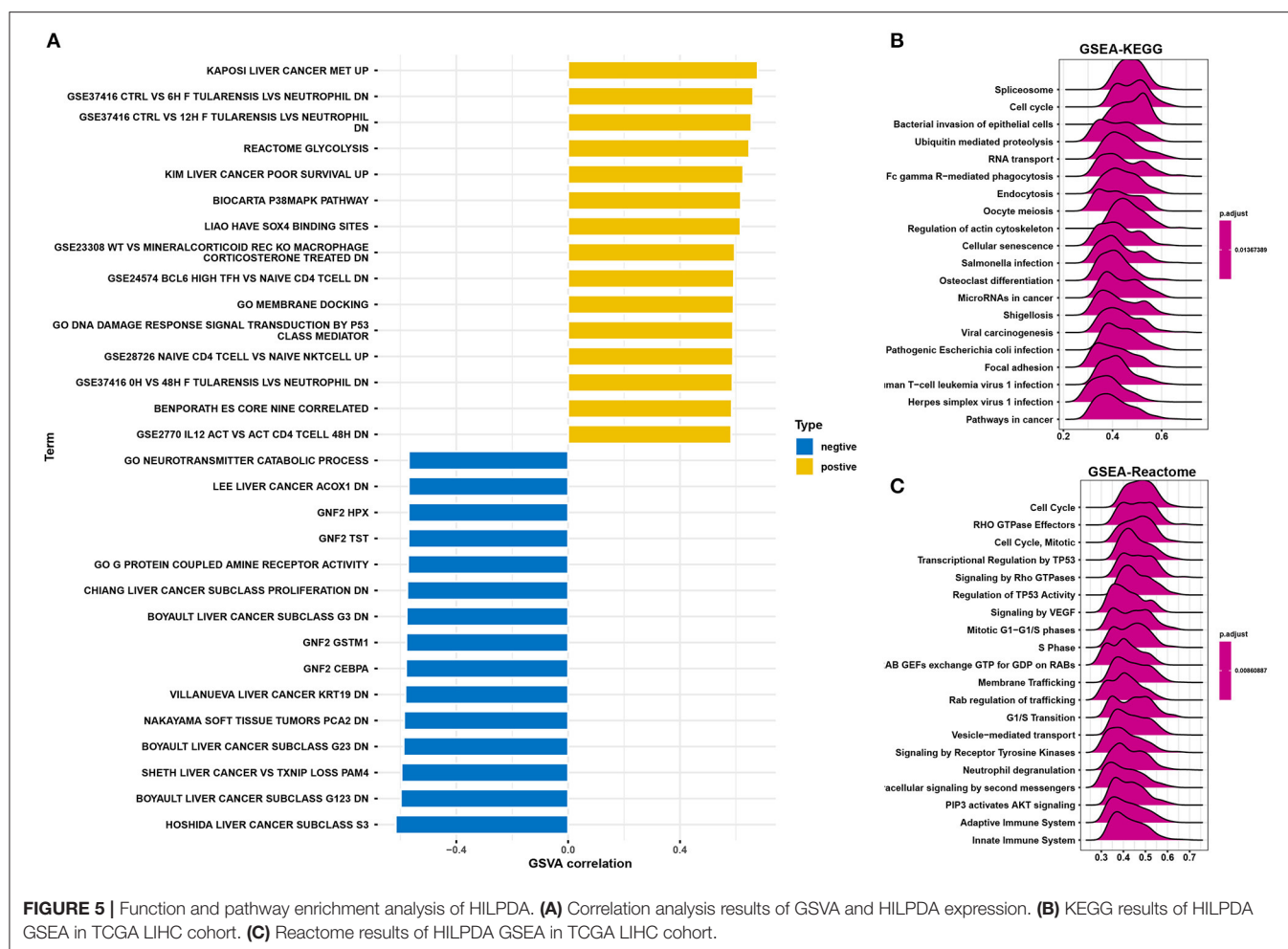
## HILPDA High Expression Correlates With Poor Cancer Prognosis

To evaluate the value of HILPDA in predicting the prognosis of cancer patients, the association between its expression and OS, DSS, and PFI was analyzed in TCGA cohort. Higher expression of HILPDA was significantly associated with worse OS in ACC ( $p = 0.029$ ), KICH ( $p = 0.0012$ ), LGG ( $p = 0.00097$ ), LIHC ( $p < 0.0001$ ), LUAD ( $p = 0.046$ ), MESO ( $p = 0.0028$ ), PAAD ( $p = 0.018$ ), and PRAD ( $p < 0.048$ ) (Figures 3A–H). Similarly,

higher HILPDA expression was significantly associated with a reduction in DSS in ACC ( $p = 0.031$ ), HNSC ( $p = 0.011$ ), KICH ( $p = 0.0037$ ), LGG ( $p = 0.011$ ), LIHC ( $p < 0.0001$ ), MESO ( $p < 0.0018$ ), and PAAD ( $p = 0.0033$ ) (Figures 4A–G). In addition, the PFI was reduced in the high HILPDA expression groups in ACC ( $p = 0.0084$ ), HNSC ( $p = 0.003$ ), KICH ( $p = 0.011$ ), KIRC ( $p = 0.005$ ), LGG ( $p = 0.0038$ ), LIHC ( $p = 0.0043$ ), LUAD ( $p = 0.01$ ), MESO ( $p = 0.042$ ), PAAD ( $p = 0.035$ ), and UVM ( $p = 0.01$ ) (Figures 4H–P).

## HILPDA Is Involved in Pathways Related to Malignancy

To predict the functions of HILPDA, we conducted a GSEA analysis based on gene sets from the MSigDB database v7.1. Results showed the scores of “Liver cancer MET up,” “Glycolysis,” and “Liver cancer poor survival up” pathways were positively correlated with HILPDA expression, indicating a role in these malignant processes (Figure 5A). We further conducted a GSEA analysis of HILPDA using TCGA LIHC data. The GSEA results



showed that cell cycle-related pathways, including the cell cycle pathway in Kyoto Encyclopedia of Genes and Genomes (KEGG) and cell cycle, transcriptional regulation by P53, mitotic G-G1/S phases, and S phase in Reactome, were significantly enriched (Figures 5B,C). These results suggest that HILPDA is associated with many malignancy-related pathways, especially those related to the cell cycle and glycolysis.

## High HILPDA Expression Correlates With High Immune Cell Infiltration and Immunosuppressive Genes in Most Tumors

We further analyzed the effect of HILPDA on the tumor immune microenvironment. We noticed that macrophages, M0 macrophage or M2 macrophage infiltration levels were higher in the high HILPDA expression group in most tumor types, especially in BRCA, CESC, LIHC, PAAD, PCPG, SKCM, and STAD (Figure 6). Correlation analysis revealed that HILPDA expression was positively correlated with infiltration levels of macrophages in most tumor types, including BRCA, CESC, LIHC, PAAD, PCPG, SKCM, STAD, and UCS (Supplementary Figure 1). Tumor-associated macrophage (TAM) infiltration and TMB status are closely related to the immunosuppressive state of the tumor (8). We further analyzed

the relationship of HILPDA with TMB and immunosuppressive genes using TCGA pan-cancer data. As shown in Figure 7A, HILPDA expression was positively correlated with TMB in LUAD, MESO, PCPG, TGCT, STAD, OV, BLCA, and HNSC, and negatively correlated with TMB in THCA and COAD. In addition, HILPDA expression was positively correlated with immunosuppressive genes, especially *PD-L1* (*CD274*), *PD-1* (*PDCD1*), *TGFB1*, and *TGFB1R1*, in most tumors (Figures 7B–F). Moreover, we validated the expression of HILPDA and the correlation between the expression of HILPDA and *TGFB1/CD274* using 13 paired samples from liver cancer patients. The results revealed that HILPDA was highly expressed in liver cancer tissues (Figure 7G). HILPDA expression was positively correlated with *TGFB1* and *CD274* expression in liver cancer tissues (Figures 7H,I). These results suggest that the high expression of HILPDA is closely related to the immunosuppressive status.

## DISCUSSION

HILPDA is involved in the progression of many diseases, including several tumor types (9, 10). Previous studies have shown the oncogenic role of HILPDA in head and neck

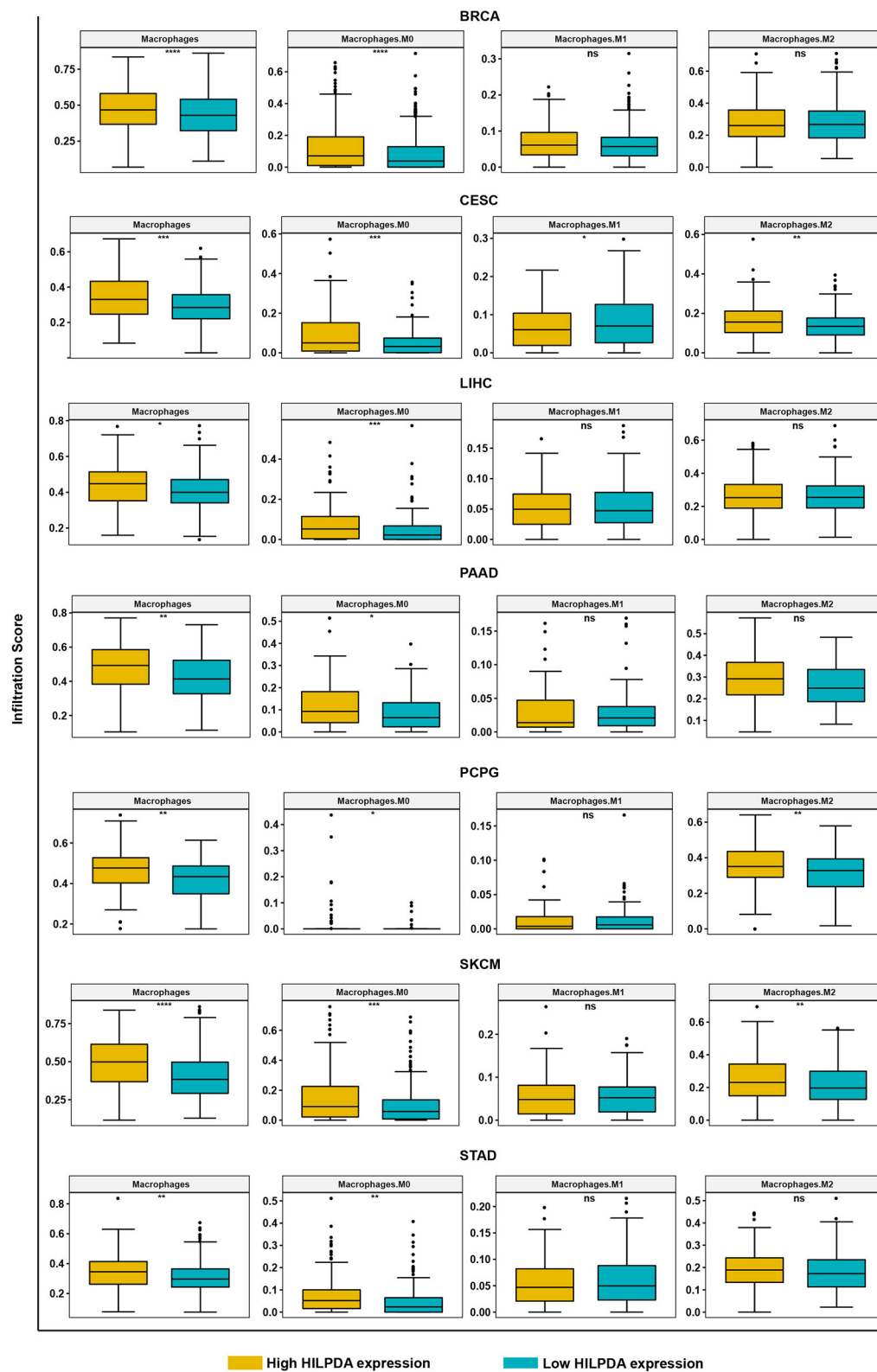


**FIGURE 6 |** Analysis of TAM infiltration in high and low HILPDA expression groups. The TAM infiltration levels in high HILPDA expression group and low HILPDA expression group in TCGA cohort. Data shown as mean  $\pm$  SD. \* $p < 0.05$ , \*\* $p < 0.01$ , \*\*\* $p < 0.001$ , \*\*\*\* $p < 0.0001$ .

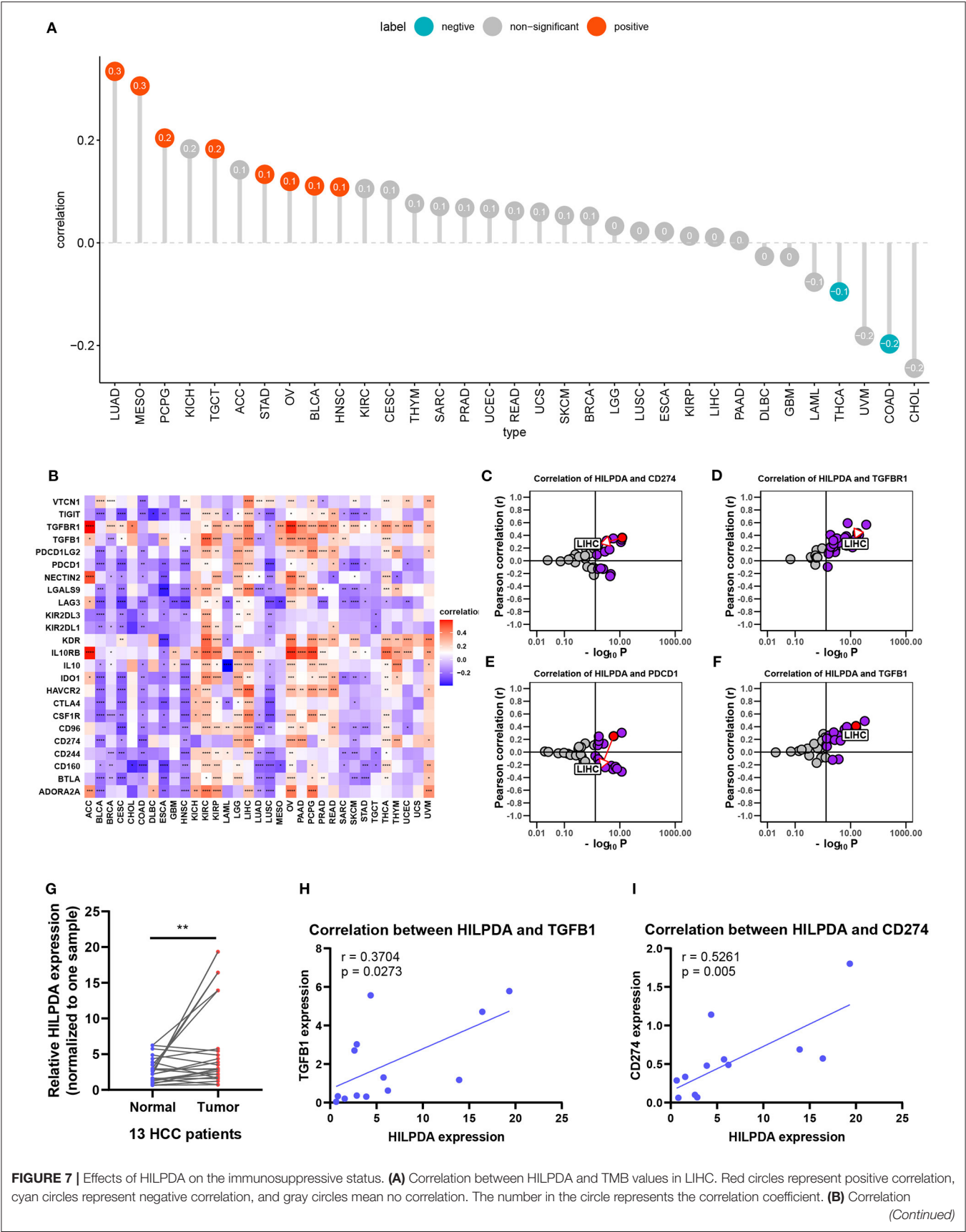




**FIGURE 7 |** between HILPDA and immunosuppressive genes is shown in the heatmap, red represents positive correlation, blue represents negative correlation, and the deeper the color, the stronger the correlation. **(C–F)** Correlation coefficient and  $-\log_{10}$  ( $p$ -value) of HILPDA with CD274, TGFB1, PD1, and TIGIT are shown. Each circle represents a different tumor from TCGA. Red circle is marked for LIHC. Gray circles mean no correlation. **(G)** qRT-PCR results showed the expression of HILPDA in liver cancer tissues. **(H,I)** The correlation between the expression of HILPDA and TIGIT/CD274 based on qRT-PCR results. Data shown as mean  $\pm$  SD. \* $p < 0.05$ , \*\* $p < 0.01$ , \*\*\* $p < 0.001$ , \*\*\*\* $p < 0.0001$ .

carcinoma (10), neuroblastoma (11), and mantle cell lymphoma (12) amongst others. However, HILPDA has not been extensively studied. Therefore, it is urgent to clarify the role of HILPDA in tumor progress and treatment.

In our study, we examined HILPDA expression levels and prognostic function in pan-cancer data using TCGA data from UCSC Xena. Based on our results, we found that HILPDA, compared to normal tissues, was overexpressed in BLCA, BRCA, CHOL, COAD, ESCA, HNSC, KIRC, KIRP, LIHC, LUAD, LUSC, PRAD, READ, and UCEC, while lower expression was observed in THCA in TCGA. The difference in HILPDA expression levels in different tumor types may reflect the distinct underlying functions and mechanisms. We further found that overexpression of HILPDA generally predicts poor prognosis in tumors with high HILPDA expression, such as ACC, KICH, LGG, LIHC, LUAD, MESO, PAAD, and PRAD. These results indicate that HILPDA is a prognostic biomarker for tumor patients.

The tumor microenvironment, especially the immune microenvironment, constitutes a vital element of tumor biology. Increasing evidence has revealed its clinicopathological significance in predicting outcomes and therapeutic efficacy (13, 14). The infiltration of TAMs facilitates the progression of tumors (15, 16). Our results proved that HILPDA has a close relationship with TAM infiltration as TAM infiltration levels were significantly higher in the high HILPDA expression group in BRCA, CESC, LIHC, PAAD, PCPG, SKCM, and STAD. Moreover, HILPDA expression was positively correlated with TAM infiltration level in most tumor types. As the high infiltration of TAMs in tumor often indicates the immunosuppressive microenvironment (17), we further investigated the relationship between HILPDA expression and tumor immunosuppressive microenvironment. We found the positive correlation between HILPDA expression and immunosuppressive genes, such as *PD-L1*, *PD-1*, *TGFB1*, and *TGFB1*, indicates the key role of HILPDA in regulating tumor immunosuppressive microenvironment. The high expression of HILPDA indicates the immunosuppression of most tumors, providing a potential target for immunotherapy.

In summary, we demonstrate that TAM infiltration was significantly increased in tissues with high HILPDA expression and that HILPDA positively correlated with immunosuppressive genes. Our results offer novel insights into the functional role of HILPDA and further highlight a potential mechanistic basis whereby HILPDA influences TAM infiltration and immunosuppressive gene expression in the tumor microenvironment. Collectively, our findings show

that HILPDA could be a valuable prognostic biomarker and a potential target for immunotherapy.

## DATA AVAILABILITY STATEMENT

The original contributions presented in the study are included in the article/**Supplementary Material**, further inquiries can be directed to the corresponding author/s.

## ETHICS STATEMENT

The studies involving human participants were reviewed and approved by The Institutional Review Board of Nanfang Hospital, Southern Medical University of Guangdong, China. The patients/participants provided their written informed consent to participate in this study.

## AUTHOR CONTRIBUTIONS

LL, DW, CL, and XZ designed the study. CL and XZ performed the data analysis. CL and HZ wrote the manuscript and helped with the validation. All authors contributed to the article and approved the submitted version.

## FUNDING

This work was supported by the National Nature Science Foundation of China (grant numbers 81773008, 81672756, 81872399, 81972897), Guangdong Province Universities and Colleges Pearl River Scholar Funded Scheme (2015), the Natural Science Foundation of Guangdong Province (grant number 2017A030311023), the Local Innovative and Research Teams Project of Guangdong Pearl River Talents Program: 2017BT01S131, and the Guangzhou Technology Project (grant number 201804010044).

## SUPPLEMENTARY MATERIAL

The Supplementary Material for this article can be found online at: <https://www.frontiersin.org/articles/10.3389/fonc.2021.597860/full#supplementary-material>

**Supplementary Figure 1 |** Correlation analysis between TAM infiltration and HILPDA expression. Plots represent correlation analyses between HILPDA and TAM infiltration in indicated tumor types.

**Supplementary Table 1 |** Pancancer TMB results.

## REFERENCES

- Kim SH, Wang D, Park YY, Katoh H, Margalit O, Sheffer M, et al. HIG2 promotes colorectal cancer progression via hypoxia-dependent and independent pathways. *Cancer Lett.* (2013) 341:159–65. doi: 10.1016/j.canlet.2013.07.028
- Togashi A, Katagiri T, Ashida S, Fujioka T, Maruyama O, Wakumoto Y, et al. Hypoxia-inducible protein 2 (HIG2), a novel diagnostic marker for renal cell carcinoma and potential target for molecular therapy. *Cancer Res.* (2005) 65:4817–26. doi: 10.1158/0008-5472.CAN-05-0120
- Siegel RL, Miller KD, Fuchs HE, Jemal A. Cancer statistics, 2021. *CA Cancer J Clin.* (2021) 71:7–33. doi: 10.3322/caac.21654
- Vitale I, Manic G, Coussens LM, Kroemer G, Galluzzi L. Macrophages and metabolism in the tumor microenvironment. *Cell Metab.* (2019) 30:36–50. doi: 10.1016/j.cmet.2019.06.001
- Liang B, Tao Y, Wang T. Profiles of immune cell infiltration in head and neck squamous carcinoma. *Biosci Rep.* (2020) 40:BSR20192724. doi: 10.1042/BSR20192724
- Desrichard A, Kuo F, Chowell D, Lee KW, Riaz N, Wong RJ, et al. Tobacco smoking-associated alterations in the immune microenvironment of squamous cell carcinomas. *J Natl Cancer Inst.* (2018) 110:1386–92. doi: 10.1093/jnci/djy060
- Thorsson V, Gibbs DL, Brown SD, Wolf D, Bortone DS, Ou YT, et al. The immune landscape of cancer. *Immunity.* (2018) 48:812–30. doi: 10.1016/j.immuni.2018.03.023
- Ngambenjawong C, Gustafson HH, Pun SH. Progress in tumor-associated macrophage (TAM)-targeted therapeutics. *Adv Drug Deliv Rev.* (2017) 114:206–21. doi: 10.1016/j.addr.2017.04.010
- VandeKopple MJ, Wu J, Auer EN, Giaccia AJ, Denko NC, Papandreou I. HILPDA regulates lipid metabolism, lipid droplet abundance, and response to microenvironmental stress in solid tumors. *Mol Cancer Res.* (2019) 17:2089–101. doi: 10.1158/1541-7786.MCR-18-1343
- van der Mijn JC, Fu L, Khani F, Zhang T, Molina AM, Barbieri CE, et al. Combined metabolomics and genome-wide transcriptomics analyses show multiple HIF1 $\alpha$ -induced changes in lipid metabolism in early stage clear cell renal cell carcinoma. *Transl Oncol.* (2020) 13:177–85. doi: 10.1016/j.tranon.2019.10.015
- Applebaum MA, Jha AR, Kao C, Hernandez KM, DeWane G, Salwen HR, et al. Integrative genomics reveals hypoxia inducible genes that are associated with a poor prognosis in neuroblastoma patients. *Oncotarget.* (2016) 7:76816–26. doi: 10.18632/oncotarget.12713
- Kuci V, Nordström L, Conrotto P, Ek S. SOX11 and HIG-2 are cross-regulated and affect growth in mantle cell lymphoma. *Leuk Lymphoma.* (2016) 57:1883–92. doi: 10.3109/10428194.2015.1121257
- Bai X, Wu DH, Ma SC, Wang J, Tang XR, Kang S, et al. Development and validation of a genomic mutation signature to predict response to PD-1 inhibitors in non-squamous NSCLC: a multicohort study. *J Immunother Cancer.* (2020) 8:e000381. doi: 10.1136/jitc-2019-000381
- Guo L, Li X, Liu R, Chen Y, Ren C, Du S. TOX correlates with prognosis, immune infiltration, and T cells exhaustion in lung adenocarcinoma. *Cancer Med.* (2020) 9:6694–709. doi: 10.1002/cam4.3324
- Shiau DJ, Kuo WT, Davuluri G, Shieh CC, Tsai PJ, Chen CC, et al. Hepatocellular carcinoma-derived high mobility group box 1 triggers M2 macrophage polarization via a TLR2/NOX2/autophagy axis. *Sci Rep.* (2020) 10:13582. doi: 10.1038/s41598-020-70137-4
- Wu J, Gao W, Tang Q, Yu Y, You W, Wu Z, et al. M2 macrophage-derived exosomes facilitate hepatocarcinoma metastasis by transferring  $\alpha(M)\beta(2)$  integrin to tumor cells. *Hepatology.* (2020). doi: 10.1002/hep.31432. [Epub ahead of print].
- Chen X, Gao A, Zhang F, Yang Z, Wang S, Fang Y, et al. ILT4 inhibition prevents TAM- and dysfunctional T cell-mediated immunosuppression and enhances the efficacy of anti-PD-L1 therapy in NSCLC with EGFR activation. *Theranostics.* (2021) 11:3392–416. doi: 10.7150/thno.52435

**Conflict of Interest:** The authors declare that the research was conducted in the absence of any commercial or financial relationships that could be construed as a potential conflict of interest.

Copyright © 2021 Liu, Zhou, Zeng, Wu and Liu. This is an open-access article distributed under the terms of the Creative Commons Attribution License (CC BY). The use, distribution or reproduction in other forums is permitted, provided the original author(s) and the copyright owner(s) are credited and that the original publication in this journal is cited, in accordance with accepted academic practice. No use, distribution or reproduction is permitted which does not comply with these terms.



# Serum Biomarker Panel for Diagnosis and Prognosis of Pancreatic Ductal Adenocarcinomas

Shreya Mehta<sup>1,2</sup>, Nazim Bhimani<sup>3</sup>, Anthony J. Gill<sup>1,2,4,5,6</sup>, Jaswinder S. Samra<sup>1,3,5</sup>, Sumit Sahni<sup>1,2,5\*†</sup> and Anubhav Mittal<sup>1,3,5\*†</sup>

<sup>1</sup> Northern Clinical School, Faculty of Medicine and Health, University of Sydney, Sydney, NSW, Australia, <sup>2</sup> Kolling Institute of Medical Research, University of Sydney, Sydney, NSW, Australia, <sup>3</sup> Upper Gastro Intestinal (GI) Surgical Unit, Royal North Shore Hospital and North Shore Private Hospital, Sydney, NSW, Australia, <sup>4</sup> Cancer Diagnosis and Pathology Group, Kolling Institute of Medical Research, Royal North Shore Hospital, St Leonards, NSW, Australia, <sup>5</sup> Australian Pancreatic Centre, Sydney, NSW, Australia, <sup>6</sup> NSW Health Pathology, Department of Anatomical Pathology, Royal North Shore Hospital, St Leonards, NSW, Australia

## OPEN ACCESS

### Edited by:

Brendan Jenkins,  
Hudson Institute of Medical Research,  
Australia

### Reviewed by:

Joanne Lundy,  
Hudson Institute of Medical Research,  
Australia  
Daniel Croagh,  
Monash University, Australia

### \*Correspondence:

Anubhav Mittal  
anubhav.mittal@sydney.edu.au  
Sumit Sahni  
sumit.sahni@sydney.edu.au

<sup>†</sup>These authors share senior  
authorship

### Specialty section:

This article was submitted to  
Gastrointestinal Cancers,  
a section of the journal  
Frontiers in Oncology

**Received:** 13 May 2021

**Accepted:** 08 June 2021

**Published:** 05 July 2021

### Citation:

Mehta S, Bhimani N, Gill AJ,  
Samra JS, Sahni S and Mittal A  
(2021) Serum Biomarker  
Panel for Diagnosis and  
Prognosis of Pancreatic  
Ductal Adenocarcinomas.  
Front. Oncol. 11:708963.  
doi: 10.3389/fonc.2021.708963

**Background:** Patients with pancreatic ductal adenocarcinoma (PDAC) have late diagnosis which results in poor prognosis. Currently, surgical resection is the only option for curative intent. Identifying high-risk features for patients with aggressive PDAC is essential for accurate diagnosis, prognostication, and personalised care due to the disease burden and risk of recurrence despite surgical resection. A panel of three biomarkers identified in tumour tissue (S100A4, Ca125 and Mesothelin) have shown an association with poor prognosis and overall survival. The diagnostic and prognostic value of the serum concentration of this particular biomarker panel for patients with PDAC has not been previously studied.

**Methods:** Retrospectively collected blood samples of PDAC patients (n =120) and healthy controls (n =80) were evaluated for the serum concentration of select biomarkers – S100A4, S100A2, Ca-125, Ca 19-9 and mesothelin. Statistical analyses were performed for diagnostic and prognostic correlation.

**Results:** A panel of four biomarkers (S100A2, S100A4, Ca-125 and Ca 19-9) achieved high diagnostic potential (AUROC 0.913). Three biomarkers (S100A4, Ca-125 and Ca 19-9) correlated with poor overall survival in a univariable model ( $p < 0.05$ ). PDAC patients with abnormal levels of 2 or more biomarkers in their serum demonstrated significantly lower survival compared to patients with abnormal levels of one or less biomarker ( $p < 0.05$ ).

**Conclusion and Impact:** The identified biomarker panels have shown the potential to diagnose PDAC patients and stratify patients based on their prognostic outcomes. If independently validated, this may lead to the development of a diagnostic and prognosticating blood test for PDAC.

**Keywords:** pancreatic ductal adenocarcinoma, diagnostic biomarkers, prognostic biomarkers, S100A4, Ca-125 and Ca 19-9, survival analysis

## INTRODUCTION

Pancreatic ductal adenocarcinoma (PDAC) has the highest mortality of all major cancers and is projected to become the second most common cause of cancer related death by 2030 (1, 2). Currently, clinical decision making is based on the radiological staging, vascular involvement, overall disease burden and the patient's premorbid status. However, current algorithms used to treat PDAC do not specifically take into account the biological behaviour of each tumour. Recent work on the genetic variability and biology of PDAC highlights the importance of tumour biology in chemosensitivity and overall survival (3, 4). Hence, there is an urgent need for an easily quantifiable and cost-effective biomarker signature to assist clinicians in taking informed treatment decisions based on an individual patient's tumor biology.

A PDAC tissue biomarker panel (S100A4, Mesothelin, Ca-125) approach has recently been shown to be successful in prognosticating pancreatic cancer outcome (5). The expression of these biomarkers in the tumour tissue has been shown to track with the genetic changes associated with a more aggressive (so called 'squamous') genotype of PDAC (6). However, given that these tissue sample may be difficult to obtain at first presentation, a liquid biopsy using secreted biomarkers in the patient's blood would be beneficial in diagnosis and prognostication with personalisation of treatment for patients with PDAC.

The aim of this study was to: (1) determine the diagnostic potential of this set of biomarkers individually and as a panel by comparing serum expression of these biomarkers in PDAC patients and healthy controls; (2) establish a "normal" and "abnormal" result for the expression of a set of biomarkers – Ca 19.9, Ca-125, Mesothelin, S100A2 and S100A4 by comparing serum values in patients with PDAC with healthy controls; (3) identifying the prognostic significance of these biomarkers based on serum expression in PDAC patients and correlation with overall survival.

## METHODOLOGY

### Patient Information

Patients across two tertiary centres, Royal North Shore Hospital and North Shore Private hospital, who had surgically resected PDAC, and serum collected at the time of surgery from 2007 – 2014 were included in this study. The serum was obtained from the Kolling Tumour Bank. Serum from age and sex matched healthy controls was also obtained from the Kolling Tumour Bank.

### Standard Protocol Approvals, Registrations, and Patient Consents

Ethical approval was obtained at the respective tertiary centres (references HREC/16/HAWKE/105 and NSPHEC 2016-007). Informed written consent was obtained from all participants and/or their designated surrogate. Northern Sydney Local Health District reference: RESP/16/76.

## ELISA Assay

ELISA assay was performed for S100A4 (Circulex S100A4 ELISA Kit Version 2 Cat# CY-8086, MBL Life Science, Japan), S100A2 (Cat# SEC009Hu, Cloud-clone Corp, Wuhan, China) and Mesothelin (Mesomark ELISA Kit; Fujirebio Diagnostics, PA, USA), following manufacturer's guidelines. Each sample was performed in duplicate. Assay for Ca-125 and Ca 19-9 was performed at the Pathology North, RNSH, using their standard protocol.

## Data Analysis

The biomarker concentrations between PDAC and Healthy Controls were compared and analysed for diagnostic potential using AUROC curves. The cut-off values used for multivariable analysis (**Supplementary Table 1**) were determined based on optimum sensitivity and specificity in univariable analysis.

Patient characteristics were compared for survival using Cox Proportional Hazard Model. Univariable survival analysis for biomarkers was performed using Kaplan-Meier curves, and statistical significance was achieved using the Log-rank test with a  $p$ -value  $<0.05$ . The biomarker cut-off values for the survival analysis were based on either clinically used values or values where high specificity was achieved with minimum loss of sensitivity (**Supplementary Table 2**). PDAC patients were divided into two groups based on normal or abnormal levels of biomarker concentration. The cut-offs were established based on the observed direction of change in biomarkers. Biomarkers with significantly elevated levels in the serum of PDAC patients compared to healthy controls (*i.e.*, S100A2, Ca-125, Mesothelin and Ca 19-9), patients were classified with abnormal levels when their biomarker level was more than cut-off. In contrast, for the biomarkers with significantly decreased levels in PDAC serum, patients were classified with abnormal levels when their biomarker level was less than cut-off. All statistical analyses were performed using Stata SE, IBM SPSS Statistics for Windows 2019 (Version 26.0 Armonk, NY, IBM Corp) or GraphPad Prism Software (Version 8.4.2).

## RESULTS

### Population Demographics

Patient characteristics are described in **Table 1**. There were 120 patients with PDAC included in this study and 80 healthy controls.

### Diagnostic Biomarkers

Initially, the ability of each biomarker (*i.e.*, S100A4, S100A2, Mesothelin, Ca-125 and Ca 19-9) to diagnose PDAC was assessed by comparing expressions with healthy controls. Serum levels of S100A4, S100A2, Ca-125 and Ca19-9 demonstrated moderate to high ability to diagnose PDAC with AUROC values of 0.613, 0.634, 0.755 and 0.869, respectively (**Figure 1**). In contrast, mesothelin showed poor diagnostic ability (AUROC: 0.525; **Figure 1**).



**TABLE 1 |** Patient and tumour characteristics and correlation with survival status.

	Total n (%)	HR	95% CI	p-value
Age				0.237
<70 years	72 (60.0)	Reference		
≥70 years	48 (40.0)	1.27	0.85-1.90	
Gender				0.706
Male	61 (50.8)	Reference		
Female	59 (49.2)	0.93	0.62-1.38	
Tumour size				0.009
<35mm	55 (45.8)	Reference		
≥35mm	65 (54.2)	1.70	1.14-2.55	
T Stage				0.041
T1 & T2	9 (7.5)	Reference		
T3 & T4	111 (92.5)	2.56	1.04-6.33	
Node Positive				0.001
No	26 (21.7)	Reference		
Yes	94 (78.3)	2.68	1.51-4.76	
Vascular Invasion				<0.001
No	46 (38.3)	Reference		
Yes	74 (61.7)	2.49	1.61-3.87	
Perineural Invasion				0.024
No	38 (31.7)	Reference		
Yes	82 (68.3)	1.66	1.07-2.58	
Grade				0.021
0 or 1	84 (70.0)	Reference		
2 or 3	36 (30.0)	1.65	1.08-2.54	
Blood loss				0.873
<450mL	52 (43.3)	Reference		
≥450mL	68 (56.7)	1.03	0.69-1.54	
Length of stay				0.347
<12 days	45 (37.5)	Reference		
≥12 days	75 (62.5)	0.82	0.54-1.24	
Margin Status				0.002
R0	49 (40.8)	Reference		
R1	71 (59.2)	1.89	1.25-2.85	

Next, a multivariable model for a panel of S100A4, S100A2, Ca-125 and Ca 19-9 was generated to assess its diagnostic ability. A diagnostic cut-off based on optimum sensitivity and selectivity was selected for diagnostic multivariable model. The cut-off, sensitivity and selectivity values are described in **Supplementary Table 1**. The panel showed very high diagnostic ability (AUROC: 0.913; **Supplementary Table 3**), which was superior to the current clinically used biomarker Ca 19-9 alone (AUROC: 0.869).

## Survival Analysis Based on Serum Biomarker Levels

Survival correlation with abnormal serum biomarker levels were determined using Kaplan Meier curves. Abnormal serum levels of S100A4 (median survival (m.s.): 28 vs 24 months; **Figure 2**), Ca-125 (m.s.: 27 vs 22.5 months; **Figure 2**) and Ca19-9 (m.s.: 33 vs 23 months; **Figure 2**) led to reduction in the median overall survival time. In contrast, abnormal serum levels of S100A2 resulted in increased median survival time (m.s.: 23 vs 28 months; **Figure 2**). However, none of the biomarkers individually corresponded with overall survival.

The panel of S100A4, Ca-125 and Ca 19-9 was further analysed to determine its ability to stratify patients based on their overall survival. Initially, patients were divided into four groups: (1) none of the biomarkers with abnormal levels (n = 6); (2) one biomarker with abnormal levels (n = 31);

(3) two biomarkers with abnormal levels (n = 56); (4) three biomarkers with abnormal levels (n = 27). Multiple comparison Kaplan Meier curve analysis did not achieve statistical significance (p = 0.22; **Supplementary Figure 1**), potentially due to very small number of patients in some categories. The combination of first two and last two categories was able to stratify patients based on their overall survival (**Figure 3**). The patients with abnormal levels of one or less of the biomarker (n = 37) had significantly improved survival outcomes, compared to those with abnormal levels of two or more biomarkers (n = 83; m.s.: 39 vs 20 months, p < 0.05; **Figure 3**). Patient distribution based on tumour characteristics was also analysed (**Supplementary Table 4**), which showed uniform distribution in both biomarker groups.

## DISCUSSION

The study demonstrates that of the select group of biomarkers included in this study, a panel of four (S100A4, S100A2, Ca-125 and Ca 19-9) have superior diagnostic potential compared to the current biomarker used in clinical practice, Ca 19-9 alone. Additionally, the abnormal expression of two or more biomarkers correlated with worse survival (median survival:

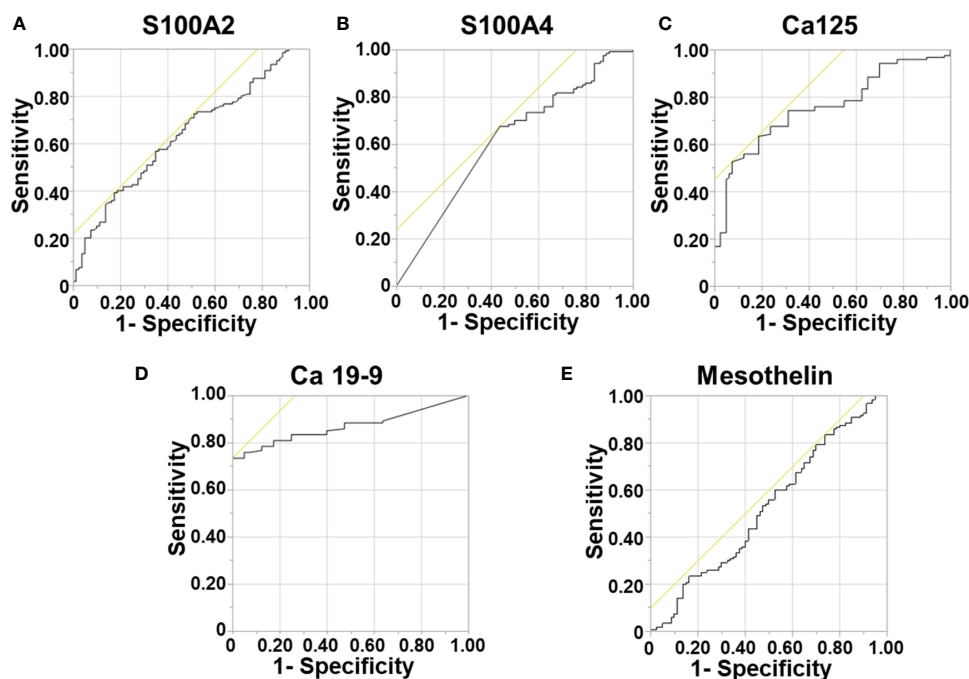


**FIGURE 1 |** Diagnostic Ability of Biomarkers. Receiver Operator Curves were generated to determine the diagnostic potential of individual biomarkers. for: **(A)** S100A2; **(B)** S100A4; **(C)** Ca-125; **(D)** Ca 19-9; and **(E)** Mesothelin.

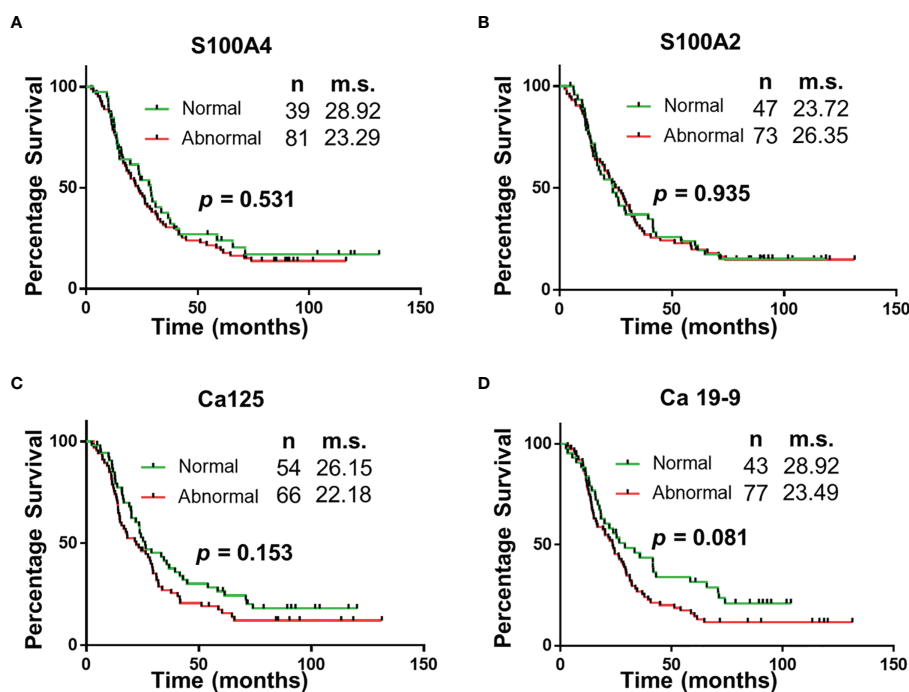


**FIGURE 2 |** Univariable Survival Analysis of Individual Biomarkers. **(A–D)** Kaplan Meier survival curves for individual biomarkers were generated using prognostic cut-offs (**Supplementary Table 3**). n, number of patients; m.s., median survival in months.

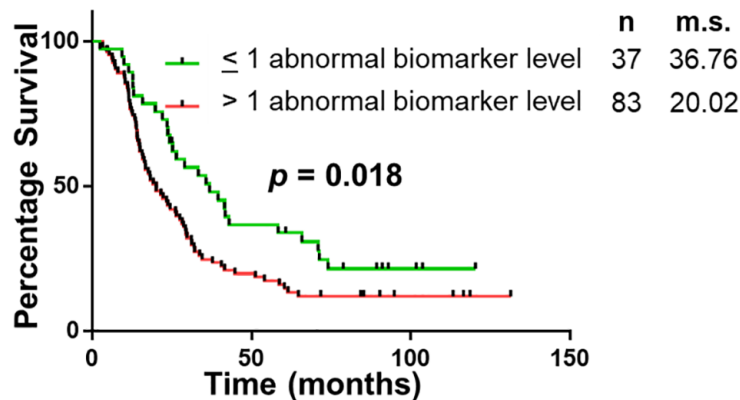


**FIGURE 3 |** Univariable Survival Analysis of Biomarker Panel. Kaplan Meier survival curves comparing patients with abnormal biomarker levels of one or less biomarker and patients with abnormal biomarker levels of two or more biomarkers. n, number of patients; m.s., median survival in months.

39.46 vs 20.04 months;  $p < 0.05$ ). The utility of this biomarker panel in the accurate diagnosis of PDAC and implications of biomarker expression on prognosis may assist with personalization of treatment and improved survival outcomes.

PDAC has one of the lowest rates of survival with a 5-year survival of between 5–10% (7–9). Most patients are diagnosed with an advanced disease stage, and of the 15–20% of patients who are candidates for surgical resection with curative intent at the time of diagnosis (10), more than 50% recur within 12 months of surgery (11). Survival rates in PDAC have changed little over the last 50 years (8), highlighting the complexity of accurate diagnosis and limitations of treatment. This failure of treatment highlights the inability of current decision-making strategies, which are primarily radiological and clinical, to accurately stratify patients into different prognostic groups based on actual tumour biology. Part of the reason is that it is often difficult to obtain adequate amount of tumour tissue sample for analysis and the associated costs of genetic analysis. Identification of a prognostic biomarker signature in pre-operative PDAC patient's blood will help clinicians recommend informed decisions regarding the appropriate treatment strategy for each individual patient and has potential to markedly improve the standard of care for these patients. The ability to select patients for personalized neoadjuvant chemotherapy will revolutionize care for PDAC. For example, it was recently reported that combinations of SRC proto-oncogene or mitogen-activated protein kinase 1/2 inhibitors with gemcitabine possess synergistic effects on the squamous subtype of PDAC cells which correlates with a triple positive on our tissue biomarker panel (12).

The identification of specific serum biomarkers that have diagnostic and prognostic potential is of high utility in accurate diagnosis and improving survival outcomes (13). Biomarker expression in serum is easily obtainable in the form of a liquid biopsy of the patient's blood. This test eradicates factors such as cost, availability of expertise, equivocal results as seen in cases

of inadequate tissue sampling from FNA or ductal brushings, risk of injury to intra-abdominal structures, acute pancreatitis and potential for needle-track seeding (14). Our study reveals a panel of biomarkers that can be utilized as a method of accurate diagnosis of PDAC. Ca 19-9 is a biomarker that is most widely used in diagnosis and monitoring progression of PDAC. Our novel biomarker panel has a sensitivity and specificity which has been demonstrated to be superior to the presently used tumor marker Ca 19-9. However, this increase was only modest (AUROC: 0.913 vs 0.869) and a future larger multi-institutional study will be required to further corroborate these findings.

Looking ahead, there are other potential applications for a liquid biopsy panel for PDAC. For example, there are a certain percentage of patients with intraductal papillary mucinous neoplasm (IPMN) and mucinous cystic neoplasms (MCN) that have an associated ductal adenocarcinoma. It is often difficult to accurately select patients for surgery vs observation, and this group may be suitable for liquid serum biopsy in attempt to gain an accurate diagnosis of PDAC to improve survival outcomes. The biomarker panel may also have utility in the follow-up of resected PDAC patients to diagnose recurrence early. These applications will be the focus of future studies.

The major limitation of this study is the retrospective nature of this analysis, a relatively smaller cohort, lack of external validation cohort, only a single timepoint for analysis at the time of surgery and lack of other comparator groups for determining diagnostic accuracy (e.g., patients with pancreatitis). Future, multi-institutional cohort with prospective design would serve to further validate this identified biomarker panel for PDAC prognosis. In addition, future studies will also involve serum specimens collected at multiple longitudinal time points and will include patients with other benign pancreatic conditions such as pancreatitis.

In conclusion, this study forms a critical basis for the future development of a minimally invasive blood test for accurate diagnosis and prognostication of PDAC patients.

## DATA AVAILABILITY STATEMENT

The raw data supporting the conclusions of this article will be made available by the authors, without undue reservation.

## ETHICS STATEMENT

The studies involving human participants were reviewed and approved by Northern Sydney Local Health District HREC. The patients/participants provided their written informed consent to participate in this study.

## AUTHOR CONTRIBUTIONS

SM, NB, AM, and SS were involved in analysis and interpretation of data. SS, JS, and AM contributed to conception of idea and design. All authors contributed to the article and approved the submitted version.

## REFERENCES

- Rahib L, Smith BD, Aizenberg R, Rosenzweig AB, Fleshman JM, Matrisian LM. Projecting Cancer Incidence and Deaths to 2030: The Unexpected Burden of Thyroid, Liver, and Pancreas Cancers in the United States. *Cancer Res* (2014) 74:2913–21. doi: 10.1158/0008-5472.CAN-14-0155
- Sung H, Ferlay J, Siegel RL, Laversanne M, Soerjomataram I, Jemal A, et al. Global Cancer Statistics 2020: GLOBOCAN Estimates of Incidence and Mortality Worldwide for 36 Cancers in 185 Countries. *CA Cancer J Clin* (2021) 71:209–249. doi: 10.3322/caac.21660
- Bailey P, Chang DK, Nones K, et al. Genomic Analyses Identify Molecular Subtypes of Pancreatic Cancer. *Nature* (2016) 531:47–52. doi: 10.1038/nature16965
- Hoyer K, Habesreiter R, Inoue Y, Yoshida K, Briest F, Christen F, et al. A Genetically Defined Signature of Responsiveness to Erlotinib in Early-Stage Pancreatic Cancer Patients: Results From the CONKO-005 Trial. *EBioMedicine* (2021) 66:103327. doi: 10.1016/j.ebiom.2021.103327
- Nahm CB, Turchini J, Jamieson N, Moon E, Sioson L, Itchins M, et al. Biomarker Panel Predicts Survival After Resection in Pancreatic Ductal Adenocarcinoma: A Multi-Institutional Cohort Study. *Eur J Surg Oncol* (2019) 45:218–24. doi: 10.1016/j.ejso.2018.10.050
- Sahni S, Moon EA, Howell VM, Mehta S, Pavlakis N, Chan D, et al. Tissue Biomarker Panel as a Surrogate Marker for Squamous Subtype of Pancreatic Cancer. *Eur J Surg Oncol* (2020) 46:1539–42. doi: 10.1016/j.ejso.2020.02.001
- Dreyer SB, Chang DK, Bailey P, Biankin AV. Pancreatic Cancer Genomes: Implications for Clinical Management and Therapeutic Development. *Clin Cancer Res* (2017) 23:1638–46. doi: 10.1158/1078-0432.CCR-16-2411
- Ansari D, Torén W, Zhou Q, Hu D, Andersson R. Proteomic and Genomic Profiling of Pancreatic Cancer. *Cell Biol Toxicol* (2019) 35:333–43. doi: 10.1007/s10565-019-09465-9
- Zhou B, Xu J-W, Cheng Y-G, Gao J-Y, Hu S-Y, Wang L, et al. Early Detection of Pancreatic Cancer: Where Are We Now and Where Are We Going? *Int J Cancer* (2017) 141:231–41. doi: 10.1002/ijc.30670
- Klaiber U, Hackert T. Conversion Surgery for Pancreatic Cancer—The Impact of Neoadjuvant Treatment. *Front Oncol* (2020) 9:1501. doi: 10.3389/fonc.2019.01501
- Groot VP, Rezaee N, Wu W, Cameron JL, Fishman EK, Hruban RH, et al. Patterns, Timing, and Predictors of Recurrence Following Pancreatectomy for Pancreatic Ductal Adenocarcinoma. *Ann Surg* (2018) 267:936–45. doi: 10.1097/SLA.0000000000002234
- Er JL, Goh PN, Lee CY, Tan YJ, Hii L-W, Mai CW, et al. Identification of Inhibitors Synergizing Gemcitabine Sensitivity in the Squamous Subtype of Pancreatic Ductal Adenocarcinoma (PDAC). *Apoptosis* (2018) 23:343–55. doi: 10.1007/s10495-018-1459-6
- Ideno N, Mori Y, Nakamura M, Ohtsuka T. Early Detection of Pancreatic Cancer: Role of Biomarkers in Pancreatic Fluid Samples. *Diagnostics* (2020) 10:1056. doi: 10.3390/diagnostics10121056
- Tsutsumi H, Hara K, Mizuno N, Hijioka S, Imaoka H, Tajika M, et al. Clinical Impact of Preoperative Endoscopic Ultrasound-Guided Fine-Needle Aspiration for Pancreatic Ductal Adenocarcinoma. *Endoscopic Ultrasound* (2016) 5:94–100. doi: 10.4103/2303-9027.180472

## FUNDING

This project was supported by Philanthropic funding received by AM and JS from the RT Hall Trust.

## ACKNOWLEDGMENTS

AM would like to thank Sydney Vital for the Translational Centre for Excellence in Pancreatic Cancer Grant. SS would like to thank Mr. Guy Boncardo for the Boncardo Pancreatic Cancer Fellowship. SS would also like to thank AMP Foundation for the AMP Tomorrow Grant and Cancer Australia and Cure Cancer Australia for the Young Investigator PdCCRS grant. All authors acknowledge the Kolling Tumour Bank for providing the access to the specimens.

## SUPPLEMENTARY MATERIAL

The Supplementary Material for this article can be found online at: <https://www.frontiersin.org/articles/10.3389/fonc.2021.708963/full#supplementary-material>

**Conflict of Interest:** The authors declare that the research was conducted in the absence of any commercial or financial relationships that could be construed as a potential conflict of interest.

Copyright © 2021 Mehta, Bhimani, Gill, Samra, Sahni and Mittal. This is an open-access article distributed under the terms of the Creative Commons Attribution License (CC BY). The use, distribution or reproduction in other forums is permitted, provided the original author(s) and the copyright owner(s) are credited and that the original publication in this journal is cited, in accordance with accepted academic practice. No use, distribution or reproduction is permitted which does not comply with these terms.





# Preoperative Serum Prealbumin Level and Adverse Prognosis in Patients With Hepatocellular Carcinoma After Hepatectomy: A Meta-Analysis

Yu Fan, Yimeng Sun, Changfeng Man\* and Yakun Lang\*

*Institute of Molecular Biology & Translational Medicine, The Affiliated People's Hospital, Jiangsu University, Zhenjiang, China*

## OPEN ACCESS

### Edited by:

Alessandro Passardi,  
Romagnolo Scientific Institute for the  
Study and Treatment of Tumors  
(IRCCS), Italy

### Reviewed by:

Matteo Donadon,  
Humanitas University, Italy  
Weiqi Rong,  
Translational Research, China

### \*Correspondence:

Changfeng Man  
changfengman@njmu.edu.cn  
Yakun Lang  
lyk111223@sina.com

### Specialty section:

This article was submitted to  
Gastrointestinal Cancers: Hepato  
Pancreatic Biliary Cancers,  
a section of the journal  
Frontiers in Oncology

**Received:** 14 September 2021

**Accepted:** 04 October 2021

**Published:** 21 October 2021

### Citation:

Fan Y, Sun Y, Man C and Lang Y  
(2021) Preoperative Serum  
Prealbumin Level and Adverse  
Prognosis in Patients With  
Hepatocellular Carcinoma After  
Hepatectomy: A Meta-Analysis.  
*Front. Oncol.* 11:775425.  
doi: 10.3389/fonc.2021.775425

**Background:** Prealbumin is a sensitive indicator of liver function and nutritional status.

**Objectives:** This meta-analysis aimed to examine the association of the serum prealbumin level with the prognosis of patients with hepatocellular carcinoma (HCC) undergoing hepatectomy.

**Methods:** We comprehensively searched the PubMed, Embase, Wanfang, China Academic Journals (CNKI), and SinoMed databases up to September 1, 2021. Eligible studies should report the association of the serum prealbumin level with prognosis and provide the multivariable-adjusted risk estimates of the outcomes of interest in HCC patients undergoing hepatectomy.

**Results:** A total of 11 studies with 7,442 HCC patients were identified and analyzed. Meta-analysis of a fixed effects model showed that a low serum prealbumin level was associated with poor overall survival [hazard ratio (HR) = 1.54, 95% confidence interval (CI) = 1.42–1.68], recurrence-free survival (HR = 1.34, 95% CI = 1.17–1.52), and a higher risk of postoperative hepatic insufficiency (HR = 2.21; 95% CI = 1.36–3.60) in HCC patients. Sensitivity and subgroup analyses confirmed the robustness of low serum prealbumin in predicting poor overall survival.

**Conclusions:** This meta-analysis indicated that a low preoperative serum prealbumin level was significantly associated with adverse prognosis in HCC patients undergoing hepatectomy.

**Keywords:** prealbumin, hepatocellular carcinoma, hepatectomy, overall survival, hepatic insufficiency, meta-analysis

## INTRODUCTION

Hepatocellular carcinoma (HCC) is the principal type of primary liver cancer in adults and accounts for approximately 90% of liver malignancy (1). Despite the advances in treatment approaches for HCC, it remains the second leading cause of cancer-related mortality because of its distant metastasis and tumor recurrence (2). The 5-year survival of HCC is about 10%–20% (3, 4). Hepatectomy is the main treatment for HCC (5). However, only one-third of patients with early-stage HCC could receive surgical resection

or liver transplantation due to advanced stage of disease or cirrhosis-related hepatic insufficiency. Therefore, the prognostic assessment of HCC patients before surgery is an unmet demand.

Prealbumin, also known as transthyretin, is a homotetrameric protein synthesized by the liver (6). Serum prealbumin level is a sensitive indicator of liver function and nutritional status. Prealbumin has a short biological half-life and reflects recent status, rather in contrast to albumin (7). Thus, prealbumin is a better indicator of liver function and nutritional status (8). Several studies (9–15) have linked low serum prealbumin levels with adverse outcomes in HCC patients after hepatectomy. However, conflicting results have been obtained regarding the association of preoperative prealbumin level with overall survival (OS) (16, 17). Nevertheless, the magnitude of the reported risk estimates considerably varies among studies.

A previous meta-analysis involving 3,470 patients has evaluated the prognostic value of prealbumin in liver cancer (18). However, this well-designed meta-analysis enrolled heterogeneous patient populations, including those undergoing chemotherapy and molecular targeted therapy. To address these knowledge gaps, we performed a more focused meta-analysis in the current study to assess the association of preoperative prealbumin level with adverse outcomes in HCC patients undergoing hepatectomy.

## MATERIALS AND METHODS

### Data Sources and Literature Search

This meta-analysis was conducted according to the Preferred Reporting Items for Systematic Reviews and Meta-Analyses guidelines (19). Two independent authors comprehensively searched PubMed, Embase, Wanfang, China Academic Journals (CNKI), and SinoMed databases up to September 1, 2021. The keywords included: “prealbumin” OR “transthyretin” AND “hepatocellular carcinoma” OR “hepatocellular cancer” OR “liver cancer.” The reference lists of related studies were also manually reviewed for additional studies.

### Study Selection

The inclusion criteria were as follows: 1) population: patients with HCC undergoing hepatectomy; 2) exposure: serum prealbumin level before surgery; 3) comparison: patients with a lower prealbumin level *versus* those with a higher prealbumin level; outcome measures: overall survival, recurrence-free survival, and postoperative hepatic insufficiency; 5) study design: prospective or retrospective cohort studies; and 6) reported multivariable adjusted risk summary for the outcomes of interest according to the prealbumin category. The following exclusion criteria were used: 1) patients with a specific type of HCC; 2) patients who did not receive surgery; 3) risk estimates reported using univariate analysis; and 4) studies with overlapping patients.

### Data Extraction and Quality Assessment

The extracted data included the following: surname of the first author, publication year, country of origin, study design, number of patients, percentage of male gender, mean/median age, cutoff

value of low prealbumin, outcome measures, fully adjusted risk estimate, length of follow-up, and adjustment for confounders. The methodological quality of the eligible studies was evaluated with the Newcastle–Ottawa Scale (NOS) (20). A study with a score of 7 points or over was classified as high quality. Two independent authors conducted the data extraction and quality assessment. Any disagreement between these processes was resolved by mutual consent.

### Statistical Analysis

All meta-analyses were performed using the STATA 12.0 (STATA Corp LP, College Station, TX, USA). The impact of the preoperative serum prealbumin level on adverse outcomes was estimated by pooling the multivariable-adjusted hazard ratio (HR) and their 95% confidence interval (CI) for the lowest *versus* the highest prealbumin category. Heterogeneity was evaluated using the Cochran  $Q$  test and  $I^2$  statistic. A  $p$ -value of  $<0.10$  of the Cochran  $Q$  test or  $I^2$  statistic  $\geq 50\%$  indicated the presence of significant heterogeneity, and a random effects model was selected to pool the risk summary. Otherwise, we selected a fixed effects model if heterogeneity was not found. Leave-one-out study sensitivity analysis was conducted to investigate the stability of the pooling results. To identify potential sources of heterogeneity across studies, subgroup analyses were performed according to sample size, study design, prealbumin cutoff value, follow-up duration, and NOS points. Publication bias was examined using Begg's test (21) and Egger's test (22).

## RESULTS

### Search Results and Study Characteristics

Our literature search identified 1,265 unique publications. Among them, 1218 were scanned for their titles or abstracts and 47 were retrieved for full-text evaluation. After applying the predefined selection criteria, 11 studies (9–14, 16, 17, 23–25) satisfying our inclusion criteria were finally included in this meta-analysis (Figure 1).

Table 1 describes the baseline characteristics of the included studies. A total of 11 studies with 7,442 HCC patients were identified and analyzed. These studies were published from 2012 to 2021. One study (11) was performed in Japan, and others were conducted in China. Two studies (12, 13) adopted a prospective design, and others were retrospective studies. The reported mean/median age of patients ranged between 49.5 and 69.6 years. The mean/median follow-up duration was from 21 days to 67.7 months. Seven studies (11, 12, 14, 17, 23–25) reported the distribution of Child–Pugh classes. Approximately 90% of patients were grouped into Child–Pugh class A, and only one study (11) included the Child–Pugh class C. Substantial Child–Pugh class A patients also had a low prealbumin value (14, 23–25). Compared with the normal prealbumin group, the low prealbumin group had a significantly higher incidence of Child–Pugh grade B (14, 23, 25). Regarding the methodological quality, all included studies were considered to be of high quality, with NOS scores ranging from 7 to 8 points.

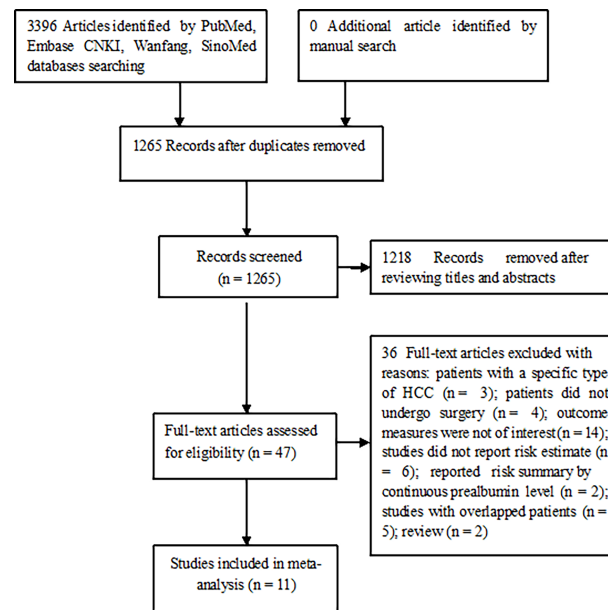


**FIGURE 1** | Flowchart of the study selection process.

## Overall Survival

Ten studies (10–14, 16, 17, 23–25) provided data on the value of prealbumin level in predicting OS. As shown in **Figure 2A**, no significant heterogeneity ( $I^2 = 7.1\%$ ,  $p = 0.377$ ) was observed. The meta-analysis indicated that a higher prealbumin level was associated with poorer OS (HR = 1.54, 95% CI = 1.42–1.68) than was a lower prealbumin level in the fixed effects model. Leave-one-out study sensitivity analysis suggested that the pooled risk estimates were statistically significant (data not shown). Additionally, the predictive value of a low prealbumin level showed no significant alterations in the different sample sizes, study designs, prealbumin cutoff values, and the follow-up duration subgroups (**Table 2**). However, Begg's test ( $p = 0.032$ ) and Egger's test ( $p = 0.099$ ) indicated clear evidence of publication bias. After imputing two potential missing studies, the pooled HR of OS was 1.53 (95% CI = 1.12–2.09) under trim-and-fill analysis (**Figure 3**).

## Recurrence-Free Survival

Two studies (10, 23) provided data on the value of prealbumin level in predicting RFS. **Figure 2B** shows no significant heterogeneity ( $I^2 = 32.8\%$ ,  $p = 0.222$ ) between studies. The pooled HR of RFS was 1.34 (95% CI = 1.17–1.52) for the higher *versus* lower prealbumin level in the fixed effects model.

## Hepatic Insufficiency

Two studies (9, 25) provided data on the value of prealbumin level in predicting postoperative hepatic insufficiency. As shown in **Figure 2C**, there was no significant heterogeneity ( $I^2 = 0.0\%$ ,  $p = 0.406$ ) between studies. The pooled HR of hepatic

insufficiency was 2.21 (95% CI = 1.36–3.60) for the higher *versus* lower prealbumin level in the fixed effects model.

## DISCUSSION

The current meta-analysis suggested that a low preoperative serum prealbumin level was independently associated with poor OS and RFS, as well as increased risk of postoperative hepatic insufficiency, in HCC patients undergoing hepatectomy. HCC patients with a low serum prealbumin level after hepatectomy had approximately 54% and 34% reduced risks of OS and RFS, respectively. Moreover, a low serum prealbumin level was associated with a 2.21-fold higher risk of postoperative hepatic insufficiency. These findings indicated that the preoperative serum prealbumin level may serve as a promising predictor of adverse outcomes in HCC patients.

Analysis of the serum prealbumin level using continuous variables also supported its predictive value. A decrease of 0.1 g/L prealbumin level increased the odds ratio of postoperative liver function insufficiency to 3.91 (15). Per standard deviation increase in the prealbumin level was associated with a 23% lower risk of mortality in HCC patients after hepatectomy (26). Our subgroup analysis further indicated that prediction of OS risk using the low prealbumin level appeared to be more pronounced in studies with a follow-up of >36 months than in those with ≤36 months of follow-up. This finding suggested that the impact of a low prealbumin level on OS tended to be stronger with increased duration of follow-up.

The serum albumin and prealbumin levels can be used to reflect the protein nutritional status, inflammatory state, and

**TABLE 1 |** Main characteristics of individual studies.

First author, year	Country	Study design	Sample size (% male)	Mean/median age (years)	Child-Pugh class	Low albumin	Prealbumin cutoff (mg/dl)	Outcome measures: HR or RR (95% CI)	Adjustment for covariates	Follow-up duration	Total NOS
Huang et al. (9)	China	R	427 (84.8)	51.1 ± 10.4	NR	NR	<17 vs. ≥17	HI: 3.19 (1.19–8.60)	Multivariate Cox proportional hazard analysis	21 days	7
Zhao et al. (10)	China	R	373 (87.9)	52 (25–81)	NR	NR	≤15.2 vs. >15.2	OS: 1.45 (1.03–2.05) RFS: 1.56 (1.18–2.07)	Multivariate Cox proportional hazard analysis	60 months	7
Shimura et al. (11)	Japan	R	25 (88)	69.6 (55–84)	A: 88%; B: 8%; C: 4%	NR	≤11.4 vs. >11.4	OS: 4.84 (1.12–20.9)	Multivariate Cox proportional hazard analysis	67.7 months	7
Wen et al. (12)	China	P	613 (81.9)	52.9 ± 10.4	A: 88.9%; B: 10.1%	10.9%	≤12 vs. >19 (men); ≤11 vs. >17 (women)	OS: 1.37 (1.13–1.65)	Multivariate Cox proportional hazard analysis	23 months	7
Zhang et al. (13)	China	P	230 (83.9)	51.6 ± 12.2	NR	NR	≤15.3 vs. >15.3	OS: 2.35 (1.25–4.39)	Age, sex, alcohol, tobacco, hypertension, diabetes, chemotherapy, tumor size, tumor number, differentiation, BCLC stage, AFP	>36 months	7
Jia, 2019 (14)	China	R	526 (85.6)	NR	A: 94.9%; B: 5.1%	10.3%	≤18.2 vs. >18.2	OS: 1.64 (1.27–2.12)	Age, sex, tumor size, tumor number, tumor capsule, albumin, ALT, TB, AFP, AST, macrovascular invasion, cirrhosis, HBsAg, Child–Pugh, BCLC stage	56 months	7
Li et al. (23)	China	R	1,483 (89)	51 ± 11	A: 90%; B: 10%	NR	≤17 vs. >17	OS: 1.45 (1.24–1.70) RFS: 1.28 (1.10–1.48)	Comorbid illness, ECOG performance status, cirrhosis, portal hypertension, TB, AST, albumin, AFP, maximum tumor size, tumor number, vascular invasion, satellites, tumor differentiation, blood loss, blood transfusion, major hepatectomy	67 months	8
Li et al. (24)	China	R	2,022 (86.0)	49.5 ± 11.2	A: 90.1%; B: 9.9%	10.7%	≤16.6 vs. >16.6	OS: 1.69 (1.44–1.98)	Age, sex, tumor number, tumor size, tumor capsule, HBsAg, cirrhosis, AFP, ALB, AST, ALT, TB, Child–Pugh, BCLC stage	37.4 months	8
Wang, 2020 (16)	China	R	142 (82.4)	NR	NR	NR	≤20 vs. >20	OS: 1.45 (0.96–2.17)	Tumor diameter, tumor number, HBsAg, cirrhosis, C-reactive protein, CNLC stage	60 months	7
Li et al. (25)	China	R	1,356 (88.9)	50.6 ± 10.6	A: 90.4%; B: 9.6%	NR	<17 vs. ≥17	OS: 2.50 (1.22–5.15) HI: 1.97 (1.12–3.43)	Sex, comorbid illness, platelets, AST, tumor size, tumor number, vascular invasion, blood loss, blood transfusion, extent of hepatectomy, type of resection, operation time	3 months	8
Xu et al. (17)	China	R	245 (88.2)	Not reported	A: 93.5%; B: 6.5%	8.98%	≤20 vs. >20	OS: 1.43 (0.66–1.78)	Multivariate Cox proportional hazard analysis	60 months	7

HR, hazard ratio; RR, risk ratio; CI, confidence interval; P, prospective; R, retrospective; NR, not reported; HCC, hepatocellular carcinoma; OS, overall survival; RFS, recurrence-free survival; HI, hepatic insufficiency; ALT, alanine transaminase; AST, aspartate aminotransferase; BCLC, Barcelona Clinic Liver Cancer; HBsAg, hepatitis B surface antigen; TB, total bilirubin; ECOG, Eastern Cooperative Oncology Group; AFP, Alpha fetoprotein; CNLC, China Liver Cancer; NOS, Newcastle–Ottawa Scale.

hepatic protein synthesis capability. Serum albumin level is more commonly used in clinical practice than is the prealbumin level. However, serum albumin level is often affected by renal function, hydration, and exogenous supplement of albumin (27). There is skepticism in using albumin as a nutritional marker because of its lack of specificity and long half-life of 20 days (28). Serum prealbumin is recommended as a nutritional biomarker, particularly in the elderly population (29). The major advantage of prealbumin as a nutritional biomarker is its short half-life of 2–3 days and its high specificity and sensitivity in the assessment of hepatic functional reserve (30, 31). Moreover, the serum prealbumin level is unaffected by intestinal protein losses

(32). Therefore, prealbumin level is a more reliable and faster indicator for assessing a patient's nutritional level. In the multivariable analysis, the preoperative prealbumin level independently predicted OS, whereas the albumin level lost its statistical significance (11, 12, 23, 25). These findings indicated that the serum prealbumin level may have better predictive value than does the albumin level in HCC patients. Notably, the above findings should be interpreted with caution due to the small number of studies included.

Our meta-analysis highlighted that the determination of preoperative prealbumin levels can improve the risk stratification of HCC patients. The identification of HCC patients with a low



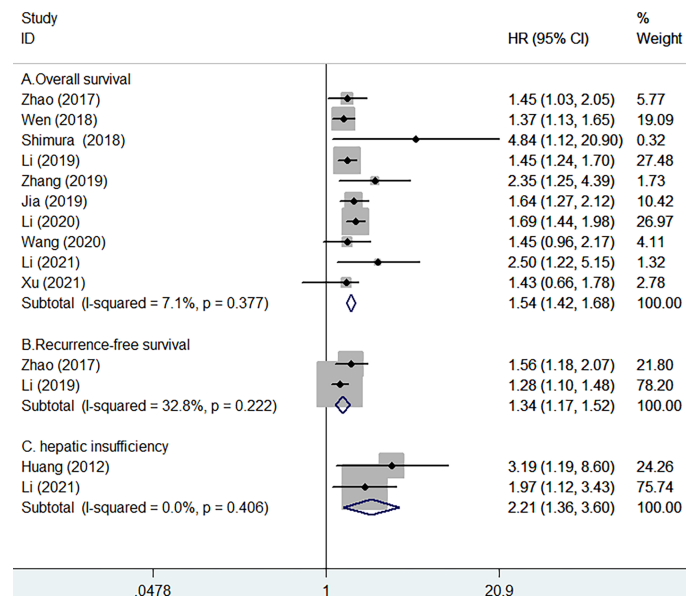


**FIGURE 2** | Forest plots showing the pooled hazard ratios (HR) and 95% CI of overall survival (A), recurrence-free survival (B), and postoperative hepatic insufficiency (C) for lower versus higher serum prealbumin levels.

prealbumin level may help clinicians estimate the liver function and nutritional status. HCC patients with a low prealbumin level should receive close monitoring and active nutritional support.

The current meta-analysis has several limitations. Firstly, selection bias may have occurred because of the retrospective nature of most eligible studies. Secondly, single determination of the prealbumin level rather than a dynamic measurement may have resulted in the misclassification of patients into categories. Thirdly, various cutoff values for low level of serum prealbumin were reported in the included studies, conferring difficulty for clinical applications. Future studies should further establish the optimal cutoff value for low level of prealbumin. Fourthly, due to insufficient data, we failed to perform subgroup analysis according to the clinicopathologic data, including cirrhosis, C-reactive protein, Barcelona Clinic Liver Cancer stage, or the alpha fetoprotein level. Fifthly, the serum prealbumin level may be affected by obstructive

jaundice, hyperthyroidism, nephritic syndrome, or ulcerative colitis. Particularly, not all included studies adjusted for the tumor factors and cirrhosis in their statistical models. The lack of adjustment for these important confounders may have led to the overestimation of the predictive value of prealbumin. Finally, apart from one study (11) originating from Japan, all the included studies were from China, where there is a predominant hepatitis B virus endemic area, thereby restricting the generalizability of our study to the West.

## CONCLUSION

A low preoperative serum prealbumin level is possibly an independent predictor of poor survival and postoperative hepatic insufficiency in HCC patients undergoing hepatectomy. The serum prealbumin level may be used for the risk

**TABLE 2** | Results of subgroup analysis on overall survival.

Subgroup	No. of studies	Pooled hazard ratio	95% confidence interval	Heterogeneity between studies
Study design				
Prospective	2	1.43	1.20–1.72	$p = 0.107$ , $I^2 = 61.5\%$
Retrospective	8	1.57	1.43–1.73	$p = 0.508$ , $I^2 = 0.0\%$
Sample size				
<1,000	7	1.50	1.32–1.69	$p = 0.438$ , $I^2 = 0.0\%$
≥1,000	3	1.58	1.42–1.77	$p = 0.184$ , $I^2 = 40.9\%$
Prealbumin cutoff				
≤18 mg/dl	7	1.54	1.41–1.69	$p = 0.158$ , $I^2 = 35.4\%$
>18 mg/dl	3	1.56	1.28–1.90	$p = 0.824$ , $I^2 = 0.0\%$
Follow-up duration				
>36 months	8	1.58	1.44–1.73	$p = 0.669$ , $I^2 = 0.0\%$
≤36 months	2	1.42	1.19–1.71	$p = 0.113$ , $I^2 = 60.1\%$

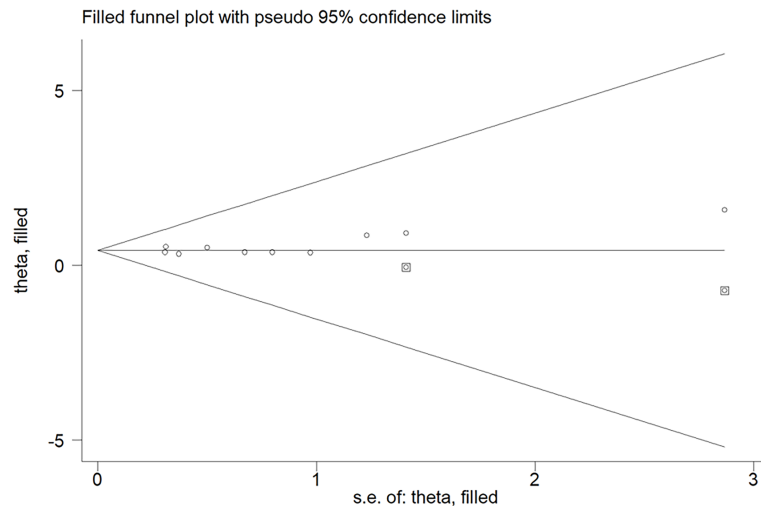


**FIGURE 3** | Funnel plot showing the impact of a lower prealbumin level on overall survival. The circles alone are real studies; circles enclosed in boxes are “filled” studies.

stratification of HCC patients. However, the current findings should be interpreted with caution due to the retrospective nature of most of the eligible studies.

## DATA AVAILABILITY STATEMENT

The original contributions presented in the study are included in the article/supplementary material. Further inquiries can be directed to the corresponding authors.

## AUTHOR CONTRIBUTIONS

CM and YL contributed to the study and guaranteed the integrity of study. YF and YS searched the literature, extracted the data,

assessed the study quality, and conducted the statistical analysis. YF wrote the manuscript. YL revised/edited the manuscript. All authors contributed to the article and approved the submitted version.

## FUNDING

This work is supported by: 1) Jiangsu Innovative Team Leading Talent Fund (CXTDC2016006); 2) Jiangsu 333 Talent Fund (BRA2020016); 3) Suqian Science and Technology Support Project Fund (S201907); 4) Jiangsu Provincial Key Research and Development Special Fund (BE2015666); 5) Jiangsu Six High Peak Talent Fund (WSW-205); and 6) Zhenjiang Key Research and Development Fund (SH2021038).

## REFERENCES

- Forner A, Reig M, Bruix J. Hepatocellular Carcinoma. *Lancet* (2018) 391 (10127):1301–14. doi: 10.1016/S0140-6736(18)30010-2
- Sung H, Ferlay J, Siegel RL, Laversanne M, Soerjomataram I, Jemal A, et al. Global Cancer Statistics 2020: GLOBOCAN Estimates of Incidence and Mortality Worldwide for 36 Cancers in 185 Countries. *CA Cancer J Clin* (2021) 71(3):209–49. doi: 10.3322/caac.21660
- Buonaguro L, Petrizzo A, Tagliamonte M, Tornesello ML, Buonaguro FM. Challenges in Cancer Vaccine Development for Hepatocellular Carcinoma. *J Hepatol* (2013) 59(4):897–903. doi: 10.1016/j.jhep.2013.05.031
- Asafo-Agyei KO, Samant H. *Hepatocellular Carcinoma*. Treasure Island (FL: StatPearls (2021).
- Chen H, Jia W. Progress in Hepatectomy for Hepatocellular Carcinoma and Peri-Operation Management. *Genes Dis* (2020) 7(3):320–7. doi: 10.1016/j.gendis.2020.02.001
- Ingenbleek Y, Young V. Transthyretin (Prealbumin) in Health and Disease: Nutritional Implications. *Annu Rev Nutr* (1994) 14:495–533. doi: 10.1146/annurev.nu.14.070194.002431
- Marcason W. Should Albumin and Prealbumin Be Used as Indicators for Malnutrition? *J Acad Nutr Diet* (2017) 117(7):1144. doi: 10.1016/j.jand.2017.04.018
- Beck FK, Rosenthal TC. Prealbumin: A Marker for Nutritional Evaluation. *Am Family Physician* (2002) 65(8):1575–8.
- Huang L, Li J, Yan JJ, Liu CF, Wu MC, Yan YQ. Prealbumin Is Predictive for Postoperative Liver Insufficiency in Patients Undergoing Liver Resection. *World J Gastroenterol* (2012) 18(47):7021–5. doi: 10.3748/wjg.v18.i47.7021
- Zhao XJ, Jin GZ, Yang N, Dong W, Yang GS. Value of Preoperative Prealbumin Content in Assessing Long-Term Prognosis of Patients With Hepatocellular Carcinoma After Hepatectomy. *Acad J Second Mil Med Univ* (2017) 38(4):463–8. doi: 10.16781/j.0258-879x.2017.04.0463
- Shimura T, Shibata M, Kofunato Y, Okada R, Ishigame T, Kimura T, et al. Clinical Significance of Serum Transthyretin Level in Patients With Hepatocellular Carcinoma. *ANZ J Surg* (2018) 88(12):1328–32. doi: 10.1111/ans.14458
- Wen X, Yao M, Lu Y, Chen J, Zhou J, Chen X, et al. Integration of Prealbumin Into Child-Pugh Classification Improves Prognosis Predicting Accuracy in HCC Patients Considering Curative Surgery. *J Clin Transl Hepatol* (2018) 6 (4):377–84. doi: 10.14218/JCTH.2018.00004

13. Zhang L, Chen QG, Li SQ, Zhang J, Min QH, Gao QF, et al. Preoperative Fibrinogen to Prealbumin Ratio as a Novel Predictor for Clinical Outcome of Hepatocellular Carcinoma. *Future Oncol* (2019) 15(1):13–22. doi: 10.2217/fon-2018-0376
14. Jia RR, Zhong JH, Huo RR, Su QB, Xiang X, Zhao FL, et al. Correlation Between Serum Prealbumin and Prognosis of Patients With Hepatocellular Carcinoma After Hepatectomy. *J Surg Oncol* (2019) 119(6):794–800. doi: 10.1002/jso.25378
15. Shen Y, Shi G, Huang C, Zhu X, Chen S, Sun H, et al. Prediction of Post-Operative Liver Dysfunction by Serum Markers of Liver Fibrosis in Hepatocellular Carcinoma. *PLoS One* (2015) 10(10):e0140932. doi: 10.1371/journal.pone.0140932
16. Wang ZY. C-Reactive Protein-to-Prealbumin Ratio Predicts Prognoses of Patients After Curative Resection for Hepatocellular Carcinoma. Master's thesis of Bengbu Medical College (2020).
17. Xu XS, Cai PP, Zhang LZ. The Value of Fibrinogen/Prealbumin Ratio in Predicting the Prognosis of Hepatocellular Carcinoma After Operation. *Mod Oncol* (2021) 29(18):3224–8. doi: 10.3969/j.issn.1672-4992.2021.18.0187
18. Qiao W, Leng F, Liu T, Wang X, Wang Y, Chen D, et al. Prognostic Value of Prealbumin in Liver Cancer: A Systematic Review and Meta-Analysis. *Nutr Cancer* (2020) 72(6):909–16. doi: 10.1080/01635581.2019.1661501
19. Liberati A, Altman DG, Tetzlaff J, Mulrow C, Gotzsche PC, Ioannidis JP, et al. The PRISMA Statement for Reporting Systematic Reviews and Meta-Analyses of Studies That Evaluate Health Care Interventions: Explanation and Elaboration. *J Clin Epidemiol* (2009) 62(10):e1–34. doi: 10.1016/j.jclinepi.2009.06.006S0895-4356(09)00180-2
20. Wells G, Shea B, O'Connell D, Peterson J, Welch V, Losos M, et al. *The Newcastle–Ottawa Scale (NOS) for Assessing the Quality If Nonrandomized Studies in Meta-Analyses*. Available at: [http://www.ohri.ca/programs/clinical\\_epidemiology/oxford.asp](http://www.ohri.ca/programs/clinical_epidemiology/oxford.asp) (Accessed September 6, 2021).
21. Begg CB, Mazumdar M. Operating Characteristics of a Rank Correlation Test for Publication Bias. *Biometrics* (1994) 50(4):1088–101. doi: 10.2307/2533446
22. Egger M, Davey Smith G, Schneider M, Minder C. Bias in Meta-Analysis Detected by a Simple, Graphical Test. *Bmj* (1997) 315(7109):629–34. doi: 10.1136/bmj.315.7109.629
23. Li JD, Xu XF, Han J, Wu H, Xing H, Li C, et al. Preoperative Prealbumin Level as an Independent Predictor of Long-Term Prognosis After Liver Resection for Hepatocellular Carcinoma: A Multi-Institutional Study. *HPB (Oxford)* (2019) 21(2):157–66. doi: 10.1016/j.hpb.2018.06.1803
24. Li MJ, Teng YX, Li Q, Xiao XC, Huo RR, Ma L, et al. Serum Prealbumin Predicts Prognosis of Hepatectomy in Patients With Hepatocellular Carcinoma. *Chin J Hepatobiliary Surg* (2020) 26(1):27–31. doi: 10.3760/cma.j.issn.1007-8118.2020.01.007
25. Li JD, Diao YK, Li J, Wu H, Sun LY, Gu WM, et al. Association Between Preoperative Prealbumin Level and Postoperative Mortality and Morbidity After Hepatic Resection for Hepatocellular Carcinoma: A Multicenter Study From a HBV-Endemic Area. *Am J Surg* (2021) 221(5):1024–32. doi: 10.1016/j.amjsurg.2020.08.036
26. Huo RR, Liu HT, Deng ZJ, Liang XM, Gong WF, Qi LN, et al. Dose-Response Between Serum Prealbumin and All-Cause Mortality After Hepatectomy in Patients With Hepatocellular Carcinoma. *Front Oncol* (2020) 10:596691. doi: 10.3389/fonc.2020.596691
27. Fuhrman MP, Charney P, Mueller CM. Hepatic Proteins and Nutrition Assessment. *J Am Diet Assoc* (2004) 104(8):1258–64. doi: 10.1016/j.jada.2004.05.213
28. Levitt DG, Levitt MD. Human Serum Albumin Homeostasis: A New Look at the Roles of Synthesis, Catabolism, Renal and Gastrointestinal Excretion, and the Clinical Value of Serum Albumin Measurements. *Int J Gen Med* (2016) 9:229–55. doi: 10.2147/IJGM.S102819
29. Ingenbleek Y. Plasma Transthyretin as a Biomarker of Sarcopenia in Elderly Subjects. *Nutrients* (2019) 11(4):895. doi: 10.3390/nu11040895
30. Huang H. An Analysis of Biochemical Parameter for Liver Reserve Function in Patients With Liver Cancer. *J Oncol* (2009) 15(3):232–3.
31. Collins N. The Difference Between Albumin and Prealbumin. *Adv Skin Wound Care* (2001) 14(5):235–6. doi: 10.1097/00129334-200109000-00009
32. Takeda H, Ishihama K, Fukui T, Fujishima S, Orii T, Nakazawa Y, et al. Significance of Rapid Turnover Proteins in Protein-Losing Gastroenteropathy. *Hepatogastroenterology* (2003) 50(54):1963–5.

**Conflict of Interest:** The authors declare that the research was conducted in the absence of any commercial or financial relationships that could be construed as a potential conflict of interest.

**Publisher's Note:** All claims expressed in this article are solely those of the authors and do not necessarily represent those of their affiliated organizations, or those of the publisher, the editors and the reviewers. Any product that may be evaluated in this article, or claim that may be made by its manufacturer, is not guaranteed or endorsed by the publisher.

Copyright © 2021 Fan, Sun, Man and Lang. This is an open-access article distributed under the terms of the Creative Commons Attribution License (CC BY). The use, distribution or reproduction in other forums is permitted, provided the original author(s) and the copyright owner(s) are credited and that the original publication in this journal is cited, in accordance with accepted academic practice. No use, distribution or reproduction is permitted which does not comply with these terms.



# ZCCHC17 Served as a Predictive Biomarker for Prognosis and Immunotherapy in Hepatocellular Carcinoma

## OPEN ACCESS

### Edited by:

Qingfeng Zhu,  
Johns Hopkins Medicine,  
United States

### Reviewed by:

Alessandro Granito,  
University of Bologna, Italy  
Neha Nanda,  
Johns Hopkins Medicine,  
United States

### \*Correspondence:

Xueming Wu  
wuxueming0120@163.com  
Chunying Luo  
lcy2005@ymcn.edu.cn

<sup>†</sup>These authors have contributed  
equally to this work and share  
first authorship

<sup>‡</sup>These authors have contributed  
equally to this work

### Specialty section:

This article was submitted to  
Gastrointestinal Cancers: Hepato  
Pancreatic Biliary Cancers,  
a section of the journal  
Frontiers in Oncology

**Received:** 21 October 2021

**Accepted:** 13 December 2021

**Published:** 06 January 2022

### Citation:

Liu F, Liang J, Long P, Zhu L,  
Hou W, Wu X and Luo C (2022)  
ZCCHC17 Served as a  
Predictive Biomarker for  
Prognosis and Immunotherapy  
in Hepatocellular Carcinoma.  
Front. Oncol. 11:799566.  
doi: 10.3389/fonc.2021.799566

Fahui Liu<sup>1†</sup>, Jiadong Liang<sup>1†</sup>, Puze Long<sup>1</sup>, Lilan Zhu<sup>2</sup>, Wanyun Hou<sup>1</sup>, Xueming Wu<sup>1‡\*</sup> and Chunying Luo<sup>1,3‡\*</sup>

<sup>1</sup> Department of Pathology, Affiliated Hospital of Youjiang Medical University for Nationalities, Baise, China, <sup>2</sup> Undergraduate Clinical Medicine, Youjiang Medical University for Nationalities, Baise, China, <sup>3</sup> Department of Cell Biology, Medical College of Guangxi University, Nanning, China

Hepatocellular carcinoma (HCC) is one of the common malignant tumors. The prognosis and five-year survival rate of HCC are not promising due to tumor recurrence and metastasis. Exploring markers that contribute to the early diagnosis of HCC, markers for prognostic evaluation of HCC patients, and effective targets for treating HCC patients are in the spotlight of HCC therapy. Zinc Finger CCHC-Type Containing 17 (ZCCHC17) encodes the RNA binding protein ZCCHC17, but its role in HCC is still unclear. Here, 90 paraffin-embedded specimens combined with bioinformatics were used to comprehensively clarify the value of ZCCHC17 in the diagnosis and prognosis of HCC and its potential functions. Paraffin-embedded specimens were used to assess ZCCHC17 protein expression and its correlation with prognosis in 90 HCC patients. The public data sets of HCC patients from TCGA, ICG, and GEO databases were also used for further analysis. It was found that protein and mRNA levels of ZCCHC17 in HCC tissues were significantly higher than those in normal tissues. The abnormally high expression may be related to the abnormal DNA methylation of ZCCHC17 in tumor tissues. The high expression of ZCCHC17 is related to AFP, histologic grade, tumor status, vascular invasion, and pathological stage. Multi-data set analysis showed that patients with high ZCCHC17 expression had a worse prognosis, and multivariate cox regression analysis showed an independent prognostic significance of ZCCHC17. The results of functional analysis, including Gene Ontology (GO), Kyoto Encyclopedia of Genes and Genomes (KEGG) and Gene Set Enrichment Analysis (GSEA), indicate that ZCCHC17 is mainly involved in immune regulation. Subsequently, further single-sample gene set enrichment analysis (ssGSEA) showed that the expression of ZCCHC17 was related to the infiltration of immune cells. Importantly, we also analyzed the relationship between ZCCHC17 and immune checkpoint genes, tumor mutation burden (TMB), microsatellite instability (MSI) and TP53 status in HCC patients and evaluated the role of ZCCHC17 in cancer immunotherapy. In summary, ZCCHC17 is a novel marker for the



diagnosis and prognostic evaluation of HCC. Concurrently, it regulates immune cells in the tumor microenvironment (TME) of HCC patients, which has a specific reference value for the immunotherapy of HCC.

**Keywords:** ZCCHC17, HCC, diagnosis, prognosis, immunotherapy

## INTRODUCTION

HCC is a common malignancy of liver cancer. Worldwide, there were 905667 new cases of HCC in 2020, accounting for 4.7% of new cancer cases in the whole year. It is the fourth leading cause of cancer death globally, and the annual mortality rate is as high as 8.3% (1). The early symptoms of most patients are usually not evident, and they have reached the middle-to-late stage when coming to medical attention. Moreover, due to tumor size and location, recurrence, and metastasis, it is difficult for many patients to undergo surgery. The overall survival after treatment is still poor. In recent years, although sorafenib has somewhat improved survival in patients with advanced HCC (2), and Nivolumab and Pembrolizumab have shown positive results in recent immunotherapy clinical trials (3, 4). However, HCC still has a dismal prognosis. Therefore, it is of great significance to explore the pathogenesis of HCC and identify new diagnostic markers and therapeutic targets.

ZCCHC17 is one of the genes encoding RNA binding proteins (RBP) (5). As an essential participant in post-transcriptional modification, RBPs often bind to RNA to form ribonucleoprotein complex (RNP). Defects in RNP structure or function can lead to disease, including tumor formation. Factors that cause abnormal function of RBPs in tumors include genomic changes (6), transcriptional and post-transcriptional modification regulation (7) and post-translational modification (8). RBPs can affect the occurrence and development of tumors by regulating the maturation, translation, localization and stability of RNA and binding DNA (9). Because of the vital role of RBP in post-transcriptional modification, even minor changes can have significant effects. The abnormal function of RBP can often affect multiple tumor signature features, such as tumor proliferation, tumor metastasis, tumor death resistance, tumor metabolic disorder, tumor immune escape, tumor genome instability (10).

In view of the close relationship between RBPs and tumorigenesis, there is insufficient evidence for the role and clinical significance of ZCCHC17 in the diagnosis, disease progression, and prognosis of HCC. In this study, the expression of ZCCHC17 in HCC tissues was studied by collecting clinical samples and bioinformatics methods. The correlation or role of ZCCHC17 in the occurrence, development and prognosis of HCC was analyzed by bioinformatics. To lay an experimental and theoretical basis for further investigation of the mechanism of ZCCHC17 in the occurrence and development of HCC and its influence on the treatment of HCC, and to provide some valuable insights and therapeutic strategies for the treatment in HCC. Importantly, ZCCHC17 appears to affect the prognosis of HCC patients partly

through regulating immune cells infiltration. These findings highlight the significant role of ZCCHC17 in HCC and suggest that ZCCHC17 may play an essential role in the regulation of immune cells infiltration in HCC and in guiding the treatment of HCC patients.

## MATERIALS AND METHODS

### Data Collection of HCC Patients

RNAseq data (level 3 HTSeq-FPKM) of 374 hepatocellular carcinoma patients was downloaded from the TCGA (<https://portal.gdc.cancer.gov/>) LIHC (hepatocellular carcinoma) project. The formatted RNAseq data were converted into TPM (transcripts per million reads) format for subsequent analysis. The TCGA methylation data evaluated by the Infinium 450K array was obtained from the Xena Public Data Center (<https://xena.ucsc.edu/>). The RNAseq data in TPM format of TCGA and GTEx processed uniformly by the Toil process (11) is downloaded from UCSC XENA (<https://xenabrowser.net/datapages/>). 231 HCC patients with complete follow-up data and RNA sequencing data were downloaded from ICGC. Gene expression profiling data sets (GSE54236, GSE84005) were obtained from the GEO database (<https://www.ncbi.nlm.nih.gov/gds>). A total of 4 sets of data downloaded from public databases were used to study the expression differences of ZCCHC17. The data of HCC patients from TCGA and ICGC with survival data were used for further survival analysis. In addition. In order to further prove the reliability of the experiment, we collected the paraffin-embedded tissues of 90 HCC patients with complete follow-up information from the Department of Pathology, Affiliated Hospital of Youjiang Medical University for Nationalities as a validation cohort. This study was reviewed and approved by the Ethics Committee of the Affiliated Hospital of Youjiang Medical University for Nationalities (YYFY-LL-2021-31), and all patients agreed with written informed consent. The criteria for inclusion were as follows: all of the HCC patients were treated for the first time, and none of the patients received radiotherapy, chemotherapy, or targeted anticancer drug treatment before surgery. The primary lesion was hepatocellular carcinoma, and the pathological type was hepatocellular carcinoma. Exclusion criteria included patients receiving chemotherapy or radiation before surgery or patients diagnosed with multiple neoplasms, cholangiocarcinoma, or metastatic HCC.

### Immunohistochemistry

The collected paraffin-embedded tissues were made into pathological sections with a diameter of 3 to 5 microns. The

pathological sections were processed through the following workflow: sliced, dewaxed, antigen repaired (EDTA PH=9.0), and blocked. Slides were incubated in primary antibody (ZCCHC17, Invitrogen, #PA5-103989, 1:1000 Dilution) overnight at 4°C. Secondary antibody incubation (MaxVision, KIT-5010), DAB staining, hematoxylin staining. After dehydration, the sections were sealed with neutral gum. The image on the sections is collected using the tissue slice digital scanner and imaging system, and the image analysis system automatically reads the tissue measurement data. Staining was scored as follows: 0: negative or no coloring; 1: weak positive light yellow; 2: medium positive brown; 3: intense positive brown. Then the positive area of weak, medium and intense in the measuring area is analyzed and calculated separately. The integrated optical density (IOD) in the positive area and the size of the positive area is measured. The mean density value (IOD/positive area) indicated the expression abundance of ZCCHC17 protein.

## Bioinformatics Analysis

The level of methylation for each CpG site is expressed as a Beta value. Beta values ranged from 0 (unmethylated) to 1 (fully methylated). The protein data file that interacts with ZCCHC17 is downloaded in the Compartmentalized Protein-Protein Interaction Database | v2.1.1 (<http://comppi.linkgroup.hu>) (12). The functions and pathway analysis of proteins that interact with ZCCHC17 for GO and KEGG were performed using the “clusterProfiler” package (13). The correlation between ZCCHC17 and HCC patients’ prognosis was analyzed using Kaplan-Meier survival analysis and Cox regression analysis. We use the ssGSEA (14) (single-sample gene set enrichment analysis) algorithm to quantify the relative abundance of 24 immune cell infiltrations in the tumor microenvironment of HCC patients. The enrichment score calculated by ssGSEA analysis represents the relative abundance of infiltrating cells in each tumor microenvironment in each sample. Potential ICB response for ZCCHC17 patients in high and low groups was predicted with the TIDE algorithm (15).

## Statistical Analysis

Clinical information was obtained from TCGA and was analyzed by R-4.0.2 and SPSS 24.0. For comparisons of two groups, paired or unpaired t-tests were used for normally distributed variables; otherwise, Wilcoxon signed-rank test was used. For correlations between two variables, Spearman’s correlation test was used. The differences in patient survival with different groups were analyzed using Kaplan-Meier analysis and uni- and multivariate analyses. For all Statistical analyses, A P-value < 0.05 was considered statistically significant in this study.

## RESULTS

### Expression of ZCCH17 in HCC and Diagnostic Efficacy for HCC

The results showed that the ZCCHC17 expression in the tumor was higher than normal, and the difference between the two groups

was 0.935 (0.755-1.114). The difference was statistically significant ( $t = 10.470$ ,  $P < 0.001$ ) (**Figure 1A**). The analysis of TCGA unpaired samples showed that the expression level of ZCCHC17 in the tumor was significantly higher than that of normal, and the difference was statistically significant ( $P < 0.001$ ) (**Figure 1B**). In addition, to further determine the accuracy of the results, we added normal samples from GTEx. The comparison results still show that the expression level of ZCCHC17 in the tumor is significantly higher than that of normal ( $P < 0.001$ ) (**Figure 1C**). In the diagnostic value of ZCCHC17, ZCCHC17 showed a high accuracy of tumor prediction in HCC. (AUC = 0.930, CI = 0.896-0.964) (**Figure 1D**). At the same time, we downloaded the expression profile data of HCC patients from GSE54236, GSE84005, and ICGC to validate the expression difference of ZCCHC17 between tumor and non-tumor samples. The results showed that the expression level of ZCCHC17 in the tumor was significantly higher than that in normal ( $P < 0.001$ ) (**Figures 1E-G**). At the same time, through immunohistochemistry experiments of clinical samples. The independent sample T-test showed that the ZCCHC17 in the tumor was higher than normal, and the difference between the two groups was 0.011 (0.008-0.014). The difference was statistically significant ( $t = 7.683$ ,  $P < 0.001$ ) (**Figure 1H**). The paired sample T-test showed that the ZCCHC17 in the tumor was higher than that in normal, and the difference between the two groups was 0.011 (0.009-0.014). The difference was statistically significant ( $t = 9.299$ ,  $P < 0.001$ ) (**Figure 1I**). It can also be observed that the staining intensity of ZCCHC17 in HCC is also significantly higher than that of paired adjacent normal tissues (20X) (**Figure 1J**). These results indicate that ZCCHC17 also has significant differences in protein expression levels. Ns,  $P \geq 0.05$ ; \*,  $P < 0.05$ ; \*\*,  $P < 0.01$ ; \*\*\*,  $P < 0.001$ .

### DNA Methylation Is Involved in Mediating Changes in ZCCHC17 Expression

As shown in Figure A, ZCCHC17 has 15 methylation sites, of which cg24317935 has the highest methylation level, and cg21417843 has the lowest methylation level (**Figure 2A**). Then we analyzed the difference in methylation level between the tumor and the normal samples. The results showed that the methylation level in the normal group was significantly higher than that in the tumor group ( $P < 0.001$ ) (**Figure 2B**). Then we analyzed 15 methylation sites. The correlation between the methylation and the expression level of ZCCHC17 showed that cg03605784 ( $r = -0.200$ ,  $P < 0.001$ ), cg03856286 ( $r = -0.260$ ,  $P < 0.001$ ), cg08734125 ( $r = -0.190$ ,  $P < 0.001$ ), cg22706424 ( $r = -0.210$ ,  $P < 0.001$ ), cg24317935 ( $r = 0.210$ ,  $P < 0.001$ ) was significantly negatively correlated with the expression of ZCCHC17 (**Figures 2C-G**). Ns,  $P \geq 0.05$ ; \*,  $P < 0.05$ ; \*\*,  $P < 0.01$ ; \*\*\*,  $P < 0.001$ .

### The Association Between ZCCHC17 Expression and Clinicopathologic Features

The characteristics of 374 HCC patients from TCGA, including T stage, N stage, M stage, Pathologic stage, Tumor status, Gender, Age, Histologic grade, AFP, Vascular invasion, were collected and shown in **Table 1**. In order to further understand

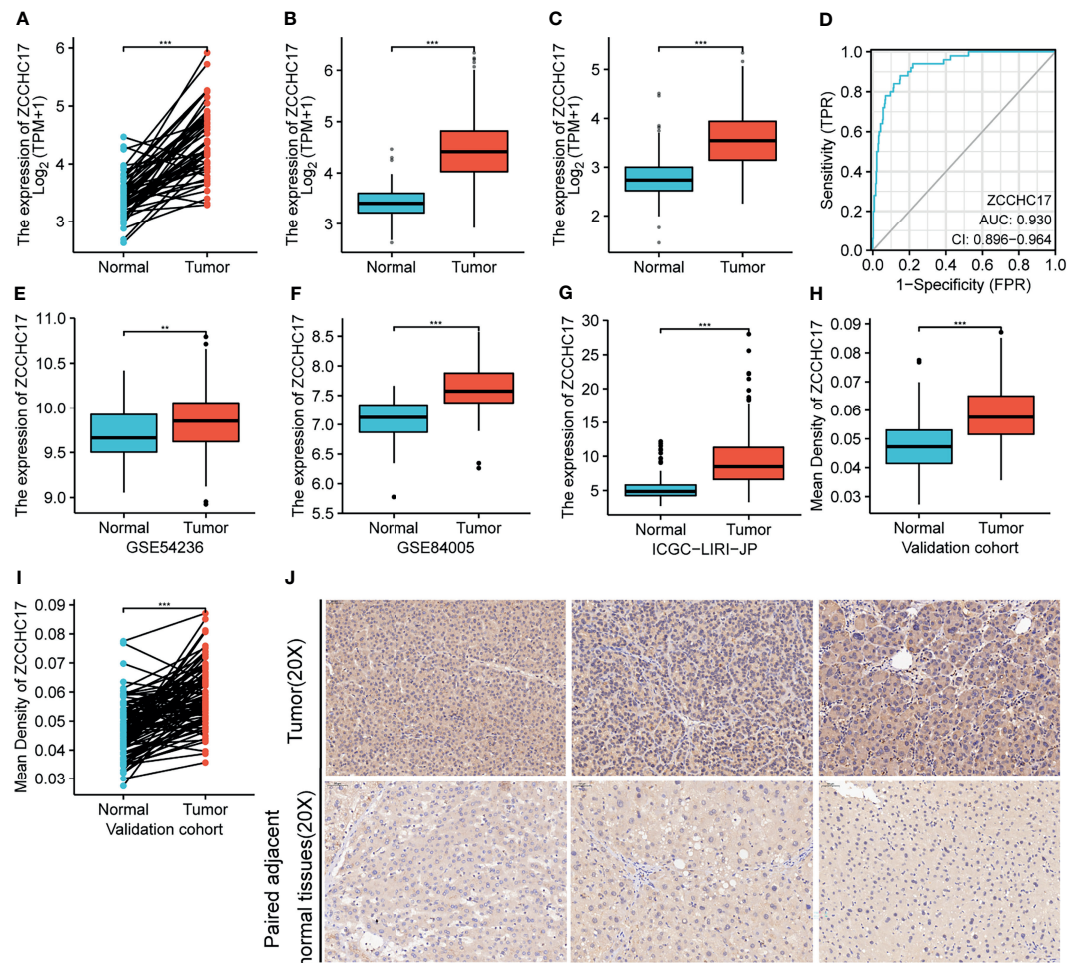


**FIGURE 1 |** Expression of ZCCHC17 in HCC and diagnostic efficacy for HCC. **(A, B)** ZCCHC17 was highly expressed in HCC in TCGA ( $P < 0.001$ ); **(C)** High expression of ZCCHC17 in HCC compared with normal tissues from GTEx and TCGA ( $P < 0.001$ ); **(D)** Diagnostic capability of ZCCHC17 in HCC; **(E)** High expression of ZCCHC17 in HCC in GSE54236 ( $P < 0.01$ ); **(F)** High expression of ZCCHC17 in HCC in GSE84005 ( $P < 0.001$ ); **(G)** High expression of ZCCHC17 in HCC in ICGC; **(H–J)** ZCCHC17 proteins were highly expressed in HCC compared with adjacent normal tissues (20X) ( $P < 0.001$ ). \*\* $P < 0.01$ ; \*\*\* $P < 0.001$ .

the clinical significance of ZCCHC17 in HCC, we compared the clinicopathological relationship between ZCCHC17 expression and different subgroups. The results showed significant differences in the expression of ZCCHC17 in different subgroups of AFP, histologic grade, tumor status, vascular invasion and pathological stage (**Figures 3A–E**). Ns,  $P \geq 0.05$ ; \*,  $P < 0.05$ ; \*\*,  $P < 0.01$ ; \*\*\*,  $P < 0.001$ .

## The Relationships Between ZCCHC17 Expression and Survival in HCC

Owing to the expression level of ZCCHC17 is closely related to the progression and malignancy of HCC, we then tested the prognostic value of ZCCHC17. The results showed that the expression of ZCCHC17 was significantly related to patients' overall survival (OS), progression-free survival (PFS) and disease-specific survival (DSS) (**Figures 4A–C**). In order to explore the relationship between different methylation sites of

ZCCHC17 and prognosis in HCC, we identified the relationship between the 15 methylation sites of ZCCHC17 and the OS, PFS of HCC patients. According to the median of the methylation value, we divided the patients into high and low groups. The results showed that the high methylation level of the methylation site cg08734125 is relevant to the patient's better OS ( $P = 0.011$ ), and the high methylation level of cg25469212 is related to the poor patient OS ( $P = 0.021$ ). In addition, the high methylation level of cg25469212 was associated with worse PFS in patients ( $P = 0.049$ ) (**Figures 4D–F**). In addition, data from ICGC and validation cohort also proved that increased expression of ZCCHC17 was significantly associated with worse OS (**Figures 4G, H**). Univariate Cox regression analysis showed that Stage III and Stage IV, With tumor, and the expression level of ZCCHC17 was a risk factor for the prognosis of HCC patients. Further multivariate Cox regression analysis showed that Stage III and Stage IV, With tumor, The expression level of ZCCHC17

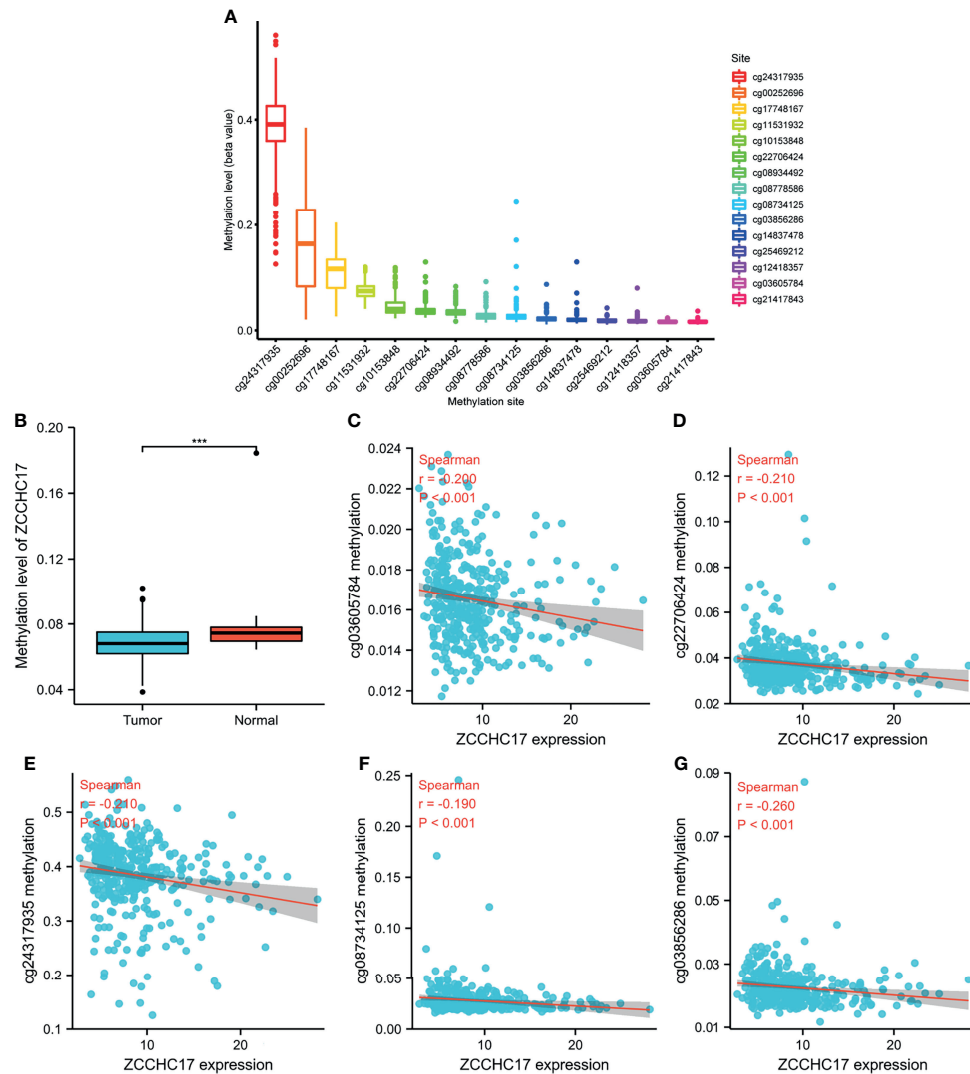


**FIGURE 2 |** ZCCHC17 methylation levels in HCC from TCGA. **(A)** The methylation level of 15 methylation sites for ZCCHC17; **(B)** Difference in ZCCHC17 methylation levels between normal and tumor tissues; **(C–G)** Correlation of ZCCHC17 methylation level with the expression level of ZCCHC17. \*\*\* $P < 0.001$ .

is an independent risk factor affecting the prognosis of HCC patients (Table 2). In summary, the above results suggest that ZCCHC17 plays a vital role in the prognostic evaluation of HCC patients.

### Functional Analysis of ZCCHC17

Figure A shows 49 proteins that interact with ZCCHC17. The number of lines between the two proteins indicates the number of evidence of the interaction between the two proteins. The lines with different colors represent the positions of the interactions between the two proteins in other evidence (Figure 5A). Then we performed KEGG and GO enrichment analysis on these 49 interacting proteins (Figures 5B, D). The analysis results show that these genes are mainly related to methylation and participate in immunotherapy-related pathways. Concurrently, we also performed GSEA enrichment analysis on ZCCHC17 in the TCGA dataset, and the

results showed that interactions between immune cells and microRNAs in the tumor microenvironment, the intestinal immune network for IgA production, PD-1 signaling, cancer immunotherapy by PD-1 blockade, immunoregulatory interactions between a lymphoid and a non-lymphoid cell (Figure 5C). It shows that the highly expressed ZCCHC17 significantly participates in multiple immunotherapy-related pathways and the vital role of ZCCHC17 in the body's immunity.

### The Correlation Between ZCCHC17 and Immune Cells Infiltration in HCC

Based on the previous functional analysis, we found that ZCCHC17 may play an important role in the immune response of HCC patients. Therefore, we used ssGSEA to analyze the infiltration of 24 kinds of immune cells in TME of HCC patients. Spearman method was used to analyze the correlation between the expression of



**TABLE 1 |** Detailed clinical information for all HCC patients from TCGA.

Characteristic	Low Expression of ZCCHC17	High Expression of ZCCHC17	p
n	187	187	
<b>T stage, n (%)</b>			<b>0.021</b>
T1	105 (28.3%)	78 (21%)	
T2	38 (10.2%)	57 (15.4%)	
T3	39 (10.5%)	41 (11.1%)	
T4	4 (1.1%)	9 (2.4%)	
<b>N stage, n (%)</b>			0.059
N0	130 (50.4%)	124 (48.1%)	
N1	0 (0%)	4 (1.6%)	
<b>M stage, n (%)</b>			1.000
M0	130 (47.8%)	138 (50.7%)	
M1	2 (0.7%)	2 (0.7%)	
<b>Pathologic stage, n (%)</b>			<b>0.032</b>
Stage I	101 (28.9%)	72 (20.6%)	
Stage II	37 (10.6%)	50 (14.3%)	
Stage III	37 (10.6%)	48 (13.7%)	
Stage IV	2 (0.6%)	3 (0.9%)	
<b>Tumor status, n (%)</b>			0.305
Tumor free	106 (29.9%)	96 (27%)	
With tumor	71 (20%)	82 (23.1%)	
<b>Gender, n (%)</b>			0.658
Female	58 (15.5%)	63 (16.8%)	
Male	129 (34.5%)	124 (33.2%)	
<b>Age, n (%)</b>			0.277
≤60	83 (22.3%)	94 (25.2%)	
>60	104 (27.9%)	92 (24.7%)	
<b>Histologic grade, n (%)</b>			<b>0.032</b>
G1	32 (8.7%)	23 (6.2%)	
G2	95 (25.7%)	83 (22.5%)	
G3	56 (15.2%)	68 (18.4%)	
G4	2 (0.5%)	10 (2.7%)	
<b>AFP(ng/ml), n (%)</b>			0.336
≤400	116 (41.4%)	99 (35.4%)	
>400	30 (10.7%)	35 (12.5%)	
<b>Vascular invasion, n (%)</b>			0.086
No	117 (36.8%)	91 (28.6%)	
Yes	50 (15.7%)	60 (18.9%)	

The bold values represent different pathological features.

The P value in bold indicates that the P value is statistically significant.

ZCCHC17 and the degree of infiltration of 24 kinds of immune cells. The lollipop graph showed the correlation and significance of the expression level of 24 kinds of immune cells and ZCCHC17 (Figure 6A). Further, we analyzed 10 types of immune cells with different infiltration degrees between groups with high and low expression of ZCCHC17 and visualized the correlation of these 10 cells (Figures 6B–L). The results showed that the infiltration degree of NK CD56bright cells ( $r=0.200$ ,  $P<0.001$ ), TFH ( $r=0.190$ ,  $P<0.001$ ), aDCs ( $r=0.190$ ,  $P<0.001$ ), Th1 cells ( $r=0.100$ ,  $P=0.048$ ), T helper cells ( $r=0.200$ ,  $P<0.001$ ) and Th2 cells ( $r=0.430$ ,  $P<0.001$ ) in the high ZCCHC17 expression group was significantly higher than that in the low ZCCHC17 expression group, and the infiltration degree of these immune cells was positively correlated with the expression level of ZCCHC17; The infiltration degree of Cytotoxic cells ( $r=0.180$ ,  $P<0.001$ ), Th17 cells ( $r=0.210$ ,  $P<0.001$ ), pDC ( $r=0.190$ ,  $P<0.001$ ) and DC ( $r=-0.180$ ,  $P=0.001$ ) in the high ZCCHC17 expression group was significantly lower than that in the low expression group, and the infiltration degree of these immune cells was negatively correlated with the expression level of ZCCHC17. These results suggest that ZCCHC17 may be involved

in regulating the TME in HCC. Ns,  $P\geq 0.05$ ; \*,  $P<0.05$ ; \*\*,  $P<0.01$ ; \*\*\*,  $P<0.001$

## Response to Immunotherapy in HCC Was Associated With ZCCHC17 Expression Levels

The previous sections suggest that ZCCHC17 may participate in the body's immune system and play an important role. Therefore, we collected more than forty common immune checkpoint genes and analyzed the expression correlation between ZCCHC17 and these genes. The analysis results show that ZCCHC17 is positively correlated with the expression of multiple immune checkpoint genes (Figure 7A). In addition, the expression level of ZCCHC17 is also significantly positively correlated with the TMB and MSI of HCC patients. That is, the higher expression of ZCCHC17, the higher TMB and MSI for HCC patients (Figures 7B, C). The TMB of the ZCCHC17 high expression group was also significantly higher than that of the low expression group (Figure 7D); the results of the chi-square test showed that the proportion of patients with TP53 mutation in HCC patients in the ZCCHC17 high

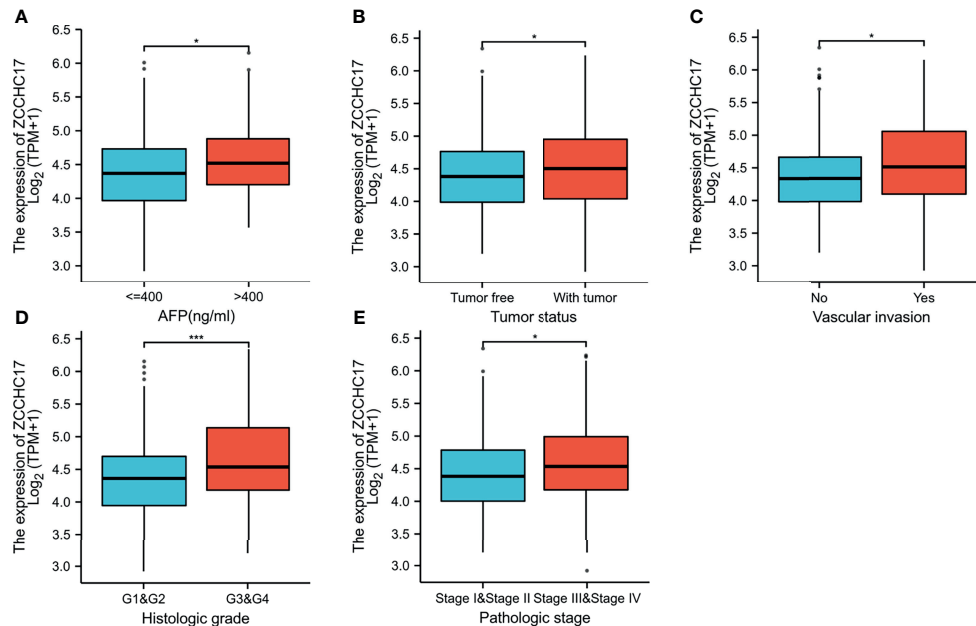


**FIGURE 3** | Expression differences of ZCCHC17 in different subgroups in TCGA. **(A)** ZCCHC17 differentially expressed in different levels of AFP ( $P < 0.05$ ); **(B)** ZCCHC17 differentially expressed in different tumor status ( $P < 0.05$ ); **(C)** ZCCHC17 differentially expressed in different groups of vascular invasion ( $P < 0.05$ ); **(D)** ZCCHC17 differentially expressed in different histologic grade ( $P < 0.001$ ); **(E)** ZCCHC17 differentially expressed in different groups of the pathological stage ( $P < 0.05$ ). \* $P < 0.05$ ; \*\*\* $P < 0.001$ .

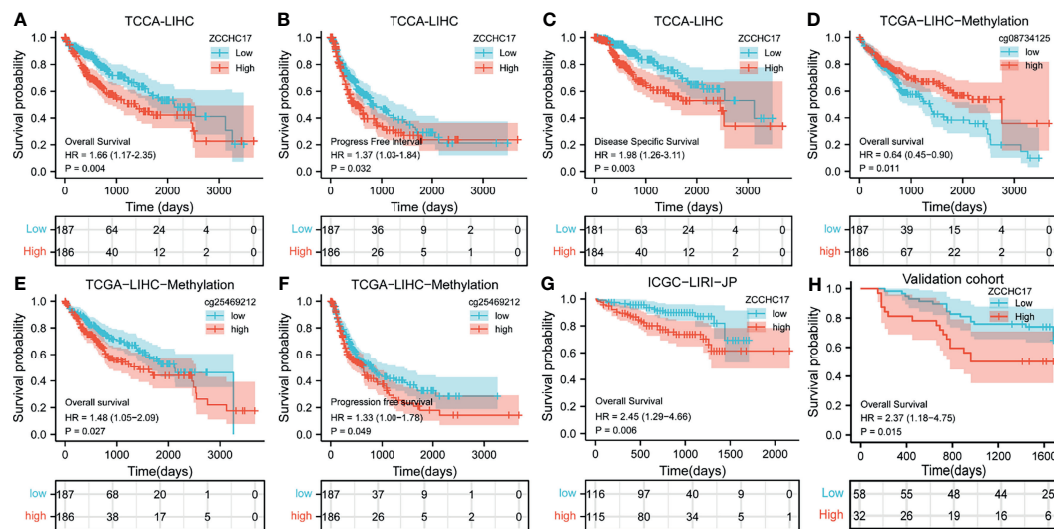


**FIGURE 4** | Impact of ZCCHC17 on survival in HCC patients from different cohorts. **(A–C)** The expression of ZCCHC17 was significantly related to patients' OS ( $P = 0.004$ ), PFS ( $P = 0.0032$ ) and DSS ( $P = 0.003$ ) in TCGA; **(D)** High methylation level of cg08734125 is relevant to the patient's better OS ( $P = 0.011$ ) in TCGA; **(E, F)** Low methylation level of cg25469212 is relevant to the patient's worse OS ( $P = 0.027$ ) and PFS ( $P = 0.049$ ) in TCGA; **(G)** The poor OS correlated with high ZCCHC17 expression in ICGC ( $P = 0.006$ ); **(H)** High expression of ZCCHC17 indicates a poor OS in the validation cohort. ( $P = 0.0015$ ).

expression group was also significantly higher than that of the ZCCHC17 low expression group (Figure 7E). Simultaneously, we also use TIDE to predict the results of immunotherapy analysis. TIDE uses a set of gene expression markers to evaluate two different

tumor immune escape mechanisms, including the dysfunction of tumor-infiltrating cytotoxic T lymphocytes (CTL) and the rejection of CTL by immunosuppressive factors. A high TIDE score indicates poor immune checkpoint blockade (ICB) treatment and prognosis

**TABLE 2 |** Univariate and multivariate Cox regression analyses.

Characteristics	Total (N)	Univariate Analysis		Multivariate Analysis	
		Hazard ratio (95% CI)	P-value	Hazard ratio (95% CI)	P-value
<b>Pathologic stage</b>	349				
Stage I & Stage II	260	Reference			
Stage III & Stage IV	90	2.504 (1.727-3.631)	<b>&lt;0.001</b>	2.049 (1.375-3.054)	<b>&lt;0.001</b>
<b>Tumor status</b>	354				
Tumor free	202	Reference			
With tumor	153	2.317 (1.590-3.376)	<b>&lt;0.001</b>	1.773 (1.183-2.657)	<b>0.006</b>
<b>Gender</b>	373				
Male	253	Reference			
Female	121	1.261 (0.885-1.796)	0.200		
<b>Age</b>	373				
<=60	177	Reference			
>60	196	1.205 (0.850-1.708)	0.295		
<b>Histologic grade</b>	368				
G1&G2	233	Reference			
G4&G3	136	1.091 (0.761-1.564)	0.636		
<b>AFP(ng/ml)</b>	279				
<=400	215	Reference			
>400	65	1.075 (0.658-1.759)	0.772		
<b>Vascular invasion</b>	317				
No	208	Reference			
Yes	110	1.344 (0.887-2.035)	0.163		
<b>ZCCHC17</b>	373	1.909 (1.442-2.526)	<b>&lt;0.001</b>	1.723 (1.269-2.339)	<b>&lt;0.001</b>

The bold values represent different pathological features.

The P value in bold indicates that the P value is statistically significant.

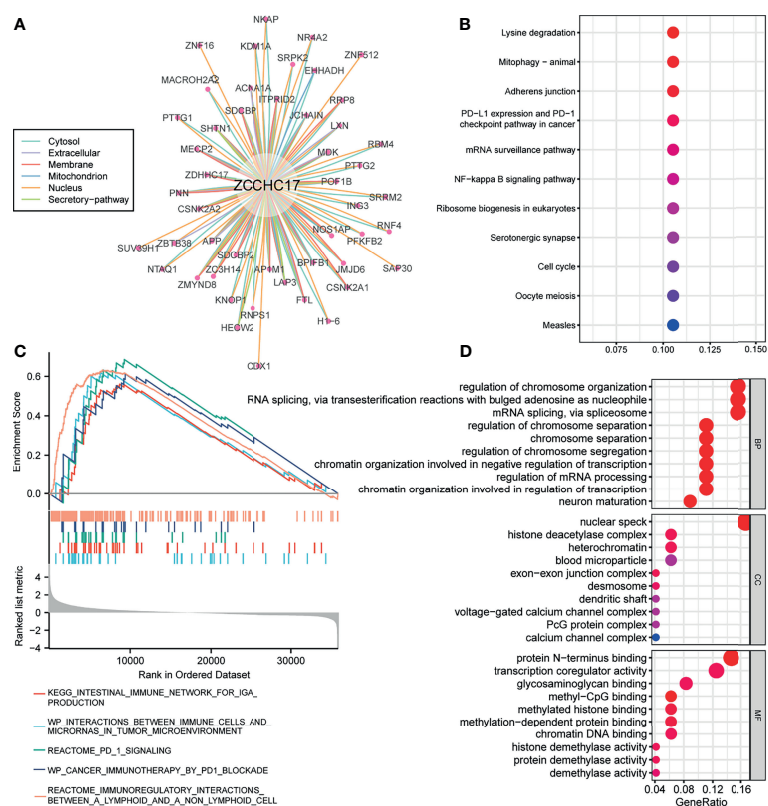


**FIGURE 5 |** Analysis of function and pathways for ZCCHC17. **(A)** The protein-protein interaction network of ZCCHC17; **(B)** KEGG pathway analysis for proteins interacted with ZCCHC17; **(C)** GSEA analysis for ZCCHC17 in TCGA; **(D)** GO analysis for proteins interacted with ZCCHC17.

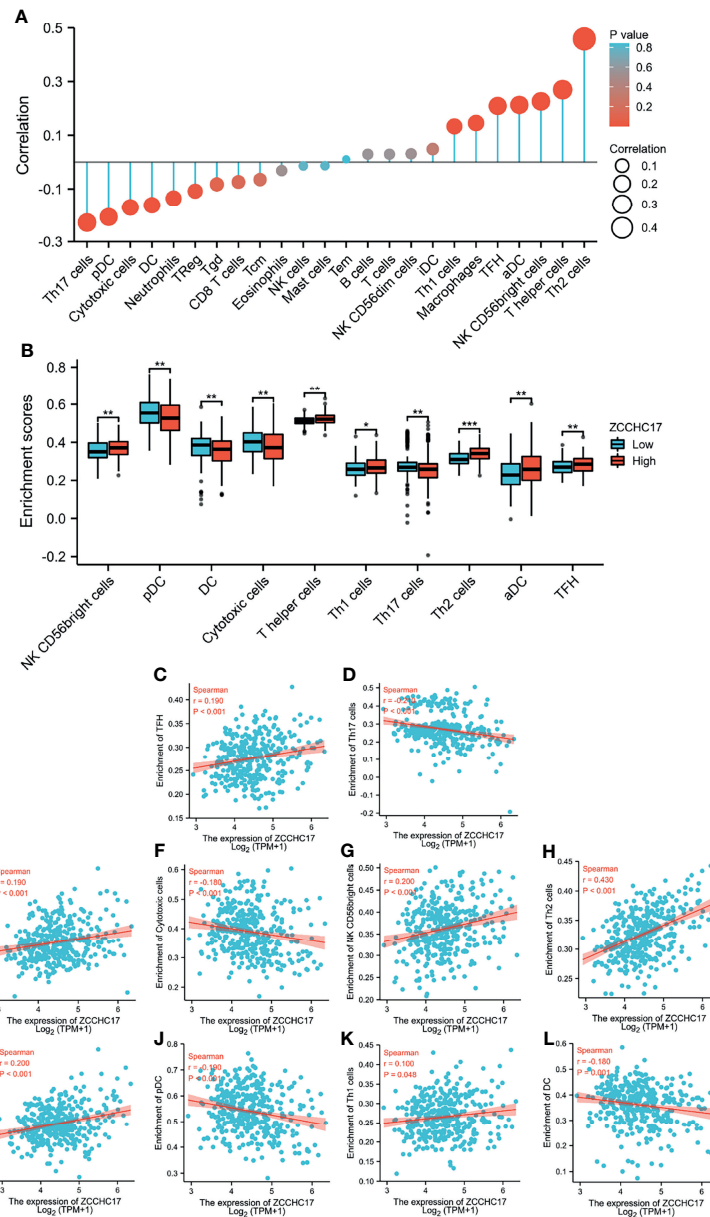


**FIGURE 6 |** The relationship between ZCCHC17 expression and immune cells infiltration in TCGA. **(A)** Lollipop diagram showing a correlation between ZCCHC17 and levels of 24 immune cell infiltrates; **(B)** 10 immune cells are differentially expressed in different groups of ZCCHC17 ( $P < 0.05$ ); **(C–L)** Scatter plot showed the correlation between the infiltration of 10 immune cells and the ZCCHC17 expression ( $P < 0.05$ ). \* $P < 0.05$ ; \*\* $P < 0.01$ ; \*\*\* $P < 0.001$ .

after ICB treatment. The results showed that the proportion of patients in the ZCCHC17 high expression group that responded to immunotherapy was significantly lower than that of the ZCCHC17 low expression group (**Figure 7F**); The TIDE score of the ZCCHC17 high expression group was significantly higher than that of the low expression group (**Figure 7G**). Collectively, these analyses suggest that HCC patients with ZCCHC17 high expression had worse therapeutic effects than those with ZCCHC17 low expression during immunotherapy. Ns,  $P \geq 0.05$ ; \*,  $P < 0.05$ ; \*\*,  $P < 0.01$ ; \*\*\*,  $P < 0.001$ .

## DISCUSSION

ZCCHC17, so far, is still a relatively unresearched human protein-coding gene. Previous research reports indicate that ZCCHC17 is involved in a series of biological processes, including transcription regulation (16) and regulation of mRNA splicing (17), suggesting that ZCCHC17 may act as a transcriptional cofactor and/or play a role in regulating mRNA splicing. Another study showed that it is the primary regulator of synaptic gene expression in Alzheimer's disease (5). However, its



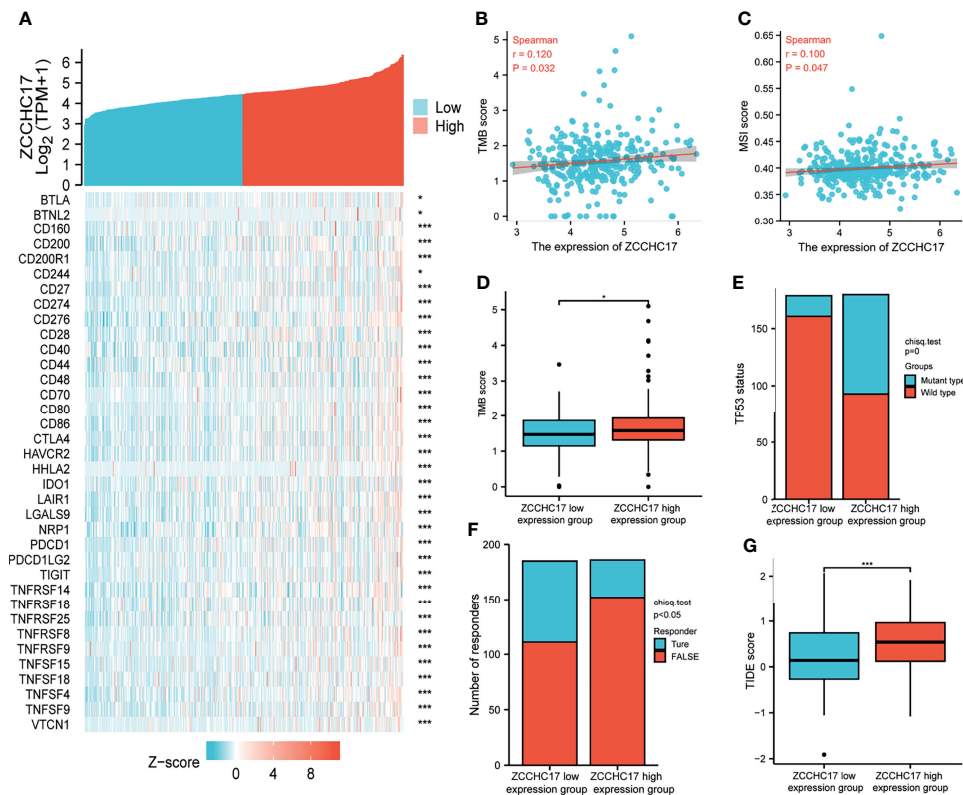


**FIGURE 7 |** Analysis of ZCCHC17 was used as a marker for immunotherapy. **(A)** Spearman correlation analysis of ZCCHC17 expression and immune checkpoint genes expression; **(B)** Spearman correlation analysis of TMB and ZCCHC17 gene expression ( $r=0.120$ ,  $P=0.032$ ); **(C)** Spearman correlation analysis of MSI and ZCCHC17 gene expression ( $r=0.100$ ,  $P=0.047$ ); **(D)** Difference analysis of TMB in different groups of samples of HCC patients ( $P<0.05$ ); **(E)** Distribution of TP53 gene mutation status in HCC patients in different groups of samples ( $P<0.001$ ); **(F)** The distribution of immune responses of samples in different groups in the prediction results ( $P<0.05$ ); **(G)** The distribution of immune response scores in different groups in the prediction results ( $P<0.001$ ). \* $P<0.05$ ; \*\*\* $P<0.001$ .

clinical significance in tumors and its role and function have not yet been elucidated. The incidence of HCC in China accounts for 55% of the world's HCC cases. It is urgent to find effective diagnostic and therapeutic targets. Therefore, in this study, we combined clinical specimens and public databases from TCGA, ICGC, GEO to analyze the role and significance of ZCCHC17 in HCC. The results show that mRNA and protein expression of ZCCHC17 in HCC tissues is higher than normal liver tissues. This abnormally high expression is related to the abnormal methylation of ZCCHC17. Subsequently, further analysis results showed that the high expression of ZCCHC17 was significantly related to multiple tumor malignant indicators. In addition, the survival rate of HCC patients with high ZCCHC17 expression was significantly lower than that of HCC patients with low expression. Finally, we further studied the function of ZCCHC17 and its potential role in clinical treatment. We found that it plays a vital role in the immune system, regulates immune cells in TME, and may serve as an important marker for immunotherapy. All in all, these results confirm that ZCCHC17 is used as an HCC diagnosis and as an independent prognostic biomarker and may promote the development of tumor-targeted therapy and tumor immunotherapy.

The hypothetical mechanism and the role of ZCCHC17 in HCC are shown in **Supplementary Figure 1**.

Unlike the routine detection of HER2, EGFR, BRAF, KRAS and other genes in breast cancer, lung cancer, colorectal cancer and other tumors, HCC has not yet an apparent gene-phenotype related to its prognosis and treatment due to its heterogeneity (18). Therefore, genetic testing is not recommended for routine clinical use in diagnosing HCC, according to the 8th edition of the American Joint Committee on Cancer. AFP (19) is more sensitive in HCC (especially hepatitis B-related HCC), but it must be combined with imaging because it is a non-specific tumor marker. For this reason, this study is the first to analyze the role of ZCCHC17 as a tumor diagnostic marker. First, ZCCHC17 in tumors is significantly higher in mRNA and protein levels than in normal adjacent tissues. We found that ZCCHC17 has strong specificity and can effectively distinguish tumor and non-tumor samples. Therefore, we did a methylation analysis to explore further the reasons for the abnormally high expression of ZCCHC17 in tumor samples. DNA methylation is an extensively researched epigenetic modification in regulating gene expression (20). Although the nucleotide sequence and composition of DNA are not changed after DNA methylation,

gene expression is affected. By downloading the methylation data of HCC patients from TCGA and analyzing the correlation between the methylation level of different CpG sites and the expression level of ZCCHC17, we found that the methylation level of ZCCHC17 in normal tissues was significantly higher than that in tumor tissues. This also explains the reason for the abnormal expression of ZCCHC17 in HCC tissues to some extent.

Because of the abnormal expression of ZCCHC17 in HCC, we analyzed its clinical significance in HCC patients. On the one hand, the significant difference between ZCCHC17 and AFP (ng/ml) at different levels emphasizes the feasibility of ZCCHC17 as a diagnostic marker, which is consistent with the results of our previous analysis. On the other hand, ZCCHC17 has significant differences in different groups' histologic grades, tumor status, vascular invasion, and pathological stage. Meanwhile, we also noticed that ZCCHC17 is always expressed higher in higher histological grades, higher pathological stages, and tissues with vascular invasion. It is well-known that high-grade tumors are poorly differentiated, and grow very fast and are prone to distant metastasis. These results indicate that ZCCHC17 is also helpful for evaluating the malignant degree of tumors. At the same time, it suggests that ZCCHC17 may promote the malignant transformation of tumors, but its specific mechanism also leads us to study further. Secondly, we use the KM-survival curve and Cox regression analysis to analyze the expression of ZCCHC17 on the prognosis of patients. Of note, the results also showed significant relationships between ZCCHC17 and the prognosis of HCC patients in the analysis of different cohorts.

In addition, for the methylation levels of different methylation sites, we also analyzed the relationship between the methylation levels of different methylation sites and the prognosis in HCC patients. The results showed that the methylation level of multiple methylation sites in ZCCHC17 was related to the prognosis of HCC patients. More than ten years ago, biomarkers based on DNA methylation were considered the next "big event" in cancer biomarker research, but so far, they have been unable to meet expectations. In addition to this, the high cost of next-generation sequencing technologies also makes it difficult for this marker to be further promoted. In addition, the complex relationship between DNA methylation and its precise genomic location is one of the main obstacles. Like the results in this study, the level of methylation at different sites has very different effects on the prognosis of patients. In recent years, studies have shown that methylation of the RIZ1 gene promoter region in HCC tissues is associated with postoperative tumor recurrence, which may be the reason for the poor prognosis of patients with RIZ1 gene methylation positive in HCC tissues (21); Similarly, another study also showed that Compared with normal tissues, the methylation level of the ADRA1A promoter region in the tumor tissues of HCC patients was significantly increased, the mRNA and protein levels of ADRA1A were decreased, and DNA methyltransferase inhibitors could increase the mRNA expression of ADRA1A (22). It shows that ADRA1A gene hypermethylation may be involved in the occurrence of HCC. These studies have shown that DNA

methylation is closely related to the progress of HCC. Nevertheless, the downside is that they all only paid attention to the impact of DNA methylation but failed to clarify the methylation sites that affect the prognosis of HCC patients in detail. This study used high-throughput sequencing data to more accurately determine the methylation sites of ZCCHC17 that affect the prognosis of patients during the development of HCC, indicating that abnormal gene methylation is also a fundamental reason for the prognosis of HCC patients. To a certain extent, this result also provides further valuable clues for the precise treatment and prognosis evaluation of HCC.

It is good to understand the complete function by analyzing its specific and mutual binding proteins and probing the signal pathway and function involved in a protein. Therefore, we analyzed the proteins that interacted with ZCCHC17. Through the enrichment analysis of KEGG and GSEA pathways, we noticed that ZCCHC17 is mainly involved in the body's immune system in terms of mechanism regulation and regulating a series of immunotherapy-related processes, including cancer immunotherapy by PD-1 blockade, PD-L1 expression and PD-1 checkpoint pathway in cancer, these analyses emphasize the link between ZCCHC17 and immune response. In the GO enrichment analysis results, ZCCHC17 and its related proteins are mainly involved in the body's methylation process, which is consistent with the results of our previous analysis and proves the reliability of this study.

More and more research has focused on immune cells' crucial role in the TME. Under normal circumstances, the immune system can recognize and eliminate tumor cells in the TME. However, tumor cells can adopt different strategies to suppress the human immune system to survive and grow. Our analysis results show that ZCCHC17 is significantly related to the infiltration of various immune cells. It was previously reported that regulatory T cells (Treg) with CD4<sup>+</sup> and CD25<sup>+</sup> are the most significant immunosuppressive cell groups in the tumor microenvironment. Their existence has prognostic significance because the accumulation of Treg is related to poor prognosis and aggressiveness of HCC (23). At the same time, we noticed the degree of correlation between ZCCHC17 and Th1 cells and Th2 cells. Th cells secrete cytokines, which can regulate the body's immune function. Th cells are divided into Th1 and Th2. Th1 cells secrete cytokines IFN- $\gamma$ , TNF- $\alpha$ , IL-12, which play an essential role in tumor immunity (24), and IL-4, IL-6, and IL-10 are cytokines secreted by Th2 cells, which can inhibit the secretion of cytokines by Th1 cells and promote humoral immunity (25). Th1/Th2 balance plays a vital role in the maintenance of normal immune function. Under normal circumstances, Th1 cell function is relatively strong. Th2 cell function is hyperactive and then synthesizes and secretes many inhibitory cytokines under an imbalance of Th1/Th2 condition, which directly leads to the decline of the body's immune function and causes the immune escape of tumor cells (26). Our research has shown that ZCCHC17 is highly correlated with immune cells in TME, indicating that ZCCHC17 may help tumor cells to immune escape by affecting the Th1/Th2 balance, thereby promoting the occurrence of HCC. However, its exact

mechanism needs to be further confirmed. Nevertheless, no matter what, these studies suggest that we pay attention to the relationship between genes and immune cells to help understand the occurrence and development of tumors and contribute to the development of immunotherapy therapies.

Based on the functional analysis of ZCHHC17 and its high correlation with the degree of immune cells infiltration in TME, it is suggested that it plays a vital role in regulating immune mechanism function. Therefore, here we have collected more than forty common immune checkpoint genes, including monoclonal antibody immune checkpoint inhibitors, therapeutic antibodies, cancer vaccines and small molecule inhibitors. We analyzed the correlation between the expression of ZCCHC17 and these immune checkpoint genes, and the results showed that ZCCHC17 is positively correlated with the expression of multiple immune checkpoints. Immunotherapy is a treatment method that restores the body's normal anti-tumor immune response by restarting and maintaining the tumor-immune cycle, thereby controlling and eliminating tumors. Nevertheless, it is difficult to find those patients who can benefit from immunotherapy. Most previous studies believe that MSI, TMB and ICB-related gene expression is closely related to response to immunotherapy (27, 28). However, they cannot independently accurately predict the treatment effect. Therefore, we further analyzed the relationship between ZCCHC17 and TMB, MSI and other immunotherapy markers, and the analysis results also showed a significant correlation between ZCCHC17 and these markers. Therefore, we infer that the expression of ZCCHC17 can be used as a marker of the immunotherapy effect of patients. We further applied TIDE to predict the immunotherapy effect of HCC patients in different ZCCHC17 expression groups. Intriguingly, the results of TIDE showed that patients in the ZCCHC17 high expression group showed a worse response to the immunotherapy. In contrast, patients in the ZCCHC17 low expression group obtained better therapeutic benefits from immunotherapy.

With the development of immunotherapy, many corresponding clinical studies have been carried out. Although specific results have been achieved, the situation is still not satisfactory. A recent study shows that the idea of immunotherapy for solid tumors with a high tumor mutation burden (TMB-H) is based on tumor mutations that may produce immunogenic neoantigens. The increase in neoantigens is positively correlated with the increase in the count of CD8<sup>+</sup> T cells, and CD8<sup>+</sup> T cells infiltrated tumors are the basis for a good response to immunotherapy (29). Therefore, TMB-H may not be suitable as a biomarker for predicting the efficacy of immunotherapy for all cancers. Cervical squamous cell carcinoma and adenocarcinoma, endometrial cancer, melanoma, lung cancer and bladder cancer are defined as type-I cancers (30). TMB-H can be used as a predictor of immunotherapy efficacy for type-I cancers. However, HCC, pancreatic cancer, esophageal cancer, and other tumors are considered type-II cancers. The evidence for TMB-H to predict the efficacy of immunotherapy for type-II cancers is still insufficient (30). The predictive value of TMB in another study

from another study is still only reflected in NSCLC, head and neck squamous cell carcinoma and melanoma. However, the predictive value of TMB-H is not observed for other cancer types (31). These conclusions also put forward the limitations of the current immunotherapy effect prediction to some extent. It indicates that the prediction of the effects of immunotherapy may require more markers or target combined analysis to predict effectively.

This study has improved our understanding of the relationship between ZCCHC17 and the development of HCC, but this study still has some limitations. First, although we analyzed different cohorts, we verified the differential expression and clinical significance of ZCCHC17 in HCC from the level of mRNA and protein. However, this study has not proven its direct mechanism of action in HCC, but this is also one of the directions we are currently working on. In addition, concerning evaluating the effects of immunotherapy in patients with HCC, although we have used the tools currently recognized as the best evaluation of the effects of immunotherapy, we have reached a different conclusion from some previous studies. However, because we are currently unable to obtain a large-scale immunotherapy cohort to verify the prediction of immunotherapy effects in this study, we conservatively propose that the evidence for TMB or MSI as a marker of immunotherapy for HCC patients is insufficient, and hope that in the future, we can collect more information to validate our conclusions.

All in all, this study started from ZCCHC17, explored the role of ZCCHC17 in HCC and clarified its clinical significance in more detail. The collection of bioinformatics and clinical samples proved that ZCCHC17 is highly expressed in HCC tissues, and this high expression is related to the poor prognosis of patients. At the same time, this study found that ZCCHC17 is involved in immune-related pathways in HCC patients and is also related to multiple immunotherapy-related targets (immune checkpoint genes, TMB, MSI). These findings provide a new and effective molecular marker for the diagnosis and targeted therapy of HCC. It also provides some new insights for judging the prognosis of HCC patients and evaluating the effects of immunotherapy. These findings can promote our current understanding of the role of ZCCHC17 in HCC and promote its transformational application in HCC diagnosis and treatment.

## DATA AVAILABILITY STATEMENT

The datasets presented in this study can be found in online repositories. The names of the repository/repositories and accession number(s) can be found in the article/**Supplementary Material**.

## ETHICS STATEMENT

The studies involving human participants were reviewed and approved by Affiliated Hospital of Youjiang Medical University for Nationalities The Ethics Committee. The patients/

participants provided their written informed consent to participate in this study.

## AUTHOR CONTRIBUTIONS

FL and JL collected the data and wrote the manuscript. PL, LZ and WH participated in data analysis and clinical sample collection. CL and XW designed the study. All authors contributed to the article and approved the submitted version.

## FUNDING

This study was supported by National Natural Science Foundation of China (Nos. 81341122, 81970462), Natural

Science Foundation of Guangxi Zhuang Autonomous Region (Nos. 2020GXNSFAA259052), High-level Talents Project of Affiliated Hospital of Youjiang Medical College for Nationalities (R202011708,Y20196301).

## SUPPLEMENTARY MATERIAL

The Supplementary Material for this article can be found online at: <https://www.frontiersin.org/articles/10.3389/fonc.2021.799566/full#supplementary-material>

**Supplementary Figure 1 |** The hypothetical mechanism and the role of ZCCHC17 in HCC.

**Supplementary Figure 2 |** The correlation between ZCCHC17 and the markers of regulatory T cells in HCC.

## REFERENCES

- Sung H, Ferlay J, Siegel RL, Laversanne M, Soerjomataram I, Jemal A, et al. Global Cancer Statistics 2020: GLOBOCAN Estimates of Incidence and Mortality Worldwide for 36 Cancers in 185 Countries. *CA: Cancer J Clin* (2021) 71(3):209–49. doi: 10.3322/caac.21660
- Llovet JM, Ricci S, Mazzaferro V, Hilgard P, Gane E, Blanc J-F, et al. Sorafenib in Advanced Hepatocellular Carcinoma. *N Engl J Med* (2008) 359(4):378–90. doi: 10.1056/NEJMoa0708857
- El-Khoueiry A, Sangro B, Yau T, Crocenzi T, Kudo M, Hsu C, et al. Nivolumab in Patients With Advanced Hepatocellular Carcinoma (CheckMate 040): An Open-Label, Non-Comparative, Phase 1/2 Dose Escalation and Expansion Trial. *Lancet (London England)* (2017) 389(10088):2492–502. doi: 10.1016/s0140-6736(17)31046-2
- Finn R, Ryoo B, Merle P, Kudo M, Bouattour M, Lim H, et al. Pembrolizumab As Second-Line Therapy in Patients With Advanced Hepatocellular Carcinoma in KEYNOTE-240: A Randomized, Double-Blind, Phase III Trial. *J Clin Oncol Off J Am Soc Clin Oncol* (2020) 38(3):193–202. doi: 10.1200/jco.19.01307
- Tomljanovic Z, Patel M, Shin W, Califano A, Teich AF. ZCCHC17 is a Master Regulator of Synaptic Gene Expression in Alzheimer's Disease. *Bioinformatics* (2018) 34(3):367–71. doi: 10.1093/bioinformatics/btx608
- Sánchez-Jiménez C, Ludeña M, Izquierdo J. T-Cell Intracellular Antigens Function as Tumor Suppressor Genes. *Cell Death Dis* (2015) 6:e1669. doi: 10.1038/cddis.2015.43
- Hopkins T, Mura M, Al-Ashtal H, Lahr R, Abd-Latif N, Sweeney K, et al. The RNA-Binding Protein LARP1 Is a Post-Transcriptional Regulator of Survival and Tumorigenesis in Ovarian Cancer. *Nucleic Acids Res* (2016) 44(3):1227–46. doi: 10.1093/nar/gkv1515
- Wang J, Liu Q, Shyr Y. Dysregulated Transcription Across Diverse Cancer Types Reveals the Importance of RNA-Binding Protein in Carcinogenesis. *BMC Genomics* (2015) 16(7):1–10. doi: 10.1186/1471-2164-16-s7-s5
- Kechavarzi B, Janga S. Dissecting the Expression Landscape of RNA-Binding Proteins in Human Cancers. *Genome Biol* (2014) 15(1):R14. doi: 10.1186/gb-2014-15-1-r14
- Nyati K, Zaman M, Sharma P, Kishimoto T. Arid5a, an RNA-Binding Protein in Immune Regulation: RNA Stability, Inflammation, and Autoimmunity. *Trends Immunol* (2020) 41(3):255–68. doi: 10.1016/j.it.2020.01.004
- Vivian J, Rao AA, Nothhaft FA, Ketchum C, Armstrong J, Novak A, et al. Toil Enables Reproducible, Open Source, Big Biomedical Data Analyses. *Nat Biotechnol* (2017) 35(4):314–6. doi: 10.1038/nbt.3772
- Veres DV, Gyurkó DM, Thaler B, Szalay KZ, Fazekas D, Korcsmáros T, et al. CompPI: A Cellular Compartment-Specific Database for Protein-Protein Interaction Network Analysis. *Nucleic Acids Res* (2015) 43(D1):D485–93. doi: 10.1093/nar/gku1007
- Yu G, Wang L-G, Han Y, He Q-Y. ClusterProfiler: An R Package for Comparing Biological Themes Among Gene Clusters. *Omic: J Integr Biol* (2012) 16(5):284–7. doi: 10.1089/omi.2011.0118
- Bindea G, Mlecnik B, Tosolini M, Kirilovsky A, Waldner M, Obenauf AC, et al. Spatiotemporal Dynamics of Intratumoral Immune Cells Reveal the Immune Landscape in Human Cancer. *Immunity* (2013) 39(4):782–95. doi: 10.1016/j.immuni.2013.10.003
- Jiang P, Gu S, Pan D, Fu J, Sahu A, Hu X, et al. Signatures of T Cell Dysfunction and Exclusion Predict Cancer Immunotherapy Response. *Nat Med* (2018) 24(10):1550–8. doi: 10.1038/s41591-018-0136-1
- Joo JH, Taxter TJ, Munguba GC, Kim YH, Dhaduvai K, Dunn NW, et al. Pinin Modulates Expression of an Intestinal Homeobox Gene, Cdx2, and Plays an Essential Role for Small Intestinal Morphogenesis. *Dev Biol* (2010) 345(2):191–203. doi: 10.1016/j.ydbio.2010.07.009
- Wang P, Lou PJ, Leu S, Ouyang P. Modulation of Alternative pre-mRNA Splicing *In Vivo* by Pinin. *Biochem Biophys Res Commun* (2002) 294(2):448–55. doi: 10.1016/s0006-291x(02)00495-3
- Kamarajah S, Frankel T, Sonnenday C, Cho C, Nathan H. Critical Evaluation of the American Joint Commission on Cancer (AJCC) 8th Edition Staging System for Patients With Hepatocellular Carcinoma (HCC): A Surveillance, Epidemiology, End Results (SEER) Analysis. *J Surg Oncol* (2018) 117(4):644–50. doi: 10.1002/jso.24908
- Singal A, Lampertico P, Nahon P. Epidemiology and Surveillance for Hepatocellular Carcinoma: New Trends. *J Hepatol* (2020) 72(2):250–61. doi: 10.1016/j.jhep.2019.08.025
- Zhang Q, Marioni RE, Robinson MR, Higham J, Sproul D, Wray NR, et al. Genotype Effects Contribute to Variation in Longitudinal Methylome Patterns in Older People. *Genome Med* (2018) 10(1):75. doi: 10.1186/s13073-018-0585-7
- Piao G, Piao W, He Y, Zhang H, Wang G, Piao Z. Hyper-Methylation of RIZ1 Tumor Suppressor Gene Is Involved in the Early Tumorigenesis of Hepatocellular Carcinoma. *Histol Histopathol* (2008) 23(10):1171–5. doi: 10.14670/HH-23.1171
- Chen G, Fan X, Li Y, He L, Wang S, Dai Y, et al. Promoter Aberrant Methylation Status of ADRA1A Is Associated With Hepatocellular Carcinoma. *Epigenetics* (2020) 15(6-7):684–701. doi: 10.1080/15592294.2019.1709267
- Granito A, Muratori L, Lalanne C, Quarneri C, Ferri S, Guidi M, et al. Hepatocellular Carcinoma in Viral and Autoimmune Liver Diseases: Role of CD4+ CD25+ Foxp3+ Regulatory T Cells in the Immune Microenvironment. *World J Gastroenterol* (2009) 15(22):2994–3009. doi: 10.3748/wjg.v15.i22.2994
- Kaji K, Mizukoshi E, Yamashita T, Arai K, Sunagazaka H, Fushimi K, et al. Cellular Immune Responses for Squamous Cell Carcinoma Antigen Recognized by T Cells 3 in Patients With Hepatocellular Carcinoma. *PLoS One* (2017) 12(1):e0170291. doi: 10.1371/journal.pone.0170291
- Jia H, Zhao T, Zou D, Jia X, Gao J, Song X. Therapeutic Injection of a C-Type CpG ODN Induced an Antitumor Immune Response in C57/BL6 Mice of



- Orthotopically Transplanted Hepatocellular Carcinoma. *Oncol Res* (2016) 23 (6):321. doi: 10.3727/096504016X14570992647041
26. Dey P, Li J, Zhang J, Chaurasiya S, Strom A, Wang H, et al. Oncogenic KRAS-Driven Metabolic Reprogramming in Pancreatic Cancer Cells Utilizes Cytokines From the Tumor Microenvironment. *Cancer Discov* (2020) 10 (4):608–25. doi: 10.1158/2159-8290.Cd-19-0297
  27. Wu X, Gu Z, Chen Y, Chen B, Chen W, Weng L, et al. Application of PD-1 Blockade in Cancer Immunotherapy. *Comput Struct Biotechnol J* (2019) 17:661–74. doi: 10.1016/j.csbj.2019.03.006
  28. Liu F, Hou W, Liang J, Zhu L, Luo C. LRP1B Mutation: A Novel Independent Prognostic Factor and a Predictive Tumor Mutation Burden in Hepatocellular Carcinoma. *J Cancer* (2021) 12(13):4039–48. doi: 10.7150/jca.53124
  29. Liu T, Tan J, Wu M, Fan W, Wei J, Zhu B, et al. High-Affinity Neoantigens Correlate With Better Prognosis and Trigger Potent Antihepatocellular Carcinoma (HCC) Activity by Activating CD39+ CD8+ T Cells. *Gut* (2021) 70(10):1965–77. doi: 10.1136/gutjnl-2020-322196
  30. McGrail D, Pilié P, Rashid N, Voorwerk L, Slagter M, Kok M, et al. High Tumor Mutation Burden Fails to Predict Immune Checkpoint Blockade Response Across All Cancer Types. *Ann Oncol Off J Eur Soc Med Oncol* (2021) 32(5):661–72. doi: 10.1016/j.annonc.2021.02.006
  31. Bersanelli M. Tumour Mutational Burden as a Driver for Treatment Choice in Resistant Tumours (and Beyond). *Lancet Oncol* (2020) 21(10):1255–7. doi: 10.1016/s1470-2045(20)30433-2

**Conflict of Interest:** The authors declare that the research was conducted in the absence of any commercial or financial relationships that could be construed as a potential conflict of interest.

**Publisher's Note:** All claims expressed in this article are solely those of the authors and do not necessarily represent those of their affiliated organizations, or those of the publisher, the editors and the reviewers. Any product that may be evaluated in this article, or claim that may be made by its manufacturer, is not guaranteed or endorsed by the publisher.

Copyright © 2022 Liu, Liang, Long, Zhu, Hou, Wu and Luo. This is an open-access article distributed under the terms of the Creative Commons Attribution License (CC BY). The use, distribution or reproduction in other forums is permitted, provided the original author(s) and the copyright owner(s) are credited and that the original publication in this journal is cited, in accordance with accepted academic practice. No use, distribution or reproduction is permitted which does not comply with these terms.



# FAM21C Promotes Hepatocellular Carcinoma Invasion and Metastasis by Driving Actin Cytoskeleton Remodeling *via* Inhibiting Capping Ability of CAPZA1

Yao Lu<sup>1</sup>, Deng Huang<sup>2</sup>, Baolin Wang<sup>1</sup>, Bowen Zheng<sup>1</sup>, Jialong Liu<sup>1</sup>, Juxian Song<sup>1</sup> and Shuguo Zheng<sup>1\*</sup>

<sup>1</sup> Institute of Hepatobiliary Surgery, Southwest Hospital, Third Military Medical University (Army Medical University), Chongqing, China, <sup>2</sup> Department of Hepatobiliary, General Hospital of Tibet Military Command Area, Tibet, China

## OPEN ACCESS

### Edited by:

Zhaohui Huang,  
Affiliated Hospital of Jiangnan  
University, China

### Reviewed by:

Pirjo Spuul,  
Tallinn University of Technology,  
Estonia  
Gianluca Baldanzi,  
Università degli Studi del Piemonte  
Orientale, Italy

### \*Correspondence:

Shuguo Zheng  
shuguo.zh@tmmu.edu.cn

### Specialty section:

This article was submitted to  
Gastrointestinal Cancers: Hepato  
Pancreatic Biliary Cancers,  
a section of the journal  
Frontiers in Oncology

**Received:** 04 November 2021

**Accepted:** 21 December 2021

**Published:** 13 January 2022

### Citation:

Lu Y, Huang D, Wang B,  
Zheng B, Liu J, Song J and  
Zheng S (2022) FAM21C Promotes  
Hepatocellular Carcinoma Invasion  
and Metastasis by Driving Actin  
Cytoskeleton Remodeling via Inhibiting  
Capping Ability of CAPZA1.  
Front. Oncol. 11:809195.  
doi: 10.3389/fonc.2021.809195

Hepatocellular carcinoma (HCC) is characterized by a high incidence of metastasis. The dynamic remodeling of the actin cytoskeleton plays an important role in the invasion and migration of HCC cells. In previous studies, we found that CAPZA1, a capping protein, can promote EMT of HCC cells by regulating the remodeling of the actin filament (F-actin) cytoskeleton, thus promoting the invasion and migration of HCC cells. In this study, we found that FAM21C may have a regulatory effect on CAPZA1, and we conducted an in-depth study on its potential regulatory mechanism. First, we found that FAM21C is highly expressed in HCC tissues and its high expression could promote the malignant progression of HCC. Meanwhile, the high expression of FAM21C promoted the invasion and migration of HCC cells *in vitro* and *in vivo*. Further, FAM21C interacted with CAPZA1, and their binding inhibited the capping capacity of CAPZA1, thus promoting the invasion and migration of HCC cells. This effect of FAM21C was abolished by mutating the CP-interacting (CPI) domain, the CAPZA1 binding site on FAM21C. In conclusion, high expression of FAM21C in HCC tissues can promote malignant progression of HCC and its potential mechanism involves FAM21C inhibition of CAPZA1 capping capacity by binding to CAPZA1, which drives F-actin cytoskeleton remodeling, and thus promotes invasion and migration of HCC cells.

**Keywords:** hepatocellular carcinoma, FAM21C, CAPZA1, actin cytoskeleton, invasion and metastasis

## INTRODUCTION

HCC is the fifth most common tumor in the world and the second leading cause of cancer-related deaths (1), and its high malignancy poses a serious threat to human health. Due to hepatitis B virus infection and aflatoxin exposure, China has become a region with the highest incidence of HCC (2). Currently, radical resection is still the most effective treatment for HCC, but its postoperative

**Abbreviations:** CAPZA1, capping actin protein of muscle Z-line alpha subunit 1; Co-IP, Co-immunoprecipitation; F-actin, actin filament; HCC, hepatocellular carcinoma; IB, Immunoblot; IP, Immunoprecipitation; MD, moderately differentiated; PD, poorly differentiated; WD, well differentiated.

survival rate at five years is only about 25% to 50%. The appearance of invasion- and metastasis-related phenotype, such as multifocal sites and invasion of the main vessel in HCC predicts the poor prognosis of patients (3). Therefore, it is very important to investigate the molecular mechanisms of invasion and migration of HCC cells to identify the corresponding therapeutic targets with the objective of improving the prognosis of patients.

HCC invasion and metastasis is a complex biological behavior of cells that involves multiple signaling pathways (4). The actin cytoskeleton not only serves as a reticular scaffold supporting cell space, but also participates in the regulation of a variety of cell biological behaviors, including migration, invasion, and cargo transport (5–7). Studies have shown that dynamic remodeling of the cytoskeleton plays an important role in the invasion and migration of tumor cells and is becoming a major focus of current cancer research. It has been reported that actin cytoskeleton remodeling promotes HCC invasion and metastasis by participating in biological events such as epithelial-mesenchymal transition (EMT), invadopodia formation, and endocytic recycling of specific cargo in HCC cells (8–10). These findings suggest that an in-depth study of the cytoskeletal remodeling mechanism during tumor cell invasion and migration may provide new ideas to reveal the mechanism of tumor invasion and metastasis. Our previous study showed that the  $\alpha 1$  subunit of the cytoskeletal protein CAPZ (CAPZA1), which can directly bind to F-actin, has low expression in HCC tissues and can also participate in the regulation of actin filament cytoskeleton remodeling to promote EMT in HCC cells (11). Therefore, we suggest that the mechanism of CAPZA1 involves the inhibition of further lengthening of F-actin by binding to the barbed end of actin filaments, which induces cytoskeleton remodeling and thus inhibits invasion and migration of HCC cells. However, it has not been reported whether CAPZA1 is regulated by other upstream molecules in HCC.

FAM21C, also known as vaccinia virus penetration factor (VPEF), because it helps the vaccinia virus enter HeLa cells by liquid-phase endocytosis (12). Subsequently, it was reported that the WASH (WASP and SCAR homologue) complex is an important member of the WASP family, consisting of five subunits including FAM21 and containing the VCA domain, which can achieve regulation of site-specific actin polymerization by recruiting and activating the Arp2/3 complex; FAM21C is a subunits of the WASH complex and plays an important role in maintaining the ability of the WASH complex to promote the localized F-actin polymerization (13, 14). Currently, the role of FAM21 in tumors is unclear. Studies have confirmed that the knockdown of FAM21 inhibits the migration of prostate cancer cells, and its expression is regulated by the nuclear translocation of IGFR (15); in pancreatic cancer studies, nuclear FAM21 was found to regulate NF- $\kappa$ B transcription, and its reduced expression increased the sensitivity of pancreatic cancer cells to gemcitabine and pentafluorouracil (16); knockdown of FAM21 expression in breast cancer cells significantly reduced the ability of cells to degrade the extracellular matrix (17). These findings suggest that FAM21C may be an important regulator in

promoting tumor cell invasion and migration, but its underlying molecular mechanisms have not been clearly reported. It is reported that Fam21-tail could interact with CAPZA in HeLa cells (18). Moreover, through the STRING database (19), we found that FAM21C could interact with CAPZA1, and it is unclear whether this interaction promotes the invasion and migration of HCC cells. Therefore, this study aimed to investigate the biological functions of FAM21C in HCC and the potential molecular mechanism involved in regulating the remodeling of the actin cytoskeleton induced by CAPZA1 to promote the invasion and migration of HCC cells.

## MATERIALS AND METHODS

### Bioinformatics Analysis

The Cancer Genome Atlas (TCGA) visualization tool found on the GEPIA (<http://gepia.cancer-pku.cn/index.html>) website was used to analyze the differences in mRNA expression levels between 369 HCC tissues and 50 normal liver tissues of FAM21C, and the relationship between FAM21C mRNA and ACTB, as well as the relationship between mRNA levels and tumor stage and the overall survival (OS) rate in HCC. This is done by enter the FAM21C in the “Search” field, and the analyses was performed *via* different option. Then the statistical graphs were generated directly. The differences in FAM21C protein levels in HCC and liver tissues were analyzed using the Human Protein Atlas (HPA) website (<https://www.proteinatlas.org/>). OS and disease-free survival (DFS) associated with FAM21C in HCC were analyzed by Kaplan–Meier Plotter (<http://kmplot.com/analysis/>) website with the option “Automatically select the best cut-off value”. The Ualcan online bioinformatics website (<http://ualcan.path.uab.edu/analysis.html>) used the same approach to obtain results of FAM21C on OS from the LIHC database. The FAM21C protein interaction network was analyzed by STRING (<https://string-db.org/>) and GeneMANIA (<http://genemania.org/>) website in the same way as above.

### Cases and Follow-Up

In this study, we collected pathological specimens from 129 patients who had undergone hepatectomy for HCC at the Southwest Hospital (Chongqing, China) from January 2010 to December 2012. The patients were followed for 5 years, and clinicopathological data including age, sex, tumor size, TNM stage, tumor classification, lymphatic metastasis, Vascular invasion, intrahepatic metastasis, postoperative recurrence, postoperative survival time were collected through medical record systems and follow-up. This study was approved by the Institutional Research Ethics Committee of Southwest Hospital (KY2020127).

### Immunohistochemical Staining Analysis

We collected 129 specimens from HCC patients as paraffin tissue sections, which were then used in tissue microarrays (TMA). After dewaxing and hydration, the chips were microwave heated in sodium citrate solution to repair the antigen. Subsequently,

endogenous peroxidase activity was removed with 3% hydrogen peroxide at room temperature for 30 min, while 10% BSA was used to block tissue at room temperature for 1 h. TMAs were incubated with anti-FAM21C antibody (1:500, Biorbyt, UK) at 4°C overnight. The next day, the immunohistochemical staining kit (Proteintech, China) was used for DAB staining according to the kit instructions. After dehydration, the slices were sealed with neutral resin. Each tissue was scored by 2 independent pathologists according to the following methods: tissue staining intensity scoring: 1 (+); 2 (++); 3 (+++) and positive cell ratio scoring: 1 (0-25%); 2 (26%-50%); 3 (51%-75%); 4 (>75%). The immunohistochemistry score is the product of the staining intensity score and the positive cell ratio score.

## Cell Line

Huh7 was obtained from the Fudan Cell Bank (China, Shanghai) and HepG2 was obtained from the American Type Culture Collection (ATCC). All cells were free of mycoplasma contamination. Both cell cultures were cultured with Dulbecco's modified Eagle's medium (DMEM) (Gibco) containing 10% fetal bovine serum (FBS) (Gibco). All cells were maintained at 37°C, 5% CO<sub>2</sub> in an incubator.

## Lentivirus Infection

The FAM21C protein sequence was taken from the UniProt database (NM\_015262). FAM21C shRNA, overexpression and mutation recombinant lentivirus (sh-FAM21C, FAM21C-OE, FAM21C $\Delta$ ) was constructed, packaged, amplified by Shanghai Genechem Co Ltd. Scramble shRNA (sh-NC, LV-NC, NC-FAM21C $\Delta$ ) served as a negative control. FAM21C overexpression and mutation lentiviruses expressed a fusion-HA/Flag-tagged protein, respectively. Specifically, amino acids were mutated at positions 1003, 1010, and 1019 to alanine (**Supplementary Figure 1**). Huh7 and HepG2 cells were seeded in 6-well plates and lentivirus transfection was performed when cells reached 20% to 30% confluence. Cells were replaced with 1 mL of fresh complete medium and the corresponding volume of lentivirus and transfection reagent was added to each well according to the instructions. Cells were selected with puromycin. The transfection efficiency was observed by fluorescence microscopy, followed by western blotting experiments to detect the expression of FAM21C and tagged proteins.

## Transwell and Invasion Assay

Transwell chambers (8.0  $\mu$ m, Corning Life Science, USA) were inserted in 24-well plates (Nest, China). A 200  $\mu$ L volume of serum-free medium containing  $1 \times 10^5$  cells and 600  $\mu$ L of complete medium containing 10% FBS were added to the upper and lower chambers of each well, respectively. The cells were further incubated for 24 h. The cells were fixed in 4% paraformaldehyde at room temperature for 30 min, followed by crystalline violet staining (Beyotime, China) for 30 min. The cells in the upper chamber were then washed in PBS, and were gently wiped with a cotton swab. Three fields of view were randomly selected under the microscope to observe the cells and were photographed for counting (20x magnification). For invasion

experiments, Matrigel (Corning Life Science, USA) was mixed with DMEM in a ratio of 1:6 and 30  $\mu$ L was added to each chamber and placed in an incubator at 37°C for 5 h. The remaining steps were performed as for Transwell experiments.

## Wound Healing

Huh7 and HepG2 were inoculated in 6-well plates and cultured until the cells reached 100% confluence. Using a pipette tip, the surface of the cell monolayer was scratched in a straight line. After washing the cell debris with PBS, the culture was changed to serum-free medium and continued for an additional 24 h. The migration area of each group was observed under the microscope and was photographed (20x magnification). Microscopic images of Huh7 and HepG2 were collected at 0, 24, and 0, 30h, respectively.

## Extraction of Cytoplasmic and Cytoskeletal Proteins

The cytoplasmic and cytoskeletal proteins were extracted with the Subcellular Structure Protein Extraction Kit (Sangon, China) according to the manufacturer's instructions. A standard number of cells ( $2 \times 10^6$ ) were used in each sample. Each sample was mixed with 500  $\mu$ L of cold Extraction buffer 1 supplemented with 5  $\mu$ L of protease inhibitor and shaken on ice for 10min. The supernatant was collected and saved after centrifugation at 3000 rpm for 8min at 4°C. The cytoplasmic proteins were present in the supernatant. The residual precipitation was re-suspended with 200  $\mu$ L of Extraction buffer 4. Then, the sample was centrifuged at 12000 g for 15 min at 4°C. The residual precipitation was dissolved with 200  $\mu$ L of 1xloading buffer after washing twice with -20°C with 90% acetone. The cytoskeletal proteins were dissolved in loading buffer. The protein levels were detected by western blotting (20).

## Western Blotting

Huh7 and HepG2 cells were lysed with RIPA buffer (Beyotime, China) containing protease inhibitors or phosphatase inhibitors (Beyotime, China) for 30 min on ice. The cell lysate was centrifuged at 13000  $\times$ g for 15 min at 4°C, and the supernatant was collected. F-actin (cytoskeletal proteins) were extracted followed by *Extraction of cytoplasmic and cytoskeletal proteins*. The lysate was heated at 100°C in a metal bath for 5 mins after mixing with 5x loading buffer. Proteins were separated by SDS-PAGE and then transferred to PVDF membranes (Millipore, USA). A solution of 5% skimmed milk was used to block the membranes at room temperature for 1 h and then incubated with a primary antibody at 4°C overnight. The next day, after washing the membranes three times with TBST, the PVDF membranes were incubated with homologous HRP-conjugated secondary antibody at room temperature for 1 h. Finally, the blots were visualized with ECL reagent using an imaging system (Vilber, France). Antibody descriptions were as follows: (FAM21C:1:1000, Millipore, USA; GAPDH:1:10,000, Proteintech, China; HA:1:1000, Roche, Switzerland; F-actin:1:1000, Abcam, USA; CAPZA1:1:5000, Abcam, USA; Flag:1: 1000, Sigma, USA).



## Co-Immunoprecipitation

The Protein A/G magnetic beads were obtained from Biomake. A 50  $\mu$ L volume of beads were transferred to eppendorf tubes, after three washes in TBST, 200  $\mu$ L PBS containing 10  $\mu$ L of anti-CAPZA1 antibody (Abcam, USA) or anti-HA antibody (Roche, Switzerland) was added to eppendorf tubes, and shaken at room temperature for 1 h. After washing with TBST three times, the beads were resuspended in 500  $\mu$ L of the antigen-containing lysate, and shaken at 4°C overnight. The next day, the supernatant was discarded by magnetic separation, TBST washed three times and then 35  $\mu$ L of 1×loading buffer was added and heated at 100°C in a metal bath for 10 min. The supernatant was collected in another eppendorf tube. The remaining steps were the same as in those for western blotting. For quantitative Co-immunoprecipitation, an equal number of cells with different treatments were extracted. Protein concentrations were determined using the BCA Protein Assay Kit (Beyotime, China). CAPZA1 was considered as a loading control. The remaining steps were the same as for Co-IP.

## Immunocytofluorescence

Huh7 cells were seeded in 24-well plates containing clean coverslips. After washing with PBS 3 times, cells were fixed in 4% paraformaldehyde and permeabilized with 0.2% Triton-100, then blocked with 5% BSA for 1 h at room temperature. Subsequently, the coverslips were incubated with primary antibody (FAM21C: 1:50, Biorbyt, UK) at 4°C overnight. The next day, the primary antibody was discarded and the cells were washed 3 times with PBS and incubated with Alexa Fluor 488-conjugated secondary antibodies (1:200, Proteintech, China) in a wet box for 1 h. Subsequently, cells were stained with TRITC Phalloidin (1:200, Solarbio, China) for 30 min at room temperature to detect the actin cytoskeleton. Finally, 10  $\mu$ L of antifluorescence quencher containing DAPI was used to stain the nuclei. Cells were examined by fluorescence microscopy and photographed (40x magnification).

## Orthotopic Xenograft Model

SPF-grade BALB/c nude mice were used to establish the orthotopic xenograft model (6-week old, males, each group  $n=6$ ). Nude mice were anesthetized with isoflurane by inhalation, a 1-cm incision was made in the midline of the abdomen to expose the left lobe of the liver, and sh-FAM21C-expressing Huh7 and negative control cells ( $1 \times 10^6$  cells/80  $\mu$ L DMEM, containing 30  $\mu$ L of Matrigel) were injected with a microinjector under the liver envelope. Continuous sutures closed the abdomen. A normal diet was maintained and mice were observed every 2 days. Six weeks later, the nude mice were euthanized under deep anesthesia, the livers were removed and photographed, and the number of metastases was counted, after which tissues were preserved in 4% paraformaldehyde. Then, the liver was sectioned and stained with haematoxylin and eosin, and tumor lesions were observed. Animal experiments were approved by the Laboratory Animal Welfare and Ethics Committee of the Third Military Medical University (Army Medical University), Chongqing, China.

## Statistical Analysis

All statistical analyses were performed with GraphPad Prism 6.0 (GraphPad Software Ltd, San Diego, CA). Images were processed with ImageJ free software. The data were expressed as mean  $\pm$  standard deviation. Comparisons between two groups were evaluated using independent sample *t* tests or paired-sample *t* tests. The Chi-square test was used to analyze the relationship between FAM21C and clinicopathological parameters. Survival analysis was performed using Kaplan–Meier survival analysis. *P*-value less than 0.05 ( $P < 0.05$ ) was considered significant.

## RESULTS

### Bioinformatics Analysis Suggested That FAM21C Expression Was Closely Related to the Malignant Progression of HCC

To gain a preliminary understanding of the role of FAM21C in HCC, we analyzed 369 HCC tissues and 50 normal liver tissues from the online database GEPIA (21), and FAM21C mRNA was found to be highly expressed in HCC tissues (**Figure 1A**). Meanwhile, the expression of FAM21C mRNA gradually increased with increasing TNM stage (I–III) of HCC but the elevated expression in stage IV HCC tissues was not significant ( $P=0.00796$ ) (**Figure 1B**). Furthermore, we searched for the expression of the FAM21C protein in HCC tissues and normal liver tissues in the HPA database and found that the immunohistochemical staining signal of the FAM21C protein was stronger in HCC tissues (representative images are shown) (**Figure 1C**) (22). Finally, we analyzed the effect of FAM21C on the prognosis of HCC patients from the GEPIA, Kaplan–Meier Plotter, and Ualcan databases, and the results showed that the OS and DFS were significantly lower in the FAM21C mRNA high-expression group than in the FAM21C mRNA low-expression group (**Figures 1D–G**) (23). The results of the above bioinformatics analysis suggested that the high expression of FAM21C in HCC could be closely related to the malignant progression of HCC.

### Case Analysis Confirms That High Expression of FAM21C in HCC Tissue Promotes Malignant Progression of HCC

To verify the prediction results of the bioinformatic analysis, a tissue microarray using primary HCC tissue samples was prepared. The tissue microarray contained 87 clinical tumor tissue samples collected from patients with HCC, 42 of which had paraneoplastic paired tissues. Seventeen (19.5%) of the 87 patients with HCC had TNM stage I, 12 (13.8%) had stage II, 44 (50.6%) had stage III, and 14 (16.1%) had stage IV. HCC was classified according to the degree of differentiation into a highly differentiated group: 8.0% ( $n=7$ ), a moderately differentiated group: 75.9% ( $n=66$ ), and a poorly differentiated group: 16.1% ( $n=14$ ). Approximately 6.9% ( $n=6$ ) of patients presented lymph node metastases, 36.8% ( $n=32$ ) had vascular invasion, 77.0% ( $n=67$ ) had recurrence within 5 years after surgery, 62.1% ( $n=54$ ) patients died from cancer-related deaths within 5 years after

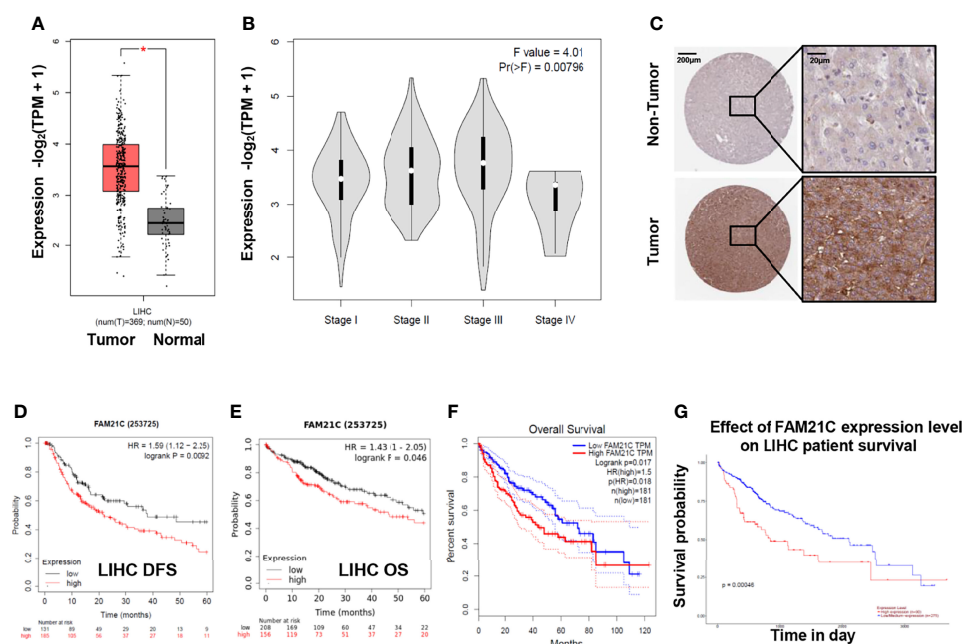


**FIGURE 1 |** FAM21C increases in HCC and is an indicator of poor prognosis by bioinformatics analysis. **(A)** The differential analysis of mRNA levels of FAM21C between 369 HCC tissue and 50 normal tissues. **(B)** Relationship between FAM21C mRNA expression levels and the HCC clinical stages in GEPIA datasets. **(C)** The protein level of FAM21C in HCC tissue and non-tumor tissues using the Human Protein Atlas (HPA) database. Representative pictures are shown. **(D, E)** DFS and OS of FAM21C in Kaplan-Meier Plotter database using the “Auto select best cutoff” option. **(F, G)** The OS of FAM21C in GEPIA and Ualcan database respectively. Survival analysis showed that high expression of FAM21C mRNA indicated a poor survival time. \* $P < 0.05$  was considered statistically significant.

surgery (**Table 1**). Subsequently, we performed immunohistochemical staining of FAM21C on HCC tissue microarrays, and the results showed that the tissues were classified as weakly positive (+), positive (++), and strongly positive (+++) according to the depth of staining (**Figure 2A**). Then we scored the 87 HCC tissues in the low expression group ( $n = 42$ ) and the high expression group ( $n = 45$ ) based on the score of the staining depth and the percentage of stained area, using the median as the cut-off value. Among the 42 pairs of cancer and para-cancer tissues, the expression of FAM21C was significantly higher in HCC tissues than in para-cancerous tissues ( $8.05 \pm 2.34$  vs.  $4.86 \pm 1.32$ ,  $P < 0.0001$ ) (**Figure 2B**). Subsequently, we statistically analyzed pathological parameters such as tumor

size, TNM stage, and vascular invasion, and postoperative follow-up data of HCC patients in the FAM21C low-expression and high-expression groups (**Supplementary Table 1**), and the results suggested that the tumor diameter of HCC in the FAM21C high-expression group was significantly greater than in the low-expression group ( $8.7 \pm 0.6$  cm vs.  $6.8 \pm 0.5$  cm,  $P = 0.0192$ ) (**Figure 2C**). Thirty-nine patients in the FAM21C high-expression group were in stage III–IV, and the number was significantly higher than that of the 19 patients in the low-expression group ( $86.7\%$  vs.  $45.2\%$ ,  $P < 0.001$ ) (**Figure 2D**). Twenty-three patients in the FAM21C high-expression group presented microvascular invasion, which was significantly more pronounced than that 9 cases in the FAM21C

**TABLE 1 |** Clinicopathologic Parameters of Patients.

Pathologic Variable	No. of Patients	Pathologic Variable	No. of Patients
TNM stage	87	Vascular invasion	87
Stage I	17 (19.5%)	Yes	32 (36.8%)
Stage II	12 (13.8%)	No	55 (63.2%)
Stage III	44 (50.6%)	Postoperative recurrence	87
Stage IV	14 (16.1%)	Yes	67 (77.0%)
HCC differentiation	87	No	20 (23.0%)
PD	14 (16.1%)	Cancer related death	87
MD	66 (75.9%)	Death	54 (62.1%)
WD	7 (8.0%)	Survival	33 (37.9%)
Lymph node metastasis	87		
Yes	6 (6.9%)		
No	81 (93.1%)		

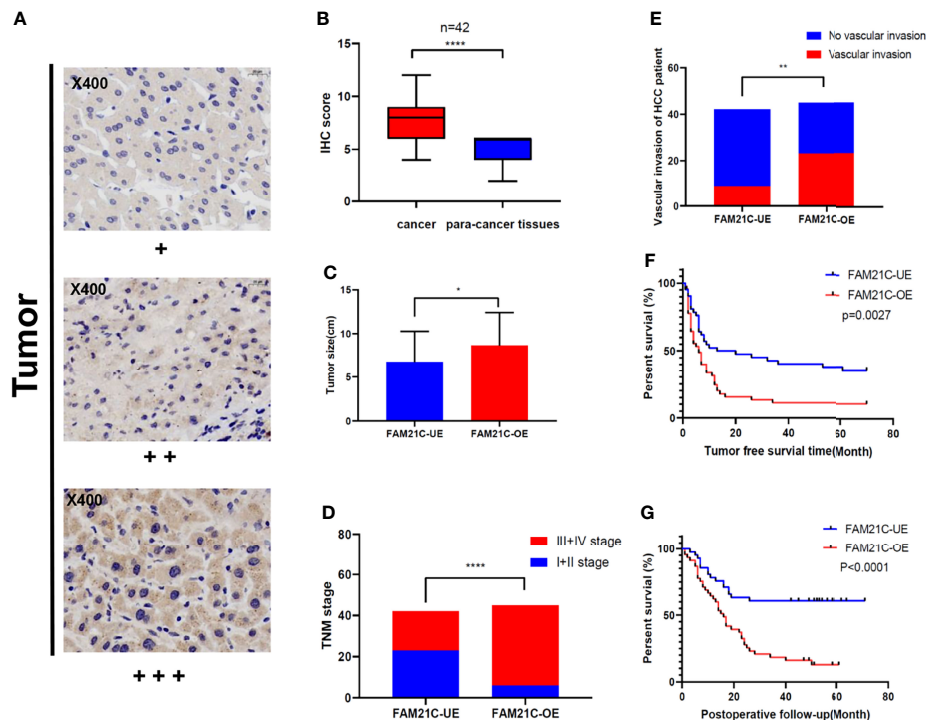


**FIGURE 2 |** Up-regulated expression of FAM21C promotes the malignant progression of HCC in patients. **(A)** Immunohistochemical staining was performed in 129 HCC tissue. The stain intensity was classified as weak (+), moderate (++), or strong intensity (+++). Representative images are presented. FAM21C expression was scored according to intensity and area as described in the Materials and Methods. **(B)** The expression of FAM21C levels in 42 paired HCC tissue analyzed by paired Student's *t* test. **(C)** The mean tumor size in HCC patient of the FAM21C low-expression and high-expression group; red indicates the overexpression and blue indicates the low-expression. **(D)** Tumor stage in HCC patients of the FAM21C overexpression and low-expression groups; red indicates the III+IV stage, and blue indicates I+II stage. **(E)** Vascular invasion in HCC patients of the FAM21C overexpression and low-expression groups; red indicates the occurrence of vascular invasion, and blue indicates no vascular invasion. **(F, G)** The Kaplan–Meier analysis of DFS and OS between FAM21C low-expression group and overexpression group. \**P* < 0.05, \*\**P* < 0.01, \*\*\*\**P* < 0.0001.

low-expression group (51.1% vs. 21.4%, *P*=0.0071) (**Figure 2E**). Finally, we performed a statistical analysis of the prognosis of patients in the FAM21C high-expression and FAM21C low-expression groups, and the results showed that the OS and DFS rates were significantly lower in the FAM21C high-expression group than in the FAM21C low-expression group (**Figures 2F, G**). These results suggest that FAM21C is highly expressed in patients with HCC and can promote the malignant progression of HCC.

### FAM21C Promotes HCC Cell Invasion and Migration *In Vitro*

The WASH complex is an important member of the WASP family that plays an important role in mediating the dynamic remodeling of the cytoskeleton. FAM21C is a key subunit of WASH; thus, we hypothesized that it might be associated with cytoskeleton-related invasion and metastasis. To investigate the role of FAM21C in HCC, we first tested the expression of FAM21C in high-invasive cells Huh7 and low-invasive cells HepG2. Our results revealed that the protein level of FAM21C in Huh7 cells was higher than in HepG2 (**Figures 3A, B**). Then we stably knocked down and overexpressed FAM21C in Huh7 and HepG2 cells respectively, while adding the HA tag to the

overexpressing lentivirus to construct the HA-FAM21C fusion protein (**Figures 3C, D**). Transwell and Wound healing assays showed that the migration ability of Huh7 cells with stably knocked down FAM21C expression was significantly reduced; and the invasion ability was also significantly reduced compared to the negative control in Matrigel-precoated chambers (**Figures 3E, F, I, J**). In contrast, in HepG2 overexpressing FAM21C, migration ability was enhanced with increased expression of FAM21C and invasion ability was also significantly increased (**Figures 3G–J**). Reciprocally, we overexpressed FAM21C in Huh7 cells and knocked it down in HepG2, finding that the invasive and migratory ability of Huh7 and HepG2 was dramatically increased and significantly decreased respectively (**Supplementary Figure 2**). These results suggested that FAM21C can promote the invasive and migratory ability of HCC cells *in vitro*.

### FAM21C Is Involved in Regulating Actin Filament Cytoskeleton Remodeling Through Binding to CAPZA1

A previous study by our group found that low expression of CAPZA1 induced the remodeling of the actin filament cytoskeleton in HCC cells, driving EMT and thus promoting

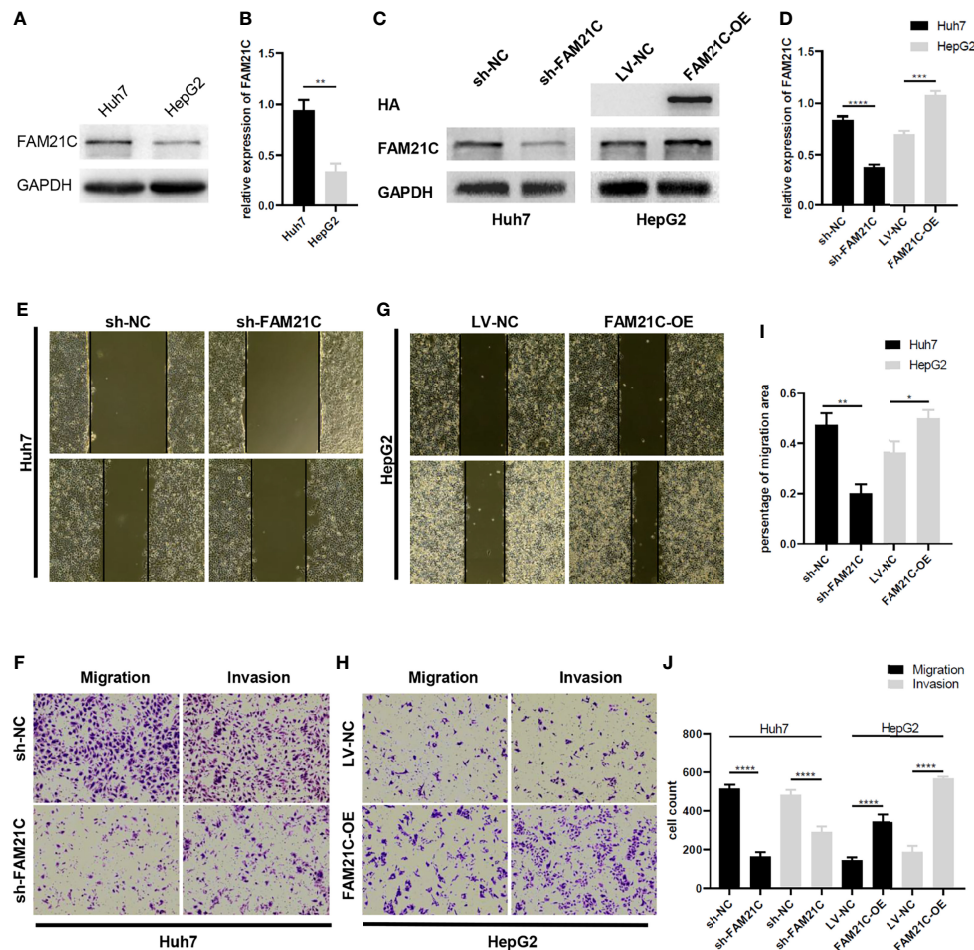


**FIGURE 3 |** FAM21C increases HCC cell invasion and migration *in vitro*. **(A)** The wild-type FAM21C content of Huh7 and HepG2 cells was detected by western blot. **(B)** Histograms show the relative expression levels of FAM21C. **(C)** Western blotting was used to detect the protein levels of FAM21C in Huh7 and HepG2 after infected with sh-FAM21C and FAM21C-OE lentivirus compared with the respective negative control. HA indicated that the overexpression of HA-FAM21C fusion protein was effective. **(D)** Histograms show the relative expression levels of proteins. **(E–H)** Wound healing, Transwell and invasion assay were used to detect the migration and invasion potential of Huh7 and HepG2 cells after transfected with knockdown or overexpression lentivirus respectively. The invasion and migration ability of Huh7 was decreased after FAM21C knockdown; the invasion and migration ability of HepG2 was increased after FAM21C overexpression. Scale bar: 200 $\times$ . **(I, J)** Histograms show the percentage of migration area and cell count after the FAM21C expression was modulated. Data are represented as the mean  $\pm$  SD,  $n=3$ . \* $P < 0.05$ , \*\* $P < 0.01$ , \*\*\* $P < 0.001$ , \*\*\*\* $P < 0.0001$ .

invasion and migration of HCC cells (11). A quantitative/TMT IP-MS analysis of KIAA0196 indicated that FAM21C could interact with CAPZA1 (24). What's more, The bioinformatics analysis also showed that the two can be combined (**Supplementary Figure 3**), but the effects of its combination on HCC cells are unclear. Thus, we used immunoprecipitation assays to first verify whether FAM21C could interact with CAPZA1 in HCC cells by constructing an FAM21C-HA fusion protein using a HA tag, and interfering FAM21C expression with shRNA. Magnetic beads encapsulated with the CAPZA1 antibody were used in pull-down HA tag from the total protein lysate. The results showed that the two could bind to each other in Huh7 overexpressing the FAM21C-HA fusion protein, indirectly verifying that FAM21C could interact with CAPZA1 (**Figures 4A, B**). Consistent with our

previous study, immunoprecipitation assays confirmed that CAPZA1 could bind to F-actin (**Figure 4A**). The effect of FAM21C bind to CAPZA1 on the F-actin cytoskeleton was then explored. Using western blotting assays, Huh7 cells with knockdown of FAM21C, CAPZA1 expression did not change, but the protein level of F-actin was decreased; in contrast, in Huh7 cells overexpressing FAM21C-HA, CAPZA1 expression was also unchanged, but the protein level of F-actin was increased (**Figures 4C, D**). The results suggest that FAM21C is not significantly related to the expression of CAPZA1, but may be involved in regulating the level of F-actin. A subsequent search of the GEPIA database revealed no significant correlation between FAM21C mRNA levels and F-actin (**Supplementary Figure 4**). This suggested to us that FAM21C may influence the intracellular



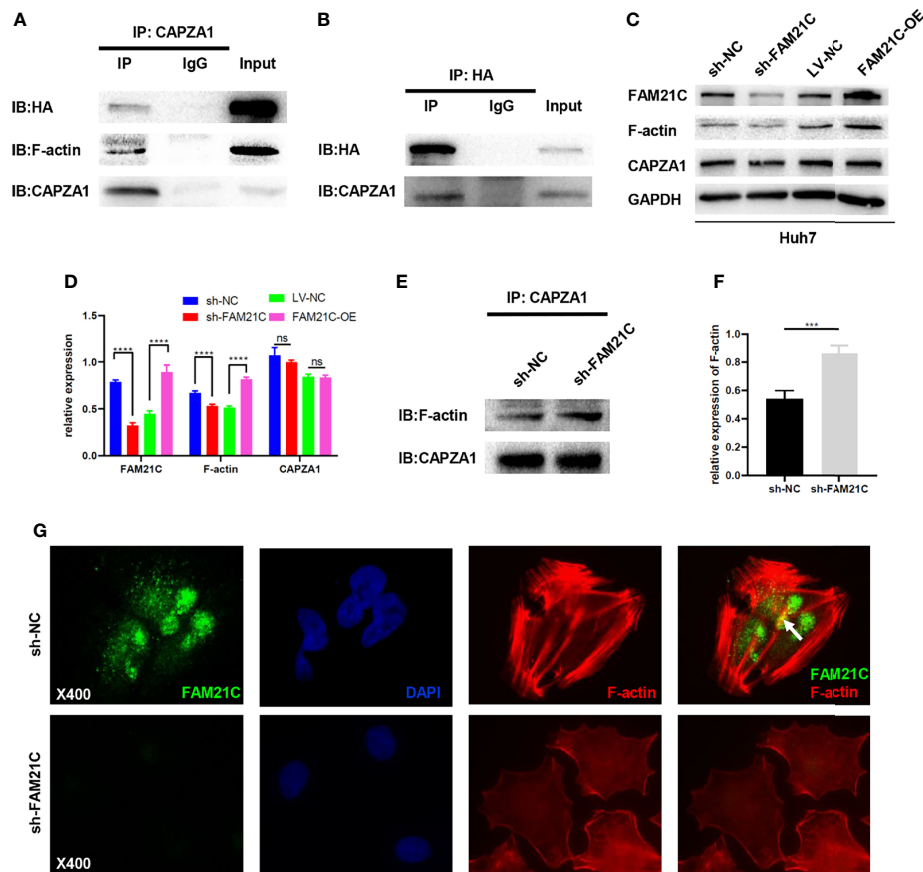


**FIGURE 4 |** FAM21C bind to CAPZA1 and inhibit the capping ability of CAPZA1 to promote cytoskeleton remodeling in HCC cells. **(A, B)** Co-Immunoprecipitation (Co-IP) was performed to validate protein interactions. The results showed that HA-FAM21C and CAPZA1 can pull each other down. Moreover, Co-IP also showed that CAPZA1 can interact with F-actin. **(C)** Western blotting was used to detect the expression of FAM21C, F-actin, and CAPZA1. GAPDH was used as the loading control. **(D)** Histograms show the relative expression. **(E)** Quantitative Co-Immunoprecipitation showed that the binding level of F-actin to CAPZA1 was increased after FAM21C knockdown. CAPZA1 level was considered loading control. **(F)** After Quantification by ImageJ software, the histograms showed the relative level of F-actin. **(G)** Immunofluorescence assay on Huh7 cells showed that with the decreased of FAM21C, actin cytoskeleton scattered arrangement, and lack of the colocalization of FAM21C and F-actin. (The arrowhead shows the colocalization). Nuclei were stained with DAPI. Scale bar = 400x. Data are represented as the mean  $\pm$  SD,  $n=3$ . \*\*\* $P < 0.001$ , \*\*\*\* $P < 0.0001$ ; ns for no significance.

level of F-actin by promoting its remodeling. Next, we performed quantitative Co-IP experiments by collecting the same number of Huh7 cells in the FAM21C knockdown and control groups, extracting the total protein and then normalizing the protein concentration, and verifying the amount of F-actin bounding by enriching CAPZA1. The results showed that after FAM21C was knocked down, the amount of F-actin bound to CAPZA1 increased significantly in contrast to the decrease in total F-actin content (**Figures 4E, F**). Meanwhile, immunofluorescence assays revealed that the amount of FAM21C was significantly reduced in the knockdown group compared to the control group, and the actin cytoskeleton was scattered, while there was a lack of colocalization of FAM21C with F-actin (**Figure 4G**). These results suggested that FAM21C can promote F-actin polymerization and thus regulate actin cytoskeleton remodeling by interacting with CAPZA1 and inhibiting the capping ability of CAPZA1 in HCC cells.

### FAM21C Binds to CAPZA1 Mainly Through the CPI Domain and Inhibits the CAPZA1 Capping Function, Thus Promoting the Invasion and Migration of HCC Cells

Protein molecules containing the CPI domain can bind to CAPZ; leucine, arginine, proline, which are 3 highly conserved amino acids exist in the CPI domain (25); thus, we performed a targeted mutation of these three conserved amino acids to alanine in the CPI domain based on the amino acid sequence of FAM21C (26) (**Supplementary Figure 1**), to further verify whether FAM21C promotes the invasion and migration of HCC cells by binding to CAPZA1. We constructed a fusion protein (FAM21CΔ-Flag) with the Flag tag protein and mutant FAM21C. An immunoprecipitation was performed to verify whether the Flag-tagged mutant FAM21C could bind to CAPZA1. The results showed that the two did not bind (**Figure 5A**). Subsequently, immunoblotting assay was performed to detect

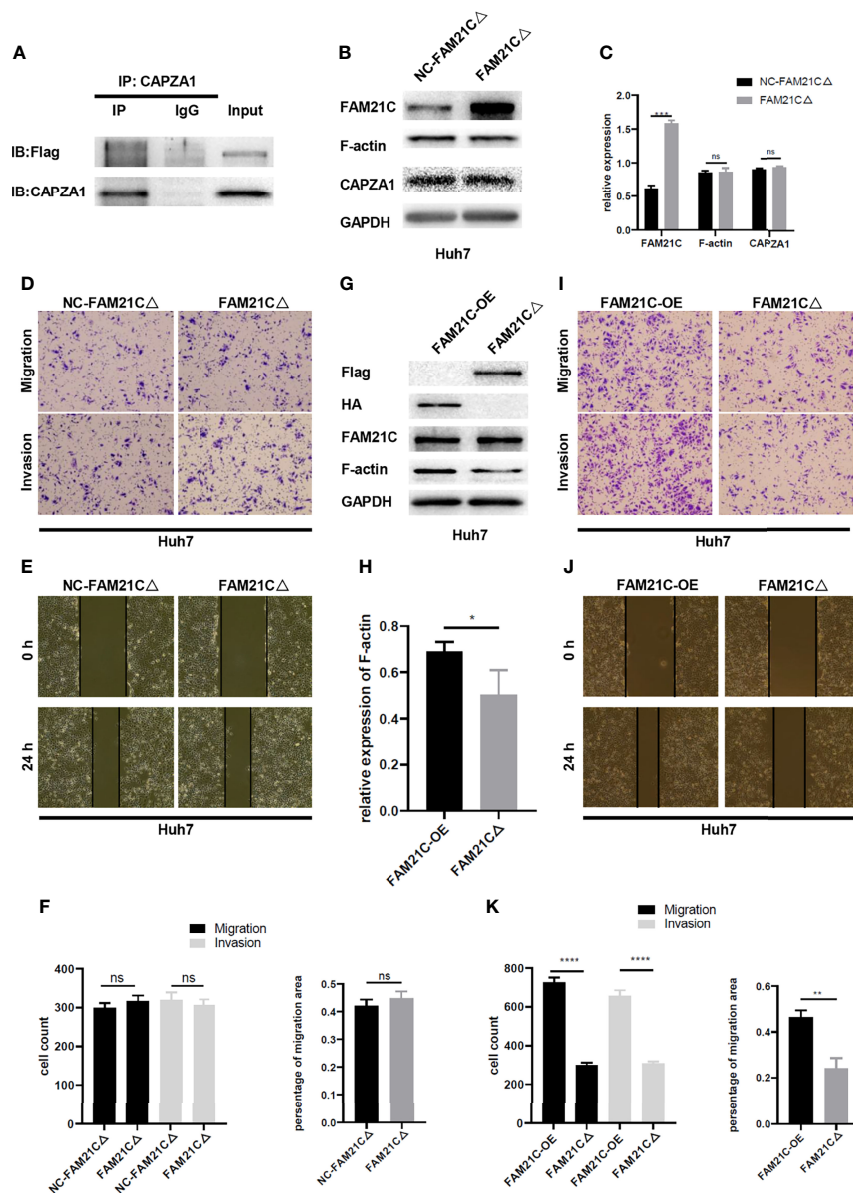


**FIGURE 5 |** FAM21C CPI mutation failed to promote the HCC cells invasion and migration. **(A)** Co-IP was used to validate the interaction between FAM21C mutation and CAPZA1. The results showed that CPI mutation interfered with binding to CAPZA1. **(B)** Western blotting was performed to detect the expression level of FAM21C, CAPZA1 and F-actin following transfected with mutation lentivirus in Huh7 cells. **(C)** Histograms showed the relative expression level. **(D, E)** Transwell, Wound healing, and invasion assays were performed to validate the migration and invasion potential of CPI mutation Huh7 cells. **(F)** Histograms showed the results were of no significant. **(G)** The protein of Flag, HA, FAM21C, F-actin, GAPDH were analyzed by western blotting. **(H)** Histograms showed the relative expression levels of F-actin. **(I, J)** Transwell, Wound healing, and invasion assays were performed to validate the migration and invasion potential of FAM21C-OE-Huh7 and FAM21CΔ-Huh7 cells. **(K)** The statistical graph indicates the cell count and percentage of the migration area. Data are represented as the mean  $\pm$  SD,  $n=3$ . \* $P < 0.05$ , \*\* $P < 0.01$ , \*\*\* $P < 0.001$ , \*\*\*\* $P < 0.0001$ ; ns for no significance.

transfection efficiency and the effect of mutant FAM21C on actin cytoskeleton. The results showed that the content of FAM21C was significantly higher in the treated group compared to the control group, but the content of CAPZA1 and F-actin were not significantly different (**Figures 5B, C**), suggesting that the mutant FAM21C failed to affect the actin cytoskeleton of Huh7 cells. Then, *in vitro* functional assays did not show any significant

differences in the migration and invasion ability of Huh7 cells transfected with mutant FAM21C compared with the control group (**Figures 5D–F**). To go a step further, we compared the biological role of wild-type FAM21C and mutant FAM21C *via* FAM21C-OE-Huh7 and FAM21CΔ-Huh7 cells. The western blotting assay showed that the F-actin level was significantly elevated in FAM21C-OE-Huh7 cells compared with FAM21CΔ-

Huh7 cells (**Figures 5G, H**). Consistent with these findings, the invasive and migratory ability of FAM21C-OE-Huh7 cells was enhanced compared to FAM21CΔ-Huh7 cells (**Figures 5I–K**). These data demonstrated that the binding of FAM21C to CAPZA1 was inhibited by the mutation of the CPI domain, resulting in an inability of FAM21C to regulate actin cytoskeleton through CAPZA1, which failed to influence the invasion and migration ability of HCC cells. In conclusion, FAM21C exerts its procarcinogenic effects by binding to the CAPZA1 through the CPI domain, which in turn induces remodeling of the F-actin cytoskeleton, thus promoting HCC cells invasion and migration.

## FAM21C Promotes Invasion and Metastasis of HCC in Nude Mice

We have demonstrated that FAM21C promotes HCC cell invasion and migration *in vitro*. To investigate the role of FAM21C *in vivo*, sh-FAM21C-expressing Huh7 and its negative control cells were injected into the left lobe of the nude mice liver (n=6). Six weeks later, all nude mice were deeply anesthetized and euthanized, and the metastatic foci on the surface of the nude mice liver was observed. The result showed that few metastatic foci were present on the liver surface of nude mice in the sh-FAM21C-expressing Huh7 group; in contrast, in the control group, more metastatic foci were diffused on the liver surface, along with the formation of localized masses (**Figures 6A, B**). Subsequently, The liver sections were confirmed as tumors tissue by hematoxylin and eosin staining. The result showed that in the control group the metastasis foci were more widely distributed in the liver tissue; Conversely, the distant metastatic lesions of the sh-FAM21C-expressing Huh7 group displayed a restricted distribution (**Figure 6C**)

(**Supplementary Figure 5**). This result suggested that FAM21C could promote the invasive and migratory ability of HCC cells *in vivo*.

## DISCUSSION

In the present study, FAM21C expression was up-regulated in HCC tissues and its high expression was significantly associated with malignant progression of HCC. Meanwhile, we confirmed that FAM21C could promote the invasion and metastasis of HCC *in vitro* and *in vivo*. Additionally, we found and confirmed that FAM21C could interact with CAPZA1 through its CPI domain in HCC cells and FAM21C inhibits the capping ability of CAPZA1, thus inducing the remodeling of the actin filament cytoskeleton, which in turn promoted HCC invasion and metastasis.

During tumor development, tumors achieve distant settlement by encroaching on surrounding tissues to break the tumor barrier (27). Dynamic remodeling of the actin filament cytoskeleton and its associated regulators play an unquestionable role in tumor spreading (28, 29). Thus it is important to investigate the mechanism of actin filament cytoskeleton remodeling during invasion and migration of HCC cells to improve the patient's prognosis. Based on the findings of a previous study, we investigated the mechanism by which FAM21C induces the remodeling of the F-actin cytoskeleton by regulating CAPZA1 to promote HCC invasion and metastasis. Consistently, the dynamic remodeling of F-actin includes nucleation, polymerization, depolymerization, and side branch formation (30). The WASP family molecules are important regulators of F-actin remodeling, and their VCA

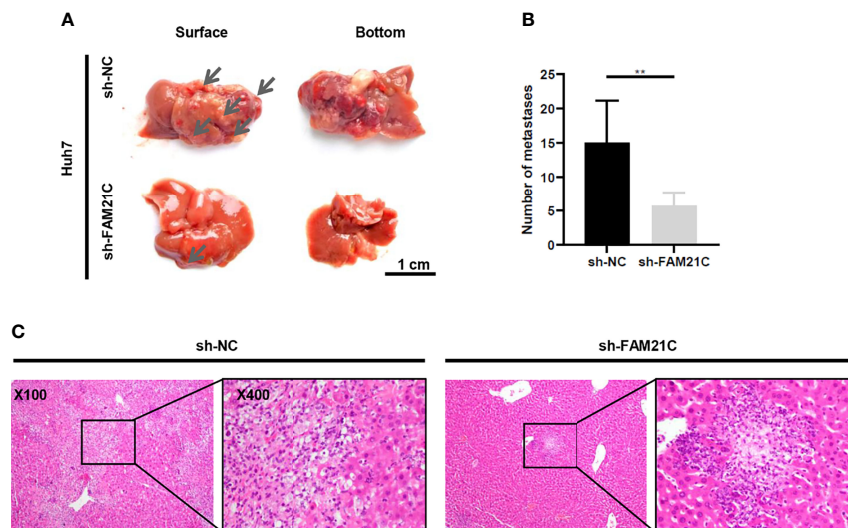


**FIGURE 6 |** FAM21C could promote HCC invasion and metastasis *in vivo*. **(A)** The metastatic tumor foci were widely distributed on the liver surface of the negative control group. The few metastatic lesions were localized predominantly on the liver lobe of the sh-FAM21C-expressing Huh7 group. Scale bar: 1 cm. **(B)** Histograms show the number of the metastatic tumor foci. Data are represented as the mean ± SD, n=6. \*\**P* < 0.01. **(C)** Haematoxylin and eosin staining was performed on xenograft liver sections. Scale bar = 100× and 400×.

domains function to promote actin filament nucleation and lengthening and can play important roles in different cellular substructures (31). For example, N-WASP, an important member of WASP, is highly expressed in HCC, and its elevated expression predicts a poor prognosis in HCC patients, and the potential mechanism maybe to promote prolongation of actin filament side branch polymerization by activating the Arp2/3 complex, which drives the formation of a bulge in the cell membrane and thus enhances cell migration (32, 33). WASH, a newly identified member of the WASP family, can regulate actin formation on the surface of the endosomal membrane to form a reticular scaffold, thus participating in regulation of transferrin recycling (34). Furthermore, in esophageal cancer, WASH overexpression improves the characteristics of tumor stem cells and is associated with a poor prognosis (35). The above results suggest that the WASP family may play a role as a pro-oncogene in tumors, in which the WASH complex may promote tumor cell development by regulating actin filament cytoskeleton remodeling, but the exact mechanism is not yet clear. FAM21C is an important subunit of the WASH complex, and studies have shown that FAM21 knockdown reduces the protein level of WASH, but WASH knockdown does not alter FAM21 expression (36). In this study, we investigated the potential mechanism of FAM21C, a key subunit of the WASH complex, to promote the invasion and metastasis of HCC through regulation of the remodeling of the F-actin cytoskeleton, furthering the understanding of the mechanism of the WASP family proteins to promote the invasion and metastasis of HCC.

CAPZA1 is an important molecule that regulates the remodeling of F-actin, which mainly regulates the prolongation of F-actin by binding at the barbed end and preventing the polymerization of G-actin. In our previous study, we found that CAPZA1 had low expression in HCC tissues and its low expression could promote the malignant progression of HCC by regulating the remodeling of the F-actin cytoskeleton to promote EMT in HCC cells (11). Furthermore, in our recent study, we found that in HCC cells, PIP2 can bind to CAPZA1, and the combination of the two led to disengaging CAPZA1 from the barbed end of F-actin, which in turn promoted the prolongation of F-actin and drove the morphogenesis of HCC cells (20). In this study, we found that FAM21C was highly expressed in HCC tissues by bioinformatics analysis, and its high expression predicted a poor prognosis for HCC patients; Meanwhile, we further verified that FAM21C was highly expressed in HCC tissues using TMAs, and its high expression could promote malignant progression of HCC, and this result was also confirmed *in vitro* and *in vivo*. Subsequently, we explored the molecular mechanisms involved in FAM21C that promotes HCC cell invasion and migration. We found that FAM21C could bind to CAPZA1, and its binding could inhibit the capping ability of CAPZA1 and thus promote the prolongation of F-actin. After mutating the binding site, FAM21C failed to regulate actin cytoskeleton *via* CAPZA1 capping ability. Therefore, we concluded that FAM21C plays an important role in the invasion and metastasis of HCC by

inhibiting capping ability by binding to CAPZA1, leaving the barbed end of F-actin in an open state and polymerizing in the positive direction, ultimately promoting dynamic remodeling of the actin cytoskeleton.

It has been reported that FAM21C can attach the WASH complex to endosomal membranes and is an essential molecule for retromer-mediated WASH-dependent sorting of cargo transport (36). In addition, WASH-mediated transport of endosomal cargo such as  $\beta 1$  integrin and MT1-MMP is important for tumor cell invasion and migration (37, 38). Furthermore, the presence of numerous retromer-binding sites in FAM21C allows the cargo, retromer, and WASH complexes to constitute a fluid sorting platform linked to the actin cytoskeleton (39). These findings suggested that FAM21C, a key subunit of the WASH complex, is not only an essential molecule to maintain the stability and function of the WASH complex, but also plays an important role in actin cytoskeleton-dependent endosomal vesicle transport. In particular, the regulation of the specific endosomal cargo transport can have a significant impact on the behavior of tumor cells such as invasion and migration. Moreover, it was also reported that DKO cells transfected with the FAM21 siRNAs, along with the loss of actin foci (comets) on endosomes (40). In this study, the co-localization of FAM21C with the actin cytoskeleton was detected using an immunofluorescence assay, suggesting a potential association between the subcellular structure in which FAM21C is located and the actin cytoskeleton. Therefore, we hypothesize that during HCC cell invasion and migration, FAM21C in endosomal membranes remodels the F-actin cytoskeleton through regulation of CAPZA1, an event that promotes endosomal membrane skeleton formation and prepares the structure for endosomal vesicle transport and sorting. The above results suggest that FAM21C-regulated remodeling of the F-actin cytoskeleton is closely related to endosome-dependent cargo transport. Unfortunately, we did not investigate the related mechanisms in depth in this study, although we plan to design a specific study in the future.

In summary, we conclude that the high expression of FAM21C in HCC tissues can promote the malignant progression of HCC, and its mechanism involves the inhibition of CAPZA1 capping function by FAM21C which binds to CAPZA1, leaving the F-actin barbed-end in an open state, which in turn induces the remodeling of the F-actin cytoskeleton, thus promoting the invasion and migration of HCC cells. The remodeling of the F-actin cytoskeleton regulated by FAM21C through CAPZA1 may be closely related to endosome-dependent cargo transport, which deserves further in-depth study and its potential to become a new target for the treatment of HCC.

## DATA AVAILABILITY STATEMENT

The original contributions presented in the study are included in the article/**Supplementary Material**. Further inquiries can be directed to the corresponding author.



## ETHICS STATEMENT

The studies involving human participants were reviewed and approved by the Institutional Research Ethics Committee of Southwest Hospital. The patients/participants provided their written informed consent to participate in this study. The animal study was reviewed and approved by the Laboratory Animal Welfare and Ethics Committee of the Third Military Medical University (Army Medical University), Chongqing, China. Written informed consent was obtained from the individual(s) for the publication of any potentially identifiable images or data included in this article.

## AUTHOR CONTRIBUTIONS

YL designed and performed experiments, analyzed data and wrote the paper. DH analyzed the data and revised the manuscript. BW, BZ, JL, and JS performed a part of experiments. SZ initiated the study, provided the financial support and supervised laboratorial processes. All the authors approved the final manuscript.

## REFERENCES

- Heimbach JK, Kulik LM, Finn RS, Sirlin CB, Abecassis MM, Roberts LR, et al. AASLD Guidelines for the Treatment of Hepatocellular Carcinoma. *Hepatology* (2018) 67(1):358–80. doi: 10.1002/hep.29086
- Bray F, Ferlay J, Soerjomataram I, Siegel RL, Torre LA, Jemal A. Global Cancer Statistics 2018: GLOBOCAN Estimates of Incidence and Mortality Worldwide for 36 Cancers in 185 Countries. *CA Cancer J Clin* (2018) 68(6):394–424. doi: 10.3322/caac.21492
- Dhir M, Melin AA, Douaiher J, Lin C, Zhen WK, Hussain SM, et al. A Review and Update of Treatment Options and Controversies in the Management of Hepatocellular Carcinoma. *Ann Surg* (2016) 263(6):1112–25. doi: 10.1097/SLA.0000000000001556
- Dang H, Takai A, Forgues M, Pomyen Y, Mou H, Xue W, et al. Oncogenic Activation of the RNA Binding Protein NELFE and MYC Signaling in Hepatocellular Carcinoma. *Cancer Cell* (2017) 32(1):101–14.e8. doi: 10.1016/j.ccell.2017.06.002
- Pollard TD, Borisov GG. Cellular Motility Driven by Assembly and Disassembly of Actin Filaments. *Cell* (2003) 112(4):453–65. doi: 10.1016/s0092-8674(03)00120-x
- Yilmaz M, Christofori G. EMT, the Cytoskeleton, and Cancer Cell Invasion. *Cancer Metastasis Rev* (2009) 28(1-2):15–33. doi: 10.1007/s10555-008-9169-0
- Kaksonen M, Toret CP, Drubin DG. Harnessing Actin Dynamics for Clathrin-Mediated Endocytosis. *Nat Rev Mol Cell Biol* (2006) 7(6):404–14. doi: 10.1038/nrm1940
- Peng JM, Bera R, Chiou CY, Yu MC, Chen TC, Chen CW, et al. Actin Cytoskeleton Remodeling Drives Epithelial-Mesenchymal Transition for Hepatoma Invasion and Metastasis in Mice. *Hepatology* (2018) 67(6):2226–43. doi: 10.1002/hep.29678
- Qi S, Su L, Li J, Zhang C, Ma Z, Liu G, et al. Arf6-Driven Endocytic Recycling of CD147 Determines HCC Malignant Phenotypes. *J Exp Clin Cancer Res* (2019) 38(1):471. doi: 10.1186/s13046-019-1464-9
- Liu Y, Lu LL, Wen D, Liu DL, Dong LL, Gao DM, et al. MiR-612 Regulates Invadopodia of Hepatocellular Carcinoma by HADHA-Mediated Lipid Reprogramming. *J Hematol Oncol* (2020) 13(1):12. doi: 10.1186/s13045-019-0841-3
- Huang D, Cao L, Zheng S. CAPZA1 Modulates EMT by Regulating Actin Cytoskeleton Remodelling in Hepatocellular Carcinoma. *J Exp Clin Cancer Res* (2017) 36(1):13. doi: 10.1186/s13046-016-0474-0

## FUNDING

This research was funded by the National Natural Science Foundation of China, grant number 81972303.

## ACKNOWLEDGMENTS

We thank Prof. Chuanming Xie (Institute of Hepatobiliary Surgery, Southwest Hospital) for his help with HCC tissue microarray. We also thank Mrs. Yujun Zhang (Institute of Hepatobiliary Surgery, Southwest Hospital) for technical assistance in Animal experiment.

## SUPPLEMENTARY MATERIAL

The Supplementary Material for this article can be found online at: <https://www.frontiersin.org/articles/10.3389/fonc.2021.809195/full#supplementary-material>

- Huang CY, Lu TY, Bair CH, Chang YS, Jwo JK, Chang W. A Novel Cellular Protein, VPEF, Facilitates Vaccinia Virus Penetration Into HeLa Cells Through Fluid Phase Endocytosis. *J Virol* (2008) 82(16):7988–99. doi: 10.1128/jvi.00894-08
- Linaropoulou EV, Parghi SS, Friedman C, Osborn GE, Parkhurst SM, Trask BJ. Human Subtelomeric WASH Genes Encode a New Subclass of the WASP Family. *PLoS Genet* (2007) 3(12):e237. doi: 10.1371/journal.pgen.0030237
- Jia D, Gomez TS, Metlagel Z, Umetani J, Otwinowski Z, Rosen MK, et al. WASH and WAVE Actin Regulators of the Wiskott-Aldrich Syndrome Protein (WASP) Family are Controlled by Analogous Structurally Related Complexes. *Proc Natl Acad Sci USA* (2010) 107(23):10442–7. doi: 10.1073/pnas.0913293107
- Aleksic T, Gray N, Wu X, Rieunier G, Osher E, Mills J, et al. Nuclear IGF1R Interacts With Regulatory Regions of Chromatin to Promote RNA Polymerase II Recruitment and Gene Expression Associated With Advanced Tumor Stage. *Cancer Res* (2018) 78(13):3497–509. doi: 10.1158/0008-5472.CAN-17-3498
- Deng ZH, Gomez TS, Osborne DG, Phillips-Krawczak CA, Zhang JS, Billadeau DD. Nuclear FAM21 Participates in NF-kappaB-Dependent Gene Regulation in Pancreatic Cancer Cells. *J Cell Sci* (2015) 128(2):373–84. doi: 10.1242/jcs.161513
- Hao YH, Doyle JM, Ramanathan S, Gomez TS, Jia D, Xu M, et al. Regulation of WASH-Dependent Actin Polymerization and Protein Trafficking by Ubiquitination. *Cell* (2013) 152(5):1051–64. doi: 10.1016/j.cell.2013.01.051
- Harbour ME, Breusegem SY, Seaman MN. Recruitment of the Endosomal WASH Complex is Mediated by the Extended 'Tail' of Fam21 Binding to the Retromer Protein Vps35. *Biochem J* (2012) 442(1):209–20. doi: 10.1042/BJ20111761
- Szklarczyk D, Gable AL, Nastou KC, Lyon D, Kirsch R, Pyysalo S, et al. The STRING Database in 2021: Customizable Protein-Protein Networks, and Functional Characterization of User-Uploaded Gene/Measurement Sets. *Nucleic Acids Res* (2021) 49(D1):D605–D12. doi: 10.1093/nar/gkaa1074
- Huang D, Cao L, Xiao L, Song JX, Zhang YJ, Zheng P, et al. Hypoxia Induces Actin Cytoskeleton Remodeling by Regulating the Binding of CAPZA1 to F-Actin via PIP2 to drive EMT Hepatocellular. *Carcinoma Cancer Lett* (2019) 448:117–27. doi: 10.1016/j.canlet.2019.01.042
- Tang Z, Li C, Kang B, Gao G, Li C, Zhang Z. GEPIA: A Web Server for Cancer and Normal Gene Expression Profiling and Interactive Analyses. *Nucleic Acids Res* (2017) 45(W1):W98–W102. doi: 10.1093/nar/gkx247

22. Sivertsson A, Lindstrom E, Oksvold P, Katona B, Hikmet F, Vuu J, et al. Enhanced Validation of Antibodies Enables the Discovery of Missing Proteins. *J Proteome Res* (2020) 19(12):4766–81. doi: 10.1021/acs.jproteome.0c00486
23. Györfi B, Surowiak P, Budzies J, Lanczky A. Online Survival Analysis Software to Assess the Prognostic Value of Biomarkers Using Transcriptomic Data in non-Small-Cell Lung Cancer. *PLoS One* (2013) 8(12):e82241. doi: 10.1371/journal.pone.0082241
24. Huttlin EL, Bruckner RJ, Paulo JA, Cannon JR, Ting L, Baltier K, et al. Architecture of the Human Interactome Defines Protein Communities and Disease Networks. *Nature* (2017) 545(7655):505–9. doi: 10.1038/nature22366
25. Edwards M, Zwolak A, Schafer DA, Sept D, Dominguez R, Cooper JA. Capping Protein Regulators Fine-Tune Actin Assembly Dynamics. *Nat Rev Mol Cell Biol* (2014) 15(10):677–89. doi: 10.1038/nrm3869
26. Fokin AI, David V, Oguievetskaia K, Derivery E, Stone CE, Cao L, et al. The Arp1/11 Minifilament of Dynactin Primes the Endosomal Arp2/3 Complex. *Sci Adv* (2021) 7(3). doi: 10.1126/sciadv.abd5956
27. Hanahan D, Weinberg RA. The Hallmarks of Cancer. *Cell* (2000) 100(1):57–70. doi: 10.1016/s0092-8674(00)81683-9
28. Haffner MC, Esopi DM, Chaux A, Gurel M, Ghosh S, Vaghasia AM, et al. AIM1 is an Actin-Binding Protein That Suppresses Cell Migration and Micrometastatic Dissemination. *Nat Commun* (2017) 8(1):142. doi: 10.1038/s41467-017-00084-8
29. Pollard TD. The Cytoskeleton, Cellular Motility and the Reductionist Agenda. *Nature* (2003) 422(6933):741–5. doi: 10.1038/nature01598
30. Ge P, Durer ZA, Kudryashov D, Zhou ZH, Reisler E. Cryo-EM Reveals Different Coronin Binding Modes for ADP- and ADP-BeFx Actin Filaments. *Nat Struct Mol Biol* (2014) 21(12):1075–81. doi: 10.1038/nsmb.2907
31. Rotty JD, Wu C, Bear JE. New Insights Into the Regulation and Cellular Functions of the ARP2/3 Complex. *Nat Rev Mol Cell Biol* (2013) 14(1):7–12. doi: 10.1038/nrm3492
32. Lorenz M, Yamaguchi H, Wang Y, Singer RH, Condeelis J. Imaging Sites of N-Wasp Activity in Lamellipodia and Invadopodia of Carcinoma Cells. *Curr Biol* (2004) 14(8):697–703. doi: 10.1016/j.cub.2004.04.008
33. Jin KM, Lu M, Liu FF, Gu J, Du XJ, Xing BC. N-WASP Is Highly Expressed in Hepatocellular Carcinoma and Associated With Poor Prognosis. *Surgery* (2013) 153(4):518–25. doi: 10.1016/j.surg.2012.08.067
34. Derivery E, Sousa C, Gautier JJ, Lombard B, Loew D, Gautreau A. The Arp2/3 Activator WASH Controls the Fission of Endosomes Through a Large Multiprotein Complex. *Dev Cell* (2009) 17(5):712–23. doi: 10.1016/j.devcel.2009.09.010
35. Huang L, Lian J, Chen X, Qin G, Zheng Y, Zhang Y. WASH Overexpression Enhances Cancer Stem Cell Properties and Correlates With Poor Prognosis of Esophageal Carcinoma. *Cancer Sci* (2017) 108(12):2358–65. doi: 10.1111/cas.13400
36. Gomez TS, Billadeau DD. A FAM21-Containing WASH Complex Regulates Retromer-Dependent Sorting. *Dev Cell* (2009) 17(5):699–711. doi: 10.1016/j.devcel.2009.09.009
37. Zech T, Calaminus SD, Caswell P, Spence HJ, Carnell M, Insall RH, et al. The Arp2/3 Activator WASH Regulates Alpha5beta1-Integrin-Mediated Invasive Migration. *J Cell Sci* (2011) 124(Pt 22):3753–9. doi: 10.1242/jcs.080986
38. Monteiro P, Rosse C, Castro-Castro A, Irondelle M, Lagoutte E, Paul-Gilloteaux P, et al. Endosomal WASH and Exocyst Complexes Control Exocytosis of MT1-MMP at Invadopodia. *J Cell Biol* (2013) 203(6):1063–79. doi: 10.1083/jcb.201306162
39. Gautreau A, Oguievetskaia K, Ungermann C. Function and Regulation of the Endosomal Fusion and Fission Machineries. *Cold Spring Harb Perspect Biol* (2014) 6(3). doi: 10.1101/cshperspect.a016832
40. Dong R, Saheki Y, Swarup S, Lucast L, Harper JW, De Camilli P. Endosome-ER Contacts Control Actin Nucleation and Retromer Function Through VAP-Dependent Regulation of PI4P. *Cell* (2016) 166(2):408–23. doi: 10.1016/j.cell.2016.06.037

**Conflict of Interest:** The authors declare that the research was conducted in the absence of any commercial or financial relationships that could be construed as a potential conflict of interest.

**Publisher's Note:** All claims expressed in this article are solely those of the authors and do not necessarily represent those of their affiliated organizations, or those of the publisher, the editors and the reviewers. Any product that may be evaluated in this article, or claim that may be made by its manufacturer, is not guaranteed or endorsed by the publisher.

Copyright © 2022 Lu, Huang, Wang, Zheng, Liu, Song and Zheng. This is an open-access article distributed under the terms of the Creative Commons Attribution License (CC BY). The use, distribution or reproduction in other forums is permitted, provided the original author(s) and the copyright owner(s) are credited and that the original publication in this journal is cited, in accordance with accepted academic practice. No use, distribution or reproduction is permitted which does not comply with these terms.



# Metabolism-Associated Gene Signatures for FDG Avidity on PET/CT and Prognostic Validation in Hepatocellular Carcinoma

Hyunjong Lee<sup>1†</sup>, Joon Young Choi<sup>1†</sup>, Je-Gun Joung<sup>2,3</sup>, Jae-Won Joh<sup>4</sup>, Jong Man Kim<sup>4</sup> and Seung Hyup Hyun<sup>1\*</sup>

## OPEN ACCESS

### Edited by:

Alessandro Passardi,  
Scientific Institute of Romagna for the  
Study and Treatment of Tumors  
(IRCCS), Italy

### Reviewed by:

Chanisa Chotipanich,  
European Association of Nuclear  
Medicine, Austria  
Soňa Balogová,  
Comenius University, Slovakia

### \*Correspondence:

Seung Hyup Hyun  
shnm.hyun@samsung.com

<sup>†</sup>These authors have contributed  
equally to this work and share  
first authorship

### Specialty section:

This article was submitted to  
Gastrointestinal Cancers: Hepato  
Pancreatic Biliary Cancers,  
a section of the journal  
Frontiers in Oncology

**Received:** 30 December 2021

**Accepted:** 17 January 2022

**Published:** 31 January 2022

### Citation:

Lee H, Choi JY, Joung J-G, Joh J-W,  
Kim JM and Hyun SH (2022)  
Metabolism-Associated Gene  
Signatures for FDG Avidity on PET/CT  
and Prognostic Validation in  
Hepatocellular Carcinoma.  
Front. Oncol. 12:845900.  
doi: 10.3389/fonc.2022.845900

<sup>1</sup> Department of Nuclear Medicine, Samsung Medical Center, Sungkyunkwan University School of Medicine, Seoul, South Korea, <sup>2</sup> Samsung Genome Institute, Samsung Medical Center, Sungkyunkwan University School of Medicine, Seoul, South Korea, <sup>3</sup> Department of Biomedical Science, College of Life Science, CHA University, Seongnam, South Korea, <sup>4</sup> Department of Surgery, Samsung Medical Center, Sungkyunkwan University School of Medicine, Seoul, South Korea

**Introduction:** The prognostic value of F-18 fluorodeoxyglucose positron emission tomography/computed tomography (FDG PET/CT) in hepatocellular carcinoma (HCC) was established in previous reports. However, there is no evidence suggesting the prognostic value of transcriptomes associated with tumor FDG uptake in HCC. It was aimed to elucidate metabolic genes and functions associated with FDG uptake, followed by assessment of those prognostic value.

**Methods:** Sixty HCC patients with Edmondson–Steiner grade II were included. FDG PET/CT scans were performed before any treatment. RNA sequencing data were obtained from tumor and normal liver tissue. Associations between each metabolism-associated gene and tumor FDG uptake were investigated by Pearson correlation analyses. A novel score between glucose and lipid metabolism-associated gene expression was calculated. In The Cancer Genome Atlas Liver Hepatocellular Carcinoma dataset, the prognostic power of selected metabolism-associated genes and a novel score was evaluated for external validation.

**Results:** Nine genes related to glycolysis and the *HIF-1* signaling pathway showed positive correlations with tumor FDG uptake; 21 genes related to fatty acid metabolism and the *PPAR* signaling pathway demonstrated negative correlations. Seven potential biomarker genes, *PFKFB4*, *ALDOA*, *EGLN3*, *EHHADH*, *GAPDH*, *HMGCS2*, and *ENO2* were identified. A metabolic gene expression balance score according to the dominance between glucose and lipid metabolism demonstrated good prognostic value in HCC.

**Conclusions:** The transcriptomic evidence of this study strongly supports the prognostic power of FDG PET/CT and indicates the potential usefulness of FDG PET/CT imaging biomarkers to select appropriate patients for metabolism-targeted therapy in HCC.

**Keywords:** hepatocellular carcinoma, prognosis, FDG PET/CT, lipid metabolism, glucose metabolism, gene signatures

## INTRODUCTION

Hepatocellular carcinoma (HCC) is the most representative malignancy in the liver and the fourth leading cause of cancer death worldwide (1). Hepatectomy, liver transplantation, and trans-arterial chemoembolization are conventional treatment options for HCC (2). Recently, targeted agents such as sorafenib and nivolumab are used in patients with advanced HCC as palliative treatment (3, 4). There have been many previous studies to explore predictive factors for the prognosis and treatment response of HCC. The concentration of alpha-fetoprotein, prothrombin induced by vitamin K absence or antagonist II, and histological grade are the most well-known prognostic factors (5–7).

F-18 fluorodeoxyglucose positron emission tomography/computed tomography (FDG PET/CT) is a robust imaging modality used to diagnose malignancy (8). CT or magnetic resonance imaging (MRI) is especially useful in the diagnosis of HCC due to its specific finding of HCC, early enhancement in arterial phase, and delayed washout in portal phase (9). The diagnostic performance of FDG PET/CT is inferior to CT and MRI as there are tumors with low FDG uptake or isometabolic uptake, which are difficult to discriminate from normal liver tissue (10, 11). Nevertheless, the prognostic value of FDG PET/CT in HCC has been revealed to be highly significant in many previous studies (12–15).

Prior research has suggested possible key proteins that affect tumor FDG uptake in HCC. Lee et al. showed that hexokinase II (*HK2*) is expressed in HCC in contrast to glucose transporter 1 (*GLUT1*), which is expressed in cholangiocarcinoma (16). They also reported genes related to cell survival to be associated with high FDG uptake (17). Recently, Xia et al. found that hypoxia-induced glucose transporters may contribute to FDG uptake in HCC based on radiogenomics results (18). However, previous studies recruited less than 20 patients. In addition, there are no previous reports suggesting the prognostic value of transcriptomes associated with FDG uptake in HCC tumors. It is expected that exploring metabolic genes or functions associated with FDG uptake and evaluating their prognostic value can strongly support not only the prognostic value of FDG PET/CT but also reveal molecular functions affecting FDG uptake in HCC.

In this study, we aimed to elucidate significant metabolic genes and functions associated with FDG uptake in HCC transcriptomes as an RNA-sequencing dataset. Subsequently, the prognostic value of the genes and gene set expression scores were assessed. Ultimately, transcriptomic evidence highlighted the prognostic power of FDG PET/CT in HCC.

## METHODS

### Subjects

Between May 2009 and August 2015, patients who underwent curative surgery for HCC and pretreatment FDG PET/CT were enrolled. We identified 120 eligible samples (60 tumor tissues

and 60 paired normal liver tissues) in 60 patients (49 males and 11 females; mean age,  $58.1 \pm 8.8$  years) from the Samsung Medical Center Biobank. A single nodule of HCC was present in all patients. Samples were obtained after surgical resection prior to radiation or chemotherapy and were stored in liquid nitrogen. In all tumor samples, the pathological diagnosis and Edmondson–Steiner grade were verified by a pathologist. Only tumor samples with Edmondson–Steiner grade II were included in the study cohort, and the other samples of other grades were excluded, as there is a high variation of FDG avidity depending on the cell differentiation grade. Samples were collected in accordance with the guidelines issued by the ethics committee of our institution, and written informed consent was obtained from all patients. Our institutional review board approved this retrospective study (IRB #2017-04-022). Demographic and clinical characteristics and survival data were obtained from electronic medical records.

### FDG PET/CT Acquisition and Image Analysis

All patients fasted for at least 6 hours and had blood glucose levels of less than 200 mg/dL at the time of FDG PET/CT. Whole-body PET and CT images from the basal skull to mid-thigh were acquired 60 minutes after 5.0 MBq/kg FDG injection without intravenous or oral contrast on a dedicated PET/CT scanner (Discovery STE, GE Healthcare, Milwaukee, WI). Continuous spiral CT was performed with a 16-slice helical CT (140 keV, 30–170 mA). An emission scan was then obtained from head to thigh for 2.5 minutes per frame in 3-dimensional mode. PET images were reconstructed using CT, and attenuation correction was performed using the ordered-subsets expectation-maximization algorithm with 20 subsets and 2 iterations (matrix size, 128×128; voxel size, 3.9×3.9×3.3 mm).

All images were reviewed by a board-certified nuclear medicine physician using volume viewer software on a GE Advantage Workstation, version 4.7. The maximum standardized uptake value (SUV<sub>max</sub>) of the primary tumor was measured using a spherical volume of interest over the primary tumor. The mean SUV (SUV<sub>mean</sub>) of the normal liver was obtained by taking the average of the three 2-cm-diameter spherical VOIs (two in the right lobe and one in the left lobe). Tumor FDG avidity was measured by tumor-to-normal liver SUV ratio (TLR), calculated with the following equation:  $TLR = SUV_{max} \text{ of the tumor} / SUV_{mean} \text{ of the normal liver}$ .

### RNA Sequencing

Frozen sections from each tissue sample were homogenized in TRIZOL reagent (Invitrogen, Carlsbad, CA, USA). Total RNA was extracted using a standard chloroform protocol followed by purification with the Qiagen RNeasy Mini Kit (QIAGEN Inc, Valencia, CA, USA). RNA integrity was evaluated using RNA 6000 Nano LabChips on an Agilent 2100 Bioanalyzer (Agilent Technologies, Foster City, CA, USA). RNA purity was assessed by the ratio of spectrophotometric absorbance at 260 and 280 nm (A<sub>260</sub>/A<sub>280</sub> nm) using NanoDrop ND-1000 (NanoDrop Inc, Wilmington, DE, USA). Library construction for RNA



sequencing was performed using a Truseq RNA Sample Preparation v2 Kit (Illumina). Isolated total RNA was used in a reverse transcription reaction with poly (dT) primers using SuperScript™ II Reverse Transcriptase (Invitrogen) according to the manufacturer's protocol. Briefly, an RNA sequencing library was prepared by cDNA amplification, end-repair, 3' end adenylation, and adapter ligation. Library quality and quantity were measured using the Agilent 2100 Bioanalyzer and Qubit. Sequencing of the RNA library was carried out using the 100 bp paired-end mode of the TruSeq Rapid PE Cluster Kit and the TruSeq Rapid SBS Kit (Illumina). Reads from the FASTQ files were mapped to the hg19 human reference genome using TopHat version 2.0.6 (<http://tophat.cbcb.umd.edu/>). Raw read counts mapped to genes were measured using the BAM format file by HTSeq, version 0.6.1 (<https://htseq.readthedocs.io>). Read counts were normalized using the TMM (Trimmed Mean of M-values normalization) method. The expression of genes in tumor tissue was divided by that in normal liver tissue to calculate the fold change of gene expression. The fold changes were normalized by  $\log_2$  transformation.

## Gene Sets and Molecular Functions Associated With FDG Uptake in HCC

Metabolism-associated genes encoding proteins involved in glucose and lipid metabolism were selected from the Molecular Signature Database (mSigDB). A set of 404 genes was manually curated for further transcriptomic analysis. Pearson correlation analyses were performed between the expression of metabolism-associated genes and TLRs. All genes with positive or negative correlations ( $p < 0.05$ ) were defined as metabolism-associated genes related to tumor FDG uptake. In each gene set, REACTOME and KEGG enrichment analysis was conducted to investigate the molecular pathways associated with tumor FDG uptake using the “signatureSearch” package in R/Bioconductor (19). In each metabolism-associated gene set, a gene expression signature score (GESS) was defined as the mean z-score of each gene expression. We calculated a novel balance score between glucose and lipid metabolism-associated gene expression in HCC (metabolic balance score) by subtracting the GESS of lipid metabolism from the GESS of glucose metabolism. The concept of subtracting the average of z-score of each gene set was already applied in a previous study to evaluate a value of epithelial-mesenchymal transition score in lung cancer (20).

## Prognostic Validation of Metabolism-Associated Genes

Among the investigated metabolism-associated genes, those with significant correlation with TLR were selected as subject genes for further analysis. Prognostic validation of metabolism-associated genes was performed in The Cancer Genome Atlas Liver Hepatocellular Carcinoma (TCGA-LIHC) dataset. Clinical and gene expression data of TCGA-LIHC patients were obtained from cBioPortal using “cgdsr” and “TCGAbiolinks” packages in R/Bioconductor. Among the whole dataset, 325 patients with

disease-free survival (DFS) data and 376 patients with overall survival (OS) data were included in this study. As previously described, the GESS of glucose metabolism, the GESS of lipid metabolism, and the metabolic balance score between them were calculated. A zero for metabolic balance score was used as a cutoff to classify subjects into two risk stratification groups.

Regarding multivariable Cox regression analysis, variables with a  $p$ -value less than 0.1 in univariable analyses were included. Variables with collinearity were excluded. Metabolism-associated genes with univariable  $p$ -values less than 0.1 for both DFS and OS were selected as potential components of the biomarker gene set. The prognostic index (PI) was developed using Cox proportional hazards regression model to validate risk stratification with the biomarker gene set. Risk stratification groups were divided by a median value of PI. The expression of each potential biomarker gene was compared between each group using independent t-test. Gene mutation data were downloaded from the genomic data commons (<https://gdc.cancer.gov/>), and a mutation annotation format file was constructed using the “read.maf” function included in the “maftools” package in R/Bioconductor (21). The difference of *TP53* and *CTNNB1* mutations between risk groups was evaluated by Chi-square test. All the statistical analyses were performed using R software (v4.0.4, R Foundation for Statistical Computing, Vienna, Austria). A  $p$ -value less than 0.05 was considered statistically significant.

## RESULTS

### Patients

The patient characteristics are summarized in **Table 1**. In 31 patients (51.7%), tumors with TLRs greater than or equal to median value of TLR presented the high TLR phenotype. In the remaining 29 patients (48.3%), tumors with TLRs less than median value of TLR were assigned to the low TLR phenotype. The median value of TLR was 1.7. TLRs ranged from 1.7 to 6.8 (mean: 2.8) for high TLR tumors and from 1.1 to 1.7 (mean: 1.4) for low TLR tumors. Milan criteria compliance ( $p = 0.014$ ), young age ( $p = 0.025$ ), large tumor size ( $p = 0.005$ ), and the presence of microvascular invasion ( $p < 0.001$ ) were significantly associated with high TLR phenotype. There were no significant associations between TLR and gender, normal liver SUV, HCC etiology, or presence of liver cirrhosis.

### Metabolism-Associated Genes and Molecular Functions Related to Tumor FDG Uptake

There were 42 genes with significant positive correlations and 87 genes with significant negative correlations ( $p < 0.05$ ) with tumor FDG uptake. The list of genes is described in **Supplementary Table 1**. Gene set enrichment analysis according to TLR using the REACTOME and KEGG databases demonstrated upregulated glucose metabolism, including glycolysis and hypoxia-inducible factor-1 (*HIF-1*) signaling pathway upregulation, and downregulated lipid metabolism, including

**TABLE 1** | Clinical characteristics of patients.

Characteristics	Overall (n = 60)	Low TLR (n = 29)	High TLR (n = 31)	p
Age (range, years)	58.1 (42-76)	60.7 (43-76)	55.6 (42-73)	0.025
Sex, male	49 (81.7%)	24 (82.8%)	25 (80.6%)	1.000
Tumor size (cm)	4.4 ± 1.4	3.8 ± 1.3	4.9 ± 1.3	0.005
Milan criteria compliance	40 (66.7%)	24 (82.8%)	16 (51.6%)	0.014
Tumor SUV	4.5 ± 2.6	3.1 ± 0.5	5.9 ± 3.1	<0.001
Normal liver SUV	2.2 ± 0.3	2.2 ± 0.3	2.1 ± 0.3	0.166
TLR	2.1 ± 1.2	1.4 ± 0.2	2.8 ± 1.4	<0.001
Etiology				
HBV	46 (76.7%)	23 (79.3%)	23 (74.2%)	0.431
HCV	5 (8.3%)	1 (3.4%)	4 (12.9%)	
Alcohol and others	9 (15.0%)	5 (17.2%)	4 (12.9%)	
Cirrhosis				
No	38 (63.3%)	20 (69.0%)	18 (58.1%)	0.544
Yes	22 (36.7%)	9 (31.0%)	13 (31.9%)	
Microvascular invasion				
No	30 (50.0%)	22 (75.8%)	8 (25.8%)	<0.001
Yes	30 (50.0%)	7 (24.2%)	23 (74.2%)	

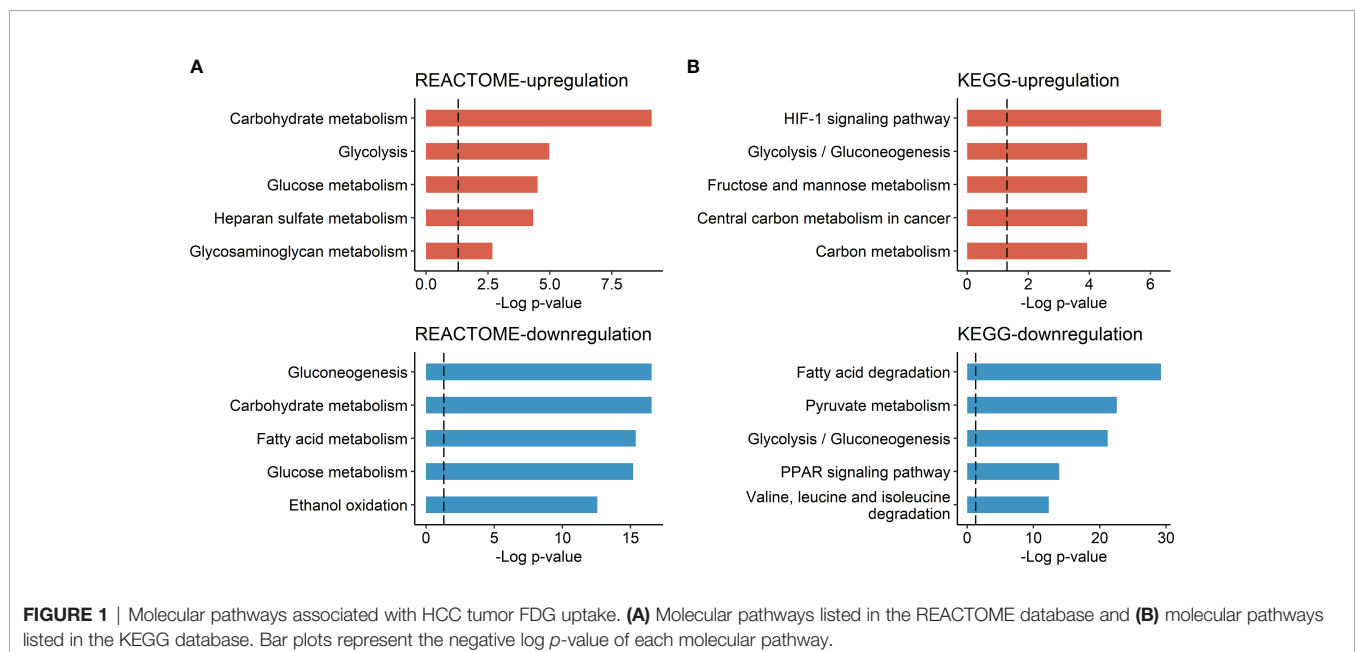
Data are numbers of patients (proportion) or mean values ± standard deviation. Tumor with TLR more than median value was assigned high TLR phenotype. SUV, standardized uptake value; TLR, Tumor-to-normal liver SUV ratio.

fatty acid metabolism and peroxisome proliferator-activated receptor (*PPAR*) signaling pathway downregulation, in HCC with high TLR phenotype (**Figure 1**).

Considering the overlap of genes in these molecular pathways, the upregulated gene sets involved in glycolysis and *HIF-1* signaling were merged into a glucose metabolism-associated gene set. The downregulated gene sets involved in fatty acid metabolism and the *PPAR* signaling pathway were merged into a lipid metabolism-associated gene set. There were nine genes with positive correlation among the glucose metabolism-associated gene set and 21 genes with negative correlation among the lipid metabolism-associated gene set.

The list of glucose metabolism-associated genes and lipid metabolism-associated genes related to tumor FDG uptake are described in **Supplementary Tables 2, 3**, respectively.

The GESS of glucose metabolism showed a positive correlation with tumor FDG uptake ( $r = 0.607$  and  $p < 0.001$ ). The GESS of lipid metabolism showed a negative correlation with tumor FDG uptake ( $r = -0.562$  and  $p < 0.001$ ). The metabolic balance score showed a positive correlation with tumor FDG uptake ( $r = 0.639$ ,  $p < 0.001$ ). A heatmap visualized the expression of the top 5 genes with high correlation coefficients, the GESSs of each metabolism, and TLR values according to the metabolic balance score (**Figure 2**).



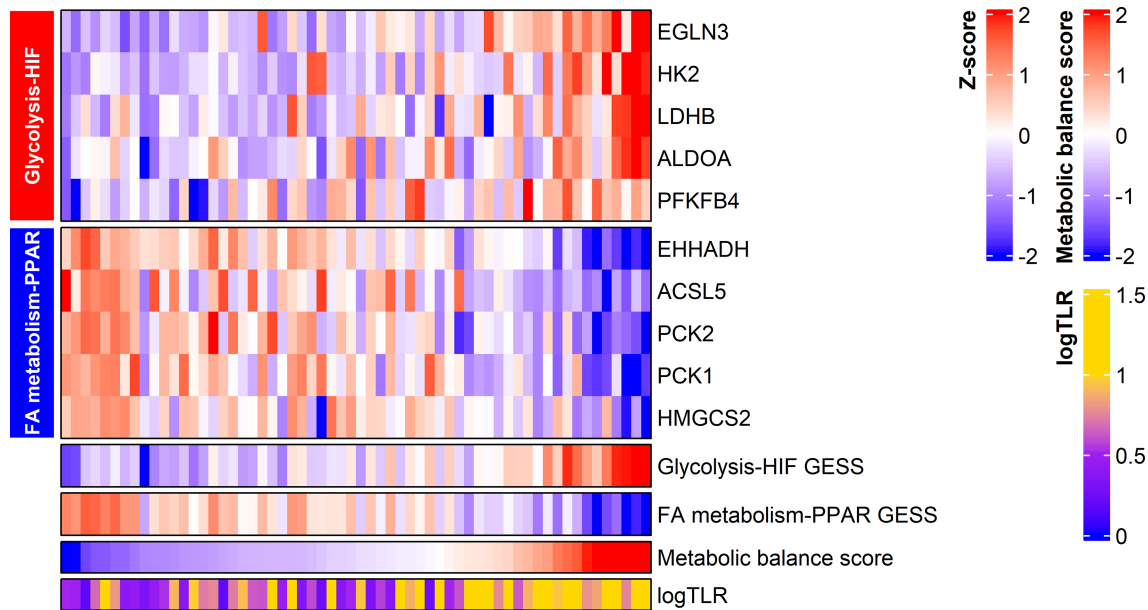


**FIGURE 2** | Expression of metabolism-associated genes related to HCC tumor FDG uptake. The expression of the top five genes from each gene set are displayed in the heatmap. Metabolic balance score showed a positive correlation with TLR in HCC. logTLR, tumor-to-normal liver standardized uptake value ratio in log scale base 2; HIF, hypoxia-inducible factor-1; FA, fatty acid.

## Prognostic Validation of Metabolism-Associated Genes in the TCGA-LIHC Dataset

By means of univariable Cox regression analysis for DFS, *PFKFB4*, *ALDOA*, *EGLN3*, *CYP4A22*, *PCK1*, *ACADL*, *CYP4A11*, *EHHADH*, *GAPDH*, *HMGCS2*, and *ENO2* genes were found to have *p*-values of less than 0.1 in Wald test. In multivariate Cox regression analysis for DFS, *PFKFB4* was an independent prognostic gene (**Table 2**). In univariable Cox regression analysis for OS, *PFKFB4*, *EGLN3*, *ALDOA*, *GAPDH*, *HK2*, *ENO2*, *PFKFB3*, *HIF1A*, *HMGCS2*, *EHHADH*, *ECI1*, and *LDHB* genes had *p*-values less than 0.1. In multivariable Cox

regression analysis for OS, *PFKFB4*, *EGLN3*, *GAPDH*, *HMGCS2*, and *ECI1* were independent prognostic genes (**Table 3**).

Seven metabolism-associated genes, including *PFKFB4*, *ALDOA*, *EGLN3*, *EHHADH*, *GAPDH*, *HMGCS2*, and *ENO2*, were potential prognostic biomarkers for HCC. Kaplan-Meier curves showed a significantly worse DFS ( $p = 0.001$ ) and OS ( $p < 0.001$ ) in patients with high-risk GESS compared to those with low-risk GESS (**Figure 3**). The expression levels of *PFKFB4*, *ALDOA*, *EGLN3*, *GAPDH*, and *ENO2* were significantly higher in the high-risk group for OS, while the expression levels of *EHHADH* and *HMGCS2* were significantly lower in the high-risk group for OS ( $p < 0.001$ , **Figure 4**).

**TABLE 2** | Cox regression analysis of disease-free survival for metabolism-associated genes.

Genes	Disease-free survival					
	Univariate			Multivariate		
	HR	95% CI	P	HR	95% CI	P
PFKFB4	1.192	1.081-1.314	< 0.001	1.208	1.049-1.390	0.009
ALDOA	1.203	1.060-1.366	0.004	1.159	0.905-1.484	0.243
EGLN3	1.094	1.028-1.166	0.005	1.061	0.967-1.164	0.212
CYP4A22	0.939	0.892-0.988	0.016	0.962	0.864-1.071	0.476
PCK1	0.942	0.897-0.990	0.019	0.992	0.922-1.068	0.832
ACADL	0.948	0.904-0.994	0.026	0.951	0.982-1.014	0.123
CYP4A11	0.937	0.883-0.995	0.033	1.061	0.941-1.196	0.335
EHHADH	0.905	0.825-0.992	0.033	1.033	0.888-1.202	0.673
GAPDH	1.185	1.005-1.397	0.043	0.889	0.681-1.161	0.388
HMGCS2	0.922	0.851-0.999	0.046	0.971	0.851-1.107	0.655
ENO2	1.085	0.998-1.179	0.055	0.884	0.769-1.015	0.081

HR, hazard ratio; CI, confidence interval.

**TABLE 3** | Cox regression analysis of overall survival for metabolism-associated genes.

Genes	Overall survival					
	Univariate			Multivariate		
	HR	95% CI	P	HR	95% CI	P
PFKFB4	1.315	1.181-1.465	< 0.001	1.174	1.004-1.373	0.045
EGLN3	1.188	1.103-1.279	< 0.001	1.134	1.006-1.278	0.039
ALDOA	1.329	1.162-1.520	< 0.001	Excluded due to collinearity		
GAPDH	1.445	1.202-1.738	< 0.001	1.383	1.058-1.809	0.018
HK2	1.147	1.061-1.241	< 0.001	1.104	0.907-1.134	0.804
ENO2	1.157	1.060-1.263	0.001	0.833	0.705-0.984	0.031
PFKFB3	1.168	1.062-1.286	0.001	1.115	0.954-1.304	0.172
HIF1A	1.228	1.070-1.411	0.004	0.937	0.754-1.165	0.560
HMGCS2	0.907	0.844-0.975	0.008	0.890	0.795-0.997	0.043
EHHADH	0.908	0.819-1.006	0.065	1.124	0.950-1.328	0.173
ECI1	0.804	0.628-1.028	0.082	0.727	0.538-0.984	0.039
LDHB	1.117	0.983-1.271	0.090	0.989	0.850-1.152	0.891

HR, hazard ratio; CI, confidence interval.

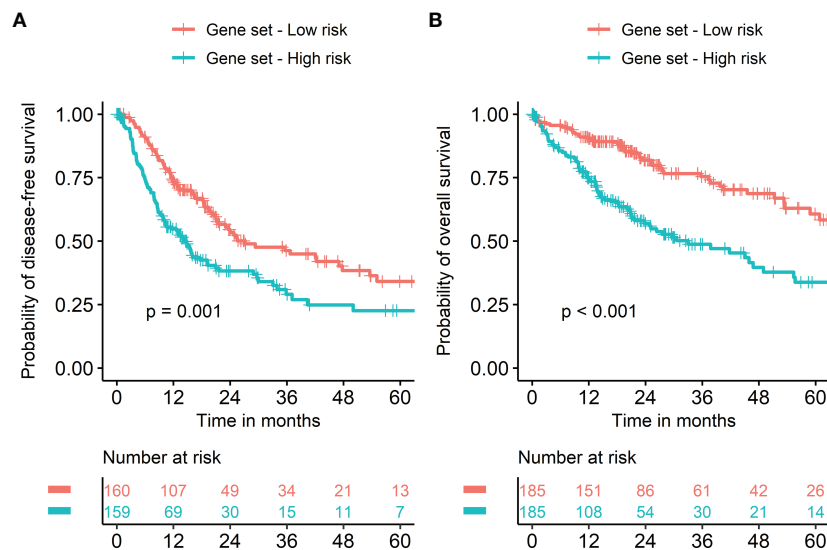


**FIGURE 3** | Survival of HCC patients according to the biomarker gene expression signature. Risk groups were classified according to prognostic index with seven biomarker genes (*PFKFB4*, *ALDOA*, *EGLN3*, *EHHADH*, *GAPDH*, *HMGCS2*, and *ENO2*). Kaplan-Meier curves showed a significantly worse prognosis in patients with high-risk gene expression signatures compared to those with low-risk gene expression signatures in terms of both disease-free (A) and overall survival (B).

Stratifying metabolic balance scores using a cutoff of zero demonstrated significant differences in DFS ( $HR = 1.22$  and  $p = 0.002$ ) and OS ( $HR = 1.33$  and  $p < 0.001$ ) according to metabolic dominance (glucose versus lipid, **Figure 5**). The proportion of high-risk patients with *TP53*-mutant HCC was significantly higher than that of those with wild-type *TP53* (57.9% vs. 36.7%,  $p < 0.001$ , **Supplementary Figure 1A**). The proportion of low-risk patients with *CTNNB1*-mutant HCC was significantly higher than that of patients with wild-type *CTNNB1* (74.7% vs. 53.0%,  $p < 0.001$ , **Supplementary Figure 1B**). A heatmap was used to visualize the expression level of 30 metabolism-associated genes according to risk group (**Supplementary Figure 2**).

## DISCUSSION

FDG PET/CT is the representative imaging modality to explore biologic tumor characteristics. Particularly in HCC, FDG PET/CT imaging findings have unique characteristics compared to other malignancies. Although many kinds of malignancies show high FDG uptake, it is not uncommon for HCC tumors to show low FDG uptake or isometabolic uptake, which is difficult to discriminate from normal liver tissue. This is not only due to the relatively high physiologic uptake of liver tissue but also due to the biologic characteristics of HCC. Therefore, previous studies have attempted to investigate proteins and genes affecting FDG



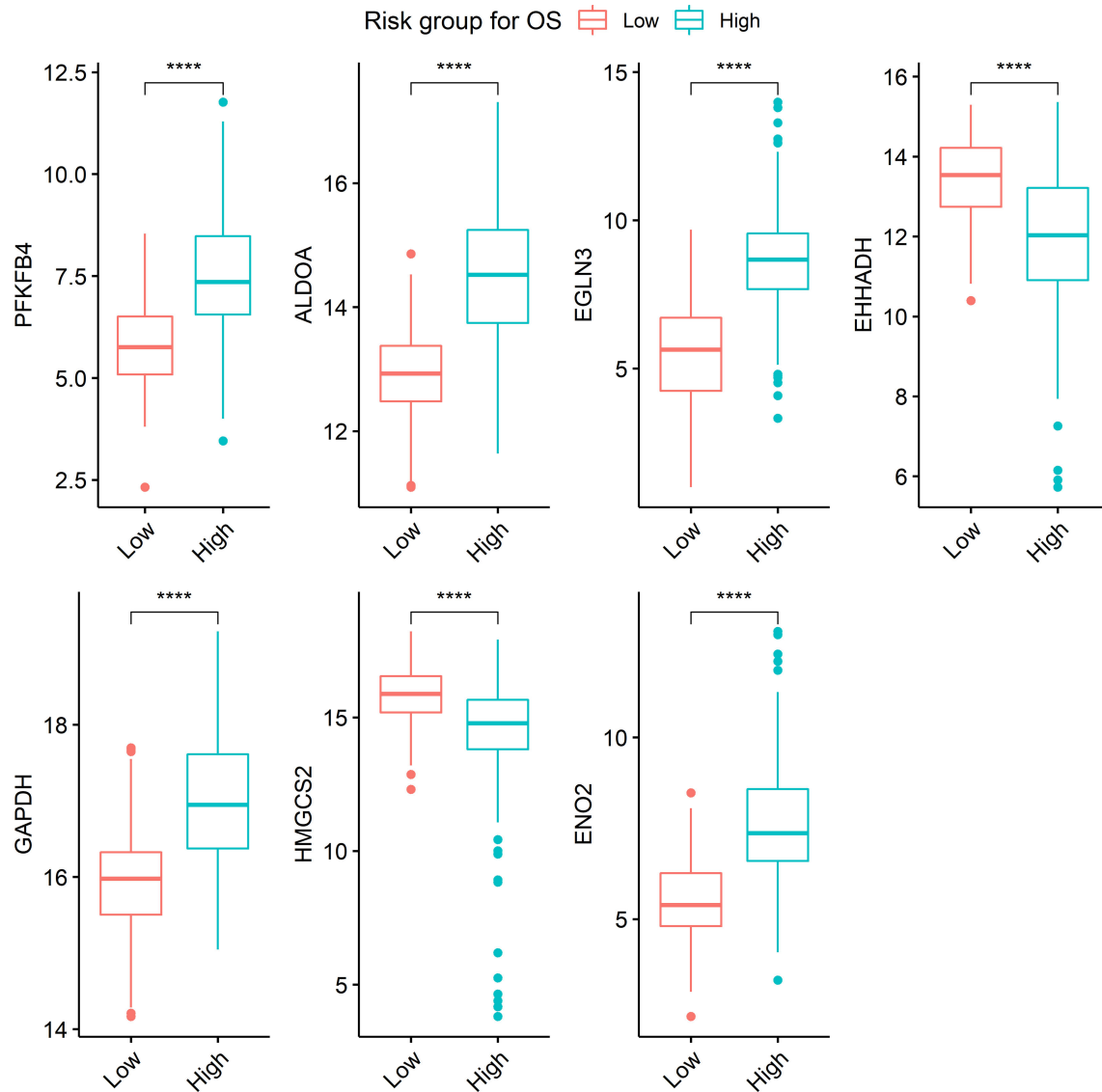


**FIGURE 4** | Boxplots visualizing the expression level of genes according to risk groups. \*\*\*\*The expression level of each gene was significantly different between risk groups ( $p < 0.001$ ). Boxplots represent the expression level of seven genes, *PFKFB4*, *ALDOA*, *EGLN3*, *EHHADH*, *GAPDH*, *HMGCS2*, and *ENO2*.

uptake in HCC. Izuishi et al. showed that increased levels of *GLUT1* and decreased levels of glucose-6-phosphatase are associated with high HCC FDG uptake (22). Chen et al. revealed an inverse correlation between the expression of fructose 1,6-bisphosphatase 1 and FDG uptake (23). Lee et al. investigated the characteristics of gene expression profiles according to FDG uptake in ten patients with HCC (17). Contrary to the aforementioned research, the present study performed an explorative investigation of metabolism-associated gene expression within 60 patients, which is the largest cohort for a radiogenomics HCC study to the best of our knowledge.

In this study, molecular pathways of glycolysis and *HIF-1* signaling were revealed to be positively associated with HCC

tumor FDG uptake. Glycolysis is the most representative mechanism to affect tumor glucose uptake. Tumor cells promote *HIF-1* signaling to resist hypoxic conditions. The *HIF-1* signaling pathway enhances the anaerobic glycolytic pathway to provide energy for tumor cells (24). The result of this study implies that resistance to hypoxic conditions mainly contributes to glucose uptake in HCC. Although there are previous reports that *HIF-1* signaling correlates with FDG uptake in other types of cancer, such as lung cancer and breast cancer (25, 26), there was no transcriptomic evidence of the association between *HIF-1* signaling and FDG uptake in HCC.

Notably, *PFKFB4* showed a significant, positive correlation with FDG uptake. It was a significant, independent prognostic gene for survival in the TCGA-LIHC dataset. *PFKFB*

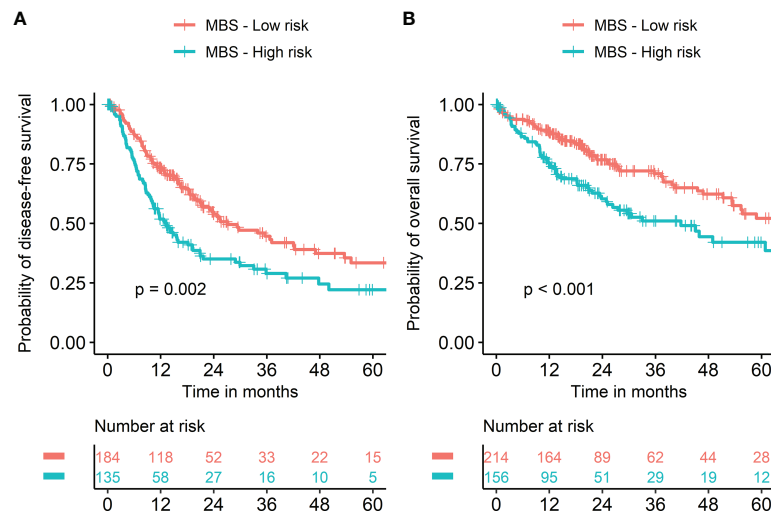


**FIGURE 5 |** Kaplan-Meier survival curves according to metabolic balance score. Risk groups were classified into two groups using metabolic balance score (MBS). Kaplan-Meier curves showed significantly worse prognosis in patients with high MBS compared to those with low MBS in terms of both disease-free (A) and overall survival (B).

enzymes produce fructose-2,6-bisphosphate, which activates 6-phosphofructo-1-kinase, a rate-limiting enzyme in glycolysis (27). It was revealed as a poor prognostic factor in HCC (28). Interestingly, *EGLN3* was another significant, independent prognostic gene for OS in the TCGA-LIHC dataset among the other metabolism-associated genes related to tumor FDG uptake. *PHD3*, which is a protein encoded by the *EGLN3* gene, has tumor suppressor functions in various cancer types (29–31). However, there is controversy surrounding the prognostic value of *PHD3* in cancer. Previous studies suggested that *PHD3* downregulation is correlated with HCC aggressiveness and poor prognosis (32, 33). On the other hand, some reports indicated that increased *PHD3* had an association with poor prognosis in other cancer subtypes (34, 35). The results of this study support the effect of increased *PHD3* on unfavorable prognosis. *EGLN3*, a target gene of the *HIF-1* protein, induces positive feedback following enhanced *HIF-1* activity (36). In this regard, increased *PHD3* expression under hypoxia was shown to enhance cancer cell survival and the progression of disease (37). In addition, *PFKFB4* is induced by *HIF-1* activation in hypoxic conditions (38). In brief, it is suggested that upregulation of the glycolytic pathway via *PFKFB4* in hypoxic conditions mainly affects poor prognosis in HCC. Furthermore, the results of the present study strongly support previous knowledge that high tumor FDG uptake in HCC is associated with poor prognosis and hypoxic tumor microenvironmental conditions (14, 15).

Fatty acid metabolism and *PPAR* signaling were downregulated functions alongside increased FDG uptake. This result is readily understandable, as the *PPAR* signaling pathway regulates fatty acid oxidation (39). Tanaka et al. suggested the de-differentiation of HCC to be correlated with reduced fatty acid oxidation and increased glycolysis (40). In this aspect, the present study is consistent with the well-established knowledge that poorly differentiated HCCs demonstrate high FDG uptake (41).

In addition, *HMGCS2* and *ECI1*, involved with fatty acid metabolism, are correlated with good prognosis with respect to OS, supported by previous knowledge that the suppression of fatty acid oxidation promotes the growth and metastasis of HCC (42). Furthermore, this result supports that PET/CT using C-11 acetate or F-18 fluorocholine tracers to visualize HCC with low FDG uptake due to enhanced fatty acid metabolism (43, 44).

We calculated the unified metabolic reprogramming scale representing the balance between glucose versus lipid metabolism gene expression in HCC. A high metabolic balance score was hypothesized to represent the metabolic shift to glycolytic process from fatty acid metabolism. This score showed an excellent correlation with tumor FDG uptake. The cutoff of zero, which is supposed as the balanced state of glucose versus lipid metabolism, showed good prognostic stratification. In brief, metabolic shift to glucose metabolism from lipid metabolism contributes to tumor FDG uptake and poor prognosis in HCC. Furthermore, there were significant differences in *TP53* and *CTNNB1* mutation between risk groups according to metabolic balance score. This suggests that metabolic characteristics may be associated with the genetic mutation profile, consistent with a previous report of HCC transcriptome classification demonstrating the associations between *TP53* mutation and the cell cycle as well as those between *CTNNB1* mutation and the *Wnt* pathway (45). In addition, there are similar studies reporting enhanced glycolysis in *TP53*-mutant HCCs and enhanced fatty acid oxidation in *CTNNB1*-mutant HCCs (46, 47).

We selected seven gene signatures associated with tumor FDG uptake in HCC. A prognostic model with those genes showed excellent stratification for both DFS and OS. In addition, those genes may have significance in selecting potential candidates for individualized therapy in terms of precision medicine. Sorafenib, as a kinase inhibitor, and nivolumab, as

an immune checkpoint inhibitor, have been recently used for molecular targeted therapy (3, 4). The therapeutic effect of sorafenib is decreased under hypoxic conditions (48). In addition, suppressing glycolysis results in re-sensitizing HCC cells to sorafenib (49). As glycolytic activity and *HIF-1* signaling are activated in tumors with high FDG uptake, the application of sorafenib may be considered referring to FDG PET/CT findings. In particular, CD147 is a favorable therapeutic target with respect to the metabolic reprogramming of HCC. Within glucose metabolism, CD147 promotes tumor growth through the regulation of glycolysis *via* degradation of p53 protein (50). In addition, p53 downregulates the expression of *PFKFB4*, which showed an excellent correlation with tumor FDG uptake and good prognostic power in the present study (51). Within fatty acid metabolism, CD147 induces tumor growth by regulating fatty acid oxidation *via* inhibition of PPAR- $\alpha$ . In brief, inhibition of CD147 may be a novel therapeutic strategy for metabolism modulation (52). One clinical study showed the treatment effects of  $^{131}\text{I}$ -metuximab, which is a radioimmunoconjugate of iodine-131, and monoclonal antibody targeting CD147. It provided profit in survival rate and recurrence rate in HCC patients that underwent radiofrequency ablation (53). This study indicates that FDG PET/CT may be a good diagnostic modality to select candidates for metabolism-targeted therapy. CD147-targeted therapy to inhibit glycolysis and disinherit fatty acid metabolism should be considered for patients with high tumor FDG uptake. Further study is warranted to evaluate the role of FDG PET/CT imaging biomarkers to select appropriate patients for metabolism-targeting therapy.

In brief, the present study has several clinical implications. First, conventional microscopic assessment of HCC is not fully standardized so that there is limitation to predict prognosis and select individualized therapeutic option accurately. The concrete transcriptomic evidence suggested in this study may be validated and utilized in personalized medicine in terms of tumor metabolism. Second, FDG PET/CT as a non-invasive functional imaging is commonly performed in initial workup for malignant disease including HCC. It is usually conducted prior to biopsy or surgery which allows obtaining histological samples. Metabolic characteristics of HCC as well as presence of metastasis provided by FDG PET/CT will contribute to predict prognosis and plan further treatment or follow-up. Furthermore, it is expected to support surrogate information for histopathologic findings as TLR showed a good association with microvascular invasion which is an important prognostic factor (data not shown). Third, transcriptomic examination is not commonly utilized in clinical field due to its high cost and requirement of high-end analytic instruments. FDG PET/CT may provide information of glucose metabolism which can be obtained from genomic analysis. In addition, a useful complementary information for lipid metabolism of HCC can be obtained with other tracers such as F-18 fluorocholine (54, 55).

There are several limitations to this study. First, a prognostic validation analysis could not be performed in subjects with both

FDG PET/CT imaging and RNA-seq data due to a limited sample size. Further study as an internal and external validation is warranted to analyze prognostic power. Second, we have focused on metabolism-associated genes related to tumor FDG uptake. Although there are many biological functions and pathways that affect tumor FDG uptake in HCC, we did not cover the whole transcriptome. Nevertheless, the limited scope of subject genes aided in the analysis of significant molecular pathways by removing genes irrelevant to key metabolic processes.

In conclusion, metabolism-associated genes and molecular functions associated with tumor FDG uptake were explored in HCC. Increased tumor FDG uptake was found to be associated with glycolysis and *HIF-1* signaling pathway upregulation, whereas fatty acid metabolism and PPAR signaling were downregulated. Metabolic balance score representing the gene expression balance between glucose versus lipid metabolism in HCC showed a good association with tumor FDG uptake. It also showed excellent prognostic power in the TCGA-LIHC dataset. Seven genes, *PFKFB4*, *ALDOA*, *EGLN3*, *EHHADH*, *GAPDH*, *HMGCS2*, and *ENO2*, related to tumor FDG uptake were revealed to have a good prognostic value for survival in HCC. This study suggested key metabolic pathways to potentially affect tumor FDG uptake in HCC. The transcriptomic evidence of this study strongly supports the prognostic power of FDG PET/CT and indicates the potential usefulness of FDG PET/CT imaging to select appropriate HCC patients for metabolism-targeted therapy.

## DATA AVAILABILITY STATEMENT

The datasets presented in this study can be found in online repositories. The names of the repository/repositories and accession number(s) can be found below: NCBI under BioProject PRJNA794275.

## ETHICS STATEMENT

The studies involving human participants were reviewed and approved by Samsung Medical Center Institutional Review Board. Written informed consent for participation was not required for this study in accordance with the national legislation and the institutional requirements.

## AUTHOR CONTRIBUTIONS

HL, JYC, and SH designed the study. J-GJ, J-WJ, and JK contributed to data collection. HL and SH performed data analysis and interpretation. HL and SH drafted the article. JYC and J-GJ provided critical revision of the article. All authors contributed to the article and approved the submitted version.

## FUNDING

This research was supported by the Basic Science Research Program through the National Research Foundation of Korea (NRF) funded by the Ministry of Science and ICT (Grant No. NRF-2017R1A2B4006598).

## SUPPLEMENTARY MATERIAL

The Supplementary Material for this article can be found online at: <https://www.frontiersin.org/articles/10.3389/fonc.2022.845900/full#supplementary-material>

## REFERENCES

- El-Serag HB. "The Liver: Biology and Pathobiology,". *Epidemiol Hepatocellular Carcinoma* (Wiley-Blackwell) (2020) 758-72. doi: 10.1002/9781119436812.ch59
- NCCN. *National Comprehensive Cancer Network Hepatobiliary Cancers (Version 5.2021)* [Online] (2021). Available at: [https://www.nccn.org/professionals/physician\\_gls/pdf/hepatobiliary.pdf](https://www.nccn.org/professionals/physician_gls/pdf/hepatobiliary.pdf) (Accessed October 21, 2021).
- Llovet J, Ricci S, Mazzaferro V, Hilgard P, Raoul J, Zeuzem S, et al. Randomized Phase III Trial of Sorafenib Versus Placebo in Patients With Advanced Hepatocellular Carcinoma (HCC). *J Clin Oncol* (2007) 25 (18\_suppl):LBA1-1. doi: 10.1200/jco.2007.25.18\_suppl.lba1
- El-Khoueiry AB, Sangro B, Yau T, Crocenzi TS, Kudo M, Hsu C, et al. Nivolumab in Patients With Advanced Hepatocellular Carcinoma (CheckMate 040): An Open-Label, non-Comparative, Phase 1/2 Dose Escalation and Expansion Trial. *Lancet* (2017) 389(10088):2492-502. doi: 10.1016/S0140-6736(17)31046-2
- Chevret S, Trinchet J-C, Mathieu D, Abou Rached A, Beaugrand M, Chastang C, et al. A New Prognostic Classification for Predicting Survival in Patients With Hepatocellular Carcinoma. *J Hepatol* (1999) 31(1):133-41. doi: 10.1016/S0168-8278(99)80173-1
- Tamura S, Kato T, Berho M, Misiakos EP, O'Brien C, Reddy KR, et al. Impact of Histological Grade of Hepatocellular Carcinoma on the Outcome of Liver Transplantation. *Arch Surg* (2001) 136(1):25-30. doi: 10.1001/archsurg.136.1.25
- Takahashi S, Kudo M, Chung H, Inoue T, Ishikawa E, Kitai S, et al. PIVKA-II is the Best Prognostic Predictor in Patients With Hepatocellular Carcinoma After Radiofrequency Ablation Therapy. *Oncology* (2008) 75(Suppl 1):91-8. doi: 10.1159/000173429
- Antoch G, Saoudi N, Kuehl H, Dahmen G, Mueller SP, Beyer T, et al. Accuracy of Whole-Body Dual-Modality Fluorine-18-2-Fluoro-2-Deoxy-D-Glucose Positron Emission Tomography and Computed Tomography (FDG-PET/CT) for Tumor Staging in Solid Tumors: Comparison With CT and PET. *J Clin Oncol* (2004) 22(21):4357-68. doi: 10.1200/JCO.2004.08.120
- Murakami T, Mochizuki K, Nakamura H. Imaging Evaluation of the Cirrhotic Liver. *Semin Liver Dis* (2001) 21(02):213-24. doi: 10.1055/s-2001-15497
- Khan MA, Combs CS, Brunt EM, Lowe VJ, Wolverson MK, Solomon H, et al. Positron Emission Tomography Scanning in the Evaluation of Hepatocellular Carcinoma. *J Hepatol* (2000) 32(5):792-7. doi: 10.1016/S0168-8278(00)80248-2
- Teefey SA, Hildeboldt CC, Dehdashti F, Siegel BA, Peters MG, Heiken JP, et al. Detection of Primary Hepatic Malignancy in Liver Transplant Candidates: Prospective Comparison of CT, MR Imaging, US, and PET. *Radiology* (2003) 226(2):533-42. doi: 10.1148/radiol.2262011980
- Lee JW, Paeng JC, Kang KW, Kwon HW, Suh K-S, Chung J-K, et al. Prediction of Tumor Recurrence by 18F-FDG PET in Liver Transplantation for Hepatocellular Carcinoma. *J Nucl Med* (2009) 50(5):682-7. doi: 10.2967/jnumed.108.060574
- Pant V, Sen IB, Soin AS. Role of 18F-FDG PET CT as an Independent Prognostic Indicator in Patients With Hepatocellular Carcinoma. *Nucl Med Commun* (2013) 34(8):749-57. doi: 10.1097/MNM.0b013e3283622eef
- Lee JW, Oh JK, Chung YA, Na SJ, Hyun SH, Hong IK, et al. Prognostic Significance of 18F-FDG Uptake in Hepatocellular Carcinoma Treated With Transarterial Chemoembolization or Concurrent Chemoradiotherapy: A Multicenter Retrospective Cohort Study. *J Nucl Med* (2016) 57(4):509-16. doi: 10.2967/jnumed.115.167338
- Na SJ, Oh JK, Hyun SH, Lee JW, Hong IK, Song B-I, et al. 18F-FDG PET/CT can Predict Survival of Advanced Hepatocellular Carcinoma Patients: A Multicenter Retrospective Cohort Study. *J Nucl Med* (2017) 58(5):730-6. doi: 10.2967/jnumed.116.182022
- Lee JD, Yang WI, Park YN, Kim KS, Choi JS, Yun M, et al. Different Glucose Uptake and Glycolytic Mechanisms Between Hepatocellular Carcinoma and Intrahepatic Mass-Forming Cholangiocarcinoma With Increased 18F-FDG Uptake. *J Nucl Med* (2005) 46(10):1753-9.
- Lee JD, Yun M, Lee JM, Choi Y, Choi Y-H, Kim JS, et al. Analysis of Gene Expression Profiles of Hepatocellular Carcinomas With Regard to 18 F-Fluorodeoxyglucose Uptake Pattern on Positron Emission Tomography. *Eur J Nucl Med Mol Imaging* (2004) 31(12):1621-30. doi: 10.1007/s00259-004-1602-1
- Xia H, Chen J, Gao H, Kong SN, Deivasigamani A, Shi M, et al. Hypoxia-Induced Modulation of Glucose Transporter Expression Impacts 18F-Fluorodeoxyglucose PET-CT Imaging in Hepatocellular Carcinoma. *Eur J Nucl Med Mol Imaging* (2020) 47(4):787-97. doi: 10.1007/s00259-019-04638-4
- Duan Y, Evans DS, Miller RA, Schork NJ, Cummings SR, Girke T. Signaturesearch: Environment for Gene Expression Signature Searching and Functional Interpretation. *Nucleic Acids Res* (2020) 48(21):e124-4. doi: 10.1093/nar/gkaa878
- Chae YK, Chang S, Ko T, Anker J, Agte S, Iams W, et al. Epithelial-Mesenchymal Transition (EMT) Signature is Inversely Associated With T-Cell Infiltration in non-Small Cell Lung Cancer (NSCLC). *Sci Rep* (2018) 8 (1):1-8. doi: 10.1038/s41598-018-21061-1
- Mayakonda A, Lin D-C, Assenov Y, Plass C, Koeffler HP. Maftools: Efficient and Comprehensive Analysis of Somatic Variants in Cancer. *Genome Res* (2018) 28(11):1747-56. doi: 10.1101/gr.239244.118
- Izuishi K, Yamamoto Y, Mori H, Kameyama R, Fujihara S, Masaki T, et al. Molecular Mechanisms of [18F] Fluorodeoxyglucose Accumulation in Liver Cancer. *Oncol Rep* (2014) 31(2):701-6. doi: 10.3892/or.2013.2886
- Chen R, Li J, Zhou X, Liu J, Huang G. Fructose-1, 6-Bisphosphatase 1 Reduces 18F FDG Uptake in Hepatocellular Carcinoma. *Radiology* (2017) 284(3):844-53. doi: 10.1148/radiol.2017161607
- Harris AL. Hypoxia—a Key Regulatory Factor in Tumour Growth. *Nat Rev Cancer* (2002) 2(1):38-47. doi: 10.1038/nrc704
- Bos R, van der Hoeven JJ, van der Wall E, van der Groep P, Van Diest PJ, Comans EF, et al. Biologic Correlates of 18fluorodeoxyglucose Uptake in Human Breast Cancer Measured by Positron Emission Tomography. *J Clin Oncol* (2002) 20(2):379-87. doi: 10.1200/JCO.2002.20.2379
- Heiden BT, Chen G, Hermann M, Brown RK, Orringer MB, Lin J, et al. 18F-FDG PET Intensity Correlates With a Hypoxic Gene Signature and Other



- Oncogenic Abnormalities in Operable non-Small Cell Lung Cancer. *PloS One* (2018) 13(7):e0199970. doi: 10.1371/journal.pone.0199970
27. Yalcin A, Telang S, Clem B, Chesney J. Regulation of Glucose Metabolism by 6-Phosphofructo-2-Kinase/Fructose-2, 6-Bisphosphatases in Cancer. *Exp Mol Med* (2009) 86(3):174–9. doi: 10.1016/j.yexmp.2009.01.003
  28. Zhang X, Li J, Ghoshal K, Fernandez S, Li L. Identification of a Subtype of Hepatocellular Carcinoma With Poor Prognosis Based on Expression of Genes Within the Glucose Metabolic Pathway. *Cancers (Basel)* (2019) 11(12):2023. doi: 10.3390/cancers11122023
  29. Su Y, Loos M, Giese N, Hines O, Diebold I, Görlach A, et al. PHD3 Regulates Differentiation, Tumour Growth and Angiogenesis in Pancreatic Cancer. *Br J Cancer* (2010) 103(10):1571–9. doi: 10.1038/sj.bjc.6605936
  30. Garvalov BK, Foss F, Henze A-T, Bethani I, Gräf-Höchst S, Singh D, et al. PHD3 Regulates EGFR Internalization and Signalling in Tumours. *Nat Commun* (2014) 5:5577. doi: 10.1038/ncomms6577
  31. Henze A-T, Garvalov BK, Seidel S, Cuesta AM, Ritter M, Filatova A, et al. Loss of PHD3 Allows Tumours to Overcome Hypoxic Growth Inhibition and Sustain Proliferation Through EGFR. *Nat Commun* (2014) 5:5582. doi: 10.1038/ncomms6582
  32. Ma M, Hua S, Li G, Wang S, Cheng X, He S, et al. Prolyl Hydroxylase Domain Protein 3 and Asparaginyl Hydroxylase Factor Inhibiting HIF-1 Levels are Predictive of Tumoral Behavior and Prognosis in Hepatocellular Carcinoma. *Oncotarget* (2017) 8(8):12983–3002. doi: 10.18632/oncotarget.14677
  33. Shi M, Dai W-Q, Jia R-R, Zhang Q-H, Wei J, Wang Y-G, et al. APC/CCD20-Mediated Degradation of PHD3 Stabilizes HIF-1 $\alpha$  and Promotes Tumorigenesis in Hepatocellular Carcinoma. *Cancer Lett* (2021) 496:144–55. doi: 10.1016/j.canlet.2020.10.011
  34. Couvelard A, Deschamps L, Rebours V, Sauvanet A, Gatter K, Pezzella F, et al. Overexpression of the Oxygen Sensors PHD-1, PHD-2, PHD-3, and FIH Is Associated With Tumor Aggressiveness in Pancreatic Endocrine Tumors. *Clin Cancer Res* (2008) 14(20):6634–9. doi: 10.1158/1078-0432.CCR-07-5258
  35. Andersen S, Donnem T, Stenvold H, Al-Saad S, Al-Shibli K, Busund L-T, et al. Overexpression of the HIF Hydroxylases PHD1, PHD2, PHD3 and FIH are Individually and Collectively Unfavorable Prognosticators for NSCLC Survival. *PloS One* (2011) 6(8):e23847. doi: 10.1371/journal.pone.0023847
  36. Luo W, Hu H, Chang R, Zhong J, Knabel M, O'Meally R, et al. Pyruvate Kinase M2 is a PHD3-Stimulated Coactivator for Hypoxia-Inducible Factor 1. *Cell* (2011) 145(5):732–44. doi: 10.1016/j.cell.2011.03.054
  37. Chu X, Xiang M, Feng L, Liu H, Zhou C. Prolyl Hydroxylase 3 Involvement in Lung Cancer Progression Under Hypoxic Conditions: Association With Hypoxia-Inducible Factor-1 $\alpha$  and Pyruvate Kinase M2. *J Thorac Dis* (2019) 11(9):3941–50. doi: 10.21037/jtd.2019.08.124
  38. Chesney J, Clark J, Klarer AC, Imbert-Fernandez Y, Lane AN, Telang S. Fructose-2, 6-Bisphosphate Synthesis by 6-Phosphofructo-2-Kinase/Fructose-2, 6-Bisphosphatase 4 (PFKFB4) is Required for the Glycolytic Response to Hypoxia and Tumor Growth. *Oncotarget* (2014) 5(16):6670–86. doi: 10.18632/oncotarget.2213
  39. Smith S. Peroxisome Proliferator-Activated Receptors and the Regulation of Mammalian Lipid Metabolism. *Biochem Soc Trans* (2002) 30(6):1086–90. doi: 10.1042/bst0301086
  40. Tanaka M, Masaki Y, Tanaka K, Miyazaki M, Kato M, Sugimoto R, et al. Reduction of Fatty Acid Oxidation and Responses to Hypoxia Correlate With the Progression of De-Differentiation in HCC. *Mol Med Rep* (2013) 7(2):365–70. doi: 10.3892/mmr.2012.1201
  41. Torizuka T, Tamaki N, Inokuma T, Magata Y, Sasayama S, Yonekura Y, et al. *In Vivo* Assessment of Glucose Metabolism in Hepatocellular Carcinoma With FDG-PET. *J Nucl Med* (1995) 36(10):1811–7.
  42. Yuan P, Mu J, Wang Z, Ma S, Da X, Song J, et al. Down-Regulation of SLC25A20 Promotes Hepatocellular Carcinoma Growth and Metastasis Through Suppression of Fatty-Acid Oxidation. *Cell Death Dis* (2021) 12(4):361. doi: 10.1038/s41419-021-03648-1
  43. Ho C-L, Simon C, Yeung DW. 11C-Acetate PET Imaging in Hepatocellular Carcinoma and Other Liver Masses. *J Nucl Med* (2003) 44(2):213–21.
  44. Talbot J-N, Gutman F, Fartoux L, Grange J-D, Ganne N, Kerrou K, et al. PET/CT in Patients With Hepatocellular Carcinoma Using [18 F] Fluorocholine: Preliminary Comparison With [18 F] FDG PET/CT. *Eur J Nucl Med Mol Imaging* (2006) 33(11):1285–9. doi: 10.1007/s00259-006-0164-9
  45. Boyault S, Rickman DS, De Reyniès A, Balabaud C, Rebouissou S, Jeannot E, et al. Transcriptome Classification of HCC is Related to Gene Alterations and to New Therapeutic Targets. *Hepatology* (2007) 45(1):42–52. doi: 10.1002/hep.21467
  46. Senni N, Savall M, Granados DC, Alves-Guerra M-C, Sartor C, Lagoutte I, et al.  $\beta$ -Catenin-Activated Hepatocellular Carcinomas are Addicted to Fatty Acids. *Gut* (2019) 68(2):322–34. doi: 10.1136/gutjnl-2017-315448
  47. Chen P-M, Li J-R, Liu C-C, Tang F-Y, Chiang E-PI. Metabolic Pathways Enhancement Confers Poor Prognosis in P53 Exon Mutant Hepatocellular Carcinoma. *Cancer Inform* (2020) 19:1176935119899913. doi: 10.1177/1176935119899913
  48. Méndez-Blanco C, Fondevila F, García-Palomo A, González-Gallego J, Mauriz JL. Sorafenib Resistance in Hepatocarcinoma: Role of Hypoxia-Inducible Factors. *Exp Mol Med* (2018) 50(10):1–9. doi: 10.1038/s12276-018-0159-1
  49. Feng J, Dai W, Mao Y, Wu L, Li J, Chen K, et al. Simvastatin Re-Sensitizes Hepatocellular Carcinoma Cells to Sorafenib by Inhibiting HIF-1 $\alpha$ /PPAR- $\gamma$ /PKM2-Mediated Glycolysis. *J Exp Clin Cancer Res* (2020) 39(1):24. doi: 10.1186/s13046-020-1528-x
  50. Huang Q, Li J, Xing J, Li W, Li H, Ke X, et al. CD147 Promotes Reprogramming of Glucose Metabolism and Cell Proliferation in HCC Cells by Inhibiting the P53-Dependent Signaling Pathway. *J Hepatol* (2014) 61(4):859–66. doi: 10.1016/j.jhep.2014.04.035
  51. Ros S, Flöter J, Kaymak I, Da Costa C, Houddane A, Dubuis S, et al. 6-Phosphofructo-2-Kinase/Fructose-2, 6-Bisphosphatase 4 is Essential for P53-Null Cancer Cells. *Oncogene* (2017) 36(23):3287–99. doi: 10.1038/onc.2016.477
  52. Li J, Huang Q, Long X, Zhang J, Huang X, Aa J, et al. CD147 Reprograms Fatty Acid Metabolism in Hepatocellular Carcinoma Cells Through Akt/mTOR/SREBP1c and P38/Ppar $\alpha$  Pathways. *J Hepatol* (2015) 63(6):1378–89. doi: 10.1016/j.jhep.2015.07.039
  53. Bian H, Zheng J-S, Nan G, Li R, Chen C, Hu C-X, et al. Randomized Trial of [131I] Metuximab in Treatment of Hepatocellular Carcinoma After Percutaneous Radiofrequency Ablation. *J Natl Cancer Inst* (2014) 106(9):dju239. doi: 10.1093/jnci/dju239
  54. Talbot J-N, Fartoux L, Balogova S, Nataf V, Kerrou K, Gutman F, et al. Detection of Hepatocellular Carcinoma With PET/CT: A Prospective Comparison of 18F-Fluorocholine and 18F-FDG in Patients With Cirrhosis or Chronic Liver Disease. *J Nucl Med* (2010) 51(11):1699–706. doi: 10.2967/jnumed.110.075507
  55. Fartoux L, Balogova S, Nataf V, Kerrou K, Huchet V, Rosmorduc O, et al. A Pilot Comparison of 18F-Fluorodeoxyglucose and 18F-Fluorocholine PET/CT to Predict Early Recurrence of Unifocal Hepatocellular Carcinoma After Surgical Resection. *Nucl Med Commun* (2012) 33(7):757–65. doi: 10.1097/MNM.0b013e328350fb9f

**Conflict of Interest:** The authors declare that the research was conducted in the absence of any commercial or financial relationships that could be construed as a potential conflict of interest.

**Publisher's Note:** All claims expressed in this article are solely those of the authors and do not necessarily represent those of their affiliated organizations, or those of the publisher, the editors and the reviewers. Any product that may be evaluated in this article, or claim that may be made by its manufacturer, is not guaranteed or endorsed by the publisher.

Copyright © 2022 Lee, Choi, Joung, Joh, Kim and Hyun. This is an open-access article distributed under the terms of the Creative Commons Attribution License (CC BY). The use, distribution or reproduction in other forums is permitted, provided the original author(s) and the copyright owner(s) are credited and that the original publication in this journal is cited, in accordance with accepted academic practice. No use, distribution or reproduction is permitted which does not comply with these terms.



# HER2 Aberrations as a Novel Marker in Advanced Biliary Tract Cancer

Hongsik Kim<sup>1,2</sup>, Ryul Kim<sup>1</sup>, Hye Ryeon Kim<sup>1</sup>, Hyunji Jo<sup>1</sup>, Hana Kim<sup>1</sup>, Sang Yun Ha<sup>3</sup>, Joon Oh Park<sup>1</sup>, Young Suk Park<sup>1</sup> and Seung Tae Kim<sup>1\*</sup>

<sup>1</sup> Division of Hematology-Oncology, Department of Medicine, Samsung Medical Center, Sungkyunkwan University School of Medicine, Seoul, South Korea, <sup>2</sup> Division of Hematology-Oncology, Department of Internal Medicine, Chungbuk National University Hospital, Cheongju, South Korea, <sup>3</sup> Department of Pathology, Samsung Medical Center, Sungkyunkwan University School of Medicine, Seoul, South Korea

## OPEN ACCESS

### Edited by:

Alessandro Passardi,  
Scientific Institute of Romagna for the  
Study and Treatment of Tumors  
(IRCCS), Italy

### Reviewed by:

Amro Abdelrahman,  
Mayo Clinic, United States  
Alessandro Rizzo,  
National Cancer Institute Foundation  
(IRCCS), Italy  
Changhoon Yoo,  
University of Ulsan, South Korea

### \*Correspondence:

Seung Tae Kim  
shty1@skku.edu

### Specialty section:

This article was submitted to  
Gastrointestinal Cancers: Hepato  
Pancreatic Biliary Cancers,  
a section of the journal  
Frontiers in Oncology

**Received:** 13 December 2021

**Accepted:** 18 January 2022

**Published:** 14 February 2022

### Citation:

Kim H, Kim R, Kim HR,  
Jo H, Kim H, Ha SY, Park JO,  
Park YS and Kim ST (2022) HER2  
Aberrations as a Novel Marker in  
Advanced Biliary Tract Cancer.  
Front. Oncol. 12:834104.  
doi: 10.3389/fonc.2022.834104

HER2 aberrations have been reported as a novel biomarker in HER2-directed therapy or as a prognostic marker in various tumor types. However, in advanced biliary tract cancer (BTC), there have been few studies regarding HER2 aberrations as a biomarker. We analyzed 121 advanced BTC patients who had been treated with Gemcitabine/Cisplatin (GP) as a 1st line therapy between November 2019 and April 2021. Next-generation sequencing (NGS), namely, HER2 aberrations was performed in all patients. The TruSight™ Oncology 500 assay from Illumina was used for the NGS panel. Among 121 patients with advanced BTC, HER2 aberrations were observed in 18 patients (14.9%). For subtypes of HER2 aberrations, point mutation was observed in 5 patients (27.8%), gene amplification in 11 patients (61.1%), and both point mutation and gene amplification in 2 patients (11.1%). The frequency of HER2 aberrations was significantly different according to the primary tumor ( $p = 0.009$ ). In gallbladder cancer, HER2 aberrations were observed at a relatively high frequency (36.4%). The tumor response to GP did not differ between patients with and without HER2 aberrations (33.3%, vs. 26.2%, respectively,  $p = 0.571$ ). The median progression-free survival (PFS) to GP was 4.7 months (95% CI, 4.0 to 5.5 months) in patients with HER2 aberrations and 7.0 months (95% CI, 5.2 to 8.8 months) without HER2 aberrations ( $p = 0.776$ ). The median overall survival (OS) was not reached and not reached in patients with and without HER2 aberrations ( $p = 0.739$ ), respectively. The univariate analysis for PFS to GP and OS showed that HER2 aberrations were not an independent factor for survival. This study showed that the HER2 aberrations were observed in 14.9% of advanced BTC and were not an independent biomarker for survival.

**Keywords:** HER2, ERBB2, biliary tract cancer, next-generation sequencing, chemotherapy

## INTRODUCTION

Biliary tract cancers (BTCs) are rare, aggressive, and heterogeneous malignancies (1, 2). Most patients present with advanced disease at the time of diagnosis. Palliative chemotherapy is the only treatment option for advanced BTC, and the gemcitabine plus cisplatin (GP) has been the standard of treatment as 1st line chemotherapy. However, the prognosis for these patients is poor, and median overall survival (OS) is less than one year with palliative chemotherapy (3–5).

Human epidermal growth factor receptor 2 (HER2) is associated with tumor proliferation by downstream signaling activation and is among the most investigated biomarker in various tumor types, namely, breast and gastric cancers (6, 7). HER2 aberrations play a role as predictive and prognostic biomarkers in various tumor types (8–11). Several studies also reported that the HER2 pathway could have a role in the development and growth of BTC (12–15) and HER2 overexpression and amplification were reported approximately 4–6% of BTC, 1–4% of intrahepatic cholangiocarcinoma, 4–9% of extrahepatic cholangiocarcinoma, and 9–14% of gallbladder cancer (11, 15, 16). Also, HER2-directed therapy has been developed in advanced BTCs (17–22). Several previous studies have assessed HER2 overexpression and amplification by immunohistochemistry (IHC) and focused only on HER2 directed therapy based on the results of IHC. However, most studies have focused only on the overexpression and/or amplification of HER2.

Recently, advances in whole-exome sequencing (WES) and next-generation sequencing (NGS) of multiple genes have defined the tumor biology of BTCs (23–25). Also, in previous studies, HER2 aberrations by NGS highly correlated with HER2 overexpression by IHC/FISH in various solid tumors (26–28). Currently, several clinical trials are evaluating the HER2-directed therapy based on HER2 aberrations detected by NGS in advanced BTCs (29, 30). However, in the era of NGS, there have been few reports on the role of HER2 aberrations, namely, gene mutation, gene amplification, and overexpression as a biomarker in advanced BTCs (31–34) and the role of HER2 aberrations to cytotoxic chemotherapy has not been evaluated yet. Therefore, we intended to explore the prevalence of HER2 aberrations using NGS in advanced BTCs and evaluate the role of HER2 aberrations as both a predictive factor for GP and a prognostic factor.

## MATERIALS AND METHODS

### Patients

We analyzed 121 advanced BTC patients who received gemcitabine and cisplatin (GP) as the 1st line treatment at the Samsung Medical Center, Korea, between November 2019 and April 2021. Molecular profiles, namely, HER2 aberrations, were available for all patients through NGS using the TruSight™ Oncology 500 assay (Illumina Inc., San Diego, CA, USA). The baseline clinicopathologic characteristics were collected for patients. The Institutional Review Board (IRB No. 2021-07-110) at the Samsung Medical Center approved this study and this retrospective analysis waived individual consent.

### TruSight™ Oncology 500 Assay

The tumor samples were obtained at the time of diagnosis in advanced or metastatic BTCs and used formalin-fixed paraffin-embedded (FFPE) material. For DNA library preparation and enrichment, the TruSight™ Oncology 500 Kit was used following the manufacturer's instructions. Post-enriched

libraries were quantified, pooled, and sequenced on a NextSeq 500. The quality of the NextSeq 500 sequencing runs was assessed using the Illumina Sequencing Analysis Viewer. Sequencing data were analyzed with the TruSight Oncology 500 Local App Version 1.3.0.39. The TruSight™ Oncology 500 is a comprehensive tumor profiling assay and biomarkers, namely, single nucleotide variants (SNVs), copy number variants (CNVs), indels, fusions, and splice variants.

## Treatment Outcomes

All 121 patients were evaluated for clinical outcomes of objective response rate (ORR), disease control rate (DCR), and progression-free survival (PFS) to gemcitabine and cisplatin as the 1st line treatment according to the Response Evaluation Criteria in Solid Tumors (RECIST) version 1.1 through computed tomography (CT). Also, overall survival (OS) was analyzed. PFS was defined as the time from the start of GP until the date of disease progression or death from any cause. OS was defined as the time from the start of GP until death from any cause. According to the RECIST, ORR was defined as the proportion of patients with a complete response (CR) or partial response (PR) to treatment and DCR was defined as the proportion of patients with a complete response (CR), partial response (PR) or stable disease (SD) to treatment.

## Statistics

The cut-off date for data collection was April 30, 2021. Descriptive statistics were used to summarize patient and tumor characteristics and treatment history and were reported as proportions and medians. Data are presented as the number (%) for categorical variables. Correlations between HER2 aberrations and clinicopathologic features were analyzed by t-test or Fisher exact test. Survival analyses were performed using the Kaplan–Meier method, and differences were analyzed by log-rank test. Hazard ratios and corresponding 95% confidence intervals were calculated using the Cox proportional hazards model. Univariate analysis of predictive and prognostic factors was performed using Cox proportional hazards models for PFS and OS. IBM SPSS Statistics 25 was used for statistical analysis.

## RESULTS

### Patient Characteristics and HER2 Aberrations

All 121 patients were analyzed in this study. Of these, 18 (14.9%) had tumors with HER2 aberrations. HER2 aberrations were found in 5.8% (3/52) of intrahepatic cholangiocarcinoma patients, 13.9% (5/36) of extrahepatic cholangiocarcinoma patients, 36.4% (8/22) of gallbladder cancer patients, and 18.2% (2/11) of ampulla of Vater cancer patients. For subtypes of HER2 aberrations, point mutation was observed in 5 patients (27.8%), gene amplification in 11 patients (61.1%), and both point mutation and gene amplification in 2 patients (11.1%). **Table 1** presents the clinical characteristics between patients with and without HER2 aberrations. HER2 aberrations were not

**TABLE 1** | Baseline patient characteristics.

	HER2 (–) (n = 103)	HER2 (+) (n = 18)	p-value
Median age (range), years	64 (47–79)	67 (33–82)	0.580
Age 65≥ years, n (%)	58 (56.3%)	8 (44.4%)	0.499
Sex, n (%)			0.556
Male	68 (66.0%)	10 (55.6%)	
Female	35 (34.0%)	8 (44.4%)	
Tumor site, n (%)			0.009
Intrahepatic	49 (47.6%)	3 (16.7%)	
Extrahepatic	31 (30.1%)	5 (27.8%)	
Gallbladder	14 (13.6%)	8 (44.4%)	
Ampulla of Vater	9 (8.7%)	2 (11.1%)	
Grade of differentiation, n (%)			0.838
Poorly	29 (28.2%)	4 (22.2%)	
Well/Moderate	67 (65.0%)	13 (72.2%)	
Unknown	7 (6.8%)	1 (5.6%)	
Disease stage, n (%)			0.626
Metastasis	77 (74.8%)	15 (83.3%)	
Locally advanced	26 (25.2%)	3 (16.7%)	
No. of metastatic sites, n (%)			0.928
≤2	90 (87.4%)	15 (83.3%)	
2<	13 (12.6%)	3 (16.7%)	
Metastatic sites, n (%)			
Abdominal lymph node (M1)	45 (43.7%)	10 (55.6%)	
Liver	41 (39.8%)	8 (44.4%)	
Peritoneum	20 (19.4%)	4 (22.2%)	
Lung	6 (5.8%)	1 (5.6%)	
Bone	4 (3.9%)	1 (5.6%)	
Others	17 (16.5%)	6 (33.3%)	

HER2, human epidermal growth factor receptor 2.

significantly correlated with any clinical baseline characteristics except the location of the primary tumor ( $p = 0.009$ ).

## Association Between the Status of HER2 Aberrations and the Efficacy of Gemcitabine Plus Cisplatin

We compared the tumor response, PFS, and OS to GP according to the status of HER2 aberrations. The ORR and DCR to GP were 33.3% (6/18, 95% CI 13.3–59.0) and 77.8% (14/18, 95% CI 52.3–93.6), respectively, in patients with HER2 aberrations and 26.2% (27/103, 95% CI 18.0–35.8) and 73.8% (76/103, 95% CI 64.2–82.0), respectively, in patients without HER2 aberrations. The ORR and DCR according to the status of HER2 aberrations were no significant differences ( $p = 0.571$  and  $p = 1.000$ , respectively) (Table 2).

The median PFS to GP values was 4.7 months (95% CI, 4.0 to 5.5 months) and 7.0 months (95% CI, 5.2 to 8.8 months) in

patients with and without HER2 aberrations, respectively ( $p = 0.776$ ) (Figure 1).

The median OS was not reached in patients with HER2 aberrations and not reached in patients without HER2 aberrations ( $p = 0.739$ ) (Figure 2).

## HER2 Aberrations—Univariate Analysis for Survivals

We conducted univariate analyses for PFS to GP and OS to evaluate the role of HER2 aberrations as an independent biomarker (Table 3). Univariate analysis for PFS to GP showed that grade of differentiation (poorly differentiated vs. well/moderate differentiated), disease stage (metastasis vs. locally advanced), and the number of metastatic sites ( $\leq 2$  vs.  $2 <$ ) were significant independent factors; however, HER2 aberrations were not.

Also, HER2 aberrations were not an independent factor in univariate analysis for OS. We additionally conducted survival

**TABLE 2** | Objective response rate to chemotherapy.

	HER2 aberrations (–) (n = 103)	HER2 aberrations (+) (n = 18)	p-value
Complete response	2 (1.9%)	1 (5.6%)	
Partial response	25 (24.3%)	5 (27.8%)	
Stable disease	49 (47.6%)	8 (44.4%)	
Progressive disease	14 (13.6%)	1 (5.6%)	
Not evaluable	13 (12.6%)	3 (16.7%)	
Objective response rate	27 (26.2%)	6 (33.3%)	0.571
Disease control rate	76 (73.8%)	14 (77.8%)	1.000

HER2, human epidermal growth factor receptor 2.



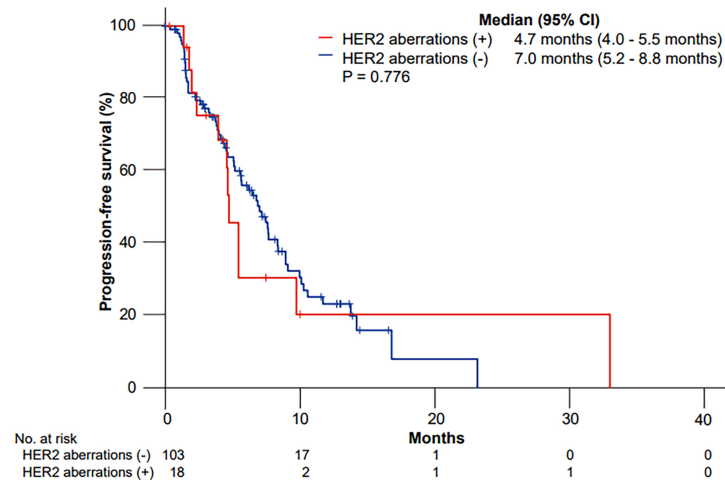


**FIGURE 1** | Kaplan-Meier curves of progression-free survival (PFS) to gemcitabine plus cisplatin according to HER2 aberrations.

analyses for PFS and OS according to HER2 amplification. HER2 amplification also was not an independent factor in univariate analysis for PFS ( $p = 0.322$ ) and OS ( $p = 0.168$ ).

## DISCUSSION

In our study, we identified that the prevalence of HER2 aberrations and the frequency of HER2 aberrations were significantly different according to the primary tumor, which was consistent with previous studies (16, 23, 35). Between the status of HER2 aberrations and treatment outcomes to GP, including ORR, DCR, and PFS were no significant differences. Also, HER2 aberrations were not an independent biomarker for PFS to GP and OS in univariate analysis. Because most clinical trials of HER2 targeted therapy included HER2 amplified BTCs, we additionally evaluate the role of HER2 amplification as a

prognostic biomarker. However, HER2 amplification was not an independent biomarker for OS.

Recently, one study described genomic characteristics focusing on the ERBB/EGFR pathway in BTC using NGS. The prevalence of HER2 aberrations by NGS was 13.9% in 1,863 BTC patients from Western countries; of these, 6.2% were point mutation, 6.8% were amplification, and 0.9% were both point mutation and amplification, which was consistent with our results (14.9% in 121 patients) (16). However, that study did not evaluate the role of HER2 aberrations as predictive and prognostic biomarkers.

The role of HER2 aberrations as a predictive and prognostic biomarker in advanced BTC to palliative chemotherapy has not previously been elucidated. One study reported that HER2 expression by IHC represented an independent poor prognostic factor in patients with BTC treated with curative surgery (31). That study evaluated the relationship between HER2 expression by IHC and survival in 100 patients with radically resected BTC. However,

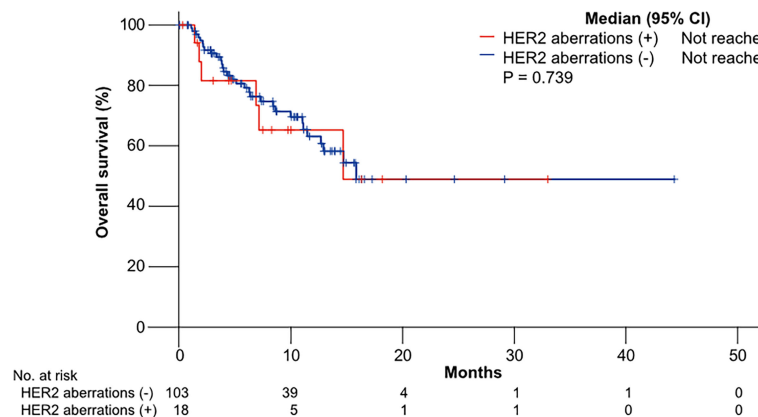


**FIGURE 2** | Kaplan-Meier curves of overall survival (OS) to gemcitabine plus cisplatin according to HER2 aberrations.

**TABLE 3 |** Univariate analysis of progression-free survival and overall survival after gemcitabine/cisplatin.

	Progression-free survival		Overall survival	
	HR (95% CI)	p-value	HR (95% CI)	p-value
<b>Age</b>		0.288		0.727
<65 years	1		1	
≥65 years	1.29 (0.81–2.07)		1.12 (0.59–2.15)	
<b>Sex</b>		0.139		0.010
Male	1		1	
Female	0.69 (0.43–1.12)		0.35 (0.16–0.78)	
<b>Tumor site</b>				
Intrahepatic	1	0.395	1	0.097
Extrahepatic	0.89 (0.51–1.56)	0.685	0.75 (0.36–1.57)	0.444
Gallbladder	0.82 (0.44–1.54)	0.537	0.54 (0.20–1.44)	0.219
Ampulla of Vater	0.46 (0.19–1.12)	0.087	0.07 (0.02–1.20)	0.074
<b>Grade of differentiation</b>		0.014		0.012
Poorly	1		1	
Well/Moderate	0.53 (0.32–0.88)		0.42 (0.22–0.83)	
<b>Disease stage</b>		0.006		0.142
Metastasis	1		1	
Locally advanced	0.27 (0.11–0.69)		0.34 (0.08–1.43)	
<b>No. of metastatic sites</b>		0.004		0.001
≥2	1		1	
<2	2.14 (1.27–3.62)		3.63 (1.87–7.03)	
<b>HER2 aberrations</b>		0.771		0.739
Negative	1		1	
Positive	1.10 (0.58–2.11)		1.16 (0.48–2.79)	

HER2, human epidermal growth factor receptor 2; HR, hazard ratio; CI, confidence interval.

there was a lack of standardized criteria of HER2 assessment in BTC, and the patient groups appeared unbalanced according to HER2 status. Meanwhile, another study reported that HER2 overexpression by IHC was not a significant difference in survival rates in BTC patients with curative surgery (36). Similarly, our results for the prognostic role of HER2 aberrations were inconsistent and inconclusive.

Several clinical trials with novel tyrosine kinase inhibitors (such as lapatinib or erlotinib) (37, 38) and monoclonal antibodies (such as cetuximab or panitumumab) (39, 40) targeting the HER pathway have been developed in HER2 overexpressing BTC and brought disappointing results. Recently, in the MyPathway HER2 basket study, combined therapy with pertuzumab plus trastuzumab resulted in an ORR of 9 of 39 patients (23%) with metastatic BTCs with HER2 amplification/overexpression, and the median OS was 10.9 months (21). Also, promising results from a phase 1 study were reported from new drugs, such as the novel HER2-targeted antibody-drug conjugate trastuzumab deruxtecan (T-DXd) (41), the anti-HER2 antibody margetuximab (MGAH22) (42), and the bispecific HER2-targeted antibody zanidatamab (ZW25) (43). Accumulating data provide the potential benefit from HER2-targeted therapies in HER2-positive BTCs.

Recently, neoadjuvant chemotherapy is considered a promising option for patients with curative intended surgery and a few clinical studies of neoadjuvant chemotherapy have been reported (44). Although our focused only on the role of HER2 aberrations as a novel biomarker by NGS in advanced BTC to palliative chemotherapy, further studies are needed to evaluate the aberrations of HER2 as a biomarker in the setting of neoadjuvant chemotherapy.

Although the role of HER2 in BTC patients is inconsistent and inconclusive, previous studies have reported HER2 overexpression

by IHC as a predictive and prognostic biomarker. Recently, in the era of NGS, clinical trials with HER2 targeting therapy included HER2 aberrations by NGS. Therefore, we reviewed the prevalence of HER2 aberrations using NGS in advanced BTCs and a new perspective which was a prognostic and predictive role of HER2 aberrations by NGS in advanced BTCs.

To the best of our knowledge, ours is the first study evaluating relationships between HER2 aberrations and GP, which is the current standard chemotherapy. We found that HER2 aberrations identified through NGS did not have a predictive or prognostic role on the standard first-line chemotherapy in advanced BTC.

This study has limitations. First, this study had a small sample size, was retrospective in nature, and utilized a heterogeneous population, which may lead to bias. However, the biliary tract cancers were a rare orphan disease. Especially, the acquisition of tumor-sample in biliary tract cancers is very difficult to work. This study tried to conduct a molecular study in biliary tract cancer. Second, only Asian patients with BTC were analyzed in the study, limiting the generalizability because of differences in molecular profiles and clinical features between Western and Eastern patients with BTC. Third, the study included various types of HER2 aberrations, making it difficult to draw definite conclusions. Therefore, findings for the HER2 aberrations as a novel biomarker in this study should be interpreted with caution. Further prospective clinical trials are required to determine whether HER2 aberrations could be a novel predictive or prognostic biomarker in BTC.

In conclusion, this retrospective study evaluated the prevalence of HER2 aberrations in BTC and the relationship between HER2 aberrations and clinical outcomes after cytotoxic chemotherapy. Our results suggest that HER2 aberrations in advanced BTC did

not have a prognostic or predictive biomarker in the first line standard cytotoxic chemotherapy (GP).

## DATA AVAILABILITY STATEMENT

The datasets presented in this article are not readily available because of the privacy restrictions at Samsung Medical Centre. Requests to access the datasets should be directed to [shty1@skku.edu](mailto:shty1@skku.edu).

## ETHICS STATEMENT

The studies involving human participants were reviewed and approved by the Institutional Review Board (IRB no. 2021-07-110) of Samsung Medical Centre.

## REFERENCES

- Hong S, Won YJ, Park YR, Jung KW, Kong HJ, Lee ES. Cancer Statistics in Korea: Incidence, Mortality, Survival, and Prevalence in 2017. *Cancer Res Treat* (2020) 52(2):335–50. doi: 10.4143/crt.2020.206
- Siegel RL, Miller KD, Jemal A. Cancer Statistics, 2020. *CA Cancer J Clin* (2020) 70(1):7–30. doi: 10.3322/caac.21590
- Lamarca A, Hubner RA, David Ryder W, Valle JW. Second-Line Chemotherapy in Advanced Biliary Cancer: A Systematic Review. *Ann Oncol* (2014) 25(12):2328–38. doi: 10.1093/annonc/mdu162
- Valle J, Wasan H, Palmer DH, Cunningham D, Anthony A, Maraveyas A, et al. Cisplatin Plus Gemcitabine Versus Gemcitabine for Biliary Tract Cancer. *N Engl J Med* (2010) 362(14):1273–81. doi: 10.1056/NEJMoa0908721
- Eckel F, Brunner T, Jelic S. Biliary Cancer: ESMO Clinical Practice Guidelines for Diagnosis, Treatment and Follow-Up. *Ann Oncol* (2011) 22:vi40–4. doi: 10.1093/annonc/mdr375
- Iqbal N, Iqbal N. Human Epidermal Growth Factor Receptor 2 (HER2) in Cancers: Overexpression and Therapeutic Implications. *Mol Biol Int* (2014) 2014:852748. doi: 10.1155/2014/852748
- Yarden Y, Sliwkowski MX. Untangling the ErbB Signalling Network. *Nat Rev Mol Cell Biol* (2001) 2(2):127–37. doi: 10.1038/35052073
- Baselga J, Swain SM. Novel Anticancer Targets: Revisiting ERBB2 and Discovering ERBB3. *Nat Rev Cancer* (2009) 9(7):463–75. doi: 10.1038/nrc2656
- Chmielecki J, Ross JS, Wang K, Frampton GM, Palmer GA, Ali SM, et al. Oncogenic Alterations in ERBB2/HER2 Represent Potential Therapeutic Targets Across Tumors From Diverse Anatomic Sites of Origin. *Oncologist* (2015) 20(1):7–12. doi: 10.1634/theoncologist.2014-0234
- Roskoski R Jr. The ErbB/HER Family of Protein-Tyrosine Kinases and Cancer. *Pharmacol Res* (2014) 79:34–74. doi: 10.1016/j.phrs.2013.11.002
- Yan M, Schwaederle M, Arguello D, Millis SZ, Gatalica Z, Kurzrock R. HER2 Expression Status in Diverse Cancers: Review of Results From 37,992 Patients. *Cancer Metastasis Rev* (2015) 34(1):157–64. doi: 10.1007/s10555-015-9552-6
- Kiguchi K, Carbajal S, Chan K, Beltrán L, Ruffino L, Shen J, et al. Constitutive Expression of ErbB-2 in Gallbladder Epithelium Results in Development of Adenocarcinoma. *Cancer Res* (2001) 61(19):6971–6.
- Pellat A, Vaquero J, Fouassier L. Role of ErbB/HER Family of Receptor Tyrosine Kinases in Cholangiocyte Biology. *Hepatology* (2018) 67(2):762–73. doi: 10.1002/hep.29350
- Trekitkarnmongkol W, Suthiphongchai T. High Expression of ErbB2 Contributes to Cholangiocarcinoma Cell Invasion and Proliferation Through AKT/P70s6k. *World J Gastroenterol* (2010) 16(32):4047–54. doi: 10.3748/wjg.v16.i32.4047
- Harder J, Waiz O, Otto F, Geissler M, Olschewski M, Weinhold B, et al. EGFR and HER2 Expression in Advanced Biliary Tract Cancer. *World J Gastroenterol* (2009) 15(36):4511–7. doi: 10.3748/wjg.15.4511

## AUTHOR CONTRIBUTIONS

Conception and design: HoK, SK. Provision of study materials or patients: HoK, SH, JP, YP, SK. Collection and assembly of data: HoK, RK, HRK, HJ, HaK, SK. Data analysis and interpretation: HoK, SK. Manuscript writing: HoK, SK. All authors listed have made a substantial, direct, and intellectual contribution to the work and approved it for publication.

## ACKNOWLEDGMENTS

A grant of the Korea Health Technology R&D Project through the Korea Health Industry Development Institute (KHIDI) supported this research and the Ministry of Health & Welfare, Republic of Korea, funded (grant number: HR20C0025).

- Jacobi O, Ross JS, Goshen-Lago T, Haddad R, Moore A, Sulkes A, et al. ERBB2 Pathway in Biliary Tract Carcinoma: Clinical Implications of a Targetable Pathway. *Oncol Res Treat* (2021) 44(1–2):20–7. doi: 10.1159/000511919
- Ramanathan RK, Belani CP, Singh DA, Tanaka M, Lenz HJ, Yen Y, et al. A Phase II Study of Lapatinib in Patients With Advanced Biliary Tree and Hepatocellular Cancer. *Cancer Chemother Pharmacol* (2009) 64(4):777–83. doi: 10.1007/s00280-009-0927-7
- Kawamoto T, Ishige K, Thomas M, Yamashita-Kashima Y, Shu S, Ishikura N, et al. Overexpression and Gene Amplification of EGFR, HER2, and HER3 in Biliary Tract Carcinomas, and the Possibility for Therapy With the HER2-Targeting Antibody Pertuzumab. *J Gastroenterol* (2015) 50(4):467–79. doi: 10.1007/s00535-014-0984-5
- Law LY. Dramatic Response to Trastuzumab and Paclitaxel in a Patient With Human Epidermal Growth Factor Receptor 2-Positive Metastatic Cholangiocarcinoma. *J Clin Oncol* (2012) 30(27):e271–3. doi: 10.1200/jco.2012.42.3061
- Javle M, Churi C, Kang HC, Shroff R, Janku F, Surapaneni R, et al. HER2/neu-Directed Therapy for Biliary Tract Cancer. *J Hemtol Oncol* (2015) 8:58. doi: 10.1186/s13045-015-0155-z
- Javle M, Borad MJ, Azad NS, Kurzrock R, Abou-Alfa GK, George B, et al. Pertuzumab and Trastuzumab for HER2-Positive, Metastatic Biliary Tract Cancer (MyPathway): A Multicentre, Open-Label, Phase 2a, Multiple Basket Study. *Lancet Oncol* (2021) 22(9):1290–300. doi: 10.1016/s1470-2045(21)00336-3
- Rizzo A, Frega G, Ricci AD, Palloni A, Abbati F, DEL S, et al. Anti-EGFR Monoclonal Antibodies in Advanced Biliary Tract Cancer: A Systematic Review and Meta-Analysis. *In Vivo* (2020) 34(2):479–88. doi: 10.21873/in vivo.11798
- Jain A, Kwong LN, Javle M. Genomic Profiling of Biliary Tract Cancers and Implications for Clinical Practice. *Curr Treat Options Oncol* (2016) 17(11):58. doi: 10.1007/s11864-016-0432-2
- Churi CR, Shroff R, Wang Y, Rashid A, Kang HC, Weatherly J, et al. Mutation Profiling in Cholangiocarcinoma: Prognostic and Therapeutic Implications. *PLoS One* (2014) 9(12):e115383. doi: 10.1371/journal.pone.0115383
- Kayhanian H, Smyth EC, Braconi C. Emerging Molecular Targets and Therapy for Cholangiocarcinoma. *World J Gastrointest Oncol* (2017) 9(7):268–80. doi: 10.4251/wjgo.v9.i7.268
- Dumbrava EEI, Balaji K, Raghav K, Hess K, Javle M, Blum-Murphy M, et al. Targeting ERBB2 (HER2) Amplification Identified by Next-Generation Sequencing in Patients With Advanced or Metastatic Solid Tumors Beyond Conventional Indications. *JCO Precis Oncol* (2019) 3:PO.18.00345. doi: 10.1200/po.18.00345
- Canaj O, Ligon AH, Hornick JL, Sholl LM. Detection of ERBB2 Amplification by Next-Generation Sequencing Predicts HER2 Expression in Colorectal Carcinoma. *Am J Clin Pathol* (2019) 152(1):97–108. doi: 10.1093/ajcp/aqz031
- Ross DS, Zehir A, Cheng DT, Benayed R, Nafa K, Hechtman JF, et al. Next-Generation Assessment of Human Epidermal Growth Factor Receptor 2 (ERBB2) Amplification Status: Clinical Validation in the Context of a

- Hybrid Capture-Based, Comprehensive Solid Tumor Genomic Profiling Assay. *J Mol Diagn* (2017) 19(2):244–54. doi: 10.1016/j.jmoldx.2016.09.010
29. Yarlagadda B, Kamatham V, Ritter A, Shahjehan F, Kasi PM. Trastuzumab and Pertuzumab in Circulating Tumor DNA ERBB2-Amplified HER2-Positive Refractory Cholangiocarcinoma. *NPJ Precis Oncol* (2019) 3:19. doi: 10.1038/s41698-019-0091-4
  30. Mondaca S, Razavi P, Xu C, Offin M, Myers M, Scaltriti M, et al. Genomic Characterization of ERBB2-Driven Biliary Cancer and a Case of Response to Ado-Trastuzumab Emtansine. *JCO Precis Oncol* (2019) 3:PO.19.00223. doi: 10.1200/po.19.00223
  31. Vivaldi C, Fornaro L, Ugolini C, Niccoli C, Musettini G, Pecora I, et al. HER2 Overexpression as a Poor Prognostic Determinant in Resected Biliary Tract Cancer. *Oncologist* (2020) 25(10):886–93. doi: 10.1634/theoncologist.2019-0922
  32. Garcia P, Lamarca A, Diaz J, Carrera E, Roa JC. On Behalf of the European-Latin American Escalon Consortium. Current and New Biomarkers for Early Detection, Prognostic Stratification, and Management of Gallbladder Cancer Patients. *Cancers (Basel)* (2020) 12(12):3670. doi: 10.3390/cancers12123670
  33. Singh A, Mishra PK, Saluja SS, Talikoti MA, Kirtani P, Najmi AK. Prognostic Significance of HER-2 and P53 Expression in Gallbladder Carcinoma in North Indian Patients. *Oncology* (2016) 91(6):354–60. doi: 10.1159/000450999
  34. Ahn DH, Javle M, Ahn CW, Jain A, Mikhail S, Noonan AM, et al. Next-Generation Sequencing Survey of Biliary Tract Cancer Reveals the Association Between Tumor Somatic Variants and Chemotherapy Resistance. *Cancer* (2016) 122(23):3657–66. doi: 10.1002/cncr.30247
  35. Galdy S, Lamarca A, McNamara MG, Hubner RA, Cella CA, Fazio N, et al. HER2/HER3 Pathway in Biliary Tract Malignancies; Systematic Review and Meta-Analysis: A Potential Therapeutic Target? *Cancer Metastasis Rev* (2017) 36(1):141–57. doi: 10.1007/s10555-016-9645-x
  36. Ogo Y, Nio Y, Yano S, Toga T, Koike M, Hashimoto K, et al. Immunohistochemical Expression of HER-1 and HER-2 in Extrahepatic Biliary Carcinoma. *Anticancer Res* (2006) 26(1b):763–70.
  37. Philip PA, Mahoney MR, Allmer C, Thomas J, Pitot HC, Kim G, et al. Phase II Study of Erlotinib in Patients With Advanced Biliary Cancer. *J Clin Oncol* (2006) 24(19):3069–74. doi: 10.1200/jco.2005.05.3579
  38. Peck J, Wei L, Zalupski M, O'Neil B, Villalona Calero M, Bekaii-Saab T. HER2/neu may Not be an Interesting Target in Biliary Cancers: Results of an Early Phase II Study With Lapatinib. *Oncology* (2012) 82(3):175–9. doi: 10.1159/000336488
  39. Leone F, Marino D, Cereda S, Filippi R, Belli C, Spadi R, et al. Panitumumab in Combination With Gemcitabine and Oxaliplatin Does Not Prolong Survival in Wild-Type KRAS Advanced Biliary Tract Cancer: A Randomized Phase 2 Trial (Vecti-BIL Study). *Cancer* (2016) 122(4):574–81. doi: 10.1002/cncr.29778
  40. Gruenberger B, Schueller J, Heubrandtner U, Wrba F, Tamandl D, Kaczirek K, et al. Cetuximab, Gemcitabine, and Oxaliplatin in Patients With Unresectable Advanced or Metastatic Biliary Tract Cancer: A Phase 2 Study. *Lancet Oncol* (2010) 11(12):1142–8. doi: 10.1016/s1470-2045(10)70247-3
  41. Tsurutani J, Iwata H, Krop I, Jänne PA, Doi T, Takahashi S, et al. Targeting HER2 With Trastuzumab Deruxtecan: A Dose-Expansion, Phase I Study in Multiple Advanced Solid Tumors. *Cancer Discov* (2020) 10(5):688–701. doi: 10.1158/2159-8290.Cd-19-1014
  42. Bang YJ, Giaccone G, Im SA, Oh DY, Bauer TM, Nordstrom JL, et al. First-In-Human Phase 1 Study of Margetuximab (MGAH22), an Fc-Modified Chimeric Monoclonal Antibody, in Patients With HER2-Positive Advanced Solid Tumors. *Ann Oncol* (2017) 28(4):855–61. doi: 10.1093/annonc/mdx002
  43. Meric-Bernstam F, Hanna DL, El-Khoueiry AB, Kang Y-K, Oh D-Y, Chaves JM, et al. Zanidatamab (ZW25) in HER2-Positive Biliary Tract Cancers (BTCs): Results From a Phase I Study. *J Clin Oncol* (2021) 39(3\_suppl):299. doi: 10.1200/JCO.2021.39.3\_suppl.299
  44. Nara S, Esaki M, Ban D, Takamoto T, Shimada K, Ioka T, et al. Adjuvant and Neoadjuvant Therapy for Biliary Tract Cancer: A Review of Clinical Trials. *Jpn J Clin Oncol* (2020) 50(12):1353–63. doi: 10.1093/jjco/hyaa170

**Conflict of Interest:** The authors declare that the research was conducted in the absence of any commercial or financial relationships that could be construed as a potential conflict of interest.

**Publisher's Note:** All claims expressed in this article are solely those of the authors and do not necessarily represent those of their affiliated organizations, or those of the publisher, the editors and the reviewers. Any product that may be evaluated in this article, or claim that may be made by its manufacturer, is not guaranteed or endorsed by the publisher.

Copyright © 2022 Kim, Kim, Kim, Jo, Kim, Ha, Park, Park and Kim. This is an open-access article distributed under the terms of the Creative Commons Attribution License (CC BY). The use, distribution or reproduction in other forums is permitted, provided the original author(s) and the copyright owner(s) are credited and that the original publication in this journal is cited, in accordance with accepted academic practice. No use, distribution or reproduction is permitted which does not comply with these terms.





# Glypican-3: A Novel and Promising Target for the Treatment of Hepatocellular Carcinoma

Xiufeng Zheng<sup>1†</sup>, Xun Liu<sup>2†</sup>, Yanna Lei<sup>1</sup>, Gang Wang<sup>2\*</sup> and Ming Liu<sup>1\*</sup>

<sup>1</sup> Department of Abdominal Oncology, West China Hospital, Sichuan University, Chengdu, China, <sup>2</sup> National Engineering Research Center for Biomaterials, Sichuan University, Chengdu, China

## OPEN ACCESS

### Edited by:

Alessandro Passardi,  
Romagnolo Scientific Institute  
for the Study and Treatment  
of Tumors (IRCCS), Italy

### Reviewed by:

Qing Zhang,  
Xuzhou Medical University, China  
Yelei Guo,  
People's Liberation Army General  
Hospital, China

### \*Correspondence:

Ming Liu  
mingliu721@aliyun.com  
Gang Wang  
wgang@scu.edu.cn

<sup>†</sup>These authors have contributed  
equally to this work

### Specialty section:

This article was submitted to  
Gastrointestinal Cancers: Hepato  
Pancreatic Biliary Cancers,  
a section of the journal  
Frontiers in Oncology

**Received:** 29 November 2021

**Accepted:** 18 January 2022

**Published:** 16 February 2022

### Citation:

Zheng X, Liu X, Lei Y, Wang G and  
Liu M (2022) Glypican-3: A Novel and  
Promising Target for the Treatment of  
Hepatocellular Carcinoma.  
Front. Oncol. 12:824208.  
doi: 10.3389/fonc.2022.824208

Glypican-3 (GPC3) is a membrane-associated proteoglycan that is specifically up-regulated in hepatocellular carcinoma (HCC) although rarely or not expressed in normal liver tissues, making it a perfect diagnostic and treatment target for HCC. Several GPC3-based clinical trials are ongoing and recently several innovative GPC3-targeted therapeutic methods have emerged with exciting results, including GPC3 vaccine, anti-GPC3 immunotoxin, combined therapy with immune checkpoint blockades (ICBs), and chimeric antigen receptor (CAR) T or NK cells. Here, we review the value of GPC3 in the diagnosis and prognosis of HCC, together with its signaling pathways, with a specific focus on GPC3-targeted treatments of HCC and some prospects for the future GPC3-based therapeutic strategies in HCC.

**Keywords:** glypican-3 (GPC3), hepatocellular carcinoma (HCC), cancer immunotherapy, immune checkpoint blockade, chimeric antigen receptor

## 1 INTRODUCTION

Liver cancer is the second-most cause of cancer death throughout the world (8.2% of the total) (1), and hepatocellular carcinoma (HCC) is the most common type of liver cancer. Despite significant advances in both diagnosis and treatment, only 40% of HCC is diagnosed at an early stage, and the results of treatment are often disappointing. Surgery is still the preferred treatment. However, only 5%-10% of HCC tumors are suitable for resection, and tumor recurrence occurs in a majority (50%-70%) of patients within five years of surgery. Although liver transplantation offers an alternative, the numbers of suitable donor liver sources are extremely limited, while waiting for the donor liver, the tumor may progress, which may lead to the loss of surgical opportunity or worsen the postoperative prognosis (2). Systemic chemotherapy with oxaliplatin-based regimens has been found to increase the overall survival (OS) by 1.47 months (3). Multiple tyrosine kinase inhibitors, sorafenib (4), used as first-line treatments, while lenvatinib (5) and donafenib were found to be superior to sorafenib in extending the OS in Chinese patients with advanced HCC (6).

Immunotherapy has become a powerful strategy for treating cancer. Anti-programmed cell death protein 1 (PD-1) inhibitors of nivolumab (7) and pembrolizumab (8), anti-CTLA-4 inhibitors of tremelimumab (9) and ipilimumab (10), the preliminary results showed promising antitumor activity in HCC. At present, the general trend in tumor treatment is the use of combination therapy, Atezolizumab combined with bevacizumab was found to improve the patient prognosis with an excellent objective response rate (ORR) in advanced HCC (11), and lenvatinib combined with

pembrolizumab or sintilimab combined with bevacizumab showed similar results (12, 13). Nevertheless, despite the progress of current treatments, there are still limited options for effective systemic treatment of HCC. As a result, its five-year survival rate is only a dismal 18% (14). Thus, the identification of specific molecular markers and targets would assist both early diagnosis and targeted therapy.

Glypian-3 (GPC3) is a heparan sulfate proteoglycan (HSPG). There are six glypican subtypes, namely, GPCs 1-6, with similar structures consisting of a 60-70 kDa protein connected to the cell membrane by a glycosylphosphatidylinositol (GPI) anchor, 14 conserved cysteine residues, and the last 50 residues at the carboxyl end modified by the heparan sulfate (HS) side-chain. GPC3 has been implicated in a variety of processes, including cell growth, differentiation, and migration (15, 16). The specific expression of GPC3 in tumor cells has received widespread attention. Here, we discuss the relevance of GPC3 to HCC diagnosis and prognosis, and also address the signaling pathways used by GPC3 to promote HCC development, and focus on the feasibility of targeting GPC3 for treating HCC.

## 2 RELEVANCE OF GPC3 TO THE DIAGNOSIS AND PROGNOSIS OF HCC

The potential of GPC3 in HCC diagnosis and prognosis is gradually being recognized. **Figure 1** compares GPC3 expression in various cancers and normal tissues (17). In 1997, Hsu et al. demonstrated that MXR7 (later shown to be GPC3)

was more strongly expressed in HCC than AFP (18), but was not visible in either normal liver or benign liver lesions (such as cirrhotic or dysplastic nodules) (19). Immunostaining also demonstrated the presence of GPC3 in small liver tumors (16). Currently, GPC3-targeted imaging includes positron emission tomography (PET) (20, 21), magnetic resonance imaging (MRI) (22), and near-infrared imaging (NIR) (23) for the early diagnosis of HCC, showing excellent results and high specificity in HCC. GPC3 is also found in the serum of many HCC patients but not in sera from healthy individuals or patients with hepatitis. Despite the presence of GPC3 being indicative of an HCC diagnosis, a single marker cannot meet the specificity and sensitivity requirements of clinical practice. GPC3 + HSP70 (heat shock protein 70) + GS (glutamine synthetase) is an optimal combination to distinguish early and grade 1 HCC from dysplastic nodules in cirrhosis, strengthening the diagnosis of suspected HCC, especially in a biopsy with few samples (24, 25). Other investigations have also proposed some combinations of potential markers, such as arginase-1/hepar-1/GPC3 (26), GP73/GPC3/CD34 (27), and GPC3/CD34 (28). Elevated levels of GPC3 in tumor cells is related to poor prognosis, as **Figure 2** shows (17). For example, the five-year survival of patients positive for GPC3 was considerably reduced compared to that of GPC3-negative patients (54.5 vs 87.7%,  $P = 0.031$ ), with this association between GPC3 level and HCC prognosis demonstrated in many studies (29). The early identification of GPC3-positivity may also predict tumor recurrence after resection, and GPC3 is recognized as an independent prognostic factor for disease-free survival (DFS) (30). A raised serum level of the GPC3 N-terminal subunit

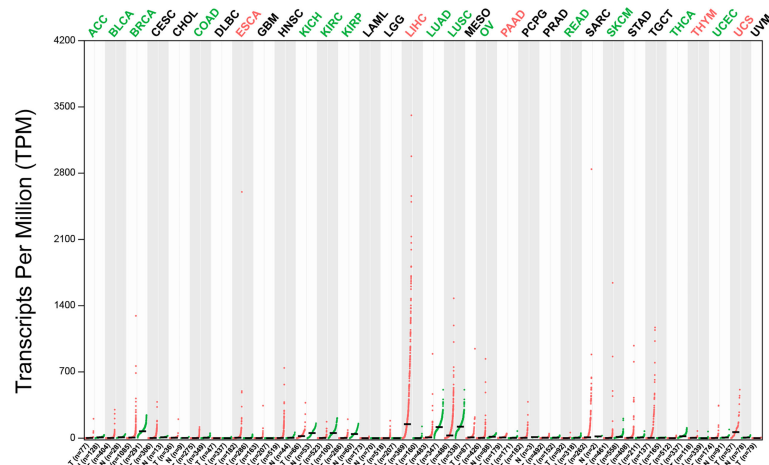
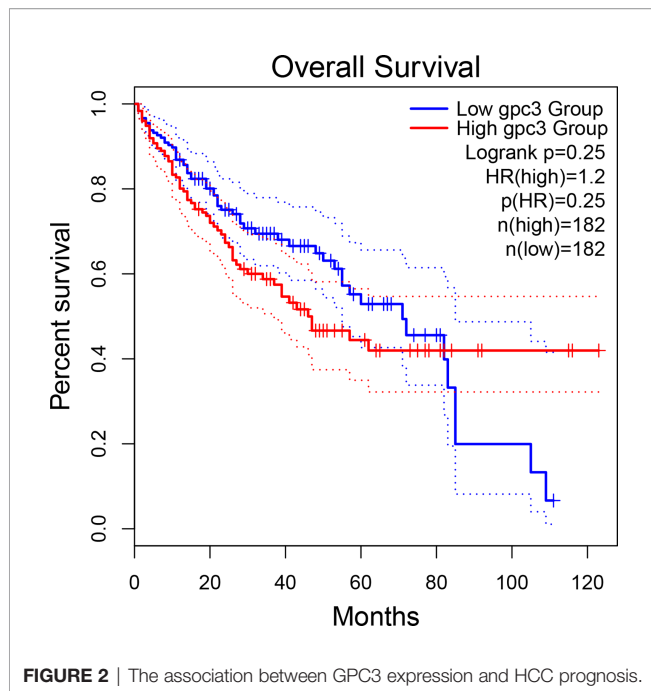


**FIGURE 1** | The expression profile of GPC3 across tumor samples and paired normal tissues (Dot plot). Each dot represents expression of samples. T, tumor samples; N, normal tissues; ACC, adrenocortical carcinoma; BLCA, bladder urothelial carcinoma; BRCA, breast invasive carcinoma; CESC, cervical squamous cell carcinoma & endocervical adeno; CHOL, cholangiocarcinoma; COAD, colon adenocarcinoma; DLBC, lymphoid neoplasm diffuse large B-cell lymphoma; ESCA, esophageal carcinoma, glioblastoma multiforme; HNSC, head & neck squamous cell carcinoma; KICH, kidney chromophobe cell carcinoma; KIRC, kidney renal clear cell carcinoma; KIRP, kidney renal papillary cell carcinoma; LAML, acute myeloid leukemia; LGG, brain lower grade glioma; LIHC, liver hepatocellular carcinoma; LUCB, lung adenocarcinoma; LUSC, lung squamous cell carcinoma; MESO, mesothelioma; OV, ovarian serous cystadenocarcinoma; PAAD, pancreatic adenocarcinoma; PCPG, pheochromocytoma & paraganglioma; PRAD, prostate adenocarcinoma; READ, rectum adenocarcinoma; SARC, sarcoma; SKCM, skin cutaneous melanoma; STAD, stomach adenocarcinoma; TGCT, testicular germ cell tumors; THCA, thyroid carcinoma; THYM, thymoma; UCEC, uterine corpus endometrial carcinoma; UCS, uterine carcinosarcoma; UVM, uveal melanoma.



antigen (sGPC3N) has also been shown to be independently related to both OS ( $p < 0.05$ ) and DFS ( $p < 0.01$ ) (31). Furthermore, both GPC3 and osteopontin (OPN) overexpression are linked to reduced DFS in HBV-positive small HCC, with elevated levels of both molecules indicative of adverse outcomes after curative resection (32). For HCV-positive patients after surgical resection, GPC3 is a prognostic indicator for reduced DFS (33). Consistently, raised levels of GPC3 mRNA have been linked to the development of HCC after liver transplantation (34). Furthermore, a viable GPC3-based immunomagnetic fluorescent system (C6/MMSN-GPC3) has been developed to identify circulating tumor cells (CTCs) in HCC patients' blood, further contributing to the early diagnosis and determination of prognosis (35).

### 3 GPC3-ASSOCIATED SIGNALING PATHWAYS IN HCC

#### 3.1 Wnt Signaling Pathway

Wnt signaling plays a major part in HCC pathology and is implicated in cell survival, proliferation, migration, and invasion. The first step in the pathway is the binding of Wnt to the membrane receptor Frizzled (FZD). Wnt signaling involves both canonical and non-canonical pathways, with the former involving the  $\beta$ -catenin protein (36, 37).  $\beta$ -catenin influences the expression of numerous genes, some of which are associated with cell proliferation and survival (38). GPC3 activates the canonical pathway, thereby stimulating HCC progression (39, 40). The human monoclonal anti-GPC3 antibody, HS20, binds the GPC3 HS moiety and has been shown to block the interaction between GPC3 and Wnt3a (41).

GPC3 also interacts with FZD through the HS chain, suggesting that GPC3 may form a signaling complex with both FZD and Wnt (42). The N-leaf cysteine-rich domain (CRD) of GPC3 has a Wnt-binding groove, and the mutation of the notch reduces binding, thereby reducing Wnt activation, and inhibiting the growth of mouse liver cancer (43).

#### 3.2 Other Signaling Pathways

The Hippo signaling pathway is responsible for reducing cell contacts and limiting both organ size and tumorigenesis (44). The Hippo pathway is frequently activated in HCC, with activation of the Yes-associated protein (YAP) (45, 46). GPC3 knockout inhibits YAP expression at both the mRNA and protein levels and induces the apoptosis of Huh7 cells (47, 48). In addition, the abnormal persistence of hedgehog signaling has been directly related to HCC (49–51), and GPC3 appears to be a negative regulator of hedgehog signaling (52–54). Transcription factors zinc-fingers and homeoboxes 2 (ZHX2) (55) and C-myc (56) are involved in the oncogenic activation of GPC3 in HCC to modulate HCC cell growth, proliferation, and differentiation. Sulfatase 2 may up-regulate GPC3 expression, promote fibroblast growth factor (FGF) signal transduction, and reduce the survival rate of HCC patients. A human monoclonal antibody against the GPC3 HS chain inhibited HGF/c-Met pathway-mediated migration and motility in hepatoma cells (41, 57–59). Furthermore, GPC3 could promote the progression and metastatic spread of HCC by influencing the functioning of tumor-associated macrophages (TAM) through macrophage recruitment (60). In **Figure 3**, we summarize the signal pathways related to GPC3.

### 4 GPC3 TARGETED THERAPY FOR HCC

Since GPC3 is overexpressed in HCC, as **Figure 4** shows, various inhibitors targeting GPC3 are under investigation.

#### 4.1 GPC3-Targeted Antibodies

##### 4.1.1 Monoclonal Antibodies

GC33 is a recombinant, humanized, high-affinity monoclonal antibody against the GPC3 C-terminus. In preclinical assessments, GC33 was found to promote antibody-dependent cellular cytotoxicity (ADCC) in an antigen-dependent manner (61). The antibody also reduced tumor growth in xenograft models, with the growth reduction correlated approximately to the cell surface antigen level (61). In clinical application, Zhu, et al. enrolled 20 patients in a dose-escalation study, showing no dose-limiting toxicities (DLT) as the maximum tolerated dose fell beyond even the highest dose planned. This suggested the potential clinical efficacy and benefit of GC33 and warrants further evaluation. The minimum serum concentrations of the antibody were above the target concentrations at doses above 5 mg/kg and there was a significant reduction in the median time to progression (TTP) between the high-GPC3 group and the low-GPC3 group (26.0 weeks vs 7.1 weeks;  $P = 0.033$ ) (62). Ikeda, et al. enrolled seven patients in a similar study in Japan to

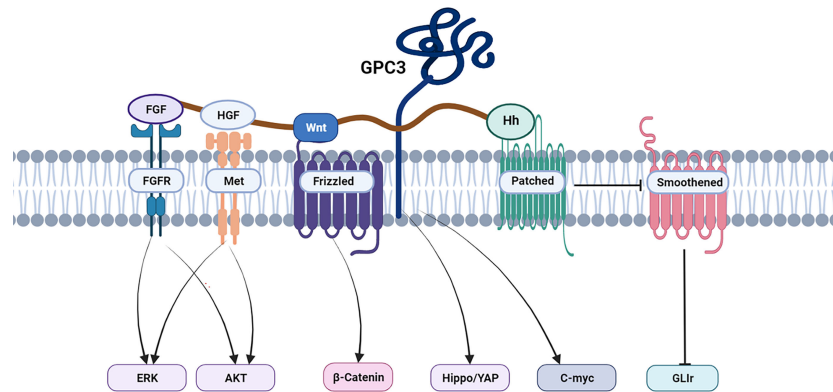


**FIGURE 3** | GPC3 associated signaling pathways in HCC.

evaluate the safety and tolerability of GC33. They observed that GC33 was well-tolerated overall, with no DLTs and with the maximum tolerated dose (MTD) not reached. These findings are consistent with those of the First-in-Human although the small sample size did not allow a clear correlation between GPC3 expression and antitumor action (63). Recently, a double-blind, phase II trial of GC33 in 185 patients with chemotherapy-unresponsive HCC showed that, although Codrituzumab therapy itself was ineffective, when increasing Codrituzumab exposure, the levels of GPC3 and CD16 in circulating immune cells could predict the efficacy of the drug, suggesting that precision Codrituzumab therapy with this perspective may have potential for treating HCC (64).

Another monoclonal antibody, 32A9, specifically targeting the middle region of GPC3, reduced the growth of HCC tumors in mice. This study then investigated two 32A9-based immunotherapeutic strategies involving an immunotoxin and

CAR-T cells. It was found that the antibody-immunotoxin complex was specifically cytotoxic to GPC3-positive tumor cells, while the 32A9-CAR-T cells destroyed the tumor cells *in vitro* and promoted regression of HCC xenograft tumors *in vivo* (65). Feng et al. described an antibody, HN3, that recognized the full GPC3 molecule with high affinity. The antibody promoted cell cycle arrest in G1, inhibiting the growth of GPC3-expressing cells and reducing the growth of xenografts in mice (66). Another human anti-GPC3 monoclonal antibody, HS20, that recognizes the HS moiety on the molecule, was shown to block Wnt signaling and inhibit tumor growth. This antibody also showed no toxicity in mice (41). Thus, although GPC3 is a well-characterized HCC-associated antigen, anti-GPC3 therapeutic strategies have had limited clinical success.

#### 4.1.2 Bispecific Antibodies

Given the low clinical response rate of monoclonal antibodies targeting GPC3, bispecific antibodies have been investigated. One such bispecific antibody, ERY974, a humanized IgG-structured T cell-redirecting antibody (TRAB) with a common light chain, could bind to both GPC3 and CD3, promoting cytotoxicity through the action of T cell effectors. ERY974 also showed significant non-immunogenic antitumor effects in tumors that were unresponsive to treatment with immune checkpoint (such as PD-1 and CTLA-4) inhibitors. Further investigation showed that ERY974 induced a high degree of inflammation in the tumor microenvironment, with toxicology studies in cynomolgus monkeys showing raised levels of cytokines in the short-term (67). A further report demonstrated a significant improvement in antitumor action in xenograft models using a combination of ERY974 and chemotherapy (68). A phase I clinical trial of this antibody is ongoing (NCT02748837). GPC3/CD47, a bispecific antibody targeting GPC3 and CD47, was effective in preventing tumor growth through recognition of both antigens. This antibody has a long serum half-life with no adverse systemic effects compared to an anti-CD47 antibody alone. The antibody was more effective than treatment with a single anti-CD47 antibody or a combination of individual anti-CD47 and anti-GPC3 antibodies in a mouse xenograft model (69). Taken together,

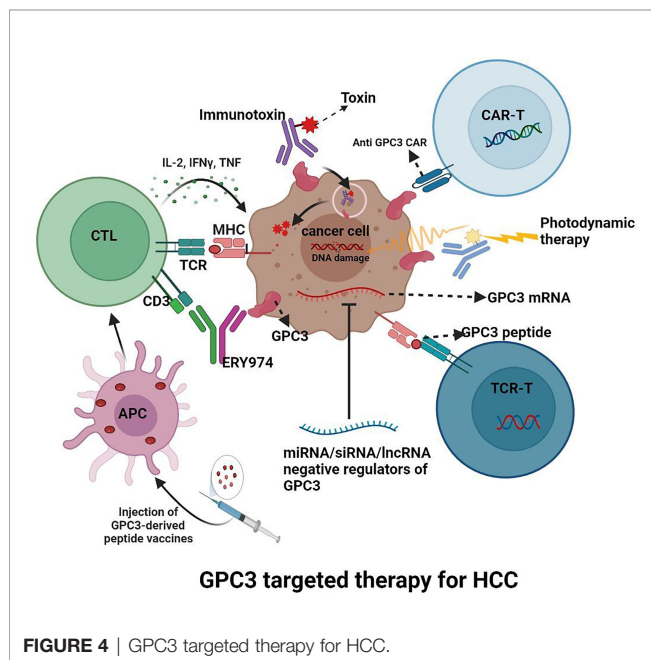


**FIGURE 4** | GPC3 targeted therapy for HCC.



these results suggest that anti-GPC3 bispecific antibodies might be potential therapeutic treatments for HCC in the future.

## 4.2 GPC3-Derived Peptide/DNA Vaccines

In addition to antibodies targeting GPC3, the application of GPC3-derived peptide/DNA vaccines is another potentially attractive option for treating HCC. Nakatsura, et al. showed that both HLA-A24(A\*2402)-restricted and H-2Kd-restricted GPC3298–306 peptide (EYILSLEEL) peptides, as well as the HLA-A2(A\*0201)-restricted GPC3<sub>144–152</sub> peptide (FVGEFFTDV), can induce GPC3-reactive cytotoxic T lymphocytes (CTLs) (70, 71). These peptides were subsequently tested as vaccines in preclinical trials using mouse models, and schedules for clinical trials were set up, testing the GPC3298–306 and GPC3144–152 peptides in a Phase I clinical trial. In the trial, one patient showed a partial response (PR), while 4 out of 19 patients with stable disease (SD) showed tumor regression or necrosis beyond the PR criteria. After two months of ongoing treatment, the disease control rate (PR+SD) was 60.6% (72). A pilot study (UMINCTR: 000005093) confirmed lymphocyte tumor infiltration by after vaccination with the GPC3 peptides. A Phase II, open-label, single-arm trial (UMIN-CTR: 000002614) enrolled 40 HCC patients who had received either surgery or radiofrequency ablation. In the year following curative treatment, 10 vaccinations were administered, resulting in a significantly lower recurrence rate in patients who had received surgery/radiofrequency ablation with vaccines than in patients who had been treated with surgery only (73). Intravenous administration of GPC3-coupled lymphocytes (LC/GPC3<sup>+</sup>) resulted in the production of both anti-GPC3 antibodies and CTLs, reducing HCC growth and lysing HCC cells in culture (74). Apart from these peptide vaccines, GPC3 DNA vaccines could elicit CTL responses against HCC cell lines, inhibit homogenous tumor growth, and increase the survival rates of xenograft-bearing mice (75). However, despite the potential attraction of a peptide vaccine, the antitumor effects are too weak for treating advanced HCC. Intratumoral peptide injection or combining the peptide vaccine with an anti-PD-1 blocking antibody could feasibly enhance the antitumor effects.

## 4.3 Immunotoxins

GPC3-targeted human nanobody (HN3) immunotoxins have been reported to have potent antitumor effects through the blocking of protein synthesis and downregulation of the Wnt signaling pathway. For example, it was found that intravenously administering the immunotoxin HN3-PE38 either individually or in combination with chemotherapeutic drugs promoted regression of Hep3B and HepG2 tumor xenografts in mice. These results indicate the potential of GPC3 use in immunotoxin-based treatment. However, a drawback was that the side effects and potential toxicity of the immunotoxin, which could thus only be used at low doses (< 0.8 mg kg<sup>-1</sup>) (76). In addition, another team of researchers constructed two mPE24-based immunotoxins (HN3-mPE24 and HN3HN3-mPE24). HN3-mPE24 had both high-affinity antigen-binding and strong anti-tumor effects in HCC cells, with minimal side

effects in mice even at high doses, and resulted in effective tumor regression and improved survival rates. However, immunogenic effects and the relatively short half-lives of immunotoxins may limit their clinical application (77). To overcome this shortcoming, another research team engineered HN3-ABD-T20 and HN3-ALB1-T20 by adding an albumin-binding domain (ABD) to prolong their half-life. This resulted in effective tumor regression at one-tenth of the dose required for HN3-T20. This increased potency was ascribed to the observed 45-fold prolongation of HN3-ABD-T20's serum retention time. Pharmacokinetic studies in mice showed that HN3-ABD-T20 had a half-life of about 5.5 hours compared to only 7 minutes for HN3-T20. HN3-ABD-T20 thus represents the best option for clinical translation because of its long serum retention, high cytotoxicity, and reduced antigenicity (78). Although further investigations, including clinical trials, are required, these findings suggest that GPC3-targeted immunotoxins have promising potential for treating HCC.

## 4.4 GPC3 CAR-T/NK Cells

In recent years, CAR-T cell therapy has proved effective for treating several cancers, especially hematological malignancies (79, 80). To date, there have been several clinical trials exploring the use of GPC3 CAR-T in HCC (Table 1). GPC3-targeted CAR-T cells are able to destroy GPC3<sup>+</sup> HCC cells *in vitro* and GPC3<sup>+</sup> HCC tumor xenografts in mice. Combinations of sorafenib and GPC3-CAR T cells have also proved effective (81). Compared with GPC3-CAR-T cells, the combination of GPC3 and epidermal growth factor receptor (EGFR)-dual-targeting CAR-T cells is more effective in reducing HCC growth (82). To further increase the specificity and decrease the off-target risk, IL-12-armored GPC3-redirected CAR-T cells were designed which showed greatly improved antitumor effects in mouse models (83). An IL-4/21 inverted cytokine receptor also improved CAR-T cell potency in an immunosuppressive tumor microenvironment (84). GPC3-specific CAR-T cells co-expressing IL-15 and IL-21 (85) or IL-7 and PH-20 (86) were found to be effective against HCC. Interestingly, disruption of PD-1 gene expression in GPC3 CAR-T cells by the CRISPR/Cas9 gene-editing system increased the *in vivo* activity of CAR-T cells against HCC, improving their infiltration levels in mouse models (87). Co-stimulation of DNAX-activating protein 10 was shown to increase the anti-tumor action of CAR-T cells (88). Interestingly, shed GPC3 competed with cell-surface GPC3 CAR-T cell binding, inhibiting the effects of the cells in HCC (89).

There are, however, side effects in the use of CAR-T cells, including tumor lysis syndrome, cytokine release syndrome, and on-target, off-tumor effects. These side-effects, rather than the neoplasm itself, may even be fatal. NK-92 cells have been developed to incorporate improved efficacy with minimal toxicity. The safety and cytotoxic specificity of genetically modified NK-92 cells have been attested to in preclinical trials, suggesting that these cells may be ideal carriers for CAR (90). The anti-tumor efficacy of NK-92/9.28.z cells has been confirmed in many HCC xenografts with different GPC3 levels (91). The combination of CAR-T and GPC3-targeted treatments appear to be highly promising, especially if combined with ICBs.

**TABLE 1 |** Clinical trials of GPC3-CAR-T for treating liver cancer.

Interventions	Study Title	Trial No.	status	Phase	Locations
<b>Monotherapy</b>					
GPC3 CAR-T cells	GPC3 CAR-T cells in patients with refractory HCC	NCT03146234	Completed	Not Applicable	Shanghai, China
	CAR-T Cells Targeting GPC3	NCT03884751	recruiting	1	Zhejiang, China
	4th generation CAR-T cells targeting GPC3	NCT03980288	recruiting	1	Zhejiang, China
	GPC3 CAR-T Cells for the Hepatocellular Carcinoma	NCT04506983	a Not yet recruiting	1	Beijing, China
	A Study of GPC3-targeted T Cells by Intratumor Injection for Advanced HCC (GPC3-CART)	NCT03130712	Unknown	1/2	Beijing, China
	A Study of GPC3 Redirected Autologous T Cells for Advanced HCC	NCT02715362	Unknown	1/2	Shanghai, China
	GPC3-CAR-T Cells for Immunotherapy of Cancer With GPC3 Expression	NCT03198546	recruiting	1	Guangdong, China
	A Study of Chimeric Antigen Receptor T Cells Combined With Interventional Therapy in Advanced Liver Malignancy	NCT02959151	Unknown	1/2	Shanghai, China
	CAR-T Cell Immunotherapy for HCC Targeting GPC3	NCT02723942	Withdrawn	1/2	Guangdong, China
	GPC3-targeted CAR-T Cell for Treating GPC3 Positive Advanced HCC	NCT04121273	recruiting	1	Jiangsu, China
anti-GPC3 CAR-T	Anti-GPC3 CAR T for Treating Patients With Advanced HCC	NCT02395250	Completed	1	Shanghai, China
<b>Combined chemotherapy</b>					
GAP T cells, Cytoxan, Fludara	GPC3-specific Chimeric Antigen Receptor Expressed in T Cells for Patients With Pediatric Solid Tumors (GAP)	NCT02932956	Recruiting	1	Texas, United States
AGAR T cells, Cytoxan, Fludara	Interleukin-15 Armored GPC3-specific Chimeric Antigen Receptor Expressed in T Cells for Pediatric Solid Tumors	NCT04377932	Not yet recruiting	1	Texas, United States
CARE T cells, Cytoxan, Fludara	Interleukin-15 and -21 Armored Glypican-3-specific Chimeric Antigen Receptor Expressed in T Cells for Pediatric Solid Tumors	NCT04715191	Not yet recruiting	1	Texas, United States
TEGAR T cells, Cytoxan, Fludarabine	T Cells co- Expressing a Second Generation GPC3-specific Chimeric Antigen Receptor With Cytokines Interleukin-21 and 15 as Immunotherapy for Patients With Liver Cancer (TEGAR)	NCT04093648	Withdrawn	1	Unknown
GLYCAR T cells, Cytoxan, Fludarabine	GPC3-specific Chimeric Antigen Receptor Expressing T Cells for Hepatocellular Carcinoma (GLYCAR)	NCT02905188	Recruiting	1	Texas, United States
Retroviral vector-transduced autologous T cells to express anti-GPC3 CARs, Fludarabine, Cyclophosphamide	Anti-GPC3 CAR-T for Treating GPC3-positive Advanced Hepatocellular Carcinoma (HCC)	NCT03084380	Unknown	1/2	Chongqing, China
<b>Combined with other immunotherapy</b>					
CAR-CD19 T cell, CAR-BCMA T cell, CAR-GPC3 T cell, (and 3 more...)	Clinical Study of Redirected Autologous T Cells With a Chimeric Antigen Receptor in Patients With Malignant Tumors	NCT03302403	Active, not recruiting	Not Applicable	Zhejiang, China

(U.S. National Library of Medicine | U.S. National Institutes of Health | U.S. Department of Health & Human Services)(Updated to 2021).

## 4.5 Gene Therapy

The use of gene therapy targeting GPC3 has also been investigated. For example, sulfatase 2 (SULF2) knockdown decreased HCC cell proliferation and migration as well as xenograft growth (58). MicroRNAs (miRNAs) targeting GPC3 have been described, with low levels of miR-1271 related to GPC3 overexpression in HCC, with the miRNA reducing HCC cell growth in a GPC3-dependent manner and inducing cell death (92). However, although the siRNA technology is effective for the specific silencing of individual genes, it is difficult to apply to a clinical setting as it requires effective delivery with high specificity and minimal toxicity. A GPC3-targeted siRNA nanovector (NP-siRNA-GPC3 antibody for HCC treatment) showed obvious antitumor efficacy *in vitro* with minimal

toxicity and significantly inhibited orthotopic HCC xenografts (93). It is known that long non-coding RNAs (lncRNAs) play significant roles in cancer, including HCC. Knockdown of the HOXA cluster antisense RNA2 (HOXA-AS2) lncRNA reduced GPC3 expression and blocked HCC cell proliferation by G1 arrest, as well as promoting apoptosis and inhibiting HCC cell migration and invasion *in vitro* (94).

## 4.6 Combination of Anti-GPC3 and ICIs

Combining anti-GPC3 antibodies and immune checkpoint inhibitors (ICIs) may be a promising strategy for GPC3-associated cancers. For example, treatment with the GC33 antibody increased the infiltration of PD-L1 positive immune cells (such as macrophages and multinucleated giant cells), and

mGC33 combined with an anti-mPD-L1 monoclonal antibody was more effective against tumors than the antibody alone in xenograft HCC models (95). A Phase I clinical trial of the anti-GPC3 monoclonal antibody Codrituzumab combined with atezozumab showed that the agents were well-tolerated and effective in reducing tumor growth in patients with advanced HCC. Among 18 evaluable patients, 1 case was diagnosed as PR, and 10 were SD (including 1 case of unconfirmed PR), of which 6 cases had SD more than 6 months before progression. No DLT was observed (96). Thus, GPC3-CAR-T in combination with anti-PD-1 has increased antitumor efficacy and may have potential for the treatment of HCC patients (97, 98).

## 4.7 Other Therapies

The direction of T cells to tumors is important in cancer therapy. For example, T cells combined with GPC3-specific antibodies are able to destroy GPC3-expressing HCC xenograft tumors in mice (99). Photodynamic therapy (PDT) is a novel method for treating tumors; this relies on the production of reactive oxygen species that induce tumor cell death. This is linked to both vascular shutdown and enhancement of immune activity, but its applications have been limited by the poor tissue penetration of visible light. The use of the near-infrared (NIR) photosensitizer may solve these limitations (100). For example, UCNPs@mSiO<sub>2</sub>-Ce6-GPC3 nanoparticles are biocompatible, have low toxicity, and produce good cell imaging and antitumor results (101). A novel multi-functional nanostructure, galactose (GAL)-golden nanorods (GNR)-siRNA of GPC3 (siGPC3) was found to produce both silencing of the GPC3 gene and photothermal action, and may be useful as a synergistic treatment for cancer (102). A study on a GPC3-targeting peptide (named G12)-modified liposome (GSI-Lip) co-loaded with sorafenib (SF) and IR780 iodide (IR780) showed promising sensitivity and specificity in detecting HCC together with synergistic effects on chemo-photothermal theranostics (103). Thus, the combination of chemotherapeutic drugs and siRNA may have potential in improving anticancer effects using synergistic interactions. SF-PL/siGPC3 with selected sizes and zeta potentials, delivered by PEI-modified liposomes, was shown to accumulate at the tumor site and to enter HCC cells, resulting in suppression of both GPC3 and the pro-proliferation gene cyclin D1 expression. Intravenous injection of SF-PL/siGPC3 into HepG2-bearing nude mice both blocked tumor growth and prolonged survival (104). GPC3 is involved in the progression of HCC, including stimulation of Wnt signaling, Hedgehog signaling. MiR-542-3p (105) and miR-485-5p (106) block the Wnt signaling pathway, while GANT61 (107) and bufalin (108) affect the Hedgehog signaling pathway to inhibit HCC.

## 4.8 Toxicities for Targeting GPC3

While exhibiting great efficacy, toxicities for targeting GPC3 must be attention. In GPC3 antibody therapy, GC33 was well tolerated in HCC, the most common adverse events (AEs) were the decrease of lymphocyte count (77%) and NK cell count (77%), no grade 4 or 5 AEs were reported (63). When GC33 combined with anti-PD-L1 antibody, grade  $\geq 3$  AEs were increased aspartate aminotransferase and decreased

lymphocyte count (96). Although the phase I clinical data of ERY974 have not been published, in animal trials, the most prominent AEs is cytokine release syndrome (CRS), an acute inflammatory syndrome resulted from the activation of immune cells and release of pro-inflammatory cytokines, however, cytokine release can be managed by corticosteroid premedication (67). In GPC3 vaccine therapy, there are reports of patients with tumor lysis syndrome after the second GPC3 peptide injection, which led to high fever, liver failure, and death (109). Thus, researchers need to optimize the balance between superior tumor-killing abilities and severe tumor lysis syndrome. In GPC3 CAR-T therapy, the commonest grade 3/4 adverse event was hematotoxicity, mainly due to transient lymphocyte count reduction resulted from lymphatic depletion (110, 111). Moreover, cytokine release syndrome (CRS), an acute inflammatory syndrome resulted from the activation of immune cells and release of pro-inflammatory cytokines, should be taken seriously. In a phase I clinical trial of GPC3 CAR-T for HCC, CRS occurred in 9/13 patients, including 1 case of grade 5 CRS (died on day 19) (110). In another study, CRS occurred in all patients, with a 50% incidence of grade  $\geq 3$  CRS (3/6) (111). In addition, neurotoxicity is related to CRS, cytokines are elevated not only in blood, but also in cerebrospinal fluid, and its clinical symptoms mainly include headache and disturbance of consciousness (112). Fortunately, administrate high-dose corticosteroids or IL-6 receptor antagonist drug tocilizumab was able to alleviate CRS (113). In patients with high tumor load, there is a more severe CRS (114). The use of CAR-T either in the early stage of disease course or after reducing tumor burden may significantly reduce the risk of severe CRS. Despite the low expression of GPC3 in normal adult tissues (115), “on-target off-tumor” may lead to disastrous side effects. GPC3 is expressed in placenta and endometrium (116, 117), suggesting that female patients, especially pregnant patients, may have a high risk of “on-target off-tumor”. Furthermore, a small amount of GPC3 was expressed in normal renal tubular and testicular germ cells (115), so renal function should be monitored during targeted GPC3 treatment, and reproductive protection should also be paid attention to in infertile men. At present, assembling suicide genes, synthetic notch receptors, on-switch CAR, bispecific CAR-T cells can help prevent healthy cells from CAR-T attacking (118). At present, no obvious toxicity has been reported in GPC3 related gene therapy, immunotoxin and photodynamic therapy (78, 93, 101).

## 5 CONCLUSION

Hepatocellular carcinoma has an extremely poor survival rate. To improve both the outcome and quality of life of these patients, it is necessary to discover and develop new means of treating the disease. GPC3 is specifically associated with liver cancer and, although it is useful in HCC diagnosis, an individual marker is not able to meet the needs of clinical therapeutic application. While using a panel of multiple markers greatly improves the rate of early cancer detection, this only strengthens the suspected diagnosis of HCC, so further

exploration into increasing the sensitivity and specificity of these markers is required.

GPC3 has exceptional cancer specificity and is currently being investigated as a global target for cancer-targeted therapies and immunotherapies. A series of antibodies against HCC is currently in clinical and preclinical trials. However, single anti-GPC3 antibody therapy does not kill liver cancer altogether, which may need to achieve high target saturation in tumor cells to induce any beneficial effect. Bispecific antibodies recognize different epitopes on the antigen simultaneously, overcoming the shortcomings of traditional monoclonal antibodies and showing excellent results in animal experiments, but these results require verification in clinical trials; nevertheless, the promising results suggest the potential of developing combined immunotherapies by optimizing antibody structures and raising antibodies against multiple targets. Second-generation GPC3-based immunotherapies, such as CAR-T and TCR engineering T cell therapy, have attracted worldwide attention. CAR-T can effectively kill tumor cells with low expression of cell surface antigens, which will expand substantially in the body during treatment of patients. However, CAR-T cells only show moderate anti-tumor activity in patients with solid tumors, including liver cancer, partly because of their specific immune microenvironment, containing the vascular-stromal barrier reduces the expansion, persistence and penetration of CAR-T; immune checkpoints and immunosuppressive cells allow HCC to undergo immune escape (119). The CAR co-expressing IL-15 and IL-21 showed improved activity. In addition, the toxicity

caused by CAR-T has limited the application. Therefore, optimization of the CAR structure to enhance the *in vivo* peak expansion and safe half-life of CAR-T warrants further investigation. It is also possible that the surviving cells may cease to express GPC3 during the treatment, resulting in drug resistance. GPC3-negative tumors may also grow and develop drug resistance under such therapeutic pressure. Therefore, the exploration of novel targets and combination therapies are future goals for HCC research.

## AUTHOR CONTRIBUTIONS

XZ and XL gathered information and designed the review. YL drew the pictures. ML and GW critically revised the manuscript. All authors contributed to the article and approved the submitted version.

## FUNDING

This work was supported by the National Natural Science Foundation of China (31971390), Sichuan Science and Technology Program (2021YFH0142), and 1.3.5 Project for Disciplines of Excellence, West China Hospital, Sichuan University (Grant No. ZYJC21043).

## REFERENCES

- Bray F, Ferlay J, Soerjomataram I, Siegel R, Torre L, Jemal A. Global Cancer Statistics 2018: GLOBOCAN Estimates of Incidence and Mortality Worldwide for 36 Cancers in 185 Countries. *CA Cancer J Clin* (2018) 68:394–424. doi: 10.3322/caac.21492
- Forner A, Reig M, Bruix J. Hepatocellular Carcinoma. *Lancet (London England)* (2018) 391:1301–14. doi: 10.1016/S0140-6736(18)30010-2
- Qin S, Bai Y, Lim H, Thongprasert S, Chao Y, Fan J, et al. Randomized, Multicenter, Open-Label Study of Oxaliplatin Plus Fluorouracil/Leucovorin Versus Doxorubicin as Palliative Chemotherapy in Patients With Advanced Hepatocellular Carcinoma From Asia. *J Clin Oncol* (2013) 31:3501–8. doi: 10.1200/JCO.2012.44.5643
- Llovet JM, Ricci S, Mazzaferro V, Hilgard P, Gane E, Blanc J-F, et al. Sorafenib in Advanced Hepatocellular Carcinoma. *N Engl J Med* (2008) 359:378–90. doi: 10.1056/NEJMoa0708857
- Kudo M, Finn RS, Qin S, Han KH, Ikeda K, Piscaglia F, et al. Lenvatinib Versus Sorafenib in First-Line Treatment of Patients With Unresectable Hepatocellular Carcinoma: A Randomised Phase 3 Non-Inferiority Trial. *Lancet (London England)* (2018) 391:1163–73. doi: 10.1016/S0140-6736(18)30207-1
- Qin S, Bi F, Gu S, Bai Y, Chen Z, Wang Z, et al. Donafenib Versus Sorafenib in First-Line Treatment of Unresectable or Metastatic Hepatocellular Carcinoma: A Randomized, Open-Label, Parallel-Controlled Phase II-III Trial. *J Clin Oncol* (2021) 39:JCO2100163. doi: 10.1200/JCO.21.00163
- El-Khoueiry AB, Sangro B, Yau T, Crocenzi TS, Kudo M, Hsu C, et al. Nivolumab in Patients With Advanced Hepatocellular Carcinoma (CheckMate 040): An Open-Label, Non-Comparative, Phase 1/2 Dose Escalation and Expansion Trial. *Lancet (London England)* (2017) 389:2492–502. doi: 10.1016/S0140-6736(17)31046-2
- Zhu AX, Finn RS, Edeline J, Cattani S, Ogasawara S, Palmer D, et al. Pembrolizumab in Patients With Advanced Hepatocellular Carcinoma Previously Treated With Sorafenib (KEYNOTE-224): A Non-Randomised, Open-Label Phase 2 Trial. *Lancet Oncol* (2018) 19:940–52. doi: 10.1016/S1470-2045(18)30351-6
- Sangro B, Gomez-Martin C, de la Mata M, Iñarrairaegui M, Garralda E, Barrera P, et al. A Clinical Trial of CTLA-4 Blockade With Tremelimumab in Patients With Hepatocellular Carcinoma and Chronic Hepatitis C. *J Hepatol* (2013) 59:81–8. doi: 10.1016/j.jhep.2013.02.022
- Gordan J, Kennedy E, Abou-Alfa G, Beg M, Brower S, Gade T, et al. Systemic Therapy for Advanced Hepatocellular Carcinoma: ASCO Guideline. *J Clin Oncol* (2020) 38:4317–45. doi: 10.1200/JCO.20.02672
- Finn RS, Ducreux M, Qin S, Galle PR, Zhu AX, Ikeda M, et al. IMbrave150: A Randomized Phase III Study of 1L Atezolizumab Plus Bevacizumab vs Sorafenib in Locally Advanced or Metastatic Hepatocellular Carcinoma. *J Clin Oncol* (2018) 36:TPS4141–TPS4141. doi: 10.1200/JCO.2018.36.15\_suppl.TPS4141
- Finn RS, Ikeda M, Zhu AX, Sung MW, Baron AD, Kudo M, et al. Phase Ib Study of Lenvatinib Plus Pembrolizumab in Patients With Unresectable Hepatocellular Carcinoma. *J Clin Oncol Off J Am Soc Clin Oncol* (2020) 38:2960–70. doi: 10.1200/JCO.20.00808
- Ren Z, Xu J, Bai Y, Xu A, Cang S, Du C, et al. Sintilimab Plus a Bevacizumab Biosimilar (IBI305) Versus Sorafenib in Unresectable Hepatocellular Carcinoma (ORIENT-32): A Randomised, Open-Label, Phase 2–3 Study. *Lancet Oncol* (2021) 22:977–90. doi: 10.1016/S1470-2045(21)00252-7
- Liver Cancer. *Statistics.Approved by the Cancer.Net Editorial Board.* (2020).
- Filmus J, Selleck S. Glypicans: Proteoglycans With a Surprise. *J Clin Invest* (2001) 108:497–501. doi: 10.1172/JCI200113712
- De Cat B, David G. Developmental Roles of the Glypicans. *Semin Cell Dev Biol* (2001) 12:117–25. doi: 10.1006/scdb.2000.0240
- Tang Z, Kang B, Li C, Chen T, Zhang Z. GEPIA2: An Enhanced Web Server for Large-Scale Expression Profiling and Interactive Analysis. *Nucleic Acids Res* (2019) 47:W556–60. doi: 10.1093/nar/gkz430
- Hsu H, Cheng W, Lai P. Cloning and Expression of a Developmentally Regulated Transcript MXR7 in Hepatocellular Carcinoma: Biological



- Significance and Temporospacial Distribution. *Cancer Res* (1997) 57:5179–84.
19. Capurro M, Wanless I, Sherman M, Deboer G, Shi W, Miyoshi E, et al. Glypican-3: A Novel Serum and Histochemical Marker for Hepatocellular Carcinoma. *Gastroenterology* (2003) 125:89–97. doi: 10.1016/S0016-5085(03)00689-9
  20. Yang X, Liu H, Sun C, Natarajan A, Hu X, Wang X, et al. Imaging of Hepatocellular Carcinoma Patient-Derived Xenografts Using  $^{89}\text{Zr}$ -Labeled Anti-Glypican-3 Monoclonal Antibody. *Biomaterials* (2014) 35:6964–71. doi: 10.1016/j.biomaterials.2014.04.089
  21. Sham J, Kievit F, Grierson J, Miyaoka R, Yeh M, Zhang M, et al. Glypican-3-Targeted  $^{89}\text{Zr}$  PET Imaging of Hepatocellular Carcinoma. *J Nucl Med* (2014) 55:799–804. doi: 10.2967/jnumed.113.132118
  22. Li Y, Chen Z, Li F, Wang J, Zhang Z. Preparation and *In Vitro* Studies of MRI-Specific Superparamagnetic Iron Oxide Antigen-3 Probe for Hepatocellular Carcinoma. *Int J Nanomed* (2012) 7:4593–611. doi: 10.2147/IJN.S32196
  23. Zhu D, Qin Y, Wang J, Zhang L, Zou S, Zhu X, et al. Novel Glypican-3-Binding Peptide for *In Vivo* Hepatocellular Carcinoma Fluorescent Imaging. *Bioconjug Chem* (2016) 27:831–9. doi: 10.1021/acs.bioconjug.6b00030
  24. Di Tommaso L, Franchi G, Park Y, Fiamengo B, Destro A, Morenghi E, et al. Diagnostic Value of HSP70, Glypican 3, and Glutamine Synthetase in Hepatocellular Nodules in Cirrhosis. *Hepatology* (2007) 45:725–34. doi: 10.1002/hep.21531
  25. Tremosini S, Forner A, Boix L, Vilana R, Bianchi L, Reig M, et al. Prospective Validation of an Immunohistochemical Panel (Glypican 3, Heat Shock Protein 70 and Glutamine Synthetase) in Liver Biopsies for Diagnosis of Very Early Hepatocellular Carcinoma. *Gut* (2012) 61:1481–7. doi: 10.1136/gutjnl-2011-301862
  26. Timek D, Shi J, Liu H, Lin F. Arginase-1, HepPar-1, and Glypican-3 are the Most Effective Panel of Markers in Distinguishing Hepatocellular Carcinoma From Metastatic Tumor on Fine-Needle Aspiration Specimens. *Am J Clin Pathol* (2012) 138:203–10. doi: 10.1309/AJCPK1ZC9WNHCCMU
  27. Yao S, Zhang J, Chen H, Sheng Y, Zhang X, Liu Z, et al. Diagnostic Value of Immunohistochemical Staining of GP73, GPC3, DCP, CD34, CD31, and Reticulin Staining in Hepatocellular Carcinoma. *J Histochem Cytochem* (2013) 61:639–48. doi: 10.1369/0022155413492771
  28. Enan E, El-Hawary A, El-Tantawy D, Abu-Hashim M, Helal N. Diagnostic Role of Glypican 3 and CD34 for Differentiating Hepatocellular Carcinoma From Nonmalignant Hepatocellular Lesions. *Ann Diagn Pathol* (2013) 17:490–3. doi: 10.1016/j.anndiagpath.2013.08.001
  29. Shirakawa H, Suzuki H, Shimomura M, Kojima M, Gotohda N, Takahashi S, et al. Glypican-3 Expression is Correlated With Poor Prognosis in Hepatocellular Carcinoma. *Cancer Sci* (2009) 100:1403–7. doi: 10.1111/j.1349-7006.2009.01206.x
  30. Chen I, Ariizumi S, Nakano M, Yamamoto M. Positive Glypican-3 Expression in Early Hepatocellular Carcinoma Predicts Recurrence After Hepatectomy. *J Gastroenterol* (2014) 49:117–25. doi: 10.1007/s00535-013-0793-2
  31. Haruyama Y, Yorita K, Yamaguchi T, Kitajima S, Amano J, Ohtomo T, et al. High Preoperative Levels of Serum Glypican-3 Containing N-Terminal Subunit are Associated With Poor Prognosis in Patients With Hepatocellular Carcinoma After Partial Hepatectomy. *Int J Cancer* (2015) 137:1643–51. doi: 10.1002/ijc.29518
  32. Yu M, Lee Y, Lin S, Wu H, Chen T, Lee W, et al. Recurrence and Poor Prognosis Following Resection of Small Hepatitis B-Related Hepatocellular Carcinoma Lesions are Associated With Aberrant Tumor Expression Profiles of Glypican 3 and Osteopontin. *Ann Surg Oncol* (2012) 19 (Suppl 3):S455–63. doi: 10.1245/s10434-011-1946-2
  33. Yorita K, Takahashi N, Takai H, Kato A, Suzuki M, Ishiguro T, et al. Prognostic Significance of Circumferential Cell Surface Immunoreactivity of Glypican-3 in Hepatocellular Carcinoma. *Liver Int* (2011) 31:120–31. doi: 10.1111/j.1478-3231.2010.02359.x
  34. Wang Y, Zhu Z, Teng D, Yao Z, Gao W, Shen Z. Glypican-3 Expression and its Relationship With Recurrence of HCC After Liver Transplantation. *World J Gastroenterol* (2012) 18:2408–14. doi: 10.3748/wjg.v18.i19.2408
  35. Chu Q, Mu W, Lan C, Liu Y, Gao T, Guan L, et al. High-Specific Isolation and Instant Observation of Circulating Tumour Cell From HCC Patients via Glypican-3 Immunomagnetic Fluorescent Nanodevice. *Int J Nanomed* (2021) 16:4161–73. doi: 10.2147/IJN.S307691
  36. Pez F, Lopez A, Kim M, Wands J, Caron de Fromental C, Merle P. Wnt Signaling and Hepatocarcinogenesis: Molecular Targets for the Development of Innovative Anticancer Drugs. *J Hepatol* (2013) 59:1107–17. doi: 10.1016/j.jhep.2013.07.001
  37. Kolluri A, Ho M. The Role of Glypican-3 in Regulating Wnt, YAP, and Hedgehog in Liver Cancer. *Front Oncol* (2019) 9:708. doi: 10.3389/fonc.2019.00708
  38. Clevers H. Wnt/ $\beta$ -Catenin Signaling in Development and Disease. *Cell* (2006) 127:469–80. doi: 10.1016/j.cell.2006.10.018
  39. Cumberledge S, Reichsman F. Glycosaminoglycans and WNTs: Just a Spoonful of Sugar Helps the Signal Go Down. *Trends Genet* (1997) 13:421–3. doi: 10.1016/S0168-9525(97)01275-4
  40. Capurro M, Xiang Y, Lobe C, Filmus J. Glypican-3 Promotes the Growth of Hepatocellular Carcinoma by Stimulating Canonical Wnt Signaling. *Cancer Res* (2005) 65:6245–54. doi: 10.1158/0008-5472.CAN-04-4244
  41. Gao W, Kim H, Feng M, Phung Y, Xavier C, Rubin J, et al. Inactivation of Wnt Signaling by a Human Antibody That Recognizes the Heparan Sulfate Chains of Glypican-3 for Liver Cancer Therapy. *Hepatology* (2014) 60:576–87. doi: 10.1002/hep.26996
  42. Capurro M, Martin T, Shi W, Filmus J. Glypican-3 Binds to Frizzled and Plays a Direct Role in the Stimulation of Canonical Wnt Signaling. *J Cell Sci* (2014) 127:1565–75. doi: 10.1242/jcs.140871
  43. Li N, Wei L, Liu X, Bai H, Ye Y, Li D, et al. A Frizzled-Like Cysteine-Rich Domain in Glypican-3 Mediates Wnt Binding and Regulates Hepatocellular Carcinoma Tumor Growth in Mice. *Hepatology* (2019) 70:1231–45. doi: 10.1002/hep.30646
  44. Zeng Q, Hong W. The Emerging Role of the Hippo Pathway in Cell Contact Inhibition, Organ Size Control, and Cancer Development in Mammals. *Cancer Cell* (2008) 13:188–92. doi: 10.1016/j.ccr.2008.02.011
  45. Zhou D, Conrad C, Xia F, Park J, Payer B, Yin Y, et al. Mst1 and Mst2 Maintain Hepatocyte Quiescence and Suppress Hepatocellular Carcinoma Development Through Inactivation of the Yap1 Oncogene. *Cancer Cell* (2009) 16:425–38. doi: 10.1016/j.ccr.2009.09.026
  46. Lee K, Lee J, Kim T, Kim T, Park H, Byun J, et al. The Hippo-Salvador Pathway Restrains Hepatic Oval Cell Proliferation, Liver Size, and Liver Tumorigenesis. *Proc Natl Acad Sci U S A* (2010) 107:8248–53. doi: 10.1073/pnas.0912203107
  47. Li H, Wolfe A, Seftor S, Edwards G, Zhong X, Abdulkarim A, et al. Deregulation of Hippo Kinase Signalling in Human Hepatic Malignancies. *Liver Int* (2012) 32:38–47. doi: 10.1111/j.1478-3231.2011.02646.x
  48. Miao H, Pan Z, Lei C, Wen J, Li M, Liu Z, et al. Knockdown of GPC3 Inhibits the Proliferation of Huh7 Hepatocellular Carcinoma Cells Through Down-Regulation of YAP. *J Cell Biochem* (2013) 114:625–31. doi: 10.1002/jcb.24404
  49. Briscoe J, Thérond P. The Mechanisms of Hedgehog Signalling and its Roles in Development and Disease. *Nat Rev Mol Cell Biol* (2013) 14:416–29. doi: 10.1038/nrm3598
  50. Salaritabar A, Berindan-Neagoe I, Darvish B, Hadijakhond F, Manayi A, Devi K, et al. Targeting Hedgehog Signaling Pathway: Paving the Road for Cancer Therapy. *Pharmacol Res* (2019) 141:466–80. doi: 10.1016/j.phrs.2019.01.014
  51. Wang Y, Han C, Lu L, Magliato S, Wu T. Hedgehog Signaling Pathway Regulates Autophagy in Human Hepatocellular Carcinoma Cells. *Hepatology* (2013) 58:995–1010. doi: 10.1002/hep.26394
  52. Capurro M, Li F, Filmus J. Overgrowth of a Mouse Model of Simpson-Golabi-Behmel Syndrome is Partly Mediated by Indian Hedgehog. *EMBO Rep* (2009) 10:901–7. doi: 10.1038/embor.2009.98
  53. Capurro M, Xu P, Shi W, Li F, Jia A, Filmus J. Glypican-3 Inhibits Hedgehog Signaling During Development by Competing With Patched for Hedgehog Binding. *Dev Cell* (2008) 14:700–11. doi: 10.1016/j.devcel.2008.03.006
  54. Li F, Shi W, Capurro M, Filmus J. Glypican-5 Stimulates Rhabdomyosarcoma Cell Proliferation by Activating Hedgehog Signaling. *J Cell Biol* (2011) 192:691–704. doi: 10.1083/jcb.201008087
  55. Luan F, Liu P, Ma H, Yue X, Liu J, Gao L, et al. Reduced Nucleic ZHX2 Involves in Oncogenic Activation of Glypican 3 in Human Hepatocellular Carcinoma. *Int J Biochem Cell Biol* (2014) 55:129–35. doi: 10.1016/j.biocel.2014.08.021

56. Li L, Jin R, Zhang X, Lv F, Liu L, Liu D, et al. Oncogenic Activation of Glypican-3 by C-Myc in Human Hepatocellular Carcinoma. *Hepatology* (2012) 56:1380–90. doi: 10.1002/hep.25891
57. Song H, Shi W, Filmus J. OCI-5/Rat Glypican-3 Binds to Fibroblast Growth Factor-2 But Not to Insulin-Like Growth Factor-2. *J Biol Chem* (1997) 272:7574–7. doi: 10.1074/jbc.272.12.7574
58. Lai J, Sandhu D, Yu C, Han T, Moser C, Jackson K, et al. Sulfatase 2 Up-Regulates Glypican 3, Promotes Fibroblast Growth Factor Signaling, and Decreases Survival in Hepatocellular Carcinoma. *Hepatology* (2008) 47:1211–22. doi: 10.1002/hep.22202
59. Gao W, Kim H, Ho M. Human Monoclonal Antibody Targeting the Heparan Sulfate Chains of Glypican-3 Inhibits HGF-Mediated Migration and Motility of Hepatocellular Carcinoma Cells. *PLoS One* (2015) 10: e0137664. doi: 10.1371/journal.pone.0137664
60. Takai H, Kato A, Kato C, Watanabe T, Matsubara K, Suzuki M, et al. The Expression Profile of Glypican-3 and Its Relation to Macrophage Population in Human Hepatocellular Carcinoma. *Liver Int* (2009) 29:1056–64. doi: 10.1111/j.1478-3231.2008.01968.x
61. Ishiguro T, Sugimoto M, Kinoshita Y, Miyazaki Y, Nakano K, Tsunoda H, et al. Anti-Glypican 3 Antibody as a Potential Antitumor Agent for Human Liver Cancer. *Cancer Res* (2008) 68:9832–8. doi: 10.1158/0008-5472.CAN-08-1973
62. Zhu A, Gold P, El-Khoueiry A, Abrams T, Morikawa H, Ohishi N, et al. First-In-Man Phase I Study of GC33, a Novel Recombinant Humanized Antibody Against Glypican-3, in Patients With Advanced Hepatocellular Carcinoma. *Clin Cancer Res* (2013) 19:920–8. doi: 10.1158/1078-0432.CCR-12-2616
63. Ikeda M, Ohkawa S, Okusaka T, Mitsunaga S, Kobayashi S, Morizane C, et al. Japanese Phase I Study of GC33, a Humanized Antibody Against Glypican-3 for Advanced Hepatocellular Carcinoma. *Cancer Sci* (2014) 105:455–62. doi: 10.1111/cas.12368
64. Abou-Alfa G, Puig O, Daniele B, Kudo M, Merle P, Park J, et al. Randomized Phase II Placebo Controlled Study of Codrituzumab in Previously Treated Patients With Advanced Hepatocellular Carcinoma. *J Hepatol* (2016) 65:289–95. doi: 10.1016/j.jhep.2016.04.004
65. Liu X, Gao F, Jiang L, Jia M, Ao L, Lu M, et al. 32A9, a Novel Human Antibody for Designing an Immunotoxin and CAR-T Cells Against Glypican-3 in Hepatocellular Carcinoma. *J Transl Med* (2020) 18:295. doi: 10.1186/s12967-020-02462-1
66. Feng M, Gao W, Wang R, Chen W, Man Y-G, Figg WD, et al. Therapeutically Targeting Glypican-3 via a Conformation-Specific Single-Domain Antibody in Hepatocellular Carcinoma. *Proc Natl Acad Sci* (2013) 110:E1083–91. doi: 10.1073/pnas.1217868110
67. Ishiguro T, Sano Y, Komatsu S, Kamata-Sakurai M, Kaneko A, Kinoshita Y, et al. An Anti-Glypican 3/CD3 Bispecific T Cell-Redirecting Antibody for Treatment of Solid Tumors. *Sci Transl Med* (2017) 9:eal4291. doi: 10.1126/scitranslmed.aal4291
68. Sano Y, Azuma Y, Tsunenari T, Kinoshita Y, Kayukawa Y, Mutoh H, et al. Abstract 3653: Combining ERY974, a Novel T Cell-Redirecting Bispecific Antibody Targeting Glypican-3, With Chemotherapy Profoundly Improved Antitumor Efficacy Over its Monotherapy in Xenograft Model. *Cancer Res* (2017) 77:3653–3. doi: 10.1158/1538-7445.AM2017-3653
69. Du K, Li Y, Liu J, Chen W, Wei Z, Luo Y, et al. A Bispecific Antibody Targeting GPC3 and CD47 Induced Enhanced Antitumor Efficacy Against Dual Antigen-Expressing HCC. *Mol Ther* (2021) 29(4): 1572–84. doi: 10.1016/j.ymthe.2021.01.006
70. Nakatsura T, Komori H, Kubo T, Yoshitake Y, Senju S, Katagiri T, et al. Mouse Homologue of a Novel Human Oncofetal Antigen, Glypican-3, Evokes T-Cell-Mediated Tumor Rejection Without Autoimmune Reactions in Mice. *Clin Cancer Res* (2004) 10:8630–40. doi: 10.1158/1078-0432.CCR-04-1177
71. Komori H, Nakatsura T, Senju S, Yoshitake Y, Motomura Y, Ikuta Y, et al. Identification of HLA-A2- or HLA-A24-Restricted CTL Epitopes Possibly Useful for Glypican-3-Specific Immunotherapy of Hepatocellular Carcinoma. *Clin Cancer Res* (2006) 12:2689–97. doi: 10.1158/1078-0432.CCR-05-2267
72. Sawada Y, Yoshikawa T, Nobuoka D, Shirakawa H, Kuronuma T, Motomura Y, et al. Phase I Trial of a Glypican-3-Derived Peptide Vaccine for Advanced Hepatocellular Carcinoma: Immunologic Evidence and Potential for Improving Overall Survival. *Clin Cancer Res* (2012) 18:3686–96. doi: 10.1158/1078-0432.CCR-11-3044
73. Sawada Y, Sakai M, Yoshikawa T, Ofuji K, Nakatsura T. A Glypican-3-Derived Peptide Vaccine Against Hepatocellular Carcinoma. *Oncoimmunology* (2012) 1:1448–50. doi: 10.4161/onci.21351
74. Wu Q, Pi L, Le Trinh T, Zuo C, Xia M, Jiao Y, et al. A Novel Vaccine Targeting Glypican-3 as a Treatment for Hepatocellular Carcinoma. *Mol Ther* (2017) 25:2299–308. doi: 10.1016/j.ymthe.2017.08.005
75. Li S, Lin J, Qi C, Fu S, Xiao W, Peng B, et al. GPC3 DNA Vaccine Elicits Potent Cellular Antitumor Immunity Against HCC in Mice. *Hepatology* (2014) 61:278–84. doi: 10.5754/hge121031
76. Gao W, Tang Z, Zhang Y, Feng M, Qian M, Dimitrov D, et al. Immunotoxin Targeting Glypican-3 Regresses Liver Cancer via Dual Inhibition of Wnt Signalling and Protein Synthesis. *Nat Commun* (2015) 6:6536. doi: 10.1038/ncomms7536
77. Wang C, Gao W, Feng M, Pastan I, Ho M. Construction of an Immunotoxin, HN3-Mpe24, Targeting Glypican-3 for Liver Cancer Therapy. *Oncotarget* (2017) 8:32450–60. doi: 10.18632/oncotarget.10592
78. Fleming B, Urban D, Hall M, Longerich T, Greten T, Pastan I, et al. Engineered Anti-GPC3 Immunotoxin, HN3-ABD-T20, Produces Regression in Mouse Liver Cancer Xenografts Through Prolonged Serum Retention. *Hepatology* (2020) 71:1696–711. doi: 10.1002/hep.30949
79. Porter D, Hwang W, Frey N, Lacey S, Shaw P, Loren A, et al. Chimeric Antigen Receptor T Cells Persist and Induce Sustained Remissions in Relapsed Refractory Chronic Lymphocytic Leukemia. *Sci Transl Med* (2015) 7:303ra139. doi: 10.1126/scitranslmed.aac5415
80. Finney O, Brakke H, Rawlings-Rhea S, Hicks R, Doolittle D, Lopez M, et al. CD19 CAR T Cell Product and Disease Attributes Predict Leukemia Remission Durability. *J Clin Invest* (2019) 129:2123–32. doi: 10.1172/JCI125423
81. Wu X, Luo H, Shi B, Di S, Sun R, Su J, et al. Combined Antitumor Effects of Sorafenib and GPC3-CAR T Cells in Mouse Models of Hepatocellular Carcinoma. *Mol Ther* (2019) 27:1483–94. doi: 10.1016/j.ymthe.2019.04.020
82. Li K, Qian S, Huang M, Chen M, Peng L, Liu J, et al. Development of GPC3 and EGFR-Dual-Targeting Chimeric Antigen Receptor-T Cells for Adoptive T Cell Therapy. *Am J Transl Res* (2021) 13:156–67.
83. Liu Y, Di S, Shi B, Zhang H, Wang Y, Wu X, et al. Armored Inducible Expression of IL-12 Enhances Antitumor Activity of Glypican-3-Targeted Chimeric Antigen Receptor-Engineered T Cells in Hepatocellular Carcinoma. *J Immunol* (2019) 203:198–207. doi: 10.4049/jimmunol.1800033
84. Wang Y, Jiang H, Luo H, Sun Y, Shi B, Sun R, et al. An IL-4/21 Inverted Cytokine Receptor Improving CAR-T Cell Potency in Immunosuppressive Solid-Tumor Microenvironment. *Front Immunol* (2019) 10:1691. doi: 10.3389/fimmu.2019.01691
85. Batra SA, Rathi P, Guo L, Courtney AN, Fleurence J, Balzeau J, et al. Glypican-3-Specific CAR T Cells Coexpressing IL15 and IL21 Have Superior Expansion and Antitumor Activity Against Hepatocellular Carcinoma. *Cancer Immunol Res* (2020) 8:309–20. doi: 10.1158/2326-6066.CIR-19-0293
86. Xiong X, Xi J, Liu Q, Wang C, Jiang Z, Yue S, et al. Co-Expression of IL-7 and PH20 Promote Anti-GPC3 CAR-T Tumour Suppressor Activity *In Vivo* and *In Vitro*. *Liver Int* (2021) 41:1033–43. doi: 10.1111/liv.14771
87. Hu W, Zi Z, Jin Y, Li G, Shao K, Cai Q, et al. CRISPR/Cas9-Mediated PD-1 Disruption Enhances Human Mesothelin-Targeted CAR T Cell Effector Functions. *Cancer Immunol Immunother CII* (2019) 68:365–77. doi: 10.1007/s00262-018-2281-2
88. Zhao R, Cheng L, Jiang Z, Wei X, Li B, Wu Q, et al. DNAX-Activating Protein 10 Co-Stimulation Enhances the Anti-Tumor Efficacy of Chimeric Antigen Receptor T Cells. *Oncoimmunology* (2019) 8:e1509173. doi: 10.1080/2162402X.2018.1509173
89. Sun L, Gao F, Gao Z, Ao L, Li N, Ma S, et al. Shed Antigen-Induced Blocking Effect on CAR-T Cells Targeting Glypican-3 in Hepatocellular Carcinoma. *J Immunother Cancer* (2021) 9:e001875. doi: 10.1136/jitc-2020-001875
90. Wang W, Zhou G, Zhang WJL. NK-92 Cell, Another Ideal Carrier for Chimeric Antigen Receptor. *Immunotherapy* (2017) 9:753–65. doi: 10.2217/imt-2017-0022
91. Yu M, Luo H, Fan M, Wu X, Shi B, Di S, et al. Development of GPC3-Specific Chimeric Antigen Receptor-Engineered Natural Killer Cells for the

- Treatment of Hepatocellular Carcinoma. *Mol Ther* (2018) 26:366–78. doi: 10.1016/j.ymthe.2017.12.012
92. Maurel M, Jalvy S, Ladeiro Y, Combe C, Vachet L, Sagliocco F, et al. A Functional Screening Identifies Five microRNAs Controlling Glypican-3: Role of miR-1271 Down-Regulation in Hepatocellular Carcinoma. *Hepatology* (2013) 57:195–204. doi: 10.1002/hep.25994
  93. Wang K, Kievit F, Sham J, Jeon M, Stephen Z, Bakthavatsalam A, et al. Iron-Oxide-Based Nanovector for Tumor Targeted siRNA Delivery in an Orthotopic Hepatocellular Carcinoma Xenograft Mouse Model. *Small* (2016) 12:477–87. doi: 10.1002/smll.201501985
  94. Zhang Y, Xu J, Zhang S, An J, Zhang J, Huang J, et al. HOXA-AS2 Promotes Proliferation and Induces Epithelial-Mesenchymal Transition via the miR-520c-3p/GPC3 Axis in Hepatocellular Carcinoma. *Cell Physiol Biochem* (2018) 50:2124–38. doi: 10.1159/000495056
  95. Endo M, Kinoshita Y, Adachi K, Narita Y, Amano J, Kato A, et al. Abstract 2747: Anti-Glypican-3 Monoclonal Antibody (Codrituzumab/GC33/RO5137382) Treatment Enhances Tumor Infiltration of PD-L1-Positive Macrophages, and Combination Therapy With Anti-PD-L1 Monoclonal Antibody Promotes Antitumor Effects. *Cancer Res* (2018) 78:2747–7. doi: 10.1158/1538-7445.AM2018-2747
  96. Cheng A-L, Yen C-J, Okusaka T, Ikeda M, Hsu C-H, Wu S-Y, et al. A Phase I, Open-Label, Multi-Center, Dose-Escalation Study of Codrituzumab, an Anti-Glypican-3 Monoclonal Antibody, in Combination With Atezolizumab in Patients With Locally Advanced or Metastatic Hepatocellular Carcinoma. *Ann Oncol* (2018) 29:viii234–5. doi: 10.1093/annonc/mdy282.080
  97. Guo X, Jiang H, Shi B, Zhou M, Zhang H, Shi Z, et al. Disruption of PD-1 Enhanced the Anti-Tumor Activity of Chimeric Antigen Receptor T Cells Against Hepatocellular Carcinoma. *Front Pharmacol* (2018) 9:1118. doi: 10.3389/fphar.2018.01118
  98. Pan Z, Di S, Shi B, Jiang H, Shi Z, Liu Y, et al. Increased Antitumor Activities of Glypican-3-Specific Chimeric Antigen Receptor-Modified T Cells by Coexpression of a Soluble PD1-CH3 Fusion Protein. *Cancer Immunol Immunother CII* (2018) 67:1621–34. doi: 10.1007/s00262-018-2221-1
  99. Dargel C, Bassani-Sternberg M, Hasreiter J, Zani F, Bockmann J, Thiele F, et al. T Cells Engineered to Express a T-Cell Receptor Specific for Glypican-3 to Recognize and Kill Hepatoma Cells In Vitro and in Mice. *Gastroenterology* (2015) 149:1042–52. doi: 10.1053/j.gastro.2015.05.055
  100. Baskaran R, Lee J, Yang S. Clinical Development of Photodynamic Agents and Therapeutic Applications. *Biomater Res* (2018) 22:25. doi: 10.1186/s40824-018-0140-z
  101. Hu J, Shi J, Gao Y, Yang W, Liu P, Liu Q, et al. 808 Nm Near-Infrared Light-Excited UCNP@SiO<sub>2</sub>-Ce6-GPC3 Nanocomposites For Photodynamic Therapy In Liver Cancer. *Int J Nanomed* (2019) 14:10009–21. doi: 10.2147/IJN.S221496
  102. Liu Y, Tan M, Fang C, Chen X, Liu H, Feng Y, et al. A Novel Multifunctional Gold Nanorod-Mediated and Tumor-Targeted Gene Silencing of GPC-3 Synergizes Photothermal Therapy for Liver Cancer. *Nanotechnology* (2021) 32:175101. doi: 10.1088/1361-6528/abdbd
  103. Mu W, Jiang D, Mu S, Liang S, Liu Y, Zhang N. Promoting Early Diagnosis and Precise Therapy of Hepatocellular Carcinoma by Glypican-3-Targeted Synergistic Chemo-Photothermal Theranostics. *ACS Appl Mater Interfaces* (2019) 11:23591–604. doi: 10.1021/acsami.9b05526
  104. Sun W, Wang Y, Cai M, Lin L, Chen X, Cao Z, et al. Codelivery of Sorafenib and GPC3 siRNA With PEI-Modified Liposomes for Hepatoma Therapy. *Biomater Sci* (2017) 5:2468–79. doi: 10.1039/C7BM00866J
  105. Wu W, Dang S, Feng Q, Liang J, Wang Y, Fan N. MicroRNA-542-3p Inhibits the Growth of Hepatocellular Carcinoma Cells by Targeting FZD7/Wnt Signaling Pathway. *Biochem Biophys Res Commun* (2017) 482:100–5. doi: 10.1016/j.bbrc.2016.10.136
  106. Gao J, Dai C, Yu X, Yin X-B, Zhou F. microRNA-485-5p Inhibits the Progression of Hepatocellular Carcinoma Through Blocking the WBP2/Wnt Signaling Pathway. *Cell Signal* (2020) 66:109466. doi: 10.1016/j.cellsig.2019.109466
  107. Wang S, Wang Y, Xun X, Zhang C, Xiang X, Cheng Q, et al. Hedgehog Signaling Promotes Sorafenib Resistance in Hepatocellular Carcinoma Patient-Derived Organoids. *J Exp Clin Cancer Res* (2020) 39:22. doi: 10.1186/s13046-020-1523-2
  108. Sheng X, Sun X, Sun K, Sui H, Qin J, Li Q. Inhibitory Effect of Bufalin Combined With Hedgehog Signaling Pathway Inhibitors on Proliferation and Invasion and Metastasis of Liver Cancer Cells. *Int J Oncol* (2016) 49:1513–24. doi: 10.3892/ijo.2016.3667
  109. Sawada Y, Yoshikawa T, Fujii S, Mitsunaga S, Nobuoka D, Mizuno S, et al. Remarkable Tumor Lysis in a Hepatocellular Carcinoma Patient Immediately Following Glypican-3-Derived Peptide Vaccination: An Autopsy Case. *Hum Vaccin Immunother* (2013) 9:1228–33. doi: 10.4161/hv.24179
  110. Shi D, Shi Y, Kaseb AO, Qi X, Zhang Y, Chi J, et al. Chimeric Antigen Receptor-Glypican-3 T-Cell Therapy for Advanced Hepatocellular Carcinoma: Results of Phase I Trials. *Sci Transl Med* (2020) 26:3979–89. doi: 10.1158/1078-0432.CCR-19-3259
  111. Fang W, Fu Q, Zhao Q, Zheng Y, Liu L, Li Z, et al. Phase I Trial of Fourth-Generation Chimeric Antigen Receptor T-Cells Targeting Glypican-3 for Advanced Hepatocellular Carcinoma, Wolters Kluwer Health. *J Clin Oncol* (2021) 39(15\_suppl):4088. doi: 10.1200/JCO.2021.39.15\_suppl.4088
  112. Lee DW, Santomasso BD, Locke FL, Ghobadi A, Turtle CJ, Brudno JN, et al. ASTCT Consensus Grading for Cytokine Release Syndrome and Neurologic Toxicity Associated With Immune Effector Cells. *Biol Blood Marrow Transplant* (2019) 25:625–38. doi: 10.1016/j.bbmt.2018.12.758
  113. Le RQ, Li L, Yuan W, Shord SS, Nie L, Habtemariam BA, et al. FDA Approval Summary: Tocilizumab for Treatment of Chimeric Antigen Receptor T Cell-Induced Severe or Life-Threatening Cytokine Release Syndrome. *Oncologist* (2018) 23:943–7. doi: 10.1634/theoncologist.2018-0028
  114. Wei J, Liu Y, Wang C, Zhang Y, Tong C, Dai G, et al. The Model of Cytokine Release Syndrome in CAR T-Cell Treatment for B-Cell Non-Hodgkin Lymphoma. *Signal Transduct Target Ther* (2020) 5:134. doi: 10.1038/s41392-020-00256-x
  115. Baumhoer D, Tornillo L, Stadlmann S, Roncalli M, Diamantis E, Terracciano L. Glypican 3 Expression in Human Nonneoplastic, Preneoplastic, and Neoplastic Tissues: A Tissue Microarray Analysis of 4,387 Tissue Samples. *Am J Clin Pathol* (2008) 129:899–906. doi: 10.1309/HCQWPWD50XHD2DW6
  116. Iglesias BV, Centeno G, Pascucci H, Ward F, Peters MG, Filmus J, et al. Expression Pattern of Glypican-3 (GPC3) During Human Embryonic and Fetal Development. *Histol Histopathol* (2008) 23:1333–40. doi: 10.14670/HH-23.1333
  117. Maeda D, Ota S, Takazawa Y, Aburatani H, Nakagawa S, Yano T, et al. Glypican-3 Expression in Clear Cell Adenocarcinoma of the Ovary. *Modern Pathol An Off J United States Can Acad Pathol Inc* (2009) 22:824–32. doi: 10.1038/modpathol.2009.40
  118. Yu S, Yi M, Qin S, Wu K. Next Generation Chimeric Antigen Receptor T Cells: Safety Strategies to Overcome Toxicity. *Mol Cancer* (2019) 18:125. doi: 10.1186/s12943-019-1057-4
  119. Hou AJ, Chen LC, Chen YY. Navigating CAR-T Cells Through the Solid-Tumour Microenvironment. *Nat Rev Drug Discov* (2021) 20:531–50. doi: 10.1038/s41573-021-00189-2

**Conflict of Interest:** The authors declare that the research was conducted in the absence of any commercial or financial relationships that could be construed as a potential conflict of interest.

**Publisher's Note:** All claims expressed in this article are solely those of the authors and do not necessarily represent those of their affiliated organizations, or those of the publisher, the editors and the reviewers. Any product that may be evaluated in this article, or claim that may be made by its manufacturer, is not guaranteed or endorsed by the publisher.

Copyright © 2022 Zheng, Liu, Lei, Wang and Liu. This is an open-access article distributed under the terms of the Creative Commons Attribution License (CC BY). The use, distribution or reproduction in other forums is permitted, provided the original author(s) and the copyright owner(s) are credited and that the original publication in this journal is cited, in accordance with accepted academic practice. No use, distribution or reproduction is permitted which does not comply with these terms.



# The Value of Serum Tumor Markers and Blood Inflammation Markers in Differentiating Pancreatic Serous Cystic Neoplasms and Pancreatic Mucinous Cystic Neoplasms

## OPEN ACCESS

### Edited by:

Brendan Jenkins,  
Hudson Institute of Medical Research,  
Australia

### Reviewed by:

Stefano Francesco Crinò,  
University of Verona, Italy  
Alessandro Esposito,  
Verona Integrated University Hospital,  
Italy

### \*Correspondence:

Huifang Xiong  
happyjenny8485@126.com  
Yin Zhu  
zhuyin27@sina.com.cn

<sup>†</sup>These authors share first authorship

### Specialty section:

This article was submitted to  
Gastrointestinal Cancers: Hepato  
Pancreatic Biliary Cancers,  
a section of the journal  
Frontiers in Oncology

**Received:** 08 December 2021

**Accepted:** 27 January 2022

**Published:** 25 February 2022

### Citation:

Wang H, Chen S, Shu X, Liu Z, Liu P,  
Zhu Y, Zhu Y and Xiong H (2022) The  
Value of Serum Tumor Markers and  
Blood Inflammation Markers in  
Differentiating Pancreatic Serous  
Cystic Neoplasms and Pancreatic  
Mucinous Cystic Neoplasms.  
Front. Oncol. 12:831355.  
doi: 10.3389/fonc.2022.831355

Huan Wang<sup>†</sup>, Sihai Chen<sup>†</sup>, Xu Shu, Zhijian Liu, Pi Liu, Yong Zhu, Yin Zhu<sup>\*</sup>  
and Huifang Xiong<sup>\*</sup>

The First Affiliated Hospital of Nanchang University, Nanchang, China

Although many studies have emphasized the prognostic and diagnostic value of tumor markers and various inflammation-related markers, their clinical significance in differentiating benign and malignant pancreatic cystic neoplasms (PCNs) remains to be clarified. The present study explored the value of serum tumor markers and inflammation-related biomarkers in the differentiation of pancreatic serous cystic neoplasms (SCNs) and pancreatic mucinous cystic neoplasms (MCNs). A total of 79 patients with PCNs were included in this study, including 35 patients with SCNs and 44 patients with MCNs. Comparison of baseline data with preoperative results of serum tumor markers and associated inflammatory markers revealed significant differences in carbohydrate antigen 199 (CA199) and "lymphocyte × ALB" (LA) between the two groups ( $p = 0.0023$ ,  $p = 0.0149$ , respectively). Univariate and multivariate regression analyses showed that an increase in CA199 and a decrease in LA were relevant risk factors for MCNs. Finally, the receiver operating characteristic (ROC) curve was generated, and the area under the ROC curve (AUC) was calculated to evaluate the prediction efficiency of each indicator. The results showed that CA199 and LA had good differential diagnostic efficacy for SCNs and MCNs. This is the first to report to demonstrate that LA can be used for the differential diagnosis of SCNs and MCNs.

**Keywords:** pancreatic cystic neoplasms, serous cystic neoplasms, mucinous cystic neoplasms, diagnose, CA199

## INTRODUCTION

Pancreatic cystic neoplasms (PCNs) are a group of tumors characterized by cystic lesions formed by pancreatic duct epithelial cells or acinar hyperplasia and retention of pancreatic secretions (1). The latest "European guidelines" suggest that PCN detection rates in the general population range from 2% to 45% (2), and the incidence rate of patients aged 70 years or above reaches 10% (3).



PCNs mainly include three clinical subtypes as follows: intraductal papillary mucinous neoplasms (IPMNs), mucinous cystic neoplasms (MCNs), and serous cystic neoplasms (SCNs). Among them, SCNs has no malignant potential and rarely requires surgical treatment. MCNs may deteriorate and are potential malignant tumors that can show a series of biological behavior processes of different degrees of dysplasia and finally to invasive cancer (1). Moreover, due to the differences in biological behavior and the degree of benignity and malignancy between different subtypes, overtreatment or untimely diagnosis and treatment can easily occur, which makes the diagnosis and treatment of PCNs a difficult problem in the clinic. Therefore, there is an urgent need for an accurate preoperative assessment of the benign and malignant degree of PCNs to facilitate subsequent rational clinical treatment. Pathological diagnosis is the gold standard for identifying the nature of PCNs, but it is an invasive operation that causes unnecessary damage to the patient, resulting in certain limitations in clinical application (4).

Numerous studies have shown that laboratory examination is becoming increasingly important to help diagnose PCNs and to distinguish between benign and malignant PCNs. Inflammation plays a key role in the occurrence and progression of tumors. The systemic inflammatory response acts on the occurrence and development of malignant tumors by releasing cytokines and other inflammatory mediators (5–7). Some inflammatory markers based on circulating blood cells can be used as a simple and convenient way to measure the systemic inflammatory response and as independent predictors of survival in a variety of malignancies, including pancreatic cancer (8–10). Recently, there has been much evidence that inflammatory indices, such as the neutrophil-to-lymphocyte ratio (NLR) and platelet-to-lymphocyte ratio (PLR), also play an important role in predicting benign and malignant PCNs (11–13). Tumor markers can reflect the ability of tumor proliferation and metastasis to a certain extent. Studies in recent years have shown that cyst fluid carcinoembryonic antigen (CEA) and cyst fluid carbohydrate antigen 199 (CA199) in PCNs provide great accuracy in distinguishing mucinous and non-mucinous PCNs (14), while the identification value of CEA and CA199 in blood needs to be further studied. The purpose of the present study was to investigate the application value of CEA, CA199, and various inflammatory indicators in the blood in the differential diagnosis of SCNs and MCNs.

## MATERIALS AND METHODS

### Patients and Methods

In total, 79 patients with PCNs diagnosed at the First Affiliated Hospital of Nanchang University from April 2011 to April 2021 were selected. All patients were diagnosed by surgical pathology or endoscopic ultrasound-guided fine-needle aspiration (EUS-FNA) cytopathology. The results showed that among the 79 patients, 35 had SCNs, and 44 had MCNs. Details of patients are shown in **Supplementary Table 2**. The inclusion criteria were as

follows: 1) meet the diagnostic criteria of PCNs; 2) all patients were diagnosed for the first time, and tumor markers and related tests were performed; and 3) gender and age were not limited. The exclusion criteria were as follows: 1) complicated with other pancreatic diseases; 2) combined with other malignant tumors; 3) secondary metastatic carcinoma of pancreas; 4) the nature of the tumor was not confirmed by pathology; and 5) no tumor markers or related tests were performed.

### Data Collection

General information (sex and age), symptoms, preoperative laboratory examination data (CEA, CA199, and inflammatory index in the blood), pathological information, and auxiliary examination information (estimated tumor size and location) were collected.

### Statistical Analysis

Statistical analysis was performed using SPSS 26.0 statistical software (version 1.2.5001) and R language software (R packages “ggplot2”, “pROC”, “Hmisc”, “PerformanceAnalytics”, “corrplot”, “GGally”, and “rms”). For continuous measurement data, such as age, the mean  $\pm$  standard deviation was used if they were in line with a normal distribution, and a t test was used for comparisons between two groups. Percentiles were used for enumeration data, such as gender, and the chi-square test or Fisher’s exact probability method was used for comparisons between two groups. The receiver operating characteristic (ROC) curve was used to further analyze the diagnostic efficacy of laboratory indices that were meaningful for predicting SCNs and MCNs (15).  $p < 0.05$  was considered statistically significant.

## RESULTS

### Comparison of Preoperative Indices Between SCN and MCN Patients

As shown in **Table 1**, the following 79 patients were enrolled in this study: 35 patients (11 males and 24 females) were confirmed to have SCNs by pathology with an average age of  $54.49 \pm 12.71$  (range, 28–78) years, and 44 patients (11 males and 33 females) were diagnosed with MCNs with an average age of  $55.80 \pm 15.50$  (range, 24–79) years. There was no significant difference in age ( $p = 0.6878$ ) or sex ( $p = 0.5266$ ) between the SCN and MCN groups. The average tumor size of the SCN group was 5.44 cm, and the average tumor size of the MCN group was 5.74 cm. There was no significant difference in tumor size between the two groups ( $p = 0.6725$ ). Additionally, 11/35 SCNs were detected in a head/neck location, and 24/35 SCNs were detected in a body/tail location. Notably, only 8/44 MCNs were detected in a head/neck location, and 36/44 MCNs were detected in a body/tail location. In addition, 21/35 SNC and 32/44 MCN patients had obvious symptoms (such as abdominal pain, abdominal distension, weight loss, fatigue). Among the 44 MCN patients in this study, 8 were pathologically reported to have malignant

**TABLE 1 |** Comparison of preoperative indices between patients with SCNs and MCNs.

Characteristics	SCNs (n = 35)	MCNs (n = 44)	p value
Gender			0.5266
Male	11 (31.43%)	11 (25%)	
Female	24 (68.57%)	33 (75%)	
Age (year) (mean ± SD)	54.49 ± 12.71	55.80 ± 15.50	0.6878
Size (cm) (mean ± SD)	5.44 ± 2.98	5.74 ± 3.32	0.6725
Location			0.1712
Head/neck	11 (31.43%)	8 (18.18%)	
Body/tail	24 (68.57%)	36 (81.82%)	
Complain			0.2317
Symptomatic	21 (60%)	32 (72.73%)	
Asymptomatic	14 (40%)	12 (27.27%)	
CEA (ng/mL)	2.91 ± 4.31	18.00 ± 72.79	0.1771
CA199 (U/mL)	41.73 ± 167.13	236.20 ± 360.23	0.0023*
WBC (×10 <sup>9</sup> /L)	6.58 ± 3.29	6.61 ± 3.57	0.9708
Platelet (×10 <sup>9</sup> /L)	215.54 ± 64.61	216.86 ± 85.47	0.9398
Lymphocyte (×10 <sup>9</sup> /L)	1.61 ± 0.51	1.38 ± 0.57	0.0560
Neutrophil (×10 <sup>9</sup> /L)	4.32 ± 3.27	4.65 ± 3.38	0.6603
Monocyte (×10 <sup>9</sup> /L)	0.49 ± 0.28	0.46 ± 0.27	0.6317
ALB (g/L)	41.22 ± 4.15	39.47 ± 4.21	0.0717
PLR	145.11 ± 58.28	171.73 ± 71.80	0.0796
NLR	3.60 ± 4.81	4.09 ± 4.24	0.6279
PAR	5.34 ± 1.51	5.60 ± 2.57	0.5966
NAR	0.11 ± 0.10	0.13 ± 0.12	0.5678
LMR	4.10 ± 1.86	3.78 ± 2.00	0.4746
LA	67.49 ± 24.83	54.17 ± 21.98	0.0149*
NP	903.92 ± 607.28	984.57 ± 679.03	0.5844

PLR, platelet-lymphocyte ratio; NLR, neutrophil-lymphocyte ratio; PAR, platelet-ALB ratio; NAR, neutrophil-ALB ratio; LMR, lymphocyte-monocyte ratio; LA, lymphocyte × ALB; NP, neutrophil × platelet. \*Means statistically significant.

transformation, and the malignant transformation rate was 18.18%. The preoperative examination of the two groups revealed significant differences in serum CA199 ( $p = 0.0023$ ) and “lymphocyte × ALB” (LA) ( $p = 0.0149$ ), but there were no significant differences in other indicators.

## Univariate and Multivariate Analyses of Risk Factors Associated With MCNs

According to pathology, the 79 patients were divided into the SCN group and MCN group. Univariate analysis showed that two factors were significantly correlated with MCNs, including increased serum CA199 levels (OR = 1.0034,  $p = 0.0256$ ) and decreased LA (OR = 0.9752,  $p = 0.0205$ ). In addition, there was no statistically significant difference ( $p > 0.05$ ) between SCNs and MCNs in terms of serum CEA level, white blood cell count (WBC), platelets, lymphocytes, neutrophils, monocytes, albumin (ALB), platelet-lymphocyte ratio (PLR), neutrophil-lymphocyte ratio (NLR), platelet-ALB ratio (PAR), neutrophil-ALB ratio (NAR), lymphocyte-monocyte ratio (LMR), or “neutrophil × platelet” (NP) (Table 2). The meaningful indexes of univariate analysis were included in logistic regression for multivariate analysis. The results showed that the increase in serum CA199 levels (OR = 1.0031,  $p = 0.0489$ ) and the decrease in LA (OR = 0.9788,  $p = 0.0489$ ) were independent predictors of MCNs (Table 3). In addition, we analyzed the correlations between all variables and the results were added in the supplementary material (Supplementary Figure 1), suggesting that CA199 was related to ALB and CEA. In order to further verify the test efficiency of CA199 and avoid multicollinearity, we selected variables with meaningless

**TABLE 2 |** Univariate analysis of risk factors associated with MCNs.

Characteristics	OR	95% CI	p value
Gender	1.3750	0.4892–3.8650	0.5273
Age	1.0065	0.2637–3.8424	0.6835
Size	1.0320	0.2786–3.8228	0.6681
Location	2.0625	1.4626–2.9085	0.1754
Complain	1.7778	1.1240–2.8118	0.2339
CEA	1.0552	0.6726–1.6554	0.2298
CA199	1.0034	0.9544–1.0549	0.0256*
WBC	1.0025	0.1497–6.7148	0.9703
Platelet	1.0002	0.1588–6.2986	0.9388
Lymphocyte	0.4260	0.3739–0.4854	0.0666
Neutrophil	1.0318	0.2850–3.7349	0.6563
Monocyte	0.6718	0.1963–2.2984	0.6276
ALB	0.8998	0.7741–1.0460	0.0768
PLR	1.0065	0.8517–1.1894	0.0852
NLR	1.0261	0.3017–3.4903	0.6246
PAR	1.0608	0.3319–3.3912	0.5929
NAR	3.6114	1.1932–10.9300	0.565
LMR	0.9179	0.3656–2.3045	0.4697
LA	0.9752	0.9367–1.0152	0.0205*
NP	1.0002	0.3211–3.1159	0.5797

PLR, platelet-lymphocyte ratio; NLR, neutrophil-lymphocyte ratio; PAR, platelet-ALB ratio; NAR, neutrophil-ALB ratio; LMR, lymphocyte-monocyte ratio; LA, lymphocyte × ALB; NP, neutrophil × platelet. \*Means statistically significant.

correlation to further analyze CA199, and the relevant results were added to the supplementary materials (Supplementary Table 1). The results showed that CA199 was still meaningful after calibration of other variables.

**TABLE 3 |** Multivariate analysis of risk factors associated with MCNs.

Characteristics	OR	95% CI	p value
CA199	1.0031	1.0000–1.0062	0.0489*
LA	0.9788	0.9581–0.9999	0.0489*

LA, lymphocyte  $\times$  ALB. \*Means statistically significant.

## Diagnostic Efficacy of the Preoperative Indices in Differentiating SCNs and MCNs

ROC curves were generated, and the area under the ROC curve (AUC) was calculated to evaluate the prediction efficiency of each indicator. The ROC curve was drawn with the preoperative indices as test variables and SCNs/MCNs as state variables (**Figure 1**). The results of the ROC curve showed that the AUC values of serum CA199 and LA in differentiating SCNs and MCNs were 0.6734 and 0.6765, respectively, indicating that they have a certain value in the differential diagnosis of SCNs and MCNs (**Table 4**). According to the Youden index, the diagnostic cutoff point of serum CA199 was 31.315 U/ml (sensitivity,

0.4773; and specificity, 0.9143). The diagnostic cutoff point of LA was 65.45, and the sensitivity and specificity of the differential diagnosis of SCNs and MCNs with LA < 65.45 were 0.7907 and 0.5294, respectively.

## DISCUSSION

SCNs and MCNs have different biological characteristics. SCNs are usually benign with only 1% to 3% malignant potential (16), and they can be followed up (17), while MCNs have malignant potential, and surgical resection is recommended after adequate diagnosis (18, 19). Therefore, correctly distinguishing SCNs from MCNs is of great significance for appropriate treatment. Although there are many better methods for preoperative identification of SCNs and MCNs, such as contrast-enhanced endoscopic ultrasonography (20), endoscopic ultrasound-guided fine-needle aspiration of pancreatic cysts (21), and lesion punctures with fluid aspiration followed by through-the-needle biopsies (22), these methods are either invasive or expensive.

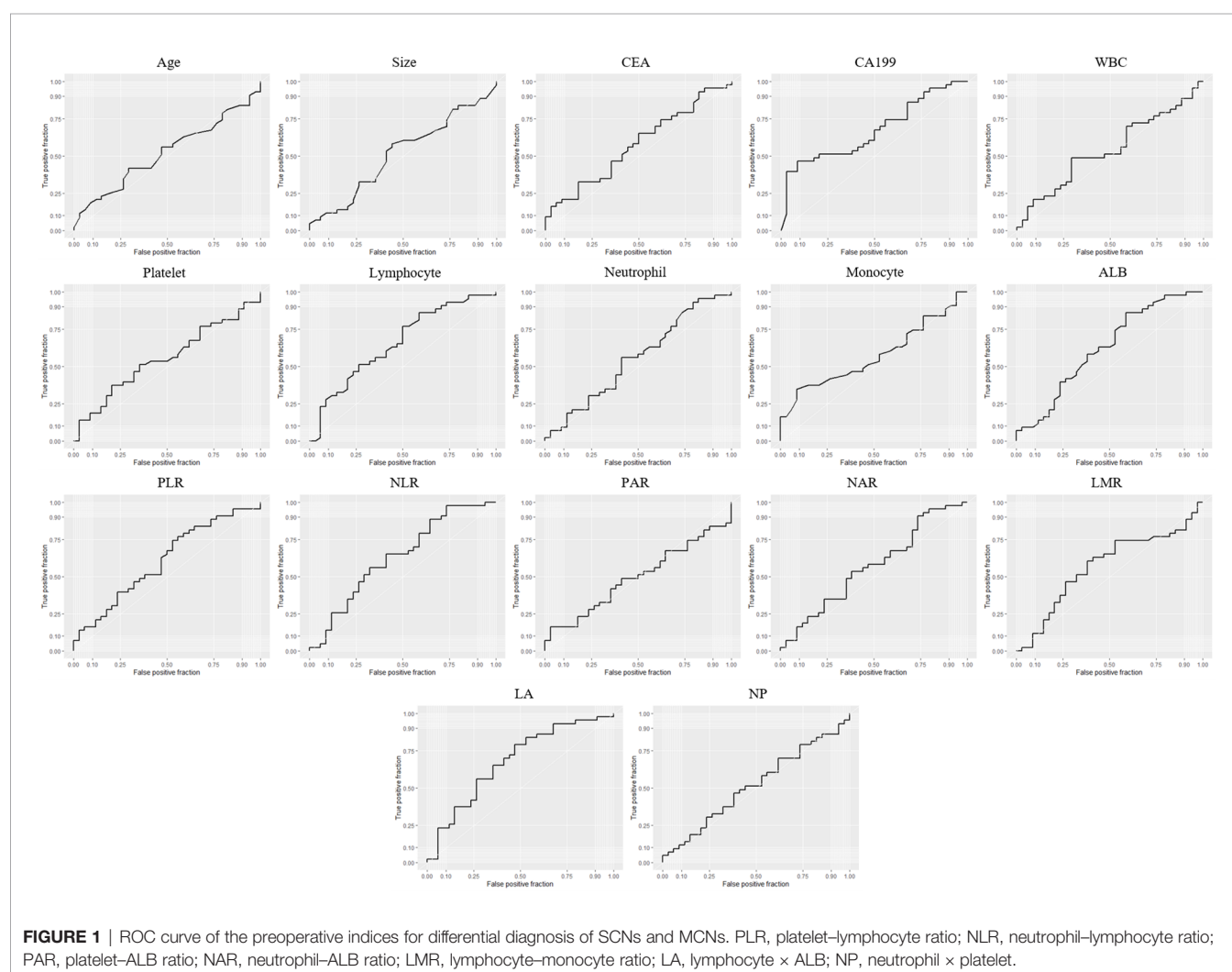


**TABLE 4 |** Diagnostic efficacy of the indices in differentiating SCNs and MCNs.

	AUC	95% CI	Cutoff	Sensitivity	Specificity	p value
Age	0.5386	0.4104–0.6668	62.50 year	0.4318	0.7143	0.8662
Size	0.5187	0.3873–0.6501	4.65 cm	0.5909	0.5588	0.6799
CEA	0.5831	0.4561–0.7101	1.745 ng/ml	0.6591	0.5143	0.2399
CA199	0.6734	0.5541–0.7926	31.315 U/ml	0.4773	0.9143	0.0336*
WBC	0.5312	0.3398–0.5979	$5.595 \times 10^9/l$	0.5000	0.5714	0.9665
Platelet	0.5331	0.4038–0.6624	$184.50 \times 10^9/l$	0.3636	0.7714	0.8791
Lymphocyte	0.6584	0.5355–0.7813	$1.62 \times 10^9/l$	0.7727	0.5143	0.0735
Neutrophil	0.5591	0.4288–0.6894	$3.38 \times 10^9/l$	0.5682	0.6000	0.7078
Monocyte	0.562	0.4342–0.6898	$0.30 \times 10^9/l$	0.3409	0.9143	0.5695
ALB	0.6228	0.4927–0.7528	43.3000 g/l	0.8605	0.4118	0.0768
PLR	0.6146	0.4878–0.7414	121.02	0.7500	0.4857	0.1177
NLR	0.6403	0.5141–0.7664	2.10	0.6591	0.6000	0.6585
PAR	0.5062	0.3636–0.6241	7.74	0.1628	0.9706	0.5929
NAR	0.567	0.4355–0.6986	0.06	0.9070	0.2647	0.5650
LMR	0.5782	0.4477–0.7088	3.816	0.6136	0.6286	0.5594
LA	0.6765	0.5529–0.8000	65.45	0.7907	0.5294	0.0205*
NP	0.5331	0.4036–0.6626	795.90	0.4773	0.6286	0.6889

PLR, Platelet–lymphocyte ratio; NLR, Neutrophil–lymphocyte ratio; PAR, Platelet–ALB ratio; NAR, Neutrophil–ALB ratio; LMR, Lymphocyte–monocyte ratio; LA, Lymphocyte×ALB; NP, Neutrophil×Platelet. \*Means statistically significant.

Therefore, there is an urgent need to find non-invasive, convenient, and inexpensive tests for differential diagnosis.

In this study, the baseline data of the included patients indicated that there were more female patients with SCNs and MCNs than male patients, and the lesions were mostly located in the body or tail of the pancreas, which is consistent with previous research reports (23). At present, many studies have shown that cyst fluid CEA has a good diagnostic effect in differentiating SCNs and MCNs, while blood CEA has a poor diagnostic effect (24). Similarly, the results of the present study also showed that there was no significant difference in serum CEA levels between the SCN group and the MCN group. In contrast, serum CA199 showed good discrimination efficiency. In the present study, the ROC curve was generated, which demonstrated that when serum CA199 was higher than 31.315 U/ml, the occurrence of MCNs was indicated with a sensitivity and specificity of 0.4773 and 0.9143, respectively. The serum tumor marker, CA199 (a tumor-related carbohydrate protein), plays an important role in the diagnosis, treatment, and postoperative follow-up of pancreatic cancer. Increasing evidence indicates that serum CA199 levels play an important role in differentiating the benign and malignant properties of PCNs (25–27). Postlewait et al. (28) analyzed the preoperative blood CA199 level of 349 cases of MCNs and found that the median CA199 level in the malignant group was 210 U/ml; in the nonmalignant group, the median CA199 level was only 15 U/ml ( $p = 0.001$ ), suggesting that the elevated level of serum CA199 indicated malignant MCNs, which was consistent with the results of the present study.

Recent studies have shown that not only the internal characteristics of tumor cells but also the host inflammatory response determine the occurrence and development of tumors (29). In patients with malignant tumors, host factors, such as weight loss, malnutrition, and systemic inflammatory response, are interrelated, and systemic inflammatory response can be used as a predictor of benign and malignant tumors (30). Some inflammatory indicators (NLR, PLR, and LMR) based on

circulating blood cells can be used as a simple and convenient way to measure systemic inflammatory response and as an independent predictor of survival and prognosis in various malignant tumors, including pancreatic cancer (8–10). Recently, there has been much evidence that inflammatory indicators also play an important role in predicting benign and malignant PCNs (12, 13, 31). Our study discovered that LA had good discrimination efficiency between SCNs and MCNs with an AUC of 0.6765 and a diagnostic cutoff point of 65.45. Thus, LA values <65.45 indicate MCNs. Although the potential causal effects behind the association between LA and differential SCNs and MCNs are unclear, the following hypotheses can be proposed. The high density of tumor-infiltrating lymphocytes is closely related to the good prognosis of several cancers, indicating that the antitumor immune response is mainly mediated by lymphocytes (32). Serum ALB is produced by the liver and is known as one of the negative acute phase proteins in response to inflammation. In addition, low ALB concentrations also indicate malnutrition, which can negatively affect tumor immunity in the microenvironment. Given these findings, LA may reflect both the immune response, as represented by lymphocyte count, and nutritional status, as represented by serum albumin levels.

When the two risk factors mentioned above are present at the same time, it indicates a higher risk of MCNs. Surgical treatment and regional pancreatectomy according to imaging results can be considered. In addition, intraoperative frozen pathological results should be considered to prevent more extensive pancreatic parenchymal invasion. Therefore, the present study provides clinicians with a simple, effective, and non-invasive method to identify SCNs and MCNs, thereby facilitating the management and treatment of PCN patients.

The present study had several limitations. First, this study was a retrospective analysis. Only cases with PCNs clearly indicated by surgical pathology or EUS-FNA cytopathology were included, which may have led to selection bias. In addition, due to the



limited sample size, we failed to analyze the differential value of these indicators in other types of PCNs, and the predictive efficacy of CA199 and LA still needs to be verified in future clinical work. Importantly, there are an increasing number of studies on PCNs that are exploring the risk factors for the preoperative prediction of malignant PCNs. For clinicians, comprehensive analysis of various risk factors before surgery and accurate balance between the risk of surgery and the risk of malignancy will bring maximum benefits to patients with PCNs.

## CONCLUSION

In conclusion, as a non-invasive method, tumor markers and inflammatory indicators can complement each other, and joint detection can play an important role in distinguishing SCNs and MCNs. The present study found that serum CA199 and LA can be used independently in the differential diagnosis of SCNs and MCNs. It is worth noting that this is the first report that reveals the value of LA in identifying SCNs and MCNs. The new marker is easily evaluated by routine blood tests, which could provide an opportunity for further investigation.

## DATA AVAILABILITY STATEMENT

The raw data supporting the conclusions of this article will be made available by the authors, without undue reservation.

## REFERENCES

- van Huijgevoort N, Del CM, Wolfgang CL, van Hooft JE, Besselink MG. Diagnosis and Management of Pancreatic Cystic Neoplasms: Current Evidence and Guidelines. *Nat Rev Gastroenterol Hepatol* (2019) 16:676–89. doi: 10.1038/s41575-019-0195-x
- European Study Group on Cystic Tumours of the Pancreas. European Evidence-Based Guidelines on Pancreatic Cystic Neoplasms. *Gut* (2018) 67:789–804. doi: 10.1136/gutjnl-2018-316027
- Kromrey ML, Bulow R, Hubner J, Paperlein C, Lerch MM, Ittermann T, et al. Prospective Study on the Incidence, Prevalence and 5-Year Pancreatic-Related Mortality of Pancreatic Cysts in a Population-Based Study. *Gut* (2018) 67:138–45. doi: 10.1136/gutjnl-2016-313127
- Talukdar R, Nageshwar RD. Treatment of Pancreatic Cystic Neoplasm: Surgery or Conservative? *Clin Gastroenterol Hepatol* (2014) 12:145–51. doi: 10.1016/j.cgh.2013.08.031
- Bausch D, Pausch T, Krauss T, Hopt UT, Fernandez-del-Castillo C, Warshaw AL, et al. Neutrophil Granulocyte Derived MMP-9 Is a VEGF Independent Functional Component of the Angiogenic Switch in Pancreatic Ductal Adenocarcinoma. *Angiogenesis* (2011) 14:235–43. doi: 10.1007/s10456-011-9207-3
- Gong L, Cumpian AM, Caetano MS, Ochoa CE, de la Garza MM, Lapid DJ, et al. Promoting Effect of Neutrophils on Lung Tumorigenesis Is Mediated by CXCR2 and Neutrophil Elastase. *Mol Cancer* (2013) 12:154. doi: 10.1186/1476-4598-12-154
- Coussens LM, Werb Z. Inflammation and Cancer. *Nature* (2002) 420:860–7. doi: 10.1038/nature01322
- Raungkaewmanee S, Tangjitgamol S, Manusirivithaya S, Srijaipracharoen S, Thavaramara T. Platelet to Lymphocyte Ratio as a Prognostic Factor for Epithelial Ovarian Cancer. *J Gynecol Oncol* (2012) 23:265–73. doi: 10.3802/jgo.2012.23.4.265

## ETHICS STATEMENT

Ethical approval/written informed consent was not required for the study of animals/human participants in accordance with the local legislation and institutional requirements.

## AUTHOR CONTRIBUTIONS

HW and SC performed this study and wrote the manuscript as co-first authors; XS and ZL checked the statistics; PL and YoZ revised the manuscript; HX and YoZ designed this study and edited the manuscript. All authors contributed to the article and approved the submitted version.

## FUNDING

This study was supported by the National Natural Science Foundation of China (No. 82060108) and the Youth Project of the Jiangxi Natural Science Foundation (20202BABL216007).

## SUPPLEMENTARY MATERIAL

The Supplementary Material for this article can be found online at: <https://www.frontiersin.org/articles/10.3389/fonc.2022.831355/full#supplementary-material>

- Sugiura T, Uesaka K, Kanemoto H, Mizuno T, Okamura Y. Elevated Preoperative Neutrophil-to-Lymphocyte Ratio as a Predictor of Survival After Gastroenterostomy in Patients With Advanced Pancreatic Adenocarcinoma. *Ann Surg Oncol* (2013) 20:4330–7. doi: 10.1245/s10434-013-3227-8
- Luo G, Guo M, Liu Z, Xiao Z, Jin K, Long J, et al. Blood Neutrophil-Lymphocyte Ratio Predicts Survival in Patients With Advanced Pancreatic Cancer Treated With Chemotherapy. *Ann Surg Oncol* (2015) 22:670–6. doi: 10.1245/s10434-014-4021-y
- Goh BK, Tan DM, Chan CY, Lee SY, Lee VT, Thng CH, et al. Are Preoperative Blood Neutrophil-to-Lymphocyte and Platelet-to-Lymphocyte Ratios Useful in Predicting Malignancy in Surgically-Treated Mucin-Producing Pancreatic Cystic Neoplasms? *J Surg Oncol* (2015) 112:366–71. doi: 10.1002/jso.23997
- Gemenetzi G, Bagante F, Griffin JF, Rezaee N, Javed AA, Manos LL, et al. Neutrophil-to-Lymphocyte Ratio Is a Predictive Marker for Invasive Malignancy in Intraductal Papillary Mucinous Neoplasms of the Pancreas. *Ann Surg* (2017) 266:339–45. doi: 10.1097/SLA.0000000000001988
- Lan C, Li X, Wang X, Hao J, Ren H. A New Combined Criterion to Better Predict Malignant Lesions in Patients With Pancreatic Cystic Neoplasms. *Cancer Biol Med* (2018) 15:70–8. doi: 10.20892/j.issn.2095-3941.2017.0152
- Yoon WJ, Brugge WR. Pancreatic Cystic Neoplasms: Diagnosis and Management. *Gastroenterol Clin North Am* (2012) 41:103–18. doi: 10.1016/j.gtc.2011.12.016
- Yin J, Tian L. Joint Confidence Region Estimation for Area Under ROC Curve and Youden Index. *Stat Med* (2014) 33:985–1000. doi: 10.1002/sim.5992
- Van Dyke TJ, Johlin FC, Bellizzi AM, Howe JR. Serous Cystadenocarcinoma of the Pancreas: Clinical Features and Management of a Rare Tumor. *Dig Surg* (2016) 33:240–8. doi: 10.1159/000444721
- Khashab MA, Shin EJ, Amateau S, Canto MI, Hruban RH, Fishman EK, et al. Tumor Size and Location Correlate With Behavior of Pancreatic Serous Cystic Neoplasms. *Am J Gastroenterol* (2011) 106:1521–6. doi: 10.1038/ajg.2011.117

18. Kloppel G, Kosmahl M. Cystic Lesions and Neoplasms of the Pancreas. The Features Are Becoming Clearer. *Pancreatology* (2001) 1:648–55. doi: 10.1159/000055876
19. Tanaka M, Fernandez-del CC, Adsay V, Chari S, Falconi M, Jang JY, et al. International Consensus Guidelines 2012 for the Management of IPMN and MCN of the Pancreas. *Pancreatology* (2012) 12:183–97. doi: 10.1016/j.pan.2012.04.004
20. Lisotti A, Napoleon B, Facciorusso A, Cominardi A, Crino SF, Brighi N, et al. Contrast-Enhanced EUS for the Characterization of Mural Nodules Within Pancreatic Cystic Neoplasms: Systematic Review and Meta-Analysis. *Gastrointest Endosc* (2021) 94:881–9. doi: 10.1016/j.gie.2021.06.028
21. Facciorusso A, Mohan BP, Tacelli M, Crino SF, Antonini F, Fantin A, et al. Use of Antibiotic Prophylaxis Is Not Needed for Endoscopic Ultrasound-Guided Fine-Needle Aspiration of Pancreatic Cysts: A Meta-Analysis. *Expert Rev Gastroenterol Hepatol* (2020) 14:999–1005. doi: 10.1080/17474124.2020.1797486
22. Crino SF, Bernardoni L, Gabbriellini A, Capelli P, Salvia R, Rusev BC, et al. Beyond Pancreatic Cyst Epithelium: Evidence of Ovarian-Like Stroma in EUS-Guided Through-The-Needle Micro-Forceps Biopsy Specimens. *Am J Gastroenterol* (2018) 113:1059–60. doi: 10.1038/s41395-018-0124-6
23. Kearns M, Ahmad NA. Diagnosis and Management of Pancreatic Cystic Neoplasms. *Curr Treat Options Gastroenterol* (2017) 15:587–602. doi: 10.1007/s11938-017-0162-y
24. Moris D, Damaskos C, Spartalis E, Papalampros A, Vernadakis S, Dimitroulis D, et al. Updates and Critical Evaluation on Novel Biomarkers for the Malignant Progression of Intraductal Papillary Mucinous Neoplasms of the Pancreas. *Anticancer Res* (2017) 37:2185–94. doi: 10.21873/anticancer.11553
25. Efe C. Role of Serum Carbohydrate Antigen 19-9 and Carcinoembryonic Antigen in Distinguishing Between Benign and Invasive Intraductal Papillary Mucinous Neoplasm of the Pancreas (Br J Surg 2011; 98: 104-110). *Br J Surg* (2012) 99:1315–6. doi: 10.1002/bjs.7280
26. Bai X, Ye L, Zhang Q, Prasoon P, Wang J, Liang T. Surgical Resection and Outcome of Pancreatic Cystic Neoplasms in China: Analysis Of a 16-Year Experience From a Single High-Volume Academic Institution. *World J Surg Oncol* (2014) 12:228. doi: 10.1186/1477-7819-12-228
27. Fritz S, Hackert T, Hinz U, Hartwig W, Buchler MW, Werner J. Role of Serum Carbohydrate Antigen 19-9 and Carcinoembryonic Antigen in Distinguishing Between Benign and Invasive Intraductal Papillary Mucinous Neoplasm of the Pancreas. *Br J Surg* (2011) 98:104–10. doi: 10.1002/bjs.7280
28. Postlewait LM, Ethun CG, McInnis MR, Merchant N, Parikh A, Idrees K, et al. Association of Preoperative Risk Factors With Malignancy in Pancreatic Mucinous Cystic Neoplasms: A Multicenter Study. *JAMA Surg* (2017) 152:19–25. doi: 10.1001/jamasurg.2016.3598
29. Greten FR, Grivennikov SI. Inflammation and Cancer: Triggers, Mechanisms, and Consequences. *Immunity* (2019) 51:27–41. doi: 10.1016/j.immuni.2019.06.025
30. Nakamura K, Smyth MJ. Myeloid Immunosuppression and Immune Checkpoints in the Tumor Microenvironment. *Cell Mol Immunol* (2020) 17:1–12. doi: 10.1038/s41423-019-0306-1
31. Zhou W, Rong Y, Kuang T, Xu Y, Shen X, Ji Y, et al. The Value of Systemic Inflammatory Markers in Identifying Malignancy in Mucinous Pancreatic Cystic Neoplasms. *Oncotarget* (2017) 8:115561–9. doi: 10.18632/oncotarget.23310
32. Fridman WH, Pages F, Sautes-Fridman C, Galon J. The Immune Contexture in Human Tumours: Impact on Clinical Outcome. *Nat Rev Cancer* (2012) 12:298–306. doi: 10.1038/nrc3245

**Conflict of Interest:** The authors declare that the research was conducted in the absence of any commercial or financial relationships that could be construed as a potential conflict of interest.

**Publisher's Note:** All claims expressed in this article are solely those of the authors and do not necessarily represent those of their affiliated organizations, or those of the publisher, the editors and the reviewers. Any product that may be evaluated in this article, or claim that may be made by its manufacturer, is not guaranteed or endorsed by the publisher.

Copyright © 2022 Wang, Chen, Shu, Liu, Liu, Zhu, Zhu and Xiong. This is an open-access article distributed under the terms of the Creative Commons Attribution License (CC BY). The use, distribution or reproduction in other forums is permitted, provided the original author(s) and the copyright owner(s) are credited and that the original publication in this journal is cited, in accordance with accepted academic practice. No use, distribution or reproduction is permitted which does not comply with these terms.



## OPEN ACCESS

## Edited by:

Qingfeng Zhu,  
Johns Hopkins Medicine,  
United States

## Reviewed by:

Andrea Laurenzi,  
University Hospital of Bologna  
Policlinico S. Orsola-Malpighi, Italy  
Yang Deng,  
Shandong First Medical University,  
China

## \*Correspondence:

Juan Zhou  
zhoujuan39@qq.com  
Binwu Ying  
docbwy@126.com

<sup>†</sup>These authors have contributed  
equally to this work and share  
first authorship

## Specialty section:

This article was submitted to  
Gastrointestinal Cancers: Hepato  
Pancreatic Biliary Cancers,  
a section of the journal  
Frontiers in Oncology

Received: 11 January 2022

Accepted: 11 February 2022

Published: 04 March 2022

## Citation:

Liu W, Zhang L, Xin Z,  
Zhang H, You L, Bai L, Zhou J  
and Ying B (2022) A Promising  
Preoperative Prediction Model  
for Microvascular Invasion  
in Hepatocellular Carcinoma  
Based on an Extreme Gradient  
Boosting Algorithm.  
Front. Oncol. 12:852736.  
doi: 10.3389/fonc.2022.852736

# A Promising Preoperative Prediction Model for Microvascular Invasion in Hepatocellular Carcinoma Based on an Extreme Gradient Boosting Algorithm

Weiwei Liu<sup>1†</sup>, Lifan Zhang<sup>2†</sup>, Zhaodan Xin<sup>1</sup>, Haili Zhang<sup>3</sup>, Liting You<sup>1</sup>, Ling Bai<sup>1</sup>,  
Juan Zhou<sup>1\*</sup> and Binwu Ying<sup>1\*</sup>

<sup>1</sup> Department of Laboratory Medicine, West China Hospital, Sichuan University, Chengdu, China, <sup>2</sup> Department of Gastroenterology and Hepatology, West China Hospital, Sichuan University, Chengdu, China, <sup>3</sup> Department of Liver Surgery & Liver Transplantation Center, West China Hospital, Sichuan University, Chengdu, China

**Background:** The non-invasive preoperative diagnosis of microvascular invasion (MVI) in hepatocellular carcinoma (HCC) is vital for precise surgical decision-making and patient prognosis. Herein, we aimed to develop an MVI prediction model with valid performance and clinical interpretability.

**Methods:** A total of 2160 patients with HCC without macroscopic invasion who underwent hepatectomy for the first time in West China Hospital from January 2015 to June 2019 were retrospectively included, and randomly divided into training and a validation cohort at a ratio of 8:2. Preoperative demographic features, imaging characteristics, and laboratory indexes of the patients were collected. Five machine learning algorithms were used: logistic regression, random forest, support vector machine, extreme gradient boosting (XGBoost), and multilayer perception. Performance was evaluated using the area under the receiver operating characteristic curve (AUC). We also determined the Shapley Additive exPlanation value to explain the influence of each feature on the MVI prediction model.

**Results:** The top six important preoperative factors associated with MVI were the maximum image diameter, protein induced by vitamin K absence or antagonist-II,  $\alpha$ -fetoprotein level, satellite nodules, alanine aminotransferase (AST)/aspartate aminotransferase (ALT) ratio, and AST level, according to the XGBoost model. The XGBoost model for preoperative prediction of MVI exhibited a better AUC (0.8, 95% confidence interval: 0.74–0.83) than the other prediction models. Furthermore, to facilitate use of the model in clinical settings, we developed a user-friendly online calculator for MVI risk prediction based on the XGBoost model.

**Conclusions:** The XGBoost model achieved outstanding performance for non-invasive preoperative prediction of MVI based on big data. Moreover, the MVI risk calculator would assist clinicians in conveniently determining the optimal therapeutic remedy and ameliorating the prognosis of patients with HCC.

**Keywords:** microvascular invasion, non-invasive predictive models, machine learning, extreme gradient boosting (XGBoost), hepatocellular carcinoma

## 1 INTRODUCTION

Hepatocellular carcinoma (HCC) is one of the most common malignancies and the third leading cause of cancer-related death worldwide (1). Surgical resection is one of the predominant treatments for early-stage HCC; however, the high incidence of postoperative recurrence and metastasis largely threatens the long-term survival of patients (2). Microvascular invasion (MVI), the embolus of cancer cells with micro-metastasis in liver vessels, is an independent prognostic factor for recurrence and metastasis in HCC (3). Recently, an increasing number of studies (4, 5) have shown that a precise surgical approach and timely postoperative adjuvant therapy for patients with HCC and MVI could reduce recurrence and improve survival.

Patients with HCC and MVI have been demonstrated to achieve better prognosis through anatomical resection than through non-anatomical resection (6). In addition, scholars have suggested that patients with HCC and MVI should be treated with wide margin resection rather than narrow margin resection, as it achieves better relapse-free survival (7). Besides, surgical resection provides better tumor control than radiofrequency ablation (RFA) treatment in patients with small HCC, especially those with a high risk of MVI (8). MVI status is crucially important for clinicians to choose the optimal therapy, while MVI can only be confirmed by postoperative histopathological examination; therefore, preoperative prediction of MVI is urgent.

Early studies have focused on blood biomarkers that can predict MVI; among these,  $\alpha$ -fetoprotein (AFP) is considered one of the most notable biomarkers (9). However, its predictive efficacy for MVI was poor in univariate analysis (10, 11), while the combination of multiple biomarkers showed greater potential (12, 13). With the development of big-data-driven approaches, machine learning (ML) has been extensively used in various diseases, such as cardiac abnormalities (14), pulmonary diseases (15), neurological disorders (16), and oncology (17–20), showing great ability in prediction model construction. ML algorithms demonstrate the advantages of robust feature selection and the ability to identify clinically important risks among patients, are dedicated to finding complex patterns in big data with high accuracy and are suitable for constructing predictive models from numerous multidimensional factors, especially non-linear complex data.

However, different ML algorithms have their own advantages and disadvantages. Recently, Deng et al. combined the neutrophil-to-lymphocyte ratio, tumor size, and AFP to establish a nomogram for predicting MVI in 513 patients with HCC, but the sensitivity and specificity of the model were only

61.64% and 71.53%, respectively (21). Lei et al. constructed a nomogram to predict MVI in 1004 patients with HCC, but the high false-positive (23.4%) and false-negative rates (26.5%) still need to be considered when it is applied in clinical decision-making (22). These models were based on logistic regression algorithms; although simple to construct, they were prone to underfitting, and the clinical application accuracy was not ideal. Therefore, more ML algorithms have been applied to predict the occurrence of MVI and achieve better performance. Chen et al. proposed an MVI prediction model by integrating blood tests based on a deep learning method with concordance indexes of 0.9341 and 0.9052 in the training and validation cohorts, respectively (23). Additionally, the inclusion of radiomic features and multi-omics data improved the model's predictive performance of MVI. Xu et al. integrated radiomics, clinical features, and liver and renal function indicators and developed a multivariate logistic regression MVI prediction model in 495 patients with HCC, with an area under the receiver operating characteristic curve (AUC) of 0.889 (24). However, these radiomic features require sophisticated techniques and experts and are not easy to popularize. Overall, the sample size of previous studies was small, ranging from 150 to 1004 patients (24, 25), and it was demonstrated that the robustness of the model based on big data was better than that based on small data (26). Therefore, it is necessary to establish an MVI prediction model with reliable and excellent performance using conveniently available clinical indicators and big data.

The noninvasive preoperative diagnosis of MVI in HCC is vital for precise surgical decision-making and patient prognosis. In this study, we attempted to use multiple ML algorithms to develop a preoperative MVI prediction model and select an optimal one, based on the big data of patients with HCC at the West China Hospital, from multidimensional and conveniently available variables. Simultaneously, we quantified and explained the important variables related to MVI, visually exhibiting them using the Shapley Additive exPlanation (SHAP) algorithm. Remarkably, to make it more convenient in clinical situations, we created an MVI risk online calculator for clinicians to assist in precise HCC treatment visually and operationally.

## 2 METHODS

### 2.1 Ethics and Statements

This study was approved by the Institutional Ethics Committee of the West China Hospital, Sichuan University [number: 2019 (203)].



## 2.2 Study Design and Patients

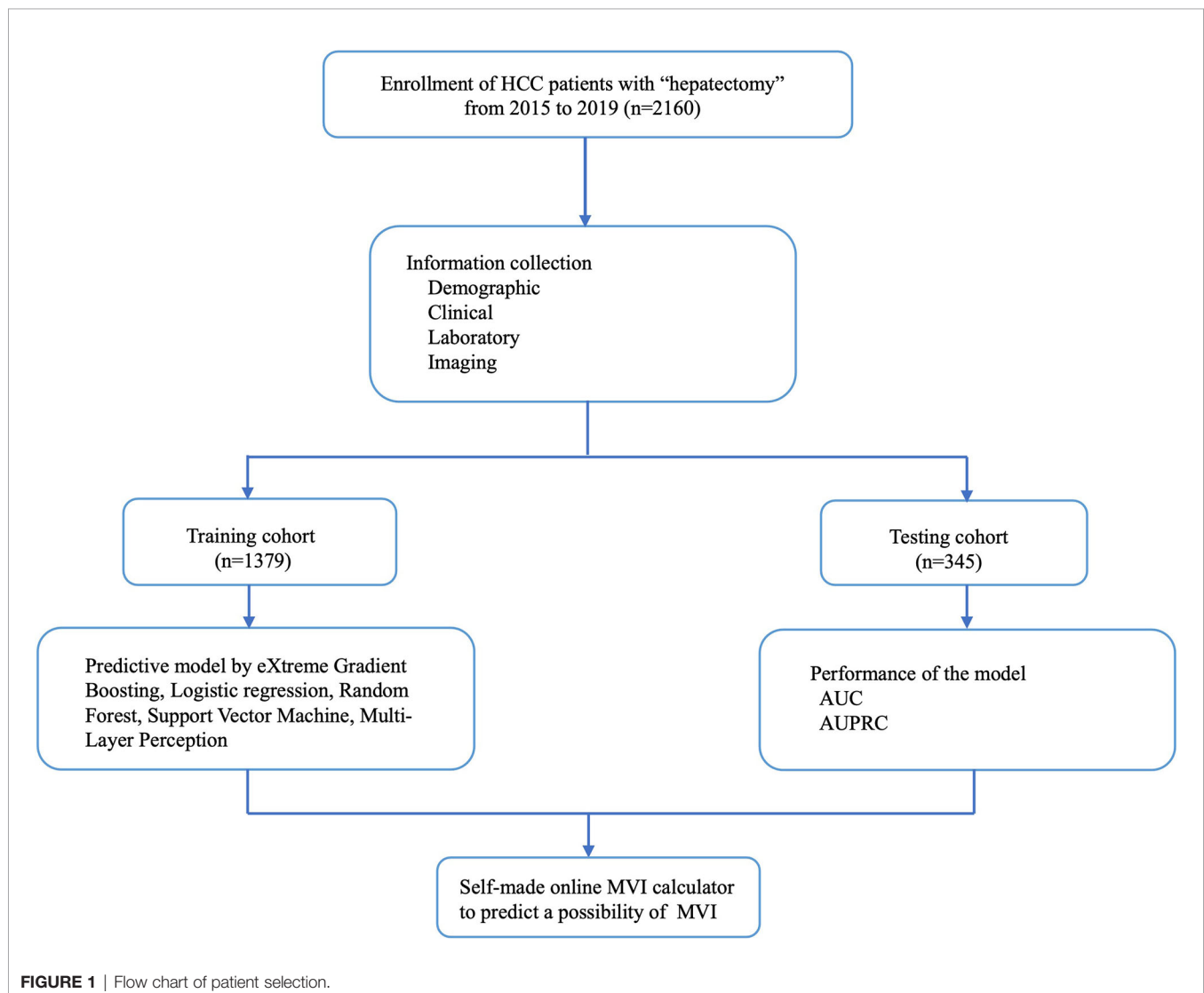
Patients with HCC who underwent surgery at the West China Hospital between January 2015 and June 2019 were retrospectively enrolled (**Figure 1**). The inclusion criteria were as follows: 1) patients who had undergone hepatectomy or liver transplantation for the first time and were pathologically diagnosed with HCC alone, regardless of whether they had received transcatheter arterial chemoembolization (TACE) before; and 2) the Guidelines for Diagnosis and Treatment of Primary Liver Cancer in China (2017 Edition) (27) were used as diagnostic criteria. The exclusion criteria were as follows: 1) Patients with HCC with recurrence who had previously undergone hepatectomy or RFA; 2) HCC with macroscopic invasion; 3) Patients with HCC and tumors at other sites; and 4) Patients with HCC and other tumors, such as bile duct adenocarcinoma, intrahepatic cholangiocarcinoma, and sarcoma.

MVI diagnosis has relied on the judgment of two or more experienced pathologists based on seven-point sampling (28) to

ensure MVI detection ability since 2015 in our hospital; hence, we used data from 2015.

## 2.3 Preoperative Examination and Clinicopathologic Variables

In total, 88 indicators were extracted from Electronic Health Records (EHR) of all patients. All of the indicators were all collected within 1 month before surgery, including three categories of characteristics: 1) demographic data: age, gender, height, weight, body mass index, ethnicity, preoperative TACE (yes or no), hepatitis B, and hepatitis C; 2) imaging features: single or multiple tumors, maximum diameter of the tumors, imaging cirrhosis, tumor margin, etc.; 3) laboratory examination results: routine blood test results, biochemical test results (hepatic function indexes, kidney function indexes, glucose, etc.), routine coagulation test results (activated partial thromboplastin time [APTT], prothrombin time, etc.), hepatitis B virus (HBV)-DNA load and tumor markers (AFP,



carbohydrate antigen, carcinoembryonic antigen, cancer antigen 125, protein induced by vitamin K absence or antagonist-II [PIVKA-II]). The details of all indicators are listed in **Supplemental Table 1**.

## 2.4 Statistical Analysis

Continuous variables with normal distribution are expressed as mean  $\pm$  standard deviation and were compared between the MVI and non-microvascular invasion (NMVI) groups using Student's *t*-test. Non-normal variables were analyzed using the Kruskal-Wallis rank sum test. Categorical variables are expressed as frequency (%), and chi-square tests or Fisher exact tests were applied to these data, as appropriate. All statistical analyses were performed using Python (version 3.7.9), and  $p < 0.05$  indicated statistical significance.

## 2.5 Machine Learning Models Establishment

The patients with HCC in this study were randomly divided into a training cohort and a validation cohort at a ratio of 8:2. To overcome the imbalance in the data, an under-sampling approach was applied (29). We attempted to develop MVI predictive models using five ML algorithms: logistic regression (LR), random forest (RF), support vector machine (SVM), multilayer perception (MLP), and extreme gradient boosting (XGBoost). LR involves modeling the relationship between explanatory variables and the log odds of a binary outcome by employing the maximum likelihood algorithm (30). RF, a tree-like model, integrates multiple decision trees through major voting, reducing variance, and increasing robustness (31). SVM is a computational algorithm that separates binary labeled data based on a line to realize the maximum distance between the labeled data using hinge loss to calculate the empirical risk (32). An MLP is typically built into structured node groups with activation functions and connection weights that mimic the behavior of biological neural networks and processes distributed and parallel information (33). XGBoost is an optimized distributed gradient boosting algorithm that uses a second-order Taylor expansion to approximate the loss function, which efficiently avoids overfitting problems by adding a regularization term to the objective function, providing excellent predictions by transforming a set of weak learners into strong learners (34).

In this study, we randomly divided the data into five equal subsets. Four subsets were used to train the model and were then validated in the remaining subsets. In this process, hyperparameter adjustment was performed for the higher area under the receiver operating characteristic curve (AU-ROC), which could evaluate the prediction ability of the model. The hyperparameters were determined using a grid search, which can be tuned and scored in a loop. Changing the subset ratio to display the learning curve of the AU-ROC model helps prevent overfitting and underfitting. After adjusting the hyperparameters, the final model of the entire training set was obtained, and then the model was evaluated on the test set. The LR, RF, SVM, and MLP models were implemented in Python (version 3.7.9) using the scikit-learn

package. The XGBoost model was implemented using the Python XGBoost package.

## 2.6 Hyperparameters Adjustment of Microvascular Invasion-Predicting Model

Hyperparameters were fully optimized since the training log-loss decreased as the number of trees increased; when the test log-loss was  $< 0.693$  ( $-\log 0.5 = 0.693$ , the test log-loss of blind guess was 0.693; a lower log-loss means a better prediction) or only slightly larger than the training log-loss, the hyperparameters were fully adjusted. We ran 100 bootstrap iterations to determine the number of trees in the final model, as recommended in previous literature. Based on the grid search, the hyperparameters used in XGBoost were set as follows: learning rate = 0.13, minimum child weight = 1, maximum tree depth = 6, and number of rounds = 100. The hyperparameters used in the other models are presented in **Supplemental Table 2**.

## 2.7 Model Performance Evaluation

To evaluate the prediction performance of the various ML models, the AUC was measured and compared. We also used precision recall curve (PRC) to measure the number of positive examples that were correctly classified, which better reflecting the predictive performance when an imbalance between the groups exists. The confusion matrix was used to visually describe the accuracy of XGBoost in identifying the MVI and NMVI statuses, including true positive (TP), false positive (FP), true negative (TN), and false negative (FN).

$$\text{Accuracy} = (\text{TP} + \text{TN}) / (\text{TP} + \text{FN} + \text{TN} + \text{FP})$$

$$\text{Specificity} = \text{TN} / (\text{TN} + \text{FP})$$

## 2.8 Interpretation of the Model by the SHapley Additive exPlanation

It is critical to correctly interpret the prediction model. Thus, the SHAP algorithm (35), a game-theoretic approach to explain the output of any ML model, was employed to obtain accurate attribution values for each feature within the prediction model. The SHAP value can be considered a quantified contribution. We can easily determine the contribution of all features and which contribution is the most.

# 3 RESULTS

## 3.1 Basic Characteristics

The characteristics of the 2160 patients with HCC are summarized in **Table 1**; 575 (27%) had MVI and 1585 (73%) had NMVI. The mean age of the patients was 53.2 years. The Han ethnic group accounted for 94.7% of the population. HBV positivity was found in 1773 (82%) cases. Hepatitis C virus positivity was observed in 23 cases (1.1%). HCC with cirrhosis was observed in 911 (42.2%) patients. We randomly divided these patients and allocated 80% of them to the training set and the remaining 20% to the test set. For all variables, the differences

**TABLE 1 |** The participant baseline characteristics data.

Variables	Total (N=2160)	NMVI (N=1585)	MVI (N=575)	P Value
Age (years)	53.2 (11.6)	53.6 (11.4)	52.0 (12.0)	0.004
Gender, n (%)				0.239
Male	1813 (83.9)	1321 (83.3)	492 (85.6)	
Female	347 (16.1)	264 (16.7)	83 (14.4)	
Height, mean (SD)	165.1 (7.0)	165.1 (7.0)	165.2 (7.0)	0.857
Weight, mean (SD)	63.2 (10.2)	63.5 (10.40)	62.5 (9.6)	0.051
BMI, mean (SD)	23.2 (3.1)	23.3 (3.2)	22.9 (2.9)	0.008
Nation, n (%)				0.313
Tibetan	76 (3.5)	50 (3.2)	26 (4.5)	
Han	2046 (94.7)	1507 (95.1)	539 (93.7)	
Others	38 (1.8)	28 (1.8)	10 (1.7)	
HBV, n (%)				0.113
Yes	1773 (82)	1314 (82.9)	459 (79.8)	
No	387 (18)	271 (17.1)	116 (20.2)	
HCV, n (%)				0.768
Yes	23 (1.1)	18 (1.1)	5 (0.9)	
No	2137 (98.9)	1567 (98.9)	570 (99.1)	
cirrhosis, n (%)				0.114
Yes	911 (42.2)	685 (43.2)	226 (39.3)	
No	1249 (57.8)	900 (56.8)	349 (60.7)	

between the training and test sets were not significant. Details are presented in **Supplemental Table 3**.

## 3.2 Clinical Characteristic Differences Between the Study Groups

The preoperative clinical characteristics of all the patients are shown in **Table 2**. Overall, in terms of imaging features, the MVI group had a larger maximum tumor diameter than the NMVI group ( $7.1 \text{ cm} \pm 3.7 \text{ cm}$  versus  $4.9 \text{ cm} \pm 3.1 \text{ cm}$ ,  $p < 0.001$ ). The occurrence frequency of satellite nodules (19.5% vs. 7.4%,  $p < 0.001$ ) and intra-tumoral artery (29.1% vs. 14.4%,  $p < 0.001$ ) were higher in the MVI group than in the NMVI group. Regarding laboratory examinations, the MVI group had a higher PLT count ( $158.9 \times 10^9/\text{L} \pm 77.9 \times 10^9/\text{L}$  vs.  $136.2 \times 10^9/\text{L} \pm 67.6 \times 10^9/\text{L}$ ,  $p < 0.001$ ), aspartate aminotransferase (AST) level ( $55.3 \text{ IU/L} \pm 49.1 \text{ IU/L}$  vs.  $43.7 \text{ IU/L} \pm 38.3 \text{ IU/L}$ ,  $p < 0.001$ ), AST/alanine aminotransferase (ALT) ratio ( $1.3 \pm 0.9$  vs.  $1.1 \pm 0.5$ ,  $p < 0.001$ ),  $\gamma$ -glutamyl transferase (GGT) level ( $116.7 \text{ IU/L} \pm 127.2 \text{ IU/L}$  vs.  $85.6 \text{ IU/L} \pm 122.8 \text{ IU/L}$ ,  $p < 0.001$ ), lactate dehydrogenase level ( $215.2 \text{ IU/L} \pm 118.9 \text{ IU/L}$  vs.  $186.8 \text{ IU/L} \pm 69.5 \text{ IU/L}$ ,  $p < 0.001$ ), hydroxybutyrate dehydrogenase (HBDH) level ( $160.6 \text{ IU/L} \pm 83.1 \text{ IU/L}$  vs.  $146.1 \text{ IU/L} \pm 54.7 \text{ IU/L}$ ,  $p < 0.001$ ), AFP level  $>400 \text{ ng/mL}$  (50.0% vs. 28.9%,  $p < 0.001$ ), and PIVKA-II level ( $11905 \text{ mAU/mL} \pm 21680.9 \text{ mAU/mL}$  vs.  $3009.1 \text{ mAU/mL} \pm 9716.8 \text{ mAU/mL}$ ,  $p < 0.001$ ) than the NMVI group. Moreover, the MVI group had more abnormal imaging and laboratory examination results than the NMVI group (**Supplemental Table 1**).

## 3.3 Development and Validation of the MVI-Predicting Model

### 3.3.1 Development of the MVI-Predicting Model

All models were parameterized with these hyperparameters, and bootstrap validation training log-loss decreased as the number of integration trees increased. The bootstrap validation testing log-loss was  $<0.693$ , which was only slightly higher than the training

log-loss when the number of rounds increased. Here, we only show the training curve of the XGBoost model as an example, which indicated a good fitting (**Figure 2A**). When the sample size reached 200 rounds, the log-loss of the training and test sets gradually tended to be stable, indicating that the model was well turned.

The learning curve showed that as the score of the training cohort decreased, the score of the validation cohort increased with an increase in training samples. We also used the XGBoost model for demonstration (**Figure 2B**). This revealed that as the sample size increased, the model had not been overfitted or underfitted, indicating a robust predictive performance.

### 3.3.2 Model Performance

We used RF, SVM, LR, XGBoost, and MLP algorithms to construct and optimize the MVI prediction model, and found that the XGBoost model achieved the highest AUC (0.8, 95% confidence interval [CI]: 0.74–0.83) (**Figure 3A**), followed by the RF (0.77, 95% CI: 0.73–0.81), LR (0.73, 95% CI: 0.70–0.77), SVM (0.66, 95% CI: 0.61–0.71), and MLP models (0.65, 95% CI: 0.60–0.70). Since the positive and negative samples were highly skewed datasets in our study, we used PRC to reflect the performance of the classifier more effectively. The area under the precision recall curve (AUPRC) value of the XGBoost model was much higher (0.71, 95% CI: 0.64–0.78) than that of the other models (**Figure 3B**). Other algorithms showed the following AUPRC values: RF model, 0.7, 95% CI: 0.65–0.77; LR model, 0.65, 95% CI: 0.62–0.71; SVM model, 0.53, 95% CI: 0.41–0.60; and MLP model, 0.53, 95% CI: 0.47–0.61. Additionally, the confusion matrix showed that the accuracy and specificity of the XGBoost model were 73% and 84%, respectively (**Figure 3C**).

## 3.4 Model Interpretation

The feature importance matrix plot sorted the most important variables, revealing the contribution of each variable to MVI versus NMVI. The top six factors associated with MVI were the

**TABLE 2 |** The clinical characteristic differences between MVI and NMVI group.

Variables	Total (N=2160)	NMVI (N=1585)	MVI (N=575)	P Value
<b>Imaging result</b>				
<b>Satellite nodules, n (%)</b>				<0.001
Yes	230 (10.6)	118 (7.4)	112 (19.5)	
No	1930 (89.4)	1467 (92.6)	463 (80.5)	
<b>Maximum image diameter, mean (SD)</b>	5.5 (3.4)	4.9 (3.1)	7.1 (3.7)	<0.001
<b>Intratumorally artery, n (%)</b>				<0.001
Yes	343 (18.3)	198 (14.4)	145 (29.1)	
No	1527 (81.7)	1173 (85.6)	354 (70.9)	
<b>Laboratory result</b>				
<b>PLT, mean (SD)</b>	142.2 (71.2)	136.2 (67.6)	158.9 (77.9)	<0.001
<b>NEUT%, mean (SD)</b>	60.2 (10.0)	59.6 (10.1)	61.7 (9.7)	<0.001
<b>LYMPH%, mean (SD)</b>	28.9 (8.8)	29.4 (8.8)	27.5 (8.7)	<0.001
<b>NLR, mean (SD)</b>	2.5 (1.5)	2.4 (1.4)	2.7 (1.7)	<0.001
<b>FIB, mean (SD)</b>	2.7 (1.0)	2.6 (0.9)	2.9 (1.0)	<0.001
<b>AST, mean (SD)</b>	46.8 (41.8)	43.7 (38.3)	55.3 (49.1)	<0.001
<b>A/A, mean (SD)</b>	1.2 (0.7)	1.1 (0.5)	1.3 (0.9)	<0.001
<b>ALP, mean (SD)</b>	103.9 (62.2)	100.4 (61.1)	113.7 (64.3)	<0.001
<b>GGT, mean (SD)</b>	93.9 (124.8)	85.6 (122.8)	116.7 (127.2)	<0.001
<b>LDL-C, mean (SD)</b>	2.4 (0.8)	2.4 (0.7)	2.5 (0.9)	<0.001
<b>LDH, mean (SD)</b>	194.4 (86.4)	186.8 (69.5)	215.2 (118.9)	<0.001
<b>HBDH, mean (SD)</b>	150.0 (63.8)	146.1 (54.7)	160.6 (83.1)	<0.001
<b>HBV DNA, n (%)</b>				<0.001
Negative	616 (38.2)	484 (41.8)	132 (29.2)	
Positive	995 (61.8)	675 (58.2)	320 (70.8)	
<b>HBV DNA Log, mean (SD)</b>	3.2 (2.1)	3.0 (2.1)	3.5 (2.0)	<0.001
<b>AFP, n (%)</b>				<0.001
<400	1404 (65.5)	1118 (71.1)	286 (50.0)	
>400	740 (34.5)	454 (28.9)	286 (50.0)	
<b>CA-125, n (%)</b>				<0.001
<35	1270 (78.1)	969 (81.4)	301 (69.0)	
>35	357 (21.9)	222 (18.6)	135 (31.0)	
<b>PIVKA-II, n (%)</b>	5597.0 (14822.6)	3009.1 (9716.8)	11905.3 (21680.9)	<0.001
<2000	628 (29.1)	524 (33.1)	104 (18.1)	
>2000	503 (23.3)	278 (17.5)	225 (39.1)	

maximum image diameter, PIVKA-II level, AFP level, satellite nodules, AST/ALT ratio, and AST level (**Figure 4A**). To illustrate the influence of each feature on model prediction, we drafted the SHAP value summary chart, and only the top 15 variables of the model are shown (**Figure 4B**). The chart shows the correlation between the high or low SHAP values and the prediction model.

We observed that the red dots, which represent the high values of the maximum image diameter, AFP level, satellite nodules, AST/ALT ratio, and AST level, appeared more on the side of the higher probability risk of MVI. This indicates that the SHAP values of these indicators were positively correlated with the possibility of the occurrence of MVI. The red dots representing

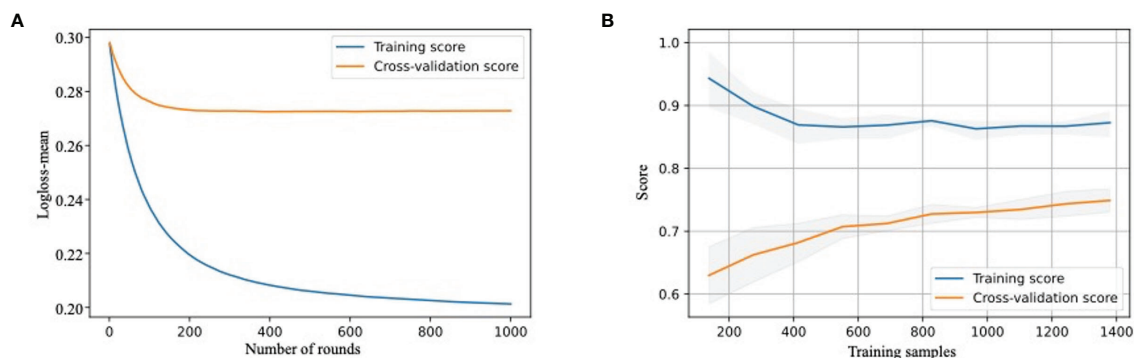


**FIGURE 2 |** Development and validation of MVI-prediction model (A) The training process of XGBoost model. Train-log-loss-mean value for the training datasets is shown in the vertical axis. The horizontal axis represents the number of times iterative cross-validation. (B) The learning curve of the score of training cohort and testing cohort. The score for training and test cohorts is shown in the vertical axis. The horizontal axis represents the number of samples trained.



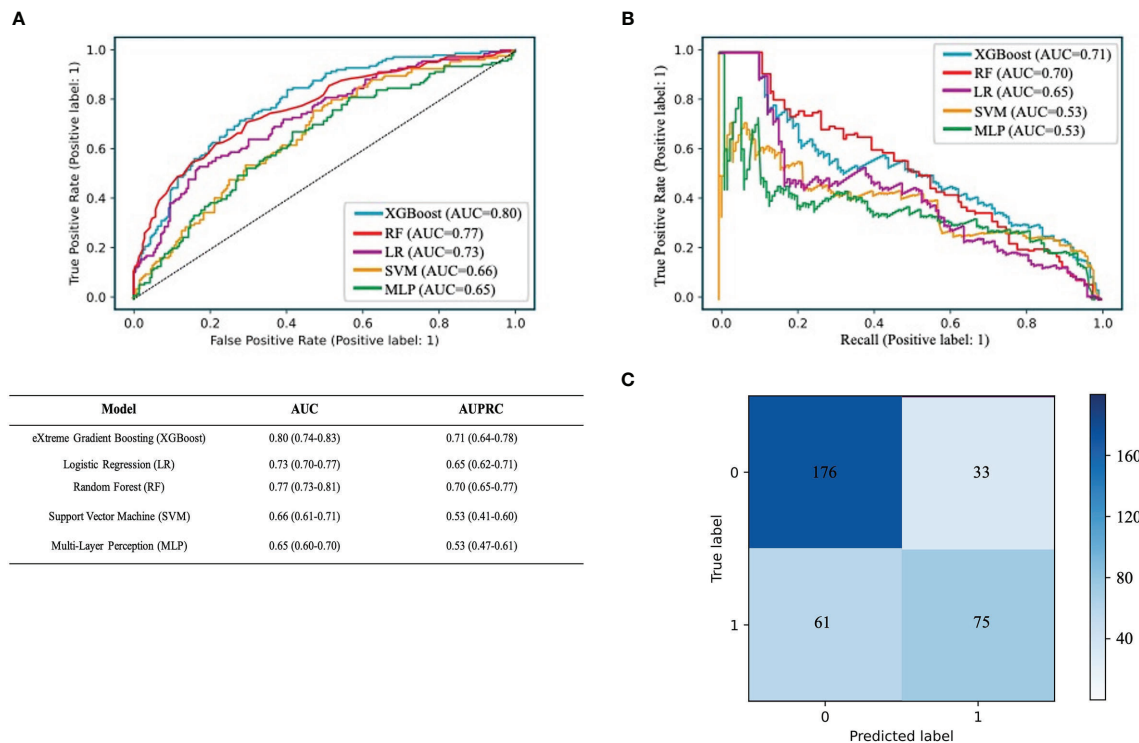


**FIGURE 3 |** Performance of the predictive models. **(A)** The ROC curve analysis of various prediction model. **(B)** The PRC curve of different models. The confusion matrix of XGBoost model in the validation cohort. **(C)** The confusion matrix of XGBoost model. The confusion matrix was composed of the True negative in the first quadrant, the false negative samples in the second quadrant, the true positive example in the third quadrant and the false positive example in the fourth quadrant.

the high values of the PIVKA-II level were covered by blue dots, indicating lower values of the PIVKA-II level. This indicated that predication was affected by the extreme values, and even if the PIVKA-II values were high, some points were still blue and tended to predict the occurrence of NMVI. Furthermore, the SHAP values of the above features are displayed, which show a clear distinction between MVI and NMVI. The cutoff values of the maximum image diameter, PIVKA-II level, AFP level, satellite nodules, AST/ALT ratio, and AST level were 5 cm, 500 mAU/mL, 200 ng/mL, one nodule, 1, and 50 U/L, respectively (**Figure 4C**). By integrating the SHAP value summary chart and the SHAP scatter plot, the sensitivity of PIVKA-II was found to be good, while the specificity of PIVKA-II was not. Other indicators showed good specificity and sensitivity.

### 3.5 Online Calculator Based on the Extreme Gradient Boosting Microvascular Invasion Prediction Model

We established a website based on the XGBoost model to predict the risk of MVI (<https://260147169.github.io/MVI-calculator/MVI-calculator.html>). We only needed to fill in the corresponding parameters of each indicator, including the maximum image diameter, PIVKA-II level, AFP level, satellite nodules, AST/ALT ratio, AST levels, HBV, total bile acid level, PLT count, GGT level, APTT, HBDH level, mean red blood cell volume, and white blood cell count. The online calculator

automatically and promptly converted the MVI risk score (**Supplemental Figure 1**).

## 4 DISCUSSION

In this study, we developed an XGBoost model for the preoperative prediction of MVI based on the EHR information of 2160 patients with HCC at the West China Hospital, and it exhibited the best AUC in the validation set compared with the other ML algorithms and showed good interpretability, as well as the importance of MVI-related factors. Furthermore, we built an online calculator based on this model to make prediction of MVI more practical. Overall, we provide a valuable and reliable preoperative MVI prediction model, which may be effective in optimizing surgical treatment and further improving the survival of patients with HCC.

Notably, the lack of specific and effective preoperative indicators is one of the bottlenecks in the diagnosis of MVI. In this retrospective cohort study, we developed an XGBoost model using 88 objective preoperative demographic, imaging, and laboratory indicators to predict the possibility of MVI. AUC analysis alone is often insufficient for comparing predictive models, particularly in an imbalanced dataset. Therefore, we used both the AUC and AUPRC to evaluate the performance of the five ML methods. Compared with other models, the XGBoost

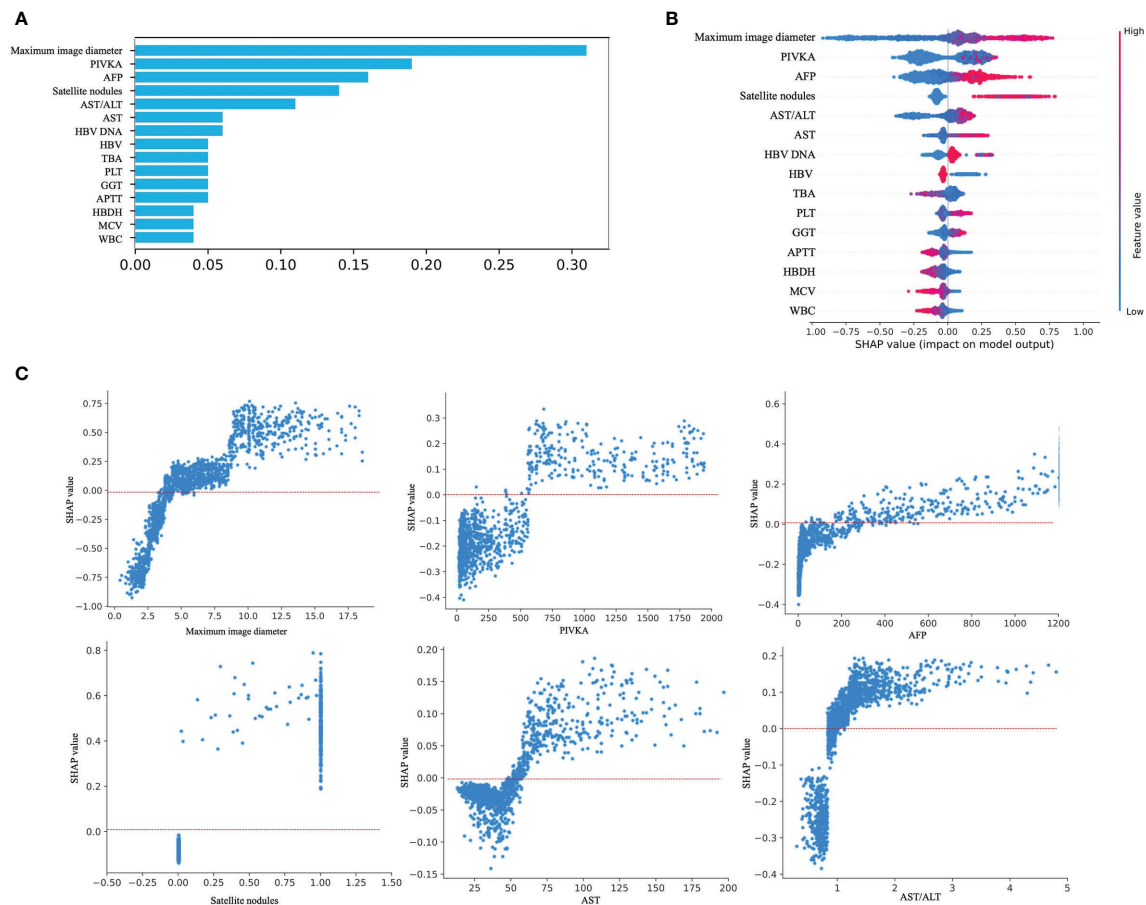


**FIGURE 4 |** Model interpretation. **(A)** Feature importance matrix plot derived from XGBoost model. **(B)** SHAP summary plot of the XGBoost model. The higher the SHAP value for each feature, the higher risk of MVI development. A dot represents each feature contribution for each patient in the model. Red indicates a high SHAP value, blue indicates a low SHAP value. **(C)** SHAP dependence plot of XGBoost model. The SHAP dependence plot represents the contribution of each feature that we care about to the output of the XGBoost model. If the SHAP value of the feature we care about is exceeds zero, the higher the risk of MVI will be.

model exhibited a better performance with an AUC of 0.8 and an AUPRC of 0.71.

Several ML methods have been developed to predict the risk of MVI. Some methods were based on radiomics or included only a few vital tumor biomarkers to build ML algorithms to predict MVI (36). Dong et al. (37) established a radiomic algorithm to make preoperative predictions of MVI based on grayscale ultrasonograms. The radiomic signatures based on the features of the gross tumor region (GTR), peri-tumoral region, and gross peritumoral region (GPTR) showed AUCs of 0.708, 0.710, and 0.726, respectively. After incorporating some important tumor biomarkers, the AUC of the GPTR radiomic signature was 0.744, and the AUC of the GTR radiomic signature was 0.806. This might ignore useful information, especially some serum biomarkers. It is worth noting that our model was built based on three multidimensional preoperative indicators, including patient clinical characteristics, imaging examination features, and laboratory examination results, without invasive examination. Compared with the MVI prediction models using

radiomics as the only predictor (25, 38), the potential significance of this model with multivariable predictors was that we could predict the possibility of MVI using routine clinical information before surgery.

Our work also has the advantages of convenient data collection, ready availability, and objectivity, which are suitable for use in the evaluation of MVI in most clinical situations. Remarkably, all the variables in our model have a short detection time, which can help clinicians quickly obtain reference diagnostic information for patients with no immediate access to pathological diagnosis. Additionally, previous studies constructed an MVI prediction model based on a small sample size (25). Studies have shown that the models with a large sample size have higher robustness than those with a small sample size (26); the sample size of our study was much bigger than that of previous studies as far as we know. Furthermore, our model showed consistent performance between the observed and predicted MVI risks by SHAP values, implying the interpretation and robustness of the model.

The importance ranking of the correlation between the top 15 conventional imaging and laboratory variables with the occurrence of MVI was identified through XGBoost model learning. Specifically, the maximum image diameter, PIVKA-II level, AFP level, satellite nodules, AST/ALT ratio, and AST level showed the top six significant contributions to the prediction of MVI, whether using the importance matrix plot or SHAP summary plot of the XGBoost model. Among them, the maximum image diameter was ranked first. In addition, satellite nodules, one of the imaging indicators, were in the top six importance rankings. Roayaie et al. defined satellite nodules as tumors  $\leq 2$  cm in size located  $\leq 2$  cm from the main tumor (39). In our SHAP scatter plot of satellite nodules, most of the scatter point values were 1. Our SHAP scatter plot of the maximum image diameter showed that the cutoff value was 5 cm. Recently, Zhang et al. (40) demonstrated that the maximum image diameter and emergence of satellite nodules aggravated the MVI of HCC. Their studies set the cutoff value of the maximum image diameter to 5 cm by referring to different guidelines. They also indicated that the presence of satellite nodules might be a risk factor for predicting the occurrence of MVI. This finding is consistent with our results.

In addition to imaging indicators, laboratory indicators, such as the PIVKA-II level, AFP level, AST/ALT ratio, and AST level, also appeared in the top six SHAP value rankings. This observation was consistent with that of a previous report in which high levels of AFP and PIVKA-II were found to be closely related to MVI (41, 42). Meanwhile, in the SHAP scatter plot, the cutoff of our PIVKA-II level was  $>500$  mAU/L. There were some patients with NMVI even though PIVKA-II values were high; our data showed that the specificity of the PIVKA-II level was relatively poor, and we thought that the cutoff value should be improved. In previous studies, Fumitoshi et al. (43) performed a univariate analysis of 167 patients, revealing that a PIVKA-II level  $\geq 150$  mAU/mL on preoperative examination was a high risk factor for MVI. In a study by Pote et al., a PIVKA-II level  $>90$  mAU/mL was an independent predictor of MVI (10). However, this finding is in line with the clinical expectation that a larger PIVKA-II value is more strongly correlated with HCC.

In our research, a consistent tendency was found in that the SHAP values with scattered points above 0 was almost always  $>200$  ng/mL on the SHAP plot of the AFP level. You et al. (44) analyzed 215 patients who underwent liver resection using univariate and multivariate analyses, and showed that an AFP cutoff level of 400 ng/mL was an independent risk factor associated with MVI. The cutoff value of the AFP level in the present study was slightly smaller than that reported in previous studies.

As indicators of impaired liver function, the AST/ALT ratio and AST level were also ranked in importance. In our study, patients with a higher AST/alkaline phosphatase (ALP) ratio and AST level were more likely to develop MVI than those with a lower AST/ALP ratio and AST level, and the cutoff value of the AST/ALT ratio was almost higher than 1 on the SHAP scatter plot. The SHAP-scattered points of serum AST levels were almost greater than 50 U/L. A previous study reported that ALT is mainly present in the cytoplasm of hepatocytes; whereas,

AST mainly exists in the mitochondria of hepatocytes, and an increase in its level indicates that hepatocytes have damaged organelles. Therefore, an increased AST/ALT ratio could generally be considered indicative of the deterioration of liver cell damage in patients with cirrhosis and HCC (45). Yang et al. (46) reported that the AST/ALT ratio is often  $>1$  due to the invasion of hepatic carcinoma cells. Dong et al. revealed that an AST level  $>40$  U/L was an independent factor for overall survival in HCC (47). Our SHAP scatter plot confirmed this. Overall, the variables selected for our prediction model were the most clinically common, readily available, and short-duration imaging and laboratory indicators, and they showed good interpretability and consistency with clinical experience, further proving the reliability of the model. This also shows the possibility that our model can be applied to countries and regions with relatively limited medical resources.

The strengths of this study are as follows. First, we used a large dataset to build an ML model for the preoperative prediction of MVI. This could contribute to improving the effective training and rational explanation of the prediction model so that the model was closer to the real situation of the prediction power. Second, we used multiple dimensional indicators to build the prediction model, thus improving its performance. All predictors have the advantages of convenient data collection, ready availability, and objectivity. Third, we used a variety of ML algorithms to select the optimal model that best fits this dataset. Finally, we transformed the model into a visual software based on the selected 15 common clinical indicators that facilitate rapid detection. Thus, the prediction model can be easily applied to countries and regions with relatively limited medical resources.

Despite these advantages, our study also has some limitations. First, this was a retrospective study, and the findings need to be validated in prospective studies. Second, our model was developed based on a single center, so its generalizability needs to be verified in multiple centers. Third, we only constructed a preoperative MVI prediction model; therefore, the clinical benefit of precise surgical choice based on the model needs to be evaluated in the future.

## 5 CONCLUSION

In conclusion, our study constructed and validated different ML algorithm models for the preoperative diagnosis of MVI by utilizing preoperative readily available, short-duration, and general noninvasive preoperative indicators. In the final model, we chose the XGBoost algorithm because it had the best performance in predicting MVI. The maximum image diameter, PIVKA-II level, AFP level, satellite nodules, AST/ALT ratio, and AST level were found to be important for predicting the occurrence of MVI. Further, development of the MVI risk-scoring web-calculator based on this model is convenient for clinical application. Meanwhile, the developed model is helpful in preoperatively predicting MVI and assists

clinicians in conveniently determining the optimal therapeutic remedy and ameliorating the prognosis of patients with HCC.

## DATA AVAILABILITY STATEMENT

The datasets presented in this study can be found in online repositories. The names of the repository/repositories and accession number(s) can be found in the article/**Supplementary Material**.

## ETHICS STATEMENT

The studies involving human participants were reviewed and approved by This study was approved by the Institutional Ethics Committee of the West China Hospital, Sichuan University [No. 2019 (203)]. The patients/participants provided their written informed consent to participate in this study.

## AUTHOR CONTRIBUTIONS

Research conception: BY, JZ, and WL. Data processing: LZ and WL. Drafting of the manuscript: WL, LZ, ZX, LY, and LB. Data

acquisition: HZ and JZ. Revision of the manuscript: BY and JZ. All authors contributed to the article and approved the submitted version.

## FUNDING

This work was supported by the National Natural Science Foundation of China (NO. 81873979), the Project of Sichuan Provincial Department of Science and Technology (NO. 2020YFS0214, 2020YJ0106).

## ACKNOWLEDGMENTS

We would like to thank all the researchers who participated in this study.

## SUPPLEMENTARY MATERIAL

The Supplementary Material for this article can be found online at: <https://www.frontiersin.org/articles/10.3389/fonc.2022.852736/full#supplementary-material>

## REFERENCES

- Sung H, Ferlay J, Siegel RL, Laversanne M, Soerjomataram I, Jemal A, et al. Global Cancer Statistics 2020: GLOBOCAN Estimates of Incidence and Mortality Worldwide for 36 Cancers in 185 Countries. *CA: A Cancer J Clin* (2021) 71(3):209–49. doi: 10.3322/caac.21660
- He W, Peng B, Tang Y, Yang J, Zheng Y, Qiu J, et al. Nomogram to Predict Survival of Patients With Recurrence of Hepatocellular Carcinoma After Surgery. *Clin Gastroenterol Hepatol* (2018) 16(5):756–64.e10. doi: 10.1016/j.cgh.2017.12.002
- Erstad DJ, Tanabe KK. Prognostic and Therapeutic Implications of Microvascular Invasion in Hepatocellular Carcinoma. *Ann Surg Oncol* (2019) 26(5):1474–93. doi: 10.1245/s10434-019-07227-9
- Lu L, Wei W, Huang C, Li S, Zhong C, Wang J, et al. A New Horizon in Risk Stratification of Hepatocellular Carcinoma by Integrating Vessels That Encapsulate Tumor Clusters and Microvascular Invasion. *Hepatol Int* (2021) 15(3):651–62. doi: 10.1007/s12072-021-10183-w
- Chen Z, Zhang X, Feng J, Li L, Zhang F, Hu Y, et al. Actual Long-Term Survival in Hepatocellular Carcinoma Patients With Microvascular Invasion: A Multicenter Study From China. *Hepatol Int* (2021) 15(3):642–50. doi: 10.1007/s12072-021-10174-x
- Jiao S, Li G, Zhang D, Xu Y, Liu J, Li G. Anatomic Versus Non-Anatomic Resection for Hepatocellular Carcinoma, Do We Have an Answer? A Meta-Analysis. *Int J Surg* (2020) 80:243–55. doi: 10.1016/j.ijsu.2020.05.008
- Yamashita Y, Tsujita E, Takeishi K, Fujiwara M, Kira S, Mori M, et al. Predictors for Microinvasion of Small Hepatocellular Carcinoma  $\leq 2$  Cm. *Ann Surg Oncol* (2012) 19(6):2027–34. doi: 10.1245/s10434-011-2195-0
- Lee S, Kang TW, Song KD, Lee MW, Rhim H, Lim HK, et al. Effect of Microvascular Invasion Risk on Early Recurrence of Hepatocellular Carcinoma After Surgery and Radiofrequency Ablation. *Ann Surg* (2021) 273(3):564–71. doi: 10.1097/sla.0000000000003268
- McHugh PP, Gilbert J, Vera S, Koch A, Ranjan D, Gedaly R. Alpha-Fetoprotein and Tumour Size Are Associated With Microvascular Invasion in Implanted Livers of Patients Undergoing Transplantation With Hepatocellular Carcinoma. *HPB (Oxford)* (2010) 12(1):56–61. doi: 10.1111/j.1477-2574.2009.00128.x
- Poté N, Cauchy F, Albuquerque M, Voitot H, Belghiti J, Castera L, et al. Performance of PIVKA-II for Early Hepatocellular Carcinoma Diagnosis and Prediction of Microvascular Invasion. *J Hepatol* (2015) 62(4):848–54. doi: 10.1016/j.jhep.2014.11.005
- Zheng J, Seier K, Gonen M, Balachandran VP, Kingham TP, D'Angelica MI, et al. Utility of Serum Inflammatory Markers for Predicting Microvascular Invasion and Survival for Patients With Hepatocellular Carcinoma. *Ann Surg Oncol* (2017) 24(12):3706–14. doi: 10.1245/s10434-017-6060-7
- Liu J, Kuang S, Zheng Y, Liu M, Wang L. Prognostic and Predictive Significance of the Tumor Microenvironment in Hepatocellular Carcinoma. *Cancer Biomarkers: Section A Dis Markers* (2021) 32(1):99–100. doi: 10.3233/cbm-203003
- Qi L, Ma L, Wu F, Chen Y, Xing W, Jiang Z, et al. S100P as a Novel Biomarker of Microvascular Invasion and Portal Vein Tumor Thrombus in Hepatocellular Carcinoma. *Hepatol Int* (2021) 15(1):114–26. doi: 10.1007/s12072-020-10130-1
- Diller G-P, Kempny A, Babu-Narayan SV, Henrichs M, Brida M, Uebing A, et al. Machine Learning Algorithms Estimating Prognosis and Guiding Therapy in Adult Congenital Heart Disease: Data From a Single Tertiary Centre Including 10 019 Patients. *Eur Heart J* (2019) 40(13):1069–77. doi: 10.1093/eurheartj/ehy915
- Moll M, Qiao D, Regan EA, Hunninghake GM, Make BJ, Tal-Singer R, et al. Machine Learning and Prediction of All-Cause Mortality in COPD. *Chest* (2020) 158(3):952–64. doi: 10.1016/j.chest.2020.02.079
- Heo J, Yoon JG, Park H, Kim YD, Nam HS, Heo JH. Machine Learning-Based Model for Prediction of Outcomes in Acute Stroke. *Stroke* (2019) 50(5):1263–5. doi: 10.1161/STROKEAHA.118.024293
- Mobadersany P, Yousefi S, Amgad M, Gutman DA, Barnholtz-Sloan JS, Velázquez Vega JE, et al. Predicting Cancer Outcomes From Histology and Genomics Using Convolutional Networks. *Proc Natl Acad Sci USA* (2018) 115(13):E2970–E9. doi: 10.1073/pnas.1717139115
- Tao K, Bian Z, Zhang Q, Guo X, Yin C, Wang Y, et al. Machine Learning-Based Genome-Wide Interrogation of Somatic Copy Number Aberrations in Circulating Tumor DNA for Early Detection of Hepatocellular Carcinoma. *EBioMedicine* (2020) 56:102811–. doi: 10.1016/j.ebiom.2020.102811
- Ji G-W, Zhu F-P, Xu Q, Wang K, Wu M-Y, Tang W-W, et al. Machine-Learning Analysis of Contrast-Enhanced CT Radiomics Predicts Recurrence



- of Hepatocellular Carcinoma After Resection: A Multi-Institutional Study. *EBioMedicine* (2019) 50:156–65. doi: 10.1016/j.ebiom.2019.10.057
20. Leung WK, Cheung KS, Li B, Law SYK, Lui TKL. Applications of Machine Learning Models in the Prediction of Gastric Cancer Risk in Patients After Helicobacter Pylori Eradication. *Alimentary Pharmacol Ther* (2021) 53(8):864–72. doi: 10.1111/apt.16272
  21. Deng G, Yao L, Zeng F, Xiao L, Wang Z. Nomogram for Preoperative Prediction of Microvascular Invasion Risk in Hepatocellular Carcinoma. *Cancer Manage Res* (2019) 11:9037–45. doi: 10.2147/CMAR.S216178
  22. Lei Z, Li J, Wu D, Xia Y, Wang Q, Si A, et al. Nomogram for Preoperative Estimation of Microvascular Invasion Risk in Hepatitis B Virus-Related Hepatocellular Carcinoma Within the Milan Criteria. *JAMA Surg* (2016) 151(4):356–63. doi: 10.1001/jamasurg.2015.4257
  23. Chen G, Wang R, Zhang C, Gui L, Xue Y, Ren X, et al. Integration of Pre-Surgical Blood Test Results Predict Microvascular Invasion Risk in Hepatocellular Carcinoma. *Comput Struct Biotechnol J* (2021) 19:826–34. doi: 10.1016/j.csbj.2021.01.014
  24. Xu X, Zhang HL, Liu QP, Sun SW, Zhang J, Zhu FP, et al. Radiomic Analysis of Contrast-Enhanced CT Predicts Microvascular Invasion and Outcome in Hepatocellular Carcinoma. *J Hepatol* (2019) 70(6):1133–44. doi: 10.1016/j.jhep.2019.02.023
  25. Feng S, Jia Y, Liao B, Huang B, Zhou Q, Li X, et al. Preoperative Prediction of Microvascular Invasion in Hepatocellular Cancer: A Radiomics Model Using Gd-EOB-DTPA-Enhanced MRI. *Eur Radiol* (2019) 29(9):4648–59. doi: 10.1007/s00330-018-5935-8
  26. Wu C, Zhou M, Liu P, Yang M. Analyzing COVID-19 Using Multisource Data: An Integrated Approach of Visualization, Spatial Regression, and Machine Learning. *GeoHealth* (2021) 5(8):e2021GH000439. doi: 10.1029/2021gh000439
  27. Zhou J, Sun HC, Wang Z, Cong WM, Wang JH, Zeng MS, et al. Guidelines for Diagnosis and Treatment of Primary Liver Cancer in China (2017 Edition). *Liver Cancer* (2018) 7(3):235–60. doi: 10.1159/000488035
  28. Sheng X, Ji Y, Ren G-P, Lu C-L, Yun J-P, Chen L-H, et al. A Standardized Pathological Proposal for Evaluating Microvascular Invasion of Hepatocellular Carcinoma: A Multicenter Study by LCPGC. *Hepatol Int* (2020) 14(6):1034–47. doi: 10.1007/s12072-020-10111-4
  29. *Imbalanced-Learn: A Python Toolbox to Tackle the Curse of Imbalanced Datasets in Machine Learning*. Available at: <https://jmlr.org/papers/v18/16-365>.
  30. Richardson AM, Joshy G, D'Este CA. Understanding Statistical Principles in Linear and Logistic Regression. *Med J Aust* (2018) 208(8):332–4. doi: 10.5694/mja17.00222
  31. Janßen R, Zabel J, von Lukas U, Labrenz M. An Artificial Neural Network and Random Forest Identify Glyphosate-Impacted Brackish Communities Based on 16S Rrna Amplicon Miseq Read Counts. *Marine Pollution Bull* (2019) 149:110530. doi: 10.1016/j.marpolbul.2019.110530
  32. Almansour NA, Syed HF, Khayat NR, Altheeb RK, Juri RE, Alhiyafi J, et al. Neural Network and Support Vector Machine for the Prediction of Chronic Kidney Disease: A Comparative Study. *Comput Biol Med* (2019) 109:101–11. doi: 10.1016/j.combiomed.2019.04.017
  33. Su F, Yuan P, Wang Y, Zhang C. The Superior Fault Tolerance of Artificial Neural Network Training With a Fault/Noise Injection-Based Genetic Algorithm. *Protein Cell* (2016) 7(10):735–48. doi: 10.1007/s13238-016-0302-5
  34. Bi Y, Xiang D, Ge Z, Li F, Jia C, Song J. An Interpretable Prediction Model for Identifying N(7)-Methylguanosine Sites Based on Xgboost and SHAP. *Mol Ther Nucleic Acids* (2020) 22:362–72. doi: 10.1016/j.omtn.2020.08.022
  35. Hathaway QA, Roth SM, Pinti MV, Sprando DC, Kunovac A, Durr AJ, et al. Machine-Learning to Stratify Diabetic Patients Using Novel Cardiac Biomarkers and Integrative Genomics. *Cardiovasc Diabetol* (2019) 18(1):78–. doi: 10.1186/s12933-019-0879-0
  36. Chen Y, Xia Y, Tolat PP, Long L, Jiang Z, Huang Z, et al. Comparison of Conventional Gadoxetate Disodium-Enhanced MRI Features and Radiomics Signatures With Machine Learning for Diagnosing Microvascular Invasion. *AJR Am J Roentgenol* (2021) 216(6):1510–20. doi: 10.2214/ajr.20.23255
  37. Dong Y, Zhou L, Xia W, Zhao X, Zhang Q, Jian J, et al. Preoperative Prediction of Microvascular Invasion in Hepatocellular Carcinoma: Initial Application of a Radiomic Algorithm Based on Grayscale Ultrasound Images. *Front Oncol* (2020) 10:353. doi: 10.3389/fonc.2020.00353
  38. Chen Y, Xia Y, Tolat PP, Long L, Jiang Z, Huang Z, et al. Comparison of Conventional Gadoxetate Disodium-Enhanced MRI Features and Radiomics Signatures With Machine Learning for Diagnosing Microvascular Invasion. *Am J Roentgenology* (2021) 216(6):1510–20. doi: 10.2214/AJR.20.23255
  39. Roayaie S, Blume IN, Thung SN, Guido M, Fiel MI, Hiotis S, et al. A System of Classifying Microvascular Invasion to Predict Outcome After Resection in Patients With Hepatocellular Carcinoma. *Gastroenterology* (2009) 137(3):850–5. doi: 10.1053/j.gastro.2009.06.003
  40. Zhang K, Tao C, Siqin T, Wu J, Rong W. Establishment, Validation and Evaluation of Predictive Model for Early Relapse After R0 Resection in Hepatocellular Carcinoma Patients With Microvascular Invasion. *J Transl Med* (2021) 19(1):293. doi: 10.1186/s12967-021-02940-0
  41. Hwang S, Song GW, Lee YJ, Kim KH, Ahn CS, Moon DB, et al. Multiplication of Tumor Volume by Two Tumor Markers Is a Post-Resection Prognostic Predictor for Solitary Hepatocellular Carcinoma. *J Gastrointest Surg* (2016) 20(11):1807–20. doi: 10.1007/s11605-016-3187-y
  42. Qi F, Zhou A, Yan L, Yuan X, Wang D, Chang R, et al. The Diagnostic Value of PIVKA-II, AFP, AFP-L3, CEA, and Their Combinations in Primary and Metastatic Hepatocellular Carcinoma. *J Clin Lab Anal* (2020) 34(5):e23158. doi: 10.1002/jcla.23158
  43. Hirokawa F, Hayashi M, Miyamoto Y, Asakuma M, Shimizu T, Komeda K, et al. Outcomes and Predictors of Microvascular Invasion of Solitary Hepatocellular Carcinoma. *Hepatol Res* (2014) 44(8):846–53. doi: 10.1111/hepr.12196
  44. You Z, Chen LP, Ye H. Predictors of Microvascular Invasion in Patients With Solitary Small Hepatitis B Related Hepatocellular Carcinoma. *Pak J Med Sci* (2014) 30(2):331–4. doi: 10.12669/pjms.302.4652
  45. Åberg F, Danford CJ, Thiele M, Talbäck M, Rasmussen DN, Jiang ZG, et al. A Dynamic Aspartate-to-Alanine Aminotransferase Ratio Provides Valid Predictions of Incident Severe Liver Disease. *Hepatol Commun* (2021) 5(6):1021–35. doi: 10.1002/hep4.1700
  46. Yang J, He X, Huang B, Zhang H, He Y. Rule of Changes in Serum GGT Levels and GGT/ALT and AST/ALT Ratios in Primary Hepatic Carcinoma Patients With Different AFP Levels. *Cancer biomarkers: section A Dis Markers* (2018) 21(4):743–6. doi: 10.3233/cbm-170088
  47. Dong W, Yan K, Yu H, Huo L, Xian Z, Zhao Y, et al. Prognostic Nomogram for Sorafenib Benefit in Hepatitis B Virus-Related Hepatocellular Carcinoma After Partial Hepatectomy. *Front Oncol* (2020) 10:605057. doi: 10.3389/fonc.2020.605057

**Conflict of Interest:** The authors declare that the research was conducted in the absence of any commercial or financial relationships that could be construed as a potential conflict of interest.

**Publisher's Note:** All claims expressed in this article are solely those of the authors and do not necessarily represent those of their affiliated organizations, or those of the publisher, the editors and the reviewers. Any product that may be evaluated in this article, or claim that may be made by its manufacturer, is not guaranteed or endorsed by the publisher.

Copyright © 2022 Liu, Zhang, Xin, Zhang, You, Bai, Zhou and Ying. This is an open-access article distributed under the terms of the Creative Commons Attribution License (CC BY). The use, distribution or reproduction in other forums is permitted, provided the original author(s) and the copyright owner(s) are credited and that the original publication in this journal is cited, in accordance with accepted academic practice. No use, distribution or reproduction is permitted which does not comply with these terms.

## GLOSSARY

AFP	$\alpha$ -fetoprotein
AI	artificial intelligence
ALB	albumin
ALP	alkaline phosphatase
ALP/GGT (A/G)	alkaline phosphatase/ $\gamma$ -glutamyl transferase
ALT	alanine aminotransferase
APTT	activated partial thromboplastin time
AST	aspartate aminotransferase
AST/ALT (A/A)	aspartate aminotransferase/alanine aminotransferase
AUC	the area under the receiver operating characteristic curve
BASO%	basophil percentage
BMI	body mass index
CA-125	carbohydrate antigen 125
CA19-9	carbohydrate antigen
CEA	carcinoembryonic antigen
CHOL	cholesterol
CK	creatinine kinase
CREA	creatinine
Cys-C	cystatin C
DBIL	Direct bilirubin
eGFR	estimated glomerular filtration rate
EHR	electronic health record
EO%	Percentage of eosinophils
FIB	fibrinogen
FN	False Negative
FP	False Positive
GGT	$\gamma$ -glutamyl transferase
GGTP	gamma glutamyl transpeptidase
GLB	globulin
GLU	glucose
Hb	hemoglobin
HBcAb	hepatitis B core antibody
HBDH	hydroxybutyrate dehydrogenase
HBeAb	hepatitis B e antibody
HBeAg	hepatitis B e antigen
HBsAb	hepatitis B s antibody
HBsAg	hepatitis B s antigen
HBV	hepatitis B virus
HBV DNA	hepatitis B virus DNA

(Continued)

Continued

HCV	hepatitis C virus
HCC	hepatocellular carcinoma
Hct	hematocrit
HDL-C	high-density lipoprotein cholesterol
IBIL	indirect bilirubin
IG%	Percentage of naive granulocytes
IG	absolute value of immature granulocytes
LDH	lactate dehydrogenase
LDL-C	low-density lipoprotein cholesterol
LYMPH%	percentage of lymphocytes
MCH	mean corpuscular hemoglobin
MCHC	mean corpuscular hemoglobin concentration
MCV	mean red blood cell volume
MONO%	monocyte percentage
ML	machine learning
MLP	Multi-Layer Perception
MVI	microvascular invasion
NEUT%	neutral lobulated granulocyte percentage
NLR	the neutrophilic lymphocyte ratio
PIVKA-II	protein induced by vitamin K absence or antagonist-II
PLT	platelets
PRC	precision recall curve
PT	prothrombin time
RBC	red blood cells
RDW-CV	RBC distribution width-coefficient of variation
RDW-SD	RBC distribution width-standard deviation
RF	random forest
RFA	radiofrequency ablation
RFS	relapse free survival
SHAP	Shapley Addictive explanation
SVM	support vector machine
TACE	transcatheter arterial chemoembolization
TBA	total bile acid
TBIL	total bilirubin
TN	Ture Negative
TP	True Positive
TT	thrombin time
UREA	uric acid
WBCs	white blood cells
XGBoost	extreme gradient boosting



# Diagnostic Value, Prognostic Value, and Immune Infiltration of LOX Family Members in Liver Cancer: Bioinformatic Analysis

Chenyu Sun<sup>1†</sup>, Shaodi Ma<sup>2†</sup>, Yue Chen<sup>3†</sup>, Na Hyun Kim<sup>1</sup>, Sujatha Kailas<sup>4</sup>, Yichen Wang<sup>5</sup>, Wenchao Gu<sup>6</sup>, Yisheng Chen<sup>7</sup>, John Pocholo W. Tuason<sup>1</sup>, Chandur Bhan<sup>1</sup>, Nikitha Manem<sup>1</sup>, Yuting Huang<sup>8</sup>, Ce Cheng<sup>9,10</sup>, Zhen Zhou<sup>11</sup>, Qin Zhou<sup>12</sup> and Yanzhe Zhu<sup>13\*</sup>

<sup>1</sup> AMITA Health Saint Joseph Hospital Chicago, Chicago, IL, United States, <sup>2</sup> Department of Epidemiology and Health Statistics, School of Public Health, Anhui Medical University, Hefei, China, <sup>3</sup> Department of Clinical Medicine, School of the First Clinical Medicine, Anhui Medical University, Hefei, China, <sup>4</sup> Gastroenterology, AMITA Health Saint Joseph Hospital Chicago, Chicago, IL, United States, <sup>5</sup> Mercy Internal Medicine Service, Trinity Health of New England, Springfield, MA, United States, <sup>6</sup> Department of Diagnostic Radiology and Nuclear Medicine, Gunma University Graduate School of Medicine, Maebashi, Japan, <sup>7</sup> Department of Orthopedics, Shanghai General Hospital, Shanghai Jiao Tong University School of Medicine, Shanghai Jiao Tong University, Shanghai, China, <sup>8</sup> University of Maryland Medical Center Midtown Campus, Baltimore, MD, United States, <sup>9</sup> College of Medicine, The University of Arizona, Tucson, AZ, United States, <sup>10</sup> Banner-University Medical Center South, Tucson, AZ, United States, <sup>11</sup> Menzies Institute for Medical Research, University of Tasmania, Hobart, TAS, Australia, <sup>12</sup> Department of Radiation Oncology, Mayo Clinic, Rochester, MN, United States, <sup>13</sup> Department of Oncology, The First Affiliated Hospital of Anhui Medical University, Hefei, China

## OPEN ACCESS

### Edited by:

Alessandro Passardi,  
Scientific Institute of Romagna for the  
Study and Treatment of Tumors  
(IRCCS), Italy

### Reviewed by:

Shih-Min Hsia,  
Taipei Medical University, Taiwan  
Carolina Añazco,  
Universidad San Sebastián, Chile

### \*Correspondence:

Yanzhe Zhu  
drzhuyanzhe@126.com

<sup>†</sup>These authors have contributed  
equally to this work

### Specialty section:

This article was submitted to  
Gastrointestinal Cancers: Hepato  
Pancreatic Biliary Cancers,  
a section of the journal  
Frontiers in Oncology

Received: 27 December 2021

Accepted: 08 February 2022

Published: 04 March 2022

### Citation:

Sun C, Ma S, Chen Y, Kim NH,  
Kailas S, Wang Y, Gu W, Chen Y,  
Tuason JPW, Bhan C, Manem N,  
Huang Y, Cheng C, Zhou Z, Zhou Q  
and Zhu Y (2022) Diagnostic Value,  
Prognostic Value, and Immune  
Infiltration of LOX Family Members in  
Liver Cancer: Bioinformatic Analysis.  
Front. Oncol. 12:843880.  
doi: 10.3389/fonc.2022.843880

**Background:** Liver cancer (LC) is well known for its prevalence as well as its poor prognosis. The aberrant expression of lysyl oxidase (LOX) family is associated with liver cancer, but their function and prognostic value in LC remain largely unclear. This study aimed to explore the function and prognostic value of LOX family in LC through bioinformatics analysis and meta-analysis.

**Results:** The expression levels of all LOX family members were significantly increased in LC. Area under the receiver operating characteristic curve (AUC) of LOXL2 was 0.946 with positive predictive value (PPV) of 0.994. LOX and LOXL3 were correlated with worse prognosis. Meta-analysis also validated effect of LOX on prognosis. Nomogram of these two genes and other predictors was also plotted. There was insufficient data from original studies to conduct meta-analysis on LOXL3. The functions of LOX family members in LC were mostly involved in extracellular and functions and structures. The expressions of LOX family members strongly correlated with various immune infiltrating cells and immunomodulators in LC.

**Conclusions:** For LC patients, LOXL2 may be a potential diagnostic biomarker, while LOX and LOXL3 have potential prognostic and therapeutic values. Positive correlation between LOX family and infiltration of various immune cells and immunomodulators suggests the need for exploration of their roles in the tumor microenvironment and for potential immunotherapeutic to target LOX family proteins.

**Keywords:** liver cancer, lysyl oxidase, bioinformatic analysis, receiver operating curve, nomogram, prognostic value, immune infiltration

## BACKGROUND

Liver cancer (LC) is the sixth most common malignant tumor and the third leading cause of cancer-associated mortality worldwide. Hepatocellular carcinoma (HCC) accounts for 75%–85% of all LC, according to the GLOBOCAN 2020 estimation (1). In east Asia, especially China, a high incidence of HCC was noted, and similarly, the incidence and mortality of LC in developing countries are significantly higher than those in developed countries (2, 3). The variations in the prevalence of LC amongst different populations and regions are attributed to a variety of environmental and genetic factors, such as aflatoxin, alcohol, smoking, chronic hepatitis virus infection, and type 2 diabetes (4–6). Despite significant advances in diagnosis and treatment of LC, including surgical resection, local ablation, liver transplantation, and sorafenib–regorafenib sequential therapy, the prognosis of LC remains poor (6). Based on most recent data, 841,000 new cases and 782,000 deaths of LC around the globe was estimated to occur each year (1). Therefore, it is of great value to explore novel diagnostic and prognostic biomarkers that are sensitive and specific, and to identify potential targets for medications (7).

With the advent of next-generation sequencing (NGS) and other techniques, increasing amount of information has become available for a variety of cancer types and other diseases (8–11). Thus, the mechanisms of cancers, as well as other diseases, have become more widely investigated based on bioinformatic methods, by combining information technology and molecular biology. Bioinformatics methods, such as data-mining, are also widely applied for identification of potential biomarkers as therapeutic targets, as well as diagnostic and prognostic predictors, and to explore the pathogenesis of malignancies at the molecular level (12–14).

As an extracellular enzyme, lysyl oxidase (LOX) oxidatively deaminates specific lysine and hydroxylysine residues to form allysines in the telopeptide domains of the collagen molecule, and thus plays a critical role in covalent cross-link formation in collagen fibrils (15). LOX is highly expressed in tissues containing elastic fibers and fibrillar collagen, such as skin, lung, and the fibrous lamina propria in the small intestine, stomach, and liver (16). In addition to LOX, four LOX-like proteins (LOXL-1, -2, -3, and -4) have also been identified in the LOX family (17–19). Studies have found that the LOX family was involved in carcinogenesis and tumor metastasis, through angiogenesis promotion, formation of mature extracellular matrix at the secondary site, focal adhesion kinase (FAK) activation, and other mechanisms (19–22).

The lysyl oxidase (LOX) family consists of five members: LOX, the first described member of this family, and its four related members called lysyl oxidase-like genes (LOXL1–4). Recent evidence suggests that the LOX family play important

roles in liver cancer. LOX secreted by HCC promotes tube formation of endothelial cells through upregulation of VEGF, and overexpressed LOX increases angiogenesis, whereas LOXL1 was found to be increased in liver fibrosis models (23–25). As for LOXL2, its expression level was found to be higher in HCC tissues compared with non-tumor tissue (26). Although LOXL3 has been studied in different types of cancer, studies on its roles in liver cancer are limited (25). LOXL4 was found to increase the risk of invasion and metastasis, promote angiogenesis, and play a role in the immunosuppressive microenvironment in HCC (25, 27, 28).

Although previous studies have investigated the roles of the LOX family in LC, their exact roles and mechanisms, especially for LOXL1 and LOXL3, have yet to be further investigated (25). Previous studies have shown evidence of the potential prognostic values and therapeutic values of LOX family members (25, 26). Thus, online databases were mined to analyze the expression, mutation, function, and immune infiltration of LOX family members in LC, with the goal to determine their potential oncogenic role, as well as their diagnostic and prognostic value in LC.

## RESULTS

### Differential Expression Levels of LOX Family in LC

All five members of LOX family demonstrated higher expression in liver cancer tumor tissues than normal tissues (**Figure 1A** and **Table 1**). These findings were consistent with results from UALCAN, which confirmed that the expression of all LOX family members was statistically significantly higher in tumor tissue (**Figure 1B**), and from TIMER, which showed higher expression of LOX ( $P=1.5E-11$ ), LOXL1 ( $P=2.39E-04$ ), LOXL2 ( $P=4.02E-25$ ), LOXL3 ( $P=1.53E-04$ ), and LOXL4 ( $P=7.15E-05$ ). Further analysis of ROC curve showed that AUC of LOXL2 was 0.946 (95%CI:0.915–0.978, with positive predictive value (PPV) of 0.994 and a cutoff value of 1.050 (**Figure 2**).

### Prognostic Value of LOX Family in LC

Evaluation of the value of differential expression of LOX family members in LC prognosis found that LOX, LOXL3, and LOXL4 were associated with poor overall survival (OS) (**Figure 3A** and **Table 1**). UALCAN was utilized for verification which found that only LOX ( $P=0.023$ ) and LOXL3 ( $P=0.031$ ) were associated with poor OS (**Figure 3B**). Further verification via TIMER also only identified poor prognosis of LOX ( $P=0.003$ ) and LOXL3 ( $P=0.023$ ) (**Table 1**). The combined results indicated that high expression of LOX and LOXL3 was associated with worse OS.

A nomogram model incorporating the overexpressed LOX family members that were associated with poor prognosis, namely LOX and LOXL3 and other predictors (pathologic stage, histologic grade, AFP (ng/ml), Child-Pugh grade, albumin (g/dl), adjacent hepatic tissue inflammation, vascular invasion, Ishak Fibrosis score, prothrombin time, age, gender,

**Abbreviations:** LC, Liver cancer; HCC, Hepatocellular carcinoma; LOX, lysyl oxidase; LOXL, lysyl oxidase-like; FAK, focal adhesion kinase; BAPN,  $\beta$ -aminopropionitrile; ECM, extracellular matrix; SRCR, scavenger receptor cysteine-rich; TME, tumor microenvironment; ECM, extracellular matrix; MMP, matrix metalloproteinase.



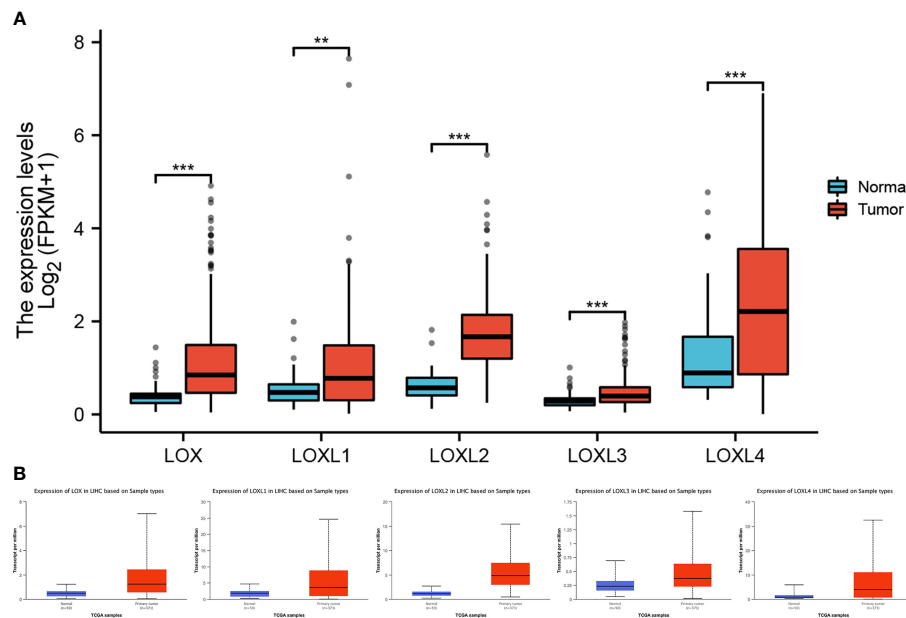


**FIGURE 1** | Expression level of *LOX* family members between normal tissue and tumor tissue in liver cancer. **(A)** analysis via R software, **(B)** analysis via ULCAN. \*\* means  $P < 0.01$ , \*\*\* means  $P < 0.001$ .

weight) is shown in **Figure 4**. The C-index of the nomogram was 0.738 (95% CI, 0.697–0.778).

## Analysis of Genetic Mutations of *LOX* Family in LC

Next, the genetic alterations of the *LOX* family in LC patients were evaluated with the cBioPortal online tool. Among 1,066 LC patients, 55 samples had genetic alteration of *LOX* family members, with a mutation rate of 5.16%. The mutation rate of *LOXL2* was the highest (4%) (**Figures 5A, B**). Using cBioPortal and TIMER online tools, we found significant ( $p < 0.01$ ) and positive correlations amongst *LOX* family member proteins: *LOX* with *LOXL1*, *LOXL2*, *LOXL3*, and *LOXL4*; *LOXL1* with *LOX*, *LOXL2*, *LOXL3*, and *LOXL4*; *LOXL2* with *LOX*, *LOXL1*, *LOXL3*, and *LOXL4*; *LOXL3* with *LOX*, *LOXL1*, *LOXL2*, and *LOXL4*; *LOXL4* with *LOX*, *LOXL1*, *LOXL2*, and *LOXL3* (**Figures 5C, D**).

## Exploration of Potential Drugs That Are Interacted With *LOX* Family Members in LC

As *LOX* and *LOXL3* were both found to be overexpressed in LC and associated with worse OS, further exploration of potential interacting drugs was conducted by using Coremine Medical, which identified 30 drugs that were associated with both *LOX* and *LOXL3* in liver neoplasms (**Figure 6**). The top three drugs were Aminopropionitrile, quinone, and copper.

## Analysis of Interaction of *LOX* Family Members in Patients With LC

Using the STRING database, PPI network analysis was performed on the differentially expressed *LOX* family members and 10 proteins (*BMP1*, *ELN*, *EFEMP2*, *FBLN5*, *FN1*, *MFAP2*, *MFAP5*, *PCOLCE*, *TLL1*, *TLL2*) that significantly interacted with *LOX* family members to further explore their potential interactions (**Figure 7A**). The results from GeneMANIA also

**TABLE 1** | Expression level of *LOX* family members between normal tissue and tumor tissue in liver cancer, and overall survival of overexpressing *LOX* family members in liver cancer.

Gene name	Mean			TCGA			TIMER		
	Normal tissue group	Tumor tissue group	P value	HR	95%CI	P value	HR	95%CI	P value
<i>LOX</i>	0.418 ± 0.268	1.112 ± 0.898	< 0.001	1.53	1.08–2.16	0.017	1.223	1.073–1.416	0.003
<i>LOXL1</i>	0.540 ± 0.381	1.018 ± 0.944	= 0.001	0.93	0.66–1.32	0.693	0.999	0.897–1.113	0.986
<i>LOXL2</i>	0.623 ± 0.311	1.725 ± 0.735	< 0.001	1.19	0.84–1.68	0.333	1.188	0.984–1.434	0.073
<i>LOXL3</i>	0.312 ± 0.178	0.463 ± 0.300	< 0.001	1.65	1.16–2.35	0.005	1.524	1.059–2.194	0.023
<i>LOXL4</i>	1.307 ± 1.092	2.300 ± 1.625	< 0.001	1.44	1.02–2.05	0.038	1.080	0.980–1.191	0.119

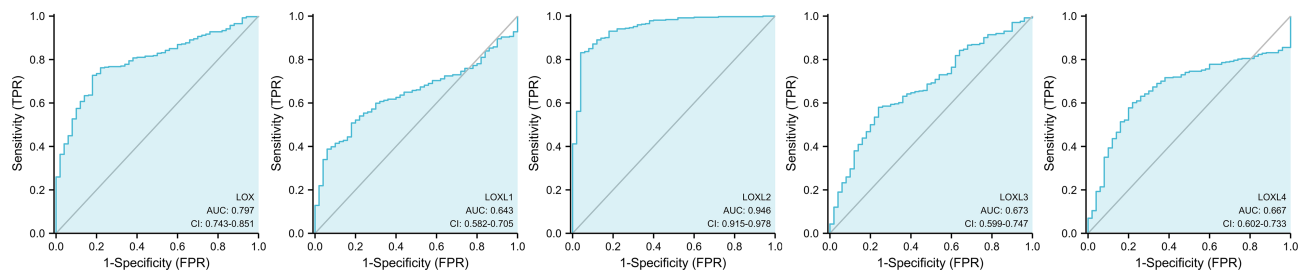


**FIGURE 2** | ROC curve analysis for *LOX* family members in liver cancer.

revealed the function of differentially expressed *LOX* family members. Their top 20 associated interactors were primarily related to extracellular matrix organization, extracellular structure organization, extracellular matrix, proteinaceous extracellular matrix, extracellular matrix part, extracellular matrix disassembly, and extracellular matrix structural constituent (Figure 7B).

### GO Enrichment and KEGG Pathway Analysis of *LOX* Family Members in LC

GO enrichment and KEGG pathway analysis of *LOX* family members and their 20 interactors were conducted by using DAVID. Receptor-mediated endocytosis, extracellular matrix organization, and extracellular matrix disassembly were the top three biological processes that were associated with *LOX* family members and their interactors (Figure 8A). The extracellular region, proteinaceous extracellular matrix, and extracellular matrix were the top three major cellular components of the target genes (Figure 8B). As for molecular function, scavenger receptor activity, oxidoreductase activity (acting on the CH-NH2 group of donors, oxygen as acceptor), and copper ion binding

were the top three functions (Figure 8C). In regard to KEGG pathways, protein digestion and absorption, PI3K-Akt signaling pathway, and ECM-receptor interaction were the top three pathways involved in LC (Figure 8D).

### Immune Cell Infiltration of *LOX* Family Members in LC

The TIMER database was utilized to investigate the association between *LOX* family members and immune cell infiltration, as immune cell level correlates with the proliferation and progression of cancer cells (Figure 9). The expression of each *LOX* family member was positively correlated with the infiltration of B cell, CD8+ T cells, CD4+ T cells, macrophages, neutrophils, and dendritic cells (DCs). Among them, Macrophage and CD4+ T Cells demonstrated the strongest positive correlation. In addition, the Cox proportional hazard model showed that B cells ( $p=0.031$ ), CD8+ T cells ( $p=0.036$ ), macrophages ( $p=0.027$ ), and DCs ( $p=0.004$ ) were significantly associated with adverse clinical outcomes in LC patients (Table 2). The association between immunomodulators and *LOX* family members with poor prognosis, namely,

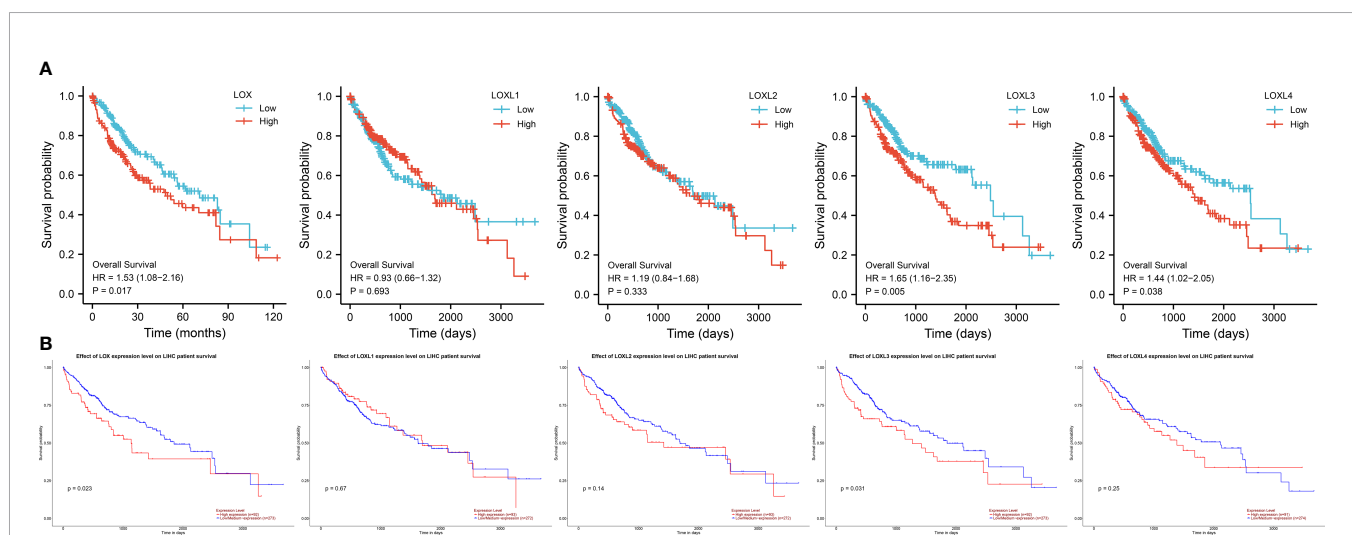


**FIGURE 3** | Survival analysis of *LOX* family members in liver cancer. (A) analysis via R software, (B) analysis via ULCAN.

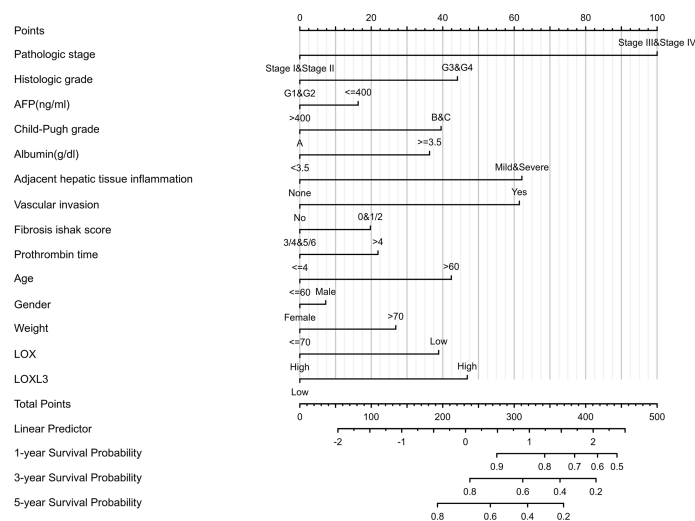


**FIGURE 4 |** Nomogram for liver cancer based on overexpressed *LOX* and *LOXL3*. The nomogram was developed in the cohort, with pathologic stage, histologic grade, AFP (ng/ml), Child-Pugh grade, albumin (g/dl), adjacent hepatic tissue inflammation, vascular invasion, Ishak Fibrosis score, prothrombin time, age, gender, weight. (C-index: 0.738, 95% CI, 0.697-0.778).

*LOX* and *LOXL3*, were then further explored. The top three immunoinhibitors associated with *LOXL3* were CSF1R, HAVCR2, and LGALS9, whilst the top three immunostimulators correlated with *LOXL3* were CD86, TNSF13B, and CXCR4. MHCs associated with *LOXL3* were HLA-DOA, HLA-DPA1, and HLA-DPB1. As for *LOX*, TGFB1, TGFBR1, and VTCN1 were the most positively correlated immunoinhibitors. TNFRSF9, CXCR4, and TNFSF15 were the three most positively associated immunostimulators. However, for MHC molecules, their associations were relatively low, with HLA-DQA2, HLA-DOA, and HLA-DPA1 as the top three molecules (Figure 10).

## Co-Expression Network and GSEA Analysis of Each Member of *LOX* Family in LC

For each member of *LOX* family, more genes (dark red dots) are positively correlated than negatively correlated (dark green dots) (Figure 11 and Table 2). GO term annotation of co-expressed genes of each member of *LOX* family as well as KEGG pathway analysis were shown in Figure 12. These results showed a wide range of influence of *LOX* family expression network in LC.

## Meta-Analysis of the Prognosis of *LOX*, *LOXL2* and *LOXL4* in LC

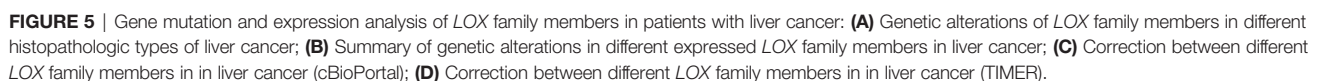
Based on the search strategy, four studies (28–31) investigating *LOX*, *LOXL2* and *LOXL4* were included for the meta-analysis, while no potential literature on other *LOX* family members were found. We combined the results of our bioinformatics analysis from the TCGA with those retrieved in the database and obtained the HR values. One study (29) provided results regarding lower expressed *LOXL2* compared with higher expressed *LOXL2*, therefore, the HR was transformed using the

formula new  $HR = e^{(-\ln HR)}$  to convert the result to the OS of higher expressed *LOXL2* compared to lower expressed *LOXL2*. This resulted in the new HR of 1.761 (95% CI: 1.215-2.551).

The pooled results revealed that overexpression of *LOX* and *LOXL4* were associated with worse OS of LC patients (HR: 1.59, 95% CI: 1.19-2.12,  $I^2 = 0\%$ ; HR: 1.58, 95% CI: 1.28-1.96,  $I^2 = 0\%$ ), while the association between overexpression of *LOXL2* and OS of LC patients showed no statistical significance (HR: 1.33, 95% CI: 0.99-1.79,  $I^2 = 29.5\%$ ) (Figure 13). Sensitivity analysis indicated stable results of this meta-analysis.

## DISCUSSION

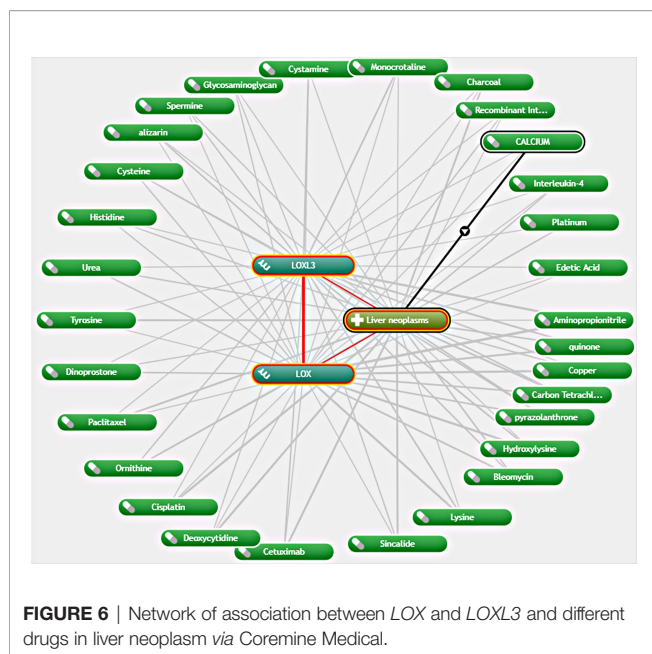
As a common malignancy with the third leading cause of cancer-related mortality (1), LC risk is influenced by various environmental and genetic factors (4–6). Previous studies have demonstrated that *LOX* is highly expressed in the fibrous lamina propria in the small intestine, stomach, and liver, as well as other tissues that contain elastic fibers and fibrillar collagen (16). *LOX*, *LOXL*, *LOXL2*, *LOXL3* and *LOXL4* were to be in intracellular locations, perinuclear regions and intranuclear locations, and are secreted to exert their functions, such as extracellular enzyme for initiating covalent cross-link formation in collagen fibrils (15, 19, 32–35). After secretion, *LOX* family members oxidase crosslink collagen and elastin (19, 36). *LOXs* were found to be involved in various physiological or pathological pathways, both in extracellular modulation and intracellular signaling (32). Studies have found *LOX* family members to be involved in carcinogenesis and tumor metastasis by formation of mature extracellular matrix at the secondary site, FAK activation, and promotion of angiogenesis (19–22). Overexpressed *LOX* was



mutation, prognostic value, and functional enrichment of *LOX* family in LC.

We found that all five members of *LOX* family are higher expressed in LC tissues than in the normal tissues and their overexpression are positively correlated with each other, which is consistent with previous findings that the expression of *LOX*, *LOXL2*, and *LOXL4* are upregulated in HCC (25). A previous study found a 30-fold increase of *LOXL1* level in a liver fibrosis model (24). However, the role of *LOXL3* in LC was not yet clear

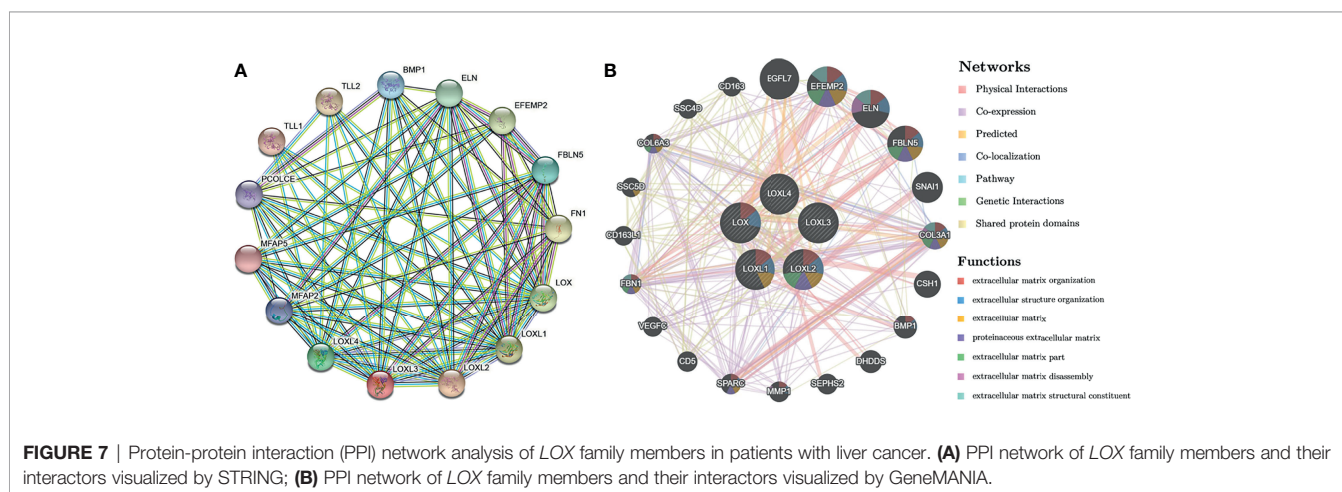




(25), and our results provided evidence that not only *LOX1* but also *LOXL3* is highly expressed in LC. As shown by the cBioPortal analysis, 5.16% of LC patients were found to have genetic mutation of *LOX* family members, and the mutation rate of *LOXL2* was the highest. Further analysis of ROC curve showed that the AUC of *LOXL2* was above 0.9 with a PPV of 0.994, indicating its potential role in diagnosis. These findings are consistent with those reported by Wong et al, in which the AUC of *LOXL2* to distinguish non-HCC and HCC patients was 0.896 (26). Therefore, *LOXL2* is a good candidate for a diagnostic marker in LC, especially HCC.

Based on the analyses through various tools, high expression of *LOX* and *LOXL3* was found to predict worse prognosis. This proves the previous hypothesis of upregulation of the *LOX* level as a predictive sign for HCC, proposed by Lin et al. (25). *LOX* gene, located at chromosome 5q23.1, is consist of a variable N-

terminal domain and a highly conserved C-terminal domain (25). *LOX* itself is an extracellular, matrix-embedded protein that plays an essential role in the cross-linking of the collagen fibrils and the deposition of insoluble collagen fibers (37, 38). Previous studies indicated that *LOX* overexpression induced the Epithelial-Mesenchymal Transition (EMT) (39). In addition, Yang et al. proved that the overexpression of *LOX* activated the angiogenesis partially through increasing the VEGF and enhancing the tube formation ability of endothelial cells in tumor initiating cells (TICs)-enriched HCC, and *LOX* inhibitor  $\beta$ -aminopropionitrile (BAPN) reverses the angiogenesis (40). Zhu et al. also found that the proliferative, migratory, and invasive abilities of HCC cells were attenuated, and the expression of vascular endothelial growth factor (VEGF) was decreased by the silencing of *LOX*, through the p38 mitogen-activated protein kinase (MAPK) signaling pathway (30). *LOX3*, located at chromosome 2p13.1, plays an important role in remodeling the cross-linking of the structural extracellular matrix (ECM) of fibrotic organs such as the liver (25, 41). It was also shown that higher expression of *LOXL3* was regulated by TGF- $\beta$  in gastric cancer (42). However, studies on the biological function of *LOXL3* in HCC are still limited (25, 39, 43). Previous literature on the prognostic role of *LOXL3* in LC patients was also minimal. Therefore, meta-analysis on *LOXL3* was not conducted. Nevertheless, the result of this analysis added new evidence that *LOXL3* could be potentially used a prognostic biomarker in addition to *LOX*. A nomogram based on *LOX*, *LOXL3*, and other predictors were developed which can help predict the mortality risk for an individual LC patient. Moreover, given their negative impacts on the survival in LC patients, *LOX* and *LOXL3* may also serve as potential therapeutic targets. Although the ULCAN and TIMER did not verify the worse prognosis associated with *LOXL4*, our result based on TCGA data indicated the potential clinical significance of *LOXL4* for worse outcome. As part of the *LOX* family, *LOXL4* gene is located at chromosome 10q24.2 (25). The *in vitro* study suggested that TGF- $\beta$  might induce *LOXL4* upregulation in several different HCC cell lines, and *LOXL4* mediated cell-matrix adhesion and cell migration in HCC *via* upregulation of



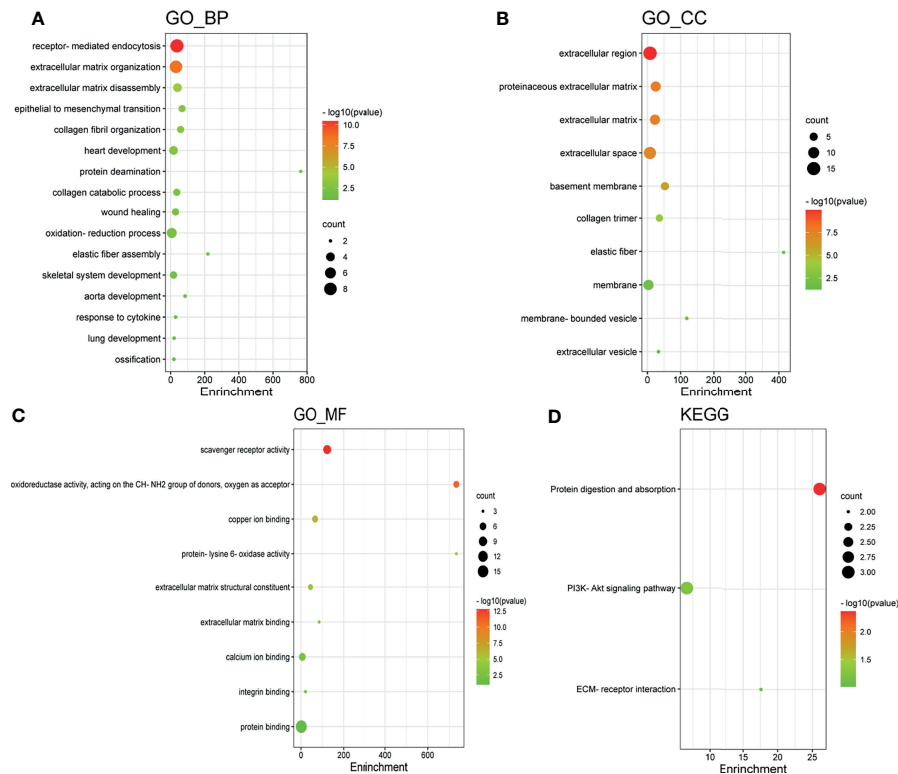


**FIGURE 8 |** Gene Ontology (GO) enrichment and Kyoto Encyclopedia of Genes and Genomes (KEGG) pathway analysis of *LOX* family members and their interactors. GO enrichment analysis of target genes based on (A) biological process, (B) cellular component, and (C) molecular function. (D) KEGG pathway enrichment analysis of target genes.

Src and FAK phosphorylation (43). Although *LOXL4* is an important extracellular protein, the HCC cell migration was promoted more by the intracellular *LOXL4* (43). In contrast, other study revealed that 5-azacytidine (5-aza-CR)-mediated overexpression of *LOXL4* reactivated wild-type p53 and promoted cancer cell death, thus suppressing the development of HCC cancers, which might indicate an improved clinical outcomes of HCC patients (28, 44). These complicated and even contradicting mechanism of *LOXL4* in HCC might partially explained the inconsistent findings of its role in HCC prognosis from TCGA, TIMER and ULCAN database.

Further exploration of potential drugs associated with *LOX* and *LOXL3* in LC by using Coremine Medical found 30 drugs. The drug that demonstrated the strongest interaction was aminopropionitrile.  $\beta$ -aminopropionitrile (BAPN), obtained from a natural source, was the first compound found to have inhibitory effect on *LOX* (45). A previous study suggested the potential therapeutic value of BAPN for liver metastasis in gastric cancer (46). Another animal study demonstrated antifibrotic effect of BAPN through reducing collagen fiber bundles and *LOX* level, which indicates its potential role in attenuating the development of liver fibrosis (47). It was also found that that BAPN acts by reversing the angiogenesis that was activated by the overexpression of *LOX* (40). Although quinone and copper

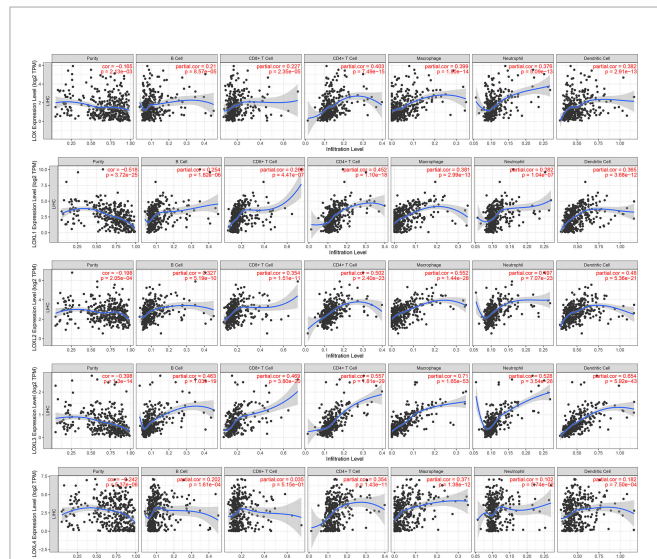


**FIGURE 9 |** Correlations between differentially expressed *LOX* family members and immune cell infiltration in liver cancer (TIMER).

**TABLE 2 |** The Cox proportional hazard model of *LOX* family members and six tumor-infiltrating immune cells in liver cancer (TIMER), and Number of genes that are positively and negative correlated with *LOX* family members.

	coef	HR	95%CI_l	95%CI_u	p.value	sig	Number of positively correlated genes	Number of positively correlated genes
B_cell	-7.875	0	0	0.484	0.031	*		
CD8_Tcell	-5.339	0.005	0	0.714	0.036	*		
CD4_Tcell	-4.127	0.016	0	11.792	0.220			
Macrophage	5.800	330.240	1.925	56641.590	0.027	*		
Neutrophil	-0.054	0.947	0	54322.082	0.992			
Dendritic	5.245	189.571	5.129	7006.334	0.004	**		
<i>LOX</i>	0.087	1.091	0.919	1.296	0.321		13085	6837
<i>LOXL1</i>	-0.159	0.853	0.716	1.015	0.073		12853	7069
<i>LOXL2</i>	0.019	1.020	0.742	1.401	0.905		13393	6529
<i>LOXL3</i>	-0.022	0.979	0.446	2.148	0.957		13866	6056
<i>LOXL4</i>	0.073	1.076	0.959	1.207	0.213		11983	7939

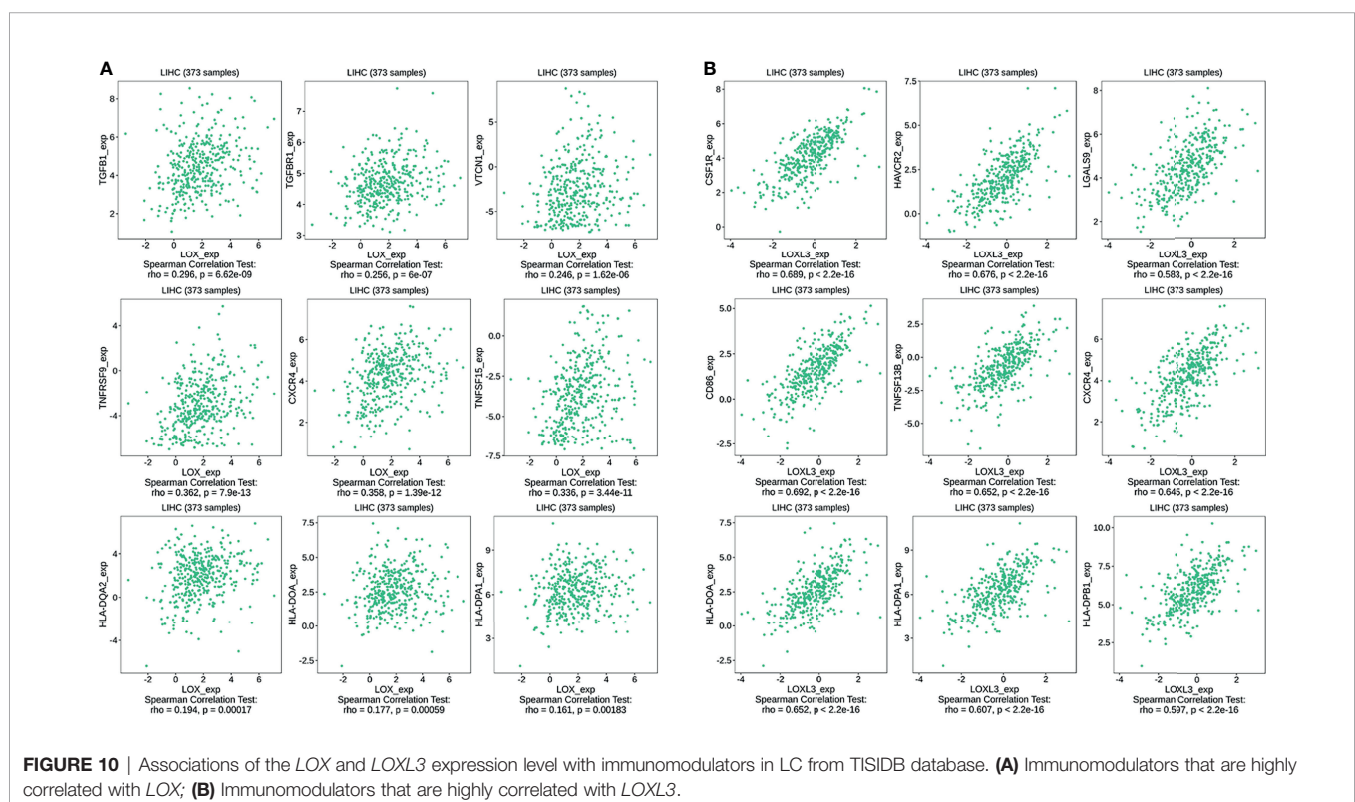
\* $p < 0.05$ , \*\* $p < 0.01$ .

95%CI\_l: Lower limit of 95% Confidential Interval; 95%CI\_u: Upper limit of 95% Confidential Interval.

were found to be potential interacting drugs, they are more likely to be identified because their own function and roles in the *LOX* proteins. Quinone is part of the redox cofactor of *LOX*s, which is a functional group in the catalytic domain of *LOX* proteins (48). *LOX* family members also contain a conserved copper-binding site in the C-terminal half of the protein (49). Copper binding to key histidine residues facilitates the formation of quinone-contained redox factor which in turn leads to the oxidase activity (48, 49). Therefore, quinone and copper can be potential research targets in the future to explore any potential practical use or potential use as therapeutic target. In addition, other drugs found through the exploration, such as cetuximab,

bleomycin, cisplatin, paclitaxel, were known to have anti-cancer effects in various types of cancer, including LC, and anti-fibrosis effects in other diseases such as pulmonary fibrosis (50–59). Their exact roles and effects in LC may need to be clarified in future studies.

Exploration of the PPI network of *LOX* family and their top interactors found that these genes are primarily related to extracellular structures and functions. GO enrichment and KEGG pathway analysis of these genes also found they are mostly involved extracellular functions and structures. This is not surprising as it is well known that members of *LOX* family contribute to structural integrity and increased tensile strength





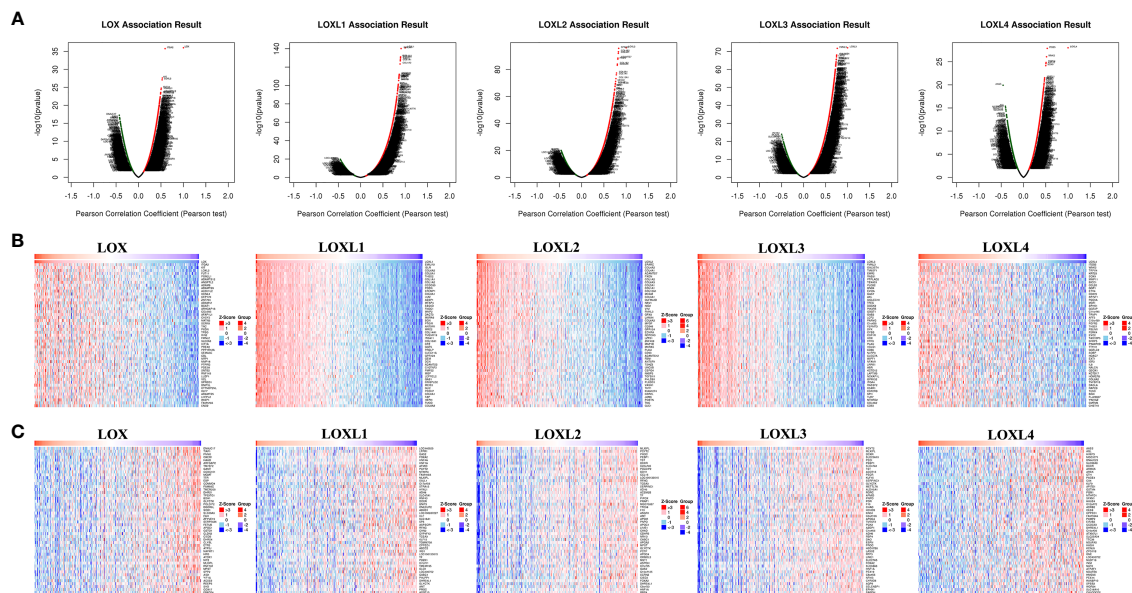


**FIGURE 11** | The co-expression genes with *LOX* family members in LC from the LinkedOmics database. **(A)** The whole significantly associated genes with *LOX* family member distinguished by Pearson test in LC cohort. **(B)** Top 50 genes positively related to *LOX* family member in LC showed by heat maps. **(C)** Top 50 genes negatively related to *LOX* family member in LC showed by heat maps. Red represents positively linked genes and blue represents negatively linked genes.

by their catalytic activity, and exert roles in remodeling the cross-linking of the structural extracellular matrix (ECM) of fibrotic organs such as the liver (25). In addition, LOX family members are involved in scavenger receptor activity, oxidoreductase activity, and copper ion binding. Multiple scavenger receptor cysteine-rich (SRCR) domains exist in *LOXL2* and *LOXL3* (60, 61). As *LOX* family are copper-dependent amine oxidases (25), it is not unexpected that oxidoreductase activity and copper ion binding are involved. Further analysis *via* LinkedOmics database also identified a significant amount of co-expressed genes associated with each *LOXL* family members, and found that these co-expressed genes are also largely involved in extracellular and functions and structures, or participate in human tissues that contain elastic fibers, fibrillar collagen, and organs with a great amount of fibrous lamina propria.

The growth and metastasis of tumor cells depend on a complex tumor microenvironment (TME) (62). TME comprises of cells of hematopoietic origin, such as lymphocytes and myeloid cells, cells of mesenchymal origin, including mesenchymal stem cells, endothelial cells, adipocytes, fibroblasts, and myofibroblasts, and the ECM (63). ECM is a complex network providing structural support, biochemical reagents and biomechanical signals for the growth of cancer cells, and it consists of multiple components, including collagen, integrin, laminin, fibronectin, glycosaminoglycans, matrix metalloproteinases (MMP) and secreted cysteine-rich acidic proteins (64). Further analysis on the relationship of *LOX* family members and tumor-infiltrating immune cells in LC found positive correlations between the infiltration of B cell, CD8+ T cells, CD4+ T cells, macrophages, neutrophils, and DCs

and all *LOX* family members. Moreover, the infiltration of B cells, CD8+ T cells, macrophages, and DCs were associated with worse outcomes. Immune cell infiltration in HCC under different conditions, such as bile acid-mediated immune cell infiltration (65) and TP53 mutations (66), have been investigated in the past. However, evidence on the associations between *LOX* family members and tumor-infiltrating immune cells in LC is limited. In addition, immunomodulatory drugs are under development for various conditions and have been approved in recent years for certain tumors such as multiple myeloma (67, 68). Therefore, we explored and identified a list of immunoinhibitors, immunostimulators, and MHC molecules that are positively correlated with *LOX* and *LOXL3*, the two *LOX* family members with poor prognosis. These immunomodulators could be potential immunotherapeutic targets. The immune environment is thought to be critical in tumor progression and may even play a crucial role in different treatments for cancers, including chemotherapy, radiotherapy, and especially immunotherapy (69–71). Our findings suggest that there is a significant role of the *LOX* family in the tumor microenvironment. Therefore, comprehensive studies on the association of tumor-infiltrating immune cells, as well as immunomodulators, and *LOX* family in LC are needed.

It is well known that tumor heterogeneity relies on the TME, including both the cancer cells themselves and different types of immune cells and the surrounding stroma. TME closely correlates with the response to immunotherapy and the prognosis in multiple cancers (72). TME tends to be involved in the immunosuppression and drug resistance, resulting in less satisfactory responses to immunotherapy. In addition, immune

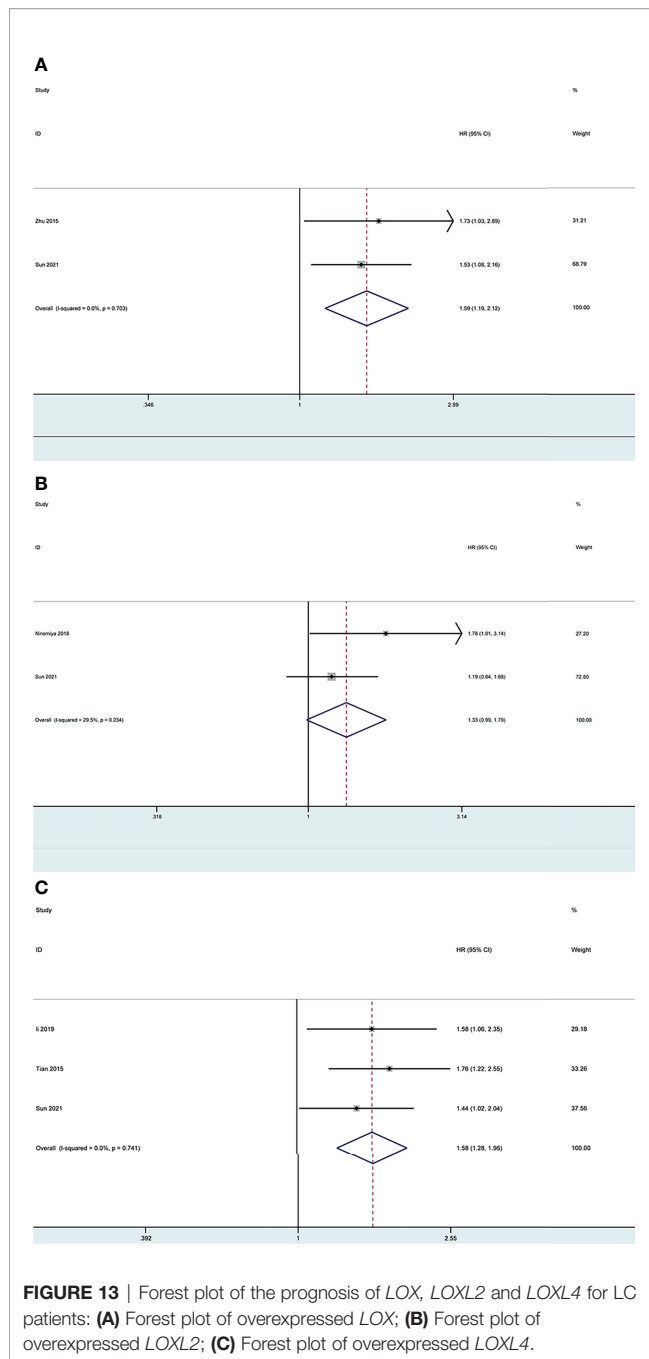




**FIGURE 12 |** GO annotations and KEGG pathways of LOX family and their associated genes in LC cohort: **(A)** results of LOX; **(B)** results of LOXL1; **(C)** results of LOXL2; **(D)** results of LOXL3; **(E)** results of LOXL4.

checkpoint blockade (ICB) relies on restoring the function of T cell to eliminate tumors (70). Moreover, as part of the adaptive immune resistance, tumor cells could upregulate the immune checkpoint gene expression to suppress T cell activity that eventually leads to immune escape (73). Thus, our findings of positive association between CD8+ T cells and CD4+ T cells, as well as other immune cells, and LOX family members suggest that ICB and other immunotherapy could have a promising

potential in LC treatment as high expression of LOX family members in tumor tissues facilitates immune cells infiltration, which could induce the immune response exerting the antitumor efficiency. It would particularly helpful to investigate compounds target on immunoinhibitors and immunostimulators identified in our study. As demonstrated in our study immunoinhibitors, CSF1R, HAVCR2, and LGALS9, were found to be associated with LOXL3, while TGFBI, TGFBR1, and VTCN1 correlated



with *LOX*. CSF-1R plays critical roles in regulating tumor-associated macrophages in TME, and targeted inhibition of the CSF-1/CSF-1R signal axis has broad application prospects in immunotherapy of malignant tumors (74). Pexidartinib is an orally administered small-molecule tyrosine kinase inhibitor that selectively inhibits CSF1R, and is currently being assessed for other types of cancer (75). Another kinase inhibitor, Derazantinib, also found to have activity against CSF1R and is under investigation for cholangiocarcinoma (76). Their potential use in LC also deserves further exploration. HAVCR2, also

known as TIM-3 and CD366, enhances T cell inhibition and apoptosis and immune-suppressive activity of Tregs (77). Antibodies against HAVCR2 disrupt the binding of the ligands to HAVCR2 are under investigation as a potential combination partner of anti-PD-1/L1 therapy (78). Previous study also found that HAVCR2 receptor limits T-cell responses by interacting with LGALS9 (79). A recent study also demonstrated that chemoradiation could induce increased expression of PD-L1 and LGALS9 in gastric cancer (80), however, whether similar result can be found in LC needs further study. TGF- $\beta$ 1 is a potent inhibitor of T cell growth, partly by inhibiting IL-2 expression and secretion by T cells themselves (81), and interestingly, it can also affect anti-tumor T cell responses by downregulating MHC molecules on the surface of tumor cells. Despite its critical roles, the development of TGFB1-targeting therapies has not been progressed well, probably due to concern of severe toxicities that could arise from blocking tumor suppression exerted by TGF- $\beta$ 1 at early stages of tumorigenesis as TGFB1 exerts potent cytostatic and pro-apoptotic activities in pre-malignant cells (82, 83). In addition, blocking TGFB1 activities on normal cells outside of the TME may also lead to toxicities (82). Nevertheless, certain antibodies are still under investigation. For example, studies on Fresolizumab, a fully human monoclonal IgG4 antibody that neutralizes mature TGFB1, were conducted for malignant pleural mesothelioma, melanoma and renal cell carcinoma (82). Galunisertib, another TGFB1 inhibitor, was found to have 16% of objective responses in glioblastoma patients with no serious treatment-related toxicities (82, 84). Another clinical trial for pancreatic cancer patients showed that combination of chemotherapy (gemcitabine) and galunisertib was associated with increased survival compared to chemotherapy alone (85), and it is now also tested for combination with anti-PD-1 antibodies (82). In addition, a new TGFB1 kinase inhibitor called vactosertib, currently tested in early-stage clinical trial for several cancer types (83). VTCN1, also known as B7S1, is also a negative regulator of tumor immunity by various mechanisms such as dampening the anti-tumor Th1 responses (86). Recently, an early-stage clinical study of FPA150, an antibody targeted on B7S1 and other the anti-B7x family members, was started for patients with advanced solid tumors to assess preliminary efficacy of FPA150 alone or in combination anti-PD, as well its safety, tolerability, pharmacokinetics, and pharmacodynamics (87). In addition to immunoinhibitors, the immunostimulators CD86, TNSF13B, and CXCR4, were found to be associated with *LOXL3*, while TNFRSF9, CXCR4, and TNFSF15 correlated with *LOX*. CD86, also known as B7-2, is an immune checkpoint molecule of B7 family and binds to CD28 and Cytotoxic T-Lymphocyte Antigen 4 (CTLA-4). Interaction of CD86 with CTLA-4 inactivates T lymphocytes, causing the escape of tumor cells from the immune system. Therefore, immunotherapy using CTLA-4 antibodies might promote T cell activation to help eliminating tumor cells (88). Ipilimumab, an CTLA-4 antibody, is currently approved by Food and Drug Administration (FDA) for HCC treatment in combination with nivolumab. In addition, Tremelimumab, fully human immunoglobulin G2 monoclonal antibody directed against

CTLA-4, is also under investigation for HCC treatment (89). TNSF14B, also known as B cell-activating factor of the TNF family (BAFF), together with its receptor, BAFFR, are important in early B-cell homeostasis and regulatory T-cell function (90). BAFF inhibitors have been tested for certain diseases. For instance, belimumab, a fully human monoclonal antibody against BAFF, has been shown to have a modest effect for active systemic lupus erythematosus (SLE), and another BAFF inhibitor Blisibimod is also under investigation for SLE (90, 91). Tabalumab is another BAFF inhibitor, and has been evaluated as a combined therapy with bortezomib for multiple myeloma (90). However, the roles of BAFF inhibitors in HCC still yet to be explored. TNFRSF9, also known as CD137, a surface glycoprotein belonging to a member of the tumor necrosis factor receptor superfamily (TNFRSF). It is expressed on activated T cells that have encountered cognate antigen, activated NK cells, and mature DCs (92). Two clinical trials have been initiated for two anti- TNFRSF9 monoclonal antibodies urelumab (BMS-663513) and utomilumab (PF-05082566) (93, 94). TNFSF15, also called TNF-like molecule 1A (TL1A), is expressed on multiple immune cells such as DCs and B cells. It binds to DR3 receptor, leading to cell apoptosis by activating the caspase cascade through interaction with TRADD and FADD, and the activation of multiple cell survival signaling pathways including NF- $\kappa$ B, STAT3, JNK, p38 MAPK and ERK (95, 96). TNFSF15 can also suppress endothelial cell proliferation and angiogenesis through the binding of DR3, and this was verified in a mouse xenograft tumor model (97, 98). Moreover, TNFSF15 also can be induced in T cells, macrophages, monocytes, and DCs in response to stimulation with immune complexes, Toll-like receptor ligands, inflammatory cytokines, and T-cell receptor activator (99). Current studies mostly focus on the role of TNFSF15 in inflammatory diseases such as SLE and psoriasis (100), its potential roles in HCC yet to be further investigated. Apart from the above immunostimulators, the CXCR4 was associated with both LOX and LOXL3. It is expressed on various pro- and anti-inflammatory immune cells, especially in macrophages and T cells (101). Multiple drugs targeted on CXCR4 have been under investigation (102). AMD3100, also known as plerixafor (Mozobil), was the FDA-approved CXCR4 antagonist used for peripheral blood stem cell transplantation, but its clinical use in LC and other solid tumors is limited due to its poor pharmacokinetics and toxic adverse effects (102, 103). Recently, other CXCR4 antagonists have been developed. For example, BPRCX807 has been experimentally validated in different HCC models (103), and it deserves further investigation. The MHCs, HLA-DOA, HLA-DPA1, and HLA-DPB1, positively associated with LOXL3 all belongs to MHC Class II molecules (104). MHC class II molecules were found to be expressed by antigen-presenting cells, including antigen-presenting cancer-associated fibroblasts (apCAFs) (105, 106). Therefore, these positive association of the MHC Class II molecules might be indirect evidence of apCAFs in HCC, and drugs targeted on these apCAFs might have potential therapeutic values and future studies are needed for further clarification.

This bioinformatic study also acknowledges some limitations: First, as all data were retrieved from online databases, the results still need to be validated with other experiments and cohorts. Second, as this study was mainly aimed at exploring the potential diagnostic, prognostic, and therapeutic values of the LOX family members in LC patients, the details of their mechanisms were not comprehensively explored. Third, most of the samples on the online databases were HCC, therefore their values on other types of LC still need further investigation. Fourth, meta-analysis found that *LOXL4* was associated with poor OS, while results from TIMER and UALCAN did not yield the same conclusion. However, only two studies on the survival effect of overexpressed *LOXL4* were found, therefore, more studies are urgently needed to validate its effect of the prognosis for LC patients.

## CONCLUSIONS

This bioinformatics analysis investigated the expression levels, diagnostic and prognostic values, genetic alterations, PPI network, functional enrichment, tumor microenvironment factors, and potential mechanisms of LOX family members in LC. Our results found that all LOX family members are overexpressed in LC tumors, and *LOXL2* is good candidate as a diagnostic marker. *LOX* and *LOXL3* are associated with poor prognosis and carry potential as therapeutic targets. The effect of *LOXL4* on survival remains equivocal and prompts more studies. The infiltration of a variety of immune cells and a list of immunomodulators were positive correlated with LOX family members. These results highlight the need to explore the roles of LOX family in the tumor microenvironment and their potential as immunotherapeutic targets.

## METHODS

### Analysis of LOX Family Expression Levels

The expression levels of LOX family members between LC and normal tissue were first compared by using the Wilcoxon rank sum test, and visualized by 'ggplot2' package of R software version v3.6.3 (The R Foundation for Statistical Computing, 2020).  $p < 0.05$  was considered statistically significant. Data extracted from The Cancer Genome Atlas Liver Hepatocellular Carcinoma (TCGA-LIHC) database (<https://portal.gdc.cancer.gov/>), and Log2 transformed FPKM (fragments per kilobase exon-model per million reads mapped) were used.

To further verify the expression levels of the 5 members of LOX family between LC tissues and adjoining normal tissues, the difference in transcriptional levels were assessed using students' t-test through the UALCAN online tool (<http://ualcan.path.uab.edu/analysis.html>), in which a statistically significant value was defined as  $p$ -value  $< 0.05$  (107). These findings were then verified through Tumor Immune Estimation Resource (TIMER) (<https://cistrome.shinyapps.io/timer/>), an online tool based on data of

more than ten-thousand tumors from 32 types of cancer (108, 109).

The optimal discriminate cut-off point between the high and low expression groups was evaluated by the receiver operating characteristic (ROC) curve and area under the curve (AUC) values for overexpressed *LOX* family members, with data obtained from the TCGA-LIHC database. Log2 transformed FPKM were used for downstream analyses. ROC curve was created by using pROC and ggplot2 packages of R software.

## Analysis of Prognostic Value of *LOX* Family Expression in LC

The prognostic value of *LOX* family expression was first explored based on the TCGA-LIHC data with Log2 transformed FPKM. We applied the Kaplan-Meier (KM) survival analysis with log-rank test to compare the survival difference between high expression group and low expression group. The KM curves, with p-values and hazard ratio (HR) with 95% confidence interval (CI), were generated by log-rank tests and univariate Cox proportional hazards regression. These calculations were performed using R software with 'survminer', and 'survival' packages. The results were verified by through the UALCAN online tool (107) and TIMER (108, 109).

A predictive model based on TCGA-LIHC data was also established to predict the mortality risk based on overexpressed members of *LOX* family and all other potential predictors (110–112). A nomogram using 'rms' and 'survival' R packages was developed, based on multivariate Cox proportional hazards analysis for predicting the 1,3,5-year overall survival. A graphical representation of potential predicting factors was provided by the nomogram to calculate the risk of mortality for an individual patient. In order to assess the discriminatory performance of the model, C-index was also calculated (112–114).

## Analysis of Genetic Mutations of *LOX* Family in LC

Five datasets, including "TCGA, Firehose Legacy", "RIKEN, Nat Genet 2012", "AMC, Hepatology 2014", "INSERM, Nat Genet 2015", and "MSK, Clin Cancer Res 2018" were applied to analyze gene mutations of *LOX* family members via cBioPortal (<http://www.cbioportal.org/>). cBioPortal is a comprehensive web resource providing visualization, analysis, and download of large-scale cancer genomics data sets (115). The correlation of *LOX* family members with each other was calculated by analyzing mRNA expressions (RNA sequencing [RNA-seq] version (v.2) RSEM) in the cBioPortal online tool for Liver Hepatocellular Carcinoma (TCGA, Firehose Legacy). Pearson's correction was included. TIMER was also used to verify the correlation of *LOX* family members using the Correlation module (108, 109).

## Exploration of Potential Drugs That Are Interacted With *LOX* Family in LC

Potential drugs that interact with members of the *LOX* family and demonstrated significant difference in expression and

survival between LC and normal tissues were investigated through text mining. Coremine Medical (<http://www.coremine.com/medical/>) was used to visualize the connections among genes and pathways (116, 117).

## Analysis of Interaction of *LOX* Family Members in LC

Protein-protein interaction (PPI) network analysis was performed on differentially expressed *LOX* family members and their most significantly interacted proteins via STRING online database (<https://string-db.org/>) (118) and GeneMANIA (<http://www.genemania.org>) (119).

## GO Enrichment and KEGG Pathway Analysis of *LOX* Family Members

Functions of *LOX* family members and their top 20 most associated genes identified from GeneMANIA (119) were analyzed by Gene Ontology (GO) and Kyoto Encyclopedia of Genes and Genomes (KEGG) in the DAVID database (<https://david.ncifcrf.gov/summary.jsp>) (120, 121). GO enrichment analysis predicted the function based on biological processes (BP), cellular components (CC), and molecular functions (MF), while KEGG analysis determined the related pathways of *LOX* family members and their associated interactors. The results of GO and KEGG analyses were visualized by the Bioinformatics online tool (<http://www.bioinformatics.com.cn>) (122, 123). KEGG online web tool (<http://www.genome.jp/kegg/>), an integrated database for biological interpretation of genome sequences and other large-scale molecular datasets, was also used to verify crucial pathways (123–126).

## Immune Cell Infiltration of *LOX* Family Members in LC

The infiltration of different immune cells and their clinical impact were assessed through TIMER, an online tool for comprehensive molecular characterization of tumor-immune interactions (108, 109). Plots were generated using the Gene module in TIMER, through which we analyzed the correlation between the expression of *LOX* family members and immune infiltration level in LC. Cutoff value of Cor >0.2 and p<0.05 were used to determine a significant correlation (127, 128). To further explore the interactions between immune system and *LOX* family members that are associated with poor prognosis, the TISIDB database (<http://cis.hku.hk/TISIDB>) was used. TISIDB is a web portal for analyzing immune system and tumor interaction, including nearly one thousand reported immune-related anti-tumor genes, etc., and immunological data gathered from seven public databases (129–131). Here, TISIDB was used for exploring the immunomodulators associated with *LOX* family members in LC.

## Association Analysis of Each Member of *LOX* Family and GSEA Analysis

The LinkedOmics (<http://www.linkedomics.org/login.php>) is an online tool with multi-omics data from 32 types of cancer based on TCGA (132). *LOX* family members were screened from the



TCGA-LIHC cohort by choosing HiSeq RNA as platform and RNAseq as data type in both search dataset and target dataset. The genes associated with each member of LOX family member were explored through the LinkFinder module, and the correlation of results was tested by the Pearson correlation coefficient and presented respectively in volcano plot and heat maps. Function module analysis of GO and KEGG pathways were explored by the gene set enrichment analysis (GSEA) in the LinkInterpreter module.

## Meta-Analysis of the Prognosis of Overexpressed LOX Family Members in LC

A meta-analysis was performed to verify the results of OS of overexpressed LOX family members in LC. Two authors (S. Mao and Y. Chen) independently searched the potential articles related to LOX family members and LC published until May 2021 via the Cochrane Library, PubMed, Web of Science and CNKI (Chinese National Knowledge Infrastructure). To find all eligible literature, the following search strategy was used: (LOXL1 OR LOXL2 OR LOXL3 OR LOXL4 OR LOX OR lysyl oxidase like 1 OR lysyl oxidase like 2 OR lysyl oxidase like 3 OR lysyl oxidase like 4 OR lysyl oxidase) AND (liver cancer OR hepatocellular carcinoma OR LC OR HCC). Chinese phrases replaced the English terms in the CNKI database. Before conducting this study, we consulted the Preferred Reporting Items declared by the Systematic Review and Meta-Analysis (PRISMA) (133). Then, the strength of associations between LOX family members and OS in LC was evaluated by calculating the combined HRs with the corresponding 95% confidence interval (CI).  $I^2$  statistics were used to assess the degree of heterogeneity across the incorporated original studies (134). If  $I^2 > 50\%$ , the

random-effects model was used to estimate the HR to account for heterogeneity; otherwise, the fixed-effects model was applied (135). In addition, we performed sensitivity analysis by switching between the random-effects model and fixed-effects model and observing for significant differences in the results (136, 137). The above statistical analysis was performed using STATA 15.1. statistical software (Stata Corp., College Station, TX).

## DATA AVAILABILITY STATEMENT

The datasets presented in this study can be found in online repositories. The names of the repository/repositories and accession number(s) can be found in the article/supplementary material.

## AUTHOR CONTRIBUTIONS

YZ and CS designed the research study. CS, YC, and SM selected and collected the data. CS, YC, SM, and WG analyzed the data. CS, YC, SM, and NK wrote the manuscript. ZZ participated in the statistical analysis. SK, YW, WG, YC, JT, CB, NM, YH, CC, and QZ provided critical opinions and revised the manuscript. All authors read and approved the final manuscript.

## FUNDING

The Training Program Foundation of Youth Scholars by the First Affiliated Hospital of Anhui Medical University (2020kj24).

## ACKNOWLEDGMENTS

We acknowledge TCGA database for providing their platforms and contributors for uploading their meaningful datasets.

## REFERENCES

- Sung H, Ferlay J, Siegel RL, Laversanne M, Soerjomataram I, Jemal A, et al. Global Cancer Statistics 2020: GLOBOCAN Estimates of Incidence and Mortality Worldwide for 36 Cancers in 185 Countries. *CA Cancer J Clin* (2021) 71(3):209–49. doi: 10.3322/caac.21660
- Tan Z. Recent Advances in the Surgical Treatment of Advanced Gastric Cancer: A Review. *Med Sci Monit* (2019) 25:3537–41. doi: 10.12659/MSM.916475
- Wallace MC, Preen D, Jeffrey GP, Adams LA. The Evolving Epidemiology of Hepatocellular Carcinoma: A Global Perspective. *Expert Rev Gastroenterol Hepatol* (2015) 9(6):765–79. doi: 10.1586/17474124.2015.1028363
- Chen JG, Zhang SW. Liver Cancer Epidemic in China: Past, Present and Future. *Semin Cancer Biol* (2011) 21(1):59–69. doi: 10.1016/j.semcancer.2010.11.002
- Petrizzo A, Caruso FP, Tagliamonte M, Tornesello ML, Ceccarelli M, Costa V, et al. Identification and Validation of HCC-Specific Gene Transcriptional Signature for Tumor Antigen Discovery. *Sci Rep* (2016) 6:29258. doi: 10.1038/srep29258
- Niu J, Lin Y, Guo Z, Niu M, Su C. The Epidemiological Investigation on the Risk Factors of Hepatocellular Carcinoma: A Case-Control Study in Southeast China. *Med (Baltimore)* (2016) 95(6):e2758. doi: 10.1097/MD.0000000000002758
- Yang JD, Hainaut P, Gores GJ, Amadou A, Plymth A, Roberts LR. A Global View of Hepatocellular Carcinoma: Trends, Risk, Prevention and Management. *Nat Rev Gastroenterol Hepatol* (2019) 16(10):589–604. doi: 10.1038/s41575-019-0186-y
- Zhang G, Kang Z, Mei H, Huang Z, Li H. Promising Diagnostic and Prognostic Value of Six Genes in Human Hepatocellular Carcinoma. *Am J Transl Res* (2020) 12(4):1239–54.
- Shirdarreh M, Aziza O, Pezo RC, Jerzak KJ, Warner E. Patients' and Oncologists' Knowledge and Expectations Regarding Tumor Multigene Next-Generation Sequencing: A Narrative Review. *Oncologist* (2021) 26(8):e1359–71. doi: 10.1002/onco.13783
- Giunchi F, Franceschini T, Fiorentino M. A Narrative Review of Individualized Treatments of Genitourinary Tumors: Is the Future Brighter With Molecular Evaluations? *Transl Androl Urol* (2021) 10(3):1553–61. doi: 10.21037/tau-20-1185
- Levy SE, Myers RM. Advancements in Next-Generation Sequencing. *Annu Rev Genomics Hum Genet* (2016) 17:95–115. doi: 10.1146/annurev-genom-083115-022413
- Behjati S, Tarpey PS. What is Next Generation Sequencing? *Arch Dis Child Educ Pract Ed* (2013) 98(6):236–8. doi: 10.1136/archdischild-2013-304340
- Li S, Yang R, Sun X, Miao S, Lu T, Wang Y, et al. Identification of SPP1 as a Promising Biomarker to Predict Clinical Outcome of Lung Adenocarcinoma Individuals. *Gene* (2018) 679:398–404. doi: 10.1016/j.gene.2018.09.030
- Shen Y, Liu J, Zhang L, Dong S, Zhang J, Liu Y, et al. Identification of Potential Biomarkers and Survival Analysis for Head and Neck Squamous Cell Carcinoma Using Bioinformatics Strategy: A Study Based on TCGA and GEO Datasets. *BioMed Res Int* (2019) 2019:7376034. doi: 10.1155/2019/7376034
- Cox TR, Erler JT. Remodeling and Homeostasis of the Extracellular Matrix: Implications for Fibrotic Diseases and Cancer. *Dis Model Mech* (2011) 4(2):165–78. doi: 10.1242/dmm.004077

16. Fogelgren B, Polgar N, Szauter KM, Ujfaludi Z, Laczko R, Fong KS, et al. Cellular Fibronectin Binds to Lysyl Oxidase With High Affinity and Is Critical for its Proteolytic Activation. *J Biol Chem* (2005) 280(26):24690–7. doi: 10.1074/jbc.M412979200
17. Stewart GD, Nanda J, Brown DJ, Riddick AC, Ross JA, Habib FK. NO-Sulindac Inhibits the Hypoxia Response of PC-3 Prostate Cancer Cells via the Akt Signalling Pathway. *Int J Cancer* (2009) 124(1):223–32. doi: 10.1002/ijc.23934
18. Rodriguez HM, Vaysberg M, Mikels A, McCauley S, Velayo AC, Garcia C, et al. Modulation of Lysyl Oxidase-Like 2 Enzymatic Activity by an Allosteric Antibody Inhibitor. *J Biol Chem* (2010) 285(27):20964–74. doi: 10.1074/jbc.M109.094136
19. Kumari S, Panda TK, Pradhan T. Lysyl Oxidase: Its Diversity in Health and Diseases. *Indian J Clin Biochem* (2017) 32(2):134–41. doi: 10.1007/s12291-016-0576-7
20. Lucero HA, Ravid K, Grimsby JL, Rich CB, DiCamillo SJ, Maki JM, et al. Lysyl Oxidase Oxidizes Cell Membrane Proteins and Enhances the Chemotactic Response of Vascular Smooth Muscle Cells. *J Biol Chem* (2008) 283(35):24103–17. doi: 10.1074/jbc.M709897200
21. Erler JT, Giaccia AJ. Lysyl Oxidase Mediates Hypoxic Control of Metastasis. *Cancer Res* (2006) 66(21):10238–41. doi: 10.1158/0008-5472.CAN-06-3197
22. Miller BW, Morton JP, Pinese M, Saturno G, Jamieson NB, McGhee E, et al. Targeting the LOX/hypoxia Axis Reverses Many of the Features That Make Pancreatic Cancer Deadly: Inhibition of LOX Abrogates Metastasis and Enhances Drug Efficacy. *EMBO Mol Med* (2015) 7(8):1063–76. doi: 10.15252/emmm.201404827
23. Yang M, Liu J, Wang F, Tian Z, Ma B, Li Z, et al. Lysyl Oxidase Assists Tumorinitiating Cells to Enhance Angiogenesis in Hepatocellular Carcinoma. *Int J Oncol* (2019) 54(4):1398–408. doi: 10.3892/ijo.2019.4705
24. Zhao W, Yang A, Chen W, Wang P, Liu T, Cong M, et al. Inhibition of Lysyl Oxidase-Like 1 (LOXL1) Expression Arrests Liver Fibrosis Progression in Cirrhosis by Reducing Elastin Crosslinking. *Biochim Biophys Acta Mol Basis Dis* (2018) 1864(4 Pt A):1129–37. doi: 10.1016/j.bbdis.2018.01.019
25. Lin HY, Li CJ, Yang YL, Huang YH, Hsiao YT, Chu PY. Roles of Lysyl Oxidase Family Members in the Tumor Microenvironment and Progression of Liver Cancer. *Int J Mol Sci* (2020) 21(24):9751. doi: 10.3390/ijms21249751
26. Wong CC, Tse AP, Huang YP, Zhu YT, Chiu DK, Lai RK, et al. Lysyl Oxidase-Like 2 is Critical to Tumor Microenvironment and Metastatic Niche Formation in Hepatocellular Carcinoma. *Hepatology* (2014) 60(5):1645–58. doi: 10.1002/hep.27320
27. Tan HY, Wang N, Zhang C, Chan YT, Yuen MF, Feng Y. Lysyl Oxidase-Like 4 Fosters an Immunosuppressive Microenvironment During Hepatocarcinogenesis. *Hepatology* (2020) 73(6):2326–41. doi: 10.1002/hep.31600
28. Li R, Wang Y, Zhang X, Feng M, Ma J, Li J, et al. Exosome-Mediated Secretion of LOXL4 Promotes Hepatocellular Carcinoma Cell Invasion and Metastasis. *Mol Cancer* (2019) 18(1):18. doi: 10.1186/s12943-019-0948-8
29. Tian M, Liu W, Jin L, Jiang X, Yang L, Ding Z, et al. LOXL4 Is Downregulated in Hepatocellular Carcinoma With a Favorable Prognosis. *Int J Clin Exp Pathol* (2015) 8(4):3892–900.
30. Zhu J, Huang S, Wu G, Huang C, Li X, Chen Z, et al. Lysyl Oxidase Is Predictive of Unfavorable Outcomes and Essential for Regulation of Vascular Endothelial Growth Factor in Hepatocellular Carcinoma. *Dig Dis Sci* (2015) 60(10):3019–31. doi: 10.1007/s10620-015-3734-5
31. Ninomiya G, Yamada S, Hayashi M, Takeda S, Suenaga M, Takami H, et al. Significance of Lysyl Oxidase-Like 2 Gene Expression on the Epithelial-mesenchymal Status of Hepatocellular Carcinoma. *Oncol Rep* (2018) 39(6):2664–72. doi: 10.3892/or.2018.6349
32. Wei S, Gao L, Wu C, Qin F, Yuan J. Role of the Lysyl Oxidase Family in Organ Development (Review). *Exp Ther Med* (2020) 20(1):163–72. doi: 10.3892/etm.2020.8731
33. Molnar J, Fong KS, He QP, Hayashi K, Kim Y, Fong SF, et al. Structural and Functional Diversity of Lysyl Oxidase and the LOX-Like Proteins. *Biochim Biophys Acta* (2003) 1647(1–2):220–4. doi: 10.1016/S1570-9639(03)00053-0
34. Iturbide A, García de Herreros A, Peiró S. A New Role for LOX and LOXL2 Proteins in Transcription Regulation. *FEBS J* (2015) 282(9):1768–73. doi: 10.1111/febs.12961
35. Shao B, Zhao X, Liu T, Zhang Y, Sun R, Dong X, et al. LOXL2 Promotes Vasculogenic Mimicry and Tumour Aggressiveness in Hepatocellular Carcinoma. *J Cell Mol Med* (2019) 23(2):1363–74. doi: 10.1111/jcmm.14039
36. Xiao Q, Ge G. Lysyl Oxidase, Extracellular Matrix Remodeling and Cancer Metastasis. *Cancer Microenviron* (2012) 5(3):261–73. doi: 10.1007/s12307-012-0105-z
37. López B, González A, Hermida N, Valencia F, de Teresa E, Díez J. Role of Lysyl Oxidase in Myocardial Fibrosis: From Basic Science to Clinical Aspects. *Am J Physiol Heart Circ Physiol* (2010) 299(1):H1–9. doi: 10.1152/ajpheart.00335.2010
38. Smith-Mungo LI, Kagan HM. Lysyl Oxidase: Properties, Regulation and Multiple Functions in Biology. *Matrix Biol* (1998) 16(7):387–98. doi: 10.1016/S0945-053X(98)90012-9
39. Ye M, Song Y, Pan S, Chu M, Wang ZW, Zhu X. Evolving Roles of Lysyl Oxidase Family in Tumorigenesis and Cancer Therapy. *Pharmacol Ther* (2020) 215:107633. doi: 10.1016/j.pharmthera.2020.107633
40. Yang M, Liu J, Wang F, Tian Z, Ma B, Li Z, et al. Lysyl Oxidase Assists Tumor-Initiating Cells to Enhance Angiogenesis in Hepatocellular Carcinoma. *Int J Oncol* (2019) 54(4):1398–408. doi: 10.3892/ijo.2019.4705
41. Ribeiro AL, Kaid C, Silva PB, Cortez BA, Okamoto OK. Inhibition of Lysyl Oxidases Impairs Migration and Angiogenic Properties of Tumor-Associated Pericytes. *Stem Cells Int* (2017) 2017:4972078. doi: 10.1155/2017/4972078
42. Kasashima H, Yashiro M, Okuno T, Miki Y, Kitayama K, Masuda G, et al. Significance of the Lysyl Oxidase Members Lysyl Oxidase Like 1, 3, and 4 in Gastric Cancer. *Digestion* (2018) 98(4):238–48. doi: 10.1159/000489558
43. Wang N, Zhou X, Tang F, Wang X, Zhu X. Identification of LOXL3-Associating Immune Infiltration Landscape and Prognostic Value in Hepatocellular Carcinoma. *Virchows Arch* (2021) 479(6):1153–65. doi: 10.1007/s00428-021-03193-4
44. Shao J, Lu J, Zhu W, Yu H, Jing X, Wang YL, et al. Derepression of LOXL4 Inhibits Liver Cancer Growth by Reactivating Compromised P53. *Cell Death Differ* (2019) 26(11):2237–52. doi: 10.1038/s41418-019-0293-x
45. Madden MZ, Rathmell JC. The Complex Integration of T-Cell Metabolism and Immunotherapy. *Cancer Discov* (2021) 11(7):1636–43. doi: 10.1158/2159-8290.CD-20-0569
46. Ferreira S, Saraiva N, Rijo P, Fernandes AS. LOXL2 Inhibitors and Breast Cancer Progression. *Antioxidants (Basel)* (2021) 10(2):312. doi: 10.3390/antiox10020312
47. Li Q, Zhu CC, Ni B, Zhang ZZ, Jiang SH, Hu LP, et al. Lysyl Oxidase Promotes Liver Metastasis of Gastric Cancer via Facilitating the Reciprocal Interactions Between Tumor Cells and Cancer Associated Fibroblasts. *EBioMedicine* (2019) 49:157–71. doi: 10.1016/j.ebiom.2019.10.037
48. Grau-Bové X, Ruiz-Trillo I, Rodríguez-Pascual F. Origin and Evolution of Lysyl Oxidases. *Sci Rep* (2015) 5:10568. doi: 10.1038/srep10568
49. Noda K, Kitagawa K, Miki T, Horiguchi M, Akama TO, Taniguchi T, et al. A Matricellular Protein Fibulin-4 Is Essential for the Activation of Lysyl Oxidase. *Sci Adv* (2020) 6(48):eabc1404. doi: 10.1126/sciadv.abc1404
50. Mohseni R, Arab Sadeghabadi Z, Goodarzi MT, Karimi J. Co-Administration of Resveratrol and Beta-Aminopropionitrile Attenuates Liver Fibrosis Development via Targeting Lysyl Oxidase in CCl4-Induced Liver Fibrosis in Rats. *Immunopharmacol Immunotoxicol* (2019) 41(6):644–51. doi: 10.1080/08923973.2019.1688829
51. Shah R, Chan KKW. The Impact of Socioeconomic Status on Stage at Presentation, Receipt of Diagnostic Imaging, Receipt of Treatment and Overall Survival in Colorectal Cancer Patients. *Int J Cancer* (2021) 49(5):1031–43. doi: 10.1002/ijc.33622
52. Viswanadh MK, Agrawal N, Azad S, Jha A, Poddar S, Mahto SK, et al. Novel Redox-Sensitive Thiolated TPGS Based Nanoparticles for EGFR Targeted Lung Cancer Therapy. *Int J Pharm* (2021) 602:120652. doi: 10.1016/j.ijpharm.2021.120652
53. Conforti F, Davies ER, Calderwood CJ, Thatcher TH, Jones MG, Smart DE, et al. The Histone Deacetylase Inhibitor, Romidepsin, as a Potential Treatment for Pulmonary Fibrosis. *Oncotarget* (2017) 8(30):48737–54. doi: 10.18632/oncotarget.17114
54. Perrone AM, Ravegnini G, Miglietta S, Argenti L, Ferioli M, De Crescenzo E, et al. Electrochemotherapy in Vulvar Cancer and Cisplatin Combined With Electroporation. Systematic Review and *In Vitro* Studies. *Cancers (Basel)* (2021) 13(9):1993. doi: 10.3390/cancers13091993
55. Lee J, You JH, Shin D, Roh JL. *Ex Vivo* Culture of Head and Neck Cancer Explants in Cell Sheet for Testing Chemotherapeutic Sensitivity. *J Cancer Res Clin Oncol* (2020) 146(10):2497–507. doi: 10.1007/s00432-020-03306-7

56. Saboormaleki S, Sadeghian H, Bahrami AR, Orafaie A, Matin MM. 7-Farnesylcoumarin Exerts Anti-Cancer Effects on a Prostate Cancer Cell Line by 15-LOX-1 Inhibition. *Arch Iran Med* (2018) 21(6):251–9.
57. Sterzynska K, Klejowski A, Wojtowicz K, Swierczewska M, Nowacka M, Kazmierczak D, et al. Mutual Expression of ALDH1A1, LOX, and Collagens in Ovarian Cancer Cell Lines as Combined CSCs- and ECM-Related Models of Drug Resistance Development. *Int J Mol Sci* (2018) 20(1):54. doi: 10.3390/ijms20010054
58. Gao Y, Liu T, Liu X, Wu C. Preparation of Paclitaxel-Folic Acid Functionalized Gelatin Grafted Mesoporous Hollow Carbon Nanospheres for Enhancing Antitumor Effects Toward Liver Cancer (SMMC-7721) Cell Lines. *J Biomater Appl* (2020) 34(8):1071–80. doi: 10.1177/0885328219896457
59. Li Y, Tang T, Lee HJ, Song K. Selective Anti-Cancer Effects of Plasma-Activated Medium and Its High Efficacy With Cisplatin on Hepatocellular Carcinoma With Cancer Stem Cell Characteristics. *Int J Mol Sci* (2021) 22(8):3956. doi: 10.3390/ijms22083956
60. Csiszar K. Lysyl Oxidases: A Novel Multifunctional Amine Oxidase Family. *Prog Nucleic Acid Res Mol Biol* (2001) 70:1–32. doi: 10.1016/S0079-6603(01)70012-8
61. Schmelzer CEH, Heinz A, Troilo H, Lockhart-Cairns MP, Jowitt TA, Marchand MF, et al. Lysyl Oxidase-Like 2 (LOXL2)-Mediated Cross-Linking of Tropoelastin. *FASEB J* (2019) 33(4):5468–81. doi: 10.1096/fj.201801860RR
62. Oliver AJ, Lau PKH, Unsworth AS, Loi S, Darcy PK, Kershaw MH, et al. Tissue-Dependent Tumor Microenvironments and Their Impact on Immunotherapy Responses. *Front Immunol* (2018) 9:70. doi: 10.3389/fimmu.2018.00070
63. Hanahan D, Coussens LM. Accessories to the Crime: Functions of Cells Recruited to the Tumor Microenvironment. *Cancer Cell* (2012) 21(3):309–22. doi: 10.1016/j.ccr.2012.02.022
64. Buoncervello M, Gabriele L, Toschi E. The Janus Face of Tumor Microenvironment Targeted by Immunotherapy. *Int J Mol Sci* (2019) 20(17):4320. doi: 10.3390/ijms20174320
65. Zhang T, Nie Y, Gu J, Cai K, Chen X, Li H, et al. Identification of Mitochondrial-Related Prognostic Biomarkers Associated With Primary Bile Acid Biosynthesis and Tumor Microenvironment of Hepatocellular Carcinoma. *Front Oncol* (2021) 11:587479. doi: 10.3389/fonc.2021.587479
66. Li W, Wu H, Xu X, Zhang Y. Comprehensive Analysis of Genomic and Immunological Profiles in Chinese and Western Hepatocellular Carcinoma Populations. *Aging (Albany NY)* (2021) 13(8):11564–94. doi: 10.18632/aging.202853
67. Davis LN, Sherbenou DW. Emerging Therapeutic Strategies to Overcome Drug Resistance in Multiple Myeloma. *Cancers (Basel)* (2021) 13(7):1686. doi: 10.3390/cancers13071686
68. Maes K, Mondino A, Lasarte JJ, Agirre X, Vanderkerken K, Prosper F, et al. Epigenetic Modifiers: Anti-Neoplastic Drugs With Immunomodulating Potential. *Front Immunol* (2021) 12:652160. doi: 10.3389/fimmu.2021.652160
69. Pitt JM, Marabelle A, Eggermont A, Soria JC, Kroemer G, Zitvogel L. Targeting the Tumor Microenvironment: Removing Obstruction to Anticancer Immune Responses and Immunotherapy. *Ann Oncol* (2016) 27(8):1482–92. doi: 10.1093/annonc/mdw168
70. Kalinski P, Talmadge JE. Tumor Immuno-Environment in Cancer Progression and Therapy. *Adv Exp Med Biol* (2017) 1036:1–18. doi: 10.1007/978-3-319-67577-0\_1
71. Roma-Rodrigues C, Mendes R, Baptista PV, Fernandes AR. Targeting Tumor Microenvironment for Cancer Therapy. *Int J Mol Sci* (2019) 20(4):840. doi: 10.3390/ijms20040840
72. Bagaev A, Kotlov N, Nomie K, Svekolkina V, Gafurov A, Isaeva O, et al. Conserved Pan-Cancer Microenvironment Subtypes Predict Response to Immunotherapy. *Cancer Cell* (2021) 39(6):845–65.e7. doi: 10.1016/j.ccell.2021.04.014
73. Sanmamed MF, Nie X, Desai SS, Villaroel-Espindola F, Badri T, Zhao D, et al. A Burned-Out CD8+ T-Cell Subset Expands in the Tumor Microenvironment and Cures Cancer Immunotherapy. *Cancer Discov* (2021) 11(7):1700–15. doi: 10.1158/2159-8290.CD-20-0962
74. Li HW, Tang SL. Colony Stimulating Factor-1 and its Receptor in Gastrointestinal Malignant Tumors. *J Cancer* (2021) 12(23):7111–9. doi: 10.7150/jca.60379
75. Vaynrub A, Healey JH, Tap W, Vaynrub M. Pexidartinib in the Management of Advanced Tenosynovial Giant Cell Tumor: Focus on Patient Selection and Special Considerations. *Onco Targets Ther* (2022) 15:53–66. doi: 10.2147/OTT.S345878
76. Braun S, McSheehy P, Litherland K, McKernan P, Forster-Gross N, Bachmann F, et al. Derazantinib: An Investigational Drug for the Treatment of Cholangiocarcinoma. *Expert Opin Investig Drugs* (2021) 30(11):1071–80. doi: 10.1080/13543784.2021.1995355
77. Lee J, Han Y, Wang W, Jo H, Kim H, Kim S, et al. Phytochemicals in Cancer Immune Checkpoint Inhibitor Therapy. *Biomolecules* (2021) 11(8):1107. doi: 10.3390/biom11081107
78. Burugu S, Dancsok AR, Nielsen TO. Emerging Targets in Cancer Immunotherapy. *Semin Cancer Biol* (2018) 52(Pt 2):39–52. doi: 10.1016/j.semcancer.2017.10.001
79. Anderson AC. Tim-3: An Emerging Target in the Cancer Immunotherapy Landscape. *Cancer Immunol Res* (2014) 2(5):393–8. doi: 10.1158/2326-6066.CIR-14-0039
80. Petersen SH, Kua LF, Nakajima S, Yong WP, Kono K. Chemoradiation Induces Upregulation of Immunogenic Cell Death-Related Molecules Together With Increased Expression of PD-L1 and Galectin-9 in Gastric Cancer. *Sci Rep* (2021) 11(1):12264. doi: 10.1038/s41598-021-91603-7
81. Thomas DA, Massagué J. TGF- $\beta$  Directly Targets Cytotoxic T Cell Functions During Tumor Evasion of Immune Surveillance. *Cancer Cell* (2005) 8(5):369–80. doi: 10.1016/j.ccr.2005.10.012
82. de Streeck G, Lucas S. Targeting Immunosuppression by TGF- $\beta$ 1 for Cancer Immunotherapy. *Biochem Pharmacol* (2021) 192:114697. doi: 10.1016/j.bcp.2021.114697
83. Batlle E, Massagué J. Transforming Growth Factor- $\beta$  Signaling in Immunity and Cancer. *Immunity* (2019) 50(4):924–40. doi: 10.1016/j.immuni.2019.03.024
84. Rodon J, Carducci MA, Sepulveda-Sánchez JM, Azaro A, Calvo E, Seoane J, et al. First-In-Human Dose Study of the Novel Transforming Growth Factor- $\beta$  Receptor I Kinase Inhibitor LY2157299 Monohydrate in Patients With Advanced Cancer and Glioma. *Clin Cancer Res* (2015) 21(3):553–60. doi: 10.1158/1078-0432.CCR-14-1380
85. Melisi D, Garcia-Carbonero R, Macarulla T, Pezet D, Deplanque G, Fuchs M, et al. Galunisertib Plus Gemcitabine vs. Gemcitabine for First-Line Treatment of Patients With Unresectable Pancreatic Cancer. *Br J Cancer* (2018) 119(10):1208–14. doi: 10.1038/s41416-018-0246-z
86. Ni L, Dong C. New Checkpoints in Cancer Immunotherapy. *Immunol Rev* (2017) 276(1):52–65. doi: 10.1111/imr.12524
87. John P, Wei Y, Liu W, Du M, Guan F, Zang X. The B7x Immune Checkpoint Pathway: From Discovery to Clinical Trial. *Trends Pharmacol Sci* (2019) 40(11):883–96. doi: 10.1016/j.tips.2019.09.008
88. Bolandi N, Derakhshani A, Hemmat N, Baghbanzadeh A, Asadzadeh Z, Afrashteh Nour M, et al. The Positive and Negative Immunoregulatory Role of B7 Family: Promising Novel Targets in Gastric Cancer Treatment. *Int J Mol Sci* (2021) 22(19):10719. doi: 10.3390/ijms221910719
89. Weinmann A, Galle PR. Role of Immunotherapy in the Management of Hepatocellular Carcinoma: Current Standards and Future Directions. *Curr Oncol* (2020) 27(Suppl 3):S152–64. doi: 10.3747/co.27.7315
90. Hengeveld PJ, Kersten MJ. B-Cell Activating Factor in the Pathophysiology of Multiple Myeloma: A Target for Therapy? *Blood Cancer J* (2015) 5(2):e282. doi: 10.1038/bcj.2015.3
91. Navarra SV, Guzmán RM, Gallacher AE, Hall S, Levy RA, Jimenez RE, et al. Efficacy and Safety of Belimumab in Patients With Active Systemic Lupus Erythematosus: A Randomised, Placebo-Controlled, Phase 3 Trial. *Lancet* (2011) 377(9767):721–31. doi: 10.1016/S0140-6736(10)61354-2
92. Etxeberria I, Glez-Vaz J, Teixeira Á, Melero I. New Emerging Targets in Cancer Immunotherapy: CD137/4-1BB Costimulatory Axis. *ESMO Open* (2020) 4(Suppl 3):e000733. doi: 10.1136/esmoopen-2020-000733
93. Chester C, Ambulker S, Kohrt HE. 4-1BB Agonism: Adding the Accelerator to Cancer Immunotherapy. *Cancer Immunol Immunother* (2016) 65(10):1243–8. doi: 10.1007/s00262-016-1829-2
94. Chu DT, Bac ND, Nguyen KH, Tien NLB, Thanh VV, Nga VT, et al. An Update on Anti-CD137 Antibodies in Immunotherapies for Cancer. *Int J Mol Sci* (2019) 20(8):1822. doi: 10.3390/ijms20081822
95. Croft M. The Role of TNF Superfamily Members in T-Cell Function and Diseases. *Nat Rev Immunol* (2009) 9(4):271–85. doi: 10.1038/nri2526



96. Lin WW, Hsieh SL. Decoy Receptor 3: A Pleiotropic Immunomodulator and Biomarker for Inflammatory Diseases, Autoimmune Diseases and Cancer. *Biochem Pharmacol* (2011) 81(7):838–47. doi: 10.1016/j.bcp.2011.01.011
97. Yang CR, Hsieh SL, Teng CM, Ho FM, Su WL, Lin WW. Soluble Decoy Receptor 3 Induces Angiogenesis by Neutralization of TL1A, a Cytokine Belonging to Tumor Necrosis Factor Superfamily and Exhibiting Angiostatic Action. *Cancer Res* (2004) 64:1122–9. doi: 10.1158/0008-5472.CAN-03-0609
98. Chew LJ, Pan H, Yu J, Tian S, Huang WQ, Zhang JY, et al. A Novel Secreted Splice Variant of Vascular Endothelial Cell Growth Inhibitor. *FASEB J* (2002) 16:742–4. doi: 10.1096/fj.01-0757fje
99. Bayry J. Immunology: TL1A in the Inflammatory Network in Autoimmune Diseases. *Nat Rev Rheumatol* (2010) 6:67–8. doi: 10.1038/nrrheum.2009.263
100. Croft M, Siegel RM. Beyond TNF: TNF Superfamily Cytokines as Targets for the Treatment of Rheumatic Diseases. *Nat Rev Rheumatol* (2017) 13(4):217–33. doi: 10.1038/nrrheum.2017.22
101. Schottelius M, Herrmann K, Lapa C. *In Vivo* Targeting of CXCR4-New Horizons. *Cancers (Basel)* (2021) 13(23):5920. doi: 10.3390/cancers13235920
102. Hu F, Miao L, Zhao Y, Xiao YY, Xu Q. A Meta-Analysis for C-X-C Chemokine Receptor Type 4 as a Prognostic Marker and Potential Drug Target in Hepatocellular Carcinoma. *Drug Des Devel Ther* (2015) 9:3625–33. doi: 10.2147/DDDT.S86032
103. Song JS, Chang CC, Wu CH, Dinh TK, Jan JJ, Huang KW, et al. A Highly Selective and Potent CXCR4 Antagonist for Hepatocellular Carcinoma Treatment. *Proc Natl Acad Sci USA* (2021) 118(13):e2015433118. doi: 10.1073/pnas.2015433118
104. Doxiadis GG, Otting N, de Groot NG, Bontrop RE. Differential Evolutionary MHC Class II Strategies in Humans and Rhesus Macaques: Relevance for Biomedical Studies. *Immunol Rev* (2001) 183:76–85. doi: 10.1034/j.1600-065x.2001.1830106.x
105. Huang M, Dong J. Critical Roles of Balanced T Helper 9 Cells and Regulatory T Cells in Allergic Airway Inflammation and Tumor Immunity. *J Immunol Res* (2021) 2021:8816055. doi: 10.1155/2021/8816055
106. Geng X, Chen H, Zhao L, Hu J, Yang W, Li G, et al. Cancer-Associated Fibroblast (CAF) Heterogeneity and Targeting Therapy of CAFs in Pancreatic Cancer. *Front Cell Dev Biol* (2021) 9:655152. doi: 10.3389/fcell.2021.655152
107. Chandrashekar DS, Bashel B, Balasubramanya SAH, Creighton CJ, Ponce-Rodriguez I, Chakravarthi B, et al. UALCAN: A Portal for Facilitating Tumor Subgroup Gene Expression and Survival Analyses. *Neoplasia* (2017) 19(8):649–58. doi: 10.1016/j.neo.2017.05.002
108. Li T, Fan J, Wang B, Traugh N, Chen Q, Liu JS, et al. TIMER: A Web Server for Comprehensive Analysis of Tumor-Infiltrating Immune Cells. *Cancer Res* (2017) 77(21):e108–e10. doi: 10.1158/0008-5472.CAN-17-0307
109. Li B, Severson E, Pignon JC, Zhao H, Li T, Novak J, et al. Comprehensive Analyses of Tumor Immunity: Implications for Cancer Immunotherapy. *Genome Biol* (2016) 17(1):174. doi: 10.1186/s13059-016-1028-7
110. Iasonos A, Schrag D, Raj GV, Panageas KS. How to Build and Interpret a Nomogram for Cancer Prognosis. *J Clin Oncol* (2008) 26(8):1364–70. doi: 10.1200/JCO.2007.12.9791
111. Balachandran VP, Gonen M, Smith JJ, DeMatteo RP. Nomograms in Oncology: More Than Meets the Eye. *Lancet Oncol* (2015) 16(4):e173–80. doi: 10.1016/S1470-2045(14)71116-7
112. Liu J, Lichtenberg T, Hoadley KA, Poisson LM, Lazar AJ, Cherniack AD, et al. An Integrated TCGA Pan-Cancer Clinical Data Resource to Drive High-Quality Survival Outcome Analytics. *Cell* (2018) 173(2):400–16.e11. doi: 10.1016/j.cell.2018.02.052
113. Kramer AA, Zimmerman JE. Assessing the Calibration of Mortality Benchmarks in Critical Care: The Hosmer-Lemeshow Test Revisited. *Crit Care Med* (2007) 35(9):2052–6. doi: 10.1097/01.CCM.00000275267.64078.B0
114. Pencina MJ, D'Agostino RB. Overall C as a Measure of Discrimination in Survival Analysis: Model Specific Population Value and Confidence Interval Estimation. *Stat Med* (2004) 23(13):2109–23. doi: 10.1002/sim.1802
115. Gao J, Aksoy BA, Dogrusoz U, Dresdner G, Gross B, Sumer SO, et al. Integrative Analysis of Complex Cancer Genomics and Clinical Profiles Using the Cbioportal. *Sci Signal* (2013) 6(269):pl1. doi: 10.1126/scisignal.2004088
116. de Leeuw N, Dijkhuizen T, Hehir-Kwa JY, Carter NP, Feuk L, Firth HV, et al. Diagnostic Interpretation of Array Data Using Public Databases and Internet Sources. *Hum Mutat* (2012) 33(6):930–40. doi: 10.1002/humu.22049
117. Chu H, Zhou X, Liu G, Lv M, Zhou X, Wang Y, et al. Network-Based Detection of Disease Modules and Potential Drug Targets in Intractable Epilepsy. *2014 8th Int Conf Syst Biol (ISB)* (2014) 132–40. doi: 10.1145/2554850
118. Szklarczyk D, Gable AL, Lyon D, Junge A, Wyder S, Huerta-Cepas J, et al. STRING V11: Protein-Protein Association Networks With Increased Coverage, Supporting Functional Discovery in Genome-Wide Experimental Datasets. *Nucleic Acids Res* (2019) 47(D1):D607–13. doi: 10.1093/nar/gky1131
119. Vlasblom J, Zuberi K, Rodriguez H, Arnold R, Gagarinova A, Deineko V, et al. Novel Function Discovery With GeneMANIA: A New Integrated Resource for Gene Function Prediction in Escherichia Coli. *Bioinformatics* (2015) 31(3):306–10. doi: 10.1093/bioinformatics/btu671
120. Huang da W, Sherman BT, Lempicki RA. Bioinformatics Enrichment Tools: Paths Toward the Comprehensive Functional Analysis of Large Gene Lists. *Nucleic Acids Res* (2009) 37(1):1–13. doi: 10.1093/nar/gkn923
121. Huang da W, Sherman BT, Lempicki RA. Systematic and Integrative Analysis of Large Gene Lists Using DAVID Bioinformatics Resources. *Nat Protoc* (2009) 4(1):44–57. doi: 10.1038/nprot.2008.211
122. Zhang MM, Wang D, Lu F, Zhao R, Ye X, He L, et al. Identification of the Active Substances and Mechanisms of Ginger for the Treatment of Colon Cancer Based on Network Pharmacology and Molecular Docking. *BioData Min* (2021) 14(1):1. doi: 10.1186/s13040-020-00232-9
123. Wang T, Feng Y, Wang H, Huo G, Cai Y, Wang L, et al. The Mechanisms of Sijunzi Decoction in the Treatment of Chronic Gastritis Revealed by Network Pharmacology. *Evid Based Complement Alternat Med* (2020) 2020:8850259. doi: 10.1155/2020/8850259
124. Kanehisa M, Furumichi M, Tanabe M, Sato Y, Morishima K. KEGG: New Perspectives on Genomes, Pathways, Diseases and Drugs. *Nucleic Acids Res* (2017) 45(D1):D353–D61. doi: 10.1093/nar/gkw1092
125. Kanehisa M, Sato Y, Furumichi M, Morishima K, Tanabe M. New Approach for Understanding Genome Variations in KEGG. *Nucleic Acids Res* (2019) 47(D1):D590–D5. doi: 10.1093/nar/gky962
126. Kanehisa M, Sato Y. KEGG Mapper for Inferring Cellular Functions From Protein Sequences. *Protein Sci* (2020) 29(1):28–35. doi: 10.1002/pro.3711
127. Liu S, Geng R, Lin E, Zhao P, Chen Y. ERBB1/2/3 Expression, Prognosis, and Immune Infiltration in Cutaneous Melanoma. *Front Genet* (2021) 12:602160. doi: 10.3389/fgene.2021.602160
128. Zhong L, Yang Z, Lei D, Li L, Song S, Cao D, et al. Bromodomain 4 Is a Potent Prognostic Marker Associated With Immune Cell Infiltration in Breast Cancer. *Basic Clin Pharmacol Toxicol* (2021) 128(1):169–82. doi: 10.1111/bcpt.13481
129. Xu H, Zou R, Li F, Liu J, Luan N, Wang S, et al. MRPL15 is a Novel Prognostic Biomarker and Therapeutic Target for Epithelial Ovarian Cancer. *Cancer Med* (2021) 10(11):3655–73. doi: 10.1002/cam4.3907
130. He M, Han Y, Cai C, Liu P, Chen Y, Shen H, et al. CLEC10A is a Prognostic Biomarker and Correlated With Clinical Pathologic Features and Immune Infiltrates in Lung Adenocarcinoma. *J Cell Mol Med* (2021) 25(7):3391–9. doi: 10.1111/jcmm.16416
131. Ding Y, Liu N, Chen M, Xu Y, Fang S, Xiang W, et al. Overexpressed Pseudogene MT1L Associated With Tumor Immune Infiltrates and Indicates a Worse Prognosis in BLCA. *World J Surg Oncol* (2021) 19(1):133. doi: 10.1186/s12957-021-02231-4
132. Vasaikar SV, Straub P, Wang J, Zhang B. LinkedOmics: Analyzing Multi-Omics Data Within and Across 32 Cancer Types. *Nucleic Acids Res* (2018) 46(D1):D956–63. doi: 10.1093/nar/gkx1090
133. Page MJ, McKenzie JE, Bossuyt PM, Boutron I, Hoffmann TC, Mulrow CD, et al. The PRISMA 2020 Statement: An Updated Guideline for Reporting Systematic Reviews. *J Clin Epidemiol* (2021) 134:178–89. doi: 10.1016/j.jclinepi.2021.02.003
134. Higgins JP, Thompson SG. Quantifying Heterogeneity in a Meta-Analysis. *Stat Med* (2002) 21(11):1539–58. doi: 10.1002/sim.1186
135. DerSimonian R, Laird N. Meta-Analysis in Clinical Trials Revisited. *Contemp Clin Trials* (2015) 45(Pt A):139–45. doi: 10.1016/j.cct.2015.09.002
136. Borenstein M, Hedges LV, Higgins JP, Rothstein HR. A Basic Introduction to Fixed-Effect and Random-Effects Models for Meta-Analysis. *Res Synth Methods* (2010) 1(2):97–111. doi: 10.1002/jrsm.12



137. Hernandez AV, Marti KM, Roman YM. Meta-Analysis. *Chest* (2020) 158 (1S):S97–102. doi: 10.1016/j.chest.2020.03.003

**Conflict of Interest:** The authors declare that the research was conducted in the absence of any commercial or financial relationships that could be construed as a potential conflict of interest.

**Publisher's Note:** All claims expressed in this article are solely those of the authors and do not necessarily represent those of their affiliated organizations, or those of

the publisher, the editors and the reviewers. Any product that may be evaluated in this article, or claim that may be made by its manufacturer, is not guaranteed or endorsed by the publisher.

*Copyright © 2022 Sun, Ma, Chen, Kim, Kailas, Wang, Gu, Chen, Tuason, Bhan, Manem, Huang, Cheng, Zhou, Zhou and Zhu. This is an open-access article distributed under the terms of the Creative Commons Attribution License (CC BY). The use, distribution or reproduction in other forums is permitted, provided the original author(s) and the copyright owner(s) are credited and that the original publication in this journal is cited, in accordance with accepted academic practice. No use, distribution or reproduction is permitted which does not comply with these terms.*



# Proteomic Analyses Identify Therapeutic Targets in Hepatocellular Carcinoma

Abdulkadir Elmas<sup>1</sup>, Amaia Lujambio<sup>2</sup> and Kuan-lin Huang<sup>1\*</sup>

<sup>1</sup> Department of Genetics and Genomic Sciences, Center for Transformative Disease Modeling, Tisch Cancer Institute, Icahn Institute for Data Science and Genomic Technology, Icahn School of Medicine at Mount Sinai, New York, NY, United States,

<sup>2</sup> Department of Oncological Sciences, Liver Cancer Program, Division of Liver Diseases, Department of Medicine, Tisch Cancer Institute, Icahn School of Medicine at Mount Sinai, New York, United States

## OPEN ACCESS

### Edited by:

Alessandro Passardi,  
Scientific Institute of Romagna for the  
Study and Treatment of Tumors  
(IRCCS), Italy

### Reviewed by:

Evin Iscan,  
Dokuz Eylül University, Turkey  
Maria Jesus Herrero,  
Universidad de San Sebastián, Chile

### \*Correspondence:

Kuan-lin Huang  
kuan-lin.huang@mssm.edu

### Specialty section:

This article was submitted to  
Gastrointestinal Cancers: Hepato  
Pancreatic Biliary Cancers,  
a section of the journal  
Frontiers in Oncology

**Received:** 12 November 2021

**Accepted:** 28 February 2022

**Published:** 30 March 2022

### Citation:

Elmas A, Lujambio A and  
Huang KL (2022) Proteomic  
Analyses Identify Therapeutic  
Targets in Hepatocellular Carcinoma.  
Front. Oncol. 12:814120.  
doi: 10.3389/fonc.2022.814120

Hepatocellular carcinoma (HCC) is the fourth cause of cancer-related mortality worldwide. While many targeted therapies have been developed, the majority of HCC tumors do not harbor clinically actionable mutations. Protein-level aberrations, especially those not evident at the genomic level, present therapeutic opportunities but have rarely been systematically characterized in HCC. In this study, we performed proteogenomic analyses of 260 primary tumors from two HBV-related HCC patient cohorts with global mass-spectrometry (MS) proteomics data. Combining tumor-normal and inter-tumor analyses, we identified overexpressed targets including PDGFRB, FGFR4, ERBB2/3, CDK6 kinases and MFAP5, HMCN1, and Hsp proteins in HCC, many of which showed low frequencies of genomic and/or transcriptomic aberrations. Protein expression of FGFR4 kinase and Hsp proteins were significantly associated with response to their corresponding inhibitors. Our results provide a catalog of protein targets in HCC and demonstrate the potential of proteomics approaches in advancing precision medicine in cancer types lacking druggable mutations.

**Keywords:** hepatocellular carcinoma, proteomics, targeted therapy, precision oncology, proteogenomics

## INTRODUCTION

Hepatocellular carcinoma (HCC) is the sixth most common cancer and the fourth cause of cancer-related mortality worldwide (1). The currently FDA-approved available therapies include the multikinase inhibitors sorafenib (2), regorafenib (3), lenvatinib (4), and cabozantinib (5); the VEGFR2 antagonist ramucirumab (6), the immune checkpoint inhibitors pembrolizumab (7) and nivolumab (8) [alone or in combination with ipilimumab (9)], and the combination of atezolizumab and bevacizumab (10). Unfortunately, the survival benefits conferred by these treatments are typically limited to a few months. One grand challenge for identifying personalized and effective treatment options in HCC is the limited number of druggable mutations found in an average HCC patient (1). A compelling and underexplored strategy to identify novel drug targets and implement precision medicine for HCC patient is the discovery of aberrant protein targets not readily detected by genomic analyses that could serve as effective and selective drug targets.

Recent advancements in mass spectrometry (MS) technology have enabled the rapid expansion of global proteomic datasets that quantify almost the entirety of expressed proteins in primary tumor cohorts (11–18). The resulting proteomes of primary tumor cohorts provide ample opportunities for investigating protein-level aberrations that may be of clinical utility as prognostic biomarkers or therapeutic targets, including PAK1/PTK2/RIPK2 in breast cancer (19) and Rb phosphoprotein in colorectal cancer (13). However, protein aberrations have historically remained less characterized than genomic aberrations and systematic analyses to identify such targets are urgently needed (20–23). Further, upon the computational prioritization of protein targets, validation of their therapeutic viability requires a wide array of functional models representing inter-tumor heterogeneity observed across human tumors (24).

Herein, we identify and validate protein expression-driven therapeutic targets in HCC by utilizing recently generated global MS proteomic data from two human cohorts. Multiple kinases and other proteins showed up-regulated tumor expression and/or overexpression in primary tumors, and many of these targets show little evidence of DNA or RNA level alterations. Several targets including FGFR4 kinase and Hsp proteins further showed expression-driven dependency where the HCC cell lines with high protein expression were vulnerable to their respective targeting inhibitors. Overall, these results suggest that proteomic-based approaches could identify precision targets in HCC and cancer cases lacking actionable mutations.

## RESULTS

### HCC Proteomics Cohorts

To test whether or not proteomics data could provide interesting drug targets for HCC we compiled genomic and global MS proteomic data from two cohorts of hepatitis B virus (HBV)-

related hepatocellular carcinoma patients (**Figure 1A**). (1) The HCC-Gao cohort: the Gao et al., 2019 study of 159 cases with matched-normal samples (25), and (2) The HCC-Jiang cohort: the Jiang et al., 2019 study of 101 cases and 98 matched-normal samples (16). We applied standardized normalization procedure and quality-control criteria (Methods) and retained 6,452 quantified proteins in the HCC-Gao dataset and 4,500 proteins in the HCC-Jiang dataset. We also obtained a list of genes with corresponding drug compounds from the Drug-Gene Interaction database (DGIdb) (26); overlapping quantified proteins with this DGIdb druggable gene list, we identified 1,143 and 900 currently-druggable proteins in these HCC datasets, respectively. Given the higher coverage and larger sample size of the HCC-Gao cohort dataset, we present the HCC-Gao cohort's findings as primary results and present the HCC-Jiang cohort's findings second and confirmatory.

Oncogenic kinases are established therapeutic targets in multiple cancer types, and we further retained kinase proteins for subsequent analyses. Based on a previously curated list of 683 human kinase proteins (19, 27), the HCC-Gao and HCC-Jiang datasets included 298 and 197 well-quantified kinase proteins, respectively. Additionally, we annotated the proteins using ten oncogenic signaling pathways curated by TCGA PanCanAtlas, including the Cell Cycle, HIPPO signaling, MYC signaling, NOTCH signaling, oxidative stress response/NRF2, PI3K signaling, TGF $\beta$  signaling, receptor-tyrosine kinase (RTK)/RAS/MAP-Kinase signaling, TP53, and  $\beta$ -catenin/WNT signaling pathways (28).

### Differentially Expressed Proteins

For each cancer cohort, we performed a tumor-vs-normal paired analysis to identify differentially-expressed proteins (tumor-DEPs) by adjusting for potential confounding variables including age and gender using *limma* implementation in R (v3.42.2). DEP results from the HCC-Gao and HCC-Jiang

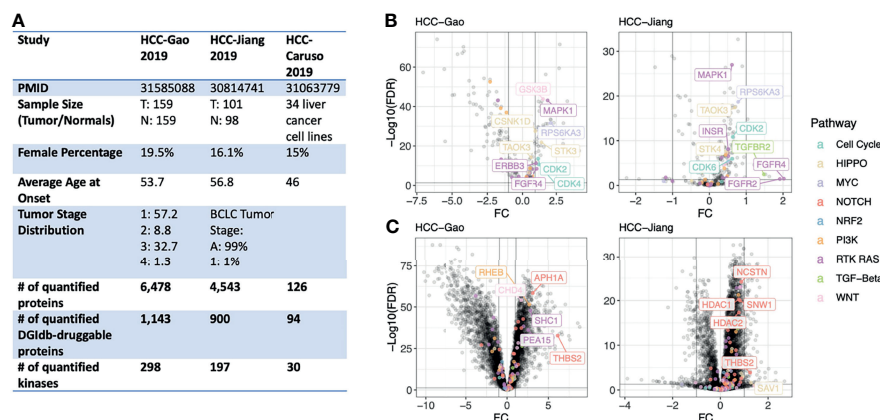


**FIGURE 1** | Study overview and differentially-expressed proteins in primary HCC tumors. **(A)** Overview of the proteogenomic datasets of human liver cancer cohorts and human liver cell lines analyzed in this study. **(B)** Volcano plots showing differentially-expressed kinase proteins between HCC tumor and normal liver samples in both the HCC-Gao and HCC-Jiang cohorts. The top differentially-expressed kinases from onco-signaling pathways are further labeled with text. **(C)** Volcano plots showing differentially-expressed non-kinase proteins between HCC tumor and normal liver samples in both the HCC-Gao and HCC-Jiang cohorts. The top differentially-expressed non-kinases from onco-signaling pathways are further labeled with text.

cohorts showed concordance (**Figure S1**). In the HCC-Gao cohort, we identified 265 significant kinase DEPs (*limma* differential expression test based on the empirical Bayes moderation of the t-statistics, false discovery rate [FDR] < 0.05), of which 31 were annotated within an oncogenic signaling pathway. Among the kinase DEPs in the HCC-Gao cohort, 9 showed over 2-fold of up-regulation in tumors, namely, MAPK1 (log2-fold-change [FC] = 1.9, FDR = 7.3e-44), GSK3B (FC = 1.6, FDR = 1.5e-44), RPS6KA3 (FC = 2.1, FDR = 2.3e-32), STK3 (FC = 1.4, FDR = 1.4e-22), CSNK1D (FC = 1, FDR = 2.9e-28), CDK2 (FC = 1.2, FDR = 2.5e-14), CDK4 (FC = 1.2, FDR = 2e-11), ERBB3 (FC = 1.1, FDR = 6e-12), and FGFR4 (FC = 1.1, FDR = 3.5e-9) (**Figure 1B**). Many of these kinases also showed significant up-regulation in tumors of the HCC-Jiang cohort, where for example FGFR4 kinase was also among the top-significant DEPs (FC = 2, FDR = 0.03) (**Figure 1B**).

Among the non-kinase proteins, we found 5,426 DEPs (FDR < 0.05) in HCC-Gao, of which 69 were annotated within an oncogenic signaling pathway. Among these, 18 showed over 2-fold of up-regulation, including THBS2 (FC = 6.1, FDR = 1.7e-33), APH1A (FC = 3.1, FDR = 3.6e-59), RHEB (FC = 2.7, FDR = 3e-52), SHC1 (FC = 2.8, FDR = 1.3e-48), and CHD4 (FC = 1.7, FDR = 6.8e-55) (**Figure 1C**). Notably, THBS2 protein was also significantly differentially-expressed (FC = 1.2, FDR = 1.3e-4) in the HCC-Jiang cohort (**Figure 1C**). HDAC1 and HDAC2 proteins showed up-regulation in tumors of both cohorts. The differential expression analyses discovered multiple proteins up-regulated in tumors compared to normal samples, and additional approaches are required to pinpoint therapeutic candidates.

## Protein Overexpression of Currently-Druggable Proteins

Many established protein targets in cancer (ex. HER2, EGFR, BRAF) are overexpressed in a fraction of tumor samples where their inhibition may show efficacy. To identify such

overexpressed proteins in global MS proteomics data, we applied our recently-developed OverExpressed Protein and Transcript target Identifier (OPPTI) algorithm (29) (Methods), which is tailored to detect overexpressed proteins from global MS proteomic cohorts that may show varied quantitative distributions due to different technical platforms.

Applying OPPTI to the HCC-Gao cohort, we identified 46 kinases that showed significant enrichment of marker overexpression (OPPTI permutation test for overexpressed markers, FDR < 0.05), including CDK6 (Protein overexpression rate [PRO] = 18.9%, FDR = 1.6e-07), EGFR (PRO = 11.9%, FDR = 0.006), and ERBB2 (PRO = 11.3%, FDR = 0.013) (**Figure 2A**). In the HCC-Jiang cohort, we identified 33 kinases that showed significant enrichment of protein overexpression (FDR < 0.05), including CDK6 (PRO = 19.2%, FDR = 5.4e-05) and PDGFRB (PRO = 24.4%, FDR = 9.5e-07) (**Figure 2A** and **Figure S2**). To ensure the robustness of the identified targets, we calculated the concordance of overexpression frequency observed in the HCC-Gao and HCC-Jiang cohorts. The kinase overexpression rates identified by OPPTI showed a high correlation between the two cohorts (Pearson correlation test,  $R = 0.44$ ,  $p = 5e-10$ ), where CDK6 and PDGFRB displayed the largest overexpression rates among the potential HCC drug targets (**Figure S3**). Despite the intrinsic and technical MS differences between the two HCC cohorts, the coherency provided cross-validating evidence for the identified targets. Among the non-kinase proteins, 1,329 markers were significantly overexpressed (OPPTI permutation test, FDR < 0.05) in the HCC-Gao cohort, and among them 359 were DGIdb druggable genes. In HCC-Jiang cohort, 641 markers were significantly overexpressed (FDR < 0.05), and among them 161 were DGIdb druggable genes. Overall, we identified 100 non-kinase DGIdb druggable proteins that were significantly overexpressed (FDR < 0.05) in both HCC cohorts, including POSTN, CYP3A5, ANXA3, ENO2, and VCAM1 (**Figure 2C** and **Figure S3**).

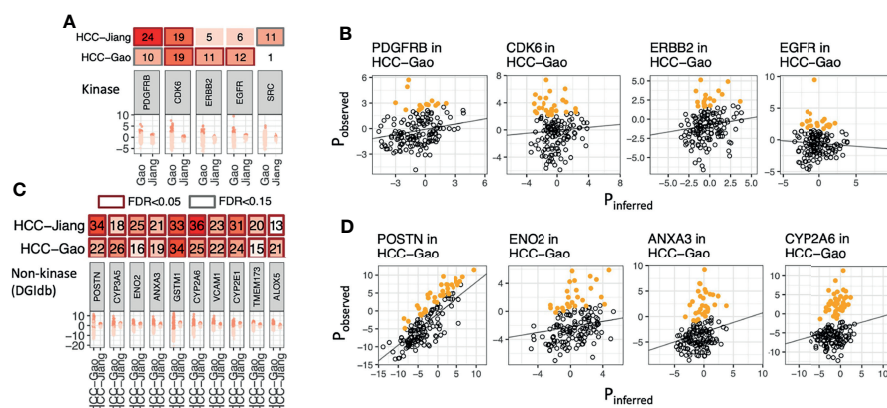


**FIGURE 2** | Overexpressed kinase and non-kinase proteins detected in human HCC tumors. **(A)** Protein kinases showing significant enrichment of overexpression as identified by OPPTI in either primary tumor cohort. **(B)** Sample-level kinase overexpression in HCC-Gao cohort of the markers shown in panel A, as identified by OPPTI through the deviation of observed protein expressions (y-axis) from the background inference (x-axis) and a cutoff value (not shown). **(C)** Ten non-kinase proteins showing the most significant enrichment of overexpression as identified by OPPTI in either primary tumor cohort. **(D)** Sample-level overexpression plots of the markers shown in panel C, as identified by OPPTI.



While both DEP and overexpressed proteins present plausible methods to identify expression-based therapeutic targets, it remains unclear whether targets discovered by the two approaches overlap. We intersected the significant DEPs and the significant overexpressed markers to enhance confidence of identifying therapeutic targets (**Figure 3C**). In the HCC-Gao cohort, 187 kinases were quantified among the DGIdb druggable genes and 75 of them showed positive values in both differential expression and protein overexpression (**Figure 3A**). Among these, 3 kinases showed significant DE (limma differential expression test based on the empirical Bayes moderation of the t-statistics,  $FC \geq 1$ ,  $FDR < 0.05$ ) and overexpression (OPPTI permutation test,  $FDR < 0.05$ ), namely, NME1 ( $FC = 1.4$ ,  $FDR = 5.0e-16$ ;  $PRO = 18.2\%$ ,  $FDR = 1.6e-07$ ), FGFR4 ( $FC = 1.1$ ,  $FDR = 3.5e-09$ ;  $PRO = 12.6\%$ ,  $FDR = 0.0026$ ), ERBB3 ( $FC = 1.1$ ,  $FDR = 6.0e-12$ ;  $PRO = 10.7\%$ ,  $FDR = 0.027$ ), as the RAS pathway (with FGFR4 and ERBB3 kinases) showed the most significant dysregulation. Other notable kinases were CDK6 from Cell Cycle pathway ( $FC = 0.8$ ,  $FDR = 2.1e-4$ ;  $PRO = 18.9\%$ ,  $FDR = 1.6e-07$ ), and PDK1 from PI3K pathway ( $FC = 0.8$ ,  $FDR = 1.5e-05$ ;  $PRO = 12.6\%$ ,  $FDR = 0.0026$ ).

Among the non-kinase targets we found 951 DGIdb druggable proteins quantified in the HCC-Gao cohort tumors, and 336 of them showed positive values in both differential expression and protein overexpression (**Figure 3B**). Among these, 68 kinases showed significant DE ( $FC \geq 1$ ,  $FDR < 0.05$ ) and overexpression ( $FDR < 0.05$ ), including, TXN ( $FC = 5.6$ ,  $FDR = 2.7e-32$ ;  $PRO = 22\%$ ,  $FDR < 1e-100$ ), POSTN ( $FC = 5$ ,  $FDR = 4.6e-17$ ;  $PRO = 22\%$ ,  $FDR < 1e-100$ ), and F5 ( $FC = 1.9$ ,  $FDR = 8.5e-26$ ;  $PRO = 13.8\%$ ,  $FDR = 4.1e-4$ ). In HCC-Jiang cohort we found 774 quantified DGIdb druggable proteins, and 366 of them showed positive values in both differential expression and protein overexpression (**Figure 3A**). Notably, 6 proteins showed significant DE ( $FC \geq 1$ ,  $FDR < 0.05$ ) and overexpression ( $FDR < 0.05$ ), including, POSTN and F5 ( $FC = 1.2$ ,

$FDR = 1.5e-08$ ;  $PRO = 34.2\%$ ,  $FDR < 1e-100$ ; and  $FC = 1.1$ ,  $FDR = 2.3e-14$ ;  $PRO = 16.5\%$ ,  $FDR = 7.8e-4$ , respectively), which were also identified in the HCC-Gao cohort. Several of the kinases have corresponding inhibitor drugs in clinical trials, and it remains to be validated whether the inhibitions of other DEP- and OPPTI-identified targets could serve as treatment strategies.

## Comparison Between DNA, RNA, and Protein-Level Alterations

Protein-level overexpression can arise from genomic alterations (i.e., copy-number amplification) but they may also arise post-transcriptionally and thus not readily observed at DNA or RNA levels. To examine these two competing hypotheses, we systematically compared the frequency of patients showing protein overexpression versus those carrying genomic mutations or transcriptomic aberrations. In the HCC-Gao cohort, we identified the fraction of cases having one or more recurrent missense or truncating mutations in the same genes. We then compared the fraction of HCC cases carrying these somatic mutations with those showing protein overexpression detected by OPPTI (**Figure 4A**). There were 127 genes with genomic alterations in the oncogenic signaling pathways with available protein quantification. HCC is known for the lack of actionable mutations, and as expected, no overexpressed kinases showed a genomic alteration rate greater than 5%. We thus investigated protein-level events that may arise independent of mutations. Five kinases from RAS pathway showed substantial protein up-regulation ( $PRO > 10\%$ ) with limited genomic alterations (likely driver), namely, ERBB2 ( $PRO = 11.3\%$ ,  $DNA = 0\%$ ), ERBB3 ( $PRO = 10.7\%$ ,  $DNA = 0\%$ ), PDGFRB ( $PRO = 10.1\%$ ,  $DNA = 0\%$ ), EGFR ( $PRO = 11.9\%$ ,  $DNA = 0\%$ ), and FGFR4 ( $PRO = 12.6\%$ ,  $DNA = 0\%$ ). (**Figures 4A, B**). Other proteins showing higher protein overexpression vs. driver genomic alteration rates include MFAP5 ( $PRO = 27.7\%$ ,  $DNA = 0\%$ ), HMCN1

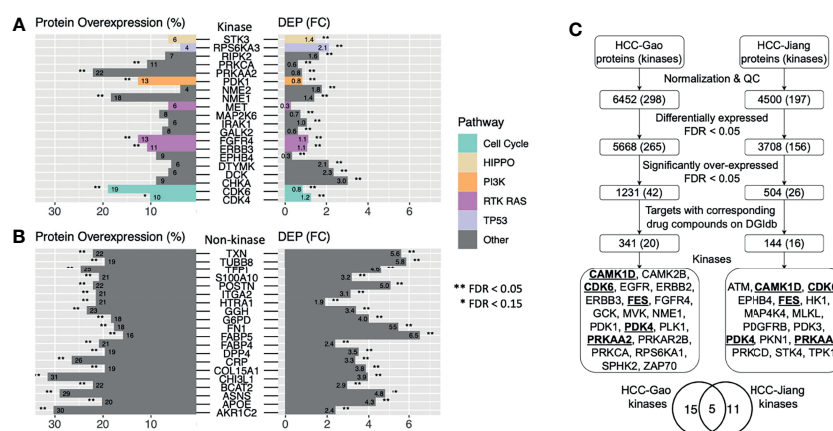


**FIGURE 3 |** Candidate HCC protein targets showing protein overexpression, differential expression in tumor vs. normal tissues, and drug compounds as indicated by DGIdb. **(A)** Druggable kinases with corresponding drug compounds based on DGIdb that showed significantly higher tumor vs. normal expression and protein overexpression in the HCC-Gao cohort. **(B)** Druggable non-kinase proteins with corresponding drug compounds based on DGIdb that showed significantly higher tumor vs. normal expression and protein overexpression in the HCC-Gao cohort. **(C)** Flowchart showing the steps in the pipeline that generated the candidate HCC protein targets from two HCC cohorts.

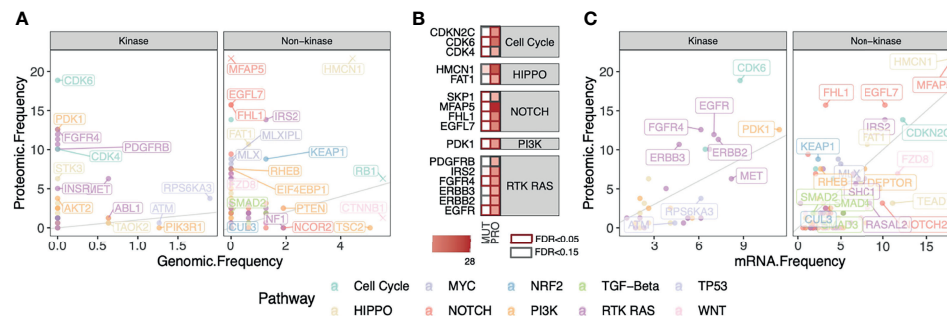


**FIGURE 4** | Comparison between fractions of cases carrying DNA, RNA, and Protein-level alterations in kinase and non-kinase targets in HCC. **(A)** Fractions of HCC cases carrying truncating or recurrent missense somatic mutations in the oncogenic signaling pathways compared to those showing protein overexpression in the HCC-Gao cohort. Top markers with high genomic and/or proteomic alterations are labeled. For better visualization of other data points, the outlying values of HMCN1 (original values: DNA = 4.4%, PRO = 22.6%), MFAP5 (DNA = 0%, PRO = 27.7%), RB1 (DNA = 5.7%, PRO = 6.3%), and CTNNB1 (original values: DNA = 18.4%, PRO = 1.3%), are truncated. **(B)** Proteins in panel A that show significant enrichment of protein overexpression (FDR < 0.15) tend to have low fractions of somatic mutations. **(C)** Fractions of HCC cases showing mRNA and protein overexpression frequencies of the genes in oncogenic signaling pathways in HCC-Gao cohort. The outlying values of HMCN1 (original values: RNA = 20%, PRO = 22.6%) and MFAP5 (RNA = 40%, PRO = 27.7%) are truncated.

(PRO = 22.6%, DNA = 4.4%), FHL1 (PRO = 15.7%, DNA = 0%), and EGFL7 (PRO = 15.7%, DNA = 0%). (**Figure 4B**).

We next compared protein overexpression to their respective mRNA overexpression by applying OPPTI with the same parameters to the RNA-Seq data available for the HCC-Gao cohort (Methods). We found two proteins with substantial rates of mRNA overexpression and protein overexpression, MFAP5 (mRNA overexpression rate [RNA] = 40%, PRO = 28%) and HMCN1 (RNA = 20%, PRO = 22.6%). We also found 4 proteins that showed significant protein up-regulation (PRO  $\geq$  10%) and higher ( $\geq$  2-fold) protein overexpression rate than transcriptomic alteration rate, including CDK6 (RNA = 8.8%, PRO = 18.9%), FHL1 (RNA = 3.2%, PRO = 15.7%), FGFR4 (RNA = 6.1%, PRO = 12.6%), ERBB3 (RNA = 4.7%, PRO = 10.7%). (**Figure 4C**). Our results confirm the paucity of targets with genomic alteration in HCC and further demonstrate that a proteomic approach can uniquely identify a considerable fraction of overexpressed targets showing apparent aberrations at the protein level but not readily identified at the mRNA level.

## Validation of Therapeutic Efficacy Using Drug Screen Data

To validate the therapeutic potential of the protein targets that we identified in the primary tumor cohorts, we integrated the *in vitro* drug screen data of 31 anticancer agents on 34 human HCC cell lines available from Caruso et al. (30). For each drug, we analyzed the association between baseline protein expression levels (measured by Reverse Phase Protein Assay [RPPA]) and cell viability after treatment to identify expression-driven dependencies (Methods), where a negative association suggested HCC cells with high protein expression showed lower viability and were more vulnerable to the targeting drug. We first analyzed expression-driven dependencies of 40 genes encoding kinases that were known targets (antibodies) of the 31 screened compounds (30). We found several drug-protein associations (**Figure 5A**).

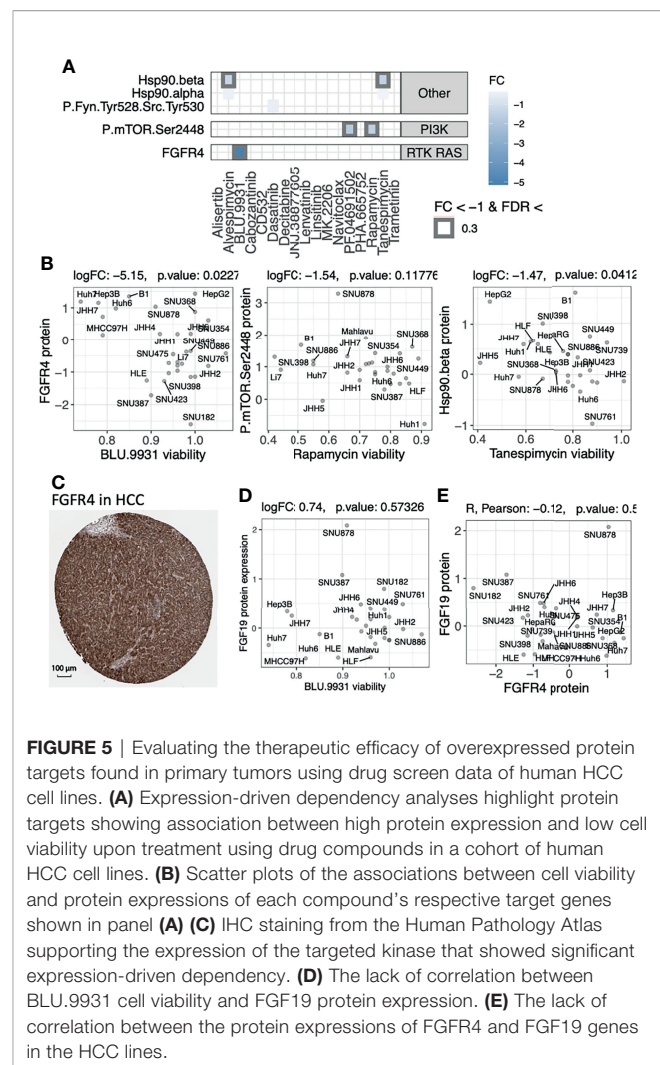


**FIGURE 5** | Evaluating the therapeutic efficacy of overexpressed protein targets found in primary tumors using drug screen data of human HCC cell lines. **(A)** Expression-driven dependency analyses highlight protein targets showing association between high protein expression and low cell viability upon treatment using drug compounds in a cohort of human HCC cell lines. **(B)** Scatter plots of the associations between cell viability and protein expressions of each compound's respective target genes shown in panel **(A)**. **(C)** IHC staining from the Human Pathology Atlas supporting the expression of the targeted kinase that showed significant expression-driven dependency. **(D)** The lack of correlation between BLU.9931 cell viability and FGF19 protein expression. **(E)** The lack of correlation between the protein expressions of FGFR4 and FGF19 genes in the HCC lines.

FGFR4 expression was negatively associated with viability of cells treated with BLU.9931 compound (FC = -5.15, p-value [p] = 0.02, **Figure 5B**), validating the FGFR4 inhibitor's efficacy in HCCs with up-regulated FGF19-FGFR4 signaling (31). FGFR4 protein expression was also orthogonally detected by immunohistochemistry (IHC) of HCC patient tumor samples in the human pathology atlas project (**Figure 5C**). MTOR expression (P.mTOR.Ser2448) was suggestively associated with the drug responses of Rapamycin (FC = -1.5, p = 0.12) and PF.04691502 (FC = -1.7, p = 0.19) (**Figure S5A**). Among the non-kinase targets, we found two associations between the expression of HSP90AB1 (Hsp90.beta) and the drug responses to Hsp90 protein inhibitors Tanespimycin (FC = -1.5, p = 0.04) and Alvospimycin (FC = -1.3, p = 0.07) (**Figure 5B** and **Figure S5B**). These results highlight FGFR4 and Hsp (HSP90AB4P) proteins as candidate therapeutic targets showing both up-regulation in HCC tumors and expression-driven dependencies.

FGFR4 is a receptor for the growth factor FGF19, whose up-regulation is thought to promote proliferation and tumorigenesis. The FGFR inhibitor BLU.9931 was previously shown to be effective against HCC xenograft tumors with amplified FGF19 (31). FGF19 protein expression (as evaluated by IHC) was further used to stratify patients for another selective FGFR4 inhibitor fisogatinib (BLU-554), where 17% (N=11/66) of the FGF19-positive patients responded compared to 0% (N=0/32) of the FGF19-negative patients (32). However, we did not observe a correlation between FGF19 upregulation and response to BLU.9931 in the human HCC cell lines (**Figure 5D**), which may be explained by the poor correlation between the FGFR4 and FGF19 protein expressions (**Figure 5E**). Analyzing data from the primary HCC tumor cohort, we also observed a lack of correlation between FGFR4 protein or mRNA expression and FGF19 gene expression levels (**Figure S6**). Phosphorylation data also showed a lack of correlation between FGFR4 (s573) phosphorylation and FGF19 gene expression levels but a strong correlation to FGFR4 protein expression (R = 0.57, p = 8.9E-13, **Figure S6**). These results imply that response to FGFR4 inhibitors and patient selection may be improved by using FGFR4 biomarkers in addition to FGF19 alone, and mechanistic intricacies in FGFR4/FGF19 signaling remain to be further determined.

## DISCUSSION

We report a proteo-genomic evaluation of aberrant protein targets in 260 primary tumors from two HBV-related HCC cohorts (**Figure 1**). Tumor-normal and inter-tumor analyses of protein expression data highlighted multiple aberrantly-expressed protein targets in key signaling pathways, including PDGFRB, CDK6, ERBB2, and EGFR (**Figures 2, 3**) whose protein overexpression in HCC tumors are also validated by IHC data from the Human Pathology Atlas (**Figure S7**). By integrating mutation, mRNA expression, and protein expression data, our proteogenomic analyses determined whether the overexpressed protein targets were concordant with genomic

evidence or arose without genomic or transcriptomic alterations (**Figure 4**). Finally, the therapeutic viability of the identified targets was evaluated by analyzing drug screen data in human cell lines, implicating proteins whose up-regulation correlate with treatment response (**Figure 5**). These series of analyses have identified a list of prominent targets in HCC-Gao/-Jiang cohorts and the HCC-Caruso study (**Supplementary Tables 1, 2**).

Genome-based precision oncology in HCC poses a challenge where potentially targetable driver alterations are only identified in less than 30% of the patients (33). Proteomic analyses enabled us to identify new potentially targetable overexpressed proteins that may correspond to limited driver alterations, such as PDGFRB, ERBB2/3, EGFR and FGFR4 kinases upregulated in HCC tumors arising from no genomic driver alterations, as well as the non-kinase proteins such as MFAP5, HMCN1, EGFL7 and FHL1. Possible therapies for the overexpressed kinases include CDK4/CDK6 inhibitors, such as Palbociclib, which has been shown effective in human liver cancer cell lines and mouse models with intact tumor suppressor Retinoblastoma (Rb1) (34). ERBB2 could also be explored as a potential target in HCC, as evidence supports its involvement in liver tumorigenesis and intravenous injection of HER2-inhibitor Trastuzumab limited HCC growth *in vivo* (35). Similarly, ERBB3 is overexpressed in hepatitis B-associated HCC, which are sensitive to ERBB3 inhibition (36). Erlotinib, an EGFR inhibitor, has been shown to be effective in patients treated with Lenvatinib as they upregulate EGFR, further supporting the role of EGFR as a biomarker (37).

By using human HCC cell lines that represent the heterogeneity observed in HCC patients, we evaluated the potential therapeutic efficacy of targets identified in primary tumors and showed protein expression of selected targets can predict treatment response. In particular, we found that the expression of FGFR4 kinase were significantly associated with drug response and may be a useful biomarker for FGFR4 inhibitors in addition to the currently-used FGF19 expression (31, 32). In addition, we observed a trend of improved recurrence-free survival in the HCC-Gao patients that did not overexpress FGFR4 protein compared to those overexpressing FGFR4 (p = 0.087; FGFR4-not-overexpressed median survival 23.2 months; FGFR4-overexpressed median survival 9.5 months) (**Figure S8**), although the association did not reach statistical significance and require validation in future larger-scale cohorts. Given the partial success of FGFR4 inhibitors in HCC patients, additional FGFR4 inhibitors have been developed and are under evaluation (38). Furthermore, tumors with elevated Hsp protein expression and MTOR phosphorylation may be more vulnerable to Hsp90 inhibitors and mTOR inhibitors such as rapamycin; other studies have also suggested that MTOR phosphorylation may be a better biomarker for mTOR inhibitors than genetic alterations in PTEN or TSC1/TSC2 (39).

In this study, the profiled primary HCC tumors collected in human cohorts are all related to HBV infection. This might pose a limitation as our findings may represent the HBV-specific



features underlying the HBV-related HCC. Expanding the generalizability of the targets identified herein requires further investigation using the HCC cases related to different primary causes. The proteomic analyses of patient cohorts herein rely on global MS data, which can be time- and resource-intensive to generate in a clinical setting. Once the relevant protein markers are identified in these discovery studies, development of targeted assays using antibody-based (ex. IHC) or targeted MS technologies (ex. selected reaction monitoring) would be required.

To conclude, by employing a multi-omics approach, we investigated protein-level aberrations showing limited DNA or RNA level alterations in two human HCC cohorts and identified potential therapeutic targets showing expression-driven dependency upon targeting inhibitory treatment in human HCC cell lines; FGFR4 kinase and Hsp proteins, lacking actionable mutations, may be targetable in a fraction of HCC as supported by the vulnerability exposed by their respective targeting inhibitors. We believe that integrating proteomics data represents an unprecedented opportunity for the discovery of effective drug targets that may not be readily observed by genomic analyses in HCC and other cancer types.

## METHODS

### Data Sources, Download, and Standardized Normalization

The proteomic and genomic datasets of HBV-related Hepatocellular Carcinoma (HCC-Gao cohort) were downloaded from The National Cancer Institute's Clinical Proteomic Tumor Analysis Consortium (CPTAC) (25). This cohort contained 159 tumor samples with matched controls, and 6,478 unique proteins were quantified (of which 298 were kinases). The transcriptomic dataset was downloaded from <https://www.biosino.org/node/project/detail/OEP000321>. Proteomic and transcriptomic datasets of the other HBV-related HCC cohort (HCC-Jiang cohort) were downloaded from related publication (16). There were 101 tumor samples in the HCC-Jiang cohort with 98 matched controls. This cohort contained 7,878 unique proteins (of which 369 were kinases). The RNA-seq data contained gene expression profiles of 35 pairs of tumor and control samples, quantified by tophat-cufflinks pipeline. 16,457 protein-coding genes were identified with FPKM > 1 in more than one sample (of which 634 were kinase-encoding). For HCC-Jiang and HCC-Gao transcriptomics data, we used the quantile normalization and log2 normalization on the FPKM-normalized RNA-seq counts and filtered out genes showing no expression in at least 20% of the samples.

We examined the data distribution of each cancer proteomic cohort and performed a standardized normalization procedure for each dataset. Each sample within a cancer cohort is normalized by its Median Absolute Deviation (MAD), so that every sample across the datasets are normalized to unit MAD. We also filtered out protein markers with high fractions (at least 20%) of missing values.

### Identification of Differentially-Expressed Proteins

For each cohort, we performed a paired (tumor against matched-normal) analysis to identify differentially-expressed proteins by using the *limma* R package (v3.42.2). We corrected our analyses for confounding variables arising from batch effects when available (TMT batch, sequencing center/operator/date) or from demographics (age, gender), and the resulting p-values were multi-testing corrected using the BH procedure for FDR. For the majority of markers, we did not observe any significant confounding effect between protein expressions and the clinical variables age and gender (**Supplementary Table 3**); the only suggestive association was observed between the HSP09AB4P protein expression showing negative correlation with patient age in HCC-Jiang cohort (**Figure S9**,  $p=0.038$  before multiple-testing correction).

### Detection of Overexpressed Proteins/Genes

To identify overexpressed markers, we used the OPPTI method (29). OPPTI is based on comparing expression levels to an inferred expression level in each tumor sample computed by a weighted k-nearest neighbor (KNN) algorithm, where the nearest features are the abundance level of other co-expressed markers. OPPTI performs a permutation test in order to evaluate the statistical significance of a marker's potential enrichment of overexpression events. For a given cancer cohort, the dysregulation scores are permuted within every sample between the proteins, and the null overexpressions are computed from this data. After iterating this process multiple times, the null overexpressions accumulated from all iterations are used to establish the permutation distribution.

### Somatic Mutations and Comparison With Proteomic Overexpression

We reasoned that protein-truncating or recurrent somatic mutations were more likely to be functional. We thus retained all truncations (i.e., frameshift/non-frameshift deletion/insertion/substitution, stop-gain, stop-loss) present in the HCC-Gao cohort. Given the smaller size of this cohort, we also considered all missense mutations that have at least three occurrences in the open-access mutation call set files from the MC3 project of TCGA PanCanAtlas that applied standardized variant-calling pipeline and quality control processes (40).

### Analyses of Drug Screening Data in HCC Cell Lines

We downloaded the *in vitro* drug screen data on human HCC cell lines from Caruso et al. (30). We calculated the association of drug response with protein expression by using *limma* implementation in R (v3.40.6). For each drug, we performed the linear regression between the cell viabilities upon drug treatment and the targeted protein's expressions across the drug-treated cell lines and obtained



the corresponding coefficient of the linear fit. The resulting p-values were multi-testing corrected using the BH procedure for FDR.

## DATA AVAILABILITY STATEMENT

The original contributions presented in the study are included in the article/**Supplementary Material**. Further inquiries can be directed to the corresponding author. OPPTI is available on GitHub: <https://github.com/Huang-lab/oppti>. Analyses were conducted based on scripts written using the R programming language version 3.6.2.

## AUTHOR CONTRIBUTIONS

AE and KH designed the analyses. AE conducted the bioinformatics analyses and KH supervised the study. AE, AL, and KH wrote and edited the manuscript. All authors contributed to the article and approved the submitted version.

## REFERENCES

- Villanueva A. Hepatocellular Carcinoma. *New Engl J Med* (2019) 380:1450–62. doi: 10.1056/NEJMra1713263
- Llovet JM, Ricci S, Mazzaferro V, Hilgard P, Gane E, Blanc JF, et al. Sorafenib in Advanced Hepatocellular Carcinoma. *New Engl J Med* (2008) 359:378–90. doi: 10.1056/NEJMoa0708857
- Bruix J, Qin S, Merle P, Granito A, Huang YH, Bodoky G, et al. Regorafenib for Patients With Hepatocellular Carcinoma Who Progressed on Sorafenib Treatment (RESORCE. A Randomised, Double-Blind, Placebo-controlled, Phase 3 Trial. *Lancet* (2017) 389(10064):56–66. doi: 10.1016/S0140-6736(16)32453-9
- Kudo M, Finn RS, Qin S, Han KH, Ikeda K, Piscaglia F, et al. Lenvatinib Versus Sorafenib in First-Line Treatment of Patients With Unresectable Hepatocellular Carcinoma: A Randomised Phase 3 Non-Inferiority Trial. *Lancet* (2018) 391:1163–73. doi: 10.1016/S0140-6736(18)30207-1
- Abou-Alfa GK, Meyer T, Cheng AL, El-Khoueiry AB, Rimassa L, Ryoo BY, et al. Cabozantinib in Patients With Advanced and Progressing Hepatocellular Carcinoma. *New Engl J Med* (2018) 379:54–63. doi: 10.1056/NEJMoa1717002
- Zhu AX, Kang YK, Yen CJ, Finn RS, Galle PR, Llovet JM, et al. Ramucirumab After Sorafenib in Patients With Advanced Hepatocellular Carcinoma and Increased  $\alpha$ -Fetoprotein Concentrations (REACH-2): A Randomised, Double-Blind, Placebo-Controlled, Phase 3 Trial. *Lancet Oncol* (2019) 20:282–96. doi: 10.1016/S1470-2045(18)30937-9
- Zhu AX, Finn RS, Cattani S, Edeline J, Ogasawara S, Palmer DH, et al. Pembrolizumab in Patients With Advanced Hepatocellular Carcinoma Previously Treated With Sorafenib (KEYNOTE-224): A non-Randomised, Open-Label Phase 2 Trial. *Lancet Oncol* (2018) 19:940–52. doi: 10.1016/S1470-2045(18)30351-6
- El-Khoueiry AB, Sangro B, Crocenzi TS, Kudo M, Hsu C, Yau T, et al. Nivolumab in Patients With Advanced Hepatocellular Carcinoma (CheckMate 040): An Open-Label, non-Comparative, Phase 1/2 Dose Escalation and Expansion Trial. *Lancet* (2017) 389:2492–502. doi: 10.1016/S0140-6736(17)31046-2
- Sangro B, Sangro B, Yau T, Crocenzi TS, Kudo M, Hsu C, et al. A Phase III, Double-Blind, Randomized Study of Nivolumab (NIVO) and Ipilimumab (IPI), Nivo Monotherapy or Placebo Plus Transarterial Chemoembolization (TACE) in Patients With Intermediate-Stage Hepatocellular Carcinoma (HCC). *J Clin Oncol* (2021) 39:TPS349–9. doi: 10.1200/JCO.2021.39.3\_suppl.TPS349

## FUNDING

This work was supported by Damon Runyon-Rachleff Innovation Award (DR52-18) and NIH/NCI R37 Merit Award (R37CA230636) to AL, as well as NIGMS R35GM138113 to KH. The Tisch Cancer Institute and related research facilities are supported by P30 CA196521.

## ACKNOWLEDGMENTS

The authors wish to acknowledge the participating patients and families who generously contributed to the datasets. We thank S. Caruso for helpful discussions on drug screen data of HCC cell lines.

## SUPPLEMENTARY MATERIAL

The Supplementary Material for this article can be found online at: <https://www.frontiersin.org/articles/10.3389/fonc.2022.814120/full#supplementary-material>

- Finn RS, Qin S, Ikeda M, Galle PR, Ducreux M, Kim TY, et al. Atezolizumab Plus Bevacizumab in Unresectable Hepatocellular Carcinoma. *New Engl J Med* (2020) 382:1894–905. doi: 10.1056/NEJMoa1915745
- Ellis MJ, Gillette M, Carr SA, Paulovich AG, Smith RD, Rodland KK, et al. Connecting Genomic Alterations to Cancer Biology With Proteomics: The NCI Clinical Proteomic Tumor Analysis Consortium. *Cancer Discov* (2013) 3:1108–12. doi: 10.1158/2159-8290.CD-13-0219
- Dou Y, Kawaler EA, Cui Zhou D, Gritsenko MA, Huang C, Blumenberg L, et al. Proteogenomic Characterization of Endometrial Carcinoma. *Cell* (2020) 180(4):729–48.e26. doi: 10.1016/j.cell.2020.01.026
- Vasaikar S, Huang C, Wang X, Petyuk VA, Savage SR, Wen B, et al. Proteogenomic Analysis of Human Colon Cancer Reveals New Therapeutic Opportunities. *Cell* (2019) 177(4):1035–49.e19. doi: 10.1016/j.cell.2019.03.030
- Clark DJ, Dhanasekaran SM, Petralia F, Pan J, Song X, Hu Y, et al. Integrated Proteogenomic Characterization of Clear Cell Renal Cell Carcinoma. *Cell* (2019) 179(4):964–83.e31. doi: 10.1016/j.cell.2019.10.007
- Mun DG, Bhin J, Kim S, Kim H, Jung JH, Jung Y, et al. Proteogenomic Characterization of Human Early-Onset Gastric Cancer. *Cancer Cell* (2019) 35(1):111–24.e10. doi: 10.1016/j.ccell.2018.12.003
- Jiang Y, Sun A, Zhao Y, Ying W, Sun H, Yang X, et al. Proteomics Identifies New Therapeutic Targets of Early-Stage Hepatocellular Carcinoma. *Nature* (2019) 567:257–61. doi: 10.1038/s41586-019-0987-8
- Sinha A, Huang V, Livingstone J, Wang J, Fox NS, Kurganovs N, et al. The Proteogenomic Landscape of Curable Prostate Cancer. *Cancer Cell* (2019) 35(3):414–27.e6. doi: 10.1016/j.ccell.2019.02.005
- Archer TC, Ehrenberger T, Mundt F, Gold MP, Krug K, Mah CK, et al. Proteomics, Post-Translational Modifications, and Integrative Analyses Reveal Molecular Heterogeneity Within Medulloblastoma Subgroups. *Cancer Cell* (2018) 34(3):396–410.e8. doi: 10.1016/j.ccell.2018.08.004
- Mertins P, Mani DR, Ruggles KV, Gillette MA, Clauser KR, Wang P, et al. Proteogenomics Connects Somatic Mutations to Signalling in Breast Cancer. *Nature* (2016) 534:55–62. doi: 10.1038/nature18003
- Huang K, Li S, Mertins P, Cao S, Gunawardena HP, Ruggles KV, et al. Proteogenomic Integration Reveals Therapeutic Targets in Breast Cancer Xenografts. *Nat Commun* (2017) 8:14864. doi: 10.1038/ncomms14864
- Huang K, Scott AD, Zhou DC, Wang LB, Weerasinghe A, Elmas A, et al. Spatially Interacting Phosphorylation Sites and Mutations in Cancer. *Nat Commun* (2021) 12:2313. doi: 10.1038/s41467-021-22481-w
- Huang K, Wu Y, Primeau T, Wang YT, Gao Y, McMichael JF, et al. Regulated Phosphosignaling Associated With Breast Cancer Subtypes and

- Druggability. *Mol Cell Proteomics* (2019) 18(8):1630–50. doi: 10.1074/mcp.RA118.001243
23. Ruggles K, Krug K, Wang X, Clauser KR, Wang J, Payne SH, et al. Methods, Tools and Current Perspectives in Proteogenomics. *Mol Cell Proteomics* (2017) 16(6):959–81. doi: 10.1074/mcp.MR117.000024
  24. Molina-Sánchez P, Ruiz de Galarreta M, Yao MA, Lindblad KE, Bresnahan E, Bitterman E, et al. Cooperation Between Distinct Cancer Driver Genes Underlies Intertumor Heterogeneity in Hepatocellular Carcinoma. *Gastroenterology* (2020) 159:2203–20.e14. doi: 10.1053/j.gastro.2020.08.015
  25. Gao Q, Zhu H, Dong L, Shi W, Chen R, Song Z, et al. Integrated Proteogenomic Characterization of HBV-Related Hepatocellular Carcinoma. *Cell* (2019) 179:561–77.e22. doi: 10.1016/j.cell.2019.08.052
  26. Cotto KC, Wagner AH, Feng YY, Kiwala S, Coffman AC, Spies G, et al. DGIdb 3.0: A Redesign and Expansion of the Drug-Gene Interaction Database. *Nucleic Acids Res* (2018) 46:D1068–73. doi: 10.1093/nar/gkx1143
  27. Manning G, Whyte DB, Martinez R, Hunter T, Sudarsanam S. The Protein Kinase Complement of the Human Genome. *Sci (New York N.Y.)* (2002) 298:1912–34. doi: 10.1126/science.1075762
  28. Sanchez-Vega F, Mina M, Armenia J, Chatila WK, Luna A, La KC, et al. Oncogenic Signaling Pathways in The Cancer Genome Atlas. *Cell* (2018) 173:321–337.e10. doi: 10.1016/j.cell.2018.03.035
  29. Elmas A, Tharakan S, Jaladanki S, Galsky MD, Liu T, Huang KL. Pan-Cancer Proteogenomic Investigations Identify Post-Transcriptional Kinase Targets. *Commun Biol* (2021) 4(1):1112. doi: 10.1038/s42003-021-02636-7
  30. Caruso S, Calatayud AL, Pilet J, La Bella T, Rekik S, Imbeaud S, et al. Analysis of Liver Cancer Cell Lines Identifies Agents With Likely Efficacy Against Hepatocellular Carcinoma and Markers of Response. *Gastroenterology* (2019) 157:760–76. doi: 10.1053/j.gastro.2019.05.001
  31. Hagel M, Miduturu C, Sheets M, Rubin N, Weng W, Stransky N, et al. First Selective Small Molecule Inhibitor of FGFR4 for the Treatment of Hepatocellular Carcinomas With an Activated FGFR4 Signaling Pathway. *Cancer Discov* (2015) 5:424–37. doi: 10.1158/2159-8290.CD-14-1029
  32. Kim RD, Sarker D, Meyer T, Yau T, Macarulla T, Park JW, et al. First-In-Human Phase I Study of Fisogatinib (BLU-554) Validates Aberrant FGF19 Signaling as a Driver Event in Hepatocellular Carcinoma. *Cancer Discov* (2019) 9:1696 LP – 1707. doi: 10.1158/2159-8290.CD-19-0555
  33. Ludmil B. Exome Sequencing of Hepatocellular Carcinomas Identifies New Mutational Signatures and Potential Therapeutic Targets Disclaimer : Europe PMC Funders Author Manuscripts Exome Sequencing of Hepatocellular Carcinomas Identifies New Mutational Signatures and. *Nat Genet* (2016) 47:505–11. doi: 10.1038/ng.3252
  34. Bollard J, Miguela V, Ruiz de Galarreta M, Venkatesh A, Bian CB, Roberto MP, et al. Palbociclib (PD-0332991), a Selective CDK4/6 Inhibitor, Restricts Tumour Growth in Preclinical Models of Hepatocellular Carcinoma. *Gut* (2017) 66:1286–96. doi: 10.1136/gutjnl-2016-312268
  35. Shi J-H, Guo WZ, Jin Y, Zhang HP, Pang C, Li J, et al. Recognition of HER2 Expression in Hepatocellular Carcinoma and its Significance in Postoperative Tumor Recurrence. *Cancer Med* (2019) 8:1269–78. doi: 10.1002/cam4.2006
  36. Chen J-Y, Chen Y-J, Yen C-J, Chen W-S, Huang W-C. HBx Sensitizes Hepatocellular Carcinoma Cells to Lapatinib by Up-Regulating Erbb3. *Oncotarget* (2016) 7:473–89. doi: 10.18632/oncotarget.6337
  37. Jin H, Shi Y, Lv Y, Yuan S, Ramirez CFA, Lieftink C, et al. EGFR Activation Limits the Response of Liver Cancer to Lenvatinib. *Nature* (2021) 595:730–4. doi: 10.1038/s41586-021-03741-7
  38. Xie H, Alem Glison DM, Kim RD. FGFR4 Inhibitors for the Treatment of Hepatocellular Carcinoma: A Synopsis of Therapeutic Potential. *Expert Opin Investigat Drugs* (2021) 1–8. doi: 10.1080/13543784.2022.2017879
  39. Harding JJ, Nandakumar S, Armenia J, Khalil DN, Albano M, Ly M, et al. Prospective Genotyping of Hepatocellular Carcinoma: Clinical Implications of Next-Generation Sequencing for Matching Patients to Targeted and Immune Therapies. *Clin Cancer Res* (2019) 25:2116–26. doi: 10.1158/1078-0432.CCR-18-2293
  40. Ellrott K, Bailey MH, Saksena G, Covington KR, Kandath C, Stewart C, et al. Scalable Open Science Approach for Mutation Calling of Tumor Exomes Using Multiple Genomic Pipelines. *Cell Syst* (2018) 6:271–281.e7. doi: 10.1016/j.cels.2018.03.002

**Conflict of Interest:** AL has received grant support from Pfizer and Genentech for unrelated projects.

The remaining authors declare that the research was conducted in the absence of any commercial or financial relationships that could be construed as a potential conflict of interest.

**Publisher's Note:** All claims expressed in this article are solely those of the authors and do not necessarily represent those of their affiliated organizations, or those of the publisher, the editors and the reviewers. Any product that may be evaluated in this article, or claim that may be made by its manufacturer, is not guaranteed or endorsed by the publisher.

Copyright © 2022 Elmas, Lujambio and Huang. This is an open-access article distributed under the terms of the Creative Commons Attribution License (CC BY). The use, distribution or reproduction in other forums is permitted, provided the original author(s) and the copyright owner(s) are credited and that the original publication in this journal is cited, in accordance with accepted academic practice. No use, distribution or reproduction is permitted which does not comply with these terms.



# Sarcopenia and Systemic Inflammation Response Index Predict Response to Systemic Therapy for Hepatocellular Carcinoma and Are Associated With Immune Cells

## OPEN ACCESS

### Edited by:

Zhaohui Huang,  
Affiliated Hospital of Jiangnan  
University, China

### Reviewed by:

Natally Horvat,  
Memorial Sloan Kettering Cancer  
Center, United States  
Guifang Guo,  
Sun Yat-sen University Cancer Center  
(SYSUCC), China

### \*Correspondence:

Fei Yin  
yinfei\_4y@sina.com

### Specialty section:

This article was submitted to  
Gastrointestinal Cancers: Hepato  
Pancreatic Biliary Cancers,  
a section of the journal  
Frontiers in Oncology

**Received:** 13 January 2022

**Accepted:** 15 March 2022

**Published:** 08 April 2022

### Citation:

Zhao M, Duan X, Han X, Wang J,  
Han G, Mi L, Shi J, Li N, Yin X, Hou J  
and Yin F (2022) Sarcopenia and  
Systemic Inflammation Response Index  
Predict Response to Systemic Therapy  
for Hepatocellular Carcinoma and  
Are Associated With Immune Cells.  
Front. Oncol. 12:854096.  
doi: 10.3389/fonc.2022.854096

Man Zhao, Xiaoling Duan, Xin Han, Jinfeng Wang, Guangjie Han, Lili Mi, Jianfei Shi,  
Ning Li, Xiaolei Yin, Jiaojiao Hou and Fei Yin\*

Department of Gastroenterology, The Fourth Hospital of Hebei Medical University, Shijiazhuang, China

**Background:** Systemic therapies, including immune checkpoint inhibitors (ICIs) and tyrosine kinase inhibitors (TKIs), have challenged the use of conventional therapies for hepatocellular carcinoma (HCC). It is crucial to determine which patients could benefit most from combination therapy. This study aims to examine the associations of sarcopenia and systemic inflammation response index (SIRI) with the treatment responses and efficacies in patients with HCC treated with ICIs and tyrosine kinase inhibitors TKIs, as well as investigate the correlation between sarcopenia and inflammatory or immune states.

**Methods:** We reviewed 160 patients with HCC treated with TKIs and ICIs. The patients' psoas muscle size was measured on axial computed tomography scans and normalized for the patients' height squared. This value was referred to as the psoas muscle index (PMI). Sarcopenia was determined from PMI and their relationships with patients' clinicopathological characteristics, inflammation indexes, peripheral blood T-cell subsets and survival were evaluated.

**Results:** Sarcopenia and systemic inflammation response index (SIRI) were independent predictors for overall survival and progression-free survival. Patients with high PMI and low SIRI demonstrated significantly better median overall survival and progression-free survival (36.0 months and 9.6 months, respectively) than those with either low PMI or high SIRI (20.8 months and 6.0 months, respectively) and those with both high SIRI and low PMI (18.6 months and 3.0 months, respectively). Portal vein tumor thrombus ( $P=0.003$ ), eastern cooperative oncology group performance status score of 1 ( $P=0.048$ ), high alkaline phosphatase ( $P=0.037$ ), high neutrophil-to-lymphocyte ratio (NLR) ( $P=0.012$ ), low lymphocyte-to-monocyte ratio (LMR) ( $P=0.031$ ), high platelet-to-

lymphocyte ratio (PLR) ( $P=0.022$ ) and high SIRI ( $P=0.012$ ) were closely associated with an increased incidence of sarcopenia. PMI was negatively correlated with SIRI ( $r = -0.175$ ,  $P=0.003$ ), NLR ( $r = -0.169$ ,  $P=0.036$ ), and PLR ( $r = -0.328$ ,  $P=0.000$ ) and was significantly positively correlated with LMR ( $r = 0.232$ ,  $P=0.004$ ). The CD3+ and CD4+ T-cell counts of the high PMI group were significantly higher than those of the low PMI group.

**Conclusion:** Sarcopenia and high SIRI were associated with reduced survival in patients with HCC treated with ICIs and TKIs. Sarcopenia could affect inflammatory states and the immune microenvironment.

**Keywords:** hepatocellular carcinoma, sarcopenia, psoas muscle index, systemic inflammatory response index, immune cell

## INTRODUCTION

Hepatocellular carcinoma (HCC) is one of the leading causes of cancer-related death; however, a limited number of systemic treatment options for advanced HCC exist. Currently, systemic therapies, including immune checkpoint inhibitors (ICIs) and tyrosine kinase inhibitors (TKIs), have challenged the use of conventional therapies for HCC. The field has witnessed substantial progress in the development of systemic therapies in the past 5 years, with studies reporting a marked increase in overall survival and in the quality of life of patients (1). For example, the natural history of advanced-stage HCC cases involves a median survival of 8 months and the approved combination of atezolizumab (anti-PDL1 antibody) and bevacizumab (anti-VEGF antibody) has more than doubled this life expectancy and improved the patient-reported outcomes (2). Although their clinical benefit is apparent, the use of ICIs and TKIs is limited owing to the associated cost. It is crucial to explore effective biomarkers for identifying patients who may benefit from combination therapy.

Sarcopenia is a progressive and generalized skeletal muscle disease characterized by accelerated loss of muscle mass and function (3). The disease has been associated with higher mortality among patients with cancer (4, 5). Sarcopenia has a negative effect on the body composition and can damage the body's immune system. For patients receiving targeted therapy and immunotherapy, the immune state of the body determines treatment response and efficacy, so sarcopenia is being recognized as increasingly important for predicting tumor prognosis and therapeutic response.

Immunity and inflammation are basic features of the tumor microenvironment. A host's inflammatory and immune response to a tumor leads to the up- or downregulation of tumor proliferation and metastasis (6). There is increasing evidence that inflammation indexes can be employed to predict the prognosis of patients with cancer. The systemic inflammation response index (SIRI), neutrophil-to-lymphocyte ratio (NLR), platelet-to-lymphocyte ratio (PLR) and lymphocyte-to-monocyte ratio (LMR) are widely studied markers that have been proven effective in predicting patient survival in various kinds of cancer (7–10). Peripheral blood T-cell subsets are effective in reflecting the systemic immune status (11, 12). For example, CD8+ T-cells

are essential immunological determinants for HBV-related HCC prognosis (13). Systematic analysis of the relationship between sarcopenia and the inflammatory indexes or immune cells would add greatly to our understanding of their role in tumor progression. Thus, the aim of this study was to investigate the role of sarcopenia as a predictor and the relationship between sarcopenia and systemic inflammation and immune status in patients with HCC.

## PATIENTS AND METHODS

### Patients and Treatments

We retrospectively enrolled HCC patients who received TKIs and ICIs from January 2018 to December 2020 at the Fourth Hospital of Hebei Medical University.

The inclusion criteria were as follows: 1) age  $\geq 18$  years; 2) histologically confirmed HCC or a clinical diagnosis based on dynamic imaging and an underlying chronic liver disease; 3) patients who were not eligible for radical treatments, such as surgery and ablation; 4) patients who had not previously taken any systemic treatment for HCC; 5) TKI in combination with ICI as first-line treatment; 6) undergoing at least one cycle of systematic treatment; 7) patients with an eastern cooperative oncology group performance status (ECOG PS) of 0–1; 8) stage B or C categorization based on the Barcelona Clinic Liver Cancer (BCLC) staging system; 9) Child-Pugh A or B; 10) patients with at least one measurable target lesion; 11) patients with available cross-sectional abdominal images with computed tomographic (CT) scans within 1 months before systematic treatment. The exclusion criteria were as follows: 1) patients with combined immune and endocrine system diseases; 2) patients with cooccurrence of other lymphatic system disorders or malignant hematologic diseases, renal and/or hepatic failure, or systematic inflammatory diseases; 3) patients with a history of malignant tumors in other organs and liver metastasis; 4) patients with concurrent hepatitis A, hepatitis E, or human immunodeficiency virus infection.

Treatment options included lenvatinib combined with pembrolizumab/nivolumab/sintilimab/camrelizumab and sorafenib combined with sintilimab/camrelizumab. The dosing of the drugs is as follows: 1) lenvatinib 12 mg (if bodyweight  $\geq 60$



kg) or 8 mg (if bodyweight <60 kg) orally once daily; 2) sorafenib starting at 200 mg orally twice daily, with subsequent dose increase to 400 mg twice daily if it is well-tolerated; 3) pembrolizumab 200 mg intravenously every 3 weeks; 4) nivolumab 240 mg intravenously every 2 weeks; 5) camrelizumab 200 mg (for bodyweight ≥50 kg) or 3 mg/kg (for bodyweight <50 kg) intravenously every 2 weeks; and 5) sintilimab 200 mg intravenously every 3 weeks.

## Data Collection

Clinical information was retrieved from electronic medical records. Baseline patient characteristics, including demographics, etiology, presence of cirrhosis, Eastern Cooperative Oncology Group-performance status (ECOG-PS), Child–Pugh Class score, tumor markers, routine blood test results, liver function parameters, peripheral blood T-cell subsets, imaging examination and treatment history were examined.

## Systemic Inflammatory Index

Routine blood results were collected within 1 week before treatment, and the SIRI, NLR, PLR and LMR were calculated. The calculations were as follows: SIRI = neutrophil count × monocyte/lymphocyte count; NLR = neutrophil count/lymphocyte count; PLR = platelet count/lymphocyte count; and LMR = lymphocyte count/monocyte count.

## Assessment of Sarcopenia and PMI

Sarcopenia was assessed by measuring the longest diameter (D1) and the perpendicular diameter (D2) of the right (ri) and left (le) psoas muscle on an axial CT scan. All diameters were measured in the same CT plane, which was usually between lumbar vertebral body (LVB) 3 and LVB 4 (14). An example image of the psoas muscle measurement is displayed in **Figure 1**.

Psoas muscle index (PMI) was calculated as follows:

$$PMI = \left[ \frac{mm}{m^2} \right] = \frac{(riD1 [mm] + riD2 [mm] + leD1 [mm] + leD2 [mm]) / 4}{Patient's height [m]^2}$$

PMI is an effective proxy for sarcopenia. The CT images were provided by trained radiologists.

## Follow-Up

All patients were assessed every 1–2 months with radiologic and laboratory evaluations. The last follow-up date was November 2021. OS was defined as the interval between the first day of therapy and the date of death or the date of the last follow-up. PFS was defined as the interval between the first day of therapy and the date of disease progression or the date of death. Radiological responses were defined using the response evaluation criteria in solid tumors v1.1. Disease control rate and overall response rate were determined by the best radiologic response after CKI and ICI treatment: disease control rate included complete response, partial response, and stable disease; overall response rate included complete and partial responses, respectively.

## Statistical Analysis

Survival analysis was performed using the Kaplan–Meier method. The differences between the survival curves were compared by the log rank test. Multivariate Cox hazard regression analysis was performed on the factors that were shown to be significant on univariate analysis. The best cutoff values were determined by receiver operating characteristic (ROC) curve analysis. Spearman correlation analysis was used to detect linear correlations. The significance level was set at 5%. All statistical data were generated using SPSS software 26.0.

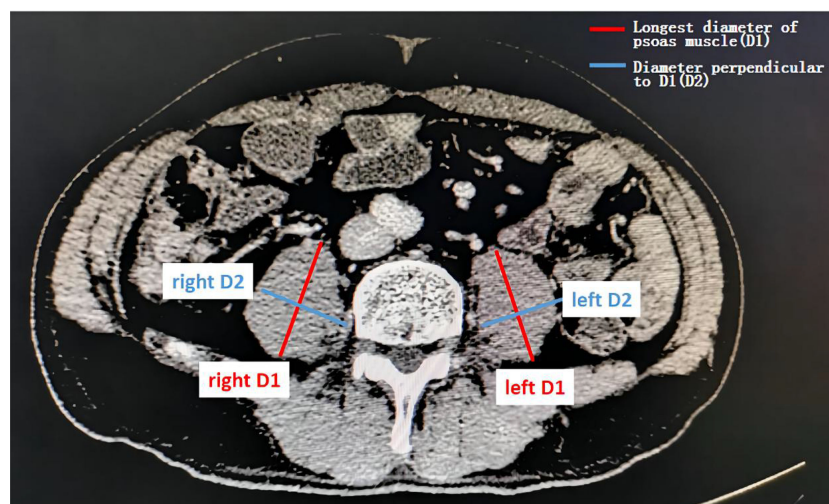


**FIGURE 1** | Assessment of the psoas muscle index (PMI). Sarcopenia was assessed by measuring the longest diameter (D1) and the perpendicular diameter (D2) of the right (ri) and left (le) psoas muscle on an axial computed tomography (CT) scan in the same plane and normalizing it for the patients' height squared. This value is referred to as the psoas muscle index (PMI).

## RESULTS

### Baseline Characteristics of Patients

The current study included a total of 160 subjects. The median age of the patients was 58 years (range: 26–86 years); 129 (80.6%) patients were male; 143 (89.4%) patients had hepatitis B virus infection; 132 (82.5%) patients exceeded the up-to-seven criteria; and 45 (28.1%) patients had portal vein tumor thrombus (PVTT). Cirrhosis was present in 114 (71.3%) patients. There were 106 (67.9%) patients with barcelona clinic liver cancer (BCLC)

stage C disease. The patients were in good physical condition; 99 (61.9%) patients had an ECOG-PS score of 0 (**Table 1**).

### Optimal Cut - Off Analysis

The optimal cutoff value for the patients was determined by ROC curve analysis as follows: NLR=3.25, PLR = 145.25, LMR = 3.59, SIRI =1.64 and PMI=14.19. The area under the receiver operating characteristic curve values for NLR, PLR, LMR, SIRI and PMI in disease control prediction were 0.622, 0.586, 0.604, 0.627, and 0.659, respectively (**Figure 2**).

**TABLE 1** | Baseline characteristics of patients stratified by sarcopenia.

Characteristics	Total(n=160)	Sarcopenia(n=120)	No sarcopenia(n=40)	P
Age				0.201
<58 years	82(51.3%)	58	24	
≥58 years	78(48.7%)	62	16	
Gender				0.083
Male	129(80.6%)	93	36	
Female	31(19.4%)	27	4	
Up-to-seven				0.118
>7	132(82.5%)	102	30	
≤ 7	37(17.5%)	17	10	
PVTT				<b>0.003</b>
Yes	45(28.1%)	41	4	
No	115(71.9%)	79	36	
ALP				<b>0.037</b>
>125U/L	58(36.3%)	49	9	
≤ 125U/L	102(63.7%)	71	31	
Liver cirrhosis				0.840
Yes	114(71.3%)	86	28	
No	46(28.7%)	34	12	
BCLC				0.177
B	54(32.1%)	37	17	
C	106(67.9%)	83	23	
ECOG-PS				<b>0.048</b>
0	99(61.9%)	69	30	
1	61(38.1%)	51	10	
AFP				0.360
>400ng/mL	74(46.3%)	58	16	
≤ 400ng/mL	86(53.7%)	62	24	
ALT				0.232
>50U/L	48(30.0%)	39	9	
≤ 50U/L	112(70.0%)	81	31	
Albumin				0.052
<35g/L	93(58.1%)	75	18	
≥ 35g/L	67(41.9%)	45	22	
NLR				<b>0.012</b>
≥ 3.25	95(59.4%)	78	17	
<3.25	65(40.6%)	42	23	
LMR				<b>0.031</b>
≥ 3.59	61(38.1%)	40	21	
<3.59	99(61.9%)	80	19	
PLR				<b>0.022</b>
≥ 145.25	79(49.4%)	53	26	
<145.25	81(50.6%)	67	14	
SIRI				<b>0.012</b>
≥ 1.64	67(41.9%)	57	10	
<1.64	93(58.1%)	63	30	

PVTT, portal vein tumor thrombus; ALP, alkaline phosphatase; BCLC, barcelona clinic liver cancer; ECOG-PS, eastern cooperative oncology group-performance status; AFP, alpha-fetoprotein; ALT, alanine transaminase; SIRI, systemic inflammation response index; NLR, neutrophil-to-lymphocyte ratio; PLR, platelet-to-lymphocyte ratio; LMR, lymphocyte-to-monocyte ratio.

Bold values means there is a statistically difference in the result.

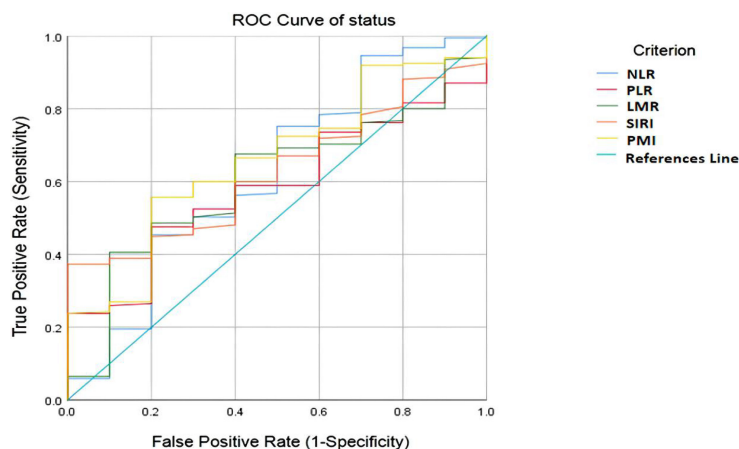


**FIGURE 2** | ROC curve analysis for optimal cut-off value of NLR, PLR, LMR, SIRI and PMI. ROC, receiver operating characteristic; NLR, neutrophil-to-lymphocyte ratio; PLR, platelet-to-lymphocyte ratio; LMR, lymphocyte-to-monocyte ratio; SIRI, systemic inflammation response index; PMI, psoas muscle index.

## The Effect of SIRI and PMI on OS and PFS

The median OS of the low SIRI group was 25.0 months, which was significantly higher than the 18.6 months of the high SIRI group ( $P=0.001$ ). The median OS of the high PMI group was 29.1 months, which was higher than the 19.7 months of the low PMI group ( $P=0.001$ ). Patients with high PMI and low SIRI demonstrated significantly better median OS (36.0 months) than those with either low PMI or high SIRI

(20.8 months) and those with both high SIRI and low PMI (18.6 months) ( $P=0.000$ ) (**Figure 3**).

The median PFS of the low SIRI group was 7.7 months, which was significantly higher than the 3.1 months of the high SIRI group ( $P=0.000$ ). The median PFS of the high PMI group was 8.5 months, which was significantly higher than the 4.1 months of the low PMI group ( $P=0.003$ ). Patients with high PMI and low SIRI demonstrated better median PFS (9.6 months) than those

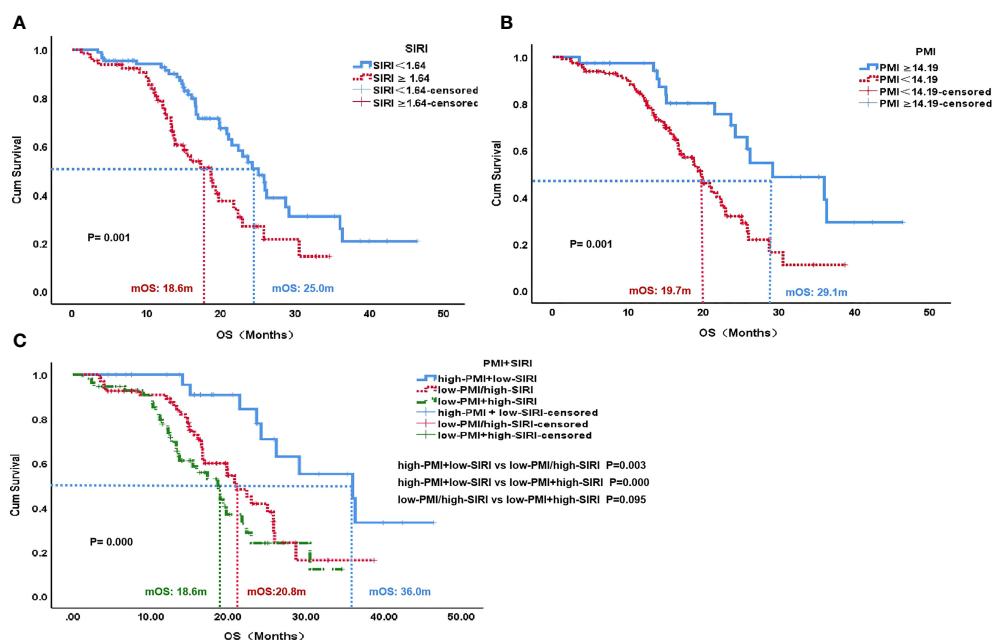


**FIGURE 3** | OS according to SIRI status (A), PMI status (B) and PMI+SIRI status (C) in the patients with HCC. OS, overall survival; SIRI, systemic inflammation response index; PMI, psoas muscle index.

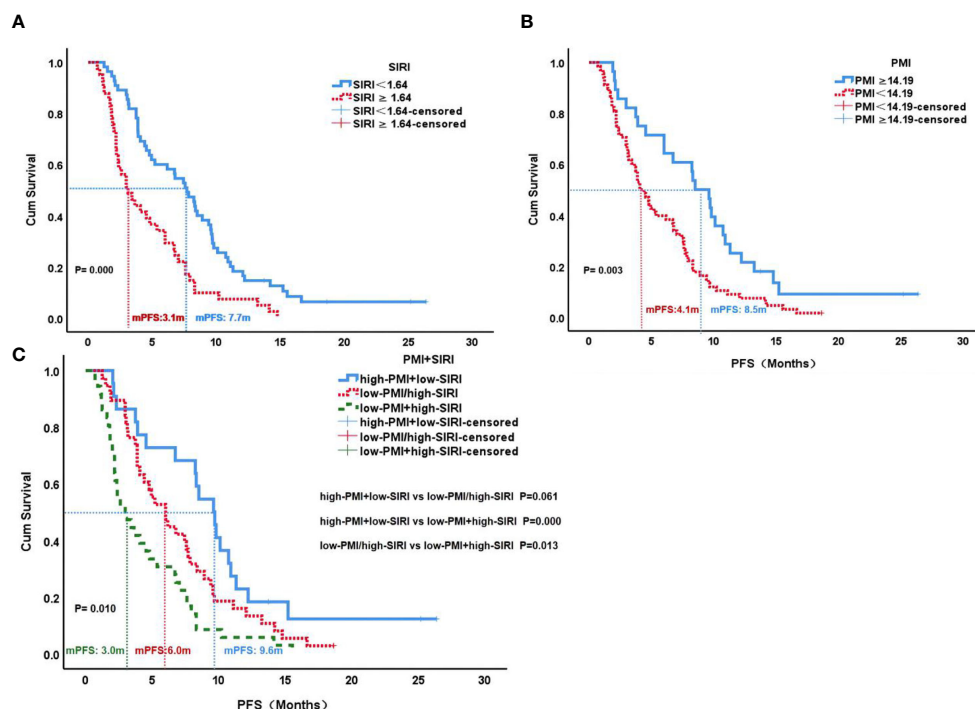


**FIGURE 4** | PFS according to SIRI status (A), PMI status (B) and PMI+SIRI status (C) in the patients with HCC. PFS, progression-free survival; SIRI, systemic inflammation response index; PMI, psoas muscle index.

with either low PMI or high SIRI (6.0 months) and those with both high SIRI and low PMI (3.0 months) ( $P=0.010$ ) (Figure 4).

For the best response after treatment, the disease control rate and overall response rate for patients were 92.5% and 36.2%, respectively. However, the disease control rate (89.6% vs. 96.6%,  $P=0.816$ ) and overall response rate (29.3% vs. 46.6%,  $P=0.272$ ) of patients with low PMI and high SIRI were lower than those of patients with high PMI and low SIRI, but there was no statistical significance (Table 2).

## Multivariate Cox Regression Analyses for PFS and OS

In the multivariate Cox regression analysis, BCLC (HR, 1.576; 95% CI, 1.010–2.458;  $P=0.045$ ), SIRI (HR, 1.817; 95% CI, 1.165–2.835;  $P=0.008$ ) and PMI (HR, 1.757; 95% CI, 1.090–2.831;  $P=0.021$ ) were independent predictors for PFS (Table 3). AFP (HR, 2.005; 95% CI, 1.251–3.213;  $P=0.004$ ), SIRI (HR, 1.800; 95% CI, 1.117–2.901;  $P=0.016$ ) and PMI (HR, 2.464; 95% CI, 1.308–4.642;  $P=0.005$ ) were independent predictors for OS (Table 4).

**TABLE 2** | Tyrosine kinase inhibitors and immune checkpoint inhibitors efficacy results.

	N	DCR %	P	ORR %	P	CR N (%)	PR N (%)	SD N (%)	PD N (%)
Overall	160	92.5		36.2		6(3.7)	52 (32.5)	90 (56.3)	12 (7.5)
PMI <14.19	120	91.7	0.892	33.4	0.373	2 (1.7)	38 (31.7)	70 (58.3)	10 (8.3)
PMI ≥14.19	40	95.0		45.0		4 (10.0)	14 (35.0)	20 (50.0)	2 (5.0)
SIRI ≥1.64	68	88.2	0.727	27.9	0.194	0 (0.0)	19 (27.9)	41 (60.3)	8 (11.8)
SIRI <1.64	92	95.7		42.4		6 (6.5)	33 (35.9)	49 (53.3)	4(4.3)
PMI+SIRI			0.122		0.540				
High PMI(≥14.19)+ Low SIRI(<1.64)	30	96.6		46.6		4 (13.3)	10 (33.3)	15 (50.0)	1 (3.4)
Low PMI(<14.19)/ High SIRI(≥1.64)	72	93.0		37.5		2 (2.8)	25(34.7)	40 (55.5)	5 (7.0)
Low PMI(<14.19)+ High SIRI(≥1.64)	58	89.6		29.3		0 (0.0)	17(29.3)	35 (60.3)	6 (10.4)

SIRI, systemic inflammation response index; PMI, psoas muscle index; DCR, disease control rate; CR, complete response; PR, partial response; SD, stable disease; ORR, overall response rate; PD, progressive disease.



**TABLE 3 |** Prognostic factors for progression-free survival.

	PFS			
	Univariate		Multivariate	
	HR(95%CI)	P	HR(95%CI)	P
Age ≥58years vs 58< years	0.982(0.651–1.482)	0.932	—	—
Gender Male vs Female	1.073(0.639–1.801)	0.790	—	—
Uptoseven >7 VS ≤7	1.661(0.978–2.821)	0.061	—	—
PVTT yes vs no	1.250(0.735–2.124)	0.410	—	—
Extrahepatic metastasis yes vs no	1.431(0.927–2.208)	0.106	—	—
BCLC C vs B	1.870(1.217–2.873)	<b>0.004</b>	1.576(1.010–2.458)	<b>0.045</b>
ECOG-PS 1 vs 0	1.627(1.059–2.500)	<b>0.026</b>	—	—
AFP >400ng/mL vs ≤400ng/mL	1.458(0.965–2.202)	0.073	—	—
ALT >50U/L vs ≤50U/L	0.751(0.427–1.195)	0.227	—	—
ALP >125U/L vs ≤125U/L	1.242(0.791–1.950)	0.346	—	—
NLR ≥3.25 vs <3.25	1.668(1.099–2.531)	<b>0.016</b>	—	—
PLR ≥145.25 vs <145.25	1.500(0.982–2.291)	0.061	—	—
LMR <3.59 vs ≥3.59	0.667(0.436–1.022)	0.063	—	—
SIRI ≥1.64 vs <1.64	2.212(1.446–3.383)	<b>0.000</b>	1.817(1.165–2.835)	<b>0.008</b>
PMI <14.19 vs ≥14.19	1.988(1.246–3.171)	<b>0.004</b>	1.757(1.090–2.831)	<b>0.021</b>

PVTT, portal vein tumor thrombus; ALP, alkaline phosphatase; BCLC, barcelona clinic liver cancer; ECOG-PS, eastern cooperative oncology group-performance status; AFP, alpha-fetoprotein; ALT, alanine transaminase; SIRI, systemic inflammation response index; NLR, neutrophil-to-lymphocyte ratio; PLR, platelet-to-lymphocyte ratio; LMR, lymphocyte-to-monocyte ratio; PMI, psoas muscle index; PFS, progression-free survival.

Bold values means there is a statistically difference in the result.

PMI and SIRI were independent risk factors for PFS and OS in patients with HCC.

## The Relationship Between PMI, SIRI and Peripheral Blood T-Cell Subsets

With PVTT ( $P=0.003$ ), ECOG-PS score of 1 ( $P=0.048$ ), high ALP ( $P=0.037$ ), high NLR ( $P=0.012$ ), low LMR ( $P=0.031$ ), high PLR ( $P=0.022$ ) and high SIRI ( $P=0.012$ ) were closely associated with an increased incidence of sarcopenia (Table 1). We further analyzed the correlation between PMI and inflammatory

indicators. Our results showed that PMI was negatively correlated with SIRI ( $r = -0.175$ ,  $P=0.003$ ), NLR ( $r = -0.169$ ,  $P=0.036$ ) and PLR ( $r = -0.328$ ,  $P=0.000$ ) and was significantly positively correlated with LMR ( $r = 0.232$ ,  $P=0.004$ ) (Figure 5). Moreover, it had been recently discovered that PMI was closely related to peripheral blood T-cell counts. The CD3+ and CD4+ T-cell counts of the high PMI group were significantly higher than those of the low PMI group. The CD8+ T-cell counts and CD4+/CD8+ ratios of the high PMI group were also higher, but without any significant difference (Table 5).

**TABLE 4 |** Prognostic factors for overall survival.

	OS			
	Univariate		Multivariate	
	HR(95%CI)	P	HR(95%CI)	P
Age ≥58years vs 58< years	1.097(0.694–1.732)	0.693	—	—
Gender Male vs Female	1.071(0.596–1.924)	0.820	—	—
Uptoseven >7 VS ≤7	1.654(0.911–3.001)	0.098	—	—
PVTT yes vs no	1.725(1.059–2.808)	<b>0.028</b>	—	—
Extrahepatic metastasis yes vs no	1.026(0.639–1.647)	0.916	—	—
BCLC C vs B	1.733(1.060–2.832)	<b>0.028</b>	—	—
ECOG-PS 0 vs 1	1.205(0.750–1.936)	0.441	—	—
AFP >400ng/mL vs ≤400ng/mL	1.952(1.228–3.102)	<b>0.005</b>	2.005(1.251–3.213)	<b>0.004</b>
ALT >50U/L vs ≤50U/L	1.147(0.684–1.921)	0.603	—	—
ALP >125U/L vs ≤125U/L	1.822(1.118–2.969)	<b>0.016</b>	—	—
NLR ≥3.25 vs <3.25	1.737(1.074–2.807)	<b>0.024</b>	—	—
PLR ≥145.25 vs <145.25	1.455(0.918–2.305)	0.110	—	—
LMR <3.59 vs ≥3.59	1.107(0.682–1.798)	0.681	—	—
SIRI ≥1.64 vs <1.64	2.034(1.274–3.248)	<b>0.003</b>	1.800(1.117–2.901)	<b>0.016</b>
PMI <14.19 vs ≥14.19	2.658(1.442–4.898)	<b>0.002</b>	2.464(1.308–4.642)	<b>0.005</b>

PVTT, portal vein tumor thrombus; ALP, alkaline phosphatase; BCLC, barcelona clinic liver cancer; ECOG-PS, eastern cooperative oncology group-performance status; AFP, alpha-fetoprotein; ALT, alanine transaminase; SIRI, systemic inflammation response index; NLR, neutrophil-to-lymphocyte ratio; PLR, platelet-to-lymphocyte ratio; LMR, lymphocyte-to-monocyte ratio; PMI, psoas muscle index; OS, overall survival.

Bold values means there is a statistically difference in the result.

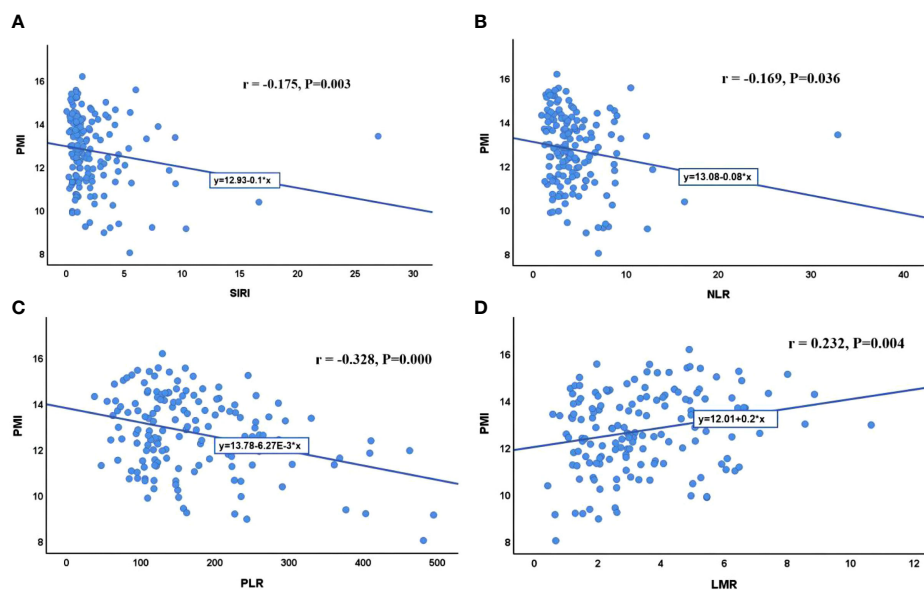


**FIGURE 5 |** Correlation between PMI and inflammatory indicators. **(A)** Correlation between PMI and SIRI; **(B)** Correlation between PMI and NLR; **(C)** Correlation between PMI and PLR; **(D)** Correlation between PMI and LMR. SIRI, systemic inflammatory response index; NLR, neutrophil-to-lymphocyte ratio; PLR, platelet-to-lymphocyte ratio; LMR, lymphocyte-to-monocyte ratio; PMI, psoas muscle index.

## DISCUSSION

When considering the limited response rate and utilization rate of TKIs and ICIs in patients with HCC, potential biomarkers for predicting treatment outcomes have attracted the attention of several physicians. This study comprehensively analyzed the predictive power of sarcopenia and inflammatory immune indicators for the treatment outcomes of patients with HCC treated with TKIs and ICIs.

Sarcopenia has been defined as the “progressive loss of muscle mass and strength with a risk of adverse outcomes such as disability, poor quality of life and death” (15). Recent studies have shown that muscle loss is associated with an impaired prognosis in patients with different solid tumors (16). In patients with HCC, sarcopenia has been associated with impaired OS and disease-free survival after surgical resection or radiofrequency ablation (17, 18). Most European and American studies have found that sarcopenia is an independent risk factor for the prognosis of HCC in patients undergoing surgical resection (19). Aliya et al. found that sarcopenia was associated with shorter survival (< 1 year) and less HCC necrosis (<50% necrosis or >50% viable tumor) with targeted therapy and was negatively associated with the efficacy of targeted

therapy (20). Kim et al. examined 102 patients with HCC treated with nivolumab and reported that patients with sarcopenia had a shorter OS than those without sarcopenia (21). A meta-analysis of 2501 patients with solid tumors reported a negative correlation between sarcopenia and ICI efficacy. Besides, the predictive power of sarcopenia was consistent across tumor types, including HCC (22). However, studies on sarcopenia and treatment response in the Chinese HCC population treated with TKIs and ICIs are relatively scarce. This study found that patients with sarcopenia before TKIs and ICIs treatment were more likely to have disease progression and had shorter survival. Sarcopenia was an independent risk factor for OS and PFS in patients with HCC.

Systemic inflammation is an important promoter of the proliferation, invasion, and metastasis of malignant cells (23–25). Many inflammatory markers, such as SIRI, LMR, NLR, and PLR, have been associated with poor prognosis for various cancers (7–10, 26). SIRI is a simple noninvasive prognostic marker based on the counts of peripheral neutrophils, monocytes and lymphocytes. High SIRI is associated with poor prognosis and has been confirmed in a variety of cancers. Survival analysis of patients with HCC treated with radiofrequency ablation revealed that OS and recurrence-free survival (RFS) were significantly higher in patients with a low SIRI than in

**TABLE 5 |** Peripheral blood T-cell subsets according to PMI.

Characteristics	CD3+T-cell counts (mean)	P	CD4+T-cell counts (mean)	P	CD8+T-cell counts (mean)	P	CD4+/CD8+ ratio (mean)	P
PMI < 14.19	$0.449 \times 10^9$	<b>0.023</b>	$0.242 \times 10^9$	<b>0.007</b>	$0.183 \times 10^9$	0.205	1.70	0.627
PMI ≥ 14.19	$0.857 \times 10^9$		$0.443 \times 10^9$		$0.376 \times 10^9$		1.91	

PMI, psoas muscle.

Bold values means there is a statistically difference in the result.

those with a high SIRI. In a multivariate analysis, SIRI was an independent predictor of RFS (27). A study of 194 patients reported that pretreatment peripheral blood SIRI was an independent predictor of tumor response and clinical outcomes in patients with HCC undergoing transcatheter arterial chemoembolization. Indeed, patients with high SIRI might have a poor prognosis (28). Another study demonstrated a correlation between SIRI ( $P = 0.002$ ) and early postoperative recurrence in patients with HCC (29). Our study evaluated the relationship between four inflammatory indicators and the clinical outcomes of HCC treated with ICIs and TKIs and proved that patients with high SIRI have a poor survival.

Among these inflammatory markers, SIRI was the best independent predictor of OS and PFS. Sarcopenia and SIRI could be potential biomarkers of response to TKIs and ICIs therapy. The current study also showed that risk groups based on sarcopenia and SIRI at baseline could successfully predict survival outcomes. Patients with high PMI and low SIRI had significantly better outcomes than those with either low PMI or high SIRI and those with both high SIRI and low PMI.

Sarcopenia and chronic inflammatory status play a role in TKIs and ICIs resistance. This study also found that PMI was negatively correlated with SIRI, NLR and PLR and was significantly positively correlated with LMR. Patients with sarcopenia had increased levels of inflammatory markers, which supports the fact that sarcopenia reflects the increased metabolic activity leading to systemic inflammation and muscle depletion (30). A possible mechanism is as follows: cytokines such as tumor necrosis factor and interleukin 6 are produced by tumor cells or surrounding cells and promote protein degradation and decreased synthesis. Tumor necrosis factor inhibits skeletal myocyte differentiation, promotes muscle atrophy, and contributes to insulin resistance by impairing the insulin signaling pathway. Interleukin 6 can further reduce muscle protein synthesis (31). Increases in inflammatory cytokines can also lead to insulin resistance and muscle wasting by activating the ubiquitin–proteasome proteolytic pathway, while muscle loss itself further exacerbates insulin resistance. Low-grade systemic inflammation caused by the tumor (and possibly exacerbated by obesity or insulin resistance) could drive local inflammation in the muscle. This effect, in turn, further contributes to systemic inflammation and muscle degradation (32).

Immunity and inflammation are essential characteristics of the tumor microenvironment. Immune-related cells in the immune microenvironment have an important influence on the occurrence and development of tumor (33). In patients with surgically resected HCC, high levels of both CD3+ and CD8+ T-cells were significantly related to a low rate of recurrence ( $P = 0.007$ ) and a prolonged RFS ( $P = 0.002$ ) (27). Sarcopenia is also closely related to the immune microenvironment. Several reports of patients with malignant melanoma or advanced lung cancer had demonstrated that patients with sarcopenia frequently had poor survival outcomes after ICIs (34–36). Because skeletal muscle cells express major histocompatibility complexes which stimulate T cells, loss of skeletal muscle may disrupt the homeostatic balance. Moreover, the drop in myokines, especially IL-15, disturbs the tight balance of different T-cell subsets (36, 37). In this study, peripheral blood T lymphocytes, especially CD3+ and CD4+ T-cell counts, were

significantly reduced in patients with sarcopenia. Thus, changes in the myokine levels as a result of sarcopenia may affect the efficacy of TKIs and ICIs treatment, indicating the predictive value of sarcopenia in this therapy.

Our approach has a few limitations. First, as the definition of sarcopenia, various cutoff values have existed in previous reports, and the authors of those reports decided the cutoff value by sex. However, we decided our cutoff values irrespective of sex because there were too few female patients in our study. Second, owing to the limited number of patients, the peripheral blood T lymphocyte subsets analysis had a limited statistical power. The statistical significance with limited number of patients need to be interpreted with caution because the observed effect may not result from true biological effect. Third, this study did not evaluate the effect of sarcopenia on drug-related adverse reactions and quality of life. We will further evaluate the impact of sarcopenia on patient safety, and finally draw more convincing conclusion.

## CONCLUSION

This study established that sarcopenia and SIRI can successfully predict the therapeutic responses of patients with HCC receiving ICIs and TKIs. Sarcopenia can objectively reflect the physical condition, nutritional status, and immune status of patients, while SIRI can reflect the inflammatory state of the body. The combination of sarcopenia and SIRI could be used to identify patients with poor treatment tolerance and high risk of tumor immune escape, as well as those who would benefit from combination therapy. In addition, sarcopenia could affect the inflammatory status and immune microenvironment, and the underlying molecular mechanisms warrant further investigation.

## DATA AVAILABILITY STATEMENT

The raw data supporting the conclusions of this article will be made available by the authors, without undue reservation.

## ETHICS STATEMENT

The studies involving human participants were reviewed and approved by Ethics Committee of The Fourth Hospital of Hebei Medical University. The patients/participants provided their written informed consent to participate in this study.

## AUTHOR CONTRIBUTIONS

Conception and design, FY and MZ. Manuscript writing, MZ. Collection and assembly of data, XD, XH, JW, GH, LM, JS, NL, XY, and JH. Data analysis and interpretation, FY and MZ. All authors contributed to the article and approved the submitted version.

## ACKNOWLEDGMENTS

The authors would like to thank Dr. Wang of imaging department who provided imaging data.

## REFERENCES

- Llovet JM, Montal R, Sia D, Finn RS. Molecular Therapies and Precision Medicine for Hepatocellular Carcinoma. *Nat Rev Clin Oncol* (2018) 15 (10):599–616. doi: 10.1038/s41571-018-0073-4
- Finn RS, Qin S, Ikeda M, Galle PR, Ducreux M, Kim TY, et al. Atezolizumab Plus Bevacizumab in Unresectable Hepatocellular Carcinoma. *N Engl J Med* (2020) 382(20):1894–905. doi: 10.1056/NEJMoa1915745
- Cruz-Jentoft AJ, Sayer AA. Sarcopenia. *Lancet* (2019) 393:2636–46. doi: 10.1016/S0140-6736(19)31138-9
- Otten L, Stobäus N, Franz K, Norman K, Genton L, Müller-Werdan U, et al. Impact of Sarcopenia on 1-Year Mortality in Older Patients With Cancer. *Age Ageing Oxf Acad* (2019) 48:413–8. doi: 10.1093/ageing/afy212
- Zhang XM, Dou QL, Zeng Y, Yang Y, Cheng ASK, Zhang WW. Sarcopenia as a Predictor of Mortality in Women With Breast Cancer: A Meta-Analysis and Systematic Review. *BMC Cancer* (2020) 20:172. doi: 10.1186/s12885-020-6645-6
- Grivennikov SI, Greten FR, Karin M. Immunity, Inflammation, and Cancer. *Cell* (2010) 140(6):883–99. doi: 10.1016/j.cell.2010.01.025
- Wang H, Ding Y, Li N, Wu L, Gao Y, Xu N, et al. Prognostic Value of Neutrophil-Lymphocyte Ratio, Platelet-Lymphocyte Ratio, and Combined Neutrophil-Lymphocyte Ratio and Platelet-Lymphocyte Ratio in Stage IV Advanced Gastric Cancer. *Front Oncol* (2020) 10:841. doi: 10.3389/fonc.2020.00841
- Zeng X, Liu G, Pan Y, Li Y. Development and Validation of Immune Inflammation-Based Index for Predicting the Clinical Outcome in Patients With Nasopharyngeal Carcinoma. *J Cell Mol Med* (2020) 24(15):8326–49. doi: 10.1111/jcmm.15097
- Cong R, Kong F, Ma J, Li Q, Wu Q, Ma X. Combination of Preoperative Neutrophil-Lymphocyte Ratio, Platelet-Lymphocyte Ratio and Monocyte-Lymphocyte Ratio: A Superior Prognostic Factor of Endometrial Cancer. *BMC Cancer* (2020) 20(1):464. doi: 10.1186/s12885-020-06953-8
- Topkan E, Mertsoylu H, Kucuk A, Besen AA, Sezer A, Sezen D, et al. Low Systemic Inflammation Response Index Predicts Good Prognosis in Locally Advanced Pancreatic Carcinoma Patients Treated With Concurrent Chemoradiotherapy. *Gastroenterol Res Pract* (2020) 2020:5701949. doi: 10.1155/2020/5701949
- Reck M, Rabe KF. Precision Diagnosis and Treatment for Advanced non-Small-Cell Lung Cancer. *N Engl J Med* (2017) 377(9):849–61. doi: 10.1056/NEJMra1703413
- Castellino F, Germain R. Cooperation Between CD4+ and CD8+ T Cells: When, Where, and How. *Annu Rev Immunol* (2006) 24:519–40. doi: 10.1146/annurev.immunol.23.021704.115825
- Xin H, Liang D, Zhang M, Li N, Chen H, Zhang H, et al. The CD68+ Macrophages to CD8+ T-Cell Ratio Is Associated With Clinical Outcomes in Hepatitis B Virus (HBV)-Related Hepatocellular Carcinoma. *HPB (Oxford)* (2021) 23(7):1061–71. doi: 10.1016/j.hpb.2020.11.002
- Loosen SH, Schulze-Hagen M, Bruners P, Tacke F, Trautwein C, Kuhl C, et al. Sarcopenia Is a Negative Prognostic Factor in Patients Undergoing Transarterial Chemoembolization (TACE) for Hepatic Malignancies. *Cancers (Basel)* (2019) 11(10):1503. doi: 10.3390/cancers11101503
- Fielding RA, Vellas B, Evans WJ, Bhasin S, Morley JE, Newman AB, et al. Sarcopenia: An Undiagnosed Condition in Older Adults. Current Consensus Definition: Prevalence, Etiology, and Consequences. International working group on sarcopenia. *J Am Med Dir Assoc* (2011) 12(4):249–56. doi: 10.1016/j.jamda.2011.01.003
- Shachar SS, Williams GR, Muss HB, Nishijima TF. Prognostic Value of Sarcopenia in Adults With Solid Tumors: A Meta-Analysis and Systematic Review. *Eur J Cancer* (2016) 57:58–67. doi: 10.1016/j.ejca.2015.12.030
- Sun G, Li Y, Peng Y, Lu D, Zhang F, Cui X, et al. Can Sarcopenia be a Predictor of Prognosis for Patients With non-Metastatic Colorectal Cancer? A Systematic Review and Meta-Analysis. *Int J Colorectal Dis* (2018) 33:1419. doi: 10.1007/s00384-018-3128-1
- Nakanishi R, Oki E, Sasaki S, Hirose K, Jogo T, Edahiro K, et al. Sarcopenia is an Independent Predictor of Complications After Colorectal Cancer Surgery. *Surg Today* (2018) 48:151–7. doi: 10.1007/s00595-017-1564-0
- van Vugt JLA, Alferink LJM, Buettner S, Gaspersz MP, Bot D, Darwish Murad S, et al. A Model Including Sarcopenia Surpasses the MELD Score in Predicting Waiting List Mortality in Cirrhotic Liver Transplant Candidates: A Competing Risk Analysis in a National Cohort. *J Hepatol* (2018) 68:707–14. doi: 10.1016/j.jhep.2017.11.030
- Qayyum A, Bhosale P, Aslam R, Avritscher R, Ma JF, Pagel MD, et al. Effect Of Sarcopenia On Systemic Targeted Therapy Response In Patients With Advanced Hepatocellular Carcinoma. *Abdom Radiol (NY)* (2021) 46 (3):1008–15. doi: 10.1007/s00261-020-02751-9
- Kim N, Yu JI, Park HC, Yoo GS, Choi C, Hong JY, et al. Incorporating Sarcopenia and Inflammation With Radiation Therapy in Patients With Hepatocellular Carcinoma Treated With Nivolumab. *Cancer Immunol Immunother* (2021) 70(6):1593–603. doi: 10.1007/s00262-020-02794-3
- Takenaka Y, Oya R, Takemoto N, Inohara H. Predictive Impact of Sarcopenia in Solid Cancers Treated With Immune Checkpoint Inhibitors: A Meta-Analysis. *J Cachexia Sarcopenia Muscle* (2021) 12(5):1122–35. doi: 10.1002/jcsm.12755
- Candido J, Hagemann T. Cancer-Related Inflammation. *J Clin Immunol* (2013) 33:S79–84. doi: 10.1007/s10875-012-9847-0
- Coussens LM, Werb Z. Inflammation and Cancer. *Nature* (2002) 420:860–7. doi: 10.1038/nature01322
- Elinav E, Nowarski R, Thaiss CA, Hu B, Jin C, Flavell RA. Inflammation-Induced Cancer: Crosstalk Between Tumours, Immune Cells and Microorganisms. *Nat Rev Cancer* (2013) 13:759–71. doi: 10.1038/nrc3611
- Van Berckelaer C, Van Geyt M, Linders S, Rypens C, Trinh XB, Tjalma WAA, et al. A High Neutrophil-Lymphocyte Ratio and Platelet-Lymphocyte Ratio are Associated With a Worse Outcome in Inflammatory Breast Cancer. *Breast* (2020) 53:212–20. doi: 10.1016/j.breast.2020.08.006
- Gabrielson A, Wu Y, Wang H, He AR, Jiang J, Kallakury B, et al. Intratumoral CD3 and CD8 T-Cell Densities Associated With Relapse-Free Survival in HCC. *Cancer Immunol Res* (2016) 4(5):419–30. doi: 10.1158/2326-6066.CIR-15-0110
- Wang TC, An TZ, Li JX, Pang PF. Systemic Inflammation Response Index is a Prognostic Risk Factor in Patients With Hepatocellular Carcinoma Undergoing Tace. *Risk Manag Healthc Policy* (2021) 14:2589–600. doi: 10.2147/RMHP.S316740
- Wu Y, Tu C, Shao C. Inflammatory Indexes in Preoperative Blood Routine to Predict Early Recurrence of Hepatocellular Carcinoma After Curative Hepatectomy. *BMC Surg* (2021) 21(1):178. doi: 10.1186/s12893-021-01180-9
- Dodson S, Baracos VE, Jatoti A, Evans WJ, Cella D, Dalton JT, et al. Muscle Wasting in Cancer Cachexia: Clinical Implications, Diagnosis, and Emerging Treatment Strategies. *Annu Rev Med* (2011) 62:265–79. doi: 10.1146/annurev-med-061509-131248
- Montesano A, Senesi P, Luzi L, Benedini S, Terruzzi I. Potential Therapeutic Role of L-carnitine in Skeletal Muscle Oxidative Stress and Atrophy Conditions. *Oxid Med Cel Longev* (2015) 2015:1–13. doi: 10.1155/2015/646171
- Feliciano EMC, Kroenke CH, Meyerhardt JA, Prado CM, Bradshaw PT, Kwan ML, et al. Association of Systemic Inflammation and Sarcopenia With Survival in Nonmetastatic Colorectal Cancer Results From the C Scans Study. *JAMA Oncol* (2017) 3(12):e172319. doi: 10.1001/jamaoncol.2017.2319
- Nishida N, Kudo M. Oncogenic Signal and Tumor Microenvironment in Hepatocellular Carcinoma. *Oncology* (2017) 93(Suppl 1):160–4. doi: 10.1159/000481246
- Shiroyama T, Nagatomo I, Koyama S, Hirata H, Nishida S, Miyake K, et al. Impact of Sarcopenia in Patients With Advanced Non-Small Cell Lung Cancer Treated With PD-1 Inhibitors: A Preliminary Retrospective Study. *Sci Rep* (2019) 9(1):2447. doi: 10.1038/s41598-019-39120-6
- Cortellini A, Bozzetti F, Palumbo P, Brocco D, Di Marino P, Tinari N, et al. Weighing the Role of Skeletal Muscle Mass and Muscle Density in Cancer Patients Receiving PD-1/PD-L1 Checkpoint Inhibitors: A Multicenter Real-Life Study. *Sci Rep* (2020) 10(1):1456. doi: 10.1038/s41598-020-58498-2
- Cortellini A, Verna L, Porzio G, Bozzetti F, Palumbo P, Masciocchi C, et al. Predictive Value of Skeletal Muscle Mass for Immunotherapy With Nivolumab in Non-Small Cell Lung Cancer Patients: A “Hypothesis-Generator” Preliminary Report. *Thorac Cancer* (2019) 10(2):347–51. doi: 10.1111/1759-7714.12965
- Afzali AM, Muntefering T, Wiendl H, Meuth SG, Ruck T. Skeletal Muscle Cells Actively Shape (Auto) Immune Responses. *Autoimmun Rev* (2018) 17 (5):518–29. doi: 10.1016/j.autrev.2017.12.005

**Conflict of Interest:** The authors declare that the research was conducted in the absence of any commercial or financial relationships that could be construed as a potential conflict of interest.

**Publisher's Note:** All claims expressed in this article are solely those of the authors and do not necessarily represent those of their affiliated organizations, or those of the publisher, the editors and the reviewers. Any product that may be evaluated in



this article, or claim that may be made by its manufacturer, is not guaranteed or endorsed by the publisher.

Copyright © 2022 Zhao, Duan, Han, Wang, Han, Mi, Shi, Li, Yin, Hou and Yin. This is an open-access article distributed under the terms of the Creative Commons

Attribution License (CC BY). The use, distribution or reproduction in other forums is permitted, provided the original author(s) and the copyright owner(s) are credited and that the original publication in this journal is cited, in accordance with accepted academic practice. No use, distribution or reproduction is permitted which does not comply with these terms.



# Challenges and Opportunities Associated With Platelets in Pancreatic Cancer

Zhou Chen<sup>1,2</sup>, Xiaodong Wei<sup>3</sup>, Shi Dong<sup>2</sup>, Fangfang Han<sup>1,2</sup>, Ru He<sup>2</sup> and Wence Zhou<sup>1,2\*</sup>

<sup>1</sup> The First Clinical Medical College, Lanzhou University, Lanzhou, China, <sup>2</sup> Department of General Surgery, The First Hospital of Lanzhou University, Lanzhou, China, <sup>3</sup> Emergency Department, Gansu Provincial Hospital, Lanzhou, China

## OPEN ACCESS

### Edited by:

Elena Campello,  
University of Padua, Italy

### Reviewed by:

Laurence Panicot-Dubois,  
INSERM U1263 Centre de Recherche  
en Cardiovasculaire et Nutrition,  
France

Iwona Inkielewicz-Stepniak,  
Medical University of Gdansk, Poland  
Shaoshan Mai,  
Medical University of Gdansk, Poland  
in collaboration with reviewer IIS.

### \*Correspondence:

Wence Zhou  
zhouwc129@163.com

### Specialty section:

This article was submitted to  
Gastrointestinal Cancers: Hepato  
Pancreatic Biliary Cancers,  
a section of the journal  
Frontiers in Oncology

**Received:** 07 January 2022

**Accepted:** 15 March 2022

**Published:** 12 April 2022

### Citation:

Chen Z, Wei X, Dong S, Han F, He R  
and Zhou W (2022) Challenges and  
Opportunities Associated With  
Platelets in Pancreatic Cancer.  
Front. Oncol. 12:850485.  
doi: 10.3389/fonc.2022.850485

Pancreatic cancer is one of the most common malignant tumors in the digestive system with a poor prognosis. Accordingly, better understanding of the molecular mechanisms and innovative therapies are warranted to improve the prognosis of this patient population. In addition to playing a crucial role in coagulation, platelets reportedly contribute to the growth, invasion and metastasis of various tumors, including pancreatic cancer. This narrative review brings together currently available evidence on the impact of platelets on pancreatic cancer, including the platelet-related molecular mechanisms of cancer promotion, pancreatic cancer fibrosis, immune evasion, drug resistance mechanisms, thrombosis, targeted platelet therapy, combined radiotherapy and chemotherapy treatment, platelet combined with nanotechnology treatment and potential applications of pancreatic cancer organoids. A refined understanding of the role of platelets in pancreatic cancer provides the foothold for identifying new therapeutic targets.

**Keywords:** platelet, molecular mechanism, immune evasion, targeted therapy, pancreatic cancer

## 1 INTRODUCTION

Pancreatic cancer (PC) is one of the most common malignant tumors and the second leading cause of death in malignant tumors of the digestive tract (1). Importantly, it has been suggested that PC will be the second most common malignancy by 2030, given the increasing incidence in recent years (2). PC characteristics, including advanced disease stage at diagnosis and high invasion and distant metastasis rates, account for the low 1-year and 5-year survival rates (3), highlighting the need to explore novel targets to enhance the diagnostic and therapeutic approach for PC. Current evidence suggests that the average platelet count of untreated cancer patients is significantly higher than non-cancer patients or patients with prior cancer history (4, 5), suggesting that platelets play an important role in the development, progression and treatment of tumors. An increasing body of evidence suggests that thrombocytosis is related to reduced survival rate, histological type, gender, age and TNM stage for various cancers (6, 7). However, little is currently known on the molecular mechanisms and therapeutic effects of platelets in PC, warranting further investigation.

## 2 INTERACTION BETWEEN VARIOUS TYPES OF CANCER AND PLATELETS

Platelets are well-established as biologically active nonnucleated cellular fragments from the cytoplasm of mature megakaryocytes in the bone marrow, playing important roles in hemostasis and thrombosis (**Figure 1**) (8). Given that an adult body contains nearly one trillion platelets in the blood circulation and the average platelet lifespan is only about eight days, our bodies must produce 100 billion new platelets every day to keep the platelet count within the normal range (8). The newly generated platelets pass through the spleen, where one-third of the platelets are stored. The stored platelets can exchange freely with circulating platelets to maintain a normal platelet count. The spleen is also the main organ for eliminating immunocompromised platelets (9). Lefrançois et al. (10) demonstrated that massive megakaryocytes were present in the pulmonary circulation in a mouse model; megakaryocytes originating from the bone marrow and spleen sinusoids could release platelets in the lungs, accounting for 50% of the platelet count. Therefore, the lungs represent the main production site of platelets besides the bone marrow, and lung pathologies can affect the quality of platelets (11). When blood loss occurs due to vascular trauma, subcutaneous collagen or/and tissue factor (TF) is exposed to the circulation, causing quick adhesion of platelets to the wound and aggregation into clusters to

form a softer hemostatic thrombus (12, 13). Under normal circumstances, the large number of circulating platelets is in dynamic equilibrium. However, platelet homeostasis is disrupted in response to different kinds of stimuli, leading to changes in platelet count and biological functions.

There is ample evidence to suggest that platelets are significantly elevated in the plasma of patients with different types of cancer (14–20). More importantly, large clinical studies showed that elevated numbers of circulating platelets were associated with tumor features, including advanced cancer and both local and distant metastasis (17, 19, 21). Meanwhile, substantial evidence suggests that thrombocytosis is predictive of poor prognosis in different cancers (22–24). Moreover, patients with higher platelet to lymphocyte ratio (PLR) were associated with shorter overall survival and disease-free survival rates (25, 26). Nevertheless, current evidence suggests poor prediction accuracy of PLR for the overall survival time of PC patients undergoing pancreatectomy (27). Thrombocytopenia induced by chemotherapeutic drugs such as gemcitabine may lead to the opposite results of the above experiments (28). In addition, increased platelet activation is a prerequisite for thrombosis. The risk of venous thromboembolism has been reported to be as high as 20% in cancer patients (29), especially in PC patients (30, 31), representing the leading cause of death in cancer patients (32). Furthermore, it has been shown that elevated platelets incredibly weaken the response and efficacy of

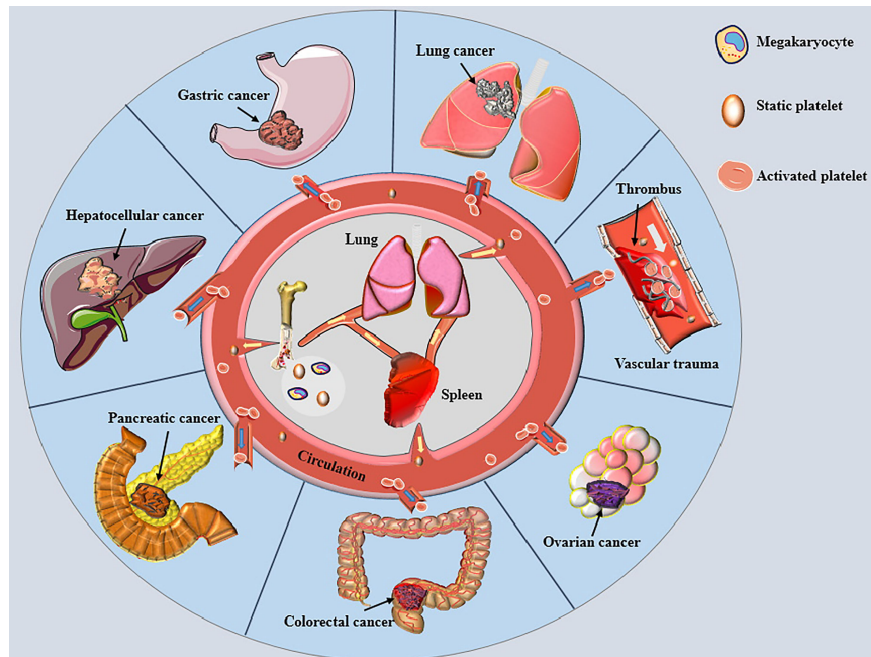


**FIGURE 1** | Platelets and various cancers. Small pieces of cytoplasm released from mature megakaryocyte cytoplasm in bone marrow and lung enter the circulation through the blood sinus to become static platelets. The newly generated platelets pass through the spleen, most of which are stored here and freely exchanged with the platelets in circulation to maintain the normal amount of platelets. Most of the aged platelets are removed in the spleen. When blood vessel is traumatized, platelets are rapidly activated and adhere to the wound, gathering together to form a soft hemostatic plug. Activated platelets change the malignant phenotype of tumor cells and encapsulate cancer cells to help cancer cells distant metastasis by escaping immune cell surveillance, thereby affecting the prognoses of various cancer patients.

chemotherapy drugs to tumor cells (33). In recent years, platelet inhibition combined with immunotherapy has achieved promising results for cancer treatment (34). Accordingly, the unique molecular mechanisms and advantages of platelets in tumor therapy make them potential targets for oncotherapy.

### 3 PC CELLS INFLUENCE THE FUNCTION OF PLATELETS

#### 3.1 PC Cells Activate and Alter the Biology of Platelets

It is widely acknowledged that platelets can be activated by various factors released by tumor cells like TF, adenosine diphosphate (ADP), thromboxane A<sub>2</sub> (TXA<sub>2</sub>) and high-mobility group box 1 (HMGB1) (35, 36). Tumor cells can activate platelets *via* direct interactions or secretion of biologically active proteins leading to tumor cell-induced platelet aggregation (TCIPA) (37, 38). During the TCIPA process, platelet  $\alpha$ Ib $\beta$ 3,  $\alpha$ 6 $\beta$ 1, platelet P-selectin, platelet Toll-like receptor (TLR) 4 and platelet CLEC-2 bind to protein molecules on the surface of the corresponding tumor cells, enhancing platelet activation and tumor cell malignant behavior (36, 39–42). In addition, the biological characteristics of platelets during the TCIPA process are subjected to significant changes, with tumor cell-induced platelet extracellular vesicle formation, granule release and alterations in platelet RNA profiles (37, 43). Moreover, activated platelets undergo various cellular responses, including morphological changes and translocation of membrane glycoproteins, and eventually release extracellular vesicles (EVs) containing bioactive substances (44). EVs are mainly composed of exosomes and microvesicles (MVs). Exosomes are intraluminal vesicles, 30–100nm in diameter, formed by the inward budding of endosomal membranes during maturation of multivesicular endosomes (MVEs), while MVs 100–1,000nm in diameter are generated by the outward budding and fission of the plasma membrane (45, 46). EVs induce different biological signals depending on the cell of origin. In this regard, platelet-derived exosomes originate from the extracellular secretion of multivesicular bodies and alpha granules, and MVs are produced by surface shedding (44). Furthermore, the number and proteomic profile of platelet-derived microvesicles (PMVs) exhibit variations with different stimuli (including pathologies). For instance, it has been shown that integrin  $\alpha$ 6 levels in shear stress-originated PMVs were significantly elevated compared to thrombin-induced PMVs (47). Importantly, integrin  $\alpha$ 6 has been documented in vascular endothelial growth factor-A (VEGF-A) and fibroblast growth factor-2-driven angiogenesis, promoting tumor growth *in vivo* and *in vitro* (48). Nevertheless, the proteomic alterations of platelet-derived MVs in PC remain unclear, emphasizing the need for further investigation. The effect of platelets on cancer cells may be attributed to the ability of exosomes to shuttle selected molecules, since EVs containing protein, mRNA and miRNA with biological functions can be delivered to PC cells (49). Similarly, tumor cell-derived exosomes can transfer mutated RNA to platelets by shuttling, a process that may involve plasma membrane fusion, clathrin-mediated endocytosis, and phagocytosis (50). The tumor

microenvironment (TME) contains various cells, cytokines and extracellular matrix components and is the main place for the interaction between the body and the tumor. Tumor cells and platelets maintain a complex, bidirectional interaction in the TME. During TCIPA, activated platelets aggregate near tumor cells to form tumor platelet clots, protecting tumor cells from T cell immune responses and NK cell surveillance and ensuring that tumor cells can persist in circulation and metastasize to distant locations (38). Moreover, platelets contain many bioactive molecules that promote the proliferation, migration and invasion of PC cells (24, 41).

#### 3.2 PC Cells Enhance Thrombopoiesis

It has been established that various cancer cells can activate platelets by secreting “activators” that result in venous thrombosis, the leading cause of death in cancer patients, especially in PC (30). Furthermore, studies have shown that cancer cells can secrete coagulants or fibrinolytic substances to induce platelet aggregation (51, 52). Mounting evidence suggests that membrane vesicles released by tumor cells called tumor-derived microvesicles (TMVs) incorporate large amounts of TF produced by tumor cells (52–55). TMVs are generated by outward budding and division of the plasma membrane, followed by vesicle release into the extracellular space. Using *in vitro* experiments, Geddings et al. (52) demonstrated that TMVs from human PC cells BxPc-3 and L3.6pl cells could interact with resting platelets to induce TF delivery and platelet aggregation in human and mouse plasma. In addition, after intravenous injection of TMV into mice, they found that femoral vein thrombosis and platelet deposition in the lungs was significantly increased. Using mouse models, researchers established that both TMV and TF could significantly activate platelets and increase the aggregation ability of platelets to form thrombosis by reducing the recalcification time (52, 56). In a study by Stark et al. (55), PC microvesicles (pcMV) derived from human PC cell line L3.6pl were injected into mice by intravenous injection. It was found that pcMV could selectively promote thrombus growth in regions with slow and turbulent flow and significantly shortened whole blood clotting time, leading to the formation of large thrombi upstream of the stenosis. Furthermore, activated platelets can directly activate neutrophils and induce the formation of neutrophil extracellular traps (NETs) (57). Conversely, NETs can induce thrombin production and activate platelets to release ATP and ADP, causing a cascade of reactions and promoting platelet aggregation (58, 59). It has been established that during NETs formation, DNA, TF, myeloperoxidase and histones are released, and DNA upregulates platelet aggregation through the platelet receptor for advanced glycation end products (RAGE) (60). Thrombosis is showed in **Figure 2**. However, NETs were not observed in the thrombi in a study where a minimally invasive laser-induced injury model was used, although neutrophils were present at the injury site (61). Interestingly, activated platelets gather into clusters and form thrombi in the TME; however, the thrombi are different from those caused by benign diseases. Histological analyses confirmed that pcMV-thrombi had a composition distinct from nonmalignant thrombi. In contrast, a study reported that the luminal area in the pancreatic TMV-thrombi



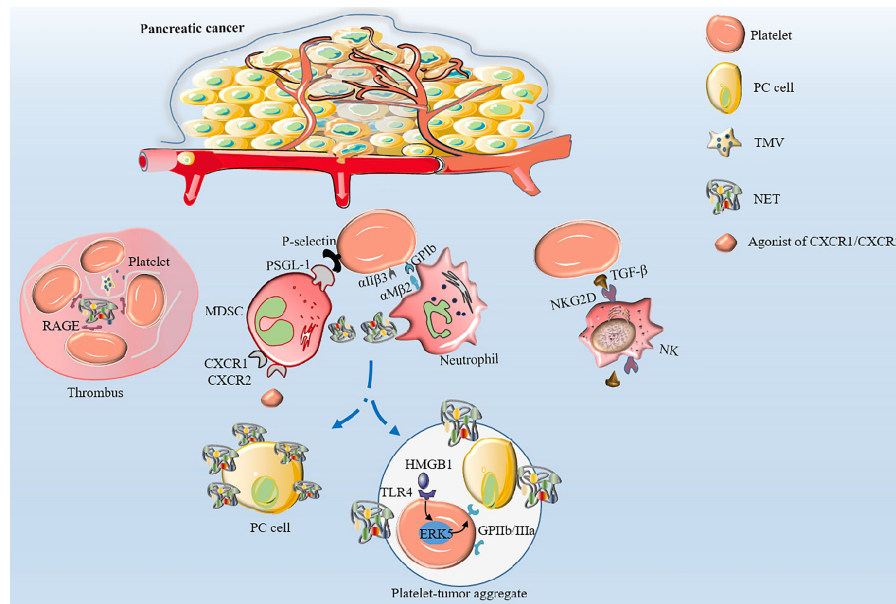


**FIGURE 2 |** The mechanisms of thrombosis and platelet-induced evasion of immune surveillance in PC. Platelets are activated by TF and TMV incorporating large amounts of TF to aggregate to form thrombi. Activated platelets interact with integrin  $\alpha\text{IIb}\beta 3$  on neutrophils via GPIb or integrin  $\alpha\text{IIb}\beta 3$  to activate and regulate the functions of neutrophils. Neutrophils release NETs, which in turn activate platelets and promote platelet aggregation via DNA-RAGE. Furthermore, tumor-produced CXCR1 and CXCR2 chemokine receptor agonists induce neutrophils and MDSCs to generate NETs. After surgical stress, activation of the TLR4-ERK5-integrin GPIIb/IIIa axis leads to platelet activation and formation of microaggregates with tumor cells and tumor platelet-neutrophil complexes, enhancing immune escape and leading to distant metastasis of tumor cells. Activated platelets assist PC cells to evade NK cell surveillance by releasing TGF- $\beta$  to recognize NKG2D on the surface of NK cells.

was filled with a loose fibrin (-proto) network, while neutrophils, monocytes and platelets were significantly reduced (55). Portal vein thrombosis is well-recognized as the most common type of thrombosis in patients with advanced PDAC, followed by mesenteric vein thrombosis and splenic vein thrombosis, suggesting its value as an indicator of poor prognosis (62, 63). Nevertheless, it has been reported that thrombocytosis has little to do with the increased incidence of thromboembolism (6) since the hypercoagulable state of the whole body is not related to an absolute increase in specific factors but the presence of activated coagulation factors (64). Overall, high expression levels of TMV, NET and TF in PC tissue participate in platelet activation and aggregation, which coupled with procoagulant molecules enzyme heparanase (HPSE), podoplanin (PDPN) and the fibrinolytic system, contribute to the high incidence of thrombosis, making it an excellent model for studying cancer-associated hypercoagulable states (65).

## 4 ACTIVATED PLATELETS PROVIDE FAVORABLE ENVIRONMENT FOR PC CELLS

### 4.1 Activated Platelets Alter the Malignant Phenotype of PC Cells

Ponert et al. (66) demonstrated that different cancer cells could easily bind to activated platelets *in vitro*, thereby accelerating the

adhesion between platelets and tumor cells; this phenomenon was particularly prominent in PC cells. In another *in vitro* experiment, investigators observed that after many platelets aggregated by binding to PC PANC-1 cells, the migration, invasion and proliferation capacity of PANC-1 cells was significantly enhanced (24, 67). The cytoplasm of platelets contains many biologically active proteins, such as growth factors, chemokines, cytokines and proteases, which are secreted by activated platelets (68). The main documented molecular pathways are shown in **Figure 3**.

#### 4.1.1 Roles of Platelet-Derived Growth Factor

Platelet-derived growth factor (PDGF) plays an important role in maintaining the integrity of blood vessels in the TME, promoting the proliferation of tumor cells, epithelial-mesenchymal transition (EMT) progression and tumor metastasis in PC (69). According to the literature, PDGF-BB exerts no effects on the proliferation of tumor cells but enhances the invasion and metastasis of tumor cells through matrigel *in vivo*, resulting in PDGFR- $\beta$ -mediated phosphorylation of MUC1 cytoplasmic tail (MUC1CT) to regulate the invasiveness of PC cells. MUC1 is a type I transmembrane protein that is overexpressed and abnormally glycosylated in ductal adenocarcinoma (70). Besides, another study revealed that autocrine PDGF-BB significantly increased the proliferation, migration and invasion of PC cells *via* the Hippo/Yes-associated protein signaling pathway (71). Metalloproteinase-9 (MMP-9) belongs to the matrix metalloprotein family, whose main function is to

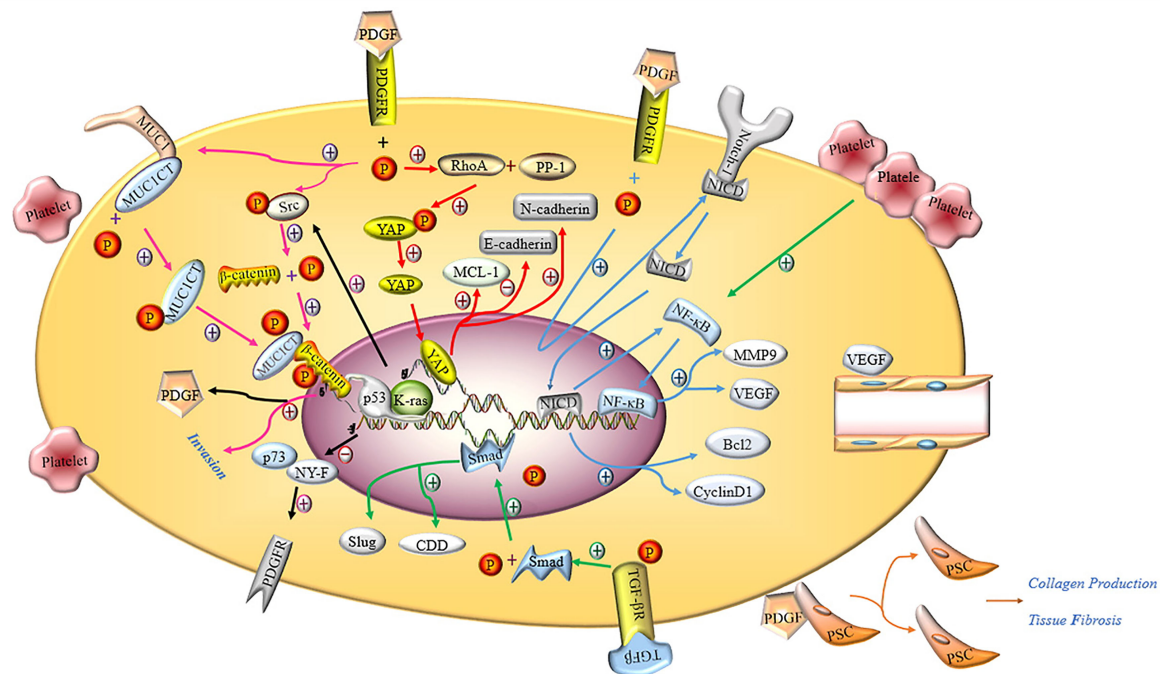


**FIGURE 3 |** Molecular mechanism of activated platelets inducing malignant phenotype of PC cells. PDGFR activated by PDGF induces the phosphorylation of tyrosine residue in the intracellular domain, activating the Hippo/Yes-associated protein signaling pathway and promoting MCL-1, N-cadherin and inhibiting E-cadherin (red arrow). Notch-1 is promoted by activated PDGFR and releases intracellular domain of Notch 1 (NICD), which enters the nucleus and increases the expression of Bcl2, Cyclin D1 and NF- $\kappa$ B. NF- $\kappa$ B promotes the expression of MMP9 and VEGF by binding nuclear genes (blue arrow). Activated PDGFR induces phosphorylation of MUC1CT and Src, phosphorylation of Src induces phosphorylation of  $\beta$ -catenin, and the combination of phosphorylated MUC1CT and  $\beta$ -catenin enhances the invasion of PC cells (pink arrow). PDGF induces PSC to proliferate and secrete collagen, thereby aggravating pancreatic fibrosis. The deletion of p53 and the mutation of K-ras not only inhibits the binding of p73 and NY-F, so that the activation of PDGFR is not inhibited, but also induces  $\beta$ -catenin phosphorylation through Src phosphorylation to promote the expression of PDGF (black arrow). Activated TGF- $\beta$ R promotes the expression of Smad, and the Smad protein enters the nucleus to promote the expression of CDD and Slug (green arrow). VEGF induces the proliferation and remodeling of endothelial cells in the TIME.

degrade and remodel the dynamic balance of the extracellular matrix. Current evidence suggests that MMP-9 is related to tumor pathological features, including invasion, metastasis, and angiogenesis (72). Suzuki et al. (7) reported that the invasive ability of PC cells co-cultured with platelets was significantly enhanced as platelets stimulated PC cells to secrete more MMP-9. It is well-recognized that Notch-1 signaling plays an important role in maintaining the balance between cell proliferation, differentiation and apoptosis (73). A study by Wang et al. (74) illustrated that downregulation of PDGF-D effectively limited the invasive ability of PC cells through inactivation of Notch-1 and NF- $\kappa$ B DNA binding activity, which in turn downregulated the expression of their target genes VEGF and MMP-9. In contrast, the opposite results were observed with overexpression of PDGF-D by cDNA transfection. In addition, the conditioned medium from cells transfected with PDGF-D siRNA showed significantly reduced levels of vascular endothelial growth factor (VEGF), which in turn inhibited tube formation by human umbilical cord vascular endothelial cells.

Studies have shown that the ligand PDGFR is indispensable for PDGF to maximize its biological function. Researchers discovered that  $\beta$ -catenin activation, coupled with K-ras

mutation and loss of p53, could activate the autocrine PDGF/ Src signal and significantly increase the proliferation and distant metastasis of PC cells, accounting for the poor prognosis of PC (75). Notably, missense mutations in the p53 tumor suppressor play an indispensable role in tumor proliferation, invasion, migration and metastasis. PDGFR is a downstream mediator of mutant p53 that has been reported to harbor huge potential for maintaining the aggressiveness of PC cells by disrupting the formation of the p73/NF-Y, a complex whose interaction prevents it from binding and activating the PDGFR promoter (76).

#### 4.1.2 Roles of Vascular Endothelial Growth Factor

VEGF is a highly specific vascular endothelial cell growth factor that increases vascular permeability and promotes the degeneration of extracellular matrix, migration and proliferation of vascular endothelial cells and blood vessel formation (77, 78). It has been shown that VEGF is abundantly stored in platelets at higher concentrations than in plasma and is related to the poor survival rate of PC patients (77, 79). Importantly, VEGF effectively promotes the proliferation, invasion and metastasis of tumor cells, as well as angiogenesis in

the TME (80, 81). Besides, VEGF overexpression-induced tumor microangiogenesis is closely related to the microvessel density (MVD) in PC tissues, promoting local tumor growth by paracrine signal transduction in stromal cells expressing VEGFR and allowing cancer cells to invade peritumoral lymphatic vessels (77). Mesenchymal stem cells (MSC) in the TME can secrete VEGF, contributing to angiogenesis in PC (82). It has been reported that PC cells express the functional P2Y<sub>12</sub> receptor required for cell proliferation by promoting EGFR-dependent and independent AKT-mediated survival signals (83). In an *in vitro* model of angiogenesis, Battinelli et al. (84) observed that activated platelets significantly released more VEGF and promoted the formation and migration of human umbilical vein endothelial cells capillary structure, and enhanced tumor growth.

#### 4.1.3 Roles of Transforming Growth Factor- $\beta$ 1

Transforming growth factor- $\beta$ 1 (TGF- $\beta$ 1) belongs to the newly discovered TGF- $\beta$  superfamily that regulates the growth and differentiation of cells. Slug is a transcription-related factor of the EMT that has been reported to be mainly regulated by TGF- $\beta$ 1 through the Smad effector pathway (85). Current evidence suggests that Slug expression is significantly increased in PC cells exposed to platelet releasate (PR)-TGF- $\beta$ 1 and can induce EMT progression. Platelet-derived TGF- $\beta$  and direct platelet-tumor cell contraction can synergistically activate the TGF- $\beta$ /Smad and NF- $\kappa$ B pathways in cancer cells, exhibiting an aggressive mesenchymal phenotype and enhanced metastasis *in vivo* (85). In addition, studies have shown that TGF- $\beta$ 1 in the TME could effectively induce pancreatic stellate cells (PSCs) to secrete alpha-smooth muscle actin ( $\alpha$ SMA), thereby exacerbating fibrosis while inhibiting the toxic response of CD8<sup>+</sup> T cells to PC cells (86).

#### 4.1.4 Roles of MiRNAs

MiRNAs are widely acknowledged to bind to specific regions of target gene mRNAs, which degrade or inhibit mRNAs and subsequently lead to inhibition of protein translation (87, 88). Serious platelet-related diseases are caused by dysfunctions of the miRNA-based regulatory system (89); the regulatory mechanism is controlled by platelet-specific signals and is not restricted by the nucleus (90). Studies have shown significant differences in the miRNA expression profiles in the blood circulation of PC patients and patients with benign pancreatic diseases (87). Recent research has demonstrated that miR-221-5p, miR-29a-3p, miR-22-3p and miR-17-3p were abundant in platelets of PC patients, and miR-29a-3p could inhibit the expression of SPARC, a multifunctional glycoprotein, and promoted proliferation, migration and invasion of PC cells *in vitro* (91). In addition, miR-221 has been reported to be essential for PDGF-mediated EMT phenotype, migration, and growth of PC cells (92). Another study showed that depletion of miRNA-rich platelets led to a marked increase in the growth rate of PC; however, the specific miRNAs and target genes have not been identified (93). Overall, platelets contain many unknown non-coding RNAs, including miRNAs, which potentially participate in the pathogenesis of PC.

#### 4.1.5 Roles of Other Protein Factors

An increasing body of evidence suggests that ADP derived from ATP released from pancreatic acinar cells and dense granules of platelets (35, 94) can effectively stimulate and activate platelets *via* Gq-coupled P2Y<sub>1</sub> and Gi-coupled P2Y<sub>12</sub> receptors located on the platelet membrane (95). The surrounding platelets are activated by ADP and trigger a cascade reaction that activates more platelets releasing VEGF and promoting tumor proliferation (84). It has been shown that platelet glycoprotein (GP) is involved in platelet adhesion, aggregation and activation and mediates the combination of platelets and CD34<sup>+</sup> cells from human blood and bone marrow *via* P-selectin (96). Increased CD34 expression has been established to promote the invasion and migration of PDAC cells (97). Nevertheless, the role of membrane glycoproteins of human platelets in PC is still unclear. Platelet thrombospondin-1 (TSP-1) is a platelet alpha-granule and matrix glycoprotein involved in tumor invasion, angiogenesis and metastasis. TSP-1 has been established as a regulator of angiogenesis that is strongly expressed in PCs, upregulates the production of MMP-9 and contributes to the extensive neovascularization and spread of highly aggressive tumors (98, 99). Boone et al. (100) demonstrated that the nucleotide-binding domain leucine-rich repeat-containing protein 3 (NLRP3) in platelets was upregulated in mice models and led to significant platelet aggregation *in vivo*. Importantly, NLRP3 forms a complex with the adaptor protein apoptosis-associated speck-like protein containing a caspase activation and recruitment domain (ASD) to promote PC progression. The opposite results were observed with NLRP3 inhibitors, with inhibited growth of PC cells and improved survival rate of mice. Moreover, P-selectin accelerates thrombus formation, induces infiltration of MDSCs and evades immune cytotoxic effect *via* PSGL-1 (101, 102). Platelet factor 4 (PF-4) reportedly regulates the activity of fibroblast growth factor 2 (FGF-2), resulting in the phosphorylation of E-cadherin and  $\beta$ -catenin on tyrosine residues leading to angiogenesis (103, 104). Activation of EGFR by epidermal growth factor (EGF) induces phosphorylation of PLC $\gamma$ , which ultimately leads to high spontaneous migratory activity in PC cells (105). Moreover, platelet-derived lysophosphatidic acid (LPA) enhances the invasion and migration of PC cells through LPAR (106). Last but not least, the Von Willebrand factor (VWF) can activate platelets to promote platelet aggregation and emboli formation *via* GPIb, promoting tumor metastasis (107, 108).

### 4.2 Activated Platelets Enhance Drug Resistance of PC Cells

The enzyme cytidine deaminase (CDD) has been reported to participate in the mechanism of gemcitabine resistance by intracellular metabolism of gemcitabine (109) after its upregulation by platelet releasate (110). Human ENT1 (hENT1) is well-known for enhancing the cellular uptake of gemcitabine, thereby enhancing its toxic effects in PC cells (111). Moreover, Slug is a master regulator of EMT that is highly expressed in CD133<sup>+</sup> human PC cell lines (Capan-1) and enhances the migration and invasion of PC cells, resulting in



gemcitabine resistance (112). *In vitro* experiments have shown that platelet-derived ADP and ATP induced high Slug expression via P2Y1 and P2X7 receptors on the surface of human PC cell lines AsPC-1 and BxPC-3. Importantly, a study demonstrated that Slug could effectively inhibit hENT1 expression, stimulate CDD expression, and enhance the resistance of PC cells to gemcitabine by inhibiting the uptake of gemcitabine by PC cells and accelerating the metabolism of gemcitabine (35, 113). Activated platelet-derived TGF- $\beta$ 1 stimulates PI3K/Akt and MEK/Erk signaling in PC cells, resulting in decreased cisplatin sensitivity (114). Nonetheless, the regulatory role of platelets on the efficacy of PC chemotherapy remains unclear, warranting further study. The above findings suggest that activated platelets can mediate drug resistance in PC cells to a certain extent.

### 4.3 Activated Platelets Contribute to PC Fibrosis

The varying degrees of fibrosis associated with PC account for the difficulty of providing effective treatment for this patient population. Tumor cells are hidden in a thick fibrotic matrix that acts as a barrier and is responsible for the poor response to chemotherapy drugs. Over the years, research on the mechanism of platelet fibrosis in PC has been limited to PSCs. PSC has been acknowledged to play a key role during pancreatic fibrosis in chronic pancreatitis and the pro-fibrotic reaction of PC by producing the stromal reaction. Studies have shown that activated platelets could effectively activate PSC and promote the formation of connective tissue (75). In a mouse model experiment, Vonlaufen et al. (115) demonstrated that the PC group co-cultured with PSC exhibited a faster growth rate, larger volume and more fibrotic bands containing activated PSC. Moreover, PSC migration was significantly increased by PC cells *in vitro*. On the contrary, the secretion of PSC could induce PC cell proliferation and migration and inhibit apoptosis. PDGF and TGF- $\beta$  released by activated platelets have been recognized as effective stimulators for PSC proliferation to accelerate extracellular matrix synthesis (115). Fitzner et al. (116) elucidated that the activation of rat PSCs *in vitro* was related to increased expression of galectin-1, and galectin-1 could mediate PSC function. PDGF stimulated the expression of the lectin galectin-1 resulting in high proliferation rates and synthesis of more collagen. Targeting platelets against PC fibrosis is a potential therapeutic approach.

### 4.4 Activated Platelets Assist PC Cells to Evade Immune Surveillance

When tumors and associated blood vessels are destroyed, cancer cells escape and slough off into the circulation to form circulating tumor cells (CTCs), which become the seeds for distant metastasis of tumors (117). Interestingly, platelets can couple to tumor cells, increase vascular permeability and induce extravasation of tumor cells (118). Tumor cells entering the circulation must deal with high shear rates and immune surveillance, such as NK cell attacks. Eventually, only a small proportion of tumor cells enter the blood

circulation for metastasis, making this process very inefficient (119). NK cells play important roles in cancer immune surveillance by mediating direct cytotoxicity and releasing immunomodulatory cytokines to form an adaptive immune response and prevent tumor progression and metastasis. During hematogenous metastasis, cancer cells are quickly encapsulated by platelets, similar to cancer cells putting on a “protective suit”, making it impossible for NK cells to recognize tumor cells allowing distant metastasis (Figure 2). Interestingly, researchers found that thrombocytopenia could effectively inhibit the ability of cancer cells to metastasize in mice models. This phenomenon was reversed by the depletion of NK cells and secretion of TGF- $\beta$  by activated platelets, thereby inhibiting immunoreceptor natural killer group 2, member D (NKG2D), indispensable for antitumor activity of NK cells (120). Okazaki et al. (121) noted that platelets could preferentially adhere to mesenchymal cells rather than epithelial cells in the TME of mouse models of infectious disease. Interestingly, cancer cells could be wrapped by activated platelets to escape immune surveillance and promote metastasis.

Neutrophils are important innate immune cells in the blood circulation that play important roles in innate and adaptive immunity. Activated platelets can recruit neutrophils by releasing chemical mediators such as CXCL4 (122) and directly interact with integrin  $\alpha$ M $\beta$ 2 on neutrophils via GPIb or integrin  $\alpha$ IIb $\beta$ 3 to activate and regulate the functions of neutrophils (123, 124). After activation by various stimuli (e.g., infection, surgery, activated platelets), neutrophils can release reticular ultrastructures composed of protein-studded chromatin called NETs (52, 125, 126). NETs play a double-edged role. On the one hand, they play a positive role in the invasion of pathogenic microorganisms. On the other hand, NET amplifies platelet activation, aggregation and thrombin activation, promotes intravascular coagulation, and promotes the attachment of cancer cells to the blood vessel wall, resulting in enhanced tumor migration (127). In this regard, it has been reported that after surgical stress, activation of the TLR4-ERK5-integrin GPIIb/IIIa axis leads to platelet activation and formation of microaggregates with tumor cells and tumor platelet-neutrophil complexes, enhancing immune escape and leading to distant metastasis of tumor cells (128). Importantly, thrombomodulin effectively prevents PC metastasis to the liver by degrading HMGB1 and thus inhibiting the induction of NETs (129). Furthermore, tumor-produced CXCR1 and CXCR2 chemokine receptor agonists induce neutrophils and granulocyte myeloid-derived suppressor cells (MDSCs) to generate NETs that encapsulate tumor cells and protect them from the cytotoxicity of CD8<sup>+</sup> T cells and NK cells by hindering the contact between immune cells and surrounding target cells (130). NETs can suppress T-cell responses through metabolic and functional exhaustion, promoting tumor growth (131). However, the role of activated platelets in evasion of immune surveillance and immune cytotoxicity by PC cells remains to be elucidated. The studies of potential markers associated with platelets in PC are summarized in Table 1.



## 5 APPLICATIONS OF PLATELETS IN THE TREATMENT OF PC

### 5.1 Platelet-Related Targeted Therapy in PC

At present, the application of platelets to enhance antitumor therapeutic effects is widely used in preclinical studies and clinical trials of PC, emphasizing the inhibition of platelet activation and abnormal pathways of cancer cells associated with activated platelets. The efficacies of single antiplatelet drugs and a combination of antiplatelet and chemotherapy drugs have been assessed in these studies. Aspirin is widely acknowledged as a derivative of salicylic acid with antiplatelet properties. It has a significant inhibitory effect on platelet aggregation and effectively prevents thrombosis by inhibiting the production of cyclooxygenase. Accordingly, it is widely used in clinical practice to prevent transient ischemic attacks, myocardial infarctions, and artificial heart thrombi formation after valve surgery. Low-dose aspirin can effectively reduce the incidence and mortality of colorectal cancer (132). In this regard, low-dose aspirin taken every other day has been reported to effectively reduce the risk of colorectal cancer in healthy women (133, 134). A study where activated platelets and PANC-1 cancer cells were co-cultivated demonstrated that the proliferation ability was increased by upregulating the expression of c-MYC. After treatment with aspirin, the proliferation rate of cancer cells was significantly reduced, and the expression of c-MYC was suppressed (72). Clopidogrel exhibits a similar antiplatelet effect as aspirin by inhibiting ADP receptors on the surface of platelets. Using an orthotopic PC mouse model, Mezouar et al. (135) revealed that clopidogrel could directly inhibit platelet activation, significantly reducing thrombus formation, tumor growth, and metastasis without increasing the risk of bleeding. Additionally,

studies have shown that the activation of EMT progression in PC cells further promoted chemotherapy resistance of PDAC (136). Low molecular weight heparin (LMWH) can reduce direct contact and interaction between platelets and tumor cells through the action of antithrombin, thereby reducing EMT progression induced by platelets (55). However, the risk of treatment-related bleeding is greatly increased by the long-term use of LMWH. Receptor tyrosine kinase (RTK) represents the largest class of enzyme-linked receptors, acting as a receptor and an enzyme that can bind to ligands and phosphorylate tyrosine residues of the target protein. It consists of a ligand-binding site in the extracellular domain, the single-pass hydrophobic  $\alpha$  helix region and an intracellular domain with tyrosine-protein kinase (PTK) activity (137). RTK mediates the connection between cells and controls a wide range of complex biological functions, including cell growth, movement, differentiation, and metabolism. Therefore, the dysregulation of the RTK signal leads to various human diseases, including cancer (138).

It has been established that PDGFRs and VEGFRs belong to the RTK supergene family, are widely distributed in the membrane of PC cells and vascular endothelial cells in the TME, and interact with abundant PDGF and VEGF released by platelets. Many experiments have been designed to explore the roles of PDGFR or/and VEGFR in PC tumorigenesis. Current evidence suggests that platelet-derived endothelial cell growth factor harbors angiogenic activity *in vitro* and *in vivo* and contributes to angiogenesis and remodeling in the TME (138). The platelet-derived endothelial cell growth factor is overexpressed in most human cancers and associated with increased microvessel density, tumor aggressiveness and poorer patient prognosis (139). In nude mouse orthotopic tumor model experiments, the phosphorylation of PDGFR in tumor and

**TABLE 1 |** Studies on potential markers associated with platelets in PC.

Potential marker	Mechanism of action	Effect on tumor	<i>In vitro/ in vivo</i>	References
PDGF	PDGF-PDGFR-MUC1CT; PDGF-PDGFR-YAP-MCL-1/N-cadherin; PDGF-PDGFR-Notch-1 and NF- $\kappa$ B-VEGF/MMP-9	Enhanced the invasion and metastasis of tumor cells; Promoted angiogenesis	Both	(70, 71, 74)
VEGF	PDGF-Notch-1 and NF- $\kappa$ B-VEGF	Increases vascular permeability; Promoted the migration and proliferation of vascular endothelial cells and blood vessel formation	Both	(74, 78)
TGF- $\beta$ 1	TGF- $\beta$ -Smad and NF- $\kappa$ B; TGF- $\beta$ 1-PI3K/Akt and MEK/Erk	Enhanced EMT and drug resistance	Both	(85, 114)
ADP/ATP	ADP-P2Y1R/P2Y12R-VEGF; ADP/ATP-P2Y1/P2X7R-CDD	Amplified platelet degranulation and aggregation; Enhanced drug resistance	Both	(95, 113)
GP	GP-P-selectin-CD34	Promoted activated platelet adhesion to PC cells and tumor proliferation	<i>In vitro</i>	(96)
TSP-1	TSP-1-MMP-9	Promoted tumor invasion, angiogenesis and metastasis	<i>In vitro</i>	(98, 99)
NLRP3	NLRP3-ASC	Promoted activity and aggregation of platelets, and PC cell progression.	<i>In vivo</i>	(100)
P-selectin	P-selectin-PSGL-1	Accelerated thrombus formation; Induced MDSCs infiltration; Evaded immune cytotoxic effect	Both	(101, 102)
EGF	EGF-EGFR-PLC $\gamma$	Enhanced the migration of PC cell	<i>In vitro</i>	(105)
VWF	VWF- GPIb	Promoted platelet aggregation and emboli formation	Both	(107, 108)
$\alpha$ 6 $\beta$ 1	$\alpha$ 6 $\beta$ 1-ADAM9	Enhanced tumor metastasis	Both	(40)
$\alpha$ IIb $\beta$ 3	$\alpha$ IIb $\beta$ 3-PI3K-c-MYC	Induced PC cell proliferation	<i>In vitro</i>	(67)
PF-4	PF-4-FGF-2-E-cadherin/ $\beta$ -catenin	Increased neovascularization	<i>In vitro</i>	(103, 104)
LPA	LPA-LPAR	Enhanced PC cell invasion and migration	<i>In vitro</i>	
miR-29a-3p	miR-29a-3p-SPARC	Promoted proliferation, migration and invasion of PC cells	<i>In vitro</i>	(91)
miR-221	miR-221-PDGF	Mediated EMT phenotype, migration and proliferation of PC cells	<i>In vitro</i>	(92)

tumor-associated endothelial cells was found to be significantly inhibited by the administration of GN963, a tyrosine kinase inhibitor against PDGFR and Src kinases. Importantly, the activity of Src and Akt kinases in tumor cells was reduced, resulting in a decrease in microvessel density and cell proliferation and increased apoptosis of tumor and tumor-associated endothelial cells (140).

Pericytes are embedded in the basement membrane of capillary endothelial cells and regulate the proliferation and differentiation of endothelial cells associated with angiogenesis. It has been shown that the surface of pericytes is rich in PDGFR- $\beta$  (141). The specific inhibition of the PDGFR- $\beta$  signal eliminates PDGFR- $\beta$ (+) progenitor perivascular cells and mature pericytes around tumor blood vessels, resulting in excessive expansion of blood vessels, endothelial cell apoptosis and low pericytes coverage in PC (142). Subsequently, eliminating pericytes is conducive to tumor vascular degeneration and significant tumor growth inhibition. Moreover, inhibitors of VEGF signaling can block VEGF-mediated endothelial cell survival, tube formation and downstream signaling, inhibit angiogenesis, and reduce tumor vascular distribution (143, 144), exhibiting no harm to the integrity of blood vessels in normal tissues and organs (145). However, due to the complexity of tumor metabolism in time and space, the efficacy of antitumor drugs is greatly affected. Bergers et al. (146) revealed that SU5416, an inhibitor that targets VEGFR in endothelial cells, was effective for early angiogenic lesions but not for large, well-vascularized tumors in mouse models of PC. In contrast, SU6668, a selective kinase inhibitor of PDGFR, has been shown to prevent further end-stage tumor growth, causing pericyte detachment and tumor blood vessel destruction. The combination of SU5416 and SU6668 was more effective than mono drug therapy at all stages of pancreatic islet carcinogenesis. Other antiplatelet drugs have also been used for the treatment of PC. For example, integrin  $\alpha$ -2 is the most expressed integrin molecule on the platelet membrane and mediates platelet adhesion and aggregation. Integrin  $\alpha$ -2 inhibitor significantly reduces the microvessel density of PC in mice and effectively inhibits tumor growth (147). In a mice model of PC with liver metastasis, the number of multiple metastatic nodules on the liver surface was significantly reduced after injection of prostaglandin before tumor formation, which might be due to inhibition of platelet aggregation by prostaglandin E1 and I2 (148).

## 5.2 Antiplatelet Combined With Chemotherapy or Radioimmunotherapy in PC

At present, although gemcitabine is still the standard first-line treatment for patients with advanced PC, the benefits of these drugs for the survival of patients with PC are below expectations (136), which may be accounted for by activated platelets weakening the therapeutic effect of antitumor drugs. Platelets interact with PC cells and stimulate the PI3K/Akt and MEK/Erk signaling by releasing activated platelet-derived TGF- $\beta$ 1, causing cancer cell tolerance to cisplatin (114). The activation of platelets

in the TME account for increased chemotherapy resistance of pancreatic ductal adenocarcinoma. In an orthotopic PC model in nude mice, the combination of VEGF receptor antibody and gemcitabine inhibited primary pancreatic tumor growth and the incidence of lymphatic metastasis and liver metastasis to a great extent compared to monotherapy, improving the survival rate of mice (149, 150). PKI 166, an EGFR protein tyrosine kinase inhibitor, combined with gemcitabine, could effectively reduce microvessel density, inhibit cell proliferation, increase tumor cell and endothelial cell apoptosis, and significantly inhibit lymph node and liver metastasis (151). Ticagrelor, which inhibits platelet activation through the ADP-P2Y<sub>12</sub> axis, can significantly reduce the proliferation ability of PC cells but not normal pancreatic cells. The combination of ticagrelor and gemcitabine significantly has been found to reduce tumor growth *in vivo* (83). In addition, gemcitabine combined with anticoagulants (e.g., dalteparin) can significantly reduce the incidence of vascular thromboembolism in advanced PC and reduce mortality due to vascular thromboembolism (152, 153). Importantly, it has been shown that radioimmunotherapy combined with imatinib (a potent inhibitor of PDGFR- $\beta$ ) significantly inhibits the growth of PC compared to radioimmunotherapy alone and does not produce any obvious side effects (154). Experimental studies have shown that SU6668 could increase the radiosensitivity of tumor blood vessels, which contributed to tumor growth inhibition and enhanced tumor response to radiotherapy (155). Adjuvant chemoradiotherapy has been established to play a minimal role in controlling advanced PC and does not improve patient prognosis (156). It remains unknown whether antiplatelet therapy combined with chemoradiotherapy will benefit patients. Overall, antiplatelet therapy can inhibit platelet-related cancer-promoting pathways, and combinations of chemotherapy and radioimmunotherapy can effectively enhance antitumor efficacy (157).

## 5.3 Platelet-Nanotechnology Treatment in PC

The barrier function of tumor vascular endothelial cells is strengthened by adhesion of the covering activated platelets, limiting penetration of chemotherapeutic drugs in the tumor cell yielding a poor antitumor effect. To overcome this problem, Cao et al. (158) constructed TM33 peptide-modified gelatin/oleic acid nanoparticles loaded with TNA that could specifically bind to P-selectin on the surface of activated platelets and release the target drug TNA into the extracellular space under the stimulation of MMP-2 secreted by activated platelets, to induce high local TNA exposure. Platelet activation was inhibited by the high concentrations of TNT on the surface of tumor blood vessels, which improved blood vessel penetration and allowed antitumor chemotherapy drugs to leak into tumor cells. Most importantly, TNT did not cause additional side effects, such as bleeding, without changing the biological functions of platelets. In addition, a small dose of nanoparticle-antitumor drugs coated with platelet membrane could selectively adhere to cells in the TME and improve the bioavailability of the antitumor drug after

local delivery. Side effects of systemic high-dose administration, including rapid white blood cell consumption and temporary local immune insufficiency, were not observed (159). Geng et al. (160) constructed a platelet camouflage nanoprobe with active targeting properties, which could escape macrophage phagocytosis and specifically bind to CD44 on the surface of most cancer cells, showing great potential for accurate diagnosis and effective treatment of cancer. Accordingly, platelet-related nanotechnology treatments can reduce the damage caused by drugs to vital human organs and accurately target PC lesions. Nano-combined targeted drug technology has great potential in the treatment of PC.

Although antiplatelet drugs combined with chemotherapeutics effectively improve the antitumor effect, the adverse events caused by these drugs should not be ignored. Common adverse events encompass fatigue, anorexia, dysphonia, nausea and decreased platelet count (161), while serious adverse events include peptic ulcer disease and gastrointestinal bleeding (133, 162). More importantly, it remains controversial whether antiplatelet drugs combined with chemotherapeutics will bring survival benefits compared with chemotherapeutics alone in advanced PC patients (161), raising awareness on the need to develop precise and individualized treatments for this patient population.

## 5.4 Platelet-Related Therapy and PC Organoid

Organoids are three-dimensional (3D) cell cultures that contain key properties of the organs they represent. These *in vitro* culture systems include self-renewing stem cells that can differentiate into multiple organ-specific cell types, exhibiting a similar spatial organization to their counterparts and reproducing some of their functions. Accordingly, they can mimic human development and disease potential, thus providing a physiologically relevant system (163). It has been shown that PC organoids can be rapidly generated from resected human or mouse tumors and biopsies with success rates as high as 75–83%. A comprehensive transcriptional and proteomic analysis of pancreatic organoids could reveal key genes and pathways altered during disease progression (164). Given that 85% of PC patients are not indicated for surgery (165), PC organoids can be generated from limited amounts of cellular material provided by endoscopic ultrasound-guided fine-needle aspiration (EUS-FNA) to detect differences in gene profile expression and find diagnostic and personalized treatment approaches (164). Moreover, a comprehensive genomic, transcriptomic and therapeutic analysis of PC patient-derived organoids (PDOs) could identify molecular and functional subtypes of PC, predict treatment response, and facilitate precision medicine for this patient population (166). Interestingly, establishing a platelet co-culture model with PC organoid can simulate the crosstalk between PC, extracellular matrix and platelets in the TME and reveal the underlying mechanisms of the interaction between PC cells and platelets (167). However, exploring the mechanisms of PC development through platelets

(platelet-related therapy) and organoid co-culture models is at an early stage, warranting more experimental data to substantiate current findings.

## 6 CONCLUSION

In conclusion, unprecedented progress has been made in better understanding platelet-mediated signaling pathways in recent years. Platelet-based studies provide novel insights into how platelets work and the basis to develop targeted therapies that can improve patient outcomes. Although the mechanisms of PC cells in escaping NK cells to lead to distant metastasis have been understood, to some extent, it remains unclear whether PC cells escape other immune cells *via* the same mechanisms. Improving immune cell monitoring and killing ability against cancer cells may be a potential approach for PC treatment. Importantly, antiplatelet therapy combined with radiotherapy or chemotherapy and platelet-related nanotechnology *in vitro* and in animal models are being investigated in ongoing studies, and the clinical efficacy has not been evaluated. Platelets and PC organoid co-culture models have important application value in discovering key points in platelet-induced PC pathogenesis and treatment. Furthermore, given the high incidence of peptic ulcers and gastrointestinal bleeding caused by antiplatelet drugs, scientific and reasonable approaches should be emphasized to ensure patient safety. A better understanding of platelet-mediated signaling pathways will provide a solid foundation for improving patient care. Indeed, comprehensive methods combining immunotherapy, chemotherapy and nanotechnology can potentially benefit PC patients.

## AUTHOR CONTRIBUTIONS

ZC, XW, and WZ conceived the review. ZC, XW, SD, FH and RH undertook the initial research. ZC, XW, SD, FH, and RH were involved in writing. ZC reviewed the manuscript, and all authors contributed to the final version. XW contributed equally to this work and should be considered co-first author. All authors contributed to the article and approved the submitted version.

## FUNDING

This article was supported by The First Hospital of Lanzhou University Intra-Hospital Fund Youth Fund, ldyyn2020-76.

## ACKNOWLEDGMENTS

We sincerely appreciate all the participants in our work.

## REFERENCES

- Illic M, Illic I. Epidemiology of Pancreatic Cancer. *World J Gastroenterol* (2016) 22:9694–705. doi: 10.3748/wjg.v22.i44.9694
- Rahib L, Smith BD, Aizenberg R, Rosenzweig AB, Fleshman JM, Matrisian LM. Projecting Cancer Incidence and Deaths to 2030: The Unexpected Burden of Thyroid, Liver, and Pancreas Cancers in the United States. *Cancer Res* (2014) 74:2913–21. doi: 10.1158/0008-5472.CAN-14-0155
- McGuire S. World Cancer Report 2014. Geneva, Switzerland: World Health Organization, International Agency for Research on Cancer, WHO Press, 2015. *Adv Nutr* (2016) 7:418–9. doi: 10.3945/an.116.012211
- Davis RB, Theologides A, Kennedy BJ. Comparative Studies of Blood Coagulation and Platelet Aggregation in Patients With Cancer and Nonmalignant Diseases. *Ann Intern Med* (1969) 71:67–80. doi: 10.7326/0003-4819-71-1-67
- Silvis SE, Turkbas N, Doscherholmen A. Thrombocytosis in Patients With Lung Cancer. *JAMA* (1970) 211:1852–3. doi: 10.1001/jama.211.11.1852
- Pedersen LM, Milman N. Prognostic Significance of Thrombocytosis in Patients With Primary Lung Cancer. *Eur Respir J* (1996) 9:1826–30. doi: 10.1183/09031936.96.09091826
- Suzuki K, Aiura K, Kitagou M, Hoshimoto S, Takahashi S, Ueda M, et al. Platelets Counts Closely Correlate With the Disease-Free Survival Interval of Pancreatic Cancer Patients. *Hepatogastroenterology* (2004) 51:847–53.
- Yeung J, Li W, Holinstat M. Platelet Signaling and Disease: Targeted Therapy for Thrombosis and Other Related Diseases. *Pharmacol Rev* (2018) 70:526–48. doi: 10.1124/pr.117.014530
- Penny R, Rozenberg MC, Firkin BG. The Splenic Platelet Pool. *Blood* (1966) 27:1–16. doi: 10.1182/blood.V27.1.1.1
- Lefrançois E, Ortiz-Muñoz G, Caudrillier A, Mallavia B, Liu F, Sayah DM, et al. The Lung is a Site of Platelet Biogenesis and a Reservoir for Haematopoietic Progenitors. *Nature* (2017) 544:105–9. doi: 10.1038/nature21706
- Lefrançois E, Looney MR. Platelet Biogenesis in the Lung Circulation. *Physiol (Bethesda)* (2019) 34:392–401. doi: 10.1152/physiol.00017.2019
- Furie B, Furie BC. Mechanisms of Thrombus Formation. *N Engl J Med* (2008) 359(9):938–49. doi: 10.1056/NEJMr0801082
- Liu Y, Jiang P, Capkova K, Xue D, Ye L, Sinha SC, et al. Tissue Factor-Activated Coagulation Cascade in the Tumor Microenvironment is Critical for Tumor Progression and an Effective Target for Therapy. *Cancer Res* (2011) 71:6492–502. doi: 10.1158/0008-5472.CAN-11-1145
- Kim HK, Song KS, Park YS, Kang YH, Lee YJ, Lee KR, et al. Elevated Levels of Circulating Platelet Microparticles, VEGF, IL-6 and RANTES in Patients With Gastric Cancer: Possible Role of a Metastasis Predictor. *Eur J Cancer* (2003) 39:184–91. doi: 10.1016/S0959-8049(02)00596-8
- Wu CK, Chang KC, Hung CH, Tseng PL, Lu SN, Chen CH, et al. Dynamic Alpha-Fetoprotein, Platelets and AST-To-Platelet Ratio Index Predict Hepatocellular Carcinoma in Chronic Hepatitis C Patients With Sustained Virological Response After Antiviral Therapy. *J Antimicrob Chemother* (2016) 71:1943–7. doi: 10.1093/jac/dkw097
- Virdee PS, Marian IR, Mansouri A, Elhussein L, Kirtley S, Holt T, et al. The Full Blood Count Blood Test for Colorectal Cancer Detection: A Systematic Review, Meta-Analysis, and Critical Appraisal. *Cancers (Basel)* (2020) 12:2348. doi: 10.3390/cancers12092348
- Herold Z, Herold M, Lohinszky J, Dank M, Somogyi A. Personalized Indicator Thrombocytosis Shows Connection to Staging and Indicates Shorter Survival in Colorectal Cancer Patients With or Without Type 2 Diabetes. *Cancers (Basel)* (2020) 12:556. doi: 10.3390/cancers12030556
- Stone RL, Nick AM, McNeish IA, Balkwill F, Han HD, Bottsford-Miller J, et al. Paraneoplastic Thrombocytosis in Ovarian Cancer. *N Engl J Med* (2012) 366:610–8. doi: 10.1056/NEJMoa1110352
- Ding N, Pang Z, Shen H, Ni Y, Du J, Liu Q. The Prognostic Value of PLR in Lung Cancer, a Meta-Analysis Based on Results From a Large Consecutive Cohort. *Sci Rep* (2016) 6:34823. doi: 10.1038/srep34823
- Geng M, Xu H, Ren R, Qu Q, Shangguan C, Wu J, et al. Prognostic Value of Clinicopathological Characteristics in Patients With Pancreatic Cancer. *Chin J Cancer Res* (2015) 27:509–15. doi: 10.3978/j.issn.1000-9604.2015.06.03
- Gay LJ, Felding-Habermann B. Contribution of Platelets to Tumour Metastasis. *Nat Rev Cancer* (2011) 11:123–34. doi: 10.1038/nrc3004
- Shirai Y, Shiba H, Sakamoto T, Horiuchi T, Haruki K, Fujiwara Y, et al. Preoperative Platelet to Lymphocyte Ratio Predicts Outcome of Patients With Pancreatic Ductal Adenocarcinoma After Pancreatic Resection. *Surgery* (2015) 158:360–5. doi: 10.1016/j.surg.2015.03.043
- Zhang SR, Yao L, Wang WQ, Xu JZ, Xu HX, Jin W, et al. Tumor-Infiltrating Platelets Predict Postsurgical Survival in Patients With Pancreatic Ductal Adenocarcinoma. *Ann Surg Oncol* (2018) 25:3984–93. doi: 10.1245/s10434-018-6727-8
- Saito R, Kawaida H, Hosomura N, Amemiya H, Itakura J, Yamamoto A, et al. Exposure to Blood Components and Inflammation Contribute to Pancreatic Cancer Progression. *Ann Surg Oncol* (2021) 28:8263–72. doi: 10.1245/s10434-021-10250-4
- Lee BM, Chung SY, Chang JS, Lee KJ, Seong J. The Neutrophil-Lymphocyte Ratio and Platelet-Lymphocyte Ratio Are Prognostic Factors in Patients With Locally Advanced Pancreatic Cancer Treated With Chemoradiotherapy. *Gut Liver* (2018) 12:342–52. doi: 10.5009/gnl17216
- Toledano-Fonseca M, Cano MT, Inga E, Gomez-Espana A, Guil-Luna S, Garcia-Ortiz MV, et al. The Combination of Neutrophil-Lymphocyte Ratio and Platelet-Lymphocyte Ratio With Liquid Biopsy Biomarkers Improves Prognosis Prediction in Metastatic Pancreatic Cancer. *Cancers (Basel)* (2021) 13:1210. doi: 10.3390/cancers13061210
- Chawla A, Huang TL, Ibrahim AM, Hardacre JM, Siegel C, Ammori JB. Pretherapy Neutrophil to Lymphocyte Ratio and Platelet to Lymphocyte Ratio do Not Predict Survival in Resectable Pancreatic Cancer. *HPB (Oxford)* (2018) 20:398–404. doi: 10.1016/j.hpb.2017.10.011
- Xiao Y, Xie H, Xie Z, Shao Z, Chen W, Qin G, et al. Kinetics of Postdiagnosis Platelet Count With Overall Survival of Pancreatic Cancer: A Counting Process Approach. *Cancer Med* (2016) 5:881–7. doi: 10.1002/cam4.644
- Haemmerle M, Stone RL, Menter DG, Afshar-Kharghan V, Sood AK. The Platelet Lifeline to Cancer: Challenges and Opportunities. *Cancer Cell* (2018) 33:965–83. doi: 10.1016/j.ccell.2018.03.002
- Stein PD, Beemath A, Meyers FA, Skaf E, Sanchez J, Olson RE. Incidence of Venous Thromboembolism in Patients Hospitalized With Cancer. *Am J Med* (2006) 119(1):60–8. doi: 10.1016/j.amjmed.2005.06.058
- Gade IL, Braekkan SK, Naess IA, Hansen JB, Cannegieter SC, Overvad K, et al. The Impact of Initial Cancer Stage on the Incidence of Venous Thromboembolism: The Scandinavian Thrombosis and Cancer (STAC) Cohort. *J Thromb Haemost* (2017) 15:1567–75. doi: 10.1111/jth.13752
- Khorana AA, Francis CW, Culakova E, Kuderer NM, Lyman GH. Thromboembolism is a Leading Cause of Death in Cancer Patients Receiving Outpatient Chemotherapy. *J Thromb Haemost* (2007) 5:632–4. doi: 10.1111/j.1538-7836.2007.02374.x
- Radziwon-Balicka A, Medina C, O'Driscoll L, Treumann A, Bazou D, Inkielewicz-Stepniak I, et al. Platelets Increase Survival of Adenocarcinoma Cells Challenged With Anticancer Drugs: Mechanisms and Implications for Chemoresistance. *Br J Pharmacol* (2012) 167:787–804. doi: 10.1111/j.1476-5381.2012.01991.x
- Rachidi S, Metelli A, Riesenberger B, Wu BX, Nelson MH, Wallace C, et al. Platelets Subvert T Cell Immunity Against Cancer via GARP-TGFbeta Axis. *Sci Immunol* (2017) 2:eai7911. doi: 10.1126/sciimmunol.aai7911
- Elaskalani O, Falasca M, Moran N, Berndt MC, Metharom P. The Role of Platelet-Derived ADP and ATP in Promoting Pancreatic Cancer Cell Survival and Gemcitabine Resistance. *Cancers (Basel)* (2017) 9:142. doi: 10.3390/cancers9100142
- Yu LX, Yan L, Yang W, Wu FQ, Ling Y, Chen SZ, et al. Platelets Promote Tumour Metastasis via Interaction Between TLR4 and Tumour Cell-Released High-Mobility Group Box1 Protein. *Nat Commun* (2014) 5:5256. doi: 10.1038/ncomms6256
- Xu XR, Yousef GM, Ni H. Cancer and Platelet Crosstalk: Opportunities and Challenges for Aspirin and Other Antiplatelet Agents. *Blood* (2018) 131:1777–89. doi: 10.1182/blood-2017-05-743187
- Sun L, Li Q, Guo Y, Yang Q, Yin J, Ran Q, et al. Extract of Caulis Spatholobi, a Novel Platelet Inhibitor, Efficiently Suppresses Metastasis of Colorectal Cancer by Targeting Tumor Cell-Induced Platelet Aggregation. *BioMed Pharmacother* (2020) 123:109718. doi: 10.1016/j.biopha.2019.109718



39. Wang Y, Ni H. Fibronectin: Extra Domain Brings Extra Risk? *Blood* (2015) 125:3043–4. doi: 10.1182/blood-2015-03-630855
40. Mammadova-Bach E, Zigrino P, Brucker C, Bourdon C, Freund M, De Arcangelis A, et al. Platelet Integrin  $\alpha 6 \beta 1$  Controls Lung Metastasis Through Direct Binding to Cancer Cell-Derived ADAM9. *JCI Insight* (2016) 1:e88245. doi: 10.1172/jci.insight.88245
41. Qi C, Wei B, Zhou W, Yang Y, Li B, Guo S, et al. P-Selectin-Mediated Platelet Adhesion Promotes Tumor Growth. *Oncotarget* (2015) 6:6584–96. doi: 10.18632/oncotarget.3164
42. Shirai T, Inoue O, Tamura S, Tsukiji N, Sasaki T, Endo H, et al. C-Type Lectin-Like Receptor 2 Promotes Hematogenous Tumor Metastasis and Prothrombotic State in Tumor-Bearing Mice. *J Thromb Haemost* (2017) 15:513–25. doi: 10.1111/jth.13604
43. In 't Veld S, Wurdinger T. Tumor-Educated Platelets. *Blood* (2019) 133:2359–64. doi: 10.1182/blood-2018-12-852830
44. Heijnen HF, Schiel AE, Fijnheer R, Geuze HJ, Sixma JJ. Activated Platelets Release Two Types of Membrane Vesicles: Microvesicles by Surface Shedding and Exosomes Derived From Exocytosis of Multivesicular Bodies and Alpha-Granules. *Blood* (1999) 94(11):3791–9. doi: 10.1182/blood.V94.11.3791.423a22\_3791\_3799
45. van Niel G, D'Angelo G, Raposo G. Shedding Light on the Cell Biology of Extracellular Vesicles. *Nat Rev Mol Cell Biol* (2018) 19:213–28. doi: 10.1038/nrm.2017.125
46. Meehan K, Vella LJ. The Contribution of Tumour-Derived Exosomes to the Hallmarks of Cancer. *Crit Rev Clin Lab Sci* (2016) 53:121–31. doi: 10.3109/10408363.2015.1092496
47. Shai E, Rosa I, Parguina AF, Motahedeh S, Varon D, García Á. Comparative Analysis of Platelet-Derived Microparticles Reveals Differences in Their Amount and Proteome Depending on the Platelet Stimulus. *J Proteom* (2012) 76:287–96. doi: 10.1016/j.jprot.2012.02.030
48. Primo L, Seano G, Roca C, Maione F, Gagliardi PA, Sessa R, et al. Increased Expression of Alpha6 Integrin in Endothelial Cells Unveils a Proangiogenic Role for Basement Membrane. *Cancer Res* (2010) 70:5759–69. doi: 10.1158/0008-5472.CAN-10-0507
49. Valadi H, Ekstrom K, Bossios A, Sjostrand M, Lee JJ, Lotvall JO. Exosome-Mediated Transfer of mRNAs and microRNAs is a Novel Mechanism of Genetic Exchange Between Cells. *Nat Cell Biol* (2007) 9:654–9. doi: 10.1038/ncb1596
50. Best MG, Sol N, Kooi I, Tannous J, Westerman BA, Rustenburg F, et al. RNA-Seq of Tumor-Educated Platelets Enables Blood-Based Pan-Cancer, Multiclass, and Molecular Pathway Cancer Diagnostics. *Cancer Cell* (2015) 28:666–76. doi: 10.1016/j.ccell.2015.09.018
51. Ho-Tin-Noé B, Goerge T, Wagner DD. Platelets: Guardians of Tumor Vasculature. *Cancer Res* (2009) 69:5623–6. doi: 10.1158/0008-5472.CAN-09-1370
52. Geddings JE, Hisada Y, Boulaftali Y, Getz TM, Whelihan M, Fuentes R, et al. Tissue Factor-Positive Tumor Microvesicles Activate Platelets and Enhance Thrombosis in Mice. *J Thromb Haemost* (2016) 14:153–66. doi: 10.1111/jth.13181
53. Davila M, Amirhosravi A, Coll E, Desai H, Robles L, Colon J, et al. Tissue Factor-Bearing Microparticles Derived From Tumor Cells: Impact on Coagulation Activation. *J Thromb Haemost* (2008) 6:1517–24. doi: 10.1111/j.1538-7836.2008.02987.x
54. Yu JL, Rak JW. Shedding of Tissue Factor (TF)-Containing Microparticles Rather Than Alternatively Spliced TF is the Main Source of TF Activity Released From Human Cancer Cells. *J Thromb Haemost* (2004) 2:2065–7. doi: 10.1111/j.1538-7836.2004.00972.x
55. Stark K, Schubert I, Joshi U, Kilani B, Hoseinpour P, Thakur M, et al. Distinct Pathogenesis of Pancreatic Cancer Microvesicle-Associated Venous Thrombosis Identifies New Antithrombotic Targets In Vivo. *Arterioscler Thromb Vasc Biol* (2018) 38:772–86. doi: 10.1161/ATVBAHA.117.310262
56. Hisada Y, Ay C, Auriemma AC, Cooley BC, Mackman N. Human Pancreatic Tumors Grown in Mice Release Tissue Factor-Positive Microvesicles That Increase Venous Clot Size. *J Thromb Haemost* (2017) 15:2208–17. doi: 10.1111/jth.13809
57. Caudrillier A, Kessenbrock K, Gilliss BM, Nguyen JX, Marques MB, Monestier M, et al. Platelets Induce Neutrophil Extracellular Traps in Transfusion-Related Acute Lung Injury. *J Clin Invest* (2012) 122:2661–71. doi: 10.1172/JCI61303
58. Wang Y, Luo L, Braun OÖ, Westman J, Madhi R, Herwald H, et al. Neutrophil Extracellular Trap-Microparticle Complexes Enhance Thrombin Generation via the Intrinsic Pathway of Coagulation in Mice. *Sci Rep* (2018) 8:4020. doi: 10.1038/s41598-018-22156-5
59. Elaskalani O, Abdol Razak NB, Metharom P. Neutrophil Extracellular Traps Induce Aggregation of Washed Human Platelets Independently of Extracellular DNA and Histones. *Cell Commun Signal* (2018) 16:24. doi: 10.1186/s12964-018-0235-0
60. Boone BA, Murthy P, Miller-Ocuin J, Doerfler WR, Ellis JT, Liang X, et al. Chloroquine Reduces Hypercoagulability in Pancreatic Cancer Through Inhibition of Neutrophil Extracellular Traps. *BMC Cancer* (2018) 18:678. doi: 10.1186/s12885-018-4584-2
61. Carminita E, Crescence L, Brouilly N, Altie A, Panicot-Dubois L, Dubois C. DNase-Dependent, NET-Independent Pathway of Thrombus Formation In Vivo. *Proc Natl Acad Sci U.S.A.* (2021) 118:e2100561118. doi: 10.1073/pnas.2100561118
62. Mier-Hicks A, Raj M, Do RK, Yu KH, Lowery MA, Varghese A, et al. Incidence, Management, and Implications of Visceral Thrombosis in Pancreatic Ductal Adenocarcinoma. *Clin Colorectal Cancer* (2018) 17:121–8. doi: 10.1016/j.clcc.2018.01.008
63. Ouassii M, Frasconi C, Mege D, Panicot-Dubois L, Boiron L, Dahan L, et al. Impact of Venous Thromboembolism on the Natural History of Pancreatic Adenocarcinoma. *Hepatobil Pancreat Dis Int* (2015) 14:436–42. doi: 10.1016/S1499-3872(15)60397-6
64. Wessler S, Yin ET. Experimental Hypercoagulable State Induced by Factor X: Comparison of the Nonactivated and Activated Forms. *J Lab Clin Med* (1968) 72:256–60.
65. Campello E, Ilich A, Simioni P, Key NS. The Relationship Between Pancreatic Cancer and Hypercoagulability: A Comprehensive Review on Epidemiological and Biological Issues. *Br J Cancer* (2019) 121:359–71. doi: 10.1038/s41416-019-0510-x
66. Ponert JM, Gockel LM, Henze S, Schlesinger M. Unfractionated and Low Molecular Weight Heparin Reduce Platelet Induced Epithelial-Mesenchymal Transition in Pancreatic and Prostate Cancer Cells. *Molecules* (2018) 23:2690. doi: 10.3390/molecules23102690
67. Mitrugno A, Sylman JL, Ngo AT, Pang J, Sears RC, Williams CD, et al. Aspirin Therapy Reduces the Ability of Platelets to Promote Colon and Pancreatic Cancer Cell Proliferation: Implications for the Oncoprotein C-MYC. *Am J Physiol Cell Physiol* (2017) 312:C176–89. doi: 10.1152/ajpcell.00196.2016
68. Nilsson RJ, Balaj L, Hulleman E, van Rijn S, Pegtel DM, Walraven M, et al. Blood Platelets Contain Tumor-Derived RNA Biomarkers. *Blood* (2011) 118:3680–3. doi: 10.1182/blood-2011-03-344408
69. Zhang Y, Cedervall J, Hamidi A, Herre M, Viitaniemi K, D'Amico G, et al. Platelet-Specific PDGFB Ablation Impairs Tumor Vessel Integrity and Promotes Metastasis. *Cancer Res* (2020) 80:3345–58. doi: 10.1158/0008-5472.CAN-19-3533
70. Singh PK, Wen Y, Swanson BJ, Shanmugam K, Kazlauskas A, Cerny RL, et al. Platelet-Derived Growth Factor Receptor Beta-Mediated Phosphorylation of MUC1 Enhances Invasiveness in Pancreatic Adenocarcinoma Cells. *Cancer Res* (2007) 67:5201–10. doi: 10.1158/0008-5472.CAN-06-4647
71. Li T, Guo T, Liu H, Jiang H, Wang Y. Platelet-derived Growth factorBB Mediates Pancreatic Cancer Malignancy via Regulation of the Hippo/Yes-associated Protein Signaling Pathway. *Oncol Rep* (2021) 45:83–94. doi: 10.3892/or.2020.7859
72. Mondal S, Adhikari N, Banerjee S, Amin SA, Jha T. Matrix Metalloproteinase-9 (MMP-9) and its Inhibitors in Cancer: A Minireview. *Eur J Med Chem* (2020) 194:112260. doi: 10.1016/j.ejmech.2020.112260
73. Miele L, Miao H, Nickoloff BJ. NOTCH Signaling as a Novel Cancer Therapeutic Target. *Curr Cancer Drug Targets* (2006) 6:313–23. doi: 10.2174/156800906777441771
74. Wang Z, Kong D, Banerjee S, Li Y, Adsay NV, Abbruzzese J, et al. Down-Regulation of Platelet-Derived Growth Factor-D Inhibits Cell Growth and Angiogenesis Through Inactivation of Notch-1 and Nuclear factor-kappaB

- Signaling. *Cancer Res* (2007) 67:11377–85. doi: 10.1158/0008-5472.CAN-07-2803
75. Kuo TL, Cheng KH, Shan YS, Chen LT, Hung WC. Beta-Catenin-Activated Autocrine PDGF/Src Signaling is a Therapeutic Target in Pancreatic Cancer. *Theranostics* (2019) 9:324–36. doi: 10.7150/thno.28201
  76. Weissmueller S, Manchado E, Saborowski M, JPt M, Wagenblast E, CA D, et al. Mutant P53 Drives Pancreatic Cancer Metastasis Through Cell-Autonomous PDGF Receptor Beta Signaling. *Cell* (2014) 157:382–94. doi: 10.1016/j.cell.2014.01.066
  77. Schneider M, Büchler P, Giese N, Giese T, Wilting J, Büchler MW, et al. Role of Lymphangiogenesis and Lymphangiogenic Factors During Pancreatic Cancer Progression and Lymphatic Spread. *Int J Oncol* (2006) 28:883–90. doi: 10.3892/ijo.28.4.883
  78. Quan L, Ohgaki R, Hara S, Okuda S, Wei L, Okanishi H, et al. Amino Acid Transporter LAT1 in Tumor-Associated Vascular Endothelium Promotes Angiogenesis by Regulating Cell Proliferation and VEGF-A-Dependent Mtorc1 Activation. *J Exp Clin Cancer Res* (2020) 39:266. doi: 10.1186/s13046-020-01762-0
  79. Morin E, Sjöberg E, Tjomsland V, Testini C, Lindskog C, Franklin O, et al. VEGF Receptor-2/Neuropilin 1 Trans-Complex Formation Between Endothelial and Tumor Cells is an Independent Predictor of Pancreatic Cancer Survival. *J Pathol* (2018) 246:311–22. doi: 10.1002/path.5141
  80. Azoitei N, Becher A, Steinestel K, Rouhi A, Diepold K, Genze F, et al. PKM2 Promotes Tumor Angiogenesis by Regulating HIF-1 $\alpha$  through NF- $\kappa$ B Activation. *Mol Cancer* (2016) 15:3. doi: 10.1186/s12943-015-0490-2
  81. Kong Y, Li Y, Luo Y, Zhu J, Zheng H, Gao B, et al. Circnfib1 Inhibits Lymphangiogenesis and Lymphatic Metastasis via the miR-486-5p/PIK3R1/VEGF-C Axis in Pancreatic Cancer. *Mol Cancer* (2020) 19:82. doi: 10.1186/s12943-020-01205-6
  82. Beckermann BM, Kallifatidis G, Groth A, Frommhold D, Apel A, Mattern J, et al. VEGF Expression by Mesenchymal Stem Cells Contributes to Angiogenesis in Pancreatic Carcinoma. *Br J Cancer* (2008) 99:622–31. doi: 10.1038/sj.bjc.6604508
  83. Elaskalani O, Domenichini A, Abdol Razak NB, ED D, Falasca M, Metharom P. Antiplatelet Drug Ticagrelor Enhances Chemotherapeutic Efficacy by Targeting the Novel P2Y12-AKT Pathway in Pancreatic Cancer Cells. *Cancers (Basel)* (2020) 12:250. doi: 10.3390/cancers12010250
  84. Battinelli EM, Markens BA, Italiano JE Jr. Release of Angiogenesis Regulatory Proteins From Platelet Alpha Granules: Modulation of Physiologic and Pathologic Angiogenesis. *Blood* (2011) 118:1359–69. doi: 10.1182/blood-2011-02-334524
  85. Labelle M, Begum S, Hynes RO. Direct Signaling Between Platelets and Cancer Cells Induces an Epithelial-Mesenchymal-Like Transition and Promotes Metastasis. *Cancer Cell* (2011) 20:576–90. doi: 10.1016/j.ccr.2011.09.009
  86. Principe DR, DeCant B, Mascariñas E, Wayne EA, Diaz AM, Akagi N, et al. Tgf $\beta$  Signaling in the Pancreatic Tumor Microenvironment Promotes Fibrosis and Immune Evasion to Facilitate Tumorigenesis. *Cancer Res* (2016) 76:2525–39. doi: 10.1158/0008-5472.CAN-15-1293
  87. Bartel DP. MicroRNAs: Target Recognition and Regulatory Functions. *Cell* (2009) 136:215–33. doi: 10.1016/j.cell.2009.01.002
  88. Agarwal V, Bell GW, Nam JW, Bartel DP. Predicting Effective microRNA Target Sites in Mammalian mRNAs. *Elife* (2015) 4:e05005. doi: 10.7554/eLife.05005
  89. Landry P, Plante I, Ouellet DL, Perron MP, Rousseau G, Provost P. Existence of a microRNA Pathway in Anucleate Platelets. *Nat Struct Mol Biol* (2009) 16:961–6. doi: 10.1038/nsmb.1651
  90. Denis MM, Tolley ND, Bunting M, Schwertz H, Jiang H, Lindemann S, et al. Escaping the Nuclear Confines: Signal-Dependent pre-mRNA Splicing in Anucleate Platelets. *Cell* (2005) 122:379–91. doi: 10.1016/j.cell.2005.06.015
  91. Mantini G, Meijer LL, Glogovitis I, In 't Veld S, Paleckyte R, Capula M, et al. Omics Analysis of Educated Platelets in Cancer and Benign Disease of the Pancreas. *Cancers (Basel)* (2020) 13:66. doi: 10.3390/cancers13010066
  92. Su A, He S, Tian B, Hu W, Zhang Z. MicroRNA-221 Mediates the Effects of PDGF-BB on Migration, Proliferation, and the Epithelial-Mesenchymal Transition in Pancreatic Cancer Cells. *PloS One* (2013) 8(8):e71309. doi: 10.1371/journal.pone.0071309
  93. Wurtzel JGT, Lazar S, Sikder S, Cai KQ, Astsaturou I, Weyrich AS, et al. Platelet microRNAs Inhibit Primary Tumor Growth via Broad Modulation of Tumor Cell mRNA Expression in Ectopic Pancreatic Cancer in Mice. *PloS One* (2021) 16:e0261633. doi: 10.1371/journal.pone.0261633
  94. Kowal JM, Yegutkin GG, Novak I. ATP Release, Generation and Hydrolysis in Exocrine Pancreatic Duct Cells. *Purinergic Signal* (2015) 11:533–50. doi: 10.1007/s11302-015-9472-5
  95. Kim S, Kunapuli SP. P2Y12 Receptor in Platelet Activation. *Platelets* (2011) 22:56–60. doi: 10.3109/09537104.2010.497231
  96. Dercksen MW, Weimar IS, Richel DJ, Breton-Gorius J, Vainchenker W, Slaper-Cortenbach CM, et al. The Value of Flow Cytometric Analysis of Platelet Glycoprotein Expression of CD34+ Cells Measured Under Conditions That Prevent P-Selectin-Mediated Binding of Platelets. *Blood* (1995) 86:3771–82. doi: 10.1182/blood.V86.10.3771.bloodjournal86103771
  97. Hsieh MJ, Chiu TJ, Lin YC, Weng CC, Weng YT, Hsiao CC, et al. Inactivation of APC Induces CD34 Upregulation to Promote Epithelial-Mesenchymal Transition and Cancer Stem Cell Traits in Pancreatic Cancer. *Int J Mol Sci* (2020) 21:4473. doi: 10.3390/ijms21124473
  98. Kasper HU, Ebert M, Malfertheiner P, Roessner A, Kirkpatrick CJ, Wolf HK. Expression of Thrombospondin-1 in Pancreatic Carcinoma: Correlation With Microvessel Density. *Virchows Arch* (2001) 438(2):116–20. doi: 10.1007/s004280000302
  99. Qian X, Rothman VL, Nicosia RF, Tuszynski GP. Expression of Thrombospondin-1 in Human Pancreatic Adenocarcinomas: Role in Matrix Metalloproteinase-9 Production. *Pathol Oncol Res* (2001) 7:251–9. doi: 10.1007/BF03032381
  100. Boone BA, Murthy P, Miller-Ocuin JL, Liang X, Russell KL, Loughran P, et al. The Platelet NLRP3 Inflammasome is Upregulated in a Murine Model of Pancreatic Cancer and Promotes Platelet Aggregation and Tumor Growth. *Ann Hematol* (2019) 98:1603–10. doi: 10.1007/s00277-019-03692-0
  101. Thomas GM, Panicot-Dubois L, Lacroix R, Dignat-George F, Lombardo D, Dubois C. Cancer Cell-Derived Microparticles Bearing P-Selectin Glycoprotein Ligand 1 Accelerate Thrombus Formation In Vivo. *J Exp Med* (2009) 206:1913–27. doi: 10.1084/jem.20082297
  102. Lu Z, Long Y, Wang Y, Wang X, Xia C, Li M, et al. Phenylboronic Acid Modified Nanoparticles Simultaneously Target Pancreatic Cancer and its Metastasis and Alleviate Immunosuppression. *Eur J Pharm Biopharm* (2021) 165:164–73. doi: 10.1016/j.ejpb.2021.05.014
  103. Perollet C, Han ZC, Savona C, Caen JP, Bikfalvi A. Platelet Factor 4 Modulates Fibroblast Growth Factor 2 (FGF-2) Activity and Inhibits FGF-2 Dimerization. *Blood* (1998) 91:3289–99. doi: 10.1182/blood.V91.9.3289.3289\_3299
  104. El-Hariry I, Pignatelli M, Lemoine NR. FGF-1 and FGF-2 Modulate the E-Cadherin/Catenin System in Pancreatic Adenocarcinoma Cell Lines. *Br J Cancer* (2001) 84:1656–63. doi: 10.1054/bjoc.2001.1813
  105. Stock AM, Hahn SA, Troost G, Niggemann B, Zänker KS, Entschladen F. Induction of Pancreatic Cancer Cell Migration by an Autocrine Epidermal Growth Factor Receptor Activation. *Exp Cell Res* (2014) 326:307–14. doi: 10.1016/j.yexcr.2014.04.022
  106. Yoshikawa K, Tanabe E, Shibata A, Inoue S, Kitayoshi M, Okimoto S, et al. Involvement of Oncogenic K-Ras on Cell Migration Stimulated by Lysophosphatidic Acid Receptor-2 in Pancreatic Cancer Cells. *Exp Cell Res* (2013) 319:105–12. doi: 10.1016/j.yexcr.2012.09.014
  107. Yang AJ, Wang M, Wang Y, Cai W, Li Q, Zhao TT, et al. Cancer Cell-Derived Von Willebrand Factor Enhanced Metastasis of Gastric Adenocarcinoma. *Oncogenesis* (2018) 7:12. doi: 10.1038/s41389-017-0023-5
  108. Qi Y, Chen W, Liang X, Xu K, Gu X, Wu F, et al. Novel Antibodies Against Gpib $\alpha$  Inhibit Pulmonary Metastasis by Affecting vWF-Gpib $\alpha$  Interaction. *J Hematol Oncol* (2018) 11:117. doi: 10.1186/s13045-018-0659-4
  109. Weizman N, Krelin Y, Shabtay-Orbach A, Amit M, Binenbaum Y, Wong RJ, et al. Macrophages Mediate Gemcitabine Resistance of Pancreatic Adenocarcinoma by Upregulating Cytidine Deaminase. *Oncogene* (2014) 33:3812–9. doi: 10.1038/onc.2013.357
  110. Mackey JR, Mani RS, Selner M, Mowles D, Young JD, Belt JA, et al. Functional Nucleoside Transporters are Required for Gemcitabine Influx and Manifestation of Toxicity in Cancer Cell Lines. *Cancer Res* (1998) 58:4349–57.
  111. Pérez-Torras S, García-Manteiga J, Mercadé E, Casado FJ, Carbó N, Pastor-Anglada M, et al. Adenoviral-Mediated Overexpression of Human

- Equilibrative Nucleoside Transporter 1 (Hent1) Enhances Gemcitabine Response in Human Pancreatic Cancer. *Biochem Pharmacol* (2008) 76:322–9. doi: 10.1016/j.bcp.2008.05.011
112. Tsukasa K, Ding Q, Yoshimitsu M, Miyazaki Y, Matsubara S, Takao S. Slug Contributes to Gemcitabine Resistance Through Epithelial-Mesenchymal Transition in CD133(+) Pancreatic Cancer Cells. *Hum Cell* (2015) 28 (4):167–74. doi: 10.1007/s13577-015-0117-3
  113. Giannuzzo A, Saccomano M, Napp J, Ellegaard M, Alves F, Novak I. Targeting of the P2X7 Receptor in Pancreatic Cancer and Stellate Cells. *Int J Cancer* (2016) 139:2540–52. doi: 10.1002/ijc.30380
  114. Chen H, Lan X, Liu M, Zhou B, Wang B, Chen P. Direct TGF- $\beta$ 1 Signaling Between Activated Platelets and Pancreatic Cancer Cells Primes Cisplatin Insensitivity. *Cell Biol Int* (2013) 37:478–84. doi: 10.1002/cbin.10067
  115. Vonlaufen A, Joshi S, Qu C, Phillips PA, Xu Z, Parker NR, et al. Pancreatic Stellate Cells: Partners in Crime With Pancreatic Cancer Cells. *Cancer Res* (2008) 68:2085–93. doi: 10.1158/0008-5472.CAN-07-2477
  116. Fitzner B, Walzel H, Sparmann G, Emmrich J, Liebe S, Jaster R. Galectin-1 is an Inductor of Pancreatic Stellate Cell Activation. *Cell Signall* (2005) 17:1240–7. doi: 10.1016/j.cellsig.2004.12.012
  117. Martin OA, Anderson RL, Narayan K, MacManus MP. Does the Mobilization of Circulating Tumour Cells During Cancer Therapy Cause Metastasis? *Nat Rev Clin Oncol* (2017) 14:32–44. doi: 10.1038/nrclinonc.2016.128
  118. Ward Y, Lake R, Faraji F, Sperger J, Martin P, Gilliard C, et al. Platelets Promote Metastasis via Binding Tumor CD97 Leading to Bidirectional Signaling That Coordinates Transendothelial Migration. *Cell Rep* (2018) 23 (3):808–22. doi: 10.1016/j.celrep.2018.03.092
  119. Schlesinger M. Role of Platelets and Platelet Receptors in Cancer Metastasis. *J Hematol Oncol* (2018) 11:125. doi: 10.1186/s13045-018-0669-2
  120. Kopp HG, Placke T, Salih RH. Platelet-Derived Transforming Growth Factor-Beta Down-Regulates NKG2D Thereby Inhibiting Natural Killer Cell Antitumor Reactivity. *Cancer Res* (2009) 69:7775–83. doi: 10.1158/0008-5472.CAN-09-2123
  121. Okazaki M, Yamaguchi T, Tajima H, Fushida S, Ohta T. Platelet Adherence to Cancer Cells Promotes Escape From Innate Immune Surveillance in Cancer Metastasis. *Int J Oncol* (2020) 57:980–8. doi: 10.3892/ijo.2020.5102
  122. Wetterholm E, Linders J, Merza M, Regner S, Thorlacius H. Platelet-Derived CXCL4 Regulates Neutrophil Infiltration and Tissue Damage in Severe Acute Pancreatitis. *Transl Res* (2016) 176:105–18. doi: 10.1016/j.trsl.2016.04.006
  123. Zucoloto AZ, Jenne CN. Platelet-Neutrophil Interplay: Insights Into Neutrophil Extracellular Trap (NET)-Driven Coagulation in Infection. *Front Cardiovasc Med* (2019) 6:85. doi: 10.3389/fcvm.2019.00085
  124. Kazzaz NM, Sule G, Knight JS. Intercellular Interactions as Regulators of NETosis. *Front Immunol* (2016) 7:453. doi: 10.3389/fimmu.2016.00453
  125. Cheng X, Zhang H, Hamad A, Huang H, Tsung A. Surgery-Mediated Tumor-Promoting Effects on the Immune Microenvironment. *Semin Cancer Biol* (2022) 20:S1044-579X(22)00012-8. doi: 10.1016/j.semcancer.2022.01.006
  126. Tohme S, Yazdani HO, Al-Khafaji AB, Chidi AP, Loughran P, Mowen K, et al. Neutrophil Extracellular Traps Promote the Development and Progression of Liver Metastases After Surgical Stress. *Cancer Res* (2016) 76:1367–80. doi: 10.1158/0008-5472.CAN-15-1591
  127. McDonald B, Davis RP, Kim SJ, Tse M, Esmon CT, Kolaczowska E, et al. Platelets and Neutrophil Extracellular Traps Collaborate to Promote Intravascular Coagulation During Sepsis in Mice. *Blood* (2017) 129:1357–67. doi: 10.1182/blood-2016-09-741298
  128. Ren J, He J, Zhang H, Xia Y, Hu Z, Loughran P, et al. Platelet TLR4-ERK5 Axis Facilitates NET-Mediated Capturing of Circulating Tumor Cells and Distant Metastasis After Surgical Stress. *Cancer Res* (2021) 81:2373–85. doi: 10.1158/0008-5472.CAN-20-3222
  129. Kajioaka H, Kagawa S, Ito A, Yoshimoto M, Sakamoto S, Kikuchi S, et al. Targeting Neutrophil Extracellular Traps With Thrombomodulin Prevents Pancreatic Cancer Metastasis. *Cancer Lett* (2021) 497:1–13. doi: 10.1016/j.canlet.2020.10.015
  130. Teixeira Á, Garasa S, Gato M, Alfaro C, Migueliz I, Cirella A, et al. CXCR1 and CXCR2 Chemokine Receptor Agonists Produced by Tumors Induce Neutrophil Extracellular Traps That Interfere With Immune Cytotoxicity. *Immunity* (2020) 52:856–871.e8. doi: 10.1016/j.immuni.2020.03.001
  131. Kaltenmeier C, Yazdani HO, Morder K, Geller DA, Simmons RL, Tohme S. Neutrophil Extracellular Traps Promote T Cell Exhaustion in the Tumor Microenvironment. *Front Immunol* (2021) 12:785222. doi: 10.3389/fimmu.2021.785222
  132. Thun MJ, Jacobs EJ, Patrono C. The Role of Aspirin in Cancer Prevention. *Nat Rev Clin Oncol* (2012) 9:259–67. doi: 10.1038/nrclinonc.2011.199
  133. Cook NR, Lee IM, Zhang SM, Moorthy MV, Buring JE. Alternate-Day, Low-Dose Aspirin and Cancer Risk: Long-Term Observational Follow-Up of a Randomized Trial. *Ann Intern Med* (2013) 159:77–85. doi: 10.7326/0003-4819-159-2-201307160-00002
  134. Randel KR, Botteri E, Romstad KMK, Frigstad SO, Bretthauer M, Hoff G, et al. Effects of Oral Anticoagulants and Aspirin on Performance of Fecal Immunochemical Tests in Colorectal Cancer Screening. *Gastroenterology* (2019) 156:1642–1649.e1641. doi: 10.1053/j.gastro.2019.01.040
  135. Mezouar S, Darbousset R, Dignat-George F, Panicot-Dubois L, Dubois C. Inhibition of Platelet Activation Prevents the P-Selectin and Integrin-Dependent Accumulation of Cancer Cell Microparticles and Reduces Tumor Growth and Metastasis In Vivo. *Int J Cancer* (2015) 136:462–75. doi: 10.1002/ijc.28997
  136. Adamska A, Elaskalani O, Emmanouilidi A, Kim M, Abdol Razak NB, Metharom P, et al. Molecular and Cellular Mechanisms of Chemoresistance in Pancreatic Cancer. *Adv Biol Regul* (2018) 68:77–87. doi: 10.1016/j.jbior.2017.11.007
  137. Manning G, Whyte DB, Martinez R, Hunter T, Sudarsanam S. The Protein Kinase Complement of the Human Genome. *Science* (2002) 298:1912–34. doi: 10.1126/science.1075762
  138. Du Z, Lovly CM. Mechanisms of Receptor Tyrosine Kinase Activation in Cancer. *Mol Cancer* (2018) 17:58. doi: 10.1186/s12943-018-0782-4
  139. Lu H, Klein RS, Schwartz EL. Antiangiogenic and Antitumor Activity of 6-(2-Aminoethyl)Amino-5-Chlorouracil, a Novel Small-Molecule Inhibitor of Thymidine Phosphorylase, in Combination With the Vascular Endothelial Growth Factor-Trap. *Clin Cancer Res* (2009) 15:5136–44. doi: 10.1158/1078-0432.CCR-08-3203
  140. Baker CH, Trevino JG, Summy JM, Zhang F, Caron A, Nesbit M, et al. Inhibition of PDGFR Phosphorylation and Src and Akt Activity by GN963 Leads to Therapy of Human Pancreatic Cancer Growing Orthotopically in Nude Mice. *Int J Oncol* (2006) 29:125–38. doi: 10.3892/ijo.29.1.125
  141. Sennino B, Falcon BL, McCauley D, Le T, McCauley T, Kurz JC, et al. Sequential Loss of Tumor Vessel Pericytes and Endothelial Cells After Inhibition of Platelet-Derived Growth Factor B by Selective Aptamer AX102. *Cancer Res* (2007) 67:7358–67. doi: 10.1158/0008-5472.CAN-07-0293
  142. Song S, Ewald AJ, Stallcup W, Werb Z, Bergers G. PDGFRbeta+ Perivascular Progenitor Cells in Tumours Regulate Pericyte Differentiation and Vascular Survival. *Nat Cell Biol* (2005) 7:870–9. doi: 10.1038/ncb1288
  143. Mancuso MR, Davis R, Norberg SM, O'Brien S, Sennino B, Nakahara T, et al. Rapid Vascular Regrowth in Tumors After Reversal of VEGF Inhibition. *J Clin Invest* (2006) 116:2610–21. doi: 10.1172/JCI24612
  144. Hu-Lowe DD, Zou HY, Grazzini ML, Hallin ME, Wickman GR, Amundson K, et al. Nonclinical Antiangiogenesis and Antitumor Activities of Axitinib (AG-013736), an Oral, Potent, and Selective Inhibitor of Vascular Endothelial Growth Factor Receptor Tyrosine Kinases 1, 2, 3. *Clin Cancer Res* (2008) 14:7272–83. doi: 10.1158/1078-0432.CCR-08-0652
  145. Ran S, Huang X, Downes A, Thorpe PE. Evaluation of Novel Antimouse VEGFR2 Antibodies as Potential Antiangiogenic or Vascular Targeting Agents for Tumor Therapy. *Neoplasia* (2003) 5:297–307. doi: 10.1016/S1476-5586(03)80023-4
  146. Bergers G, Song S, Meyer-Morse N, Bergsland E, Hanahan D. Benefits of Targeting Both Pericytes and Endothelial Cells in the Tumor Vasculature With Kinase Inhibitors. *J Clin Invest* (2003) 111:1287–95. doi: 10.1172/JCI200317929
  147. Semba T, Funahashi Y, Ono N, Yamamoto Y, Sugi NH, Asada M, et al. An Angiogenesis Inhibitor E7820 Shows Broad-Spectrum Tumor Growth Inhibition in a Xenograft Model: Possible Value of Integrin Alpha2 on Platelets as a Biological Marker. *Clin Cancer Res* (2004) 10:1430–8. doi: 10.1158/1078-0432.CCR-0109-03
  148. Kato S, Kobari M, Matsuno S, Sato T. (Inhibitory Effect of Anti-Platelet Prostaglandin on Liver Metastasis of Hamster Pancreatic Cancer). *Nihon Geka Gakkai Zasshi* (1989) 90:745–52.



149. Bruns CJ, Shrader M, Harbison MT, Portera C, Solorzano CC, Jauch KW, et al. Effect of the Vascular Endothelial Growth Factor Receptor-2 Antibody DC101 Plus Gemcitabine on Growth, Metastasis and Angiogenesis of Human Pancreatic Cancer Growing Orthotopically in Nude Mice. *Int J Cancer* (2002) 102:101–8. doi: 10.1002/ijc.10681
150. Solorzano CC, Baker CH, Bruns CJ, Killion JJ, Ellis LM, Wood J, et al. Inhibition of Growth and Metastasis of Human Pancreatic Cancer Growing in Nude Mice by PTK 787/ZK222584, an Inhibitor of the Vascular Endothelial Growth Factor Receptor Tyrosine Kinases. *Cancer Biother Radiopharm* (2001) 16:359–70. doi: 10.1089/108497801753354267
151. Solorzano CC, Baker CH, Tsan R, Traxler P, Cohen P, Buchdunger E, et al. Optimization for the Blockade of Epidermal Growth Factor Receptor Signaling for Therapy of Human Pancreatic Carcinoma. *Clin Cancer Res* (2001) 7:2563–72.
152. Maraveyas A, Waters J, Roy R, Fyfe D, Propper D, Lofis F, et al. Gemcitabine Versus Gemcitabine Plus Dalteparin Thromboprophylaxis in Pancreatic Cancer. *Eur J Cancer* (2012) 48:1283–92. doi: 10.1016/j.ejca.2011.10.017
153. Dallos MC, Eisenberger AB, Bates SE. Prevention of Venous Thromboembolism in Pancreatic Cancer: Breaking Down a Complex Clinical Dilemma. *Oncologist* (2020) 25:132–9. doi: 10.1634/theoncologist.2019-0264
154. Baranowska-Kortylewicz J, Abe M, Nearman J, Enke CA. Emerging Role of Platelet-Derived Growth Factor Receptor-Beta Inhibition in Radioimmunotherapy of Experimental Pancreatic Cancer. *Clin Cancer Res* (2007) 13:299–306. doi: 10.1158/1078-0432.CCR-06-1702
155. Griffin RJ, Williams BW, Wild R, Cherrington JM, Park H, Song CW. Simultaneous Inhibition of the Receptor Kinase Activity of Vascular Endothelial, Fibroblast, and Platelet-Derived Growth Factors Suppresses Tumor Growth and Enhances Tumor Radiation Response. *Cancer Res* (2002) 62:1702–6.
156. Neoptolemos JP, Stocken DD, Friess H, Bassi C, Dunn JA, Hickey H, et al. A Randomized Trial of Chemoradiotherapy and Chemotherapy After Resection of Pancreatic Cancer. *N Engl J Med* (2004) 350:1200–10. doi: 10.1056/NEJMoa032295
157. Yokoi K, Sasaki T, Bucana CD, Fan D, Baker CH, Kitadai Y, et al. Simultaneous Inhibition of EGFR, VEGFR, and Platelet-Derived Growth Factor Receptor Signaling Combined With Gemcitabine Produces Therapy of Human Pancreatic Carcinoma and Prolongs Survival in an Orthotopic Nude Mouse Model. *Cancer Res* (2005) 65:10371–80. doi: 10.1158/0008-5472.CAN-05-1698
158. Cao J, Yang P, Wang P, Xu S, Cheng Y, Qian K, et al. ‘Adhesion and Release’ Nanoparticle-Mediated Efficient Inhibition of Platelet Activation Disrupts Endothelial Barriers for Enhanced Drug Delivery in Tumors. *Biomaterials* (2021) 269:120620. doi: 10.1016/j.biomaterials.2020.120620
159. Bahmani B, Gong H, Luk BT, Haushalter KJ, DeTeresa E, Previti M, et al. Intratumoral Immunotherapy Using Platelet-Cloaked Nanoparticles Enhances Antitumor Immunity in Solid Tumors. *Nat Commun* (2021) 12:1999. doi: 10.1038/s41467-021-22311-z
160. Geng X, Gao D, Hu D, Liu Q, Liu C, Yuan Z, et al. Active-Targeting NIR-II Phototheranostics in Multiple Tumor Models Using Platelet-Camouflaged Nanoparticles. *ACS Appl Mater Interfaces* (2020) 12:55624–37. doi: 10.1021/acsami.0c16872
161. Ioka T, Okusaka T, Ohkawa S, Boku N, Sawaki A, Fujii Y, et al. Efficacy and Safety of Axitinib in Combination With Gemcitabine in Advanced Pancreatic Cancer: Subgroup Analyses by Region, Including Japan, From the Global Randomized Phase III Trial. *Jpn J Clin Oncol* (2015) 45:439–48. doi: 10.1093/jjco/hyv011
162. Tullemans BME, Fernandez DI, Veninga A, Baaten C, Peters LJF, Aarts MJB, et al. Tyrosine Kinase Inhibitor Sunitinib Delays Platelet-Induced Coagulation: Additive Effects of Aspirin. *Thromb Haemost* (2021) 122:92–104. doi: 10.1055/s-0041-1730312
163. Lancaster MA, Knoblich JA. Organogenesis in a Dish: Modeling Development and Disease Using Organoid Technologies. *Science* (2014) 345:1247125. doi: 10.1126/science.1247125
164. Boj SF, Hwang CI, Baker LA, Chio II, Engle DD, Corbo V, et al. Organoid Models of Human and Mouse Ductal Pancreatic Cancer. *Cell* (2015) 160:324–38. doi: 10.1016/j.cell.2014.12.021
165. Ryan DP, Hong TS, Bardeesy N. Pancreatic Adenocarcinoma. *N Engl J Med* (2014) 371:1039–49. doi: 10.1056/NEJMr1404198
166. Tiriac H, Belleau P, Engle DD, Plenker D, Deschênes A, Somerville TDD, et al. Organoid Profiling Identifies Common Responders to Chemotherapy in Pancreatic Cancer. *Cancer Discovery* (2018) 8:1112–29. doi: 10.1158/1538-7445.PANCA19-C57
167. Mai S, Inkielewicz-Stepniak I. Pancreatic Cancer and Platelets Crosstalk: A Potential Biomarker and Target. *Front Cell Dev Biol* (2021) 9:749689. doi: 10.3389/fcell.2021.749689

**Conflict of Interest:** The authors declare that the research was conducted in the absence of any commercial or financial relationships that could be construed as a potential conflict of interest.

**Publisher’s Note:** All claims expressed in this article are solely those of the authors and do not necessarily represent those of their affiliated organizations, or those of the publisher, the editors and the reviewers. Any product that may be evaluated in this article, or claim that may be made by its manufacturer, is not guaranteed or endorsed by the publisher.

Copyright © 2022 Chen, Wei, Dong, Han, He and Zhou. This is an open-access article distributed under the terms of the Creative Commons Attribution License (CC BY). The use, distribution or reproduction in other forums is permitted, provided the original author(s) and the copyright owner(s) are credited and that the original publication in this journal is cited, in accordance with accepted academic practice. No use, distribution or reproduction is permitted which does not comply with these terms.





# COMMD2 Upregulation Mediated by an ncRNA Axis Correlates With an Unfavorable Prognosis and Tumor Immune Infiltration in Liver Hepatocellular Carcinoma

Weidan Fang, Yu Gan, Ling Zhang\* and Jianping Xiong\*

Department of Oncology, The First Affiliated Hospital of Nanchang University, Nanchang, China

## OPEN ACCESS

### Edited by:

Alessandro Passardi,  
Scientific Institute of Romagna for the  
Study and Treatment of Tumors  
(IRCCS), Italy

### Reviewed by:

Louis Charles Penning,  
Utrecht University, Netherlands  
Ziheng Wang,  
Affiliated Hospital of Nantong  
University, China

### \*Correspondence:

Ling Zhang  
ndyfy1306@ncu.edu.cn  
Jianping Xiong  
jpxiong0630@outlook.com

### Specialty section:

This article was submitted to  
Gastrointestinal Cancers: Hepato  
Pancreatic Biliary Cancers,  
a section of the journal  
Frontiers in Oncology

**Received:** 12 January 2022

**Accepted:** 28 March 2022

**Published:** 29 April 2022

### Citation:

Fang W, Gan Y, Zhang L and Xiong J  
(2022) COMMD2 Upregulation  
Mediated by an ncRNA Axis Correlates  
With an Unfavorable Prognosis and  
Tumor Immune Infiltration in Liver  
Hepatocellular Carcinoma.  
Front. Oncol. 12:853026.  
doi: 10.3389/fonc.2022.853026

Liver hepatocellular carcinoma (LIHC) seriously endangers the health and quality of life of individuals worldwide. Increasing evidence has underscored that the copper metabolism MURR1 domain (COMMD) family plays important roles in tumorigenesis. However, the specific role, biological function, mechanism and prognostic value of COMMD2 and its correlation with immune cell infiltration in LIHC remain unknown. In this study, we first determined the expression and prognostic potential of COMMD2 in human tumors using The Cancer Genome Atlas (TCGA) data and identified COMMD2 as a potential oncogene in LIHC. High COMMD2 expression was associated with pathological tumor stage and metastasis. Subsequently, noncoding RNAs (ncRNAs) upregulating COMMD2 expression were identified by performing expression, correlation, and survival analyses in combination. The CRNDE/LINC00511/SNHG17/HCG18-miR-29c-3p axis was identified as the most likely ncRNA-associated pathway upstream of COMMD2 in LIHC. Next, the expression profiles of COMMD2 and ncRNAs were validated in LIHC tissues and adjacent normal tissues. Furthermore, COMMD2 was significantly positively correlated with tumor immune cell infiltration, immune cell biomarkers, and immune checkpoint molecule expression. Importantly, COMMD2 potentially influenced prognosis by regulating immune cell infiltration in LIHC. Finally, COMMD2 was knocked down in LIHC cell lines using siRNAs for functional assays *in vitro*, resulting in suppressed cell proliferation and migration. In summary, our findings showed that the ncRNA-mediated upregulation of COMMD2 was associated with an unfavorable prognosis correlated with immune cell infiltration in LIHC.

**Keywords:** COMMD2, CRNDE, LINC00511, SNHG17, HCG18, miR-29c-3p, tumor immune infiltration, liver hepatocellular carcinoma

## INTRODUCTION

Liver hepatocellular carcinoma (LIHC) is the most common type of primary cancer in the liver and third leading cause of cancer-related mortality worldwide (1). Although substantial improvements have been made in LIHC therapy, particularly in molecular targeted therapy and immunotherapy (2, 3), the 5-year survival rate of LIHC is dismal because of its high heterogeneity, complex genetics

and clinical features (4, 5). Thus, molecular biomarkers urgently need to be identified to improve the prognosis and develop novel therapeutic strategies for LIHC.

The copper metabolism MURR1 domain (COMMD) protein family comprises 10 members (COMMD1–COMMD10), all of which share a structurally conserved C-terminal motif and are implicated in regulating many biological processes through protein-protein interactions (6). COMMD proteins are frequently dysregulated in various cancers and are associated with cancer progression and metastasis (7–11). For example, decreased COMMD1 expression increased tumor invasion (12) and suppressed the sensitivity of ovarian cancer cells to cisplatin (13). COMMD7 promotes cell proliferation, migration, and invasion by upregulating NF- $\kappa$ B signaling (14) or CXCL10 (15). COMMD9 promotes the progression of non-small cell lung cancer by increasing TFDPI/E2F1 activation (8). However, the expression, biological function, possible mechanism and prognostic relevance of COMMD2 and its correlation with immune cell infiltration in human cancers, including LIHC, remain unknown.

In this study, we first performed expression profiling and survival analysis of COMMD2 in various human cancers. Additionally, COMMD2 expression was correlated with cancer stage, tumor grade, lymph node metastasis and the TP53 mutation status in LIHC. Next, the mechanism underlying the regulation of COMMD2 by noncoding RNAs (ncRNAs), including long noncoding RNAs (lncRNAs) and microRNAs (miRNAs), through a competing endogenous RNA (ceRNA) network in LIHC was explored. Furthermore, we determined the correlations of COMMD2 with tumor-infiltrating immune cells, immune cell biomarkers, and immune checkpoint molecules in LIHC and analyzed the correlations between COMMD2 and infiltrating immune cells in the tumor microenvironment. Importantly, COMMD2 influenced the overall survival (OS) of LIHC patients through immune cell infiltration. Additionally, we performed a series of functional assays to further evaluate the effects of COMMD2 knockdown on LIHC cell proliferation and migration *in vitro*. Taken together, our findings suggest that the ncRNA-mediated upregulation of COMMD2 plays crucial roles in the development of LIHC by regulating immune cell infiltration.

## MATERIALS AND METHODS

### Cell Culture and Transfection

The LIHC cell lines MHCC-97H and Huh-7 were purchased from the Cell Bank of the Chinese Academy of Sciences (Shanghai, China). MHCC-97H and Huh-7 cells were cultured in DMEM (HyClone, Logan, UT, USA) supplemented with 10% fetal bovine serum (FBS; Gibco, Grand Island, NY, USA) and 1% penicillin/streptomycin in a humidified incubator at 37°C with 5% CO<sub>2</sub>. COMMD2-targeting siRNA oligonucleotides were purchased from GenePharma (Shanghai, China). Cells were transfected with the indicated siRNAs using TurboFect transfection reagent (R0532; Thermo Scientific Scientific, Waltham, MA, United States). The siRNA sequences used in our study were as follows:

COMMD2-Homo-54: 5'-GGAAUUGUCCGAGGAGCAUT T-3', COMMD2-Homo-222: 5'-GCAUGGUGUGGAAGGAUU ATT-3'.

### Real-Time Quantitative PCR

Total RNA was extracted from cells and clinical samples using the acid guanidine method with TRIzol reagent (Thermo Fisher Scientific), chloroform and isopropanol according to the manufacturer's instructions. cDNA was obtained by reverse transcription using the PrimeScript<sup>TM</sup> RT reagent kit (Takara, Dalian, China). Real-time quantitative PCR (RT-qPCR) was performed using TB Green<sup>TM</sup> Premix Ex Taq II (Takara, Dalian, China) on an CFX96 Real-Time PCR Detection System (Bio-Rad, USA) and following minimum standard MIQE guidelines (16). The RT-qPCR cycling conditions were as follows: 95°C for 30 s, 42 cycles at 95°C for 5 s, and 60°C for 30 s. The melt curve stage was set as follows: 95°C for 15 s, 60°C for 60 s, and 95°C for 15 s. The primer sequences are shown in **Table 1**. The miRNA, mRNA and lncRNA levels were normalized to those of U6 or GAPDH. The relative expression level of mRNA from cells was calculated using the 2<sup>- $\Delta\Delta$ CT</sup> method and the miRNA, mRNA and lncRNA levels from clinical samples was assessed using the 2<sup>- $\Delta$ Ct</sup> method.

### Tissue Samples and Ethical Statement

Fresh LIHC specimens and adjacent normal tissue were obtained from 10 LIHC patients who were undergoing surgery at the First Affiliated Hospital of Nanchang University (Nanchang, China).

**TABLE 1** | Primers used in the study.

Primer	Forward (5'-3')	Reverse (5'-3')
COMMD2	TGAATTGGCACCAAGCCTTC	TGGGTCTGTCTGCAGAACTT
CRNDE	ATATTACGCCGTGGTCTTTGA	TCTGCGTGACAACTGAGGATT
LINC00511	AGGGGCGACTACTGTTACCT	CGTCCAAACAGGCTGGATCT
SNHG17	TTTTCCACGCTGTCTGTCA	CAGTTTCCCCGATGGTGAG
HCG18	ATCCTGCCAATAGATGCTGCTCAC	AGCCACCTTGGTCTCCAGTCTC
miR-29c-3p	AACACGTGTAGCACCATTGAA	CAGTGCAGGGTCCGAGGT
GAPDH	ATGGGGAAGGTGAAGGTCG	GGGGTCATTGATGGCAACAATA
U6	CGCTTCGGCAGCACATATAC	TTCACGAATTTCGCTGTCATC

The patients were treatment-naïve before surgery. This study was approved by the Ethics Committee of the First Affiliated Hospital of Nanchang University.

### CCK8 Viability and Clone Formation Assays

Cells were seeded in 96-well plates at a density of  $2 \times 10^3$  cells per well, after which 100  $\mu$ l of FBS-free medium containing 10% CCK8 was added to each well and incubated for 2 h at 37°C. Next, the OD values at 450 nm were detected using a microplate reader (Thermo Scientific) for 5 days. For the clone formation assay, cells were seeded in 6-well plates at a density of  $2 \times 10^3$  cells per well and cultured for 14 days. Next, the clones were fixed with methanol, stained with 1% crystal violet and counted.

### Wound Healing Assay

Cells were seeded in 6-well plates and cultured in serum-free DMEM to 100% density, after which wounds were created by scratching with 10  $\mu$ l pipette tips. Images were acquired at 0 and 24 h, and the wound areas were quantified using ImageJ software.

### Cell Migration Assay

Cells were seeded on the upper transwell chamber at a density of  $3 \times 10^4$  cells in 200  $\mu$ l of serum-free culture medium, and 600  $\mu$ l of medium containing 20% FBS was added to the lower chamber. After 48 h, the cells that migrated through the membranes were fixed with methanol, stained with 1% crystal violet and counted under a light microscope.

### Data Acquisition and Processing

We downloaded LIHC-related mRNA-seq expression profiles from The Cancer Genome Atlas (TCGA) database (<https://portal.gdc.cancer.gov/>). Additionally, the expression profiling data of the arrays GSE55092 and GSE107170 (GPL570 sequencing platform) from the GEO database (<http://www.ncbi.nlm.nih.gov/geo/>) were downloaded as validation datasets.

### Immune Infiltration Analysis

TIMER (<https://cistrome.shinyapps.io/timer/>) is an online database used to comprehensively analyze tumor-infiltrating immune cells in various cancer types (17). The expression levels of COMMD2 in multiple cancers and their correlation with immune cell infiltration or immune checkpoint molecules in LIHC were analyzed using TIMER. CIBERSORT is a deconvolution algorithm based on gene expression that assesses the relative variations in immune cell infiltration (18). The immune infiltration levels of 22 immune cell types in patients in the TCGA-LIHC cohort, GSE55092 and GSE107170 were analyzed using the CIBERSORT algorithm. A  $p$  value  $<0.05$  was considered to be statistically significant.

### UALCAN Analysis

UALCAN (<http://ualcan.path.uab.edu>) is a comprehensive and interactive online tool that includes 31 cancer types from the TCGA database (19). In this study, COMMD2 mRNA

expression in various cancer types and its association with survival prognosis were analyzed. Furthermore, UALCAN was used to analyze the associations of COMMD2 with clinicopathologic parameters, such as patient sex, patient age, cancer stage, tumor grade, nodal metastasis status and the TP53 mutation status in LIHC. A  $p$  value  $<0.05$  was considered to be statistically significant.

### GEPIA Database Analysis

GEPIA (<http://gepia.cancer-pku.cn/>) is an interactive analysis online tool for cancer and normal gene expression profiling using TCGA and Genotype-Tissue Expression (GTEx) data (20). GEPIA was used to determine and assess the expression and prognostic values of candidate lncRNAs in LIHC. Additionally, the correlations between COMMD2 and immune checkpoint molecules in LIHC were evaluated. A  $p$  value  $<0.05$  was considered to be statistically significant.

### Candidate miRNA Prediction

miRNAs binding upstream of COMMD2 were predicted using the TarBase (<http://www.microrna.gr/tarbase>), miRTarBase (<http://mirtarbase.mbc.nctu.edu.tw/>), miRWalk (<http://mirwalk.uni-hd.de/>) and starBase (<http://starbase.sysu.edu.cn/>) databases. Only the predicted miRNAs that commonly appeared in more than two of the abovementioned databases were considered candidate miRNAs of COMMD2.

### StarBase Database Analysis

starBase is an online database for exploring miRNA, lncRNA and RNA interaction networks (21). starBase was used to conduct the following correlation analyses in LIHC: miRNA-COMMD2, lncRNA-miR-29c-3p and lncRNA-COMMD2. The expression of candidate miRNAs in LIHC was also analyzed. Additionally, starBase was used to predict candidate lncRNAs that could potentially bind to miR-29c-3p. A  $p$  value  $<0.05$  was considered statistically significant.

### Kaplan-Meier Plotter Analysis

Kaplan-Meier plotter (<http://kmplot.com/analysis/>), an online database containing data on the relationships between gene or miRNA expression and clinical outcomes in more than 20 cancer types, was used to assess associations of miR-29c-3p with the survival of LIHC patients and the associations of COMMD2 with patient survival in various cancer types. OS and progression-free survival (PFS) with hazard ratios (HRs) with 95% confidence intervals (95% CIs) and log-rank  $p$  value were evaluated (22).

### Statistical Analysis

The statistical analyses in this study were automatically performed using the above online databases. Paired Student's  $t$  test was used to evaluate the differences in ncRNA and COMMD2 expression between the cancer and control groups. Student's  $t$  test was used for comparisons.  $P < 0.05$  was considered statistically significant. \*  $P < 0.05$  and \*\*  $P < 0.01$ .

## RESULTS

### Expression Levels of COMMD2 in Multiple Cancers

To investigate the possible roles of COMMD2 in tumorigenesis, its expression levels in tumor and normal tissue samples of multiple cancer types were analyzed using the TIMER database. COMMD2 was expressed at significantly higher levels in the tumor tissues of 10 various cancer types, including bladder cancer (BLCA), cervical squamous cell carcinoma (CESC), cholangiocarcinoma (CHOL), colorectal adenocarcinoma (COAD), esophageal cancer (ESCA), glioblastoma multiforme (GBM), head and neck squamous cell carcinoma (HNSC), LIHC, lung squamous cell carcinoma (LUSC) and stomach adenocarcinoma (STAD), than in the corresponding normal tissues. However, in breast cancer (BRCA), kidney chromophobe (KICH), lung adenocarcinoma (LUAD), prostate adenocarcinoma (PRAD) and thyroid cancer (THCA) tissues, COMMD2 expression was markedly lower than that in the corresponding normal samples (**Figure 1A**). To further evaluate COMMD2 expression in human cancers, the UALCAN database was evaluated, revealing that the COMMD2 expression levels in BLCA, CHOL, COAD, ESCA, GBM, HNSC, LIHC, LUSC and STAD tissues were significantly higher than those in the corresponding normal tissues (**Figures 1B–J**). However, compared with its levels in corresponding normal tissues, the COMMD2 expression levels in KICH, LUAD, PRAD and THCA tissues were obviously lower (**Figures 1K–N**). COMMD2 expression levels in BRCA and CESC tissues has no significantly difference than its levels in corresponding normal tissues (**Figures 1O, P**). Overall, COMMD2 expression was upregulated in BLCA, CHOL, COAD, ESCA, GBM, HNSC, LIHC, LUSC and STAD tissues and downregulated in KICH, LUAD, PRAD and THCA tissues, indicating that COMMD2 may crucially regulate carcinogenesis in these 13 types of cancer.

### Prognostic Value of COMMD2 in Various Human Cancers

The association between COMMD2 expression and prognosis was analyzed for various candidate types of cancer using the UALCAN database (**Supplementary Figure 1**). Notably, higher COMMD2 expression was significantly associated with a worse prognosis in LIHC ( $p = 0.0051$ , **Supplementary Figure 1F**), while higher expression of COMMD2 in CHOL indicated a better prognosis ( $p = 0.032$ , **Supplementary Figure 1B**). To further examine the prognostic potential of COMMD2 in different cancers, the Kaplan-Meier plotter database was used. Regarding OS, COMMD2 upregulation was associated with an unfavorable prognosis in LIHC ( $p = 0.00028$ ; **Figure 2D**), but a higher level of COMMD2 was significantly associated with a positive prognosis in LUSC ( $p = 0.018$ ; **Figure 2F**). Increased expression of COMMD2 was significantly correlated with short relapse-free survival (RFS) in BLCA, LIHC and STAD (**Figures 2I, L, O**). In other cancer types (**Figures 2A–C, E, G–H, J–K, M–N, P**), no significant correlations were found

between COMMD2 and patient prognosis. In addition, the protein expression of COMMD2 was explored with the Human Protein Atlas (HPA) database. Similarly, COMMD2 was overexpressed in LIHC tissues compared with that in normal hepatic tissue. Higher COMMD2 expression was markedly correlated with a worse OS in LIHC patients (**Supplementary Figures 2A, B**). By combining the prognostic values from various databases, we concluded that COMMD2 might be an unfavorable prognostic biomarker for LIHC.

### Association of COMMD2 Expression With the Clinicopathological Features of LIHC Patients

The relationships between COMMD2 expression and the clinicopathological parameters of LIHC patients, including patient sex, patient age, cancer stage, tumor grade, nodal metastasis status and the TP53 mutation status, were analyzed using UALCAN database. Regarding sex, COMMD2 expression was significantly upregulated in the LIHC tissues of both male and female patients compared with that in the normal tissues (**Figure 3A**). The COMMD2 level was significantly related to the age of the patient (**Figure 3B**) and remarkably correlated with cancer stage. Compared with that in normal tissues, COMMD2 expression was significantly higher in stage 1, stage 2, stage 3 and stage 4 cancers (**Figure 3C**). Concerning tumor grade, upregulation of COMMD2 expression was observed in grade 1, grade 2, grade 3, and grade 4 tumors, and COMMD2 expression increased as the pathological grade increased (**Figure 3D**). Moreover, COMMD2 expression was significantly related to the nodal metastasis status (**Figure 3E**). Furthermore, COMMD2 was expressed at a significantly higher level in the TP53 mutant than in the TP53 wild-type (**Figure 3F**). Additionally, to better understand the prognostic value of COMMD2 expression in LIHC, we explored the association between COMMD2 expression and clinical characteristics using the Kaplan-Meier database. High COMMD2 expression was significantly correlated with a poor OS in male and female patients with LIHC. Regarding the different tumor stages, upregulation of COMMD2 expression was associated with the a poor OS of patients with LIHC classified as stage 1 + 2, stage 2, and stage 2 + 3. A significant correlation between COMMD2 expression and a poor OS was observed in patients with American Joint Committee on Cancer (AJCC) stage T-2 and grade 2 LIHC. Additionally, high COMMD2 expression was significantly associated with an unfavorable OS for LIHC patients with microvascular invasion, patients who did not consume alcohol and patients without hepatitis. These results imply that COMMD2 expression possesses prognostic value in LIHC (**Figure 3G**).

### Prediction and Analysis of miRNAs Upstream of COMMD2

Increasing evidence has shown that ncRNAs play key roles in the development of cancers by regulating gene expression. To determine whether COMMD2 is modulated by ncRNAs, the



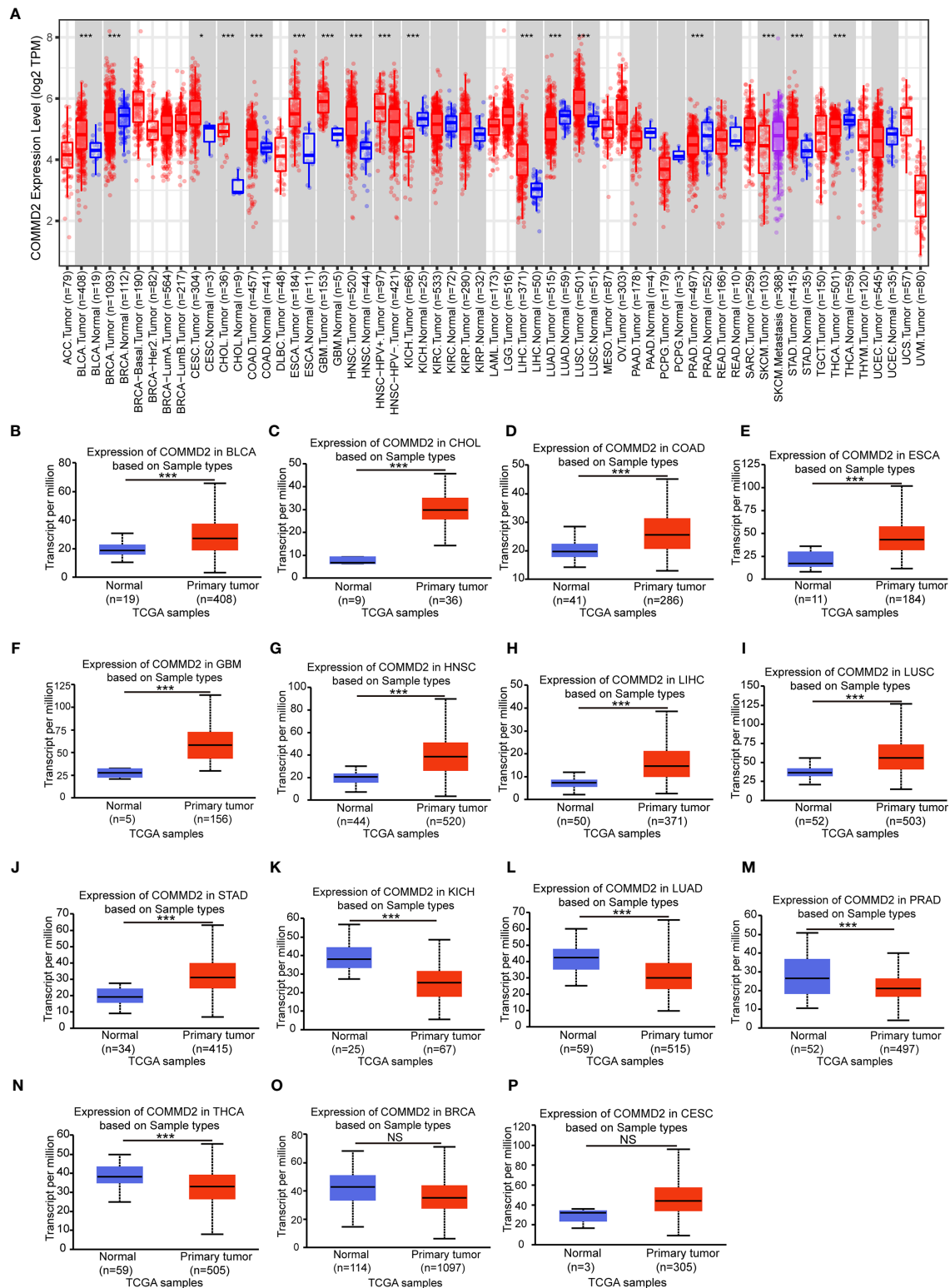


**FIGURE 1** | Expression levels of COMMD2 in different cancer types. **(A)** COMMD2 expression in different types of cancer was determined using the TIMER database. **(B–M)** COMMD2 expression in BLCA **(B)**, CHOL **(C)**, COAD **(D)**, ESCA **(E)**, GBM **(F)**, HNSC **(G)**, LIHC **(H)**, LUSC **(I)**, STAD **(J)**, KICH **(K)**, LUAD **(L)**, PRAD **(M)**, THCA **(N)**, BRCA **(O)** and CESC **(P)** tissues compared with corresponding normal tissues as determined using the UALCAN database. \*p value < 0.05, \*\*p value < 0.01, \*\*\*p value < 0.001. NS, Not Significant.

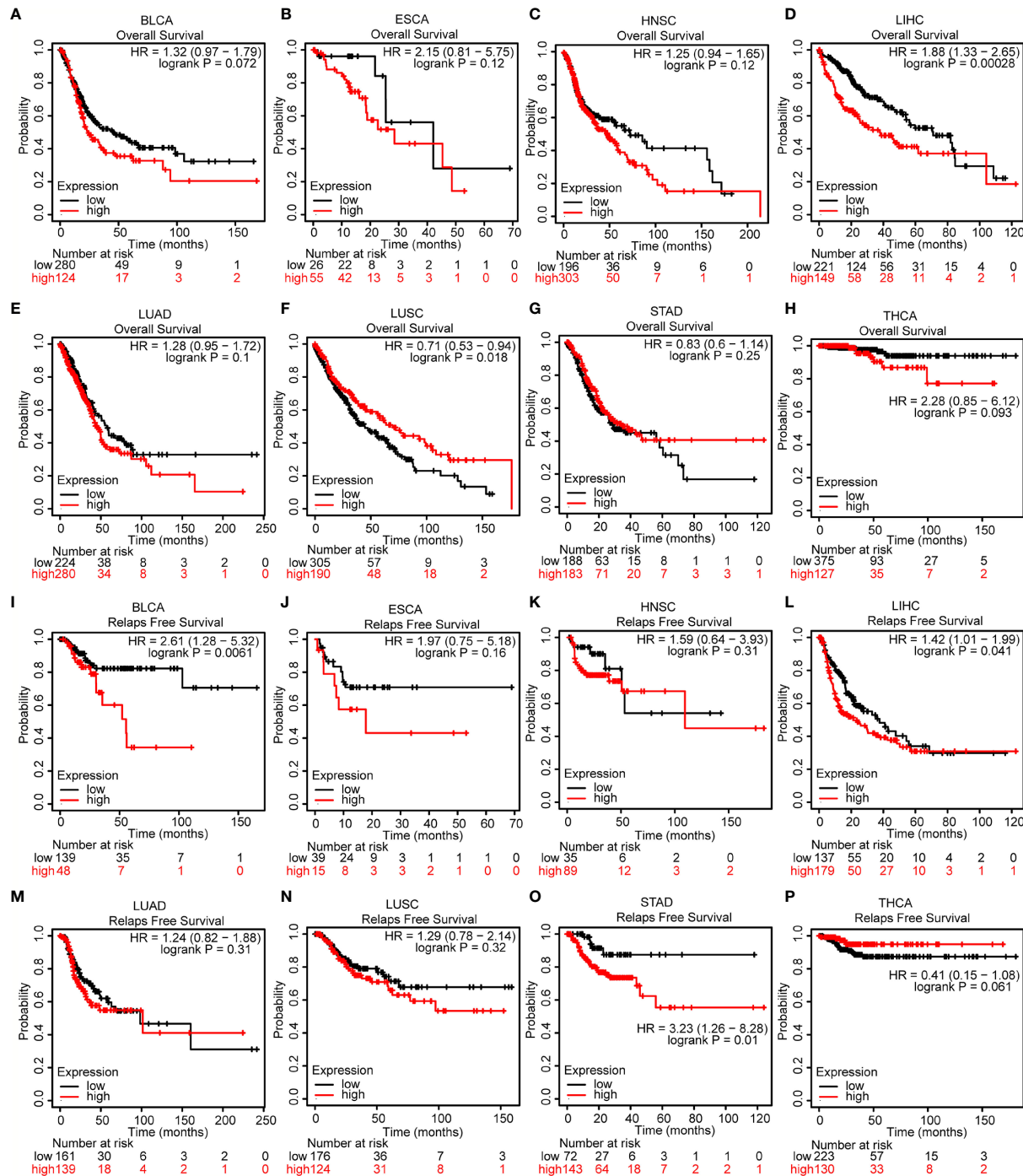


**FIGURE 2 |** Prognostic value of COMMD2 in various human cancers. (A–H) Overall survival (OS) analysis of COMMD2 in BLCA (A), ESCA (B), HNSC (C), LIHC (D), LUAD (E), LUSC (F), STAD (G) and THCA (H). (I–P) Relapse-free survival (RFS) analysis of COMMD2 in BLCA (I), ESCA (J), HNSC (K), LIHC (L), LUAD (M), LUSC (N), STAD (O) and THCA (P).

miRNAs binding upstream of COMMD2 were predicted by several target gene prediction programs, and 21 candidate miRNAs were ultimately identified (Figure 4A). The LIHC-associated miRNA-COMMD2 regulatory network was established using Cytoscape software (Figure 4B). According

to the mechanism by which miRNAs generally negatively regulate downstream target genes, miRNAs and COMMD2 should be negatively correlated. Therefore, correlation analysis was conducted. COMMD2 was significantly negatively correlated with miR-29a-3p, miR-29b-3p and miR-29c-3p and

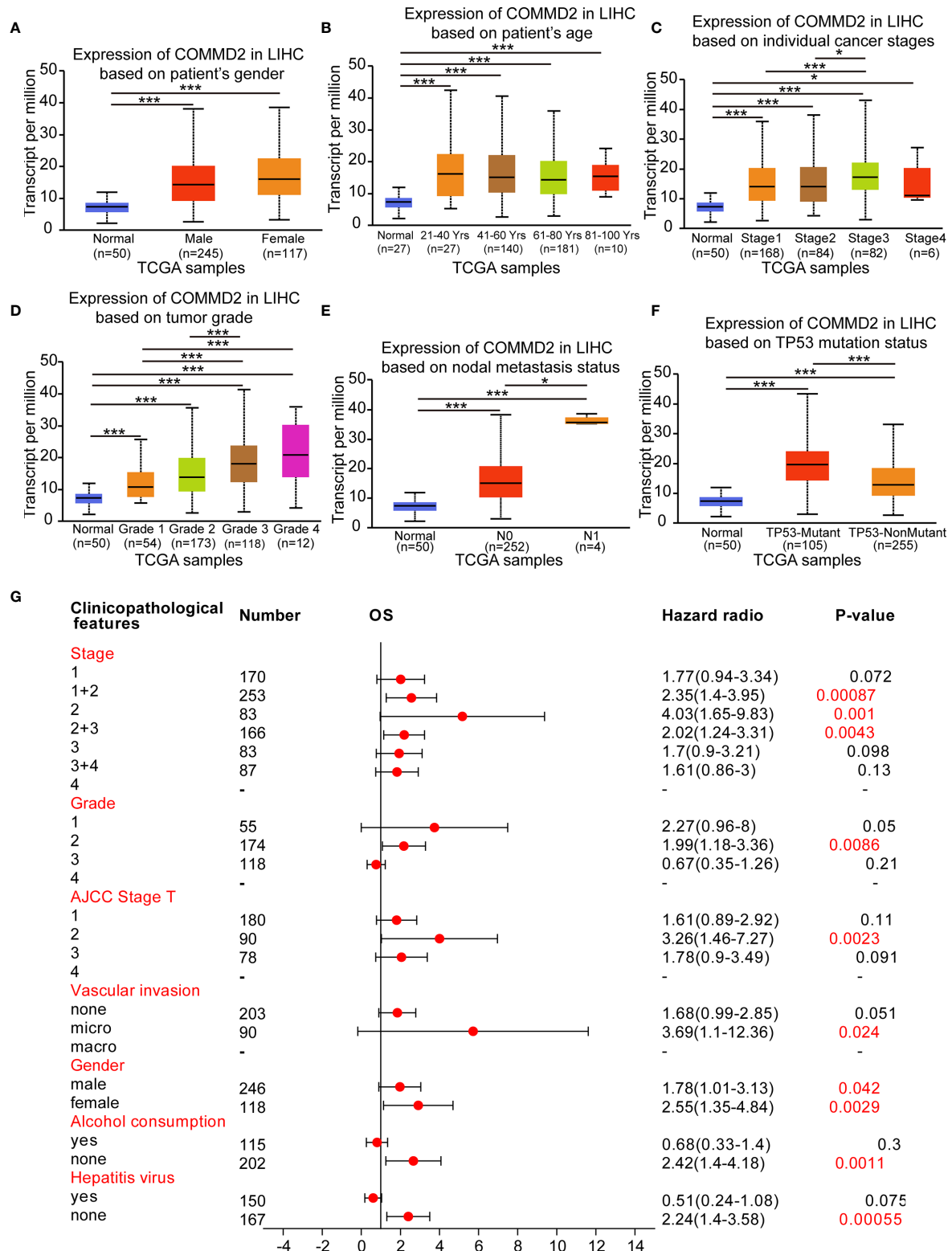


**FIGURE 3** | Association of COMMD2 expression with the clinicopathological features of LIHC patients. (A–F) Boxplot showing COMMD2 expression in normal individuals and LIHC patients based on clinicopathological features using the UALCAN database. Patient sex (A), patient age (B), cancer stage (C), tumor grade (D), nodal metastasis status (E) and TP53 mutation status parameters were analyzed (F). (G) Forest plot showing the association between COMMD2 expression and clinicopathological parameters of LIHC patients. \* $p < 0.05$ ; \*\*\* $p < 0.001$ .

positively correlated with miR-365b-5p in LIHC (**Figure 4C**). No significant relationships were observed between the expression of COMMD2 and other 17 predicted miRNAs. Finally, the expression and prognostic values of miR-29a-3p, miR-29b-3p, miR-29c-3p and miR-365b-5p in LIHC were determined. As

presented in **Figures 4D–G**, miR-29a-3p, miR-29b-3p and miR-29c-3p were markedly downregulated in LIHC, but no significant upregulation of miR-365b-5p in LIHC was observed. Furthermore, only the high expression of miR-29c-3p was associated with a positive prognosis for LIHC patients

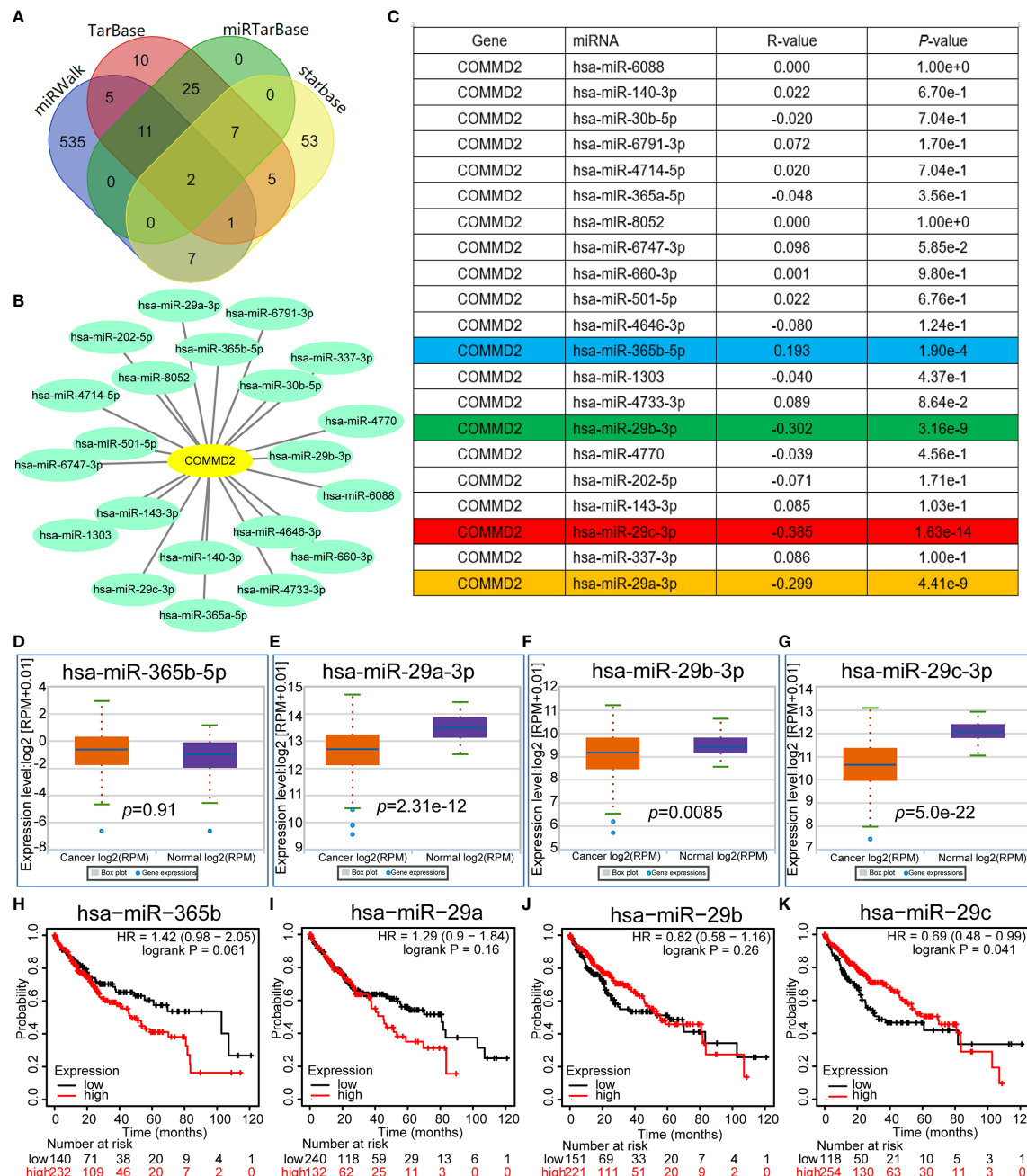


**FIGURE 4** | Prediction and analysis of miRNAs upstream of COMMD2. **(A)** miRNAs predicted to be upstream of COMMD2 using the miRWalk, TarBase, miRTarBase and starBase databases. **(B)** miRNA-COMMD2 regulatory network established using Cytoscape software. **(C)** Correlations between the predicted miRNAs and COMMD2 in LIHC as determined by the starBase database. **(D–G)** Expression of miR-365b-5p **(D)**, miR-29a-3p **(E)**, miR-29b-3p **(F)** and miR-29c-3p **(G)** in LIHC and normal tissue samples as determined by the starBase database. **(H–K)** Prognostic values of miR-365b-5p **(H)**, miR-29a-3p **(I)**, miR-29b-3p **(J)** and miR-29c-3p **(K)** in LIHC as assessed by Kaplan-Meier plotter.



(Figures 4H–K). Thus, miR-29c-3p might be the most promising miRNA that regulates COMMD2 in LIHC.

## Prediction and Analysis of lncRNAs Upstream of miR-29c-3p

Next, the lncRNAs upstream of miR-29c-3p were predicted using the starBase database. Fifty-four possible lncRNAs were predicted, and an lncRNA-miR-29c-3p regulatory network was constructed using Cytoscape software (Supplementary Figure 3). Next, the expression of these lncRNAs in LIHC was determined using GEPIA. Among the 54 predicted lncRNAs, only CRNDE, LINC00511, SNHG17, and HCG18 were expressed at significantly higher levels in LIHC tissues than in normal tissues (Figures 5A–D). Subsequently, the associations between the four lncRNAs and prognosis of LIHC patients were evaluated. High expression of CRNDE, SNHG17, or HCG18 was significantly associated with both unfavorable OS and disease-free survival (DFS) in LIHC patients (Figures 5E–L). In addition, increased expression of LINC00511 indicated a poor OS. Additionally, to further confirm the expression of ncRNAs and COMMD2 in LIHC, RT-qPCR was performed in 10 pairs of fresh LIHC specimens and adjacent normal tissue. In accordance with our previous analytic data, miR-29c-3p was significantly decreased in LIHC tissue compared with those in adjacent normal tissue (Figure 6E). In contrast, the expression levels of COMMD2, CRNDE, LINC00511, SNHG17 and HCG18 were significantly increased in LIHC tissue compared with adjacent normal tissue (Figures 6A–D, F). Based on the known interactions of these ncRNAs in ceRNA networks, lncRNAs potentially promote mRNA expression by competitively binding to matched miRNAs. Thus, negative correlations between lncRNAs and miRNAs or positive correlations between lncRNAs and mRNAs should have been observed. Correlation analysis with the starBase database indicated a positive or negative relationship between each of the four lncRNAs, particularly SNHG17 and HCG18, and COMMD2 or miR-29c-3p (Figures 6H–O). By combining expression, survival, and correlation analysis, a CRNDE/LINC00511/SNHG17/HCG18-miR-29c-3p-COMMD2 ceRNA network was constructed (Figure 6G) and could potentially serve as a prognostic model in LIHC.

## Relationship Between COMMD2 and Immune Cell Infiltration in LIHC

COMMD2 is a member of the COMMD family, the members of which affect the prognosis of patients by participating in the inflammatory response and immune cell infiltration. Therefore, the relationships between COMMD2 and infiltrating immune cells were displayed using TIMER. Positive relationships were observed between the expression of COMMD2 and the infiltration of B cells, CD8+ T cells, CD4+ T cells, macrophages, neutrophils, and dendritic cells (Figures 7B–G). Moreover, COMMD2 copy number alterations could affect the infiltration level of six dominant immune cells, especially high amplification and arm-level deletion (Figure 7A). To further understand the association between COMMD2 expression and

22 immune cell types in the TCGA-LIHC cohort, we summarized the relative fractions of these immune cells in each LIHC patient using the CIBERSORT method (Figure 8A). Patients with high COMMD2 expression exhibited significantly higher proportions of M0 macrophages and neutrophils ( $P < 0.05$ ) and lower proportions of CD8 T cells (Figure 8B). Next, we used two gene expression omnibus (GEO) datasets to determine the above results and found that patients with high COMMD2 expression had a significant increase in the abundance of M0 macrophages, neutrophils, resting dendritic cells and resting mast cells and a significant decrease in the abundance of plasma cells and resting NK cells in GSE55092 (Figures 8C, D). In GSE107170, M0 macrophages, neutrophils, naïve B cells, activated memory CD4 T cells and resting dendritic cells increased and plasma cells decreased in patients with high COMMD2 expression (Figures 8E, F). Thus, high COMMD2 expression is significantly associated with higher proportions of M0 macrophages and neutrophils. All these findings suggested that COMMD2 is closely related to the level of immune infiltration, suggesting that COMMD2 may be involved in regulating LIHC tumor immunity.

## Prognostic Analysis of COMMD2 Expression Based on Immune Cells in LIHC

Because COMMD2 expression was significantly associated with immune cell infiltration and a poor prognosis in LIHC, we next investigated whether COMMD2 expression influences the OS of LIHC patients by regulating immune cell infiltration. We performed survival analyses of LIHC patients based on COMMD2 expression in related immune cell subgroups. As shown in Figure 9 and Supplementary Figure 4, different infiltration levels of B cells, CD4+ memory T cells, CD8+ T cells, macrophages, mesenchymal stem cells, regulatory T cells, type 1 T helper cells and type 2 T helper cells were found in LIHC patients, and those with high COMMD2 expression had a poor prognosis. These results indicate that COMMD2 may influence the OS of LIHC patients by regulating immune cell infiltration.

## Correlations of COMMD2 With Immune Cell Biomarkers in LIHC

To further validate the role of COMMD2 in antitumor immunity, we explored the relationships between COMMD2 and immune cell biomarkers in LIHC using the GEPIA database. As listed in Table 2, COMMD2 was significantly positively correlated with most immune markers in various immune cell types, including B cells, CD8+ T cells, CD4+ T cells, M1 macrophages, M2 macrophages, neutrophils and dendritic cells. These results further support that COMMD2 is positively related to tumor immune cell infiltration in LIHC.

## Correlations Between COMMD2 and Immune Checkpoint Molecules in LIHC

As crucial immune checkpoint molecules, programmed death-1 (PD1), programmed death-ligand 1 (PD-L1) and cytotoxic T lymphocyte antigen-4 (CTLA-4) play important roles in

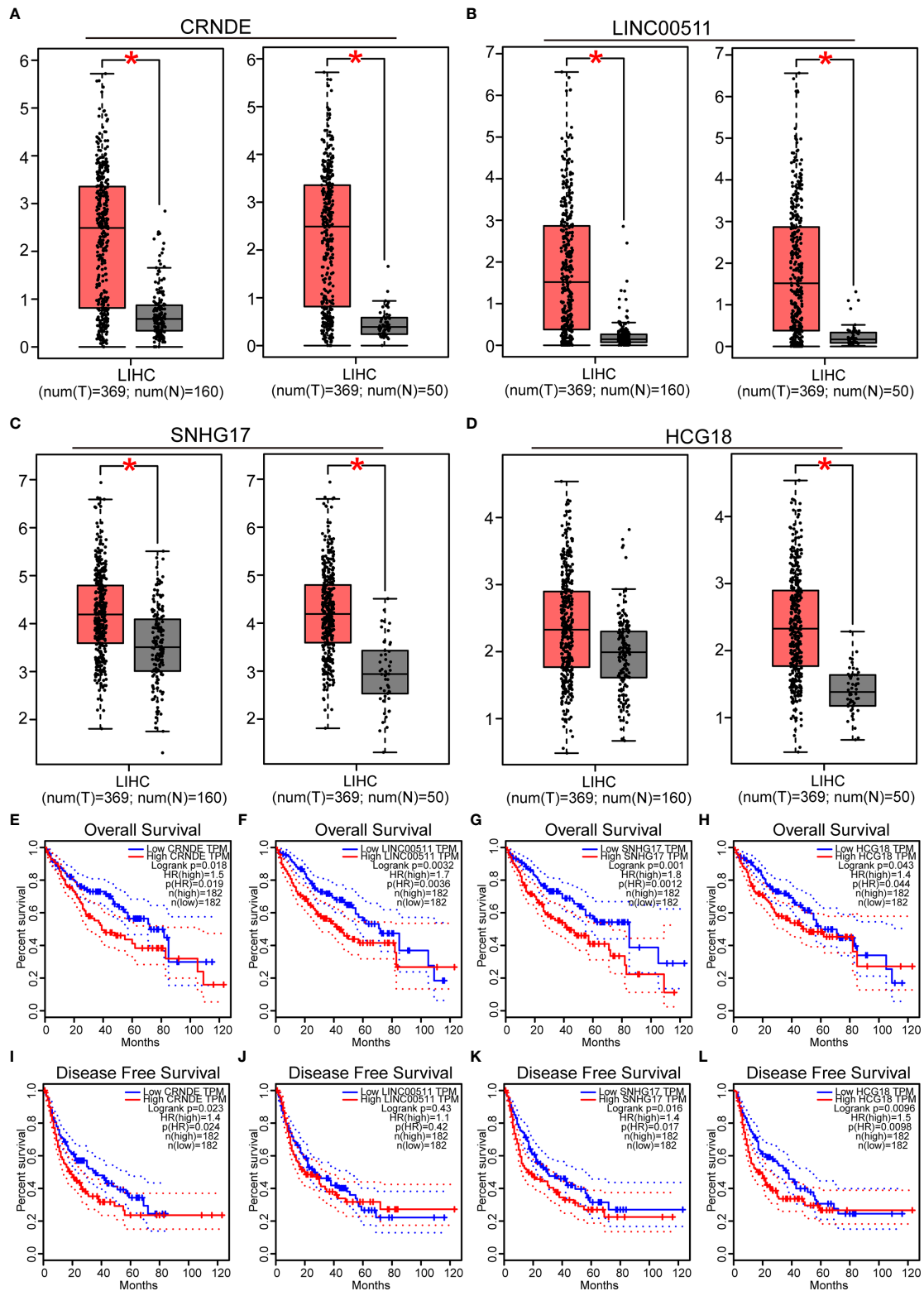


**FIGURE 5 |** Prediction and analysis of lncRNAs upstream of miR-29c-3p. (A–D) Expression of CRNDE (A), LINC00511 (B), SNHG17 (C) and HCG18 (D) in LIHC data compared with that in “TCGA normal” or “TCGA and GTEx normal” data. (E–L) OS analysis of CRNDE (E), LINC00511 (F), SNHG17 (G) and HCG18 (H) in LIHC. RFS analysis of CRNDE (I), LINC00511 (J), SNHG17 (K) and HCG18 (L) in LIHC. \*p value < 0.05.

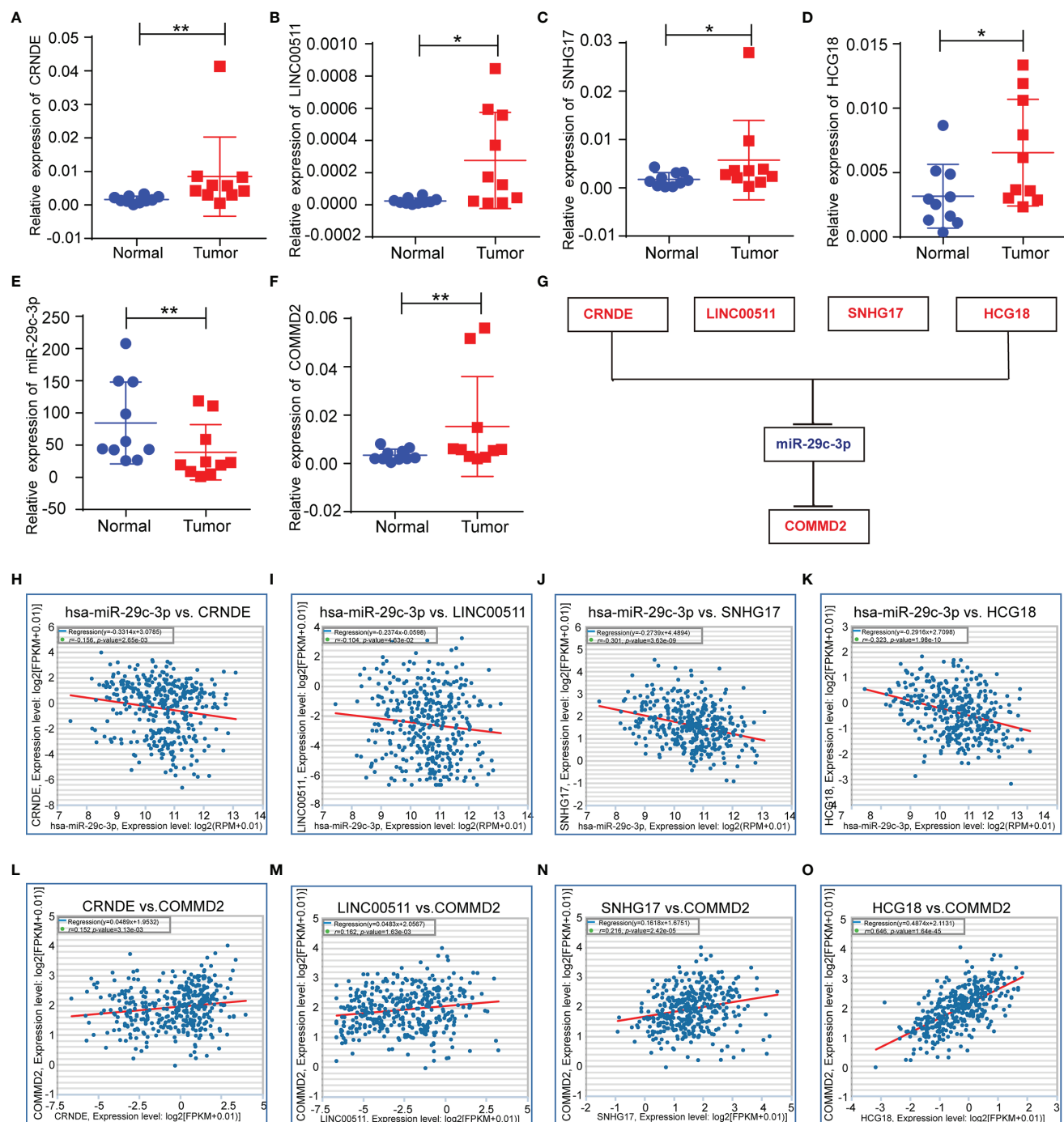


**FIGURE 6 |** Correlations of lncRNAs with miR-29c-3p and COMMD2 in LIHC. **(A–F)** Expression of crucial ncRNAs and COMMD2 in fresh LIHC specimens and adjacent normal tissue as determined by RT-qPCR. **(G)** Schematic model of the ceRNA network. Red indicates upregulation and blue indicates downregulation. **(H–K)** Correlations of CRNDE **(H)**, LINC00511 **(I)**, SNHG17 **(J)** and HCG18 **(K)** with miR-29c-3p in LIHC. **(L–O)** Correlations of CRNDE **(L)**, LINC00511 **(M)**, SNHG17 **(N)** and HCG18 **(O)** with COMMD2 in LIHC. \* $p < 0.05$ ; \*\* $p < 0.01$ .

tumor immune escape. Based on the potential oncogenic role of COMMD2 in LIHC, the correlations of COMMD2 with PD1, PD-L1 and CTLA-4 were estimated. COMMD2 was significantly positively correlated with PD1, PD-L1 and

CTLA-4 in LIHC (**Figures 10A–C**). Similar results were found using the GEPIA database, which revealed significant positive correlations of COMMD2 with PD1, PD-L1 or CTLA 4 in LIHC (**Figures 10D–F**). These results demonstrate that

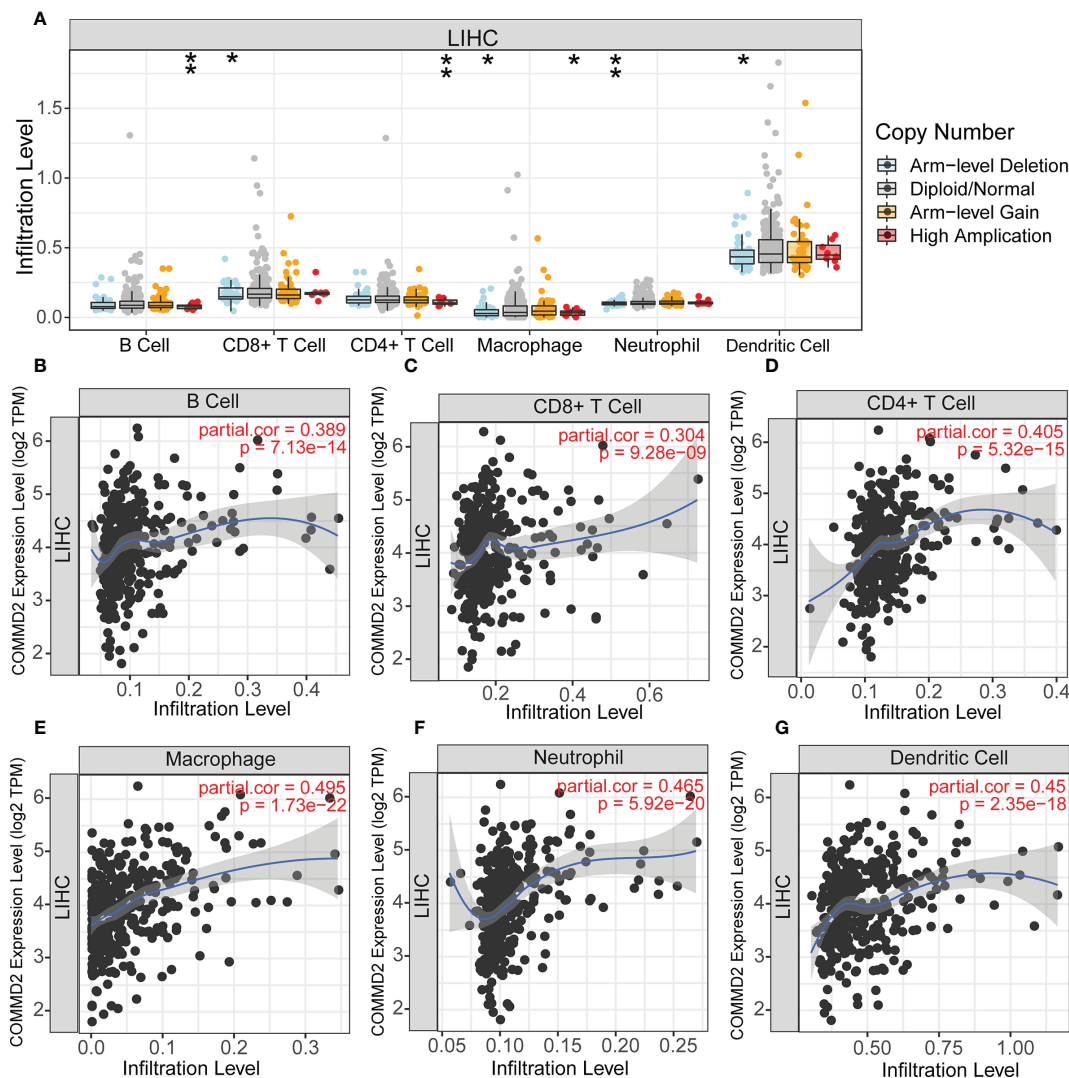


**FIGURE 7 |** Relationship Between COMMD2 and immune cell infiltration in LIHC. **(A)** Relationship Between COMMD2 copy number alterations and the infiltration level of six dominant immune cells in LIHC. **(B–G)** Correlations of COMMD2 with infiltrating B cells **(B)**, CD8+ T cells **(C)**, CD4+ T cells **(D)**, neutrophils **(E)**, macrophages **(F)** and dendritic cells **(G)** in LIHC. \* $p < 0.05$ ; \*\* $p < 0.01$ .

COMMD2 may be involved in tumor immune escape during LIHC tumorigenesis.

### Effects of COMMD2 Knockdown on the Proliferation and Migration of LIHC Cells *In Vitro*

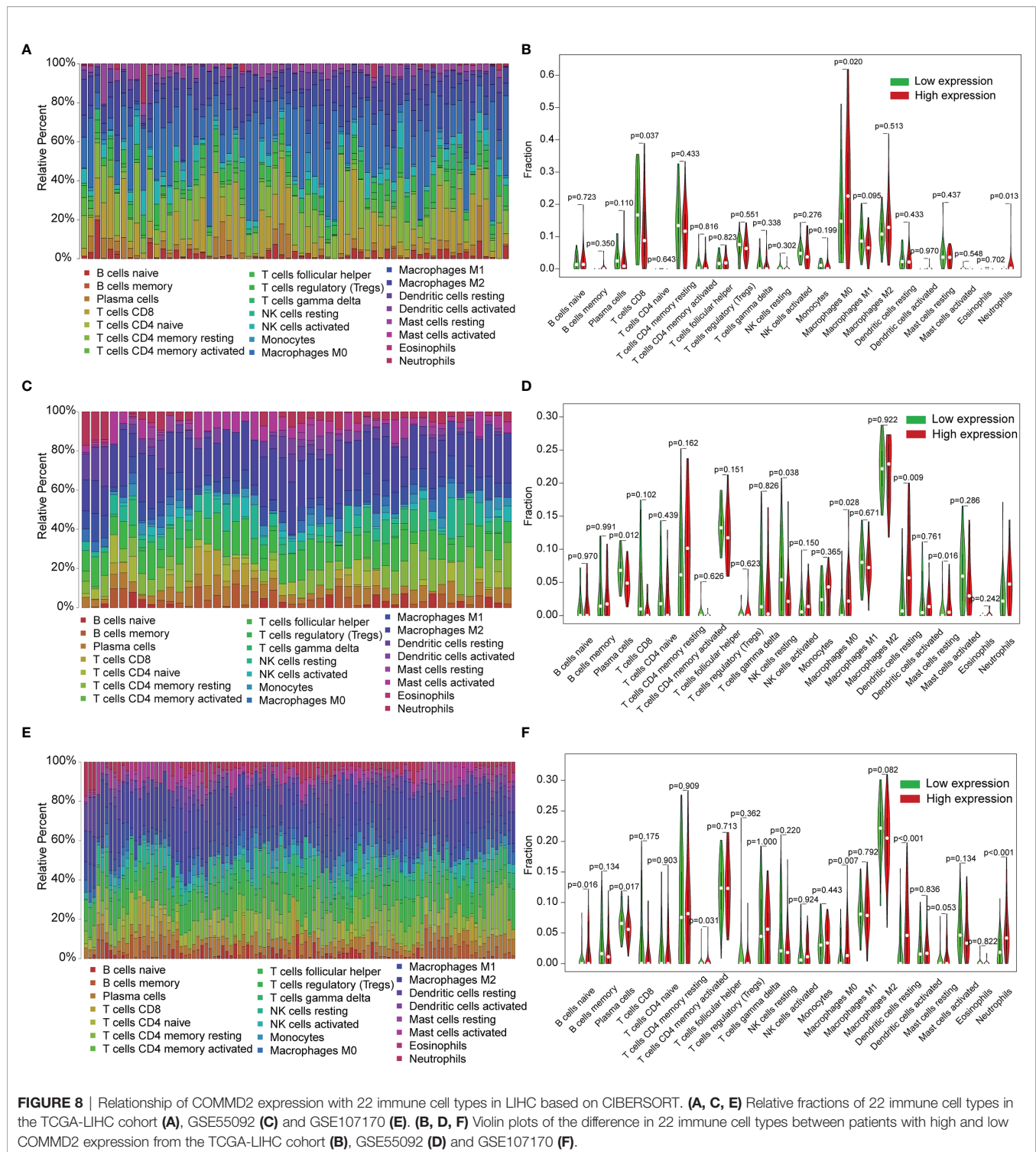
To assess the function of COMMD2 in LIHC, we knocked down its expression in HuH-7 and MHCC97-H cells using siRNAs, and the silencing efficiency was determined by RT-qPCR (**Figures 11A, B**). CCK8 and colony formation assays were performed to explore the effect of COMMD2 knockdown on LIHC cell proliferation, revealing that the proliferation of HuH-7 and MHCC97-H cells was significantly decreased after COMMD2 downregulation (**Figures 11C–F**). Subsequently, to

investigate the impacts of COMMD2 knockdown on LIHC cell migration ability, wound healing and transwell assays were performed, demonstrating that COMMD2 knockdown drastically decreased the migration ability of HuH-7 and MHCC97-H cells compared with that of control group cells (**Figures 11G–K**).

## DISCUSSION

LIHC is the third leading cause of cancer-related mortality worldwide (1). Although various therapeutic strategies have been adopted for LIHC patients, their efficacies remain





unsatisfactory (23). Identifying novel biomarkers of malignant LIHC is essential to identify new effective therapeutic targets and improve LIHC patient prognosis. Increasing evidence has demonstrated that COMMD proteins play key roles in the development and progression of multiple human

cancers (12, 13), including LIHC. However, the underlying mechanisms and clinical value of COMMD2 and its correlation with immune cell infiltration in LIHC remain unknown.

In the present study, we first performed pancancer analysis of COMMD2 expression using the TIMER and UALCAN

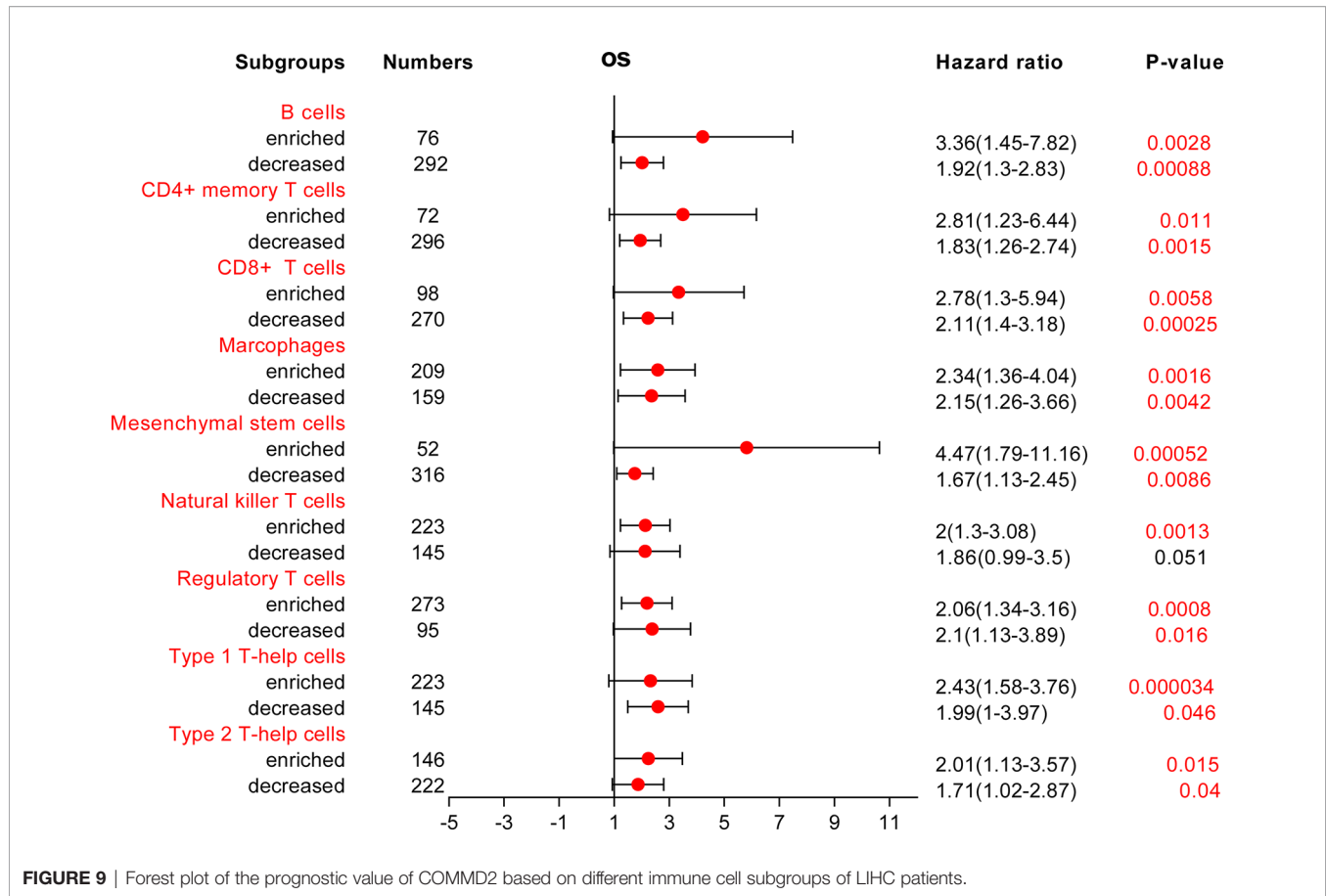


**TABLE 2 |** Correlation analysis of COMMD2 with immune cell biomarkers in LIHC.

Immune cell	Biomarker	R value	P value
B cells	CD19	0.18	0.00041***
	CD79A	0.11	0.034*
CD8+ T cells	CD8A	0.14	0.0064**
	CD8B	0.062	0.23
CD4+ T cells	CD4	0.31	8.1e-10***
M1 macrophages	NOS2	0.22	1.4e-05***
	IRF5	0.44	4e-19***
	PTGS2	0.27	8e-08***
M2 macrophages	CD163	0.031	0.55
	VSIG4	0.17	0.0014**
	MS4A4A	0.18	0.00065***
Neutrophils	CEACAM8	0.097	0.063
	ITGAM	0.35	3e-12***
	CCR7	0.13	0.01**
Dendritic cells	HLA-DPB1	0.18	0.00044***
	HLA-DQB1	-0.035	0.5
	HLA-DRA	0.24	2.4e-06***
	HLA-DPA1	0.22	1.6e-05***
	CD1C	0.2	7.3e-05***
	NRP1	0.46	1.6e-20***
	ITGAX	0.34	1.7e-11***

\*p value < 0.05, \*\*p value < 0.01, \*\*\*p value < 0.001.

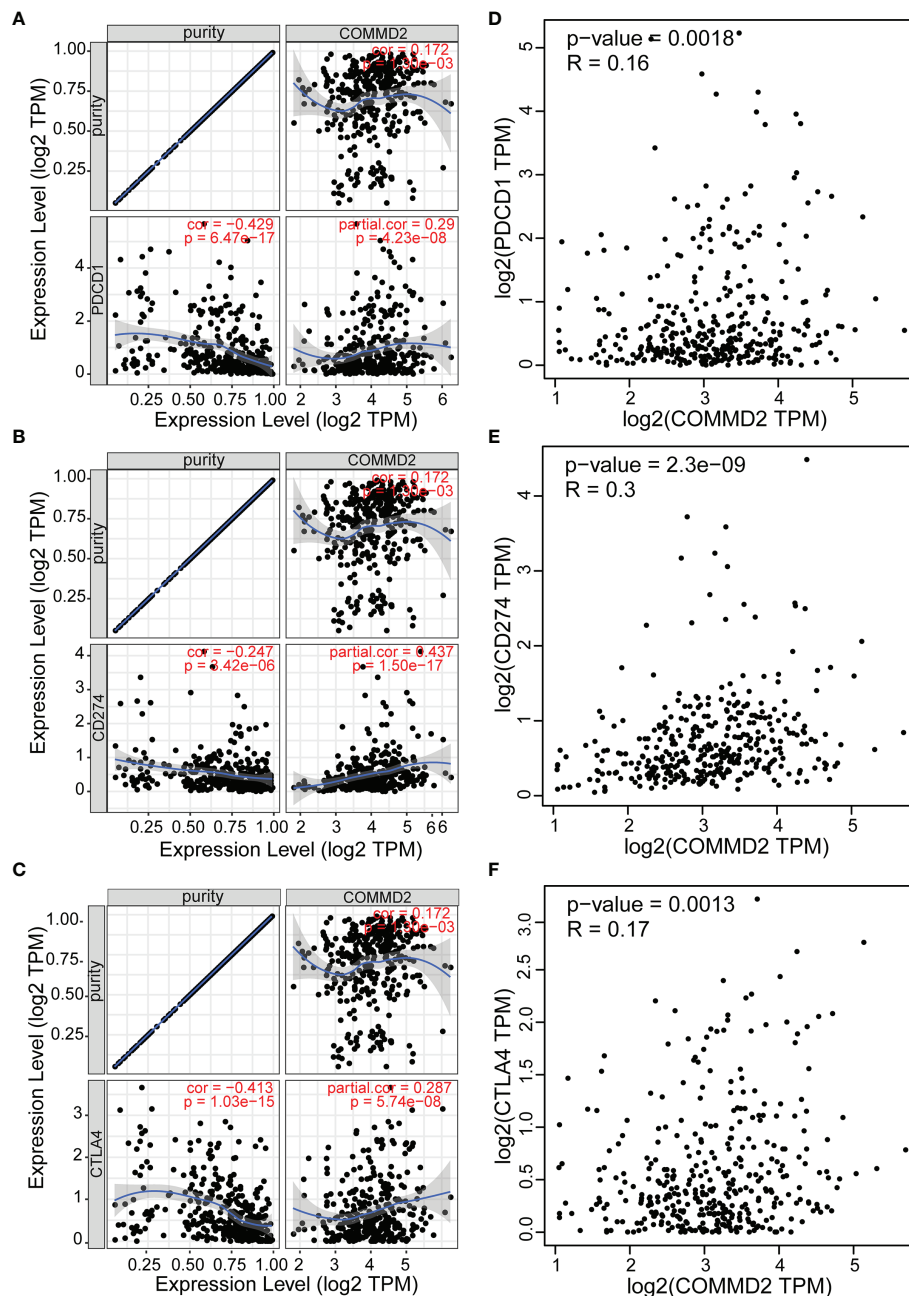


**FIGURE 10 |** Correlations between COMMD2 and PD-1, PD-L1 and CTLA-4 in LIHC. (A–C) Correlations of COMMD2 with PD-1 (A), PD-L1 (B) and CTLA-4 (C) in LIHC adjusted for purity using TIMER. (D–F) Relationships of COMMD2 with PD-1 (D), PD-L1 (E) and CTLA-4 (F) in LIHC as determined using the GEPIA database.

databases, and found that COMMD2 was abnormally expressed in the tumor tissues of 13 different cancer types compared with that in the corresponding normal tissues. Association analyses of COMMD2 with the survival of patients with candidate types of cancer indicated that high COMMD2 expression was associated with a poor prognosis in LIHC. Clinical association analyses demonstrated that increased COMMD2 expression was correlated with higher histological grade, more advanced clinical stage, lymph node metastasis and the TP53

mutation status in LIHC patients. Furthermore, COMMD2 knockdown suppresses LIHC cell proliferation and migration *in vitro* via a series of functional assays.

Previous studies have revealed that ncRNAs, particularly miRNAs, lncRNAs, and circular RNAs, are involved in the development and progression of tumors through gene regulation mechanisms involving ceRNA regulatory networks (24–27). To explore the upstream miRNAs that modulate COMMD2 expression, we used four prediction programs to predict miRNAs

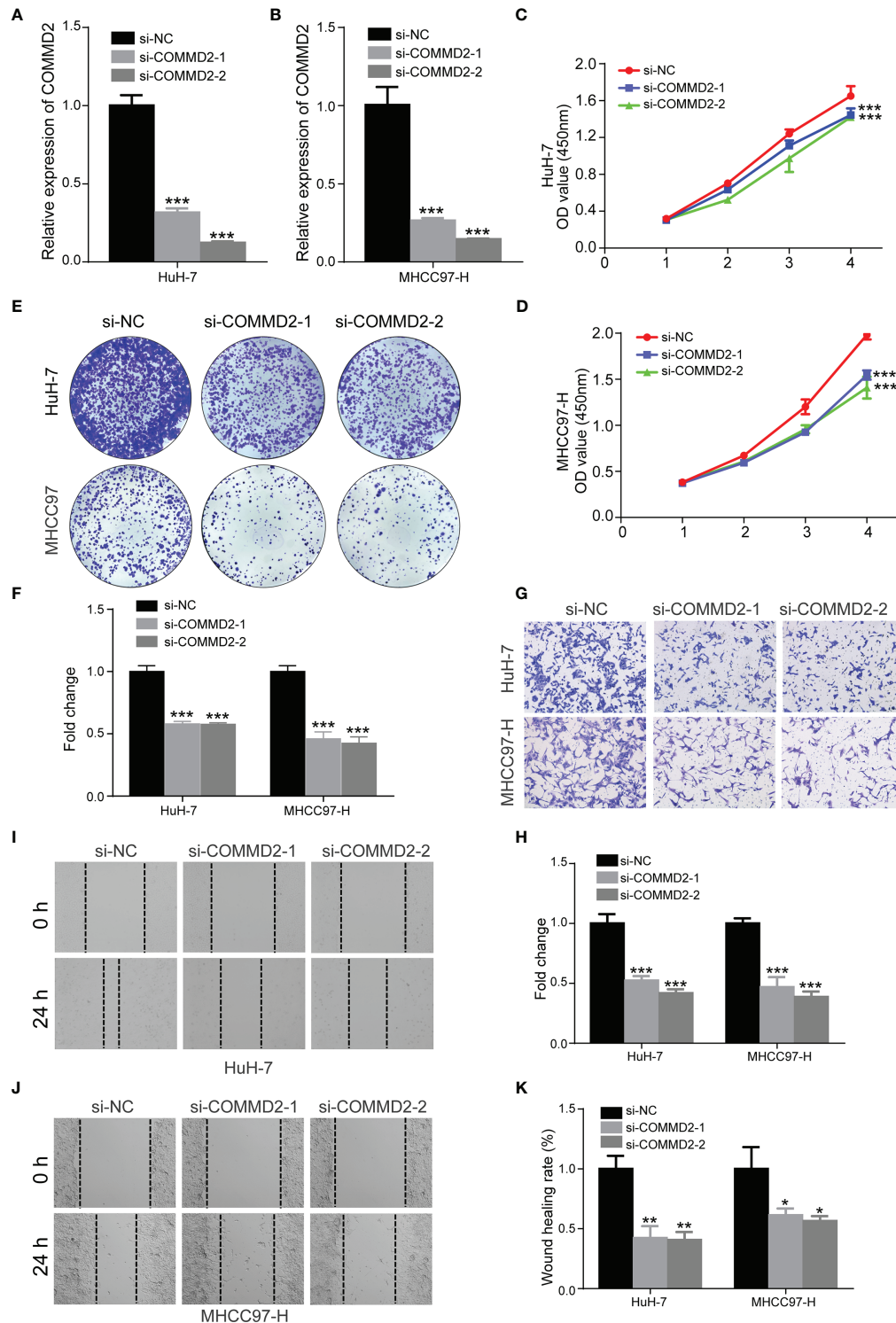


**FIGURE 11 |** Effects of COMMD2 knockdown on the proliferation and migration of LIHC cells. **(A, B)** The efficiency of COMMD2 downregulation in HuH-7 **(A)** and MHCC97-H **(B)** cells after COMMD2 siRNA transfection was detected by RT-qPCR. **(C–F)** Effect of COMMD2 knockdown on the proliferation of HuH-7 and MHCC97-H cells as determined by CCK8 **(C, D)** and colony formation assays **(E, F)**. **(G–K)** Effect of COMMD2 knockdown on the migration of HuH-7 and MHCC97-H cells as detected by transwell **(G, H)** and wound healing assays **(I–K)**. Scale bar=50  $\mu$ m. \* $P < 0.05$ ; \*\* $P < 0.01$ ; \*\*\* $P < 0.001$ .

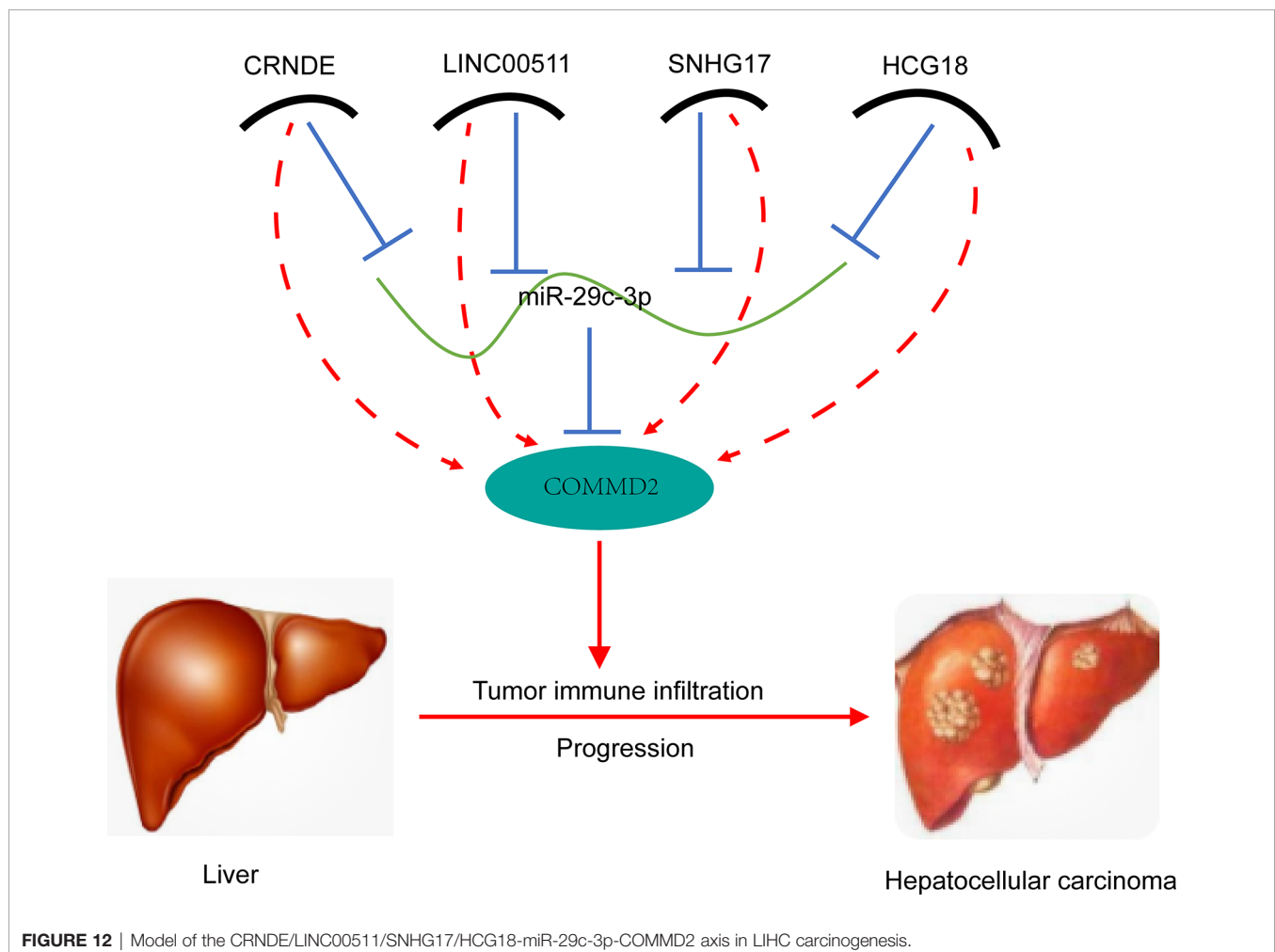


that potentially bind COMMD2 and ultimately identified 21 miRNAs. Most of these miRNAs play suppressor roles in LIHC. For example, miR-29b-3p regulates the TGF- $\beta$ 1 and p53 signaling pathways to inhibit the growth and induce the apoptosis of LIHC ascites H22 cells (28). miR-29a-3p inhibits cell proliferation and migration by targeting PTEN and thereby regulating the NF-kappaB pathway in LIHC (29). miR-29c-3p inhibits tumor progression by regulating the methylation of DNMT3B and LATS1 in LIHC (30). Among the 21 identified candidate miRNAs, only miR-29c-3p was expressed at a low level, which was negatively correlated with the high expression of COMMD2 and associated with a better prognosis for LIHC patients as determined by the combination of expression, correlation, and survival analyses. Thus, miR-29c-3p was selected as the most promising upstream miRNA of COMMD2. Previous studies also showed that miR-29c-3p inhibits LIHC proliferation (31).

According to the ceRNA hypothesis (32), the potential lncRNAs upstream of the miR-29c-3p/COMMD2 axis should be oncogenic lncRNAs in LIHC. Subsequently, lncRNAs upstream of the miR-29c-3p/COMMD2 axis were also predicted, ultimately identifying 54 possible lncRNAs. By performing expression, correlation, and survival analyses,

CRNDE, LINC00511, SNHG17 and HCG18 were identified as the most promising upregulated lncRNAs. High expression of CRNDE, LINC00511, SNHG17 and HCG18, which have positive and negative relationships with COMMD2 and miR-29c-3p, respectively, was associated with a poor prognosis in LIHC. The four lncRNAs functioned as oncogenes in multiple tumors, including LIHC. For example, the lncRNA CRNDE facilitates the proliferation, invasion, migration and chemoresistance of LIHC (33–36). LINC00511 promotes malignant cell behaviors and correlates with prognosis in LIHC (37–39). The lncRNA SNHG17 promotes cell proliferation and migration and predicts a poor prognosis in LIHC (40, 41). The lncRNA HCG18 contributes to the progression of LIHC (42, 43). Thus, the CRNDE/LINC00511/SNHG17/HCG18-miR-29c-3p-COMMD2 axis regulates the development and progression of LIHC.

Numerous recent studies have confirmed that tumor immune cell infiltration influences tumor angiogenesis and the prognosis of patients with LIHC (44–48). Herein, we found that COMMD2 was significantly positively correlated with various infiltrating immune cells in LIHC, especially M0 macrophages and neutrophils by various database. Moreover, COMMD2 was



closely related to immune markers of these tumor-infiltrating immune cells. Importantly, COMMD2 was shown to influence the OS of LIHC patients through immune cell infiltration. These findings indicate that tumor immune infiltration may partially explain the carcinogenic effect of COMMD2 in LIHC. In addition, immune checkpoint molecules, including PD-1, PD-L1, and CTLA-4, are associated with the prognosis of LIHC patients (49–51). Checkpoint inhibitors (CPIs) targeting PD-1, PD-L1, or CTLA-4 have led to clinical breakthroughs in oncological treatment (52–55). Thus, we also assessed the relationships between COMMD2 and immune checkpoint molecules. High COMMD2 expression was significantly linked to PD1, PD-L1 and CTLA-4 levels in LIHC, suggesting that targeting COMMD2 might enhance immunotherapeutic efficacy in LIHC.

However, some limitations in our study should be considered. First, our finding is mainly relies on public databases, more data and larger LIHC cohorts were required to validate its clinical suitability. Second, the role of COMMD2 in tumor immune infiltration needs to be further confirmed *in vitro* or *in vivo*. Finally, the carcinogenic mechanism of the CRNDE/LINC00511/SNHG17/HCG18-miR-29c-3p-COMMD2 axis in LIHC requires more functional studies to elucidate. Therefore, further investigations, including basic experiments and clinical trials, are needed to perform in the future.

In conclusion, our results indicate a carcinogenic effect of COMMD2 and its potential as a novel prognostic biomarker in LIHC. Furthermore, we further elucidated the underlying oncogenic mechanism of COMMD2 by constructing a CRNDE/LINC00511/SNHG17/HCG18-miR-29c-3p ceRNA network in LIHC (Figure 12). Additionally, our study showed that COMMD2 might play a cancer-promoting role by regulating tumor immune cell infiltration in patients with LIHC. Therefore, these findings provide a potentially valuable target for LIHC prognosis and immunotherapy.

## REFERENCES

1. Sung H, Ferlay J, Siegel RL, Laversanne M, Soerjomataram I, Jemal A, et al. Global Cancer Statistics 2020: GLOBOCAN Estimates of Incidence and Mortality Worldwide for 36 Cancers in 185 Countries. *CA Cancer J Clin* (2021) 71:209–49. doi: 10.3322/caac.21660
2. Kudo M, Finn RS, Qin S, Han KH, Ikeda K, Piscaglia F, et al. Lenvatinib Versus Sorafenib in First-Line Treatment of Patients With Unresectable Hepatocellular Carcinoma: A Randomised Phase 3 non-Inferiority Trial. *Lancet* (2018) 391:1163–73. doi: 10.1016/S0140-6736(18)30207-1
3. Pinter M, Scheiner B, Peck-Radosavljevic M. Immunotherapy for Advanced Hepatocellular Carcinoma: A Focus on Special Subgroups. *Gut* (2021) 70:204–14. doi: 10.1136/gutjnl-2020-321702
4. Bertuccio P, Turati F, Carioli G, Rodriguez T, La Vecchia C, Malvezzi M, et al. Global Trends and Predictions in Hepatocellular Carcinoma Mortality. *J Hepatol* (2017) 67:302–9. doi: 10.1016/j.jhep.2017.03.011
5. Villanueva A. Hepatocellular Carcinoma. *N Engl J Med* (2019) 380:1450–62. doi: 10.1056/NEJMr1713263
6. Burstein E, Hoberg JE, Wilkinson AS, Rumble JM, Csomos RA, Komarck CM, et al. COMMD Proteins, a Novel Family of Structural and Functional Homologs of MURR1. *J Biol Chem* (2005) 280:22222–32. doi: 10.1074/jbc.M501928200

## DATA AVAILABILITY STATEMENT

The original contributions presented in the study are included in the article/**Supplementary Material**. Further inquiries can be directed to the corresponding authors.

## ETHICS STATEMENT

This study was approved by the Ethics Committee of the First Affiliated Hospital of Nanchang University. The patients/participants provided their written informed consent to participate in this study.

## AUTHOR CONTRIBUTIONS

LZ and JX designed this work. WF conducted the experiments and collected the data. WF and YG analyzed the data. WF and LZ drafted the manuscript. JX revised the manuscript. All the authors approved the final version of this manuscript.

## FUNDING

This work was supported by the National Natural Science Foundation of China (grant number 81760431 and 81860427) and the Natural Science Foundation of Jiangxi Province, China (grant number 20161BAB205243).

## SUPPLEMENTARY MATERIAL

The Supplementary Material for this article can be found online at: <https://www.frontiersin.org/articles/10.3389/fonc.2022.853026/full#supplementary-material>

7. Zoubeidi A, Ettinger S, Beraldi E, Hadaschik B, Zardan A, Klomp LW, et al. Clusterin Facilitates COMMD1 and I-kappaB Degradation to Enhance NF-kappaB Activity in Prostate Cancer Cells. *Mol Cancer Res* (2010) 8:119–30. doi: 10.1158/1541-7786.MCR-09-0277
8. Zhan W, Wang W, Han T, Xie C, Zhang T, Gan M, et al. COMMD9 Promotes TFDP1/E2F1 Transcriptional Activity via Interaction With TFDP1 in non-Small Cell Lung Cancer. *Cell Signal* (2017) 30:59–66. doi: 10.1016/j.cellsig.2016.11.016
9. Yang SS, Li XM, Yang M, Ren XL, Hu JL, Zhu XH, et al. FMNL2 Destabilises COMMD10 to Activate NF-kappaB Pathway in Invasion and Metastasis of Colorectal Cancer. *Br J Cancer* (2017) 117:1164–75. doi: 10.1038/bjc.2017.260
10. Zheng L, Liang P, Li J, Huang XB, Liu SC, Zhao HZ, et al. ShRNA-Targeted COMMD7 Suppresses Hepatocellular Carcinoma Growth. *PLoS One* (2012) 7: e45412. doi: 10.1371/journal.pone.0045412
11. Yang M, Huang W, Sun Y, Liang H, Chen M, Wu X, et al. Prognosis and Modulation Mechanisms of COMMD6 in Human Tumours Based on Expression Profiling and Comprehensive Bioinformatics Analysis. *Br J Cancer* (2019) 121:699–709. doi: 10.1038/s41416-019-0571-x
12. van de Sluis B, Mao X, Zhai Y, Groot AJ, Vermeulen JF, van der Wall E, et al. COMMD1 Disrupts HIF-1alpha/Beta Dimerization and Inhibits Human Tumor Cell Invasion. *J Clin Invest* (2010) 120(6):2119–30. doi: 10.1172/JCI40583

13. Fedoseienko A, Wieringa HW, Wisman GB, Duiker E, Reyners AK, Hofker MH, et al. Nuclear COMMD1 Is Associated With Cisplatin Sensitivity in Ovarian Cancer. *PLoS One* (2016) 11(10):e0165385. doi: 10.1371/journal.pone.0165385
14. Zheng L, You N, Huang X, Gu H, Wu K, Mi N, et al. COMMD7 Regulates NF-kappaB Signaling Pathway in Hepatocellular Carcinoma Stem-Like Cells. *Mol Ther Oncol* (2019) 12:112–23. doi: 10.1016/j.omto.2018.12.006
15. You N, Li J, Huang X, Wu K, Tang Y, Wang L, et al. COMMD7 Promotes Hepatocellular Carcinoma Through Regulating CXCL10. *BioMed Pharmacother* (2017) 88:653–7. doi: 10.1016/j.biopha.2017.01.046
16. Bustin SA, Beaulieu JF, Huggett J, Jaggi R, Kibenge FS, Olsvik PA, et al. MIQE Précis: Practical Implementation of Minimum Standard Guidelines for Fluorescence-Based Quantitative Real-Time PCR Experiments. *BMC Mol Biol* (2010) 11:74. doi: 10.1186/1471-2199-11-74
17. Li T, Fan J, Wang B, Traugh N, Chen Q, Liu JS, et al. TIMER: A Web Server for Comprehensive Analysis of Tumor-Infiltrating Immune Cells. *Cancer Res* (2017) 77:e108–10. doi: 10.1158/0008-5472.CAN-17-0307
18. Newman AM, Liu CL, Green MR, Gentles AJ, Feng W, Xu Y, et al. Robust Enumeration of Cell Subsets From Tissue Expression Profiles. *Nat Methods* (2015) 12:453–7. doi: 10.1038/nmeth.3337
19. Chandrashekar DS, Bashel B, Balasubramanya SAH, Creighton CJ, Ponce-Rodriguez I, Chakravarthi B, et al. UALCAN: A Portal for Facilitating Tumor Subgroup Gene Expression and Survival Analyses. *Neoplasia* (2017) 19:649–58. doi: 10.1016/j.neo.2017.05.002
20. Tang Z, Li C, Kang B, Gao G, Li C, Zhang Z. GEPIA: A Web Server for Cancer and Normal Gene Expression Profiling and Interactive Analyses. *Nucleic Acids Res* (2017) 45:W98–W102. doi: 10.1093/nar/gkx247
21. Li JH, Liu S, Zhou H, Qu LH, Yang JH. Starbase V2.0: Decoding miRNA-ceRNA, miRNA-ncRNA and Protein-RNA Interaction Networks From Large-Scale CLIP-Seq Data. *Nucleic Acids Res* (2014) 42:D92–97. doi: 10.1093/nar/gkt1248
22. Lanczky A, Györfy B. Web-Based Survival Analysis Tool Tailored for Medical Research (KMplot): Development and Implementation. *J Med Internet Res* (2021) 23(7):e27633. doi: 10.2196/27633
23. Deng Y, Zhu J, Liu Z, Huang M, Chang DW, Gu J. Elevated Systemic Inflammatory Responses, Factors Associated With Physical and Mental Quality of Life, and Prognosis of Hepatocellular Carcinoma. *Aging (Albany NY)* (2020) 12:4357–70. doi: 10.18632/aging.102889
24. Zhan M, He K, Xiao J, Liu F, Wang H, Xia Z, et al. LncRNA HOXA11-AS Promotes Hepatocellular Carcinoma Progression by Repressing miR-214-3p. *J Cell Mol Med* (2018) 22:3758–67. doi: 10.1111/jcmm.13633
25. Lou W, Ding B, Wang J, Xu Y. The Involvement of the Hsa\_Circ\_0088494-miR-876-3p-CTNNB1/CCND1 Axis in Carcinogenesis and Progression of Papillary Thyroid Carcinoma. *Front Cell Dev Biol* (2020) 8:605940. doi: 10.3389/fcell.2020.605940
26. Gao S, Ding B, Lou W. microRNA-Dependent Modulation of Genes Contributes to ESR1's Effect on ERalpha Positive Breast Cancer. *Front Oncol* (2020) 10:753. doi: 10.3389/fonc.2020.00753
27. Qi X, Zhang DH, Wu N, Xiao JH, Wang X, Ma W. ceRNA in Cancer: Possible Functions and Clinical Implications. *J Med Genet* (2015) 52:710–8. doi: 10.1136/jmedgenet-2015-103334
28. Liu YL, Yang WH, Chen BY, Nie J, Su ZR, Zheng JN, et al. Mir29b Suppresses Proliferation and Induces Apoptosis of Hepatocellular Carcinoma Ascites H22 Cells via Regulating TGFbeta1 and P53 Signaling Pathway. *Int J Mol Med* (2021) 48:157. doi: 10.3892/ijmm.2021.4990
29. Ma JH, Bu X, Wang JJ, Xie YX. MicroRNA-29-3p Regulates Hepatocellular Carcinoma Progression Through NF-kappaB Pathway. *Clin Lab* (2019) 65:801–6. doi: 10.7754/Clin.Lab.2018.181012
30. Wu H, Zhang W, Wu Z, Liu Y, Shi Y, Gong J, et al. miR-29c-3p Regulates DNMT3B and LATS1 Methylation to Inhibit Tumor Progression in Hepatocellular Carcinoma. *Cell Death Dis* (2019) 10:48. doi: 10.1038/s41419-018-1281-7
31. Lv T, Jiang L, Kong L, Yang J. MicroRNA29c3p Acts as a Tumor Suppressor Gene and Inhibits Tumor Progression in Hepatocellular Carcinoma by Targeting TRIM31. *Oncol Rep* (2020) 43:953–64. doi: 10.3892/or.2020.7469
32. Salmena L, Poliseno L, Tay Y, Kats L, Pandolfi PP. A ceRNA Hypothesis: The Rosetta Stone of a Hidden RNA Language? *Cell* (2011) 146:353–8. doi: 10.1016/j.cell.2011.07.014
33. Wang H, Ke J, Guo Q, Barnabo Nampoukime KP, Yang P, Ma K. Long non-Coding RNA CRNDE Promotes the Proliferation, Migration and Invasion of Hepatocellular Carcinoma Cells Through miR-217/MAPK1 Axis. *J Cell Mol Med* (2018) 22:5862–76. doi: 10.1111/jcmm.13856
34. Xie SC, Zhang JQ, Jiang XL, Hua YY, Xie SW, Qin YA, et al. LncRNA CRNDE Facilitates Epigenetic Suppression of CELF2 and LATS2 to Promote Proliferation, Migration and Chemoresistance in Hepatocellular Carcinoma. *Cell Death Dis* (2020) 11:676. doi: 10.1038/s41419-020-02853-8
35. Ji D, Jiang C, Zhang L, Liang N, Jiang T, Yang B, et al. LncRNA CRNDE Promotes Hepatocellular Carcinoma Cell Proliferation, Invasion, and Migration Through Regulating miR-203/BCAT1 Axis. *J Cell Physiol* (2019) 234:6548–60. doi: 10.1002/jcp.27396
36. Chen L, Sun L, Dai X, Li T, Yan X, Zhang Y, et al. LncRNA CRNDE Promotes ATG4B-Mediated Autophagy and Alleviates the Sensitivity of Sorafenib in Hepatocellular Carcinoma Cells. *Front Cell Dev Biol* (2021) 9:687524. doi: 10.3389/fcell.2021.687524
37. Hu WY, Wei HY, Li KM, Wang RB, Xu XQ, Feng R. LINC00511 as a ceRNA Promotes Cell Malignant Behaviors and Correlates With Prognosis of Hepatocellular Carcinoma Patients by Modulating miR-195/EYA1 Axis. *BioMed Pharmacother* (2020) 121:109642. doi: 10.1016/j.biopha.2019.109642
38. Wang RP, Jiang J, Jiang T, Wang Y, Chen LX. Increased Long Noncoding RNA LINC00511 is Correlated With Poor Prognosis and Contributes to Cell Proliferation and Metastasis by Modulating miR-424 in Hepatocellular Carcinoma. *Eur Rev Med Pharmacol Sci* (2019) 23:3291–301. doi: 10.26355/eurrev\_201904\_17691
39. Peng X, Li X, Yang S, Huang M, Wei S, Ma Y, et al. LINC00511 Drives Invasive Behavior in Hepatocellular Carcinoma by Regulating Exosome Secretion and Invadopodia Formation. *J Exp Clin Cancer Res* (2021) 40:183. doi: 10.1186/s13046-021-01990-y
40. Ma T, Zhou X, Wei H, Yan S, Hui Y, Liu Y, et al. Long Non-Coding RNA SNHG17 Upregulates RFX1 by Sponging miR-3180-3p and Promotes Cellular Function in Hepatocellular Carcinoma. *Front Genet* (2020) 11:607636. doi: 10.3389/fgene.2020.607636
41. Zhu XM, Li L, Ren LL, Du L, Wang YM. LncRNA SNHG17 Predicts Poor Prognosis and Promotes Cell Proliferation and Migration in Hepatocellular Carcinoma. *Eur Rev Med Pharmacol Sci* (2021) 25:4219–27. doi: 10.26355/eurrev\_202106\_26127
42. Zou Y, Sun Z, Sun S. LncRNA HCG18 Contributes to the Progression of Hepatocellular Carcinoma via miR-214-3p/CENPM Axis. *J Biochem* (2020) 168:535–46. doi: 10.1093/jb/mvaa073
43. Zhang L, Wang Z, Li M, Sun P, Bai T, Wang W, et al. HCG18 Participates in Vascular Invasion of Hepatocellular Carcinoma by Regulating Macrophages and Tumor Stem Cells. *Front Cell Dev Biol* (2021) 9:707073. doi: 10.3389/fcell.2021.707073
44. Zhang J, Chang L, Zhang X, Zhou Z, Gao Y. Meta-Analysis of the Prognostic and Clinical Value of Tumor-Associated Macrophages in Hepatocellular Carcinoma. *J Invest Surg* (2021) 34:297–306. doi: 10.1080/08941939.2019.1631411
45. Fu J, Zhang Z, Zhou L, Qi Z, Xing S, Lv J, et al. Impairment of CD4+ Cytotoxic T Cells Predicts Poor Survival and High Recurrence Rates in Patients With Hepatocellular Carcinoma. *Hepatology* (2013) 58:139–49. doi: 10.1002/hep.26054
46. Yu S, Wang Y, Hou J, Li W, Wang X, Xiang L, et al. Tumor-Infiltrating Immune Cells in Hepatocellular Carcinoma: Tregs is Correlated With Poor Overall Survival. *PLoS One* (2020) 15:e0231003. doi: 10.1371/journal.pone.0231003
47. Xu X, Tan Y, Qian Y, Xue W, Wang Y, Du J, et al. Clinicopathologic and Prognostic Significance of Tumor-Infiltrating CD8+ T Cells in Patients With Hepatocellular Carcinoma: A Meta-Analysis. *Med (Baltimore)* (2019) 98:e13923. doi: 10.1097/MD.00000000000013923
48. Garnelo M, Tan A, Her Z, Yeong J, Lim CJ, Chen J, et al. Interaction Between Tumour-Infiltrating B Cells and T Cells Controls the Progression of Hepatocellular Carcinoma. *Gut* (2017) 66:342–51. doi: 10.1136/gutjnl-2015-310814
49. Gao Q, Wang XY, Qiu SJ, Yamato I, Sho M, Nakajima Y, et al. Overexpression of PD-L1 Significantly Associates With Tumor Aggressiveness and Postoperative Recurrence in Human Hepatocellular Carcinoma. *Clin Cancer Res* (2009) 15:971–9. doi: 10.1158/1078-0432.CCR-08-1608

50. Umemoto Y, Okano S, Matsumoto Y, Nakagawara H, Matono R, Yoshiya S, et al. Prognostic Impact of Programmed Cell Death 1 Ligand 1 Expression in Human Leukocyte Antigen Class I-Positive Hepatocellular Carcinoma After Curative Hepatectomy. *J Gastroenterol* (2015) 50:65–75. doi: 10.1007/s00535-014-0933-3
51. Chang H, Jung W, Kim A, Kim HK, Kim WB, Kim JH, et al. Expression and Prognostic Significance of Programmed Death Protein 1 and Programmed Death Ligand-1, and Cytotoxic T Lymphocyte-Associated Molecule-4 in Hepatocellular Carcinoma. *APMIS* (2017) 125:690–8. doi: 10.1111/apm.12703
52. Herbst RS, Baas P, Kim DW, Felip E, Perez-Gracia JL, Han JY, et al. Pembrolizumab Versus Docetaxel for Previously Treated, PD-L1-Positive, Advanced non-Small-Cell Lung Cancer (KEYNOTE-010): A Randomised Controlled Trial. *Lancet* (2016) 387:1540–50. doi: 10.1016/S0140-6736(15)01281-7
53. Borghaei H, Paz-Ares L, Horn L, Spigel DR, Steins M, Ready NE, et al. Nivolumab Versus Docetaxel in Advanced Nonsquamous Non-Small-Cell Lung Cancer. *N Engl J Med* (2015) 373:1627–39. doi: 10.1056/NEJMoa1507643
54. Fehrenbacher L, Spira A, Ballinger M, Kowanetz M, Vansteenkiste J, Mazieres J, et al. Atezolizumab Versus Docetaxel for Patients With Previously Treated non-Small-Cell Lung Cancer (POPLAR): A Multicentre, Open-Label, Phase 2 Randomised Controlled Trial. *Lancet* (2016) 387:1837–46. doi: 10.1016/S0140-6736(16)00587-0
55. Chae YK, Arya A, Iams W, Cruz MR, Chandra S, Choi J, et al. Current Landscape and Future of Dual Anti-CTLA4 and PD-1/PD-L1 Blockade

Immunotherapy in Cancer; Lessons Learned From Clinical Trials With Melanoma and non-Small Cell Lung Cancer (NSCLC). *J Immunother Cancer* (2018) 6:39. doi: 10.1186/s40425-018-0349-3

**Conflict of Interest:** The authors declare that the research was conducted in the absence of any commercial or financial relationships that could be construed as a potential conflict of interest.

**Publisher's Note:** All claims expressed in this article are solely those of the authors and do not necessarily represent those of their affiliated organizations, or those of the publisher, the editors and the reviewers. Any product that may be evaluated in this article, or claim that may be made by its manufacturer, is not guaranteed or endorsed by the publisher.

Copyright © 2022 Fang, Gan, Zhang and Xiong. This is an open-access article distributed under the terms of the Creative Commons Attribution License (CC BY). The use, distribution or reproduction in other forums is permitted, provided the original author(s) and the copyright owner(s) are credited and that the original publication in this journal is cited, in accordance with accepted academic practice. No use, distribution or reproduction is permitted which does not comply with these terms.



# Advantages of publishing in Frontiers



## OPEN ACCESS

Articles are free to read  
for greatest visibility  
and readership



## FAST PUBLICATION

Around 90 days  
from submission  
to decision



## HIGH QUALITY PEER-REVIEW

Rigorous, collaborative,  
and constructive  
peer-review



## TRANSPARENT PEER-REVIEW

Editors and reviewers  
acknowledged by name  
on published articles

## Frontiers

Avenue du Tribunal-Fédéral 34  
1005 Lausanne | Switzerland

Visit us: [www.frontiersin.org](http://www.frontiersin.org)

Contact us: [frontiersin.org/about/contact](http://frontiersin.org/about/contact)



## REPRODUCIBILITY OF RESEARCH

Support open data  
and methods to enhance  
research reproducibility



## DIGITAL PUBLISHING

Articles designed  
for optimal readership  
across devices



## FOLLOW US

@frontiersin



## IMPACT METRICS

Advanced article metrics  
track visibility across  
digital media



## EXTENSIVE PROMOTION

Marketing  
and promotion  
of impactful research



## LOOP RESEARCH NETWORK

Our network  
increases your  
article's readership